Utilising novel thiol-acrylate click reactions to synthesise controlled branched polymer emulsifiers

UNIVERSITY OF LIVERPOOL

Thesis submitted in accordance with the requirements of the

University of Liverpool for the degree of Doctor in Philosophy

By Samuel Edward Robert Auty

September 2014

Abstract

The formation of multi-functional thiol materials for “click” reactions in synthetic chemistry has been significantly under-represented due to added practices that are typically required when working with sulfur-containing compounds. An efficient and facile approach to approach to introducing multiple masked thiols at the surface of polyester dendritic materials is presented, avoiding these difficulties, by utilising a xanthate protecting group.

One-pot xanthate deprotection and thiol-acrylate Michael additions from the xanthate-functional dendrimers (generation zero to two) has been accomplished for the first time, using three different acrylate substrates of varying chemistry. The dendrimers were fully characterised by ^{1}H and ^{13}C NMR, SEC and either electrospray or MALDI-TOF mass spectrometry, depending upon the generation and nature of the end groups. In a similar fashion, this one-pot methodology was extended to prepare twenty different surface functional LDHs via the use of xanthate functional ATRP dendritic macroinitiators (generation one to four) and six different acrylate monomers. Model reactions and kinetics studies showed that the presence of xanthates within the initiator structure did not complicate the ATRP of ^{t}BuMA. The LDHs were fully characterised by ^{1}H NMR and SEC.

In the final study, employing one-pot xanthate deprotection and thiol-acrylate Michael addition, four dendritic ATRP macroinitiators with hydrophobic and pH responsive peripheral functionalities were prepared. Polymeric surfactants comprised of LDHs and HPDs were synthesised, varying in end group composition using different dendritic macroinitiators, and through the use of mixed initiating system, using a non-dendritic component. O/w emulsions stabilised by surfactants comprised of linear polymers, LDHs, or mixed linear polymers/LDHs architectures showed coalescence over a long term stability study under neutral and acid conditions. In contrast, o/w emulsions stabilised by surfactants comprised of branched polymers, HPDs, or mixed branched polymer/HPDs architectures showed no coalescence over a long term stability study under neutral and acid conditions. Further dilution and thermal studies to probe emulsion systems stabilised via branched surfactant architectures resulted in emulsion breakdown.

Acknowledgments

I would like to thank everyone who has been involved in the running of The University of Liverpool Department of Chemistry over the last eight years. Without the chemistry stores, facilities management, finance, electronics and workshop services this PhD thesis could not have been completed. I would also like to thank all of the staff involved in the analytical services, particularly Moya McCarron (mass spectrometry) and Jean Ellis (microanalysis) for running my samples over the last four years. I would like to thank Sean Higgins and Tony Ellis for running the NMR service and I am extremely grateful to Oliver Andrén and Michael Malkoch at the KTH Royal Institute of Technology in Stockholm, Sweden, for all the MALDI-TOF analysis results they have provided.

I would like to thank my supervisor Prof. Steve Rannard, for offering me the opportunity to begin this PhD. Steve has provided me with new ideas, enthusiasm, support, and importantly, has made the journey of my research extremely enjoyable. I am truly grateful to him for allowing me (and funding me) to go to international scientific conferences and I will miss being part of his research group. I would also like to thank everyone in the Rannard group, in particular Pierre Chambon, who has been brilliant for day-to-day advice and fixing the SEC!

Finally, I would like to thank all my family, particularly Mum, Dad and David, who have listened to various parts of science from this thesis over the past four years! I really appreciate everything, especially the support during writing.

This thesis is written in memory of James Atherton who was a close family friend who sadly passed away in January 2013.

Abbreviations

APAP - 1-[N, N-bis(2-aminopropyl)-amino]-2-propanol

BA - Benzyl acrylate

BAPA - Bis(3-aminopropyl)amine

Bis-MPA - 2,2-Bismethylolpropanoic acid

Bz - Benzyl

BTYA - Butyl acrylate

CDI - 1,1'-Carbonyldiimidazole

CI-MS - Chemical ionisation mass spectrometry

COSY - Correlation Spectroscopy

DCC - N,N'-Dicyclohexylcarbodiimide

DCU - Dicyclohexylurea

DDT - Dodecanethiol

DMAEA - 2-(Dimethylamino)ethyl acrylate

DMAP - 4-Dimethylaminopyridine

DMPP - Dimethylphenylphopshine

DPTS - 4-(Dimethylamino)pyridinium *p*-toluenesulfonate

EGDMA - Ethylene glycol dimethacrylate

ESI-MS - Electrospray mass spectrometry

G – Generation

HEA - 2-Hydroxyethyl acrylate

HPD - Hyperbranched polydendron

HPMA - Hydroxylpropyl methacrylate

IPA - Propan-2-ol

IPLA - Isopropanolamine

LDH - Linear dendritic hybrid

MALDI-TOF - Matrix-assisted laser desorption ionization time of flight spectroscopy

Mp - Morpholino

MPA - Morpholino propan-2-oyl acrylate

NHS - N-hydroxysuccinicmide

NMR - Nuclear Magnetic Resonance

OEGA - Oligo(ethylene glycol) methyl ether acrylate (M_n = 480 Da)

OEGMA - Oligo(ethyleneglycol) monomethyl ether methacrylate (M_n = 300 Da)

PAMAM - Polyamidoamine

p-TSe - Para-Toluenesulfonyl ethyl

PO - Propylene oxide

SEC - Size Exclusion Chromatography

TAEA - Tris(2-aminoethyl)amine

^{t}BOC - N-*tert*-butoxycarbonyl

TEA – Triethanolamine

THPE - 1,1,1-Tris-(hydroxyphenyl)ethane

TLC - Thin layer chromatography

TMS - Tetramethylsilane

Table of Contents

CHAPTER 1

Introduction

1.1 Overview

This chapter aims to describe the different synthetic routes that have been developed historically to synthesise and functionalise dendrimers, with particular emphasis on the evolution of "click chemistry" concepts. Further focus will be placed upon the development of dendritic "hybrid" materials which utilise and combine the monodisperse nature of dendrimers with the synthetic ease of traditional polymer chemistry. Since this study is directed towards the design and synthesis of new functionalisation chemistries for responsive amphiphilic materials, emulsion technologies will also be reviewed.

1.2 Dendritic macromolecules

Over the past 30 years, dendritic polymers have played a significant role in the evolution of macromolecular chemistry.

Dendritic polymers can be divided into two main categories; dendrimers and hyperbranched polymers. Dendrimers are theoretically structurally *perfect*, branched macromolecules that are monodisperse and synthesised by repetitive organic chemistry steps. In contrast to this, hyperbranched polymers are *irregular* branched polymeric materials that have a broad polydispersity and are synthesised by one-pot procedures using AB_x monomers. Hyperbranched polymers will be not be reviewed within this introduction, and instead the reader is directed towards a recent review for a more in-depth understanding of such materials.[1]

A dendrimer can be divided into main three architectural regions; the core, the branching units, and the peripheral groups, Figure 1.1. The number of layers within the structure is known as the generation (G) of the dendrimer.

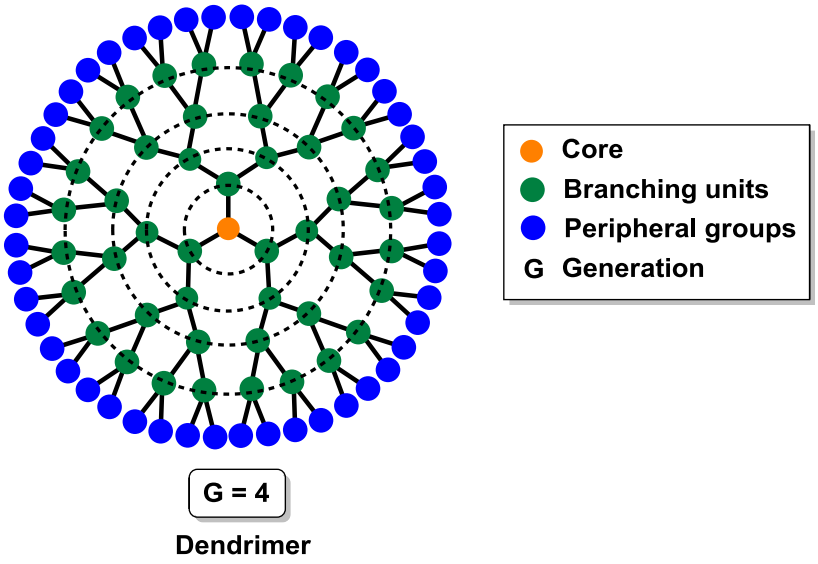

Figure 1.1 Schematic representation of a dendrimer structure

1.2.1 Divergent Synthesis

1.2.1.1 First example of divergent synthesis

The earliest example of a divergent dendrimer synthesis is widely believed to have been reported by Vögtle and coworkers in 1978.[2] These relatively small molecules (what would now be referred to as "low-generation dendrimer") were initially named "cascade molecules", and were synthesised by reacting benzyl amine with two equivalents of acrylonitrile using an amine Michael addition, to introduce a branching point. Reduction of the resulting nitrile groups, to primary amines, allowed the process to be repeated, Scheme 1.1.

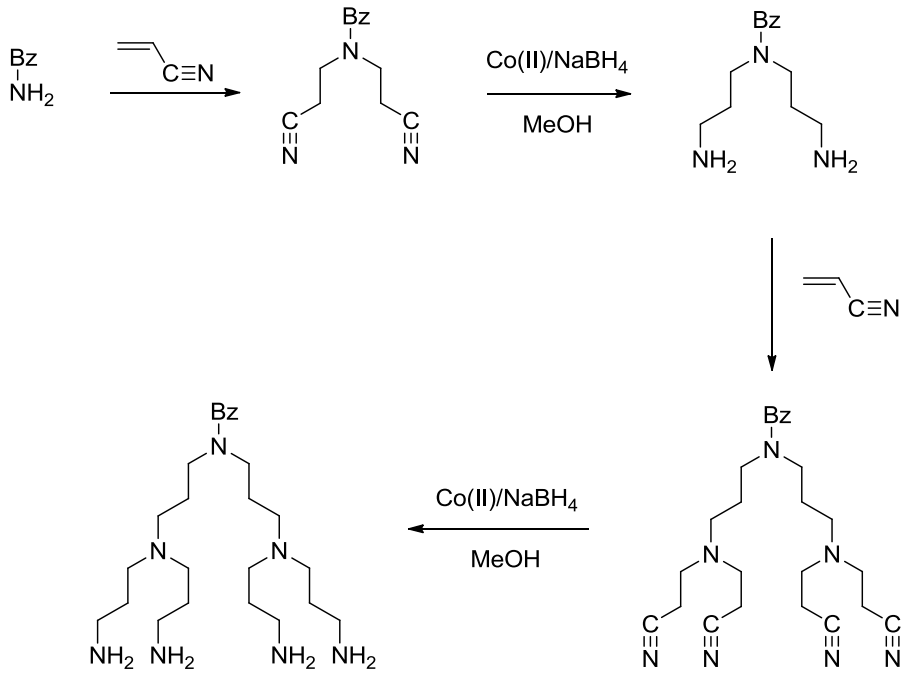

Scheme 1.1 First example of a dendrimer synthesis; originally termed "cascade molecules" by Vögtle and coworkers.[2]

1.2.1.2 Later developments for divergent growth

The most significant advances in the development of this synthesis strategy came in 1985, when Tomalia *et al.* at Dow Chemicals, published the synthesis of PAMAM dendrimers, often referred to as "Starburst™ Polymers".[3] The name PAMAM originates from the fact that these molecules contain a repeating pattern of amide linkages in the macromolecule backbone and tertiary amine branching points (**P**oly**AM**ido-**AM**ine).[4] Later in the same year, Newkome *et al.* published a similar type of branched structure which they called "Arborols".[5]

The term "dendrimer", originally used in the first PAMAM publication is the name that is used today to describe ideally branched monodisperse macromolecules of this type. The word is derived from two Greek words, "dendros" meaning "tree" or branch, and "meros" meaning "part".[4]

The synthesis of PAMAM dendrimers involves utilising an amine core molecule containing several N-H groups (such as ammonia, NH_3) that is reacted with an excess of methyl acrylate via an exhaustive Michael addition, Scheme 1.2. In a second step, each "arm" of the resulting branched

dendrimer is reactivated to form a primary amine terminated moiety by exhaustive amidation using excess ethylenediamine (EDA). Repeating this reaction sequence has allowed the synthesis and characterisation of dendritic macromolecules to very large molecular weights. Commercially, EDA is also used as the core of the PAMAM dendrimer series and materials up to G_{10} (MW = 934,720 g/mol; 4096 peripheral amine groups) have been synthesised. Very large excesses of EDA (i.e. 15-250 (EDA:ester) molar ratios) are always necessary to prevent dendrimer bridging and subsequent gelation.[3]

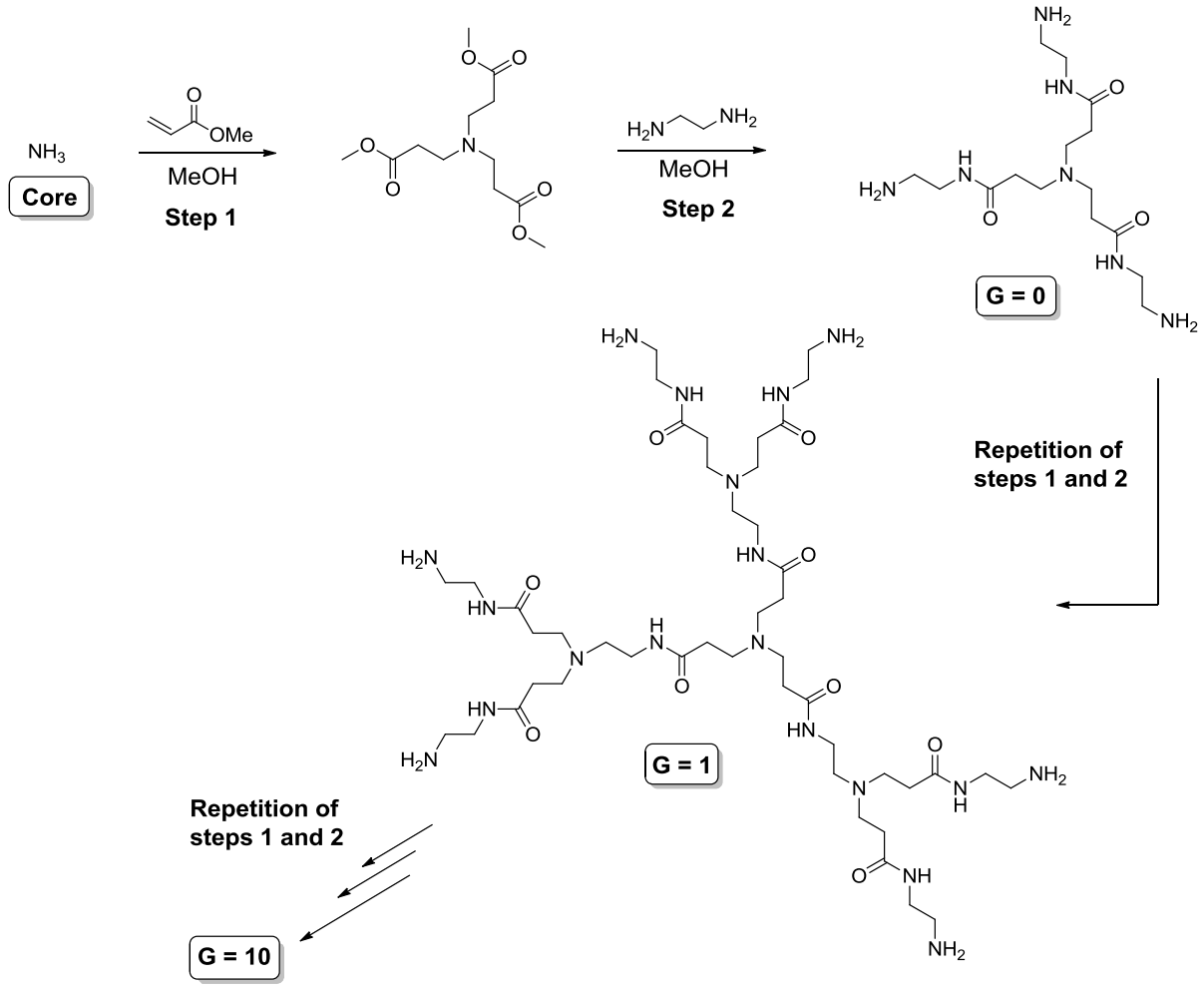

Scheme 1.2 Synthesis of a PAMAM dendrimer using an ammonia core by repetitive two step Michael addition and amidation process.

In all of these early examples, the synthesis begins from a central core, and proceeds outwards by the addition of successive layers. This route is referred to as the "divergent" approach to dendrimer synthesis, Figure 1.2.

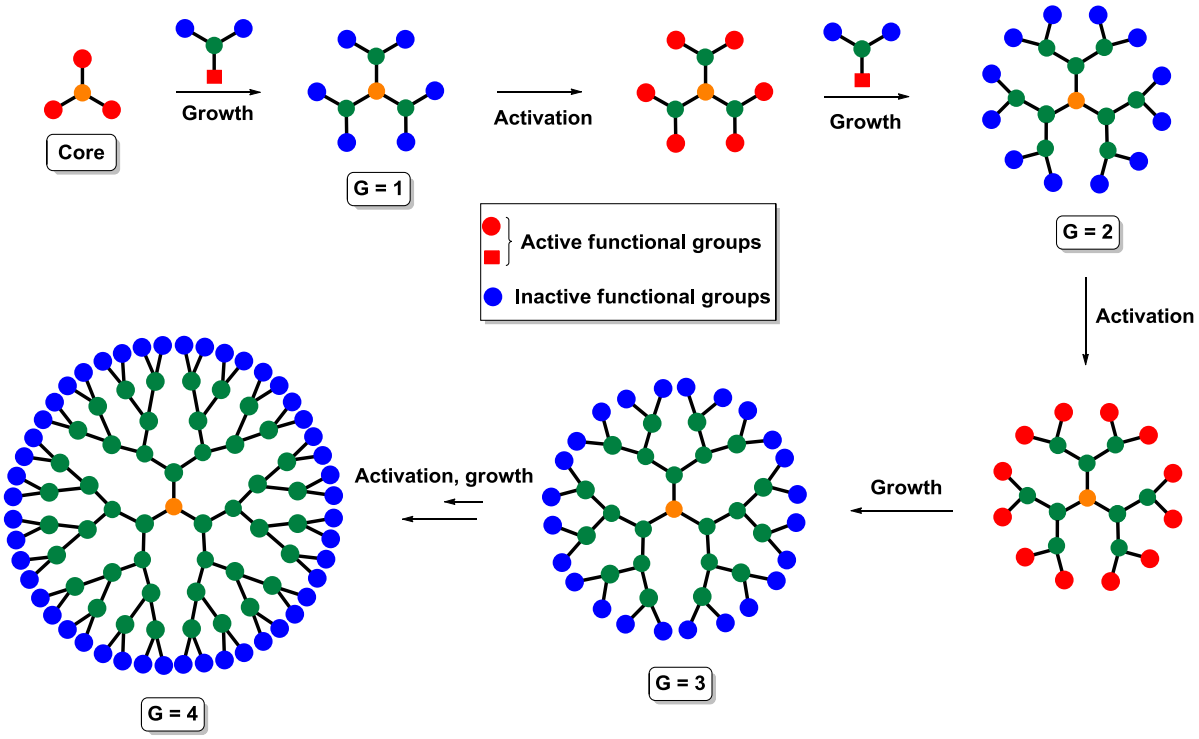

Figure 1.2 Schematic representation of dendrimer synthesis by divergent growth. (Figure adapted from Sowinska and Urbanczyk-Lipkowska).[6]

1.2.1.3 Success of divergent growth

The success of divergent growth has led to the commercialisation of PAMAM dendrimers, on multi-kilogram scales. The original divergent synthesis of "cascade molecules" by Vögtle and coworkers was hindered by problems during the reduction step. These problems were later solved by reducing the nitrile end groups to primary amines with H_2 (30-70 bar) and Raney/Cobalt as a catalyst in water.[7] Using this optimised method, multi-kilo gram scales were prepared by the Dutch company DSM and termed polypropyleneimine dendrimers (PPI dendrimers). These materials are still commercially available, but only in research quantities from SyMO-Chem.

1.2.1.4 Problems of divergent growth

A significant drawback with divergent growth is the increasing steric hindrance at the surface of the dendrimer, meaning it becomes increasingly more difficult to ensure that every reaction results in structural perfection.[8] As predicted by de Gennes and Hervet,[9] the volume of the dendrimer increases (scaling as the cube of the radius) more quickly than its surface area (scaling as the square of the radius) and, at a certain generation, the surface becomes densely packed.[6] The effect is commonly referred to as "de Gennes Dense Packing", or the "starburst effect limit". With this realisation, there has been a considerable interest in the actual purity of commercially available dendrimers synthesised by the divergent route.[8] Electrospray ionisation mass spectrometry (ESI-MS) analysis of commercially available PAMAM dendrimers has indicated structural defects arising from retro-Michael additions and intramolecular lactam formation.[10] It has been shown that a G_4 PAMAM dendrimer (48 surface groups) was found to have a dispersity (Đ) of 1.0007 (determined by ESI-MSI using a quadrupole analyser),[11] but interpretation of the published data confirmed a dendritic purity of only 8% (the dendritic purity is defined as the percentage of dendritic material that is defect-free, and is calculated by the number of error-free dendrimers divided by the total number of dendrimers multiplied by 100%).[8] Meijer and coworkers have also performed detailed analysis of a G_4 commercially available PPI dendrimer using ESI-MS.[12] Again, structures including incomplete Michael additions and cyclisation were found to make up a significant proportion of the impurities, and their approximations indicated that the dendritic purity was only 41%.[12] Efficient selectively of the chemistry is crucial to produce defect-free dendrimers by a divergent synthesis, but even then it is virtually impossible to produce perfect dendrimers beyond G_5 or G_6.[8] For example, using an average selectively of 99.5% per generation growth reaction for the synthesis of a G_5 PPI dendrimer leads to a dendrimer with a dendritic purity of 29%.[8] This is reduced to 8% at G_6 (0.995^{504} = 8%) and 0.6% (0.995^{1016} = 0.6%) at G_7.[8] As a consequence of this, the solution to defect-free dendrimers is to reduce the number of simultaneous reactions that occur during each growth step. This is achieved by using a convergent growth approach to dendrimer synthesis.

1.2.2 Convergent synthesis

1.2.2.1 First example of convergent synthesis

In 1990, after the initial patent filing,[13] Hawker *et al.* presented a new approach to dendrimer synthesis, called convergent growth,[13-15] which is complementary to the former divergent growth approaches that had been reported beforehand. The process is achieved by the formation of "wedges", also known as "dendrons", whereby instead of beginning from the core, as in the divergent approach, the synthesis begins from molecules that will ultimately form the peripheral layer of the dendrimer, and progresses inwards by coupling of the "focal point" to each branch of the monomer (growth step, Figure 1.3).[6] After successful completion of the coupling, the "focal point" is activated (selective activation step, Figure 1.3), and reacted with an additional branching monomer, which affords a higher generation dendron. After repetition of this process to build the required sized dendron, the product is attached to a polyfunctional core after activation of its focal point, to form the target dendrimer.

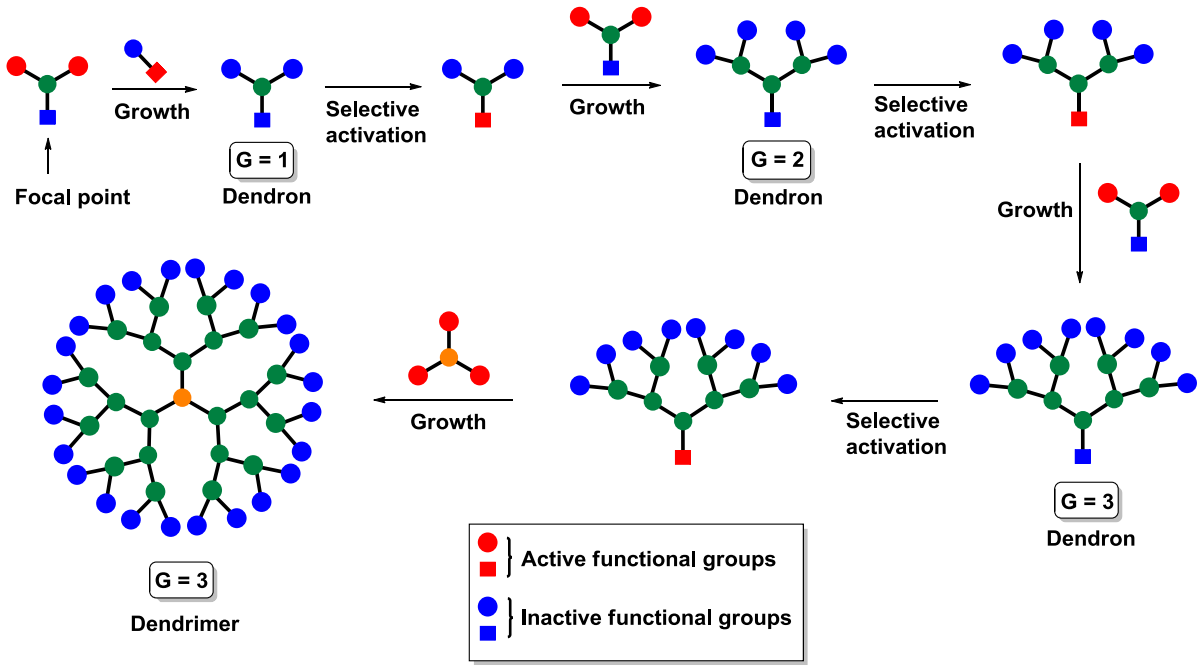

Figure 1.3 Schematic representation of dendrimer synthesis by convergent growth. (Figure adapted from Sowinska and Urbanczyk-Lipkowska).[6]

The convergent growth strategy is in sharp contrast to the divergent approach, since at any one of the growth steps, only a small number of reactions occur. Due to this, dendrimers obtained by the convergent process tend to be of higher purity, as the imperfectly branched dendrons can be removed much more easily, e.g. by liquid chromatography. Furthermore, the convergent process uses only a small number of reactions at the growth step meaning the coupling reactions can be driven to completion by using only a slight excess of reagent,[6] in contrast to the significant quantities required by the divergent process.[3]

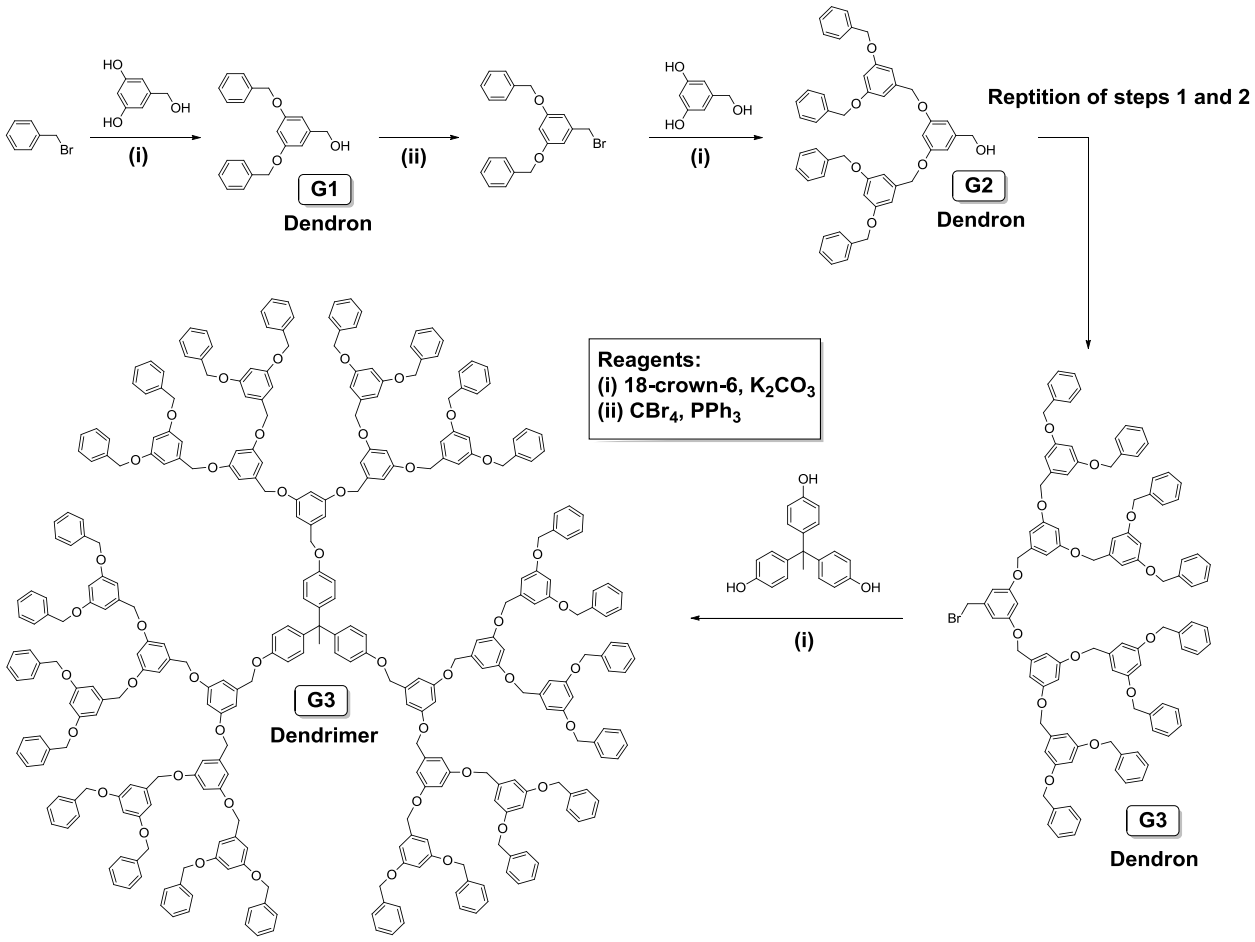

Scheme 1.3 Preparation of a G_3 poly(benzyl ether) dendrimer using the convergent synthesis developed by Hawker *et al.*[13-15].

The first example of a convergent dendrimer synthesis was for the preparation of poly(benzyl ether) dendrimers[13-15] (often called Fréchet dendrimers), Scheme 1.3. The synthesis used 3,5-dihydroxybenzyl alcohol as the AB_2 monomer, and the efficient ether forming Williamson coupling

step between a highly nucleophilic phenolate and a highly activated benzylic bromide to form a poly(benzyl ether) dendritic structure. In the first step, two equivalents of benzyl bromide were reacted with the two phenolic groups on the 3,5-dihydrobenzyl alcohol AB_2 monomer resulting in the G_1 dendron. The focal point of this G_1 dendron was then activated using carbon tetrabromide (CBr_4) and triphenylphosphine (PPh_3) resulting in an activated dendron. Reaction of this with a further unit of 3,5-dihydrobenzyl alcohol, yielded the G_2 dendron. A continuation of this two-stage process gave the G_3 dendron, which was coupled to a tris(phenolic) core, to yield the G_3 dendrimer. Due to the optimised conditions, high yields, and the ability of the benzylic substrate to prevent elimination side reactions that frequently occur during nucleophilic displacements, this method was used to construct dendrons and dendrimers up to G_6.[14]

1.2.2.2 Success of convergent growth

The design of the convergent growth means it has many advantages over the divergent growth route. As the strategy involves the construction of dendrons, the addition of the same dendrons to different cores leads to a new series of dendrimers. The convergent process has also enabled the preparation of dendrimers with layered,[16], segmented,[16] and tailored surface functionalities;[17] these are first the examples, however many further examples have been reported.[6, 18] One of the most advantageous features of the convergent growth is the ability to attach dendrons of different types to a central core. The resulting dendrimers take several names, including “Janus dendrimers”, “segmented dendrimers”, “asymmetric dendrimers” and “bow-tie dendrimers”.

1.2.2.3 Problems of convergent growth

Despite many advantages of the convergent growth method in comparison to the divergent method, it is also subject to limitations. With increasing dendron size at each generation, both the reactivity and the availability of the focal point decreases, meaning that the preparation of structurally perfect dendrimers at high generations is extremely difficult.[18] Since the growth steps are rarely quantitative, purification is achieved using liquid chromatography, resulting in loss of material at each additional generation of growth. The convergent growth method is therefore limited to the preparation of lower generation dendrimers (i.e. below G_6).[6] Both the divergent and convergent routes have their own

advantages and disadvantages, and attempts have been made to combine parts of each route to develop alternate strategies.

1.2.3 Double-stage convergent synthesis or "hypercore route"

In the first synthesis of poly(benzyl ether) dendrimers, the authors were limited to G_6, due to steric hindrance relating to the coupling of the dendron to the core. A solution to this was to construct a larger core and react this with a smaller dendron, aiming to reduce steric hindrance issues during the core coupling step. In the double-stage convergent synthesis, a low-generation dendrimer is initially constructed using a convergent synthesis pathway whereby the dendrimer has protected peripheral groups. This dendrimer is then "activated", by removing the protecting groups from the periphery, resulting in a "hypercore". Reaction of the hypercore with a dendron of choice leads to the higher generation dendrimer, Figure 1.4.

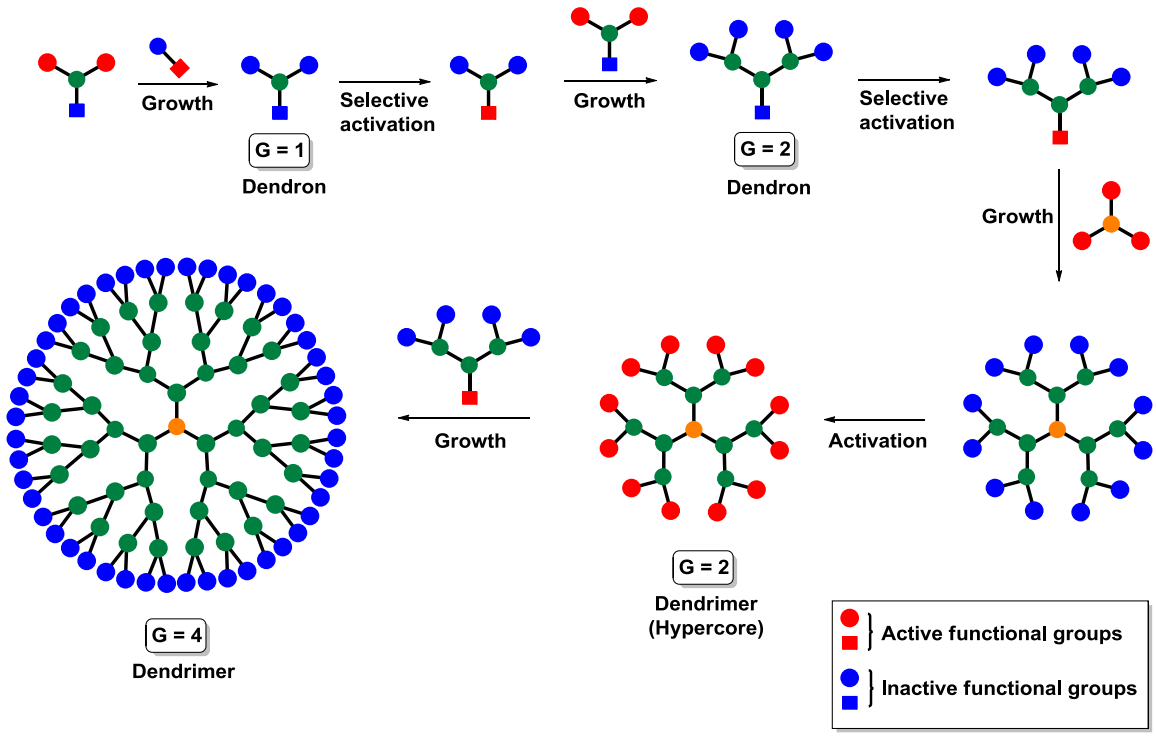

Figure 1.4 Schematic representation of dendrimer synthesis by double-stage convergent synthesis. (Figure adapted from Sowinska and Urbanczyk-Lipkowska).[6]

The route aims to limit steric hindrance by using a "hypercore", and also facilitate the construction of "layered" dendrimers.[6] Using this method, Wooley *et al.* were able to extend the synthesis of poly(benzyl ether) dendrimers to G_7,[19] Scheme 1.4.

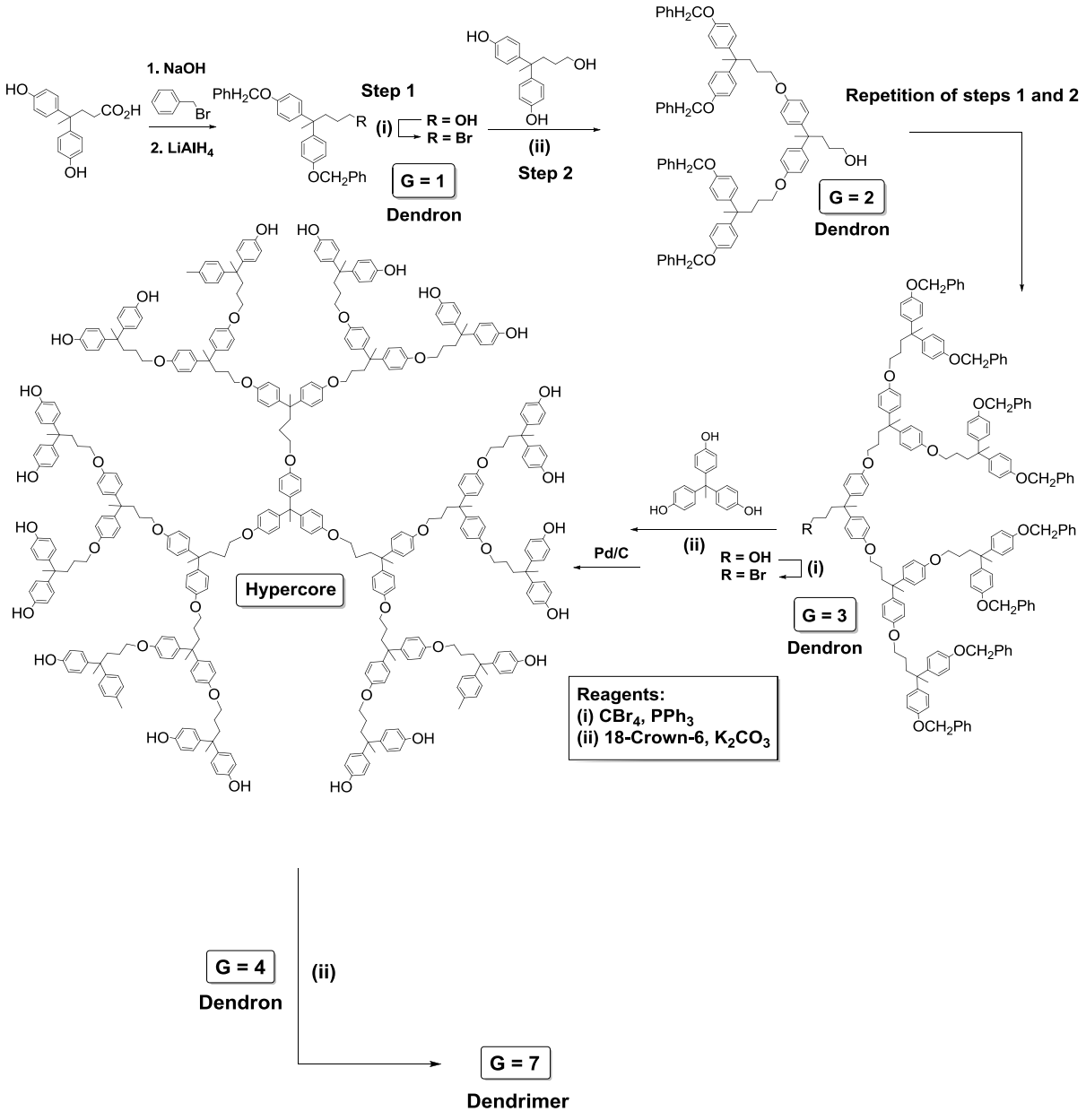

Scheme 1.4 Preparation of a G_7 poly(benzyl ether) dendrimer by double-stage convergent synthesis.[19]

1.2.4 Hypermonomer synthesis

The hypermonomer synthesis involves using a monomer that has a higher number of reactive functional groups than a conventional AB_2 monomer.[6] Monomers such as an AB_4 or AB_8 are used, which allow the synthesis of high generation dendrimers in a reduced number of steps, Figure 1.5.

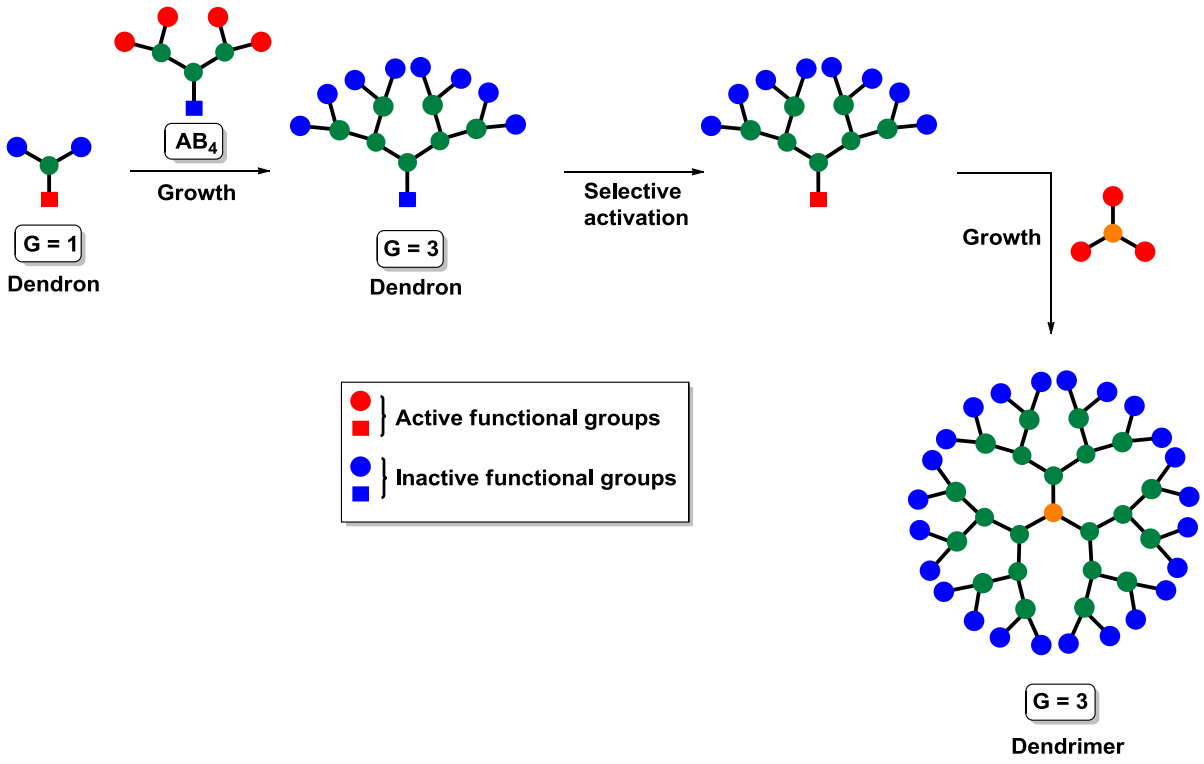

Figure 1.5 Schematic representation of dendrimer synthesis using the hypermonomer route. (Figure adapted from Sowinska and Urbanczyk-Lipkowska).[6]

This strategy was also applied to the synthesis of poly(benzyl ether) dendrimers. By using a G_2 dendron as a hypermonomer (AB_4), a G_5 dendrimer was prepared in three synthetic steps.[20]

It is worth noting that the highest generation dendrimer prepared to date (July 2014) used a hypermonomer route. Lim *et al.* recently prepared a G_{13} dendrimer utilising a hypermonomer route to add two additional generations per iteration.[21] This dendrimer has a theoretical molecular weight of 8.4 million Daltons (Da), and 16384 surface groups at the 13th generation.

1.2.5 Double-exponential growth synthesis and orthogonal approaches

Another interesting route to accelerated dendrimer synthesis is the double-exponential growth synthesis. It takes many of its features from the convergent route, relying on the synthesis of a dendron, which is later coupled to a core, but reduces the number of synthetic steps by making use of chemoselective reactions, Figure 1.6.

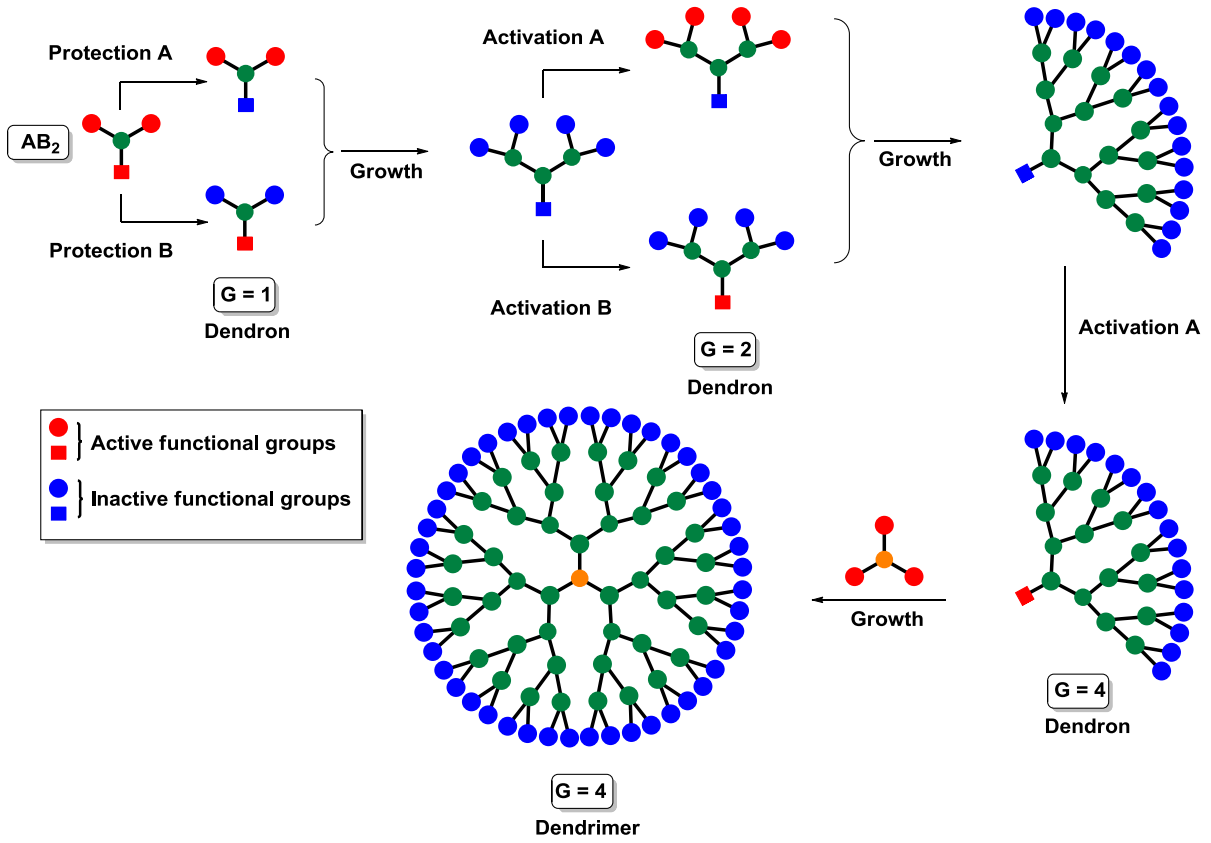

Figure 1.6 Schematic representation of dendrimer formation by the double exponential growth strategy. (Figure adapted from Sowinska and Urbanczyk-Lipkowska).[6]

An AB_2 monomer is used, which is orthogonally protected at either the focal point (A) or periphery (B), resulting in two different AB_2 monomers, Figure 1.6 (orthogonal protection is a strategy allowing the deprotection of functional groups independently of each other). Reaction of two active (A) AB_2 monomers with one active (B) AB_2 monomer results in the desired G_2 dendron.[6] Since either the focal point (A) or periphery (B) of the resulting G_2 dendron can be chemoselectively activated, repetition of this process results in the G_4 dendron. Activation of the final focal point enables the coupling to a core

to result in the desired dendrimer. The process is somewhat similar to the hypermonomer route, in that generations are "skipped" to reduce the number of synthetic steps. Kawaguchi *et al.* were the first to present this methodology in the preparation of their G_4 poly(phenylacetylene) dendrimer,[22] A further poly(ester) example, Scheme 1.5, is of particular importance, since this family of dendrimers is based on the monomer 2,2-bismethylolpropionic acid (bis-MPA), a material used widely throughout this thesis.

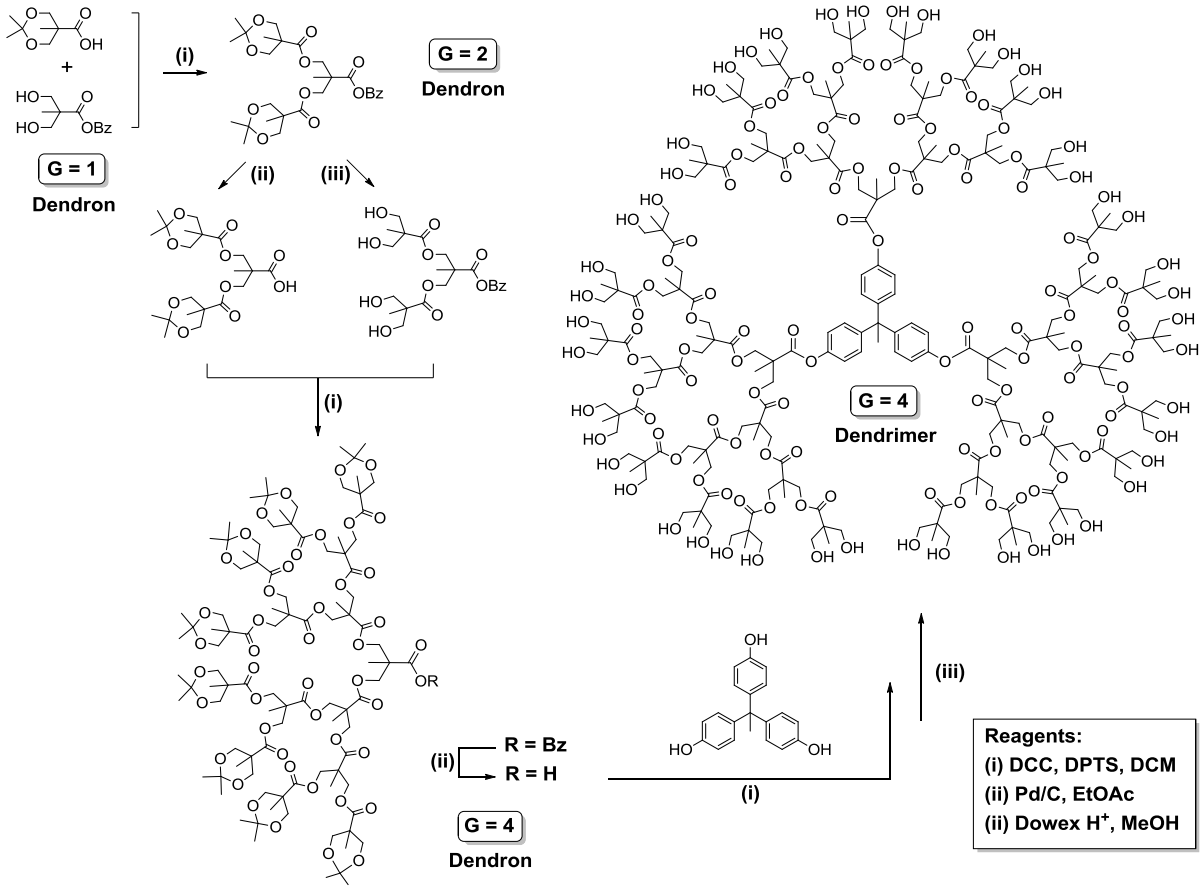

Scheme 1.5 Preparation of a G_4 polyester dendrimer using 2,2-bismethylolpropionic acid (bis-MPA) by a double-exponential growth strategy.[23]

Developments from the double-exponential growth synthesis have led to further orthogonal approaches. These routes rely on the use of two different monomers, often referred to as AB_2 and CD_2

monomers, and can occur both divergently or convergently. The monomers are used in an alternate sequence to build the structure; for example, A and C will only react with the functional groups B and D, thereby eliminating the need for activation steps, and allowing dendrimer growth to occur at every reaction step, Figure 1.7.

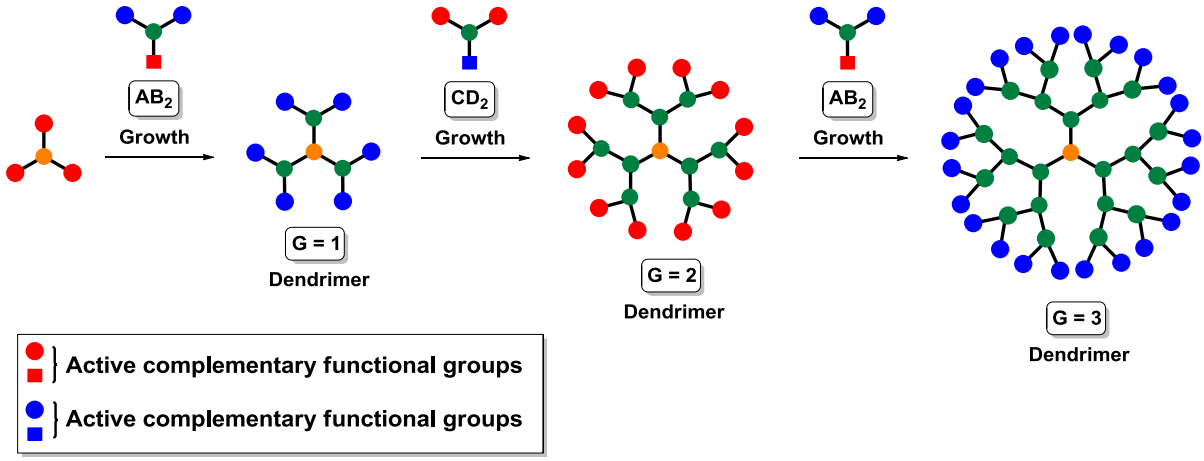

Figure 1.7 Schematic representation of dendrimer synthesis by a divergent orthogonal approach. (Figure adapted from Sowinska and Urbanczyk-Lipkowska).[6]

The first example of a orthogonal approach was reported by Spindler and Fréchet who synthesised a G_3 poly(ether-urethane) dendron in two steps, using 3,5-diisocyanatobenzyl chloride and 3,5-dihydroxybenzyl alcohol as the AB_2 and CD_2 monomers.[24] Major side reactions were observed when the typical 3,5-dihydroxybenzyl alcohol monomer was used, and therefore a protected monomer was utilised, Scheme 1.6. A more successful attempt performed by Zeng and Zimmerman *et al.* prepared a G_4 poly(alkyne-ester) dendron using alternate Mitsunobu esterification and Sonogashira coupling reactions.[25]

Since orthogonal approaches make use of highly efficient chemistries that occur independently from each other, these strategies have benefited from the development of click chemistry.

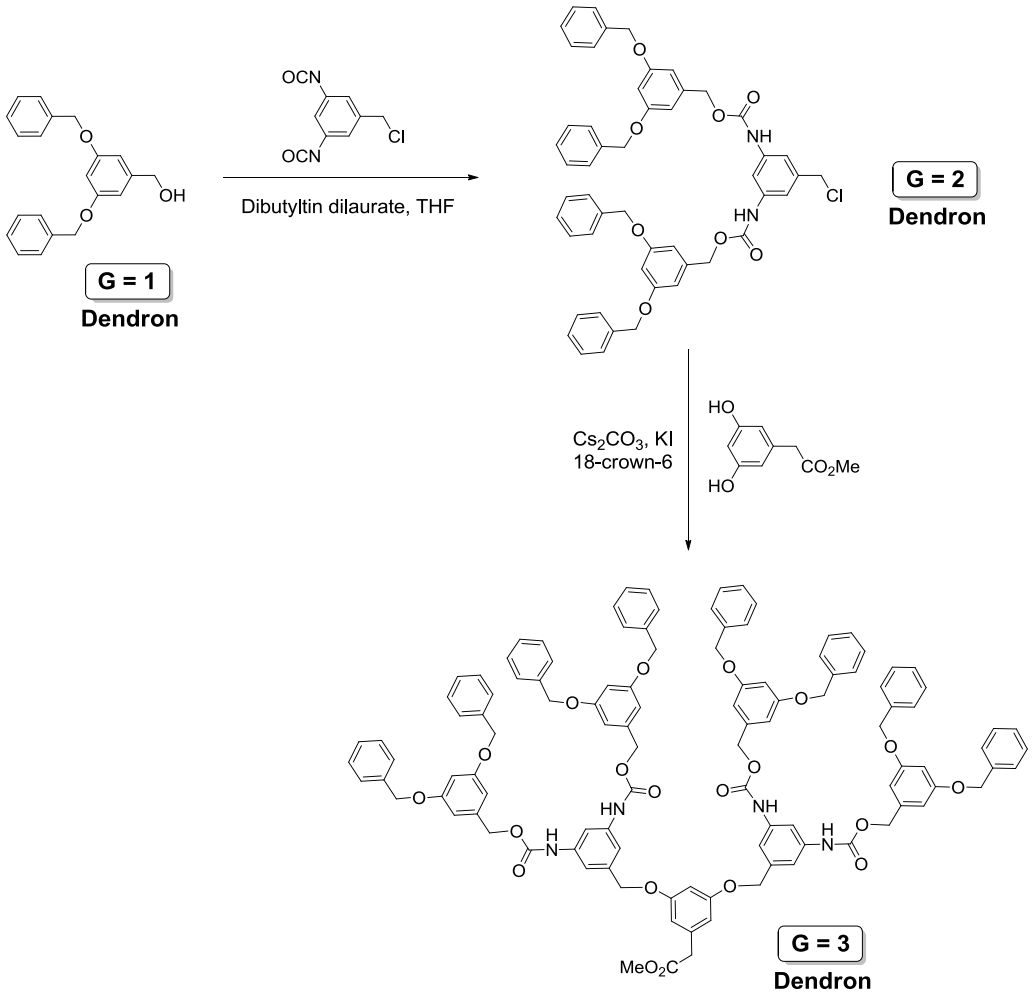

Scheme 1.6 The first example of an orthogonal approach applied to the synthesis of a poly(ether-urethane) dendron by Spindler and Fréchet.[24]

1.3 Click chemistry: Directed towards dendrimer synthesis

1.3.1 Introduction to click chemistry

The click chemistry concept was introduced by Sharpless and co-workers in 2001,[26] with the aim of highlighting chemical reactions that are highly stereo/regioselective, give yields close to 100% and produce little or no by-products. Reactions deemed "click" reactions should also be tolerant of air and moisture, use commercially available reagents and avoid tedious workup procedures such as liquid chromatography. Initially aimed for the preparation of small organic molecules,[27] click chemistry has found widespread applications in materials chemistry, particularly for the preparation of dendritic

materials.[6] The most common "click reactions" are the Cu^{I} catalysed azide-alkyne cycloaddition (CuAAC) reaction,[28] Diels-Alder cycloaddition (DA)[29] and a range of thiol-based reactions. The thiol click reactions can proceed either by an anti-Markovnikov radical addition of an alkene, also known as a "thiol-ene" reaction;[30] a "thiol-yne" route which is also radical based but uses an alkyne substrate;[31] a "thiol-bromo" reaction which is a thiol-bromide nucleophilic substitution[32] or a thiol Michael addition route, which undergoes a conjugate addition with an activated monomer, [33] Scheme 1.7.

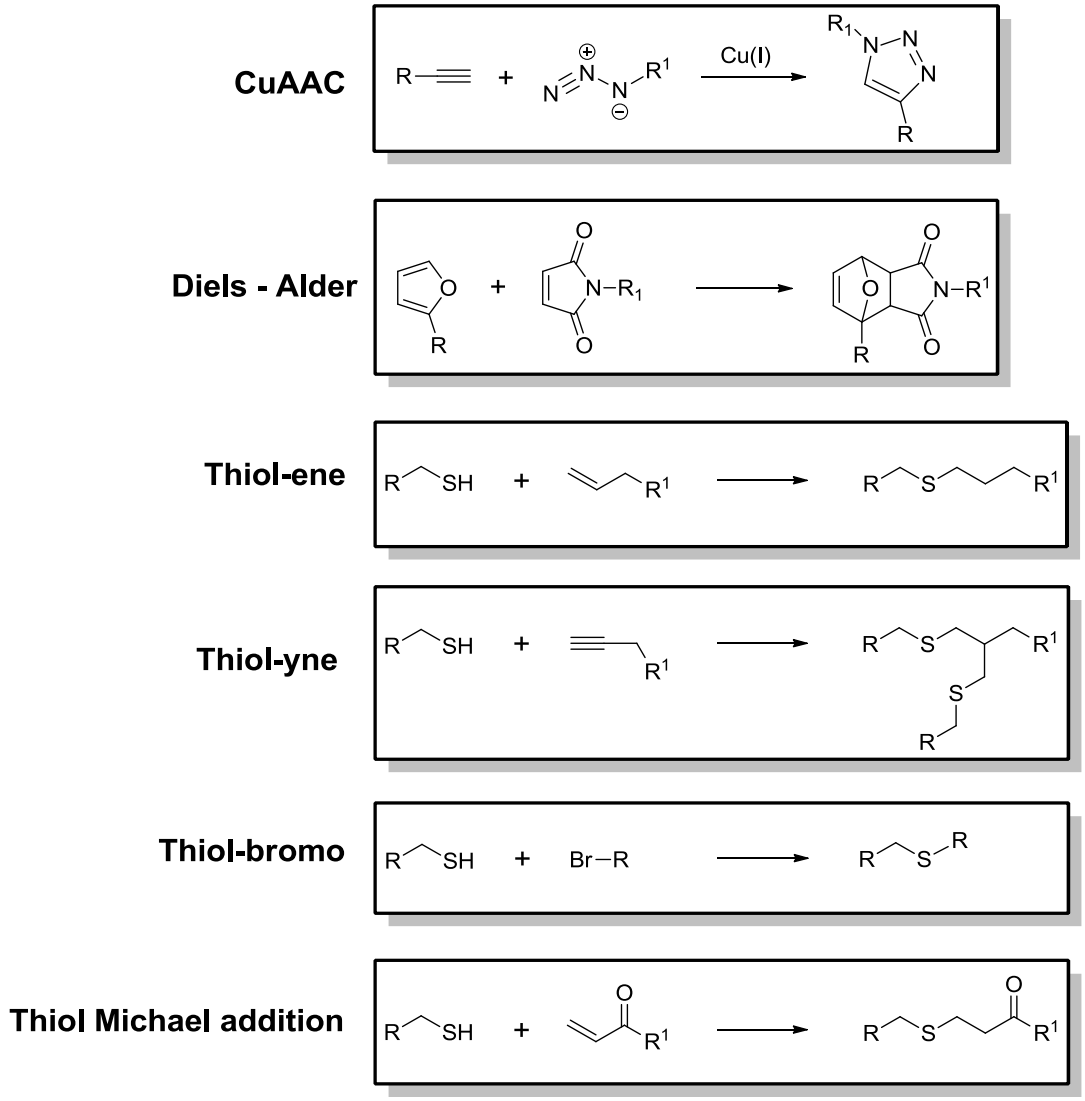

Scheme 1.7 The most widely used click reactions used within dendrimer synthesis

1.3.2 Cu^{I} catalysed azide-alkyne cycloaddition (CuAAC) click chemistry

1.3.2.1 CuAAC for dendrimer synthesis

Since the concept was introduced, the CuAAC reaction has been the most widely explored and is regarded as the original click reaction; its first introduction into a dendrimer synthesis was reported by Wu *et al.*[34] By adopting a convergent route, G_3 and G_4 dendrimers were prepared using an AB_2 monomer comprising of two alkynes and a single chloride functional group. The chloride functionality was easily re-activated with sodium azide, transforming it into an organic azide following each growth step.[6] Not long after, Joralemon *et al.* followed with a divergent synthesis based on the original poly(ether benzyl) dendrimers to synthesise dendrimers to G_3 using the CuAAC reaction.[35]

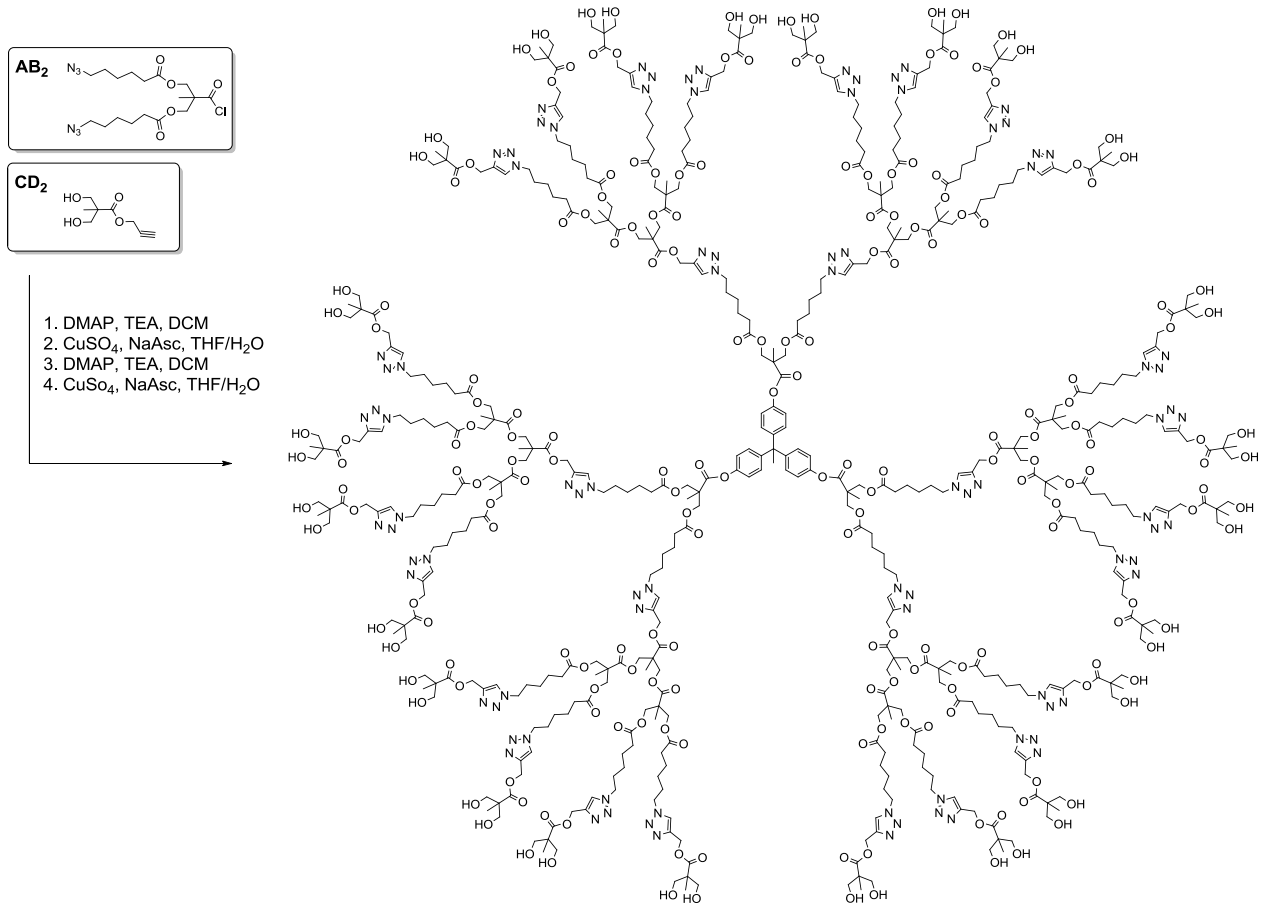

Scheme 1.8 An orthogonal approach to the synthesis of a G_4 bis-MPA dendrimer prepared in four steps utilising CuAAC and esterification reactions.[36]

The selective nature of click chemistry has led to an example of using the CuAAC towards the synthesis of a dendrimer via orthogonal routes. Antoni *et al.* made use of an AB_2 and a CD_2 monomer to prepare both bis-MPA and poly(benzyl ether) based dendrimers utilising the CuAAC reaction,[36] Scheme 1.8.

1.3.2.2 CuAAC for dendrimer functionalisation

The CuAAC reaction has also been widely used for dendrimer peripheral functionalisation. An approach to functionalise Fréchet type, bis-MPA type and PAMAM type dendrimers was demonstrated using a variety of different azide based substrates.[37] Arguably, one of the most elegant examples was reported by Wu *et al.* who prepared an asymmetrical dendrimer based on the bis-MPA scaffold, and functionalised its periphery with sixteen mannose units and two fluorescent groups using CuAAC chemistry, Figure 1.8.[38]

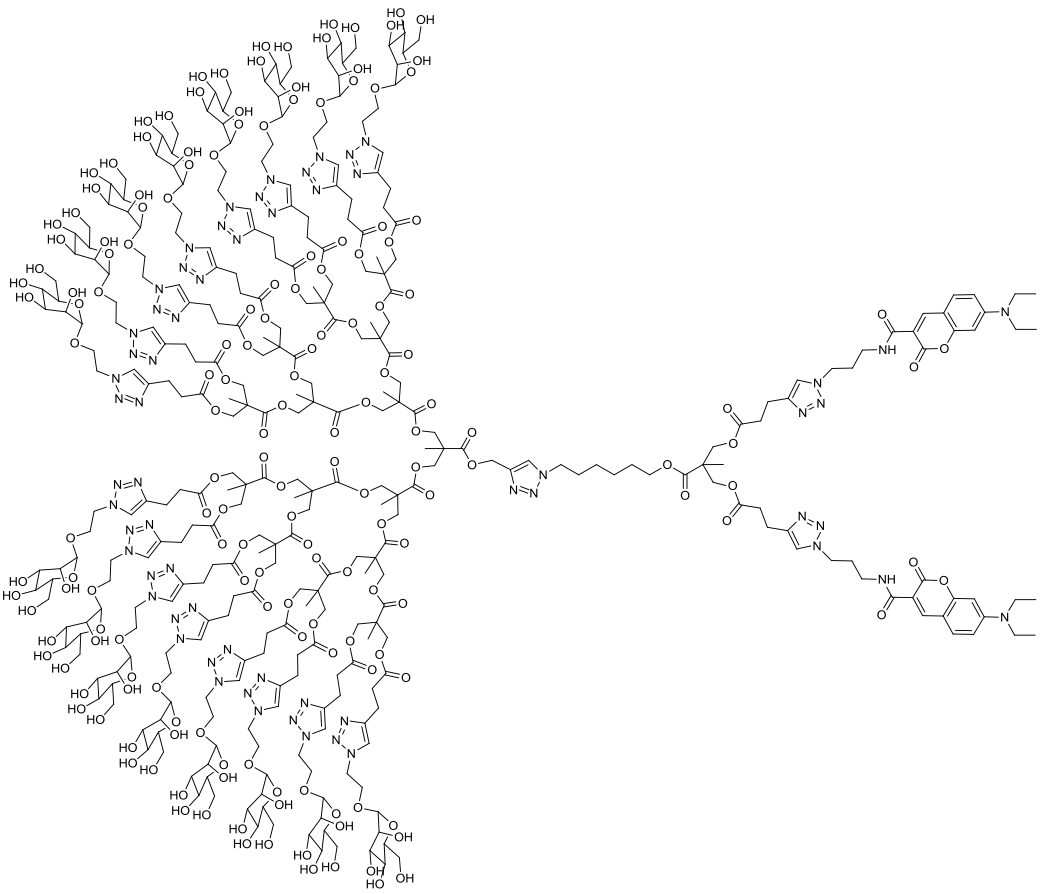

Figure 1.8 Example of an asymmetric bis-MPA dendrimer by Wu *et al.*, functionalised *via* CuAAC with sixteen mannose units and two fluorescent groups.[38]

1.3.2.3 Drawbacks with CuAAC

Unfortunately, although extremely efficient, the purification processes needed for removal of the cytotoxic copper used within the synthesis limit the CuAAC reaction predominantly to non-biomedical applications.[39] Copper-free Azide-Alkyne Cycloadditions have enabled some of the toxicity issues to be addressed,[39] but despite these attempts, azide functionalities are well known as being potentially explosive and toxic substrates to use in the laboratory.[26]

To highlight this point, at a recent conference the author of this thesis met a researcher who suffered from significant injuries whilst attempting to synthesise an azide based substrate for CuAAC chemistry. For these reasons, many chemists have turned to alternative click reactions such as the retro Diels-Alder cycloaddition and thiol-based click reactions.

1.3.3 Retro Diels-Alder cycloaddition click chemistry

The Retro Diels-Alder (DA) is becoming popular for the preparation of thermoresponsive macromolecules.[29] The reaction generates no by-products whatsoever, and its conditions are extremely simple, requiring only heat. The groups of Sanyal and co-workers and McElhanon and Wheeler have reported the first examples of thermoresponsive dendrimers based on a retro-DA between a reversible furan (diene) and malemide (dienophile) system.[40, 41] McElhanon and Wheeler were the first to report the synthesis of G_3 Fréchet type poly(benzyl-ether) dendrimers containing the thermoresponsive moieties.[40] Upon heating of the materials, the authors were able to characterise the dendrimer reducing to its former furan-malemide based monomers using ^{1}H Nuclear Magnetic Resonance (NMR) spectroscopy. Sanyal and co-workers example is similar, but is based on an asymmetric dendrimer combining the bis-MPA scaffold and the Fréchet poly(benzyl-ether) scaffold, Scheme 1.9.[41]

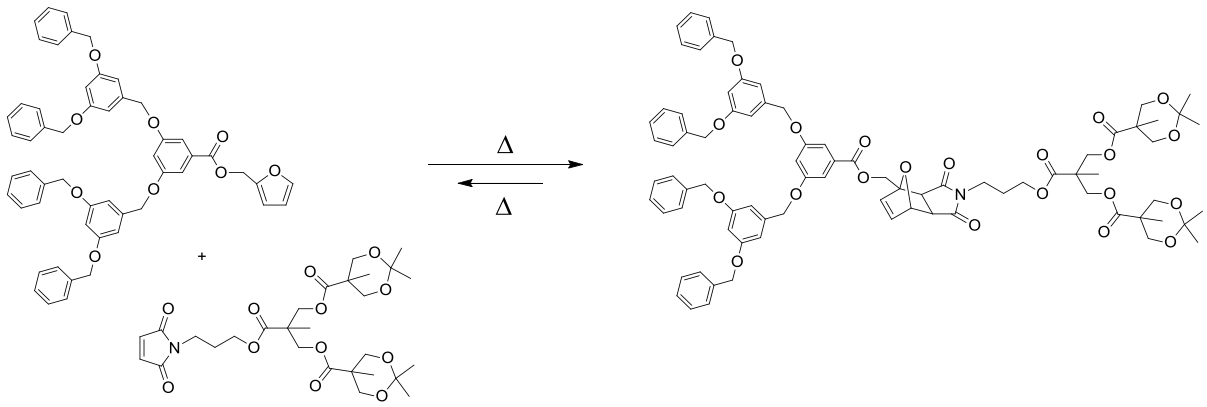

Scheme 1.9 Sanyal and co-workers example of the synthesis of an asymmetric dendrimer using a Diels Alder reaction to form the product, and a retro Diels Alder to reform the starting materials.[41]

1.3.4 Thiol-ene click chemistry

Early examples of thiol-based click reactions focussed on the radical thiol reaction, often referred to as "thiol-ene" click chemistry, with the first dendrimer example reported by Killops *et al.*[42] Using thioglycerol as an AB_2 monomer and 4-penenpoic anhydride as a CD monomer, the authors divergently synthesised a G_4 poly(thiolether) dendrimer in seven synthetic steps.[42] Soon after, an approach to synthesising bis-MPA based dendrimers using thiol-ene chemistry was reported. The orthogonal route, comprised of using AB_2 and CD_2 monomers divergently, led to the synthesis of a G_5 dendrimer in five steps,[43] Scheme 1.10. Walter *et al.* have also made use of a disulfide based core,[44] which could be cleaved and coupled to an alkylic substrate to form an asymmetric dendrimer. A very recent example of combining CuAAC and thiol-ene click chemistry reported by Antoni *et al.*, made use of the highly selective nature of the two reactions, leading to the synthesis of a G_6 dendrimer in a single day.[45]

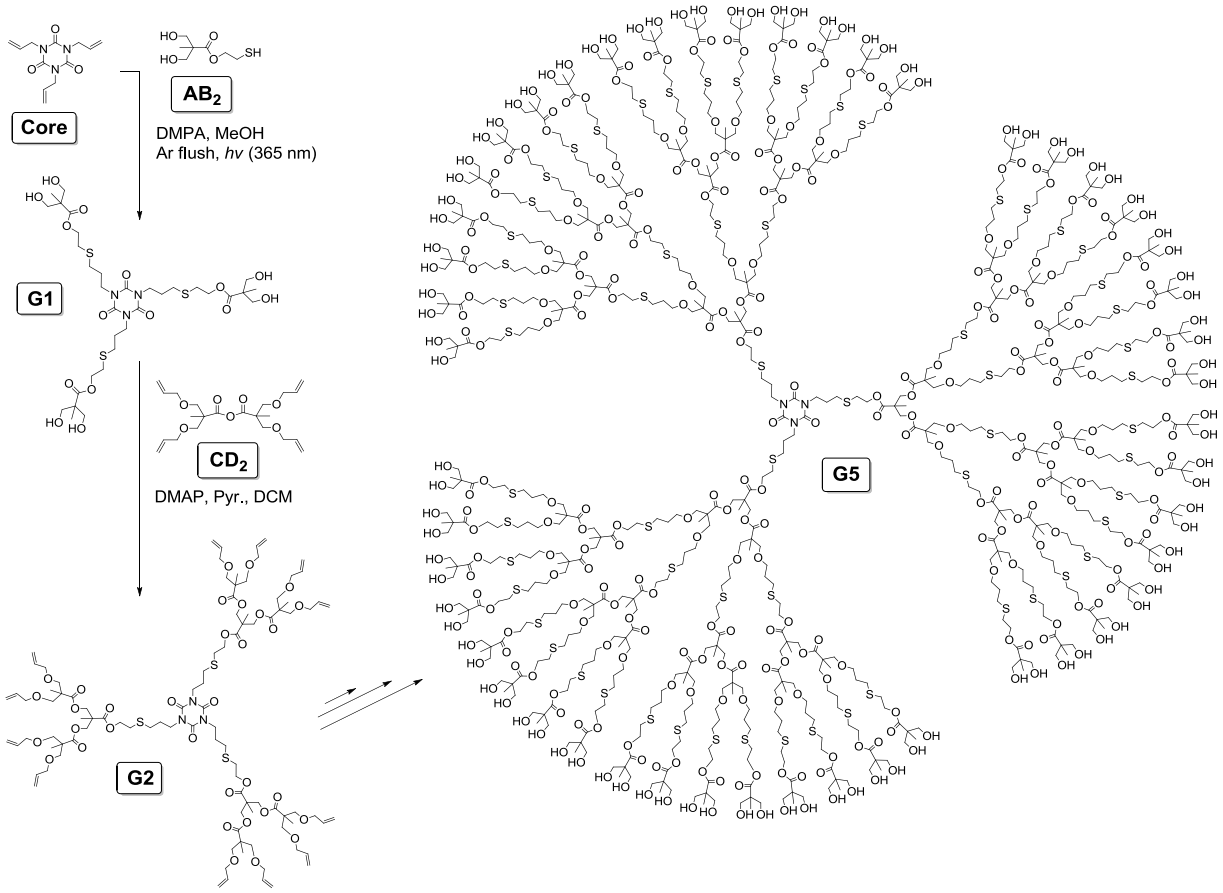

Scheme 1.10 Synthesis of a G_5 bis-MPA dendrimer by an orthogonal route, utilising thiol-ene click chemistry and traditional esterification chemistry.[43]

1.3.5 Thiol-yne click chemistry

Thiol-yne chemistry is also based on radical chemistry, and has been recently used in dendrimer synthesis. This is similar to thiol-ene chemistry, but an alkyne substrate is used in replacement to an alkene substrate.

The benefit of using thiol-yne chemistry is that two thiols react with a single alkyne, leading to a branching point at every reaction.[46] Stenzel and co-workers took full advantage of these features and adopted the synthesis of poly(thiolether) dendrimers by Killops *et al.*[42] to prepared a G_3 dendrimer comprised of 192 hydroxyl groups.[47] Using thiol-yne chemistry in replacement to thiol-ene chemistry, the authors were able to produce a G_2 dendrimer comprised of 48 hydroxyl groups in three synthetic steps, whereas seven synthetic steps were required for the same number of hydroxyl groups by the

thiol-ene route. Another particularly interesting example was reported by Shen *et al.*[48] Using a series of alternating amine Michael additions and thiol-yne click reactions, the authors prepared a G_5 dendrimer in five steps, Scheme 1.11.

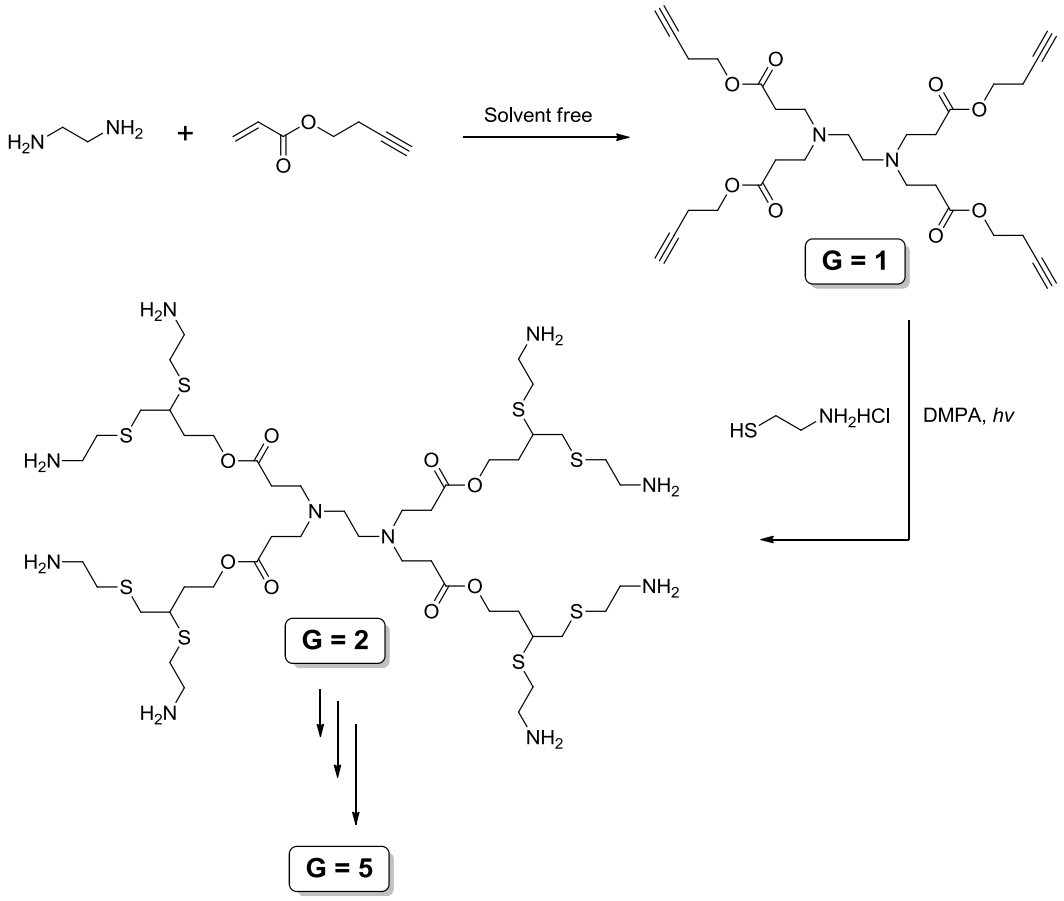

Scheme 1.11 Preparation of a G_5 dendrimer using amine Michael addition chemistry and thiol-alkyne click chemistry.[48]

Thiol-yne chemistry has also been exploited for the preparation of hyperbranched polymers. Perrier and co-workers were the first to report,[49] and further examples have since been published.[46]

1.3.5.1 Drawbacks to thiol-alkyne and thiol-ene

Drawbacks to both thiol-alkyne and thiol-ene chemistry approaches are the potential for radical-radical combination, causing cross-linking and ultimately disulfide formation.[50] Even in the discussed examples, such as Antoni *et al.* example of a G_6 dendrimer in a single day,[45] mass spectrometry characterisation such as MALDI-TOF was not shown, and SEC characterisation higher than G_5,

indicated significantly broad dispersities. As the disulfide based by-products require purification techniques to aid their removal, this suggests radical based approaches are in direct conflict with the original click concept.[26] It is for these reasons that thiol-bromo and thiol Michael addition chemistries which avoid radicals are currently of significant interest.

1.3.6 Thiol-bromo click chemistry

The only current example in the literature of a thiol-bromo click reaction applied to dendrimer synthesis is that reported by Rosen *et al.*[32] Poly(thiolglycerol-2-propionate) dendrimers to G_4 were prepared by a divergent process employing a combination of thiol-bromo click reactions and acylation reactions using 2-bromopropionyl bromide, Scheme 1.12. Analysis of the dendrimers by SEC showed no evidence of high molecular weight species.

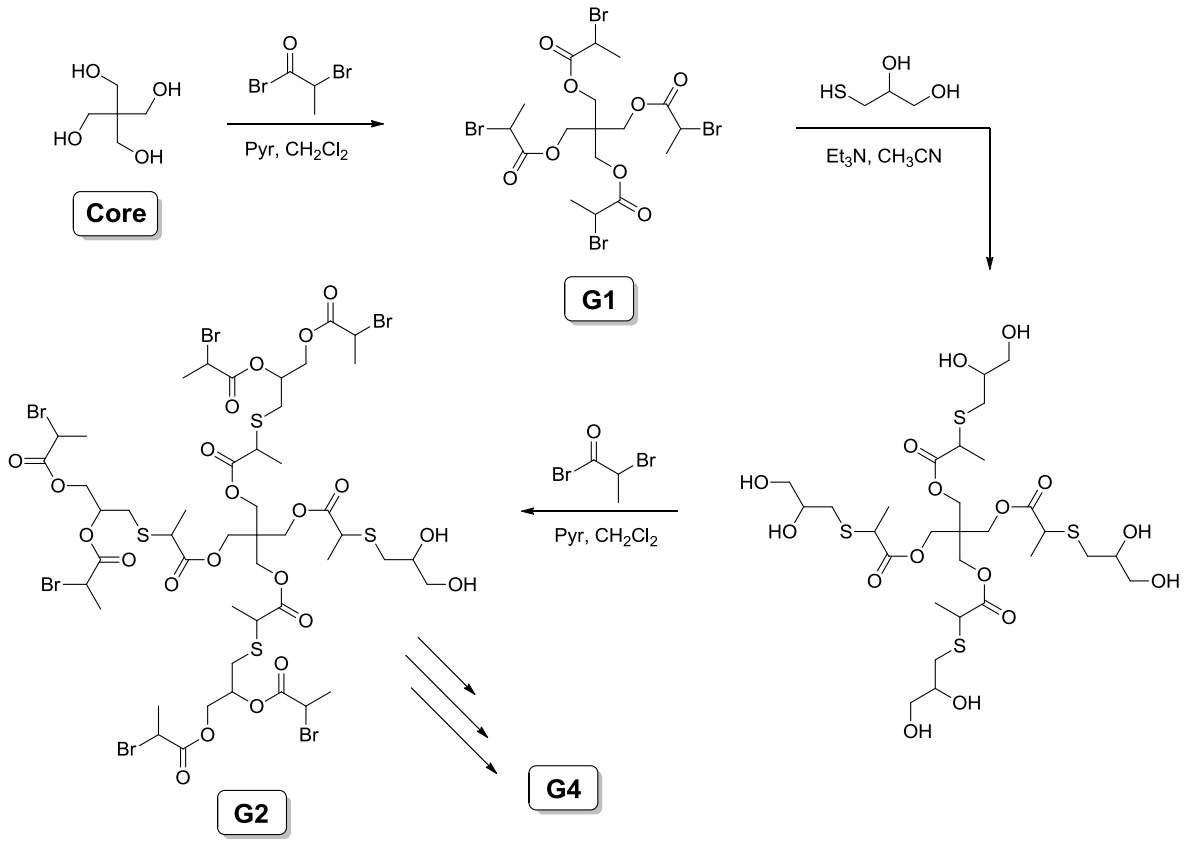

Scheme 1.12 Preparation of a G_4 dendrimer using thiol-bromo click chemistry.[32]

1.3.7 Thiol-Michael addition click chemistry

Thiol Michael addition an area of click chemistry that is receiving a considerable amount of recent attention.[33] This reaction uses an activated monomer substrate such as an acrylate or an acrylamide, which, in the presence of a highly reactive thiol, will undergo a conjugate addition. Depending on the catalyst used, the process can be either base catalysed (typically by an amine) or undergo nucleophilic catalysis (typically phosphine based).[51, 52] Since the reaction is based on an effective Michael donor (the thiol) and an effective Michael acceptor (activated double bond substrate), there are no radicals or metal catalysts required.

Largely limited by its very current status, only a handful of literature examples exist towards dendrimer synthesis using thiol-Michael addition. One early example utilised sequential thiol Michael addition/thiol-yne reactions to form octofunctional low generation dendrimers.[53] This orthogonal route demonstrated how fast thiol Michael additions can occur with optimisation of the reaction conditions, reaching completion in just 17 minutes within this report. A more recent example demonstrated the synthesis of a G_5 polyester dendrimer, via an orthogonal divergent route using a bis-MPA based moiety baring two acrylate functionalities as an AB_2 monomer and thioglycerol as a CD_2 monomer,[54] Scheme 1.13.

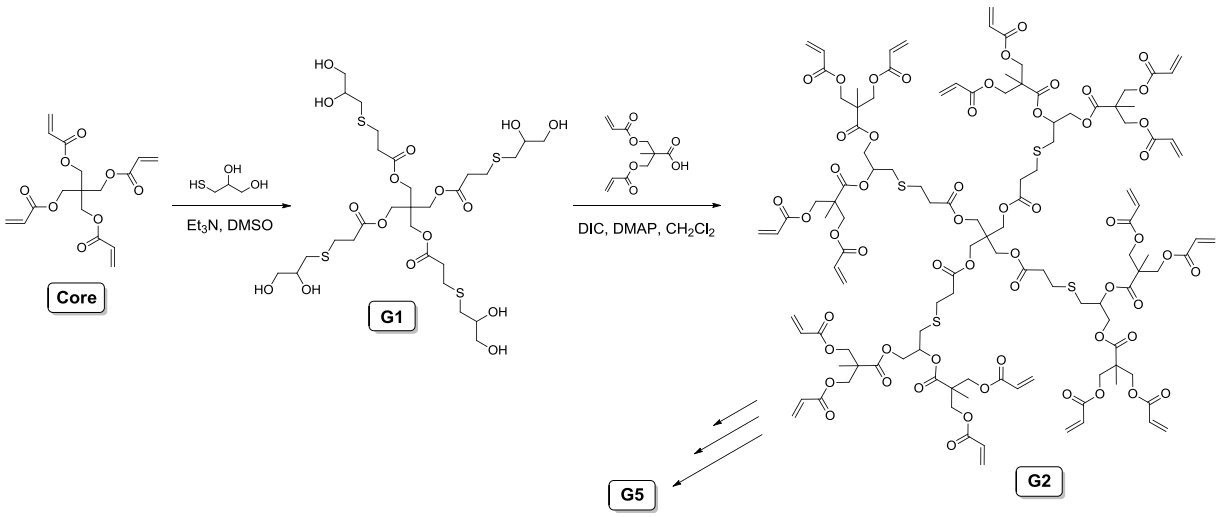

Scheme 1.13 Synthesis of a G_5 polyester dendrimer, via an orthogonal divergent route using thiol Michael addition and traditional esterification chemistry.[54]

By iterative thiol Michael additions and esterification steps, the authors synthesised a dendrimer with 128 terminal hydroxyl groups, and functionalised the surface with poly(ethylene)glycol (PEG) via traditional esterification chemistry. In another recent example, degradable bifunctional dendrimers as potential drug carriers were synthesised via thiol Michael addition chemistry. These authors made use of a thiol Michael addition between a trifunctional acrylate and dithiothreitol (DTT) to induce branching points, however an approximate 50-fold molar excess of DTT was used to generate the G_2 materials containing 12 thiol functional groups,[55] somewhat breaking the original concept of click chemistry. Apart from the first low generation octofunctional dendrimer,[53] there are no other reports that have used thiol Michael addition as a tool to induce functionalisation within dendrimer synthesis.

1.4 Dendrimers based on 2,2-bismethylolpropionic acid (bis-MPA)

A significant amount of dendrimer research now focuses on drug delivery applications,[56] with recent pharmacological results showing that dendrimers with terminal amines and multiple cationic charges such as PAMAM and PPI dendrimers can significantly induce *in-vitro* cytotoxicity,[57] whereas dendrimers based on polyester moieties remain low in toxicity.[58] The synthesis of polyester dendrimers is very well documented in the literature, and encompasses many different synthetic scaffolds.[59] One of the most widely studied polyester dendritic families is based on the monomer 2,2-bismethylolpropionic acid (bis-MPA). This simple aliphatic molecule comprises two hydroxyl groups and one carboxylic acid. It is cheap, commercially available and, as an AB_2 monomer, has been exploited for the synthesis of a large number of dendritic materials[60].

The first example of a bis-mPA based dendrimer was by Ihre *et al.* in 1996.[61] By using a convergent route, a G_4 dendrimer was synthesised comprising of a trisphenolic core and 48 peripheral acetyl groups. Oxalyl chloride was used to activate the focal point at each growth step, resulting in 10 steps of chemistry and an overall synthetic yield of 15%.[60] Unfortunately, attempting to remove the acetyl protecting groups on the periphery resulted in backbone degradation. To overcome this problem, and

to allow the synthesis of a surface reactive dendrimer, a double exponential growth strategy was developed, making use of much milder acetonide (ketal) protecting groups, Scheme 1.5. After seven steps of chemistry, comprising esterification reactions and acidic deprotections, a G_4 dendrimer with 48 peripheral hydroxyl groups was synthesised in 56% yield.[23] Although elegant, the route was plagued with low yields at high generations, and consequently a divergent synthesis based on an inexpensive and easily prepared benzylidene protected bis-MPA anhydride was reported by Ihre *et al.*[62] This synthesis was (and still is) unique, employing only extraction and/or precipitation in the purification process. Using this novel anhydride monomer, a G_5 dendrimer comprising 96 hydroxyl groups was isolated in a total yield of 52%, and is arguably the best example of a dendrimer synthesis within the literature, Scheme 1.14 (pay attention to the yields). Malkoch *et al.* extended this synthesis further, employing a similar anhydride monomer using acetonide protecting groups.[63] Both anhydride monomers have been used to prepare a variety of different bis-MPA dendrimers comprising different cores,[64] radiolabels,[65] and a disulfide bond.[44] Bis-MPA based dendrimers have also been subject to many types orthogonal approaches that use chemoselective click reactions. Of the many bis-MPA based examples that were discussed earlier (see section 1.3.2.2 and 1.3.4), arguably the most elegant example is the report of a 6^{th} G_6 bis-MPA dendrimer in a single day.[45]

1.5 Hybrid Architectures

Unlike traditional linear polymers, both dendrimers and dendrons provide a high degree of dendritic uniformity, specific sizes, shapes and controlled number of peripheral groups. However, despite the synthetic advances that have been discussed to enable the rapid synthesis of dendrimers in high purity, in reality, dendrimers are still exceptionally difficult materials to synthesise. Coupled with their synthetic expense, these problems will undoubtedly limit their commercial within low cost applications in modern day life.

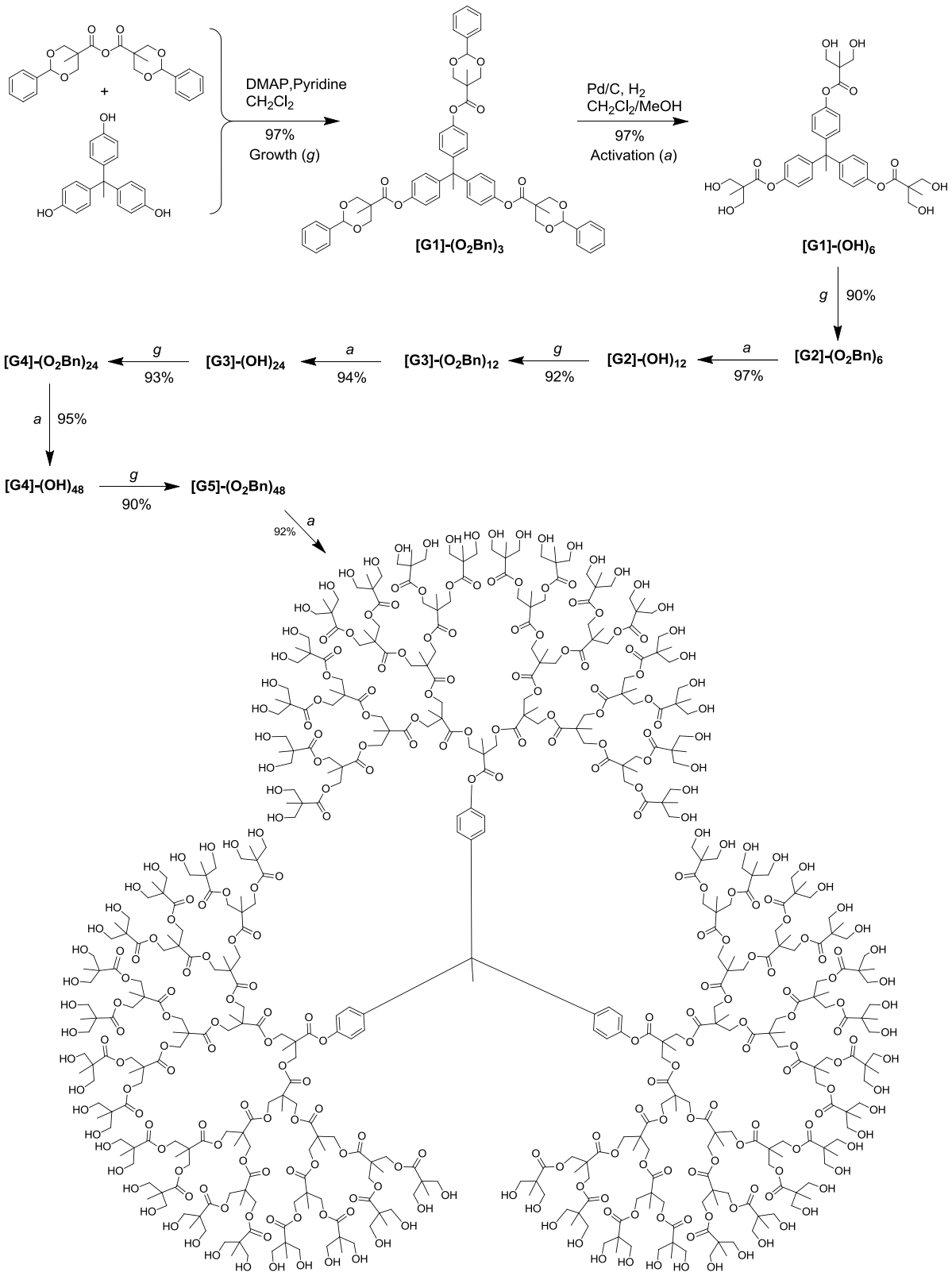

Scheme 1.14 Synthesis of a G_5 bis-MPA dendrimer reported by Ihre *et al.*[62]

As a solution to this, many hybrid structures have originated. These materials aim to combine the synthetic ease of traditional polymer synthesis with the regular and well defined structures of dendrimers and dendrons. In this section, the aim is to discuss examples of these types of structures and the synthetic routes that have been developed to make them.

1.5.1 Star-shaped materials

Star shaped materials are those which begin with a typical dendrimer, and involve growing polymer chains by initiation from the surface ("core first"), or by attachment of polymer chains to the surface by coupling chemistry ("arm first"), Figure 1.9.

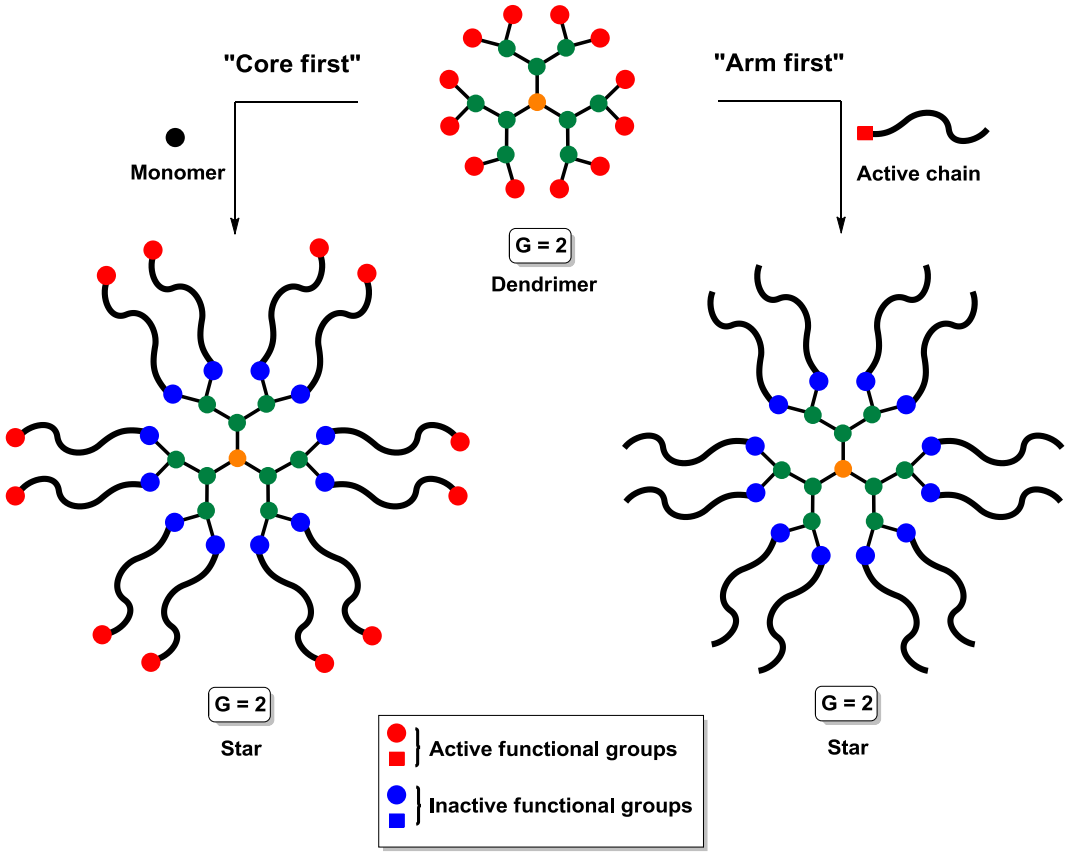

Figure 1.9 Schematic representation of star shaped hybrid architectures

1.5.1.1 Core first approach

A vast proportion of star shaped materials that are prepared via a core-first approach have been based on the bis-mPA scaffold, since their peripheral hydroxyls groups can be easily utilised to initiate

polymerisations, or modified to provide initiating sites. The groups of Hedrick and Hult were the first to utilise the hydroxyl groups of G_1 and G_2 bis-MPA dendrimers as initiators for the ring-opening polymerisation (ROP) of caprolactone and lactide acid[66, 67] to produce star shaped materials.

In a later publication, Trollsås *et al.* extended the ROP synthesis across four generations of bis-MPA dendrimers and achieved molecular weights as high as 115kDa.[68] Trollsås and Hedrick also showed that it was possible to introduce further branching points after ROP to create "dendrimer like star" structures.[69] Further examples of core first approaches have included the use of atom transfer radical polymerisation (ATRP)[70-73] and reversible addition-fragmentation chain transfer (RAFT)[74] controlled radical polymerisation processes.

1.5.1.2 Chain first approach

Another approach to form star-shaped materials is to use coupling reactions to directly attach macromolecules to the periphery of the dendrimer. Shen and co-workers recently made use of this strategy, and attached 2 kDA PEG chains to the surface of the dendrimer via dicyclohexylcarbodiimide (DCC) mediated esterification reactions.[54] Click reactions have also been used; Li *et al.* used the CuAAC reaction to attach azido terminated polystyrene residues to a dendrimer core, resulting in star shaped materials.[75]

1.5.2 Linear dendritic hybrids (LDHs)

Linear dendritic hybrids (LDHs) are materials that combine a dendron with a linear polymer chain attached at the focal point (AB type). Another variant includes dendrons attached by their focal points at both ends of a polymer chain (ABA type), Figure 1.10. Examples of different approaches to LDHs are discussed.

1.5.2.1 Coupling to a pre synthesised linear polymer chain

Coupling at the focal point of an activated dendron to the end of a reactive polymer was the first method utilised, Figure 1.10. In the first report, Gitsov *et al.* made use of use of the Williamson ether synthesis to couple the focal point of benzyl bromide functionalised poly(benzyl ether) dendrons to hydroxyl terminated PEG chain forming AB type LDHs. They investigated G_2 to G_4 and found that

the size of the dendron had no effect on the coupling efficiency.[76] In another method, reported by Gitsov and Fréchet, the authors utilised the "living" anionic nature of a poly(styrene) dianion formed under living anionic polymerisation conditions.[77] Benzyl bromide modified poly(benzyl ether) dendrons of G_2, G_3 and G_4 were successfully added and "capped" to the ends of the poly(styrene) chains resulting in ABA type LDHs. More recent examples have used either the CuAAC or thiol-ene click reactions to perform the coupling steps.[44, 78, 79]

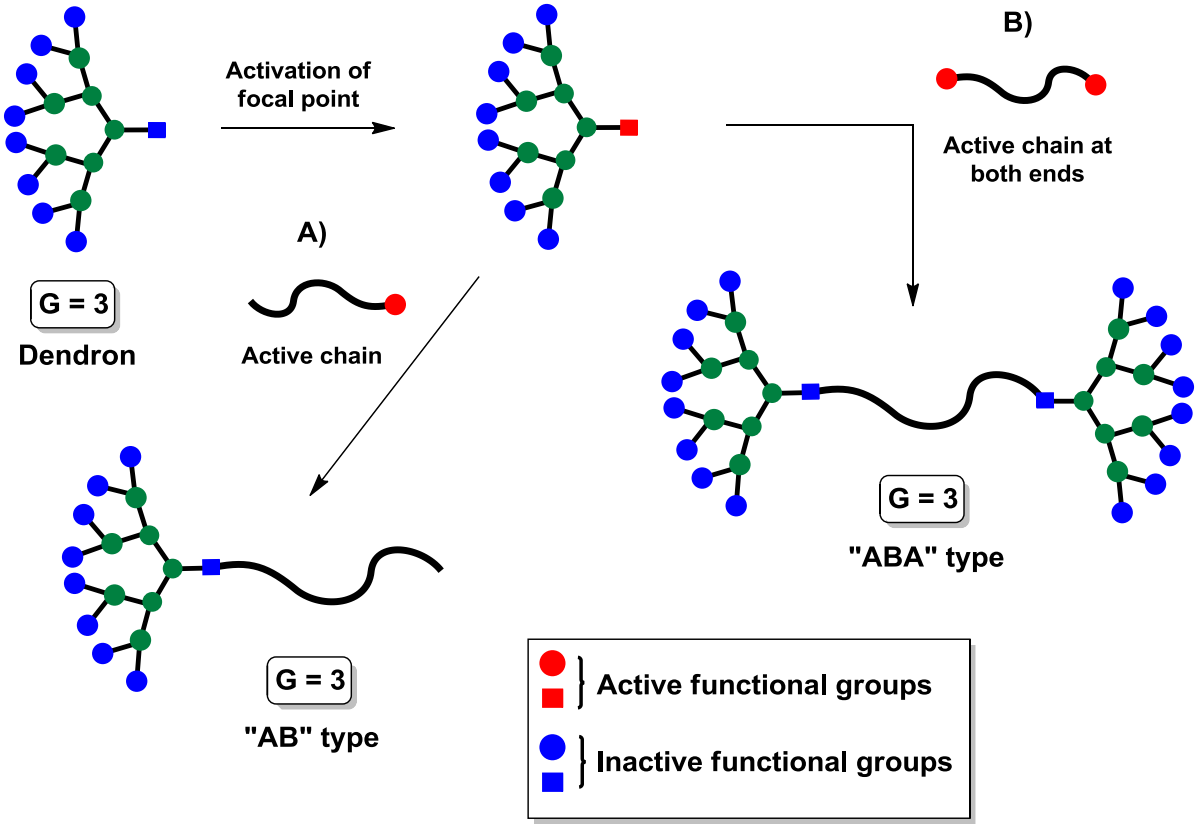

Figure 1.10 Schematic representations of LDHs synthesised by coupling a reactive dendron to a reactive polymer. Synthesis of; (A) AB type; (B) ABA type

1.5.2.2 Growth of dendron at polymer chain end or "chain first"

The second route to LDHs is to adopt a divergent synthesis of a dendron, beginning from the end of a preformed linear polymer chain, Figure 1.11. Since this is a divergent based synthesis, one of the potential drawbacks of this route is that large excesses of reagents may be required to avoid branching defeats. The first example was reported by Chapman *et al.*, who constructed a linear dendritic AB

polymer from a monofunctional PEG chain by using L-lysine and DCC mediated coupling protection/deprotection sequences.[80]. Tomalia and co-workers later followed with a LDH based on a using a PAMAM dendron.[81] Beginning from a poly(ethylene imine) linear chain, dendrons up to G_4 were constructed. However, a 10,000 fold excess of ethylene diamine was used to ensure complete amidation, requiring reaction times of between 5 and 8 days, significantly highlighting the potential drawbacks to this approach.

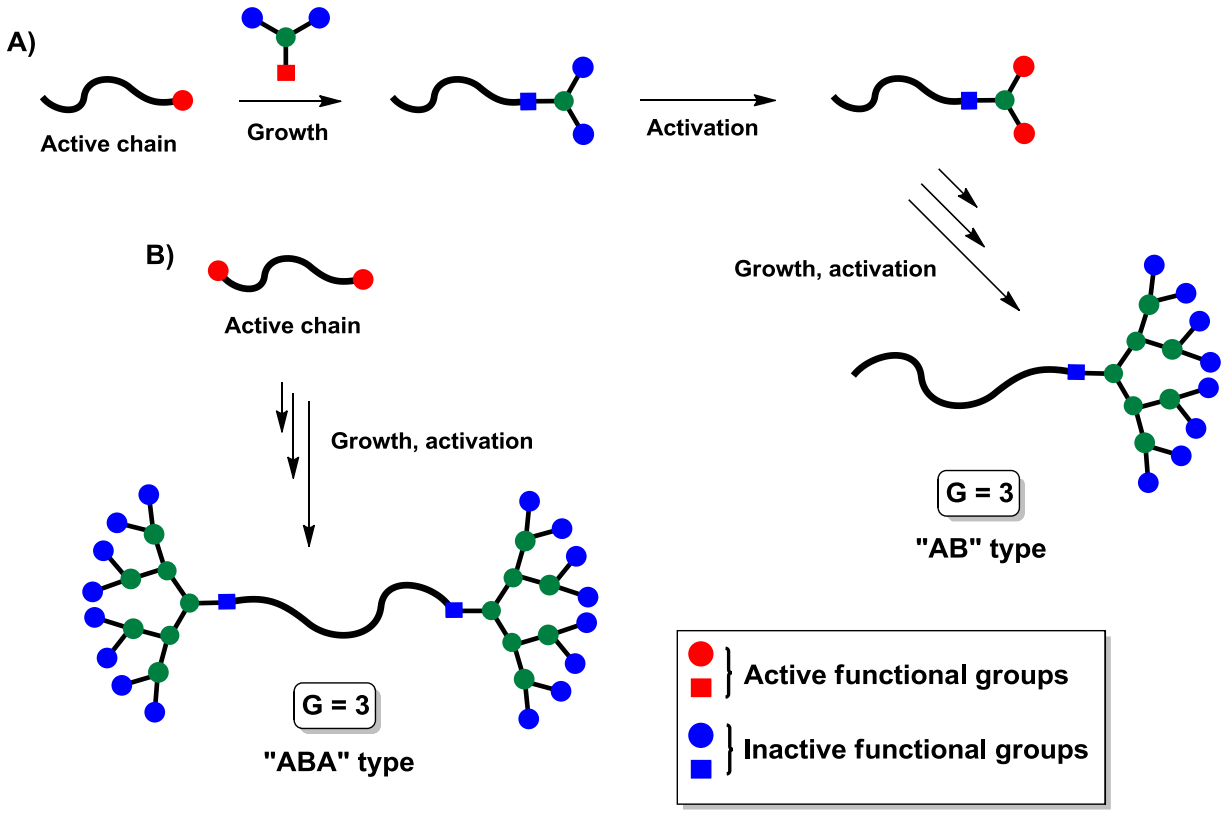

Figure 1.11 Schematic representations of LDHs synthesised by a divergent synthesis from a preformed polymer chain. Synthesis of; (A) AB type; (B) ABA type

As well as many further examples,[82] LDHs based on bis-MPA based scaffold have also been constructed by this approach. Using the reactive benzylidene protected anhydride, Ihre *et al.* demonstrated the construction of hydrophilic AB type LDHs with PEG chains having one, two or four reactive ends.[62] A similar strategy was extended by Yim *et al.* who utilised the acetonide protected bis-MPA anhydride with a hydroxyl functionalised polystyrene prepared by ATRP for the divergent

growth approach.[83] The synthesised dendron was successfully cleaved from its polystyrene chain via hydrogenation and characterised to determine the efficiency of the anhydride coupling reactions.

1.5.2.3 Macroinitiator method or "dendron first"

The final route to linear dendritic architectures is based on using a macroinitiator approach. The focal point of the dendron is modified in such a way that it can initiate a polymerisation, Figure 1.12. Several advantages of this route are that the chain length of the polymer can be easily controlled, the composition of monomers can be tailored and a variety of different polymerisation techniques can be used to suit the application.

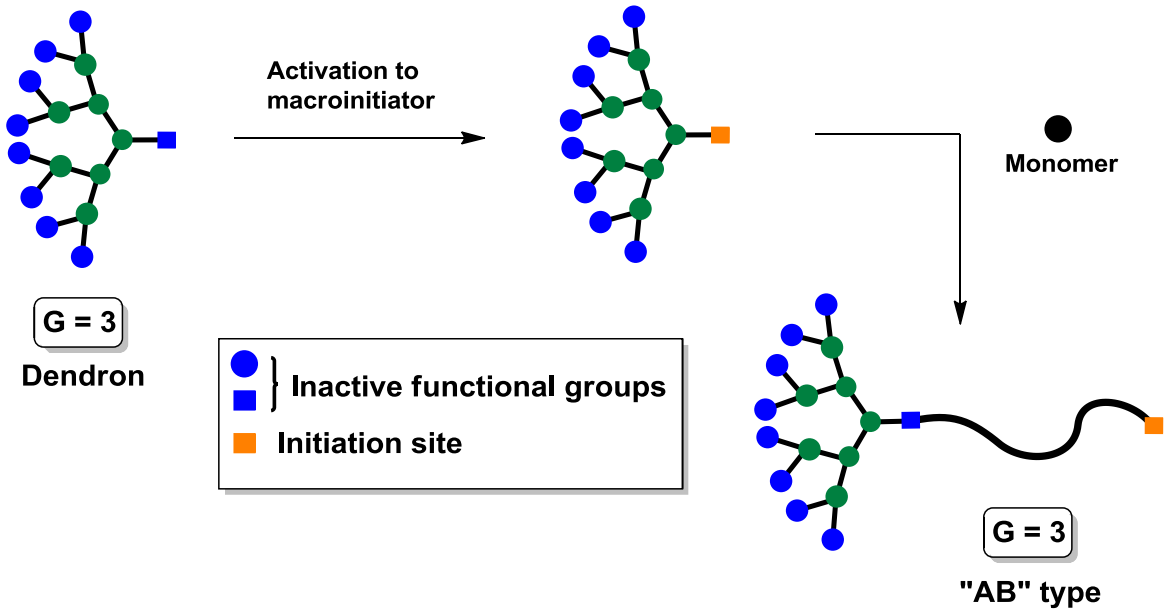

Figure 1.12 Schematic representation of an AB linear dendritic hybrid synthesised by a macroinitiator route

The first use of dendrons as macroinitiators was reported by Gitsov *et al.* in 1994[84] who made use of the benzyl alcohol moiety at the focal point of a poly(benzyl ether) dendron to ring open caprolactone. The formation of the benzyl alkoxide anion using a naphthalene potassium mirror allowed high molecular weight hybrids with narrow polydispersities to be obtained. Controlled radical polymerisation (CRP) processes have also been widely used in this approach. Early examples using nitroxide mediated radical polymerisation (NMP) and ATRP were used to synthesise AB block

hybrids with a hydrophobic poly(styrene) B block using poly(benzyl ether) dendrons.[85, 86] Further studies with poly(benzyl ether) dendron macroinitiators have also been reported using methacrylate based monomers.[87]

A noteworthy example using a poly(benzyl ether) dendron, included post modification of the dendron periphery after synthesis of the AB hybrid.[88] The authors used $LiAlH_4$ to reduce the ester moieties on the surface of the dendron to introduce carboxylic acid, alcoholic and amide functionalities. Bis-MPA dendron macroinitiators have also been utilised. Vestberg *et al.* synthesised a library of LDHs structures based on using RAFT polymerisation.[89] The bis-MPA dendrons with dithioester modified focal points allowed the controlled synthesis of AB block LDHs with a poly(methyl methacrylate) B block.

1.5.3 Dendronised polymers

Dendronised polymers are structures whereby dendrons are used as pendant functional groups along a polymer chain. Strategies to synthesising these materials include the use of dendritic monomers or the attachment of dendrons either convergently or divergently to a reactive polymer chain.

1.5.3.1 Macromonomer route

First introduced by Hawker and Fréchet in 1992,[90] the benzyl hydroxy focal points of poly(benzyl ether) dendrons (G_3 to G_5) were modified to incorporate styrenic monomer functionality via a Williamson ether synthesis with 4-chloromethyl styrene, and the resulting monomers were copolymerised with styrene, in a variety of different feed-stock ratios, Figure 1.13. An advantage of the macromonomer route is that an extremely high density of surface functionality can be introduced to the polymer, but as recently discussed;[82] a high reactivity of the groups participating in the propagation must occur; a very small size and favourable shape of the comonomer must exist, and the backbone of the polymer must be reasonably stiff.

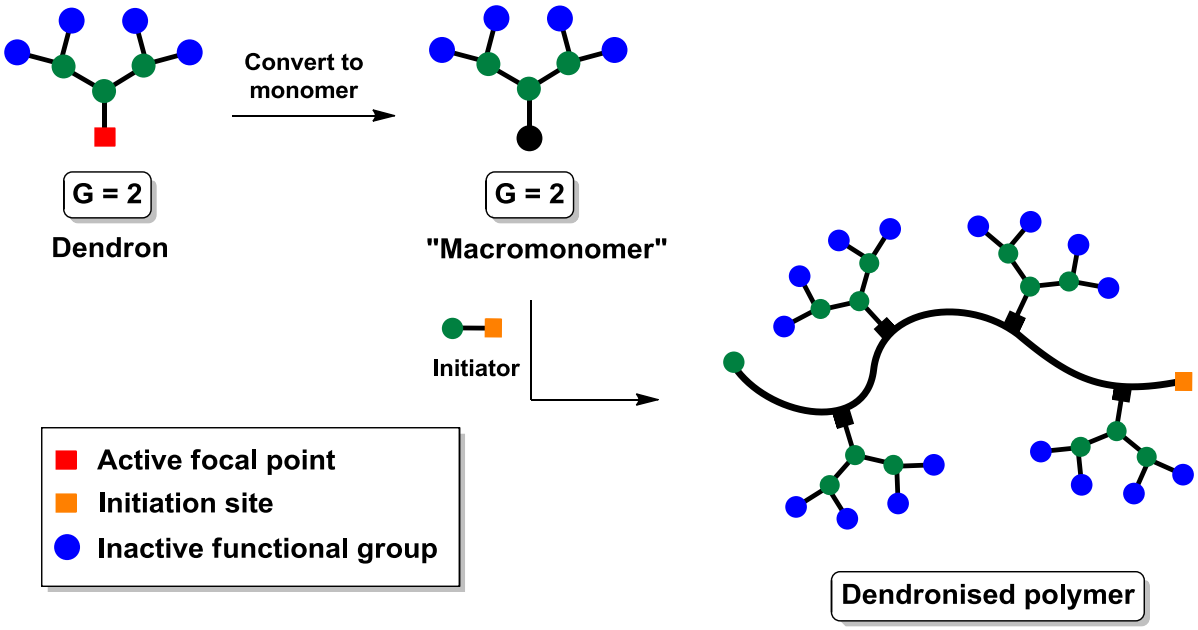

Figure 1.13 Schematic representation of dendronised polymers, formed by a macromonomer approach

For example, in the original report of this strategy,[90] G_4 and G_5 macromonomers did not form homopolymers, since their monomer size was large, and the resulting polymer chain was too flexible.[82] A solution to these problems was the incorporation of a spacer between the polymerisable group and the dendron. Using this approach, Calmark and Malmström introduced a C_{10} spacer between the bis-MPA type dendron and the acrylic polymerisable group.[91] Employing ATRP, acrylic monomers of $G_1$to G_3 were polymerised to high conversions, showing first-order kinetics.

1.5.3.2 Grafting approach

A variation to the macromonomer route is to use a "graft-to" approach, where dendrons can be either convergently coupled or divergently grown from an activated polymer chain. A recent *example* of a convergent coupling approach took advantage of the thiol-ene reaction, whereby a dendron was convergently attached to an alkene modified polymer chain.[44] Successful divergent examples have included the use of the highly reactive acetonide protected bis-MPA anhydride monomer, leading to the construction of dendronised polymers to G_3.[92]

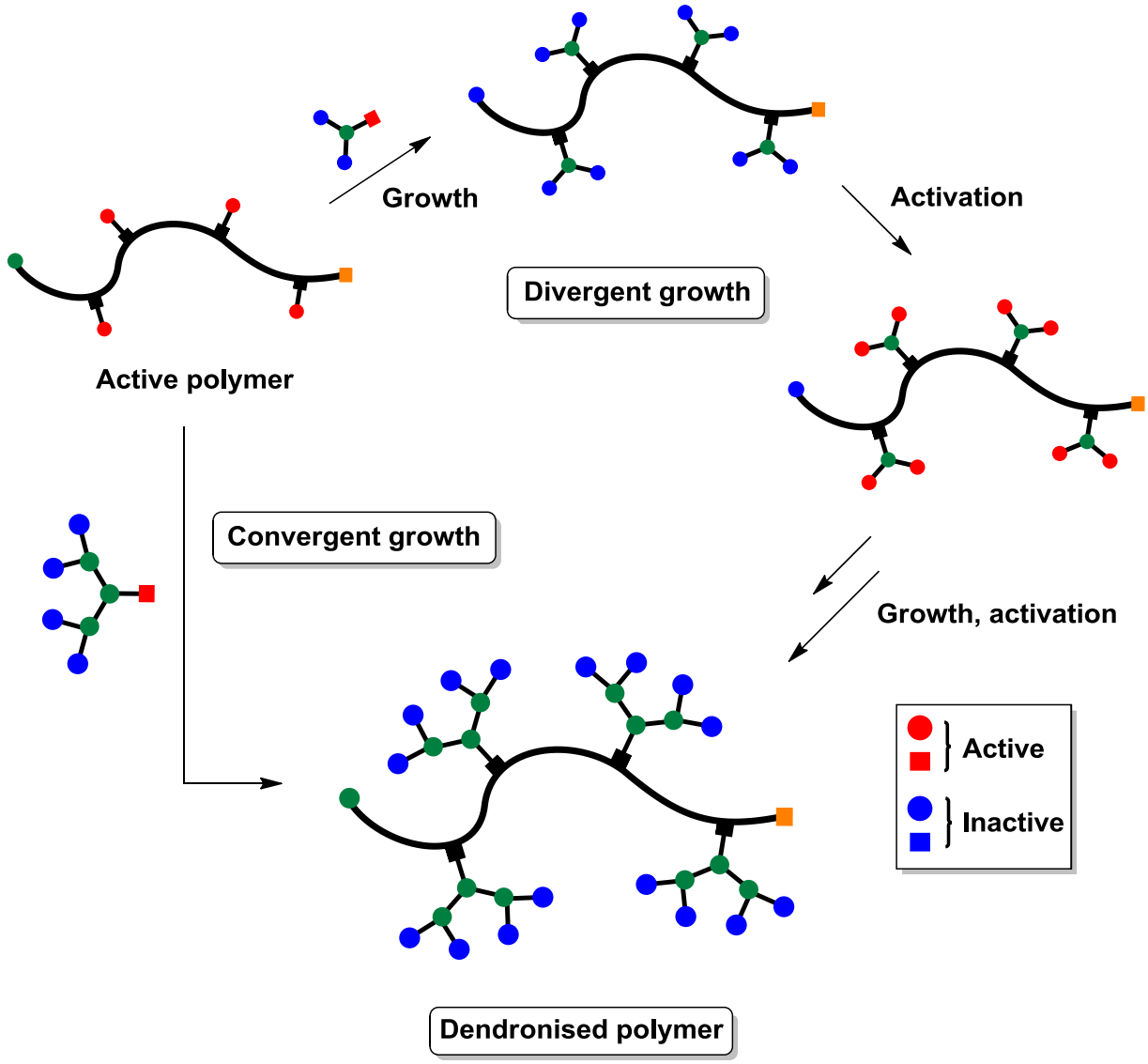

Figure 1.14 Schematic representation of dendronised polymers, formed by a grafting approach; either convergently or divergently

1.5.4 Variant hybrid structures

There are examples which include hybrid structures that do not fit into the previously discussed categories, Figure 1.15.

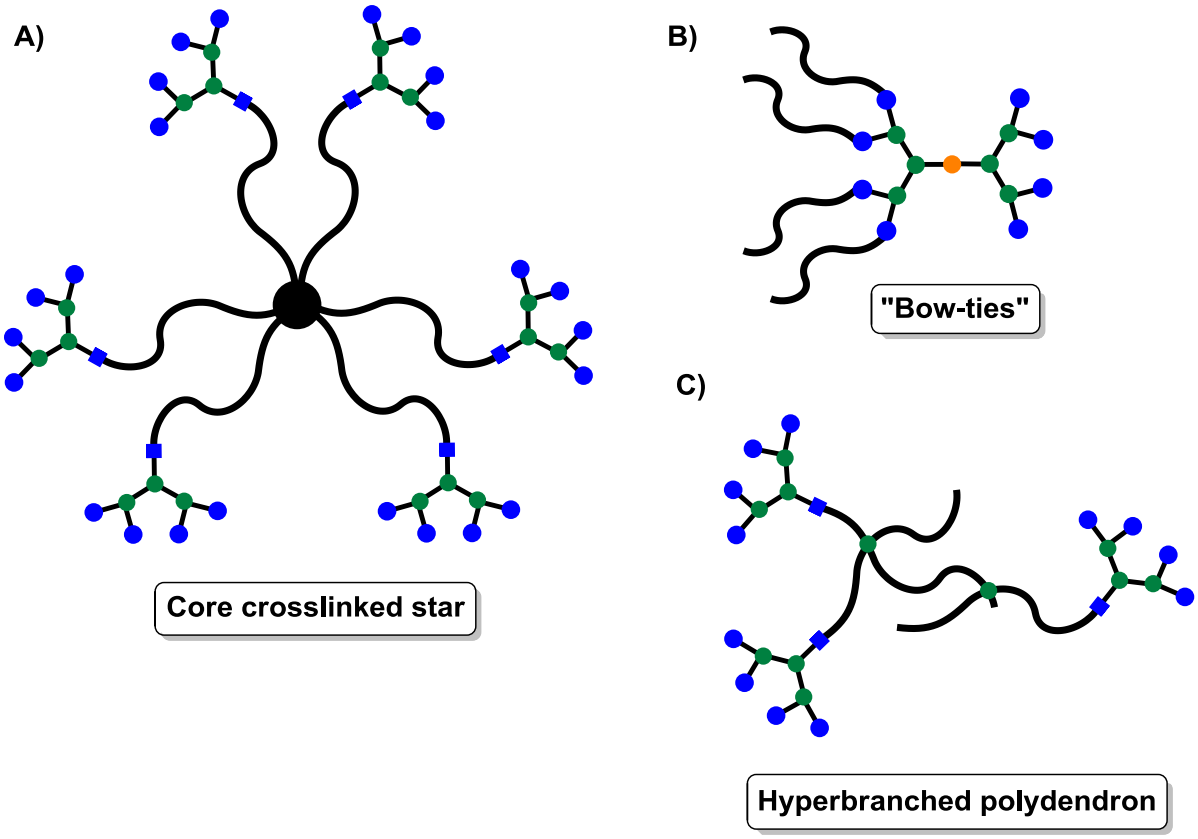

Figure 1.15 Schematic representations of variant hybrid structures; (A) Core crosslinked star polymers; (B) Bow-tie structures; (C) Hyperbranched polydendrons (HPDs)

Connal *et al.* prepared core crosslinked star polymers by a macroinitiator approach using ATRP, forming AB block linear dendritic hybrids up to G_5,[93] Figure 1.15 (A). The macroinitiator hybrids were reinitiated and crosslinked at the Br-chain site with divinyl benzene. Effects including the size of dendron and chain length were found to have a dramatic effect on the structure of the materials. Gillies and Fréchet have also prepared a class of dendritic hybrid structure which are based on an asymmetric dendrimer structure.[94] Named as "bow-ties", the structures consisted of two dendrons linked together, whereby linear PEG chains were attached to one of the dendritic segments, Figure 1.15 (B). Prepared by both divergent and convergent routes; dendritic size and length of linear PEG chains were investigated with these type of structure.

A final example of a variant hybrid structure is that recently reported by Hatton *et al.*[95] These structures, named as "Hyperbranched Polydendrons" (HPDs) consist of an AB hybrid, whereby the B

block is a soluble branched vinyl polymer, rather than a conventional linear polymer, Figure 1.15 (C). Prepared by using a macroinitiator approach and utilising ATRP, the ratio of divinyl branching group to form the branched B block was kept lower than the number of chains that were initiated (i.e. a molar ratio of brancher to initiator of less than 1), so the growing polymer cannot crosslink or gel. The resulting materials were shown to have self-assembly properties in organic and aqueous media, which was found to be linked to the surface functionalities on the dendron periphery.

1.5.5 Summary – Dendritic macromolecules

The synthesis of dendrimers and dendritic hybrids has been discussed, highlighting the key synthetic developments in both types of structures. Emphasis was placed upon click chemistry, describing the most common click reactions, and focussing on important examples. The next section introduces emulsions, aiming to link the potential of dendritic structures, towards the design of novel polymeric surfactants.

1.6 Emulsions

"Emulsions are metastable colloids made from two immiscible fluids, one being dispersed in the other, in the presence of surface active agents".[96] Since emulsions commonly contain an aqueous and an oil phase, they can be either described as an oil-in-water emulsion (o/w) or a water-in-oil emulsion (w/o), describing both the dispersed phase and continuous phase. Figure 1.16 illustrates the formation of an o/w emulsion.

Droplet diameters of emulsions can range from <1 μm[97] (often called mini or nano emulsions) to 100 μm[98], with emulsions under 100 nm typically appearing translucent. Over 100 nm, emulsions appear cloudy due to the many phase interfaces that scatter light. Emulsions are extremely important in many commercial applications because of their ability to transport or solubilise hydrophobic substances in a continuous water phase. Surface treatments such as painting and road treatments make use of emulsions, avoiding organic solvents.

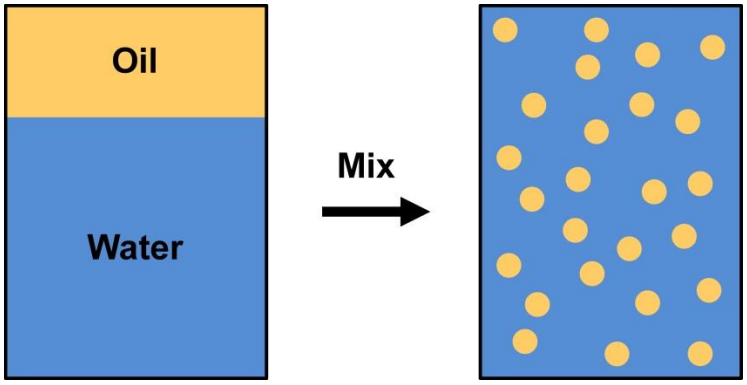

Figure 1.16 Schematic illustration of the formation of an oil-in-water (o/w) emulsion from two immiscible fluids

1.6.1 Physical chemistry of emulsions

The formation of an emulsion is not a spontaneous process, and such systems are thermodynamically unstable.[99] To emphasise this point, in Figure 1.17 an o/w system is illustrated whereby an oil phase is represented as a large oil droplet, 2, of area A_1 immersed in a liquid, 1, (state 1) which after an input of energy is subdivided into a larger number of smaller droplets with a total area A_2 (where $A_2 >> A_1$) immersed in a liquid, 1, (state 2). The following example and explanation is taken from Tadros.[99]

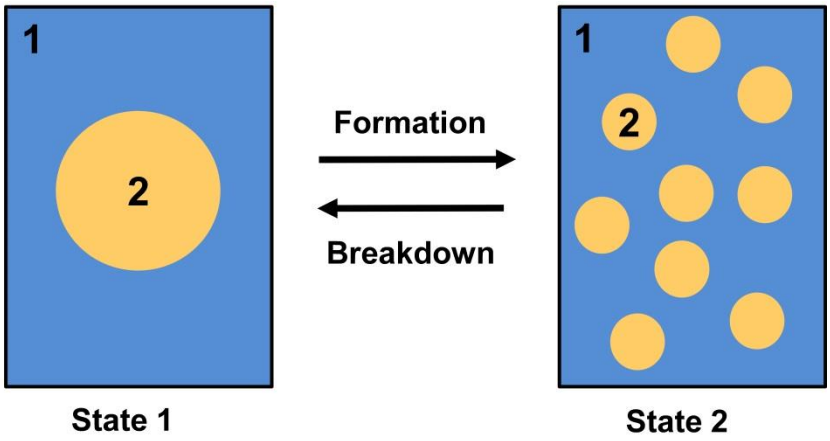

Figure 1.17 Schematic representation of emulsion formation and breakdown. (Figure adapted from Tadros).[99]

In both states 1 and 2, the interfacial tension (γ_{12}) remains approximately the same, since the size differences in this example are not significant (i.e. 0.1μm to 1-3 μm), and crucially no surfactants are

present in the system. The standard Gibbs free energy of formation (ΔG^{form}) from state 1 to state 2 is made up of two contributions, providing temperature (T) (worth noting here that temperature has an effect on the system) and interfacial tension (γ_{12}) remain constant, Equation 1.1. Firstly, a surface energy term equal to the change in area (ΔA) (where $\Delta A = A_2 - A_1$) which is positive, and secondly, a entropy of dispersions term (ΔS^{conf}) that is also positive (since producing a large number of droplets results in an increase in configurational entropy).

$$\Delta G^{form} = \Delta A \gamma_{12} - T\Delta S^{conf}$$

Equation 1.1 – Gibbs free energy of formation, from the second law of thermodynamics:

In most cases, $\Delta A\gamma_{12} >> - T\Delta S^{conf}$ meaning that ΔG^{form} is positive, and therefore the formation of emulsions is a non-spontaneous process, and the system is thermodynamically unstable. In the absence of any stabilisation mechanism, the emulsion will break down.

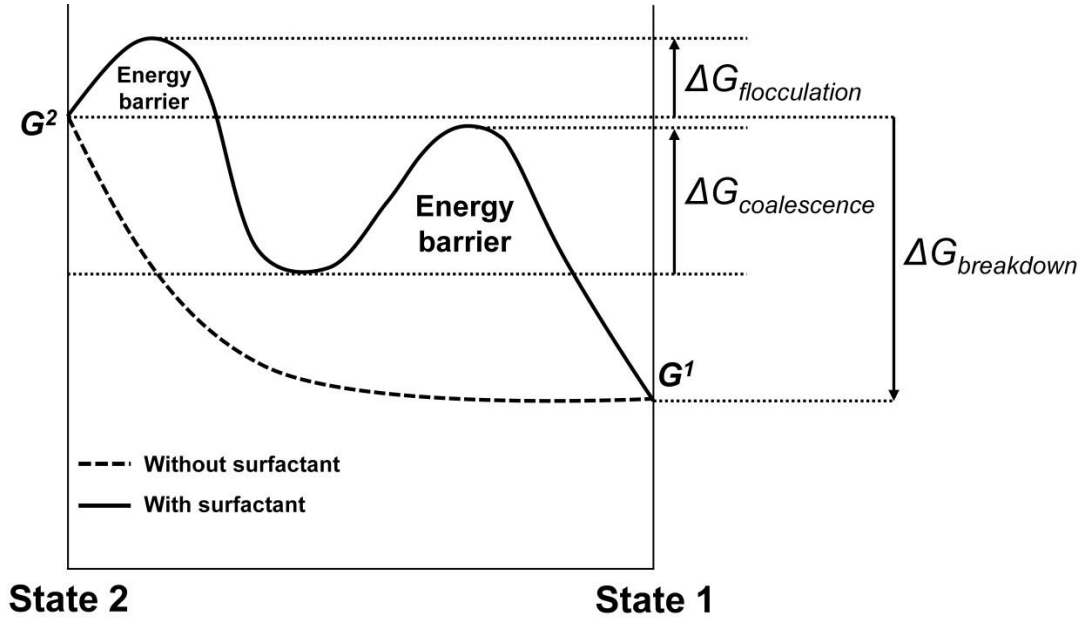

Figure 1.18 Schematic representation of free energy path for systems containing an energy barrier. (Figure adapted from Tadros).[99]

In presence of a stabiliser (i.e. a surfactant) an energy barrier is created between the droplets by reducing the interfacial tension at the liquid-liquid interface, reducing the positive ΔG^{form} term. Thus, the reversal from state 2 to state 1 becomes non-continuous as a consequence of an energy barrier created by the surfactant, therefore the system is kinetically stable. This is represented by using a free energy diagram shown in Figure 1.18.

1.6.2 Mechanisms of emulsion breakdown

There are four main instability mechanisms that can occur during the breakdown of an emulsion, Figure 1.19.[99]

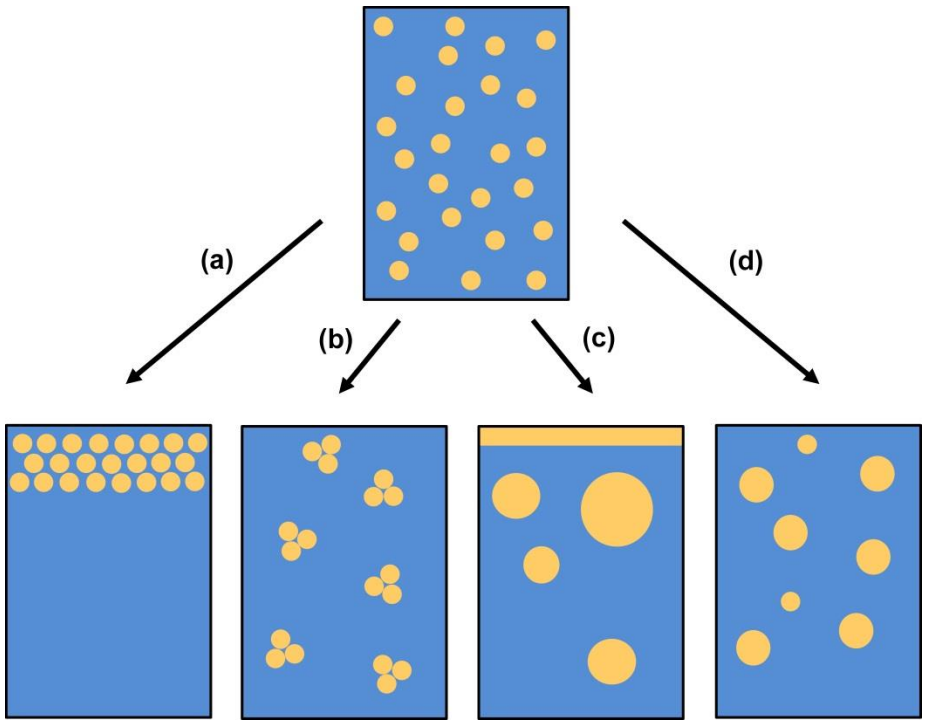

Figure 1.19 Schematic representation of the different mechanisms that lead to the emulsion breakdown;[99] (a) creaming; (b) flocculation; (c) coalescence; (d) Ostwald ripening. (Figure adopted from Tadros[99] and Woodward[100]).

Creaming and sedimentation is a process that occurs when a concentration gradient builds up, leading to larger droplets migrating to the top (or to the bottom) of the sample, depending on the densities of the dispersed and continuous phases. It is often observed after centrifugal forces, which aid the generation of a concentration gradient. Flocculation is the initial process that occurs before

coalescence, and involves the clustering (or aggregation) of droplets without any change in the primary droplet size. Coalescence is the combination of two or more droplets to form larger droplets and the result is the complete separation of the emulsion into two liquid phases.

Ostwald ripening occurs from the limited solubility of the liquid phases, which although referred to as immiscible, are often slightly soluble with each other.[99] Since emulsions have a polydispersity of droplet sizes, smaller droplets will be more soluble than larger ones, and hence smaller droplets diffuse to the bulk and become deposited on larger droplets. The net result is an overall increase in droplet size distribution, and a reduction in interfacial area. By reducing interfacial tension, surfactants create energy barriers preventing droplets from coalescing, resulting in stable emulsions. However, over time emulsions will destabilise as they are inherently thermodynamically unstable systems. During the construction of an emulsion, the surface area of the oil droplets is increased, but so is the ordering of the surrounding water molecules. Emulsion breakdown by coalescence leads to a more random distribution of the water molecules, and hence increases entropy within the system, which is a favourable process.

1.7 Surfactants

Surface active substances, or surfactants, are amphiphilic compounds that have a hydrophilic component and hydrophobic component.[101] This allows the surfactant to have an interaction between two otherwise immiscible liquid phases, reducing their interfacial tension. In a typical emulsion, the hydrophilic part of the surfactant will preferentially reside in the water phase, and the hydrophobic part, preferentially reside in the oil phase.

1.7.1 Small molecule surfactants

Most industrially prepared emulsions make use of small molecule surfactants, and are classed as either ionic (e.g. anionic, cationic) or non-ionic.

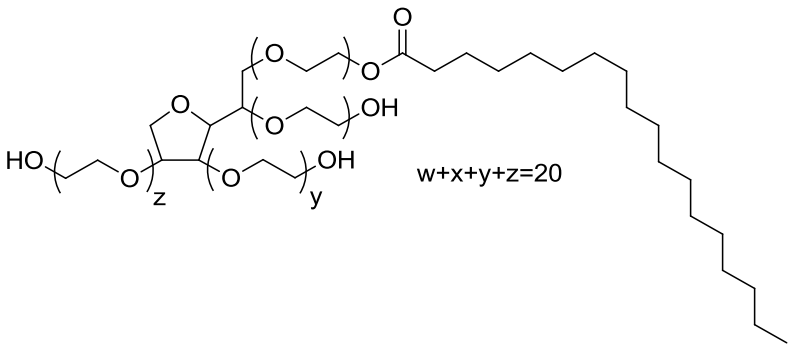

Figure 1.20 Structure of a typical non-ionic surfactant, polysorbate 60, also known as Tween 60

Non-ionic surfactants do not dissociate into ions, and typically carry no charge. However, there are examples, such as amine oxides that are able to acquire a charge depending on the pH. Therefore, a more accurate definition of a non-ionic surfactant is "a surfactant that carries no charge in the predominant working range of pH".[101] Typical non-ionic surfactants usually comprise alcohols, esters, ethers or amides. An example of a common non-ionic surfactant is Polysorbate 60, also known as Tween 60, Figure 1.20.

Of the ionic surfactants, anionic surfactants are commercially more important, reaching around 75% of the world market.[101] Anionic surfactants are often named "detergents" to emphasise their important in cleaning products. Dissociating in water, anionic surfactants form surface-active anions and hydrated cations. An example of a common anionic surfactant is sodium dodecyl sulfate (SDS), Figure 1.21, which consists of an anionic hydrophilic "head" and a hydrophobic alkyl chain "tail".

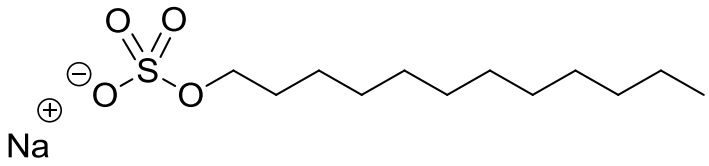

Figure 1.21 Structure of a typical ionic surfactant, sodium dodecyl sulfate (SDS)

1.7.2 Solid particulate surfactants

Stabilisation of emulsions can also be achieved using particulate surfactants often known as "Pickering" emulsions, first described by S.U. Pickering in 1907.[102] Reduction of interfacial tension is

achieved by adsorption of solid particles at the liquid-liquid interface, Figure 1.22. Both the size and stability of the emulsion droplets can be controlled by the size[103] and hydrophobicity[104] of the solid particles. By increasing the size of the solid particles this creates a greater separation between the two immiscible liquid-liquid phases, thus reducing the interfacial tension. The hydrophobic/hydrophilic nature of the solid particles can also be tuned, described in terms of their "wettability", which is expressed by their contact angle, θ. [104] If θ (expressed in terms of the water phase) is <90° then the particles are termed hydrophilic, and stabilise an o/w emulsion, but if θ is >90° then the particles are more hydrophobic and thus stabilise a w/o emulsion.[100]

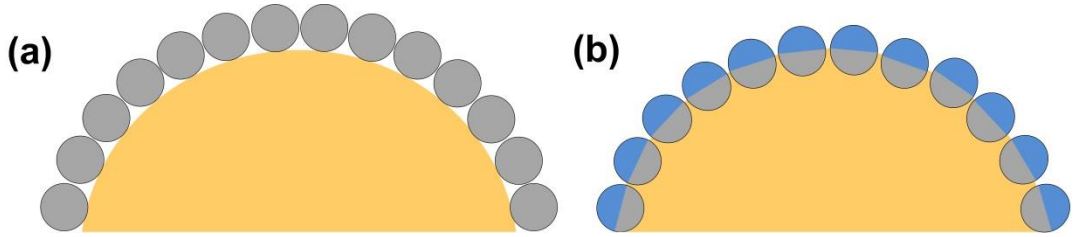

Figure 1.22 Schematic representation of Pickering emulsions stabilised by; (a) particles with uniform wettability; (b) amphiphilic particles (Janus particles). (Figure adopted from Woodward).[100]

Solid particles of amphiphilic nature, often known as "Janus particles" have also been theoretically predicted[105] and prepared.[106] The particles are able to interact with both hydrophobic and hydrophilic regions, and have been shown to be considerably more active that homogenous particles of comparable size and chemical nature.[106]

1.7.3 Linear polymeric surfactants

Amphiphilic linear copolymers can also behave as surfactants, with the hydrophilic/hydrophobic nature of the polymer allowing the interaction with both immiscible phases of the emulsion. The Hydrophilic-Lipophilic Balance (HLB) is a commonly used scale to determine how hydrophilic an amphiphilic polymer is although several approaches to calculate these values exist, Figure 1.23.

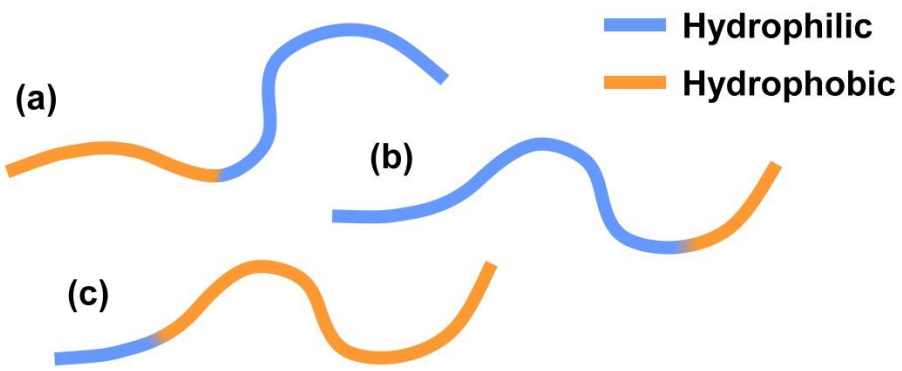

Figure 1.23 Schematic representation linear polymeric surfactants determined by their Hydrophilic-Lipophilic Balance (HLB); (a) HLB = 10; (b) HLB = >10; (c) HLB = <10

Commercially available polymeric surfactants are often graded within this scale, ranging from 1-20, with surfactants greater than 10 being more hydrophilic and surfactants less than 10 being more hydrophobic. The scale is however a very relative scale, and doesn't necessarily give a true insight into the properties of a surfactant, but rather allows the comparison between surfactants.

Responsive architectures have been the subject of many key developments in polymeric surfactants, with seminal work by Mathur *et al.* in 1998 demonstrating that "simple variations in molecular architecture may be used to tailor the pH range over which the emulsification capacities of the polymer change".[107] By synthesising a pH-responsive graft polymer comprising a poly(methacrylic acid) (PMAA) backbone and short grafts of poly(ethylene glycol) (PEG), the authors demonstrated that at high pH (basic) the polymer was hydrophilic, but by lowering the pH (acidic) caused it to develop hydrophobic segments due to the hydrogen bonding between the methacrylic acid and the ethylene glycol repeat units. This system led to formation of alternating blocks of hydrophilic (uncomplexed) and hydrophobic (complexed) segments that stabilised o/w emulsions in acidic media.

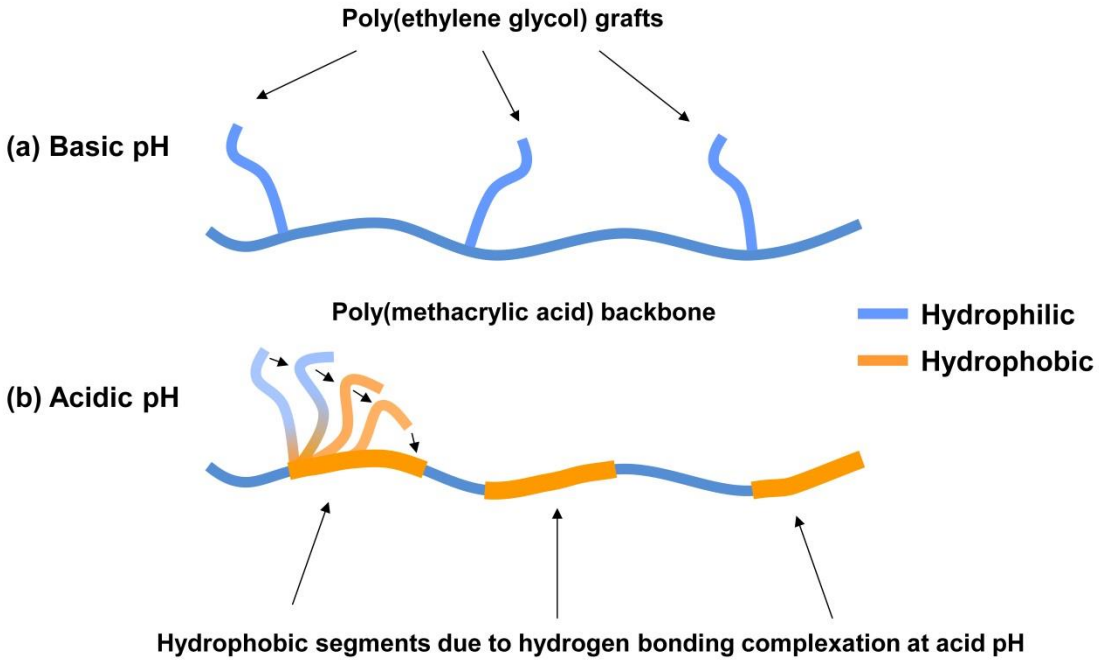

Figure 1.24 PEG-grafted PMAA polymer at; (a) basic pH; polymer remains completely hydrophilic since no hydrogen bonding; (b) acidic pH; complexation between PMAA and PEG chains, resulting in both hydrophilic and hydrophobic segments. (Figure adopted from Mathur *et al.*).[107]

The preparation of switchable amphiphilic diblock polymers have also be widely investigated.[108] Particularly interesting examples are in the approach to so-called "schizophrenic" AB diblock copolymers, which can form micelles with the A block in the micelle core, and also reverse micelles with the B block in the micelle core in aqueous solution. In the first example, a 2-(*N*-morpholino)-ethyl methacrylate-*block*-2-(diethylamino)ethyl methacrylate (MEMA-DEAEMA) polymer was prepared by group transfer polymerisation, making use of both blocks being pH responsive, therefore switchable between hydrophilic or hydrophobic,[109] Figure 1.25. At pH 8.0 the DEAEMA block was substantially deprotonated, hence hydrophobic, whereas the MEMA block remained solvated, and therefore led to micelles comprising DEAEMA cores. However, lowering the pH to 6.7 protonated the DEAEMA block, causing it to becoming hydrophilic, and by "salting out" the MEMA block, it became hydrophobic leading to micelles comprising of MEMA cores.

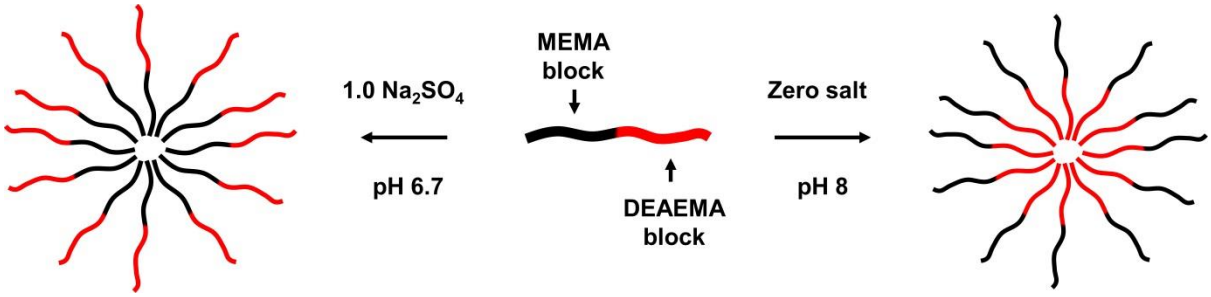

Figure 1.25 Schematic representation of the formation of micelles and reverse micelles for an AB diblock copolymer. (Figure adopted from Armes and co-workers).[109]

In a further example, Liu *et al.* made use of ATRP to prepare a diblock copolymer based on poly[propylene oxide-*block*-2-(diethylamino)ethyl methacrylate] (PPO-DEAEMA).[110] Again, the solubility of the DMAEMA block could be tuned by its pH, and similarly poly(propylene oxide) (PPO) readily dissolved in cold dilute aqueous solutions, but became insoluble at 20 °C; its lower critical solution temperature (LCST) lies between 10 °C and 20 °C. Once again, micelles and reverse micelles could be induced by changing the solution pH and the solution temperature.

Building from initial pioneering work on shell cross-linked (SCL) micelles by Wooley and co-workers,[111] the same pH responsive DMAEA-MEMA block copolymer was used to prepare SCL with tuneable hydrophilic/hydrophobic cores.[112] Lowering the temperature of the aqueous media from 60 °C to 25 °C allowed the MEMA core to switch between hydrophobic to hydrophilic, resulting in hydration and swelling. A significant drawback of these early examples of SCL micelles was that cross-linking had to be carried out at high dilution (0.1-0.5% solids) to avoid extensive inter-micellar cross-linking. Later studies found that by preparing three layer "onion" micelles using triblock polymers such as poly[ethylene oxide-*block*-2-(dimethylamino)ethyl methacrylate-*block*-2-(N-morpholino)ethyl methacrylate] (PEO-DMA-MEMA) comprising an outer PEO block prevented the DMA residues of one micelle from coming in contact with a neighbouring micelle during DMA crosslinking (10% solids); this is since a PEO-water interaction is more favourable than a PEO-PEO interaction.[113] Examples of SCL micelles using triblock polymers have also included those with pH responsive cores.[114]

Following these developments in colloidal chemistry, an example of a o/w emulsion was prepared and stabilised using SCL micelles comprising of ABC triblock copolymers.[115] At pH 9, the hydrophobic core poly[2-(diethylamin)ethyl methacrylate] (PDEA) enabled SCL micelle stabilised emulsions, with a mean oil droplet size of 18 μL by laser diffraction. Upon the addition of acid (pH 2), resulted in the protonation of the PDEA block, hence a cationic core, and ultimately led to rapid demulsification.

1.7.4 Branched polymeric surfactants

Surfactants comprising branched polymer systems have been shown to exhibit greater stability than analogous linear copolymers.[116] Results from a stability test over nine months indicated no change in the droplet size or distribution by laser diffraction of the emulsions stabilised by branched copolymers, whereas the systems incorporating linear equivalents coalesced over several weeks. This is thought to be due to the weak droplet adhesion afforded by the single hydrophobic chain end, in contrast to multiple hydrophobic chain ends which are provided by the branched architecture, Figure 1.26.

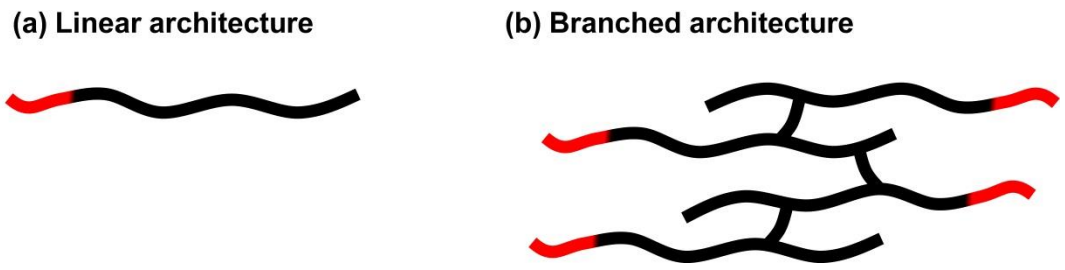

Figure 1.26 Schematic diagram comparing; (a) linear architecture; (b) branched architecture, demonstrating the multiple hydrophobic end groups (red) in the branched polymer system compared to the linear polymer system

Similar to the linear examples discussed earlier,[109, 112] branched polymers have also shown to exhibit changes in solution behaviour in response to changes in pH.[117] In this first example, Weaver *et al.* prepared branched copolymers comprising hydrophilic poly(ethyleneglycol) methacrylate (PEGMA) and pH responsive 2-(diethylamino)ethyl methacrylate (DEA) blocks. Upon dissolving the copolymer

in aqueous media at pH 2 the DEA block was fully protonated, resulting in hydrophilic particles with intensity-average hydrodynamic diameters of 46 nm. Upon increasing the pH to 10, the DEA residues became deprotonated and hydrophobic forming compact amphiphilic core-shell structures of around 24 nm. The observed variation in particle diameters via changes in pH with these branched copolymers is extremely similar to the examples of pH responsive SCL micelles which hydrate and dehydrate, discussed earlier.[112] The reader is directed to a review on such comparisons.[118]

In 2009 Woodward *et al.* combined a number of these concepts to produce branched copolymer stabilised emulsions whereby changes in the chain-end functionality, copolymer architecture and pH resulted in significant changes in the emulsion stability.[119] The branched polymers were comprised of a hydrophobic or a hydrophilic chain end (varied with different chain transfer agents) and a pH responsive 2-(diethylamino)ethyl methacrylate (DEA) block, which was branched using ethylene glycol dimethacrylate (EGDMA). Under these conditions, polymers with different hydrophobicity at the chain ends were constructed by varying the chain transfer agent (CTA) between highly hydrophobic (dodecanethiol, DDT), hydrophilic but non-ionic (1-thiolglycerol, TG), and hydrophilic and ionic (mercaptopropanoic acid, MPA). Each polymer initially stabilised o/w emulsions, but addition of acid to protonate the DEA residues resulted in demulsification by 30% using TG chain-ends and 50% using MPA chain-ends. When employing the hydrophobic DDT chain-ends, the emulsions show no signs of demulsification. These results suggested that the hydrophobicity of the chain-end which "anchors" into the oil droplet plays a vital role in emulsion stabilisation. To illustrate this theory further, the architecture was modified to become even more hydrophilic, therefore less effective at stabilising the oil phase by changing the branching agent from hydrophobic EGDMA to hydrophilic PEGMA. As expected, both polymers employing TG and MPA chain-ends led to significant demulsification, yet the polymer employing DDT chain-ends showed no sign of demulsification after 12 hours. These results reiterated that the branching process allows multiple chain ends to be anchored to the oil droplet, even when the majority of the components within the surfactant are hydrophilic.

Examples of pH responsive branched polymers have led to the development of so-called "engineered emulsions" which has allowed the assembly and disassembly of robust liquid structures.[116] Building from early concepts of hydrogen bonding between PMAA and PEG residues[107], the authors demonstrated that at basic pH the branched copolymer surfactant stabilised emulsion existed as a stable and free flowing dispersion due to the simultaneous and electrostatic stabilisation afford by the copolymer at this pH. However on lowering the pH, the electrostatic stabilisation decreases as the PMA residues are protonated and the methacrylic acid (MA) residues form hydrogen bonds with the ethylene glycol (EG) repeat units in the PEG chains. The resultant hydrogen bonding between the droplets (inter-droplet), led to emulsion gelation – so-called "emulsion engineering". Recent work has focussed on the "design principles" of these engineered emulsions, by varying their PMA to PEG copolymer compositions[120], and by also studying their kinetics using a homogeneous trigger based on the hydrolysis of glucono-δ-lactone (GδL).[121]

1.7.5 Dendrimers as surfactants

For a dendrimer to behave as a surfactant, it must possess hydrophilic and hydrophobic components. There are numerous reports on the preparation of such dendrimers, all of which use one or more combinations of the synthetic routes discussed earlier.[122] Like micelles, amphiphilic dendrimers have the capability to solubilise organic matter in aqueous media, and are considered to be model systems of the "classic micelle". However, unlike micelles which are affected by the physical environment such as pH, concentration, ionic strength and temperature, the dendrimer micelle is stable under general conditions; this is since dendrimers are covalently bonded, and do not rely on the self-assembly properties of conventional micelles. First proposed as "unimolecular micelles" by Newkome *et al.* 1986,[5] the same group prepared a saturated hydrocarbon cascade polymer with both ammonium and tetramethylammonium carboxylate end groups, resulting in an amphiphilic structure,[123] Figure 1.27.

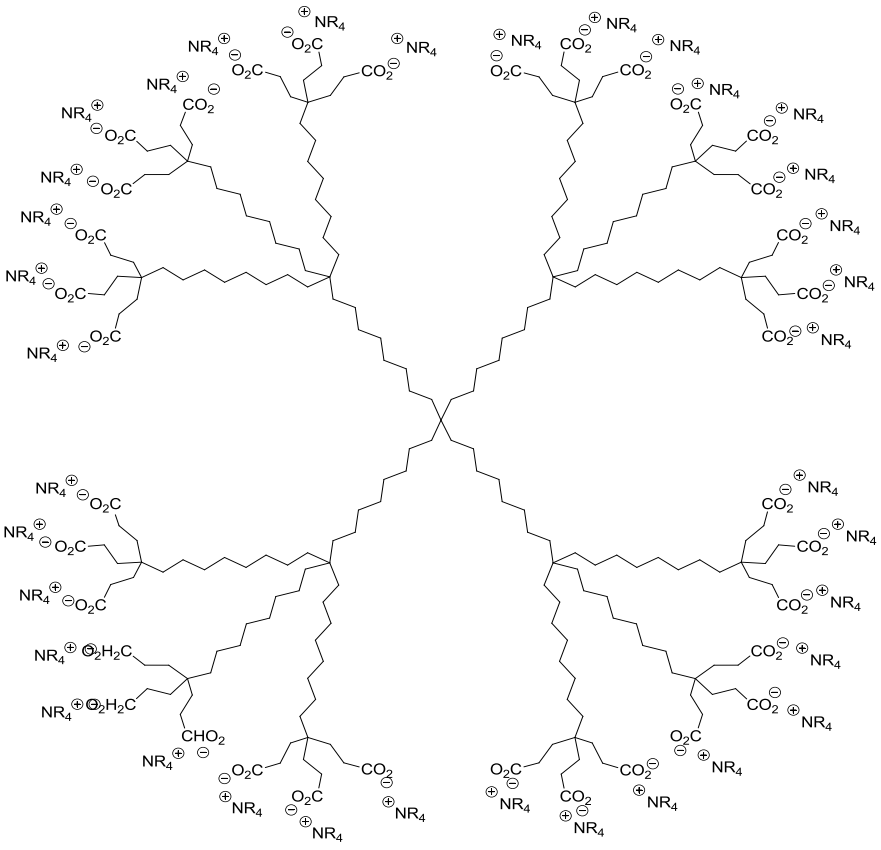

Figure 1.27 A unimolecular micelle reported by Newcome *et al.*[123]

The charged end groups solubilised the hydrophobic core in aqueous solution, resulting in a micelle-like structure. It is worth noting that the dendrimers comprising tetramethylammonium carboxylate end groups resulted in the formation of some aggregates, whereas the ammonium end groups exhibited no aggregation, demonstrating that the peripheral groups have a strong effect on the dendrimer-dendrimer interactions in solution. Many further examples of unimolecular micelles exist in the literature.[122]

Asymmetric or "Janus" type dendrimers have also played a role in dendrimer studies as surfactants. These comprise dendrimers where one segment of is hydrophilic and another segment is hydrophobic. Again these have been widely reported,[124] with the first examples being based on a poly(benzyl ether) dendrimer.[125] A particularly elegant example, (termed a "bow-tie" dendrimer in this article) was that reported by Lee *et al.* which was used for biological purposes.[126] One side of the asymmetric

dendrimer was used for inducing water solubility, by the introduction of PEO chains, and on the other side, the attachment of a drug; in this case doxorubicin (DOX, an anti-cancer drug).

The compound was extremely successful, being less than one tenth of the toxicity of free DOX, causing complete tumour regression, and showing 100% survival of the mice, comparable to no cure being achieved with mice treated with free DOX.

1.7.6 Dendritic hybrids as surfactants

When comprised of hydrophobic and hydrophilic AB or ABA blocks, LDHs have been shown to behave in a similar way in aqueous media to traditional linear block copolymer surfactants, forming supramolecular structures, such as micelles.[82] However, in comparison to linear block copolymers, it is the ability to combine the monodisperse and regular structure of the dendron, comprised of multiple surface functionalities with a traditional polymer chain, which fascinates many scientists with the potential applications of these materials.

In an early example based on a poly(benzyl ether) dendritic component, the authors showed that diblocks or triblocks were able to form mono and multimolecular micelles depending on the dendron generation (i.e. hydrophobic component), length of hydrophilic component (PEG chains), and concentration of methanol/water solvent.[127] Further specific details the on self-assembly properties of these types of structures were later reported,[128] and more recent examples have included linear dendritic micelles that are "responsive" to multiple stimuli including, pH, light and temperature changes.[129]

In comparison to unimolecular micelles, LDHs have also been shown to be far more effective at encapsulating "guest" molecules.[82] The highly ordered and covalently locked structures of dendrimers that provide unimolecular micelles with their advantages over traditional micelles in terms of stability, is in fact a problem when encapsulating molecules. It is these prearranged geometries and interior cavities limit their loading capacities, and thus only a few molecules with relatively small size can be encapsulated, even when using high generation dendrimers. To illustrate this point, a G_4 asymmetric dendrimer based on a poly(benzyl ether) structure functionalised with carboxylate moieties was

shown to encapsulate 0.45 pyrene molecules,[130] whereas a comparable triblock poly(benzyl ether) LDH was shown to encapsulate 469 molecules.[128] This not only demonstrates that the hybrid structure is nearly a thousand times more effective than the unimolecular dendritic micelle, but also shows that far more effective encapsulation can be achieved without the synthetic effect, cost, and time in synthesising the highly complex asymmetric dendrimer.[82] Multiple biological applications have since arisen from these early findings.[82, 129]

Finally, dendritic hybrids have shown some benefits in traditional emulsion systems, although it extremely surprising how few publications exist within this area comparable to studies of hybrid materials focussing on self-assembly in aqueous media.[129] In the first early example, a LDH comprising a G_4 hydrophobic lysine dendron and a hydrophilic PEO was dissolved in aqueous media and shown that the hybrid could act as an effective surfactant, demonstrating good stability over 1-2 weeks.[80]

More recent examples have since focussed on using poly(ether) based star shaped hybrids to act as demulsifiers in both w/o and o/w emulsions of crude oil.[131, 132] The emulsification of brine/water in crude oil is a common problem in the oilfield industry, and it is essential to break these emulsions before transportation and refining. In the o/w example it was found that increasing the number of PEO arms from the hydrophobic core led to a dramatic increase in the amount of water that phase separated from the emulsion.[131] In a similar investigation, using star shaped hybrids to promote the destabilisation of an o/w emulsion, it was found that there was little difference between using a core with multiple arms, comparable to a core with fewer arms, but a greater amount of emulsion destabilisation was observed when using short PEO surface chains compared to larger PEO surface chains.[132] These findings may be of particular interest when designing emulsion systems using such hybrid materials.

1.7.7 Summary - Emulsions

An understanding of emulsions has been described, reviewing the background and physical chemistry of such systems. Different types of surfactants were discussed, with key examples from linear, branched and dendritic architectures.

1.8 Research objectives

In this thesis, the design and synthesis of a new type of functionalisation chemistry will be presented, with the aim of using this new synthetic "tool" to develop responsive amphiphilic polymeric surfactants, based around hybrid dendritic architectures.

Chapter 2 will focus on the "development process" of successful functionalisation chemistries, focussing specifically on Michael addition. A one-pot, high yielding functionalisation reaction that conforms to the click chemistry concept will be sought.

Chapter 3 will use the developed chemistry within Chapter 2 to synthesise polyester dendrimers that can be functionalised at their periphery using this novel one-pot chemistry. Focus will be placed upon the synthetic design, dendritic backbone choice and chosen protecting group chemistry.

Chapter 4 will use the developed chemistry within Chapter 2 to synthesise LDHs via a macroinitiator approach, whereby the materials can be readily post modified to induce different surface functionality. Focus will be placed upon the synthesis of dendritic initiators and optimisation of polymerisation conditions.

Lastly, Chapter 5 will use the developed chemistry within Chapters 2, 3 and 4, to produce a variety of linear and branched dendritic polymeric surfactants that will vary by their surface chemistry at the periphery. An investigation into the effects of end group effect and polymer architecture will be presented. Emulsion stability, pH responsiveness, temperature response, and dilution studies will also be a priory of this final study.

1.9 References

1. B. I. Voit and A. Lederer, *Chemical Reviews*, 2009, **109**, 5924-5973.
2. E. Buhleier, W. Wehner and F. Vögtle, *Synthesis*, 1978, **1978**, 155-158.
3. D. A. Tomalia, H. Baker, J. Dewald, M. Hall, G. Kallos, S. Martin, J. Roeck, J. Ryder and P. Smith, *Polym J*, 1985, **17**, 117-132.
4. U. Boas, J. B. Christensen and P. M. H. Heegaard, *Journal of Materials Chemistry*, 2006, **16**, 3785-3798.
5. G. R. Newkome, Z. Yao, G. R. Baker and V. K. Gupta, *The Journal of Organic Chemistry*, 1985, **50**, 2003-2004.
6. M. Sowinska and Z. Urbanczyk-Lipkowska, *New Journal of Chemistry*, 2014, **38**, 2168-2203.
7. E. M. M. de Brabander-van den Berg and E. W. Meijer, *Angewandte Chemie International Edition in English*, 1993, **32**, 1308-1311.
8. A. W. Bosman, H. M. Janssen and E. W. Meijer, *Chemical Reviews*, 1999, **99**, 1665-1688.
9. P. G. de Gennes and H. Hervet, *J. Physique Lett.*, 1983, **44**, 351-360.
10. L. P. Tolić, G. A. Anderson, R. D. Smith, H. M. Brothers Ii, R. Spindler and D. A. Tomalia, *International Journal of Mass Spectrometry and Ion Processes*, 1997, **165–166**, 405-418.
11. G. J. Kallos, D. A. Tomalia, D. M. Hedstrand, S. Lewis and J. Zhou, *Rapid Communications in Mass Spectrometry*, 1991, **5**, 383-386.
12. J. C. Hummelen, J. L. J. Van Dongen and E. W. Meijer, *Chemistry – A European Journal*, 1997, **3**, 1489-1493.
13. J. M. J. Fréchet, C. J. Hawker and A. E. Philippides, *US. Patent*, 1989, US5041516.
14. C. J. Hawker and J. M. J. Fréchet, *Journal of the American Chemical Society*, 1990, **112**, 7638-7647.
15. C. Hawker and J. M. J. Fréchet, *Journal of the Chemical Society, Chemical Communications*, 1990, 1010-1013.
16. C. J. Hawker and J. M. J. Fréchet, *Journal of the American Chemical Society*, 1992, **114**, 8405-8413.
17. C. J. Hawker and J. M. J. Fréchet, *Macromolecules*, 1990, **23**, 4726-4729.
18. S. M. Grayson and J. M. J. Fréchet, *Chemical Reviews*, 2001, **101**, 3819-3868.
19. K. L. Wooley, C. J. Hawker and J. M. J. Fréchet, *Journal of the American Chemical Society*, 1991, **113**, 4252-4261.
20. K. L. Wooley, C. J. Hawker and J. M. J. Fréchet, *Angewandte Chemie International Edition in English*, 1994, **33**, 82-85.
21. J. Lim, M. Kostiainen, J. Maly, V. C. P. da Costa, O. Annunziata, G. M. Pavan and E. E. Simanek, *Journal of the American Chemical Society*, 2013, **135**, 4660-4663.

22. T. Kawaguchi, K. L. Walker, C. L. Wilkins and J. S. Moore, *Journal of the American Chemical Society*, 1995, **117**, 2159-2165.
23. H. Ihre, A. Hult, J. M. J. Fréchet and I. Gitsov, *Macromolecules*, 1998, **31**, 4061-4068.
24. R. Spindler and J. M. J. Fréchet, *Journal of the Chemical Society, Perkin Transactions 1*, 1993, 913-918.
25. F. Zeng and S. C. Zimmerman, *Journal of the American Chemical Society*, 1996, **118**, 5326-5327.
26. H. C. Kolb, M. G. Finn and K. B. Sharpless, *Angewandte Chemie International Edition*, 2001, **40**, 2004-2021.
27. P. Thirumurugan, D. Matosiuk and K. Jozwiak, *Chemical Reviews*, 2013, **113**, 4905-4979.
28. N. El Brahmi, S. El Kazzouli, S. Mignani, M. Bousmina and J. P. Majoral, *Tetrahedron*, 2013, **69**, 3103-3133.
29. A. Gandini, *Progress in Polymer Science*, 2013, **38**, 1-29.
30. C. E. Hoyle and C. N. Bowman, *Angewandte Chemie International Edition*, 2010, **49**, 1540-1573.
31. A. B. Lowe, C. E. Hoyle and C. N. Bowman, *Journal of Materials Chemistry*, 2010, **20**, 4745-4750.
32. B. M. Rosen, G. Lligadas, C. Hahn and V. Percec, *Journal of Polymer Science Part A: Polymer Chemistry*, 2009, **47**, 3931-3939.
33. D. P. Nair, M. Podgórski, S. Chatani, T. Gong, W. Xi, C. R. Fenoli and C. N. Bowman, *Chemistry of Materials*, 2013, **26**, 724-744.
34. P. Wu, A. K. Feldman, A. K. Nugent, C. J. Hawker, A. Scheel, B. Voit, J. Pyun, J. M. J. Fréchet, K. B. Sharpless and V. V. Fokin, *Angewandte Chemie International Edition*, 2004, **43**, 3928-3932.
35. M. J. Joralemon, R. K. O'Reilly, J. B. Matson, A. K. Nugent, C. J. Hawker and K. L. Wooley, *Macromolecules*, 2005, **38**, 5436-5443.
36. P. Antoni, D. Nystrom, C. J. Hawker, A. Hult and M. Malkoch, *Chemical Communications*, 2007, 2249-2251.
37. M. Malkoch, K. Schleicher, E. Drockenmuller, C. J. Hawker, T. P. Russell, P. Wu and V. V. Fokin, *Macromolecules*, 2005, **38**, 3663-3678.
38. P. Wu, M. Malkoch, J. N. Hunt, R. Vestberg, E. Kaltgrad, M. G. Finn, V. V. Fokin, K. B. Sharpless and C. J. Hawker, *Chemical Communications*, 2005, 5775-5777.
39. J.-F. Lutz, *Angewandte Chemie International Edition*, 2008, **47**, 2182-2184.
40. J. R. McElhanon and D. R. Wheeler, *Organic Letters*, 2001, **3**, 2681-2683.
41. M. M. Kose, G. Yesilbag and A. Sanyal, *Organic Letters*, 2008, **10**, 2353-2356.
42. K. L. Killops, L. M. Campos and C. J. Hawker, *Journal of the American Chemical Society*, 2008, **130**, 5062-5064.

43. M. I. Montañez, L. M. Campos, P. Antoni, Y. Hed, M. V. Walter, B. T. Krull, A. Khan, A. Hult, C. J. Hawker and M. Malkoch, *Macromolecules*, 2010, **43**, 6004-6013.
44. M. V. Walter, P. Lundberg, A. Hult and M. Malkoch, *Journal of Polymer Science Part A: Polymer Chemistry*, 2011, **49**, 2990-2995.
45. P. Antoni, M. J. Robb, L. Campos, M. Montanez, A. Hult, E. Malmström, M. Malkoch and C. J. Hawker, *Macromolecules*, 2010, **43**, 6625-6631.
46. R. Barbey and S. Perrier, in *Thiol-X Chemistries in Polymer and Materials Science*, The Royal Society of Chemistry, 2013, pp. 151-164.
47. G. Chen, J. Kumar, A. Gregory and M. H. Stenzel, *Chemical Communications*, 2009, 6291-6293.
48. Y. Shen, Y. Ma and Z. Li, *Journal of Polymer Science Part A: Polymer Chemistry*, 2013, **51**, 708-715.
49. D. Konkolewicz, A. Gray-Weale and S. Perrier, *Journal of the American Chemical Society*, 2009, **131**, 18075-18077.
50. S. P. S. Koo, M. M. Stamenović, R. A. Prasath, A. J. Inglis, F. E. Du Prez, C. Barner-Kowollik, W. Van Camp and T. Junkers, *Journal of Polymer Science Part A: Polymer Chemistry*, 2010, **48**, 1699-1713.
51. G.-Z. Li, R. K. Randev, A. H. Soeriyadi, G. Rees, C. Boyer, Z. Tong, T. P. Davis, C. R. Becer and D. M. Haddleton, *Polymer Chemistry*, 2010, **1**, 1196-1204.
52. J. W. Chan, C. E. Hoyle, A. B. Lowe and M. Bowman, *Macromolecules*, 2010, **43**, 6381-6388.
53. J. W. Chan, C. E. Hoyle and A. B. Lowe, *Journal of the American Chemical Society*, 2009, **131**, 5751-5753.
54. X. Ma, Z. Zhou, E. Jin, Q. Sun, B. Zhang, J. Tang and Y. Shen, *Macromolecules*, 2012, **46**, 37-42.
55. X. Ma, Q. Sun, Z. Zhou, E. Jin, J. Tang, E. Van Kirk, W. J. Murdoch and Y. Shen, *Polymer Chemistry*, 2013, **4**, 812-819.
56. E. R. Gillies and J. M. J. Fréchet, *Drug Discovery Today*, 2005, **10**, 35-43.
57. K. Jain, P. Kesharwani, U. Gupta and N. K. Jain, *International Journal of Pharmaceutics*, 2010, **394**, 122-142.
58. E. R. Gillies, E. Dy, J. M. J. Fréchet and F. C. Szoka, *Molecular Pharmaceutics*, 2005, **2**, 129-138.
59. J. d. A. Twibanire and T. B. Grindley, *Polymers*, 2012, **4**, 794-879.
60. A. Carlmark, E. Malmstrom and M. Malkoch, *Chemical Society Reviews*, 2013, **42**, 5858-5879.
61. H. Ihre, A. Hult and E. Söderlind, *Journal of the American Chemical Society*, 1996, **118**, 6388-6395.

62. H. Ihre, O. L. Padilla De Jesús and J. M. J. Fréchet, *Journal of the American Chemical Society*, 2001, **123**, 5908-5917.
63. M. Malkoch, E. Malmström and A. Hult, *Macromolecules*, 2002, **35**, 8307-8314.
64. M. Malkoch, H. Claesson, P. Löwenhielm, E. Malmström and A. Hult, *Journal of Polymer Science Part A: Polymer Chemistry*, 2004, **42**, 1758-1767.
65. M. C. Parrott, S. R. Benhabbour, C. Saab, J. A. Lemon, S. Parker, J. F. Valliant and A. Adronov, *Journal of the American Chemical Society*, 2009, **131**, 2906-2916.
66. M. Trollsås, J. L. Hedrick, D. Mecerreyes, P. Dubois, R. Jérôme, H. Ihre and A. Hult, *Macromolecules*, 1997, **30**, 8508-8511.
67. B. Atthoff, M. Trollsås, H. Claesson and J. L. Hedrick, *Macromolecular Chemistry and Physics*, 1999, **200**, 1333-1339.
68. M. Trollsås, H. Claesson, B. Atthoff, J. L. Hedrick, J. A. Pople and A. P. Gast, *Macromolecular Symposia*, 2000, **153**, 87-108.
69. M. Trollsås and J. L. Hedrick, *Journal of the American Chemical Society*, 1998, **120**, 4644-4651.
70. A. Heise, J. L. Hedrick, M. Trollsås, R. D. Miller and C. W. Frank, *Macromolecules*, 1998, **32**, 231-234.
71. A. Heise, J. L. Hedrick, C. W. Frank and R. D. Miller, *Journal of the American Chemical Society*, 1999, **121**, 8647-8648.
72. A. Heise, C. Nguyen, R. Malek, J. L. Hedrick, C. W. Frank and R. D. Miller, *Macromolecules*, 2000, **33**, 2346-2354.
73. D. E. Poree, M. D. Giles, L. B. Lawson, J. He and S. M. Grayson, *Biomacromolecules*, 2011, **12**, 898-906.
74. X. Hao, C. Nilsson, M. Jesberger, M. H. Stenzel, E. Malmström, T. P. Davis, E. Östmark and C. Barner-Kowollik, *Journal of Polymer Science Part A: Polymer Chemistry*, 2004, **42**, 5877-5890.
75. Y. Li, B. Zhang, J. N. Hoskins and S. M. Grayson, *Journal of Polymer Science Part A: Polymer Chemistry*, 2012, **50**, 1086-1101.
76. I. Gitsov, K. L. Wooley and J. M. J. Fréchet, *Angewandte Chemie International Edition in English*, 1992, **31**, 1200-1202.
77. I. Gitsov and J. M. J. Fréchet, *Macromolecules*, 1994, **27**, 7309-7315.
78. J. del Barrio, L. Oriol, R. Alcalá and C. Sánchez, *Macromolecules*, 2009, **42**, 5752-5760.
79. H. Altin, I. Kosif and R. Sanyal, *Macromolecules*, 2010, **43**, 3801-3808.
80. T. M. Chapman, G. L. Hillyer, E. J. Mahan and K. A. Shaffer, *Journal of the American Chemical Society*, 1994, **116**, 11195-11196.
81. R. Yin, Y. Zhu, D. A. Tomalia and H. Ibuki, *Journal of the American Chemical Society*, 1998, **120**, 2678-2679.

82. I. Gitsov, *Journal of Polymer Science Part A: Polymer Chemistry*, 2008, **46**, 5295-5314.
83. S.-H. Yim, J. Huh, C.-H. Ahn and T. G. Park, *Macromolecules*, 2006, **40**, 205-210.
84. I. Gitsov, P. T. Ivanova and J. M. J. Fréchet, *Macromolecular Rapid Communications*, 1994, **15**, 387-393.
85. K. Matyjaszewski, T. Shigemoto, J. M. J. Fréchet and M. Leduc, *Macromolecules*, 1996, **29**, 4167-4171.
86. M. R. Leduc, C. J. Hawker, J. Dao and J. M. J. Fréchet, *Journal of the American Chemical Society*, 1996, **118**, 11111-11118.
87. L. Zhu, X. Tong, M. Li and E. Wang, *Journal of Polymer Science Part A: Polymer Chemistry*, 2000, **38**, 4282-4288.
88. M. R. Leduc, W. Hayes and J. M. J. Fréchet, *Journal of Polymer Science Part A: Polymer Chemistry*, 1998, **36**, 1-10.
89. R. Vestberg, A. M. Piekarski, E. D. Pressly, K. Y. Van Berkel, M. Malkoch, J. Gerbac, N. Ueno and C. J. Hawker, *Journal of Polymer Science Part A: Polymer Chemistry*, 2009, **47**, 1237-1258.
90. C. J. Hawker and J. M. J. Fréchet, *Polymer*, 1992, **33**, 1507-1511.
91. A. Carlmark and E. E. Malmström, *Macromolecules*, 2004, **37**, 7491-7496.
92. M. Malkoch, A. Carlmark, A. Woldegiorgis, A. Hult and E. E. Malmström, *Macromolecules*, 2003, **37**, 322-329.
93. L. A. Connal, R. Vestberg, C. J. Hawker and G. G. Qiao, *Macromolecules*, 2007, **40**, 7855-7863.
94. E. R. Gillies and J. M. J. Fréchet, *Journal of the American Chemical Society*, 2002, **124**, 14137-14146.
95. F. L. Hatton, P. Chambon, T. O. McDonald, A. Owen and S. P. Rannard, *Chemical Science*, 2014, **5**, 1844-1853.
96. J. Bibette, F. L. Calderon and P. Poulin, *Reports on Progress in Physics*, 1999, **62**, 969.
97. T. Tadros, P. Izquierdo, J. Esquena and C. Solans, *Advances in Colloid and Interface Science*, 2004, **108–109**, 303-318.
98. J. I. Amalvy, G. F. Unali, Y. Li, S. Granger-Bevan, S. P. Armes, B. P. Binks, J. A. Rodrigues and C. P. Whitby, *Langmuir*, 2004, **20**, 4345-4354.
99. T. F. Tadros, in *Emulsion Formation and Stability*, Wiley-VCH Verlag GmbH & Co. KGaA, 2013, pp. 1-75.
100. R. T. Woodward, University of Liverpool, 2012.
101. R. M. D. Möbius, V.B. Fainerman, *Surfactants: Chemistry, Interfacial Properties, Applications*, Elsevier, 2001.
102. S. U. Pickering, *Journal of the Chemical Society, Transactions*, 1907, **91**, 2001-2021.
103. B. P. Binks and S. O. Lumsdon, *Langmuir*, 2001, **17**, 4540-4547.

104. B. P. Binks and S. O. Lumsdon, *Langmuir*, 2000, **16**, 8622-8631.
105. B. P. Binks and P. D. I. Fletcher, *Langmuir*, 2001, **17**, 4708-4710.
106. N. Glaser, D. J. Adams, A. Böker and G. Krausch, *Langmuir*, 2006, **22**, 5227-5229.
107. A. M. Mathur, B. Drescher, A. B. Scranton and J. Klier, *Nature*, 1998, **392**, 367-370.
108. S. Liu and S. P. Armes, *Current Opinion in Colloid & Interface Science*, 2001, **6**, 249-256.
109. V. Bütün, N. C. Billingham and S. P. Armes, *Journal of the American Chemical Society*, 1998, **120**, 11818-11819.
110. S. Liu, N. C. Billingham and S. P. Armes, *Angewandte Chemie International Edition*, 2001, **40**, 2328-2331.
111. K. B. Thurmond, T. Kowalewski and K. L. Wooley, *Journal of the American Chemical Society*, 1996, **118**, 7239-7240.
112. V. Bütün, N. C. Billingham and S. P. Armes, *Journal of the American Chemical Society*, 1998, **120**, 12135-12136.
113. V. Bütün, X. S. Wang, M. V. de Paz Báñez, K. L. Robinson, N. C. Billingham, S. P. Armes and Z. Tuzar, *Macromolecules*, 1999, **33**, 1-3.
114. S. Liu, J. V. M. Weaver, Y. Tang, N. C. Billingham, S. P. Armes and K. Tribe, *Macromolecules*, 2002, **35**, 6121-6131.
115. S. Fujii, Y. Cai, J. V. M. Weaver and S. P. Armes, *Journal of the American Chemical Society*, 2005, **127**, 7304-7305.
116. J. V. M. Weaver, S. P. Rannard and A. I. Cooper, *Angewandte Chemie International Edition*, 2009, **48**, 2131-2134.
117. J. V. M. Weaver, R. T. Williams, B. J. L. Royles, P. H. Findlay, A. I. Cooper and S. P. Rannard, *Soft Matter*, 2008, **4**, 985-992.
118. J. V. M. Weaver and D. J. Adams, *Soft Matter*, 2010, **6**, 2575-2582.
119. R. T. Woodward, R. A. Slater, S. Higgins, S. P. Rannard, A. I. Cooper, B. J. L. Royles, P. H. Findlay and J. V. M. Weaver, *Chemical Communications*, 2009, 3554-3556.
120. R. T. Woodward and J. V. M. Weaver, *Polymer Chemistry*, 2011, **2**, 403-410.
121. R. T. Woodward, L. Chen, D. J. Adams and J. V. M. Weaver, *Journal of Materials Chemistry*, 2010, **20**, 5228-5234.
122. K. Inoue, *Progress in Polymer Science*, 2000, **25**, 453-571.
123. G. R. Newkome, C. N. Moorefield, G. R. Baker, M. J. Saunders and S. H. Grossman, *Angewandte Chemie International Edition in English*, 1991, **30**, 1178-1180.
124. A.-M. Caminade, R. Laurent, B. Delavaux-Nicot and J.-P. Majoral, *New Journal of Chemistry*, 2012, **36**, 217-226.
125. K. L. Wooley, C. J. Hawker and J. M. J. Fréchet, *Journal of the Chemical Society, Perkin Transactions 1*, 1991, 1059-1076.

126. C. C. Lee, E. R. Gillies, M. E. Fox, S. J. Guillaudeu, J. M. J. Fréchet, E. E. Dy and F. C. Szoka, *Proceedings of the National Academy of Sciences*, 2006, **103**, 16649-16654.
127. I. Gitsov and J. M. J. Fréchet, *Macromolecules*, 1993, **26**, 6536-6546.
128. I. Gitsov, K. R. Lambrych, V. A. Remnant and R. Pracitto, *Journal of Polymer Science Part A: Polymer Chemistry*, 2000, **38**, 2711-2727.
129. E. Blasco, M. Piñol and L. Oriol, *Macromolecular Rapid Communications*, 2014, **35**, 1090-1115.
130. C. J. Hawker, K. L. Wooley and J. M. J. Fréchet, *Journal of the Chemical Society, Perkin Transactions 1*, 1993, 1287-1297.
131. Z. Zhang, G. Xu, F. Wang, S. Dong and Y. Chen, *Journal of Colloid and Interface Science*, 2005, **282**, 1-4.
132. J. Wang, F.-L. Hu, C.-Q. Li, J. Li and Y. Yang, *Separation and Purification Technology*, 2010, **73**, 349-354.

CHAPTER 2

Exploring amine and thiol Michael Addition

2.1 Introduction

Over the course of this thesis, the aim has been to develop a new synthetic methodology that can be used to prepare functional dendrons, dendrimers and linear dendritic hybrids (LDHs) – including a new macromolecular architecture known as Hyperbranched-Polydendrons (HPDs). The starting point in this research began by investigating amine Michael addition chemistries to assess the reaction's ability to synthesise functional macromolecules. Later in the chapter, thiol Michael addition chemistry is explored, whereby subsequent chapters will continue from these successful findings.

2.2 Amine Michael addition Chemistry

PAMAM (polyamidoamine) dendrimers, originally reported by Tomalia *et al.* in 1985,[1] are a class of dendrimers that are made divergently from an amine core molecule (see Chapter 1, section 1.2.1.2). The generations of the dendrimer are synthesised by repetitve exhaustive Michael additions using methyl acrylate, to the primary amine functionalitites of a chosen core. Subsequent amidation of the resulting ester functionality by large excesses of diamine regenerates the peripheral primary amine functionality for further exhaustive Michael addtions. The efficiency of this chemistry is demonstrated by the commerical synthesis of these macromolecules adopting this route.[2]

2.2.1 Synthesis and Characterisation of G_1 dendrimers by amine Michael addition chemistry

Amine Michael addition chemistry was evaluated using the monomers benzyl acrylate **[BA]** and 2-(dimethylamino)ethyl acrylate **[DMAEA]**, Figure 2.1, to investigate the efficiency of amine Michael addition chemistry. Analysis of the dendritic materials was performed using electrospray mass spectrometry (ESI-MS), proton (^{1}H) nuclear magnetic resonance (NMR), carbon (^{13}C) NMR and microanalysis. Triple detection size exclusion chromatography (SEC) was also used to confirm monodispersity, and significant changes to molecular weights in larger generation materials.

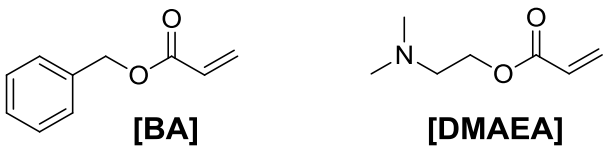

Figure 2.1 Acrylates used during amine Michael addition study; benzyl acrylate **[BA];[1]**, and 2-(dimethylamino)ethyl acrylate **[DMAEA];[2]**.

A triamine core molecule, tris(2-aminoethyl)amine **[TAEA]**, was used in model reactions to determine the efficiency of the exhaustive amine Michael addition and optimise reaction conditions including solvent type and concentration. The initial reaction conditions were adopted from the original PAMAM synthesis reports which utilised methanol as the reaction solvent and a molar ratio of 1.25:1 of acrylate monomer to each primary amine.[1] Under these conditions, the Michael addition of **[DMAEA]** to **[TAEA]**, yielding G_1 dendrimer [**Am_6-TAEA-G_1];[3]**, corresponded to 7.5:1 molar ratio of **[DMAEA]** to **[TAEA]**, Scheme 2.1.

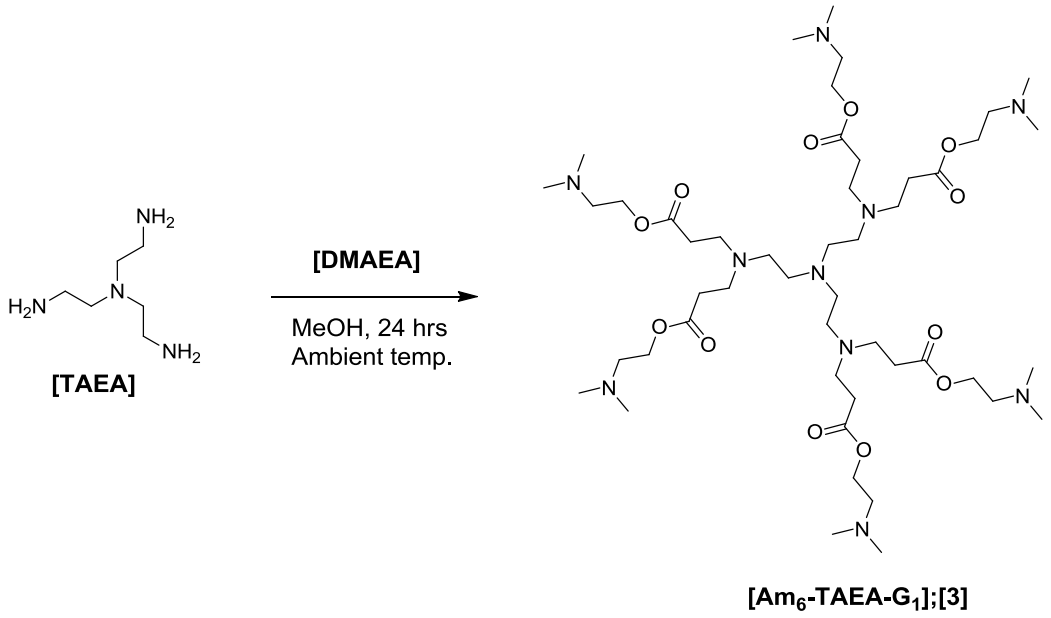

Scheme 2.1 Synthesis of G_1 dendrimer [**Am_6-TAEA-G_1];[3]**, using **[TAEA]** as a core, and the acrylate functional monomer **[DMAEA]**.

In the original synthesis of PAMAM dendrimers, non-ideal dendrimer growth, manifesting from intramolecular cyclisations occurred when the reaction conditions exceeded 50 °C.[2] Retro-Michael additions were also observed at reaction temperatures >80 °C. To avoid these side reactions, Michael

additions were performed at ambient temperature for 24 hours. Purification was achieved by removing both the solvent and excess **[DMAEA]** monomer using high vacuum.

After purification by removal of solvents, [**Am_6-TAEA-G_1];[3]** was characterised by ESI-MS. Analysis of the spectrum showed a series of adducts with molecular weights ranging from 662 Da to 1005 Da, Figure 2.2. The expected molecular weight of an exhaustively coupled dendrimer [**Am_6-TAEA-G_1];[3]** ($C_{48}H_{96}N_{10}O_{12}$) was 1004 Da (MH^+ = 1005 Da). An adduct of MH^+ = 1005 Da was present, confirming the ability to couple all six acrylates to the triamine, however, the presence of populations at 719 Da and 862 Da suggested partial Michael addition to **[TAEA]** of only four and five **[DMAEA]** acrylates respectively. The spectrum also showed a series of lower molecular weight species at 662 Da and 805 Da that could not be readily interpreted as partial Michael addition products.

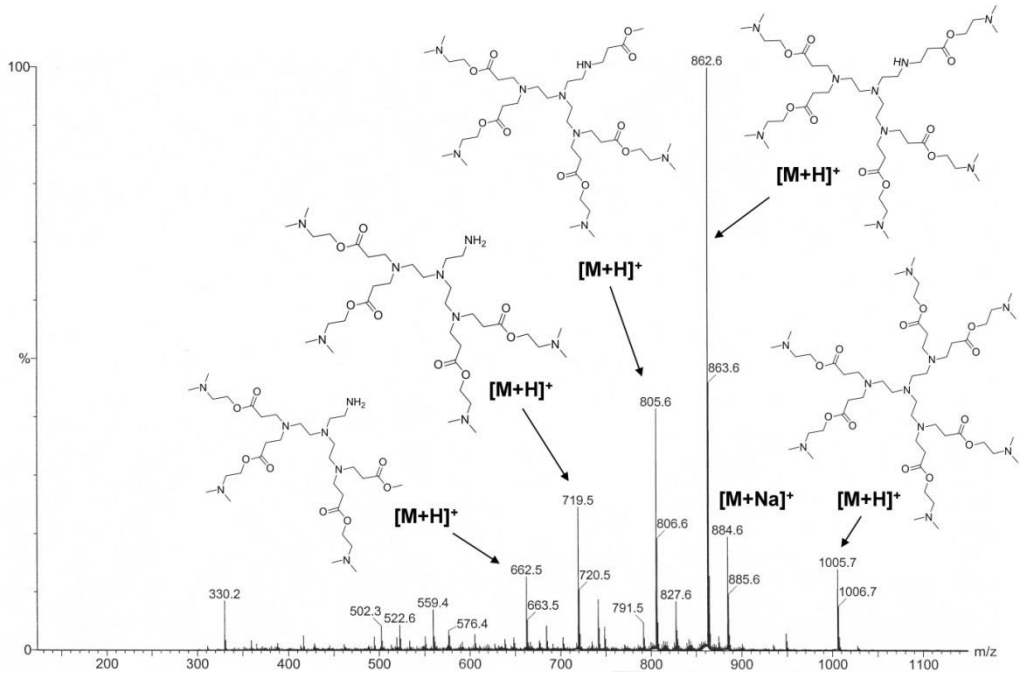

Figure 2.2 ESI-MS (MeOH) spectrum of G_1 **[DMAEA]** peripheral dendrimer [**Am_6-TAEA-G_1];[3]**

The adducts appeared to be caused by transesterification with the reaction solvent (methanol) as the systematic decrease in 56 Da corresponded to the replacement of the dimethyl amino ethanol of **[DMAEA]** with a methoxide unit, forming the corresponding methyl ester functionality, Scheme

2.2.Self-catalysed transesterification of tertiary amines with methanol at room temperature has been previously reported.[3]

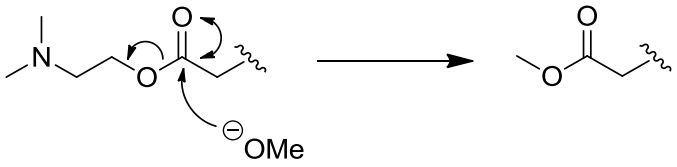

Scheme 2.2 Proposed mechanism of transesterification of **[DMAEA]** resisdues by the methoxide nucleophile generated in methanol.

It was identified that every incremental loss of 56 Da corresponded to a transesterification with methanol present in the sample. To overcome the observed partial Michael additions, the molar ratio of **[DMAEA]** to **[TAEA]** was increased to 9:1, and, to avoid transesterification species, methanol was replaced with propan-2-ol (IPA) due to its increased steric hindrance and reduced acidity (p*K*a IPA = 16.5; p*K*a methanol = 15). The reaction was repeated under these revised conditions, but analysis of [**Am_6-TAEA-G_1];[3]** using ESI-MS still resulted in several populations corresponding to partial Michael additions and transesterification products, Figure S2.1.

To determine if the optimised conditions resulted in similar effects using a different monomer, a Michael addition reaction was performed with **[BA]** to result in a benzyl (Bz) ester terminated G_1 dendrimer, [**Bz_6-TAEA-G_1];[4]**, Scheme 2.3. A 9:1 molar ratio of **[DMAEA]** to **[TAEA]** was employed in IPA under ambient temperature conditions. After reaction for 24 hours, the Bz ester functional dendrimer [**Bz_6-TAEA-G_1];[4]** was purified by high vacuum to remove the IPA and excess **[BA]** monomer. Analysis by ESI-MS showed a single population at 1119 Da (MH^+ = 1119 Da), confirming the pure exhaustive Michael adduct [**Bz_6-TAEA-G_1];[4]**, Figure 2.3. ^{1}H and ^{13}C NMR confirmed the expected number of proton and carbon environments, Figures S2.2 and S2.3.

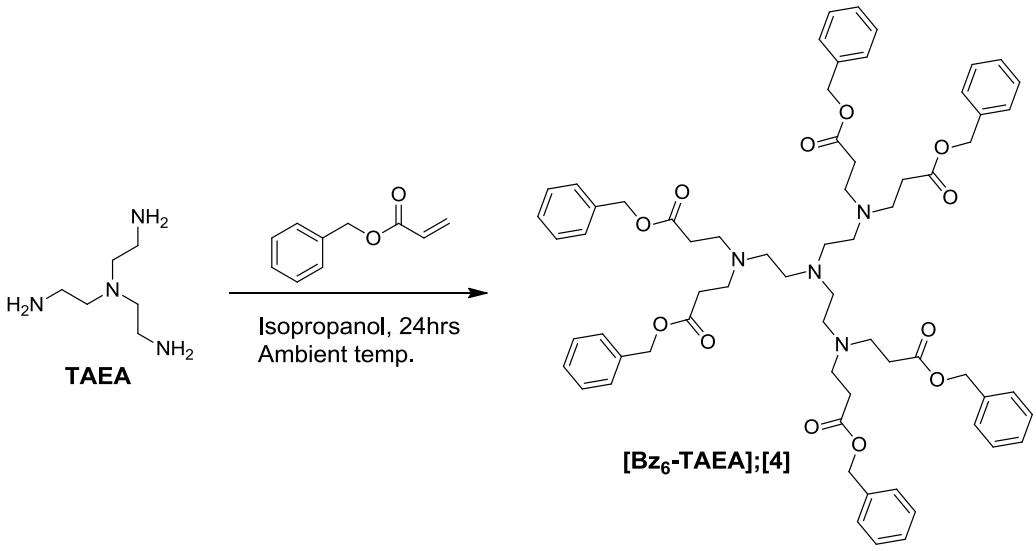

Scheme 2.3 Synthesis of G_1 dendrimer [**Bz_6-TAEA-G_1];[4]**, using **[TAEA]** and **[BA]**

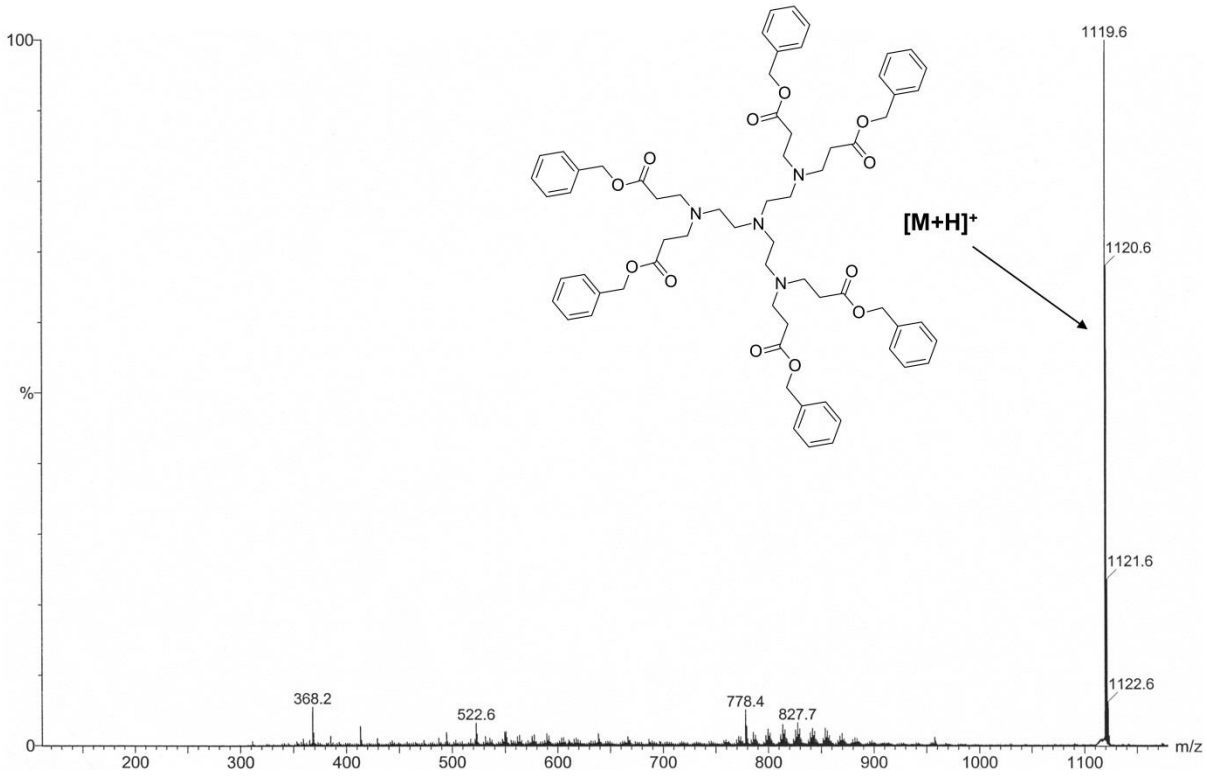

Figure 2.3 ESI-MS (MeOH) spectrum of Bz peripheral G_1 dendrimer [**Bz_6-TAEA-G_1];[4]**

It was suggested that the mixture of populations observed in the ESI-MS spectrum for [**Am_6-TAEA-G_1];[3]** could be occurring during preparation of the sample and potentially during ionisation in the mass spectrometer, particularly since analysis by ESI-MS requires MeOH to be used as the sample solvent (i.e. transesterification). At first, analysis of [**Am_6-TAEA-G_1];[3]** by ^{1}H NMR spectroscopy confirmed a series of resonances between 2.29 and 4.17 ppm, which integrated as expected; see Figure 4.20 (a) – expanded region; Figure 4.20 (b) – complete spectrum. However, further analysis of [**Am_6-TAEA-G_1];[3]** by ^{13}C NMR spectroscopy, Figure 4.21, unfortunately confirmed additional environments at 34.8, 45.3, 47.6, 52.2 and 54.8 ppm, in addition to those expected. This spectroscopic data concluded that **[Am_6-TAEA-G_1];[3]** was not pure.

2.2.2 Synthesis and Characterisation of G_1 dendrons by amine Michael addition chemistry

Of the commercially available amino alcohols, isopropanolamine **[IPLA]** was chosen to synthesise two functional G_1 dendrons using the amine Michael addition of **[BA]** and **[DMAEA]** by the reactions conditions optimised for the synthesis of functional dendrimers [**Am_6-TAEA-G_1];[3]** and [**Bz_6-TAEA-G_1];[4]**. Functional dendrons [**Bz_2-IPLA-G_1];[5]** and [**Am_2-IPLA-G_1];[6]** were prepared by exploiting the simplicity of this amine Michael addition chemistry, Scheme 2.4.

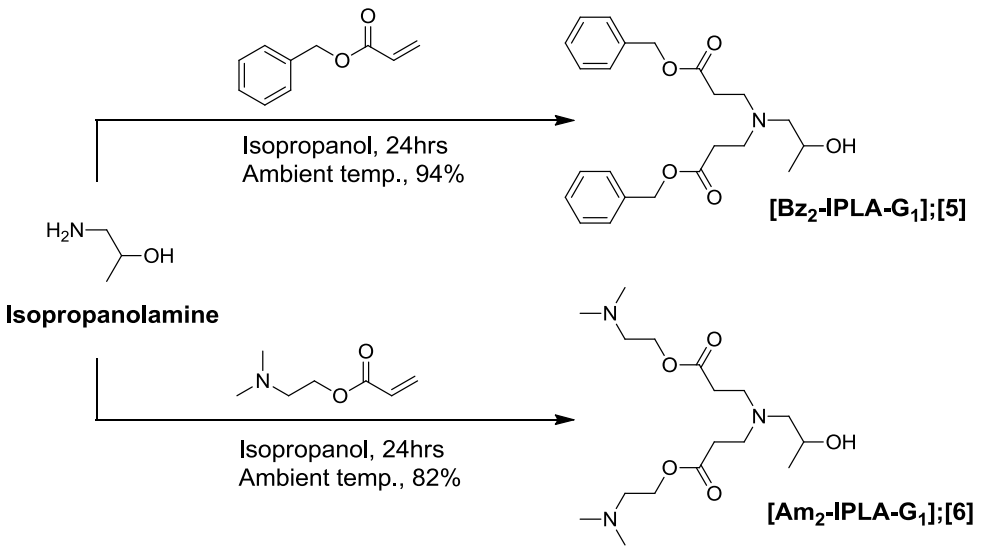

Scheme 2.4 Synthesis of G_1 functional dendrons [**Bz_2-IPLA-G_1];[5]** and [**Am_2-IPLA-G_1];[6]** using amine Michael addition chemistry

The synthesis of **[5]** resulted through using a molar ratio of 1:3 of **[IPLA]** to **[BA]** stirring in IPA for 24 hours at ambient temperature. The excess acrylate monomer and IPA were both removed under high vacuum, resulting in the Bz functional dendron [**5]** obtained in 94% yield as a pale yellow oil. Figure 2.4 illustrates the ^{1}H NMR spectrum for dendron **[5]**.

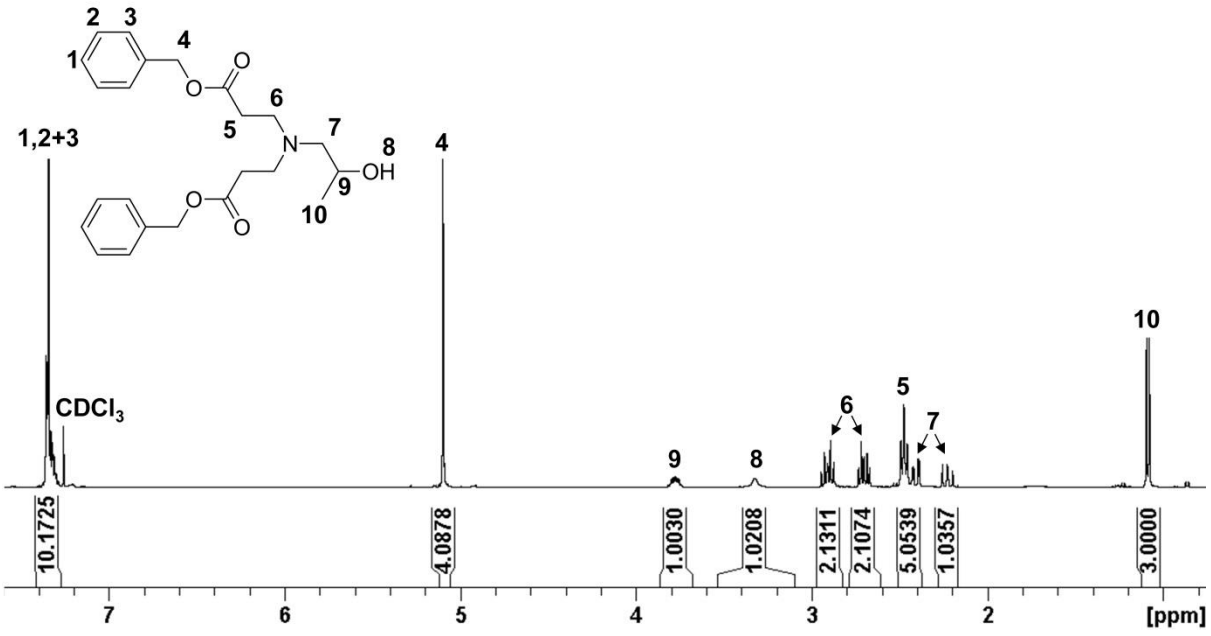

Figure 2.4 ^{1}H NMR spectrum (400 MHz, $CDCl_3$) of Bz functional dendron [**Bz_2-IPLA-G_1];[5]**

The ^{1}H NMR spectrum of dendron [**5]** was relatively straightforward to assign, with the integration of the peripheral Bz groups and branching groups being in the expected ratios. For example, calibration of the doublet at 1.10 ppm to 3 protons, resulted in an integral of 4 protons for the singlet at 5.10 ppm, Figure 2.4. Analysis of the ^{13}C NMR spectrum of [**5**] Figure 2.5, confirmed 11 total carbon environments, including a singlet ester carbonyl environment at 172 ppm. Confirmation by ESI-MS confirmed populations at 400 Da (MH^+ = 400 Da) and 422 Da (MNa^+ = 422 Da), Figure S2.6.

The tertiary amine terminated dendron [**6]** was prepared by the exact same procedure but using **[DMAEA]**, and resulted in a slightly lower yield of 82% as a yellow oil. Confirmation of the resulting dendron [**6**] was achieved using ^{1}H and ^{13}C NMR spectroscopy, confirming the correct number integrations and environments, Figures S2.7 and S2.8. ESI-MS of **[6]** confirmed two populations at

362 Da (MH^+ = 362 Da) and 384 Da (MNa^+ = 384 Da), Figure S2.9, but also indicated populations corresponding to trans-esterification products. Once again, this is believed to be occurring during analysis as no evidence was found within the NMR spectroscopy analysis.

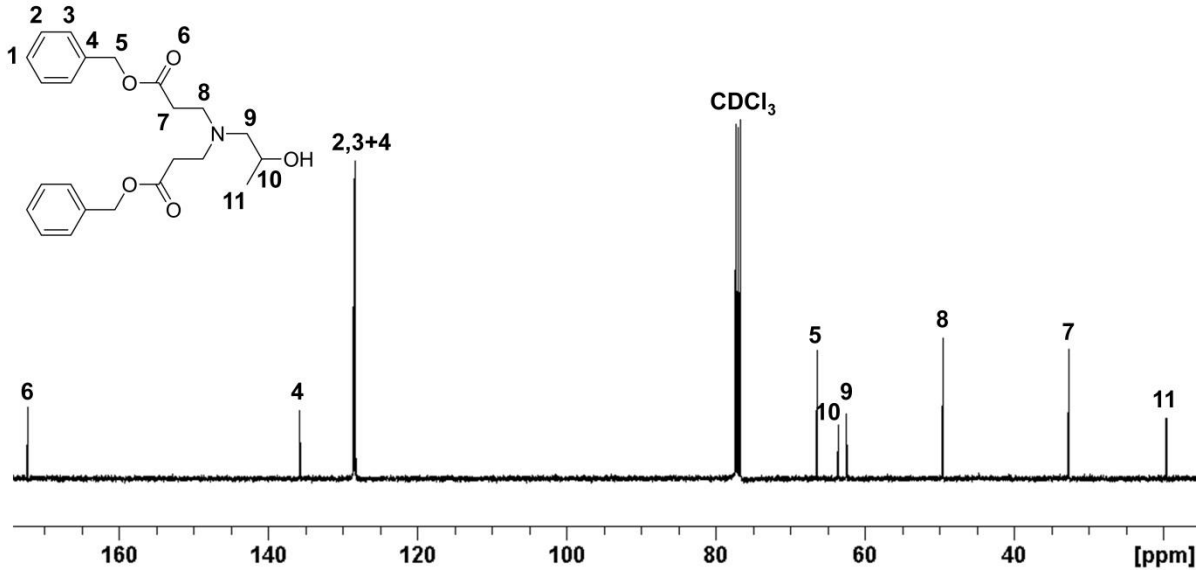

Figure 2.5 ^{13}C NMR spectrum (100 MHz, $CDCl_3$) of Bz functional dendron [**Bz_2-IPLA-G_1];[5]**

The experiments concluded that the amine Michael addition chemistry was highly efficient to synthesise G_1 materials in a single step, with typical yields exceeding 82%, without any further purification other than removal of excess reagents by vacuum. In continuing to evaluate this chemistry, a synthetic route to deriving the G_2 dendrons was sought.

2.2.3 G_2 dendritic materials

Additional dendron generation synthesis required a branching chemistry with increased functionality; hence the construction of an AB_2 branching unit resulting in two outer peripheral primary amines was attempted.

Rannard and Davis found that when an imidazole carboxylic ester, formed from the reaction of 1,1'-carbonyldiimidazole (CDI) and either a secondary or tertiary alcohol, is reacted in the presence of primary and secondary amines, it will exclusively react at the primary amine sites.[4] No reaction

occurs at the secondary amine functional groups allowing the avoidance of protection/deprotection chemistry. This is highlighted in Scheme 2.5.

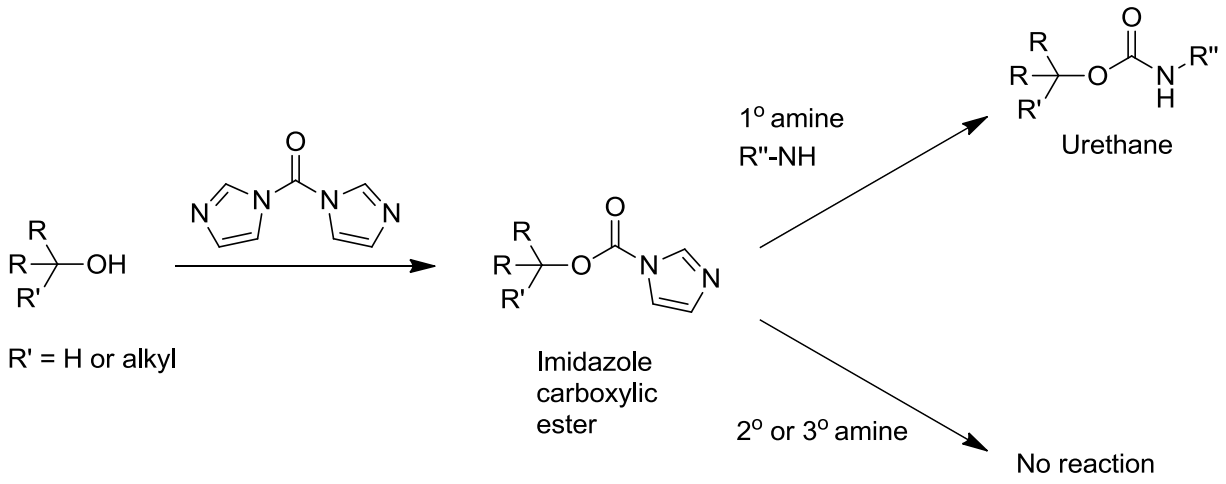

Scheme 2.5 Selective synthesis of urethanes using prepared using imidazole carboxylic esters

Using this selective methodology, an imidazole carboxylic ester intermediate was used to construct the novel AB_2 branching unit, 1-[N, N-bis (2-aminopropyl)-amino]-2-propanol **[APAP]**.

2.2.3.1 Synthesis and characterisation of 1-[N, N-bis(2-aminopropyl)-amino]-2-propanol; [APAP]

The synthesis of [**APAP]** was achieved in four synthetic steps, Scheme 2.6. In the first step, *tert*-butyl alcohol, **[7]**, was reacted in a two-fold excess with CDI at 60 °C in dry toluene under a positive flow of nitrogen for 4 hours, resulting in the selective formation of the imidazole carboxylic ester [**8**]. An excess of **[7]** was used to ensure the complete consumption of CDI, since any residual CDI present may have led to further side reactions on the triamine added in the next step. After a dropwise addition of bis(3-aminopropyl)amine **[BAPA]** to the solution, the resulting pale yellow solution was left stirring for 18 hours at 60 °C. The reaction was followed by the disappearance of the UV active molecule [**8**] using thin layer chromatography (TLC). Purification was achieved by cooling the solution to remove the imidazole byproduct formed (imidazole is soluble in toluene when warm, but

not when cool), removing the toluene, diluting the crude sample with CH_2Cl_2, washing the organic phase three times with water, drying over $MgSO_4$, and after removal of CH_2Cl_2 the pure G_1 dendron **[^{t}BOC$_2$-BAPA-G$_1$];[9]** was recovered as a white solid in 95% yield.

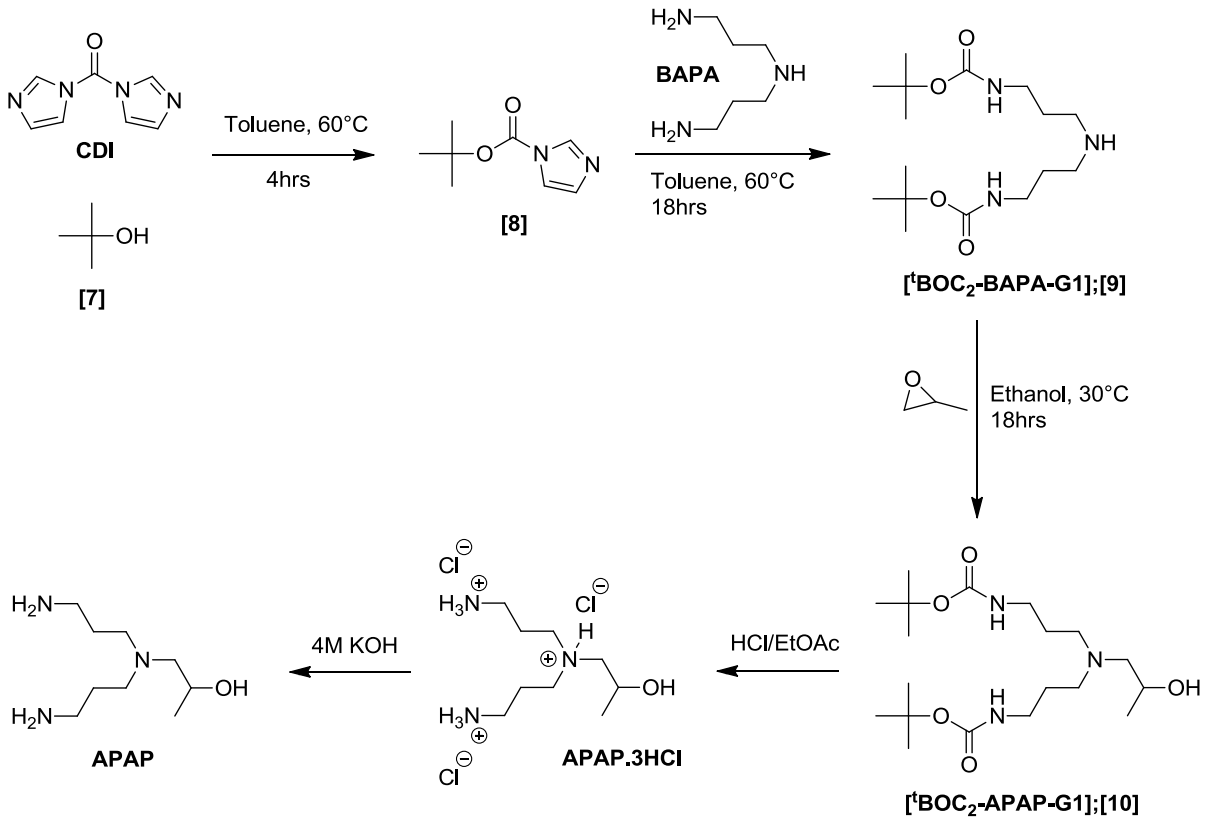

Scheme 2.6 Selective synthesis of **1-[N, N-bis (2-aminopropyl)-amino]-2-propanol;[APAP]**

ESI-MS analysis showed a single population at 332 Da (MH^+ = 332), Figure S2.10, and ^1H and ^{13}C NMR spectroscopy confirmed no trace of reaction at the secondary amine site, Figure 2.6 and Figure S2.11.

The second synthetic step utilised the ring opening of propylene oxide (PO) to functionalise the focal point of **[^{t}BOC$_2$-BAPA-G$_1$];[9]**. The ring opening of PO was used, as its conditions are mild and similar reactions have resulted in high yields.[5] PO is also low boiling (bpt: 34 °C), and when used in excess, can be removed under high vacuum. The ring opening of PO by the secondary amine functionality at the focal point of dendron **[^{t}BOC$_2$-BAPA-G$_1$];[9]** was achieved by the slow addition of a three-fold molar excess of PO to a stirring solution of [**9]** in anhydrous ethanol.

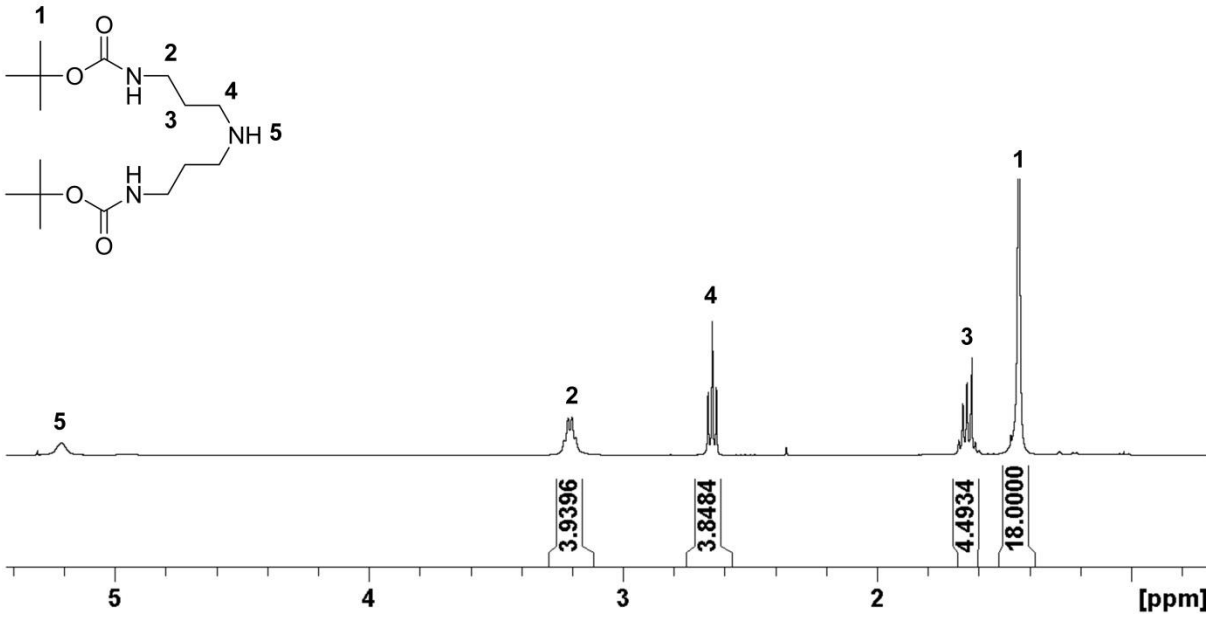

Figure 2.6 ^{1}H NMR spectrum (400 MHz, $CDCl_3$) of **[^{t}BOC$_2$-BAPA-G$_1$];[9]**

The reaction was left for 18 hours and was followed using TLC (80:20, EtOAc:MeOH). Since neither the starting material nor the product were UV active, potassium permanganate was used as a TLC stain. After purification by liquid chromatography (silica, eluting EtOAc:MeOH, 80:20) the hydroxyl-functional dendron **[^{t}BOC$_2$-APAP-G$_1$];[10]** resulted as a pale yellow solid in 85%. Analysis using ESI-MS, confirmed the presence of populations at 390 Da (MH^+ = 390 Da) and 412 Da (MNa^+ = 412 Da), Figure 2.7. ^{1}H and ^{13}C NMR spectroscopy also indicated the correct number of integrations and environments, Figures S2.12 and S2.13.

The third step of brancher synthesis involved the removal of the N-*tert*-butoxycarbonyl (^{t}BOC) protecting groups of [**10]** using concentrated hydrochloric acid in ethyl acetate to result in the tris-hydrochloride salt [**APAP.3HCl]**. The reaction was left until the evolution of CO_2 ceased, and was also monitored by using ^{1}H NMR (D_2O) until the singlet at approximately 1.50 ppm corresponding to the *t*-butyl groups, disappeared. After six hours of stirring at ambient temperature only partial deprotection resulted, and only after heating the solution at 50 °C for an additional 3 hours was the reaction driven to completion.

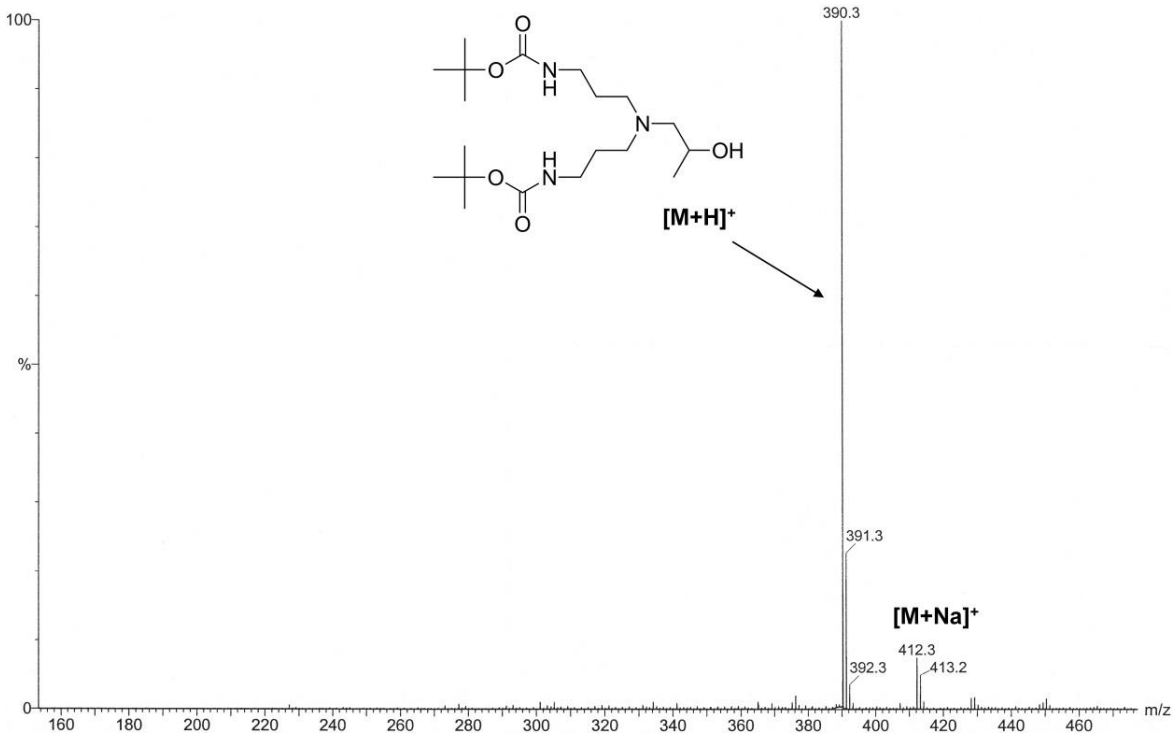

Figure 2.7 ESI-MS (MeOH) spectrum of **[^{t}BOC$_2$-APAP-G$_1$];[10]**

In the final step, the resulting tris-hydrochloride salt [**APAP.3HCl]** was converted to the free amine AB_2 branching unit [**APAP]**. The synthesis of similar molecules have used ion exchange beads to transform the salt to the free amine, but have required vacuum distillation to obtain a pure product.[5] After attempting to use ion exchange beads, which resulted in low yields (<20%), a strong base, 4M sodium hydroxide (NaOH) was used instead to deprotonate the salt counter ions. It was optimum to add a 4M NaOH aqueous solution carefully (since its exothermic) to a neat solution of [**APAP.3HCl]**, and reduce the mixture to half its volume on the rotary evaporator. In doing so, this liberated the amine product [**APAP]**, which collected on the surface of the crude solution. Extraction of the oil from the mixture using $CHCl_3$ resulted in [**APAP]** as a pure pale yellow oil in 94% yield. Characterisation of the product was obtained by ^{1}H and ^{13}C NMR, Figures S2.14 and S2.15, and chemical ionisation mass spectrometry (CI-MS), Figure 2.8. A single peak in the CI-MS spectrum confirmed the molecular ion at 190.3 Da (MH^+ = 190.3 Da).

Assignments made to the 1D ^{1}H NMR of [**APAP]** showed several relatively complicated splitting patterns, since many of the protons had similar environments, Figure S2.14. Furthermore, the

presence of a chiral centre formed from the ring opening of PO, led to multiple splitting patterns at the protons adjacent to the chiral centre, and hence some uncertainly over absolute assignments. A 2D ^{1}H-^{1}H correlation spectroscopy (COSY) experiment was therefore performed to help ensure the correct assignments were identified, Figure 2.9.

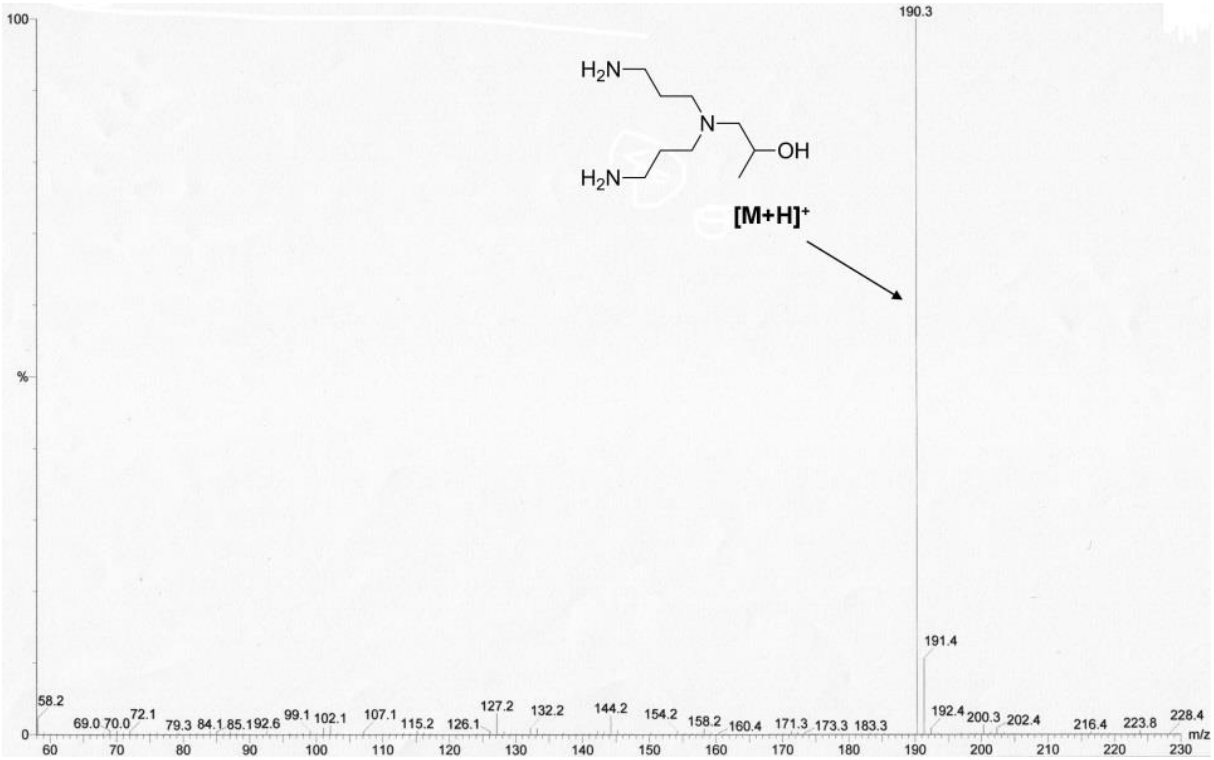

Figure 2.8 CI-MS spectrum (MeOH) of [**APAP]**

The two protons located at 2.30 ppm resonating as a doublet of doublets, were assigned correctly as environment 4, Figure 2.9, since they had a correlation with the singlet proton resonating as a multiplet at 3.78 ppm (labelled as environment 5). Similar correlational analysis was performed for environments 3, 2, 1 and 7, Figure 2.9.

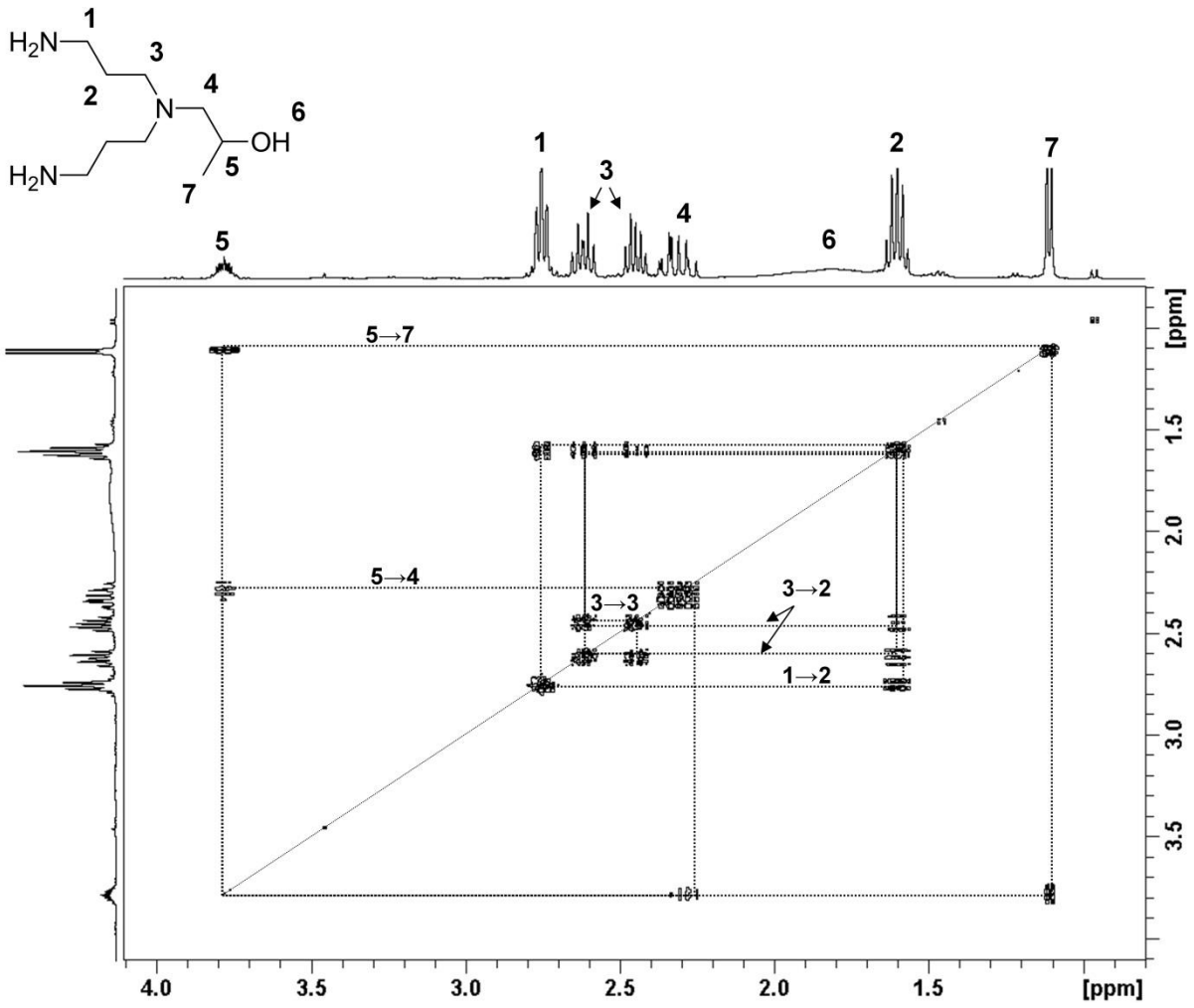

Figure 2.9 2D ^{1}H-^{1}H COSY spectrum ($CDCl_3$, 400 MHz) of **[APAP].**

2.2.3.2 Synthesis and characterisation of G_2 dendrons by amine Michael addition chemistry

Amine Michael additions used to synthesise G_2 dendrons were performed under the same conditions as the G_1dendrons, employing IPA as the reaction solvent, Scheme 2.7.

Michael additions with [**APAP]** using both **[BA]** and **[DMAEA]** yielded dendrons **[Bz_4-APAP-G_2];[11]** and **[Am_4-APAP-G_2];[12]**, and led to yields of 87% and 89% respectively, after purification by high vacuum. A single population at 838 Da (MH^+ = 838 Da) by ESI-MS was confirmed for [**11**],

Figure S2.16, and populations at 762 Da (MH^+ = 760 Da) and 784 Da (MNa^+ = 784 Da) were confirmed by ESI-MS for **[Am$_4$-APAP-G$_2$];[12]**, Figure S2.17.

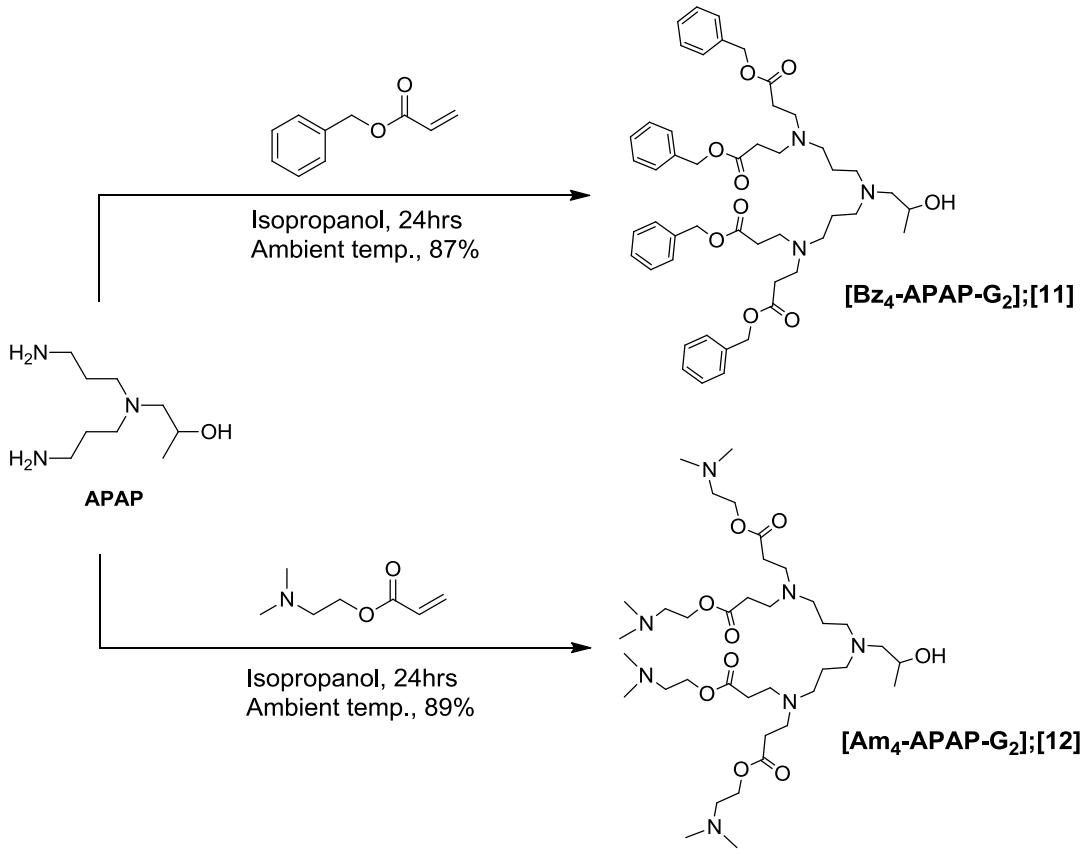

Scheme 2.7 Synthesis of G_2 functional dendrons **[Bz$_4$-APAP-G$_2$];[11]** and **[Am$_4$-APAP-G$_2$];[12]** using amine Michael addition chemistry with [**APAP]**

Analysis of each ^{1}H and ^{13}C NMR spectrum for [**11**] and [**12**] indicated the correct number of proton and carbon environments, Figures S2.18-S2.21. Further characterisation by SEC also indicated no traces of partially substituted species in either chromatogram of **[11]** or **[12]**. Molecular weights obtained by SEC were also compared to those obtained by ESI-MS, Table 2.1. Dispersities (*Đ)* for dendrons **[11]** and **[12]** were >1.0, suggesting some evidence of column interaction, leading to chromatogram broadening.

Table 2.1 SEC characterisation data of G_2 dendrons **[Bz_4-APAP-G_2];[11]** and **[Am_4-APAP-G_2];[12]**

Dendron; Entry #	ESI-MS [MH^+]		SEC (THF)		
	$M_{calc.}$ (Da)	$M_{obs.}$ (Da)	M_n (Da)	M_w (Da)	$Đ$
[Bz_4-APAP-G_2];[11]	837.5	838.5	737	843	1.14
[Am_4-APAP-G_2];[12]	761.6	762.6	471	639	1.36

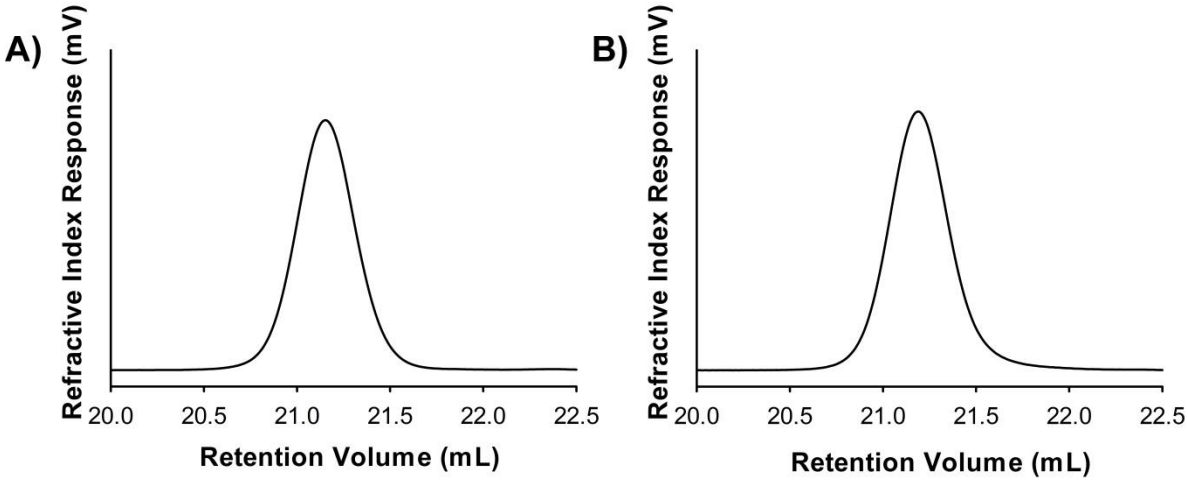

Figure 2.10 SEC chromatogram **[Bz_4-APAP-G_2];[11]** (A) and **[Am_4-APAP-G_2];[12]** (B)

2.2.4 G_3 dendritic materials

2.2.4.1 Synthesis and characterisation of [$APAP_3$-G_2];[16]

The synthesis of the G_3 dendrons was immediately more challenging since the construction of an AB_4 branching unit was required. The AB_4 branching unit, **[$APAP_3$-G_2];[16]**, Scheme 2.8, was constructed utilising the previously synthesised dendron **[^{t}BOC_2-APAP-G_1];[10]**. In the first step, the secondary hydroxyl group at the focal point of [**10]** was converted to the corresponding imidazole carboxylic ester by reaction with CDI in a 1:1 ratio for 4 hours. The reaction mixture was analysed using TLC to confirm complete conversion of the dendron [**10]** to the intermediate [**13]**.

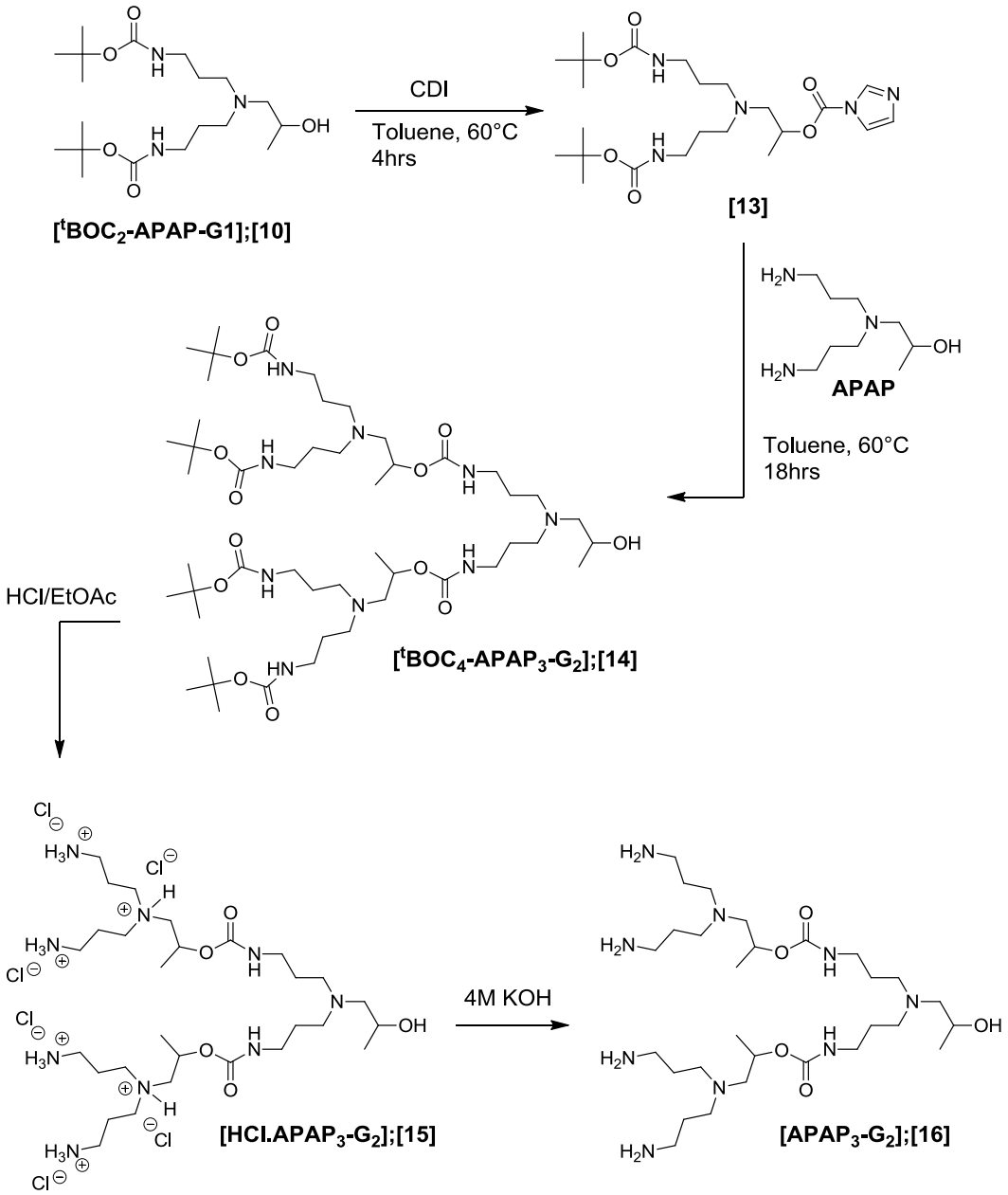

Scheme 2.8 Selective synthesis of AB_4 branching unit, **[$APAP_3$-G_2];[16]**

After complete conversion, the branching unit [**APAP]** was added and left stirring at 60 °C for 18 hours. TLC confirmed the disappearance of [**13]** after 18 hours, and the mixture was cooled, concentrated *in vacuo*, and the resulting crude product dissolved in CH_2Cl_2. Purification by washing the organic phase three times with distilled water, drying over $MgSO_4$ and removal of CH_2Cl_2 yielded **[^{t}BOC$_4$-$APAP_3$-G_2];[14]** as a crystalline glass in 78% yield. ESI-MS of [**14]**, confirmed three

populations at 1020 Da (MH^+ = 1020), 1042 Da (MNa^+ = 1042 Da) and 1058 Da (MK^+ = 1058 Da), Figure 2.11.

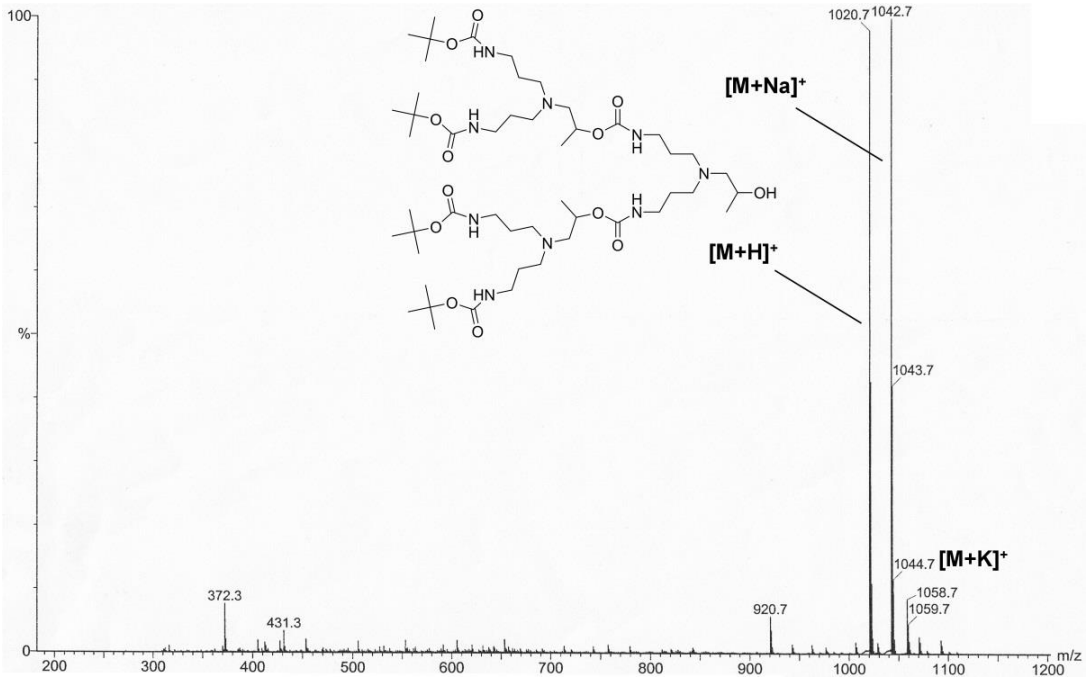

Figure 2.11 ESI-MS (MeOH) spectrum of **[^{t}BOC$_4$-APAP$_3$-G$_2$];[14]**

A species at 920 Da was identified, corresponding to the removal of 100 Da from the molecular weight of the **[14]**, resulting from the loss of one ^{t}BOC group. ^{t}BOC groups are relatively labile groups that have shown before to easily fragment under high energy conditions, such of that of ESI-MS.[6] Figure 2.12 shows the ^{1}H NMR spectrum for **[^{t}BOC$_4$-APAP$_3$-G$_2$];[14]** with the resulting spectrum fairly broad, presumably due to a hydrogen bonding effect causing reduced mobility of the macromolecule. A clear feature of the spectrum was the presence of the two broad peaks at approximately 1.1 ppm and 1.2 ppm. Relative to the peripheral *t*-butyl resonances at approximately 1.4 ppm, these broad peaks integrated in a 2:1 ratio, corresponding to the methyl environments, 6 and 12. Additional evidence of symmetrical coupling was also identified by the single hydrogen resonances 7 and 13 at both chiral centers, also integrating in a 2:1 ratio. The ^{13}C NMR spectrum of **[^{t}BOC$_4$-APAP$_3$-G$_2$];[14]** was very difficult to assign, but two urethane carbonyl resonances, at 156.2 ppm and 156.8 ppm were identified, Figure S2.22.

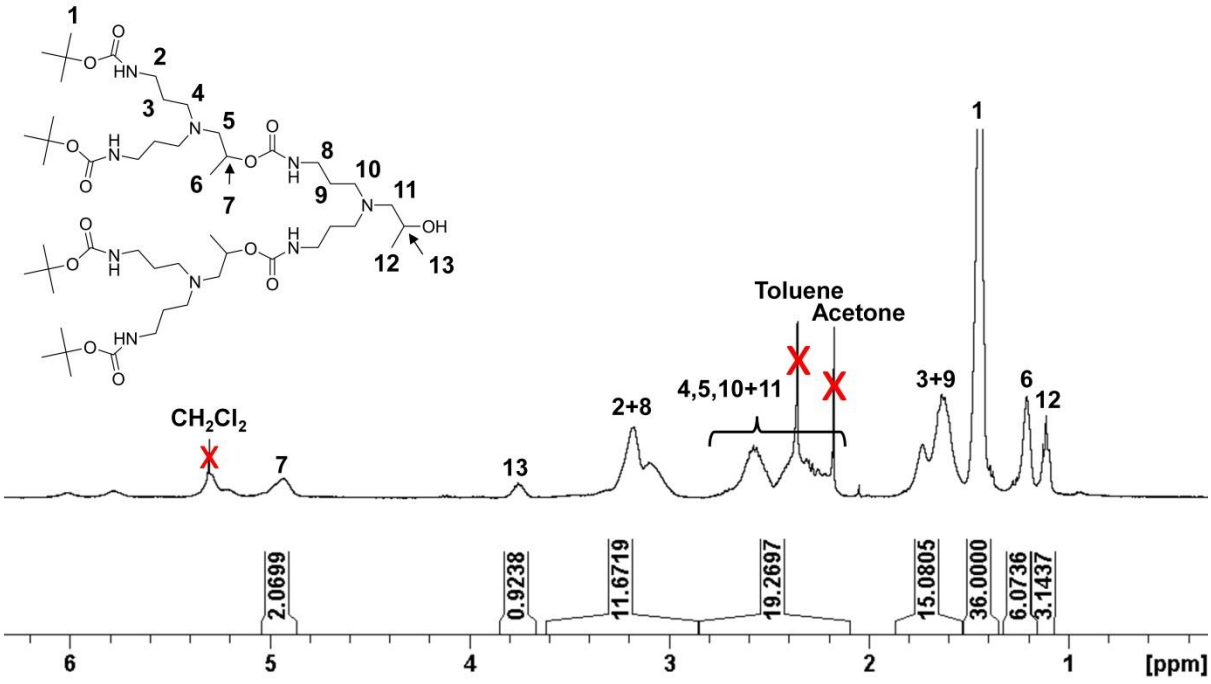

Figure 2.12 ^{1}H NMR spectrum (400 MHz, $CDCl_3$) of **[^{t}BOC$_4$-APAP$_3$-G$_2$];[14]**

The second step involved the removal of the N-tert-butoxycarbonyl (t-BOC) protecting groups of [**14]** using concentrated HCl in ethyl acetate, which followed a similar procedure to that used for the final step in the preparation of [**APAP]**. Heating at 50 °C for 3 hours fully removed the t-BOC groups, observed by the disappearance of the large singlet at 1.4 ppm by ^{1}H NMR analysis, resulting in **[HCl.APAP$_3$-G$_2$];[15]**. The final step used NaOH to deprotonate the hydrochloride salts of **[15]**, which after extraction of the resulting oil into $CHCl_3$, and removal of solvents *in vacuo*, yielded **[APAP$_3$-G$_2$];**[**16]** as very viscous yellow oil that turned orange over time in 86% yield. **[16]** was kept under N_2 to prevent the peripheral amines from reacting with CO_2 in the atmosphere.

Confirmation by ESI-MS confirmed the protonated and sodium adducts of **[APAP$_3$-G$_2$];**[**16]** observed at 620 Da (MH^+ = 620 Da) and 642 (MNa^+ = 642 Da), Figure 2.13. Assignments by ^{1}H NMR were made using a 2D ^{1}H-^{1}H COSY experiment, Figure 2.14. Peaks labelled as 6 and 12, related to the single protons at both chiral centres, and correlated as expected with peaks 5 and 11, the adjacent methyl groups. Further backbone peaks, such as the CH_2 adjacent the urethane carbonyl, labelled environment 7 were also assigned by identifying their neighbouring environments.

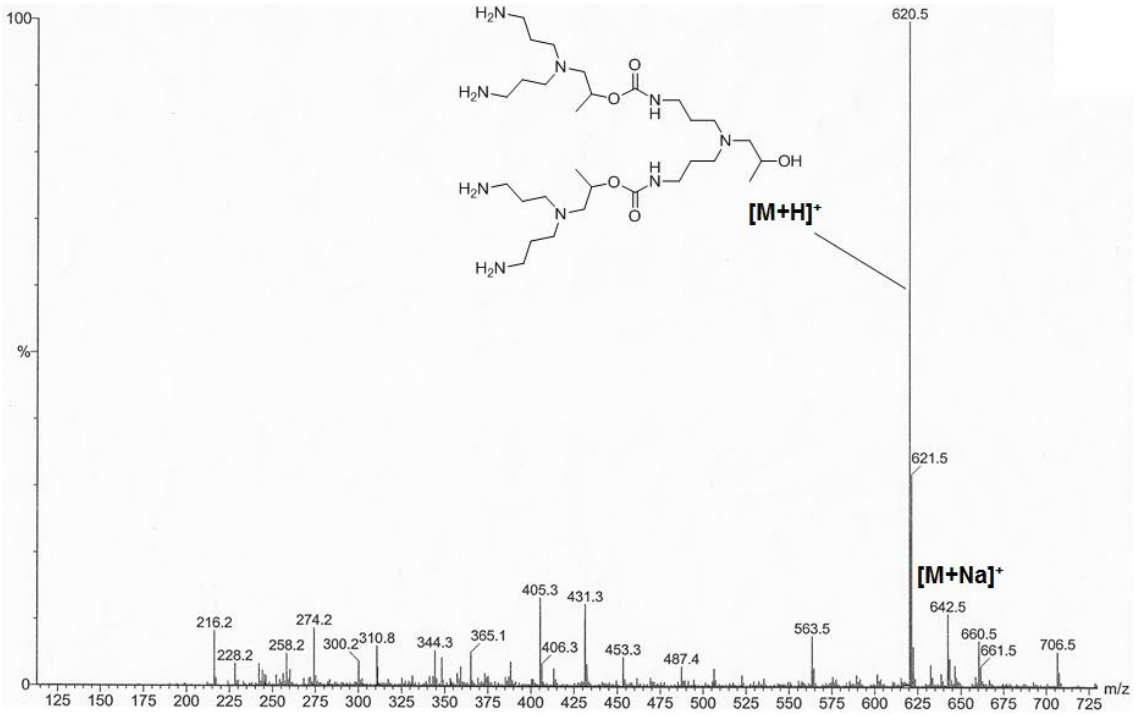

Figure 2.13 ESI-MS (MeOH) spectrum of **[APAP$_3$-G$_2$];[16]**

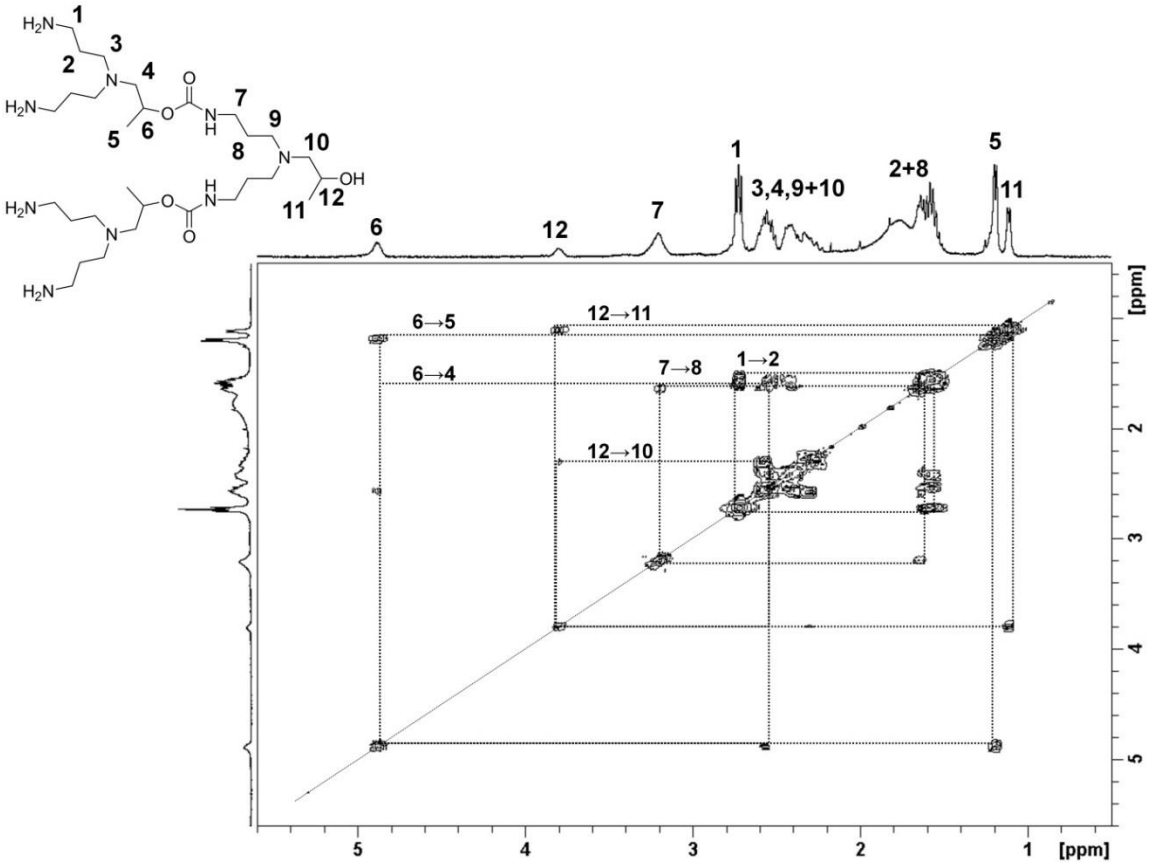

Figure 2.14 2D ^{1}H-^{1}H COSY ($CDCl_3$, 400 MHz) spectrum of **[APAP$_3$-G$_2$];[16]**

The ^{13}C NMR spectrum of **[APAP$_3$-G$_2$];[16]** was extremely difficult to interpret, even at very high concentrations (50 mg/mL), again presumably due to hydrogen bonding effects.

2.2.4.2 Synthesis and characterisation of G$_3$ dendrons by amine Michael addition chemistry

The synthesis of the G_3 dendrons **[Bz$_8$-APAP$_3$-G$_3$];[17]** and **[Am$_8$-APAP$_3$-G$_3$];[18]** were attempted using the AB_4 branching unit **[APAP$_3$-G$_2$];[16]** Scheme 2.9.

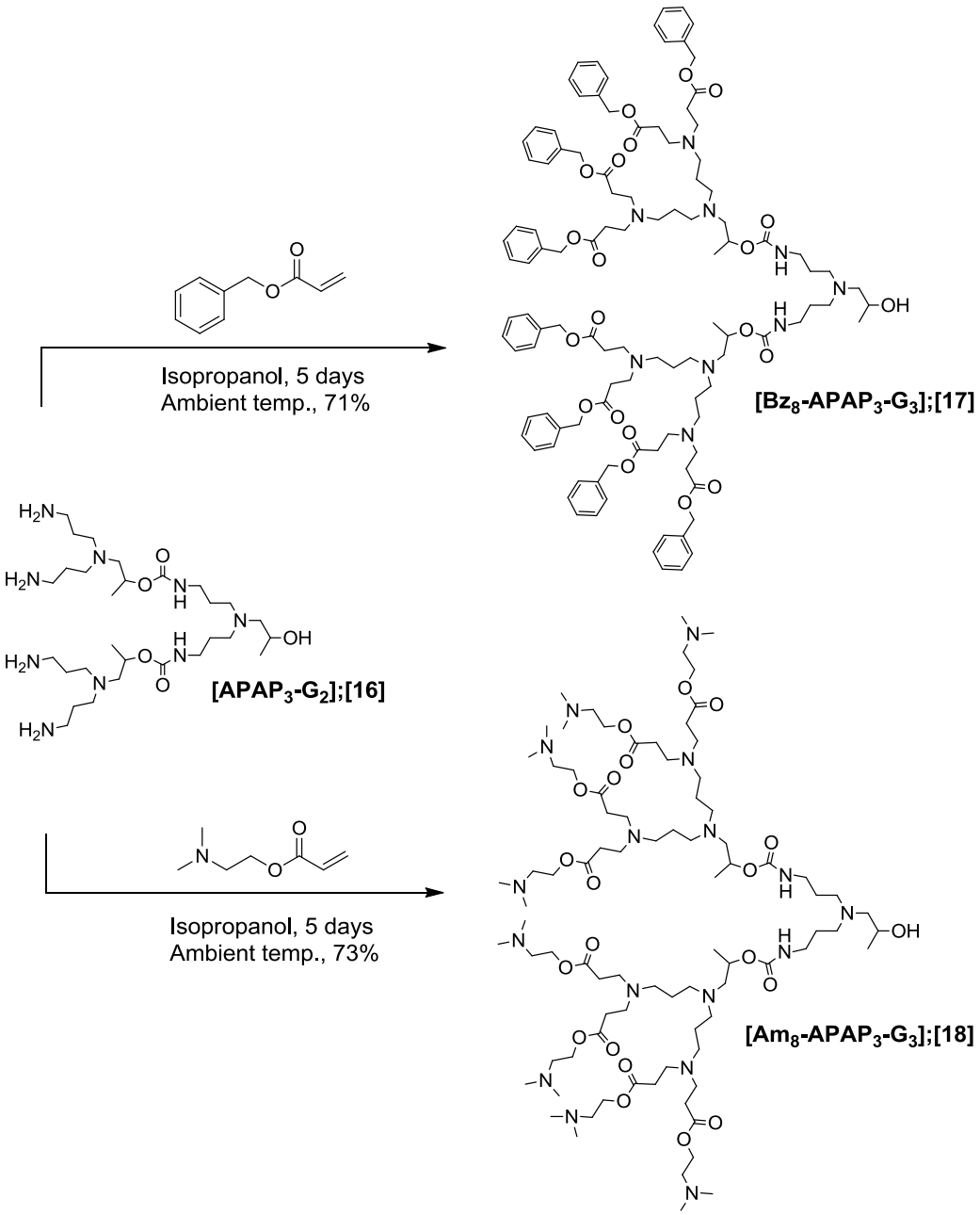

Scheme 2.9 Synthesis of G_3 dendrons **[Bz$_8$-APAP$_3$-G$_3$];[17]** and **[Am$_8$-APAP$_3$-G$_3$];[18]**

Temperature and solvent conditions were kept as previous amine Michael addition, but the molar ratio of acrylate to primary amine excess was increased from 1.5 to 2.5, to help drive the reactions to completion. The reactions were also left to react for 5 days, rather than the 24 hours, as previously. Following removal of IPA and excess acrylates by high vacuum, G_3 dendron **[Bz_8-APAP$_3$-G_3];[17]** was obtained as viscous orange oil in 71% yield, and G_3 dendron **[Am_8-APAP$_3$-G_3];[18]** as a yellow viscous oil in 73%.

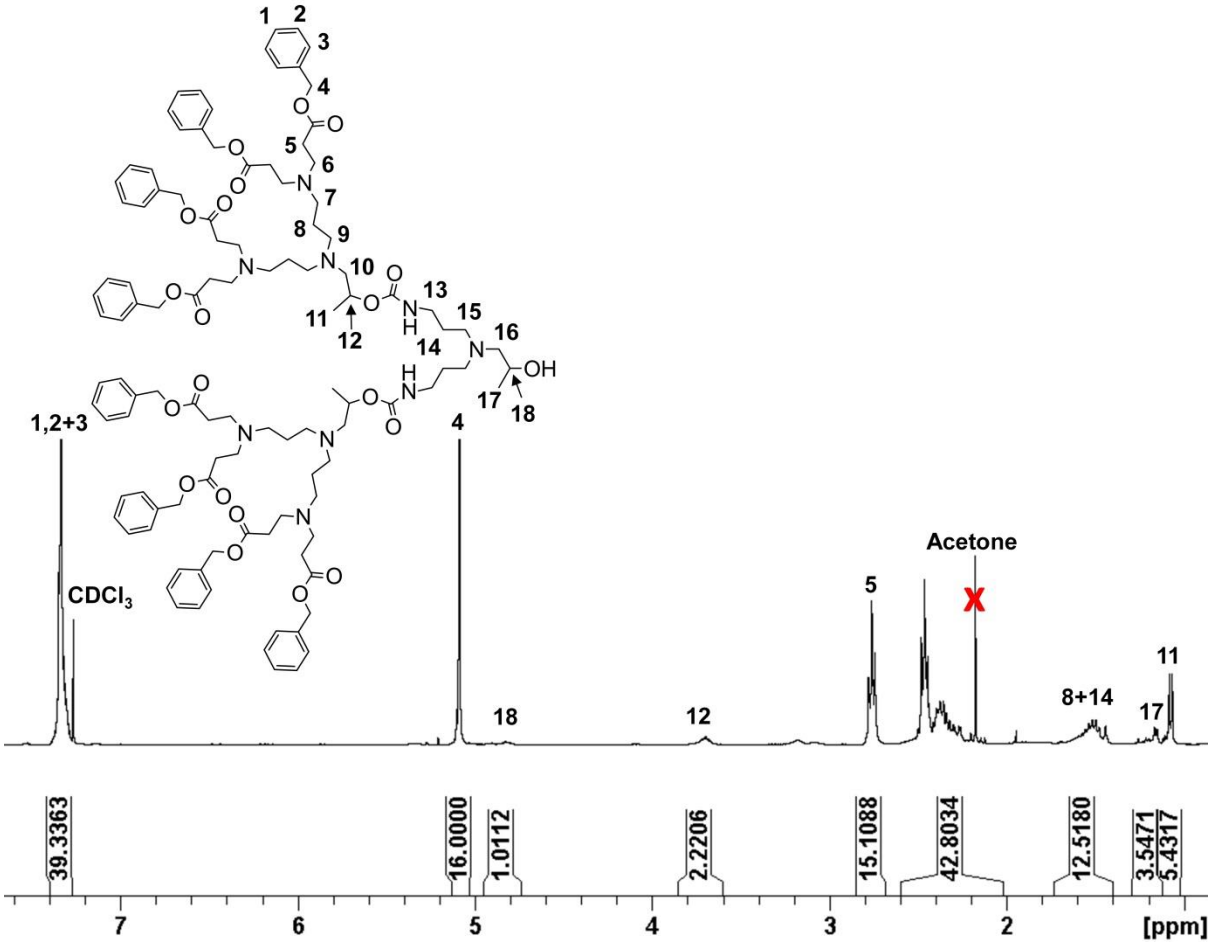

Figure 2.15 ^{1}H NMR spectrum (400 MHz, $CDCl_3$) of **[Bz_8-APAP$_3$-G_3];[17]**

The integrations of the assignments made to the ^{1}H NMR of **[17]** were promising. For example, when assignment 4, Figure 2.15, was calibrated to 16 protons relating the CH_2 methylene resonance adjacent to the Bz peripheral group, an integration of 39 protons correlating to the Bz groups was observed, with the assumption that the single proton missing from the integral (expected integral = 40) is hidden

behind the $CDCl_3$ peak. A 1:2 ratio was observed through the dendritic backbone at both chiral centres, labelled as 12 and 18, and a further integral of 15 protons seen for newly formed CH_2 after Michael addition (expected integral = 16), assigned as environment 5, Figure 2.15.

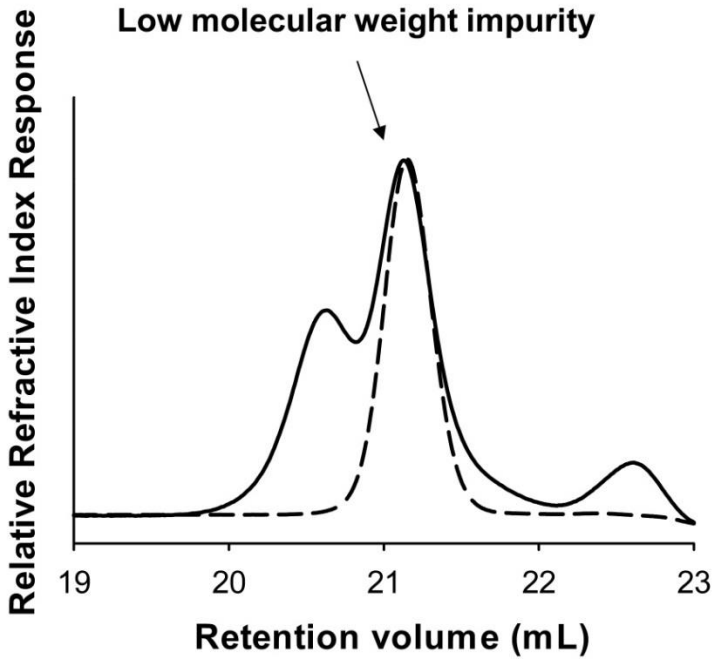

Figure 2.16 SEC chromatogram of G_3 Bz dendron **[Bz_8-$APAP_3$-G_3];[17]** (solid line). G_2 dendron Bz **[Bz_4-APAP-G_2];[11]** indicates the presence of low molecular weight impurities (dotted line)

Unfortunately mass spectral data by ESI-MS or MALDI-TOF analysis was inconclusive and adducts for **[17]** could not be observed. However, analysis using CI-MS did result in a doubly charged species $[M+2H]^{2+}$ observed at 959 Da, Figure S2.23. SEC analysis of **[17]** unfortunately indicated the presence of significant quantities of lower molecular weight impurities, as shown in Figure 2.16. The chromatogram showed one bimodal peak, the smaller of which at lower retention volume suggested the presence of complete substitution, but the larger of the two at higher retention suggested the presence of lower molecular weight impurities. An overlay of with the G_2 Bz dendron **[Bz_4-APAP-G_2];[11]** further confirmed the lower molecular weight impurities. The ^{13}C NMR spectrum of **[17]** is shown in Figure S2.24, but provided little information, since this technique was insensitive at higher generations.

Analysis of dendron **[18]** was similar to dendron **[17]**, with the ^{1}H NMR spectrum showing a high level of substitution through the backbone of the dendron, relative to the surface groups, Figure S2.25. Analysis of **[18]** using ESI-MS or MALDI-TOF analysis did not confirm any of the expected adducts, but using CI-MS resulted in a doubly charged species corresponding to $[M+2H]^{2+}$ at 883 Da, Figure S2.26. It should be noted that there were several populations present, few of which could be assigned to **[18]**. Analysis by SEC could not be performed for **[18]** since the material was found to be insoluble in the THF mobile phase.

2.2.5 Conclusions of amine Michael addition Chemistry

There are a number of conclusions to be made from using amine Michael addition chemistry for the synthesis of functional dendrons. Firstly, at low generations (i.e. G_1 and G_2), once optimised, the chemistry worked well. Yields typically exceeded 85% (calculated as a percentage from obtained yield divided by expected yield), and providing a low boiling acrylate monomer was used, purification was achieved by simply removing the solvent and excess reagents by vacuum. The synthesis of the AB_2 branching unit, [**APAP]**, to achieve the G_2 materials was also relatively straight forward, and has been recently synthesised in our research group using the described procedures in several large scale batches (>60g). However, amine Michael addition chemistry appeared to reach its limits at G_2. It was observed that for the synthesis of G_3 materials, very long reaction times (i.e. 5 days) were required for a high level of Michael addition to occur, and even after 5 days, SEC analysis confirmed the presence of significant quantities of partially functionalised materials. Furthermore, the molecular weights of the desired G_3 materials using ESI-MS or MALDI-TOF could not be readily observed.

2.3 Thiol Michael addition chemistry

Recently, there has been a significant interest in the scientific community in the use of thiol Michael addition chemistry to obtain functional polymeric materials, discussed in detail (section 1.3.7). The next part of this chapter will concentrate on the synthesis and characterisation of dendritic materials

that have thiol functionality at their peripheral groups, which can readily undergo thiol Michael addition

2.3.1 Synthesis and characterisation of thiol peripheral dendrons by a disulfide route

Disulfide bonds have been shown to be easily cleaved using a suitable reducing agent such as dithiolthreitol (DTT) to generate thiols.[7] Since thiols are nucleophilic, it was important that the thiol groups were protected or "masked", to prevent complications during the dendritic synthesis coupling steps. An asymmetric disulfide building block that could be reacted with the AB_2 branching unit [**APAP]** in a subsequent step was constructed, Schemes 2.10 and 2.11. After synthesis of the disulfide dendron, cleavage of the disulfide bonds would result in the desired thiol functional dendron.

3,3'-Dithiodipropionic acid, **[19]**, was reacted with 1.05 equivalents of CDI in THF at 35 °C, to generate the symmetrical imidazolide intermediate **[20]**, Scheme 2.10. It was important to add the CDI slowly to the vessel, since large quantities of CO_2 were generated upon the addition of CDI [Note: This was realised in error, after adding the entire quantity of CDI, resulted in the mixture foaming from out of the top of the reflux condenser! Beware!]. The reaction was monitored using TLC to confirm the appearance of the UV active intermediate **[20]** after 4 hours. After degassing the vessel with nitrogen to remove traces of CO_2, 0.33 equivalents of 4-*tert*-butylbenzylamine; **[21]** was added slowly to an excess of **[20]**, to prevent disubstitution. The reaction was left stirring overnight at 35 °C for 18 hours. Following the removal of THF, the crude product was purified by redissolving in CH_2Cl_2, washing three times with 1M HCl and twice with brine, followed by drying with anhydrous Na_2SO_4, to regenerate the desired carboxylic acid functionality. Additional purification by liquid chromatography (silica, eluting dichloromethane increasing to dichloromethane: methanol, 90:10) was required to remove impurities, resulting in the asymmetric disulfide, **[22]**, as a pure white powder.

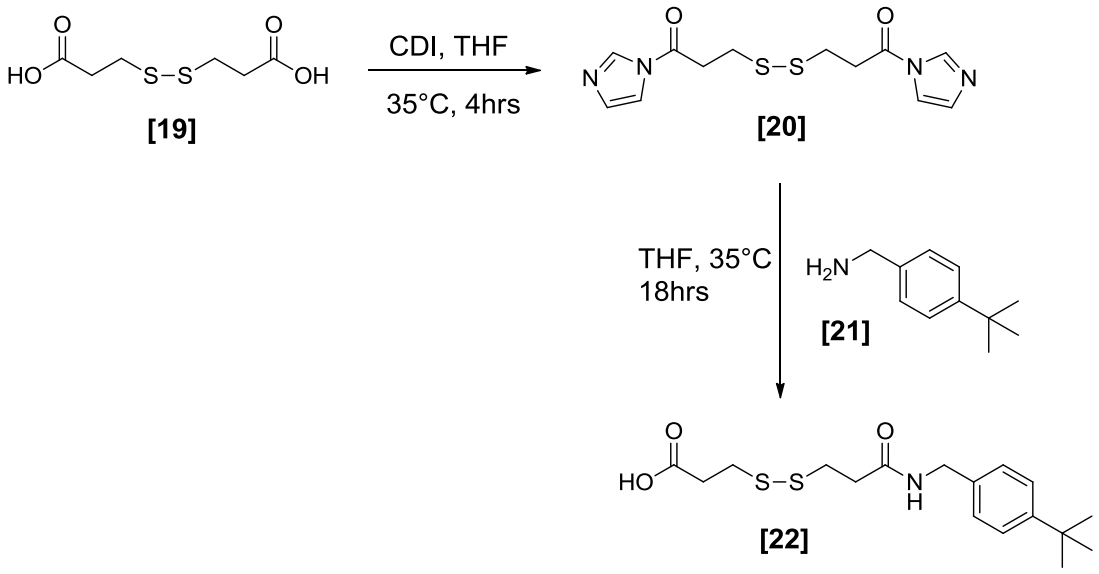

Scheme 2.10 Synthesis of **asymmetric disulfide;[22]**

The ^{1}H NMR spectrum of **[22]** confirmed the expected number of resonances with the correct integrations, Figure S2.27, and analysis of the ^{13}C NMR spectrum also confirmed the expected number of carbon environments, including two carbonyl resonances at 175.8 ppm and 171.1 ppm, each for the single acid and amide functionalities, Figure S2.28. ESI-MS confirmed a population at 378 Da (MNa^{+} = 378 Da), Figure S2.29.

To generate the G_1 disulfide protected dendron, the synthesised asymmetric disulfide **[22]** was reacted in a 1:1 ratio with CDI for 4 hours to form the selective imidazolide intermediate **[23]**, Scheme 2.11. After confirmation of the intermediate **[23]** using TLC, [**APAP]** was added dropwise to the mixture, and the resulting solution was left stirring at 35 °C for 18 hours. Purification was achieved by removing the THF, diluting the crude sample with CH_2Cl_2 and washing the organic phase three times with water. After drying the organic phase over anhydrous Na_2SO_4, and removal of solvents, a pungent viscous yellow oil resulted.

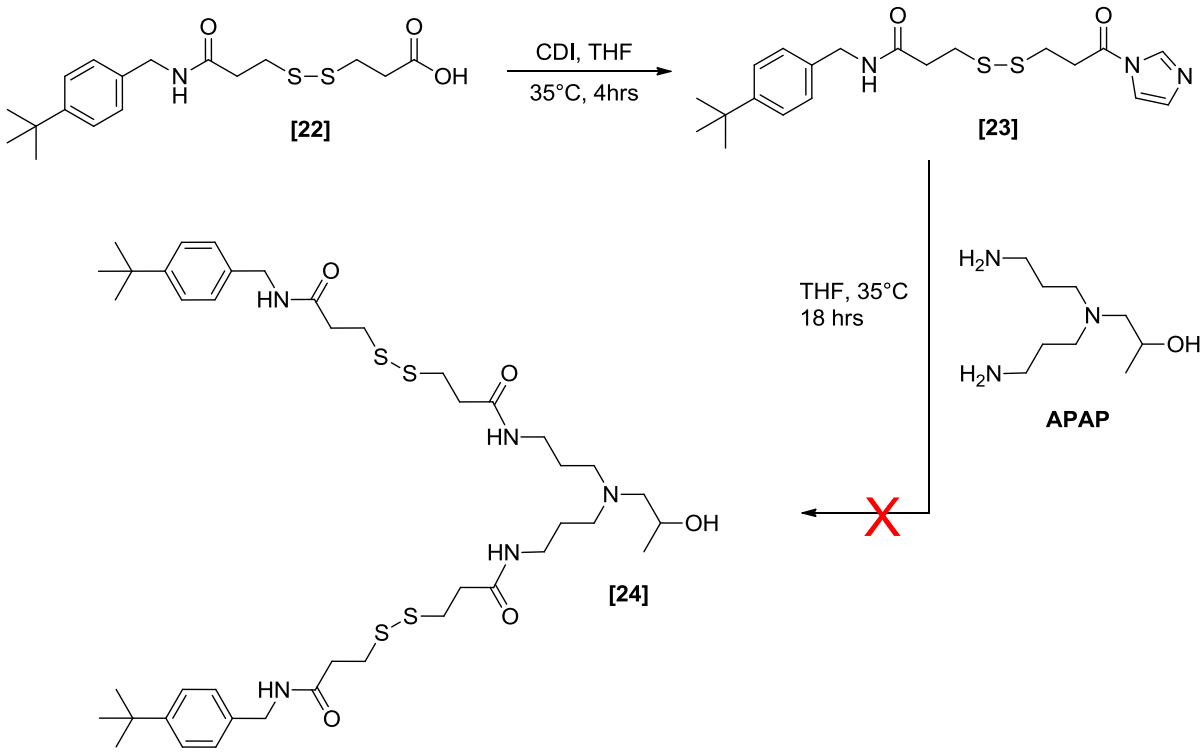

Scheme 2.11 Attempted coupling of asymmetric disulfide **[22]** to [**APAP]**

Unfortunately, analysis of the resulting oil by ^{1}H NMR and ESI-MS confirmed that the synthesis of **[24]** was unsuccessful. TLC showed a mixture of several products in the oil, and attempts to purify the resulting material by liquid chromatography was unsuccessful due to the polar nature of the materials, which caused them to bind strongly to the silica gel. The pungent odour of the oil, also suggested potential cleavage of the disulfide bond, which may have further complicated the synthesis of **[24]**. The reaction was repeated several times, under several different conditions, including ambient temperature conditions to further avoid disulfide cleavage. Unfortunately, even under modified conditions **[24]** could not be isolated. Due to the unsuccessful attempts to use a disulfide bond as a thiol protecting strategy, an alternative route was sought.

2.3.2 Synthesis and characterisation of thiol peripheral dendrons using Sanger's reagent

Sanger's reagent, otherwise known as 1-fluoro-2,4-dinitrobenzene, has been shown to be an effective protecting group for the synthesis of thiol functional dendrons and thiol functional polymers.[8, 9]

Utilising this chemistry, the Sanger's protected 11-mercaptoundecanoic acid **[Sngr-SH-COOH];[27]** was prepared, Scheme 2.12.

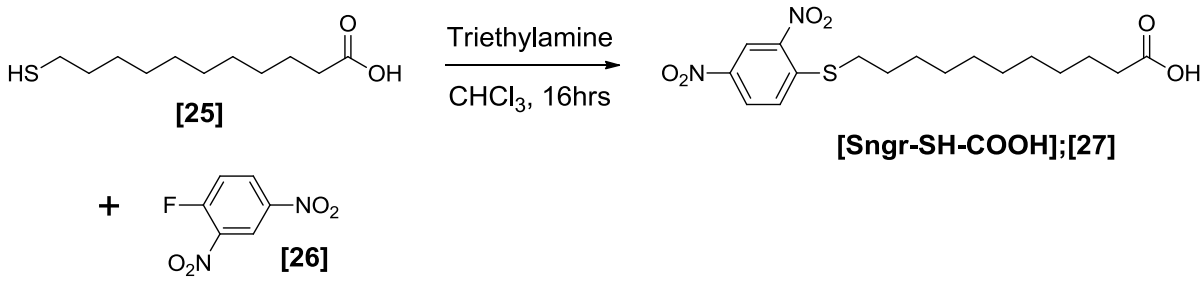

Scheme 2.12 Synthesis of **[Sngr-SH-COOH];[27]**

11-Mercaptoundercanopic acid, **[25]**, was dissolved in $CHCl_3$ and added slowly to a mixture of 1-fluoro-2,4-dinitrobenzene, **[26]**, and triethylamine in $CHCl_3$. Upon addition of **[25]** the reaction was slightly exothermic, and proceeded to turn orange. The resulting solution was sealed and left stirring overnight for 16 hours at ambient temperature. Purification was achieved by washing the organic layer twice with 1M HCl and once with brine, which yielded a yellow solid that was filtered from the mixture using a Büchner funnel. The yellow solid was recrystallized twice from hot $CHCl_3$, resulting in the pure thiol protected product **[Sngr-SH-COOH];[27]** as a yellow powder in 65%. [Note: Since most of the Sanger's protected products were solids, rather than viscous oils, recrystallisation was preferred over liquid chromatography for purification].

The ^{1}H NMR spectrum of **[27]** is shown in Figure 2.17, and appearance of resonances at 9.10, 8.35 and 7.56 ppm indicated the presence of the 2,4-dinitrobenzene functionality. The integration of the aromatic peaks relative to the CH_2 adjacent to the protected thiol, labelled environment 4, were also in the expected 1:2 ratio.

Utilising **[Sngr-SH-COOH];[27]**, the synthesis of a G_1 protected thiol dendron was attempted using CDI chemistry, and [**APAP]** as the AB_2 branching unit, Scheme 2.13.

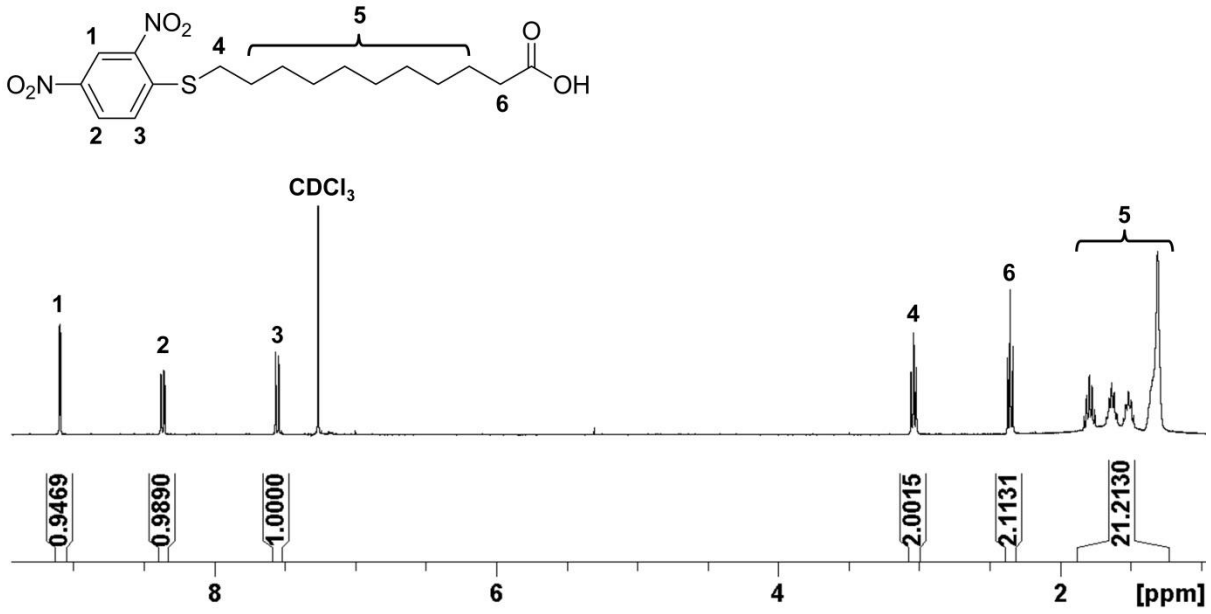

Figure 2.17 ^{1}H NMR spectrum (400 MHz, $CDCl_3$), of **[Sngr-SH-COOH];[27]**

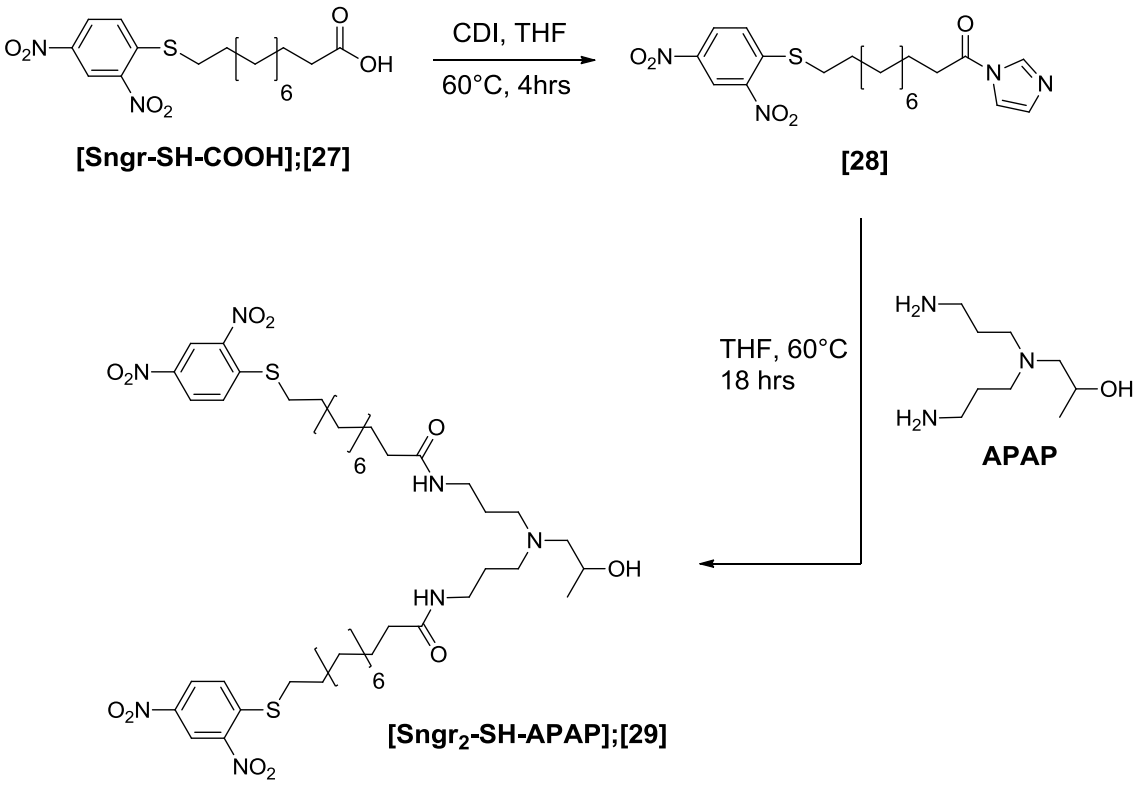

Scheme 2.13 Synthesis of **[Sngr$_2$-SH-APAP];[29]** using **[APAP]**

It was found that **[Sngr-SH-COOH];[27]**, was not soluble in toluene, therefore anhydrous THF was used as the reaction solvent; **[27]** was reacted with CDI in a 1:1 ratio for 4 hours to generate the imidazolide **[28]**. [Note: Once again, care was taken when adding the CDI to the reaction vessel, as the production of CO_2 was found to occur quickly]. After 4 hours, TLC confirmed **[28]** had been formed and [**APAP]** was added dropwise to the mixture, which was then left overnight at 60 °C for 18 hours. Purification was achieved by removing the THF, redissolving the crude mixture in CH_2Cl_2 and washing the organic layer three times with water. After drying over anhydrous Na_2SO_4, removal of solvents and recrystallisation from hot MeOH, **[Sngr$_2$-SH-APAP];[29]** was obtained as a yellow powder in 74% yield. Analysis of **[29]** using ^{1}H and ^{13}C NMR, both indicated the desired number of environments, and correct integrations, Figures S2.30 (a) and S2.30 (b). ESI-MS confirmed two populations at 922 Da (MH^+ = 922 Da) and 944 Da (MNa^+ = 944 Da) confirming the pure thiol protected dendron **[29]**, Figure 2.18.

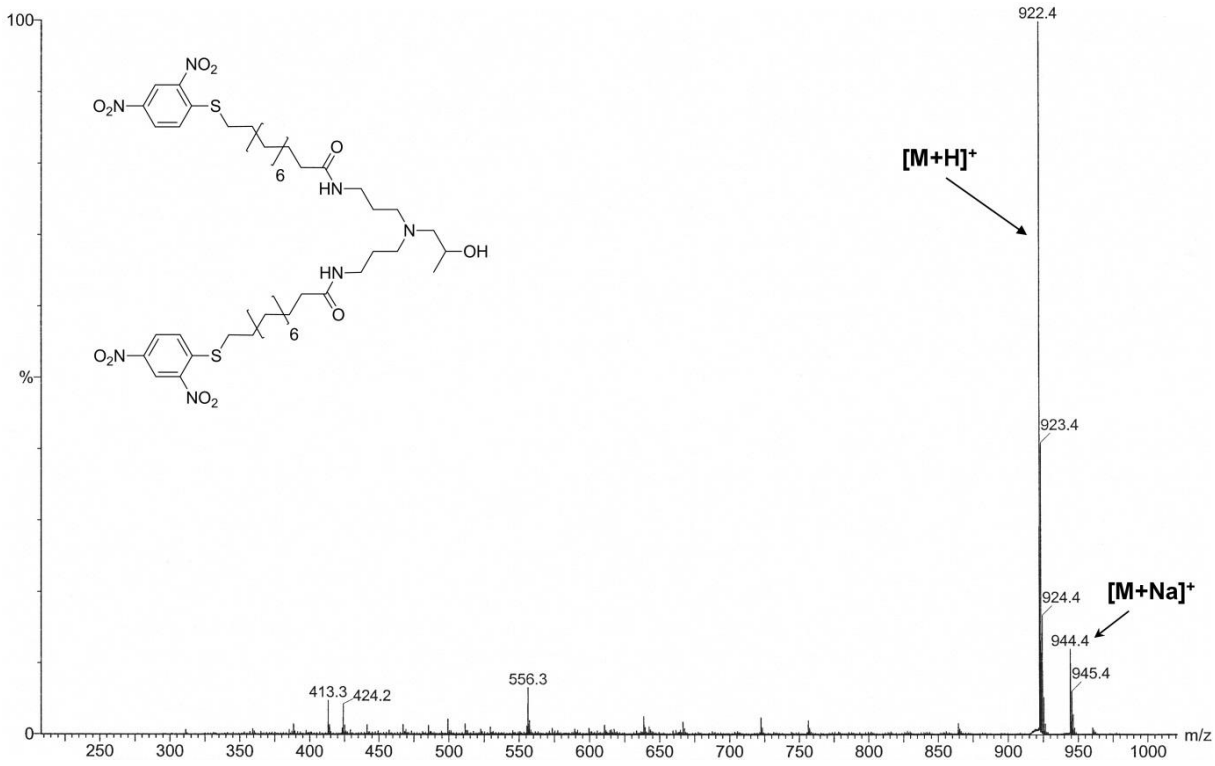

Figure 2.18 ESI-MS (MeOH) spectrum of **[Sngr$_2$-SH-APAP];[29]**

Following the synthesis of **[29]**, attempts to remove the protecting groups from the molecule, to release the peripheral thiols were made. Hawker and co-workers reported the quantitative removal of the Sanger's protecting group using an excess of mercaptoethanol or 1-propanethiol in the presence of triethylamine.[8] Neither of these thiol-based regents are particularly pleasant to work with, particularly on a large excess, and hence an excess of dodecanethiol (DDT) in the presence of triethylamine was used, Scheme 2.14. **[Sngr$_2$-SH-APAP];[29]** was dissolved in the minimum amount of DMF, a catalytic amount of TEA and 150 equivalents of DDT and left stirring in the mixture for 18 hours at ambient temperature. Purification was achieved by precipitating the mixture into hexane, which was found to remove the byproducts, excess DDT, TEA and DMF, and leave **[SH$_2$-APAP];[30]** as a red viscous oil in 40% yield. Confirmation by ^{1}H NMR confirmed the complete removal of the Sanger's protecting groups, as indicated by the disappearance of the aromatic resonances at 9.10, 8.35 and 7.56 ppm, Figure 2.19.

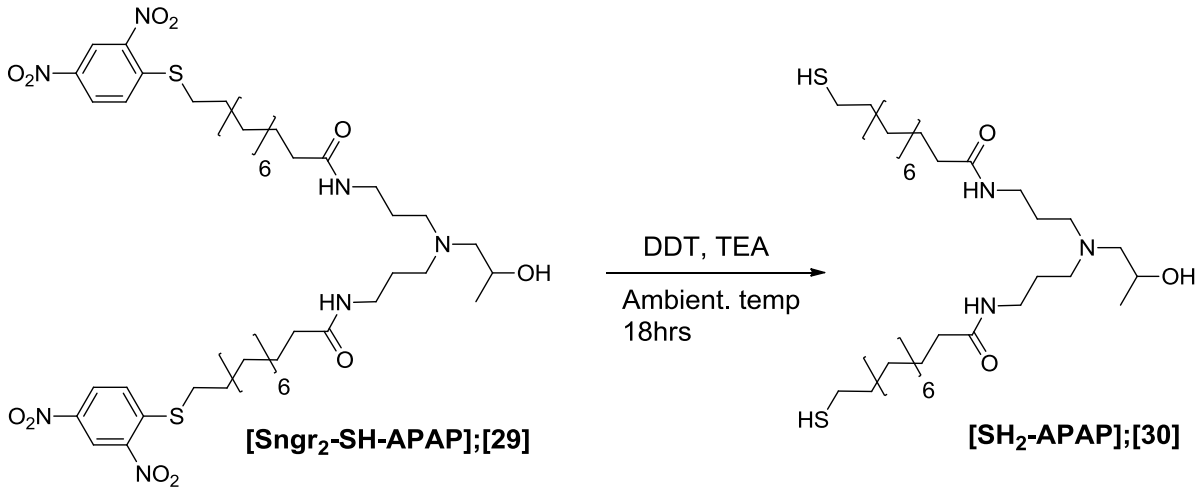

[Sngr$_2$-SH-APAP];[29] **[SH$_2$-APAP];[30]**

Scheme 2.14 Deprotection of **[Sngr$_2$-SH-APAP];[29]** to generate **[SH$_2$-APAP];[30]**

Further evidence using ESI-MS showed populations corresponding to **[SH$_2$-APAP];[30]** at 590 Da (MH^+ = 590 Da), 612 (MNa^+ = 612 Da) and 628 Da (MK^+ = 628 Da), Figure S2.31.

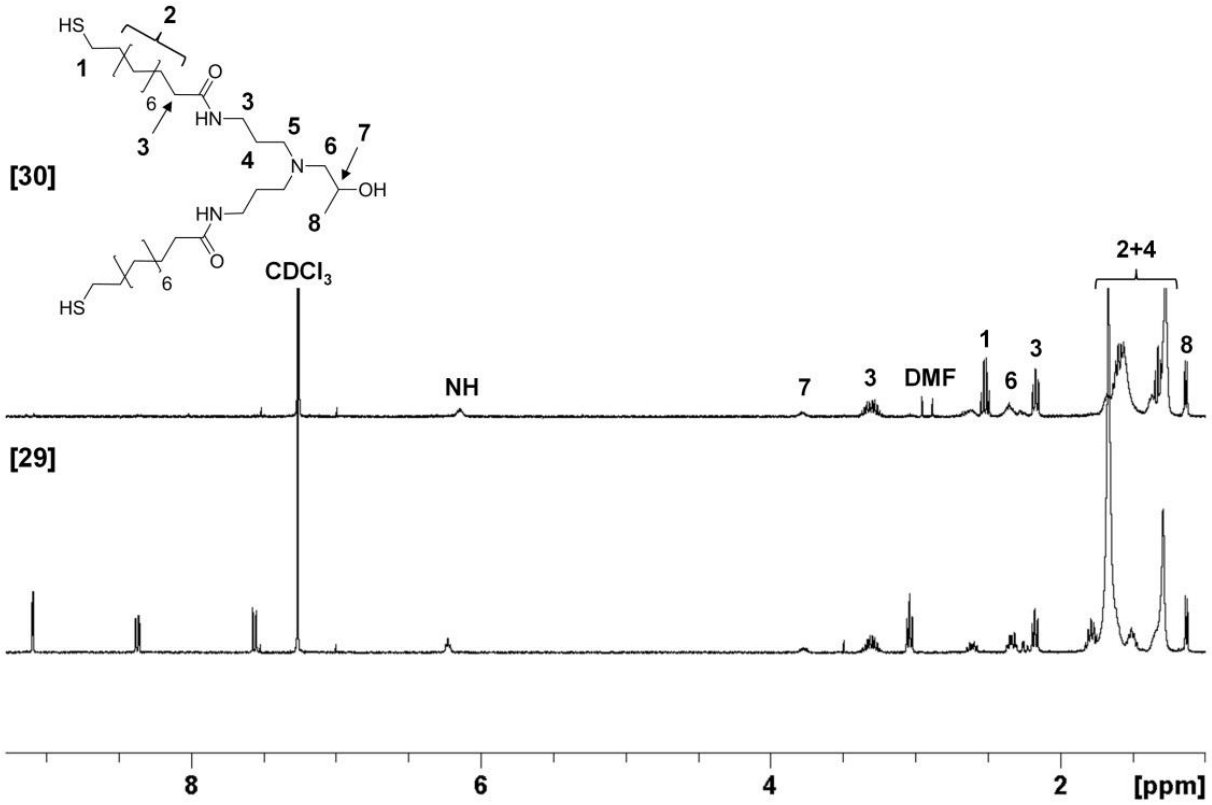

Figure 2.19 ^{1}H NMR spectra ($CDCl_3$, 400MHz) of **[Sngr$_2$-SH-APAP];[29]** and **[SH$_2$-APAP];[30]** before and after removal of the 2,4-dinitrobenzene moiety

Since **[Sngr$_2$-SH-APAP];[29]** had a secondary hydroxyl focal point, attempts were made to react this to another unit of [**APAP]** to synthesise the G_2 dendron **[Sngr$_4$-SH-APAP$_3$];[32]**, Scheme 2.15. **[Sngr$_2$-SH-APAP];[29]** was reacted in a 1:1 ratio with CDI and left for 4 hours to form the imidazolide intermediate **[31]**. After dropwise addition of **[APAP]** to the solution, the mixture was left for 18 hours at 60 °C. Purification followed a similar strategy to previous CDI reactions discussed, involving removal of solvents, dilution with CH_2Cl_2, aqueous water washes and drying over anhydrous Na_2SO_4. After removal of CH_2Cl_2, a dark orange paste was furnished. Analysis of the crude mixture by ^{1}H or ^{13}C NMR did not indicate the successful synthesis of **[Sngr$_4$-SH-APAP$_3$];[32]** and no evidence of the target molecule could be observed using ESI-MS. Attempts at further purification by recrystallisation and liquid chromatography resulted in predominantly imidazolide intermediate **[31]**.

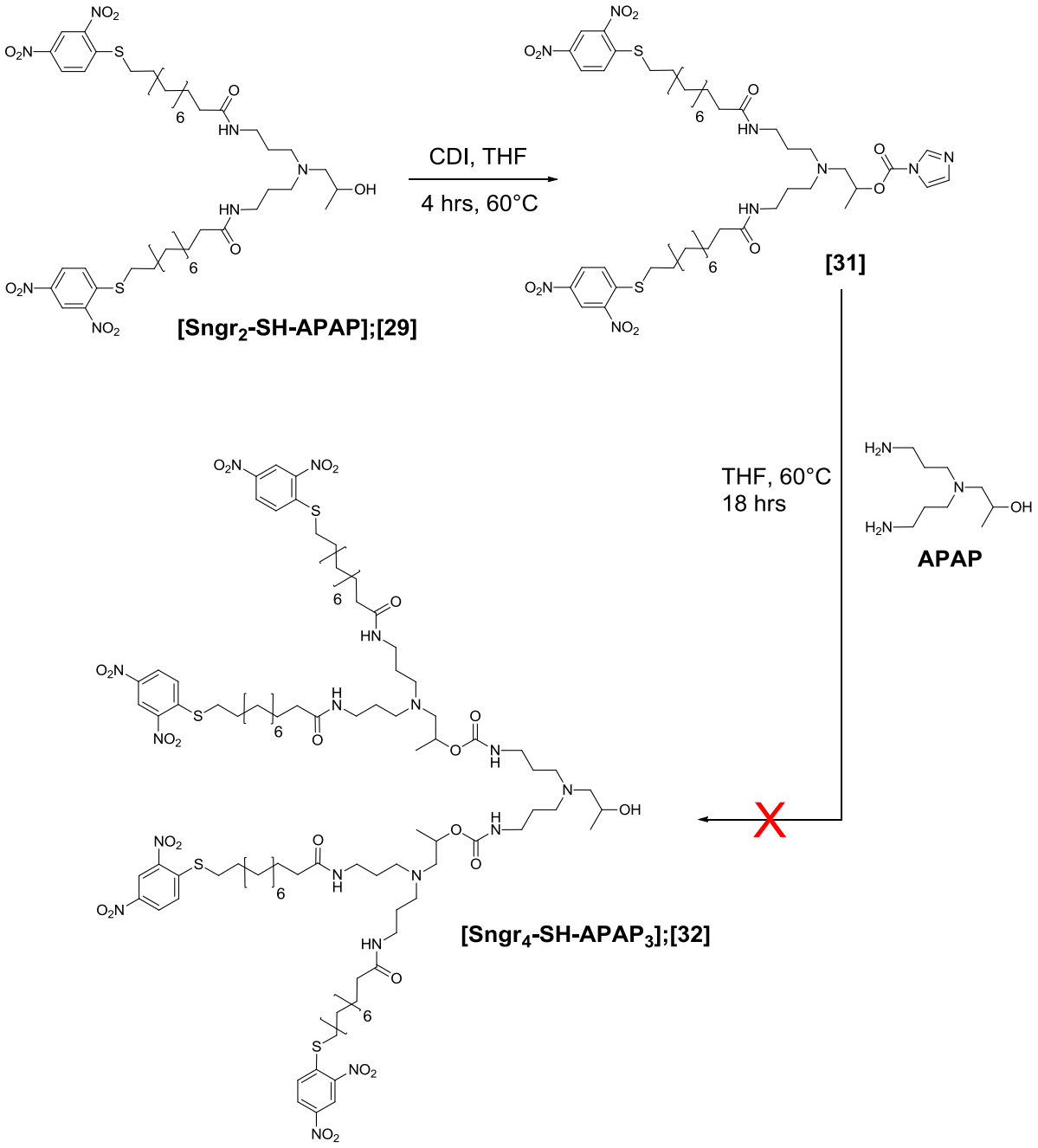

Scheme 2.15 Attempted synthesis of **[Sngr$_4$-SH-APAP$_3$];[32]**, using [**APAP]**

To reduce potential steric crowding the strategy was changed, and 4 units of **[Sngr-SH-COOH];[27]**, were reacted to one unit of **[APAP$_3$-G$_2$];[16]**, resulting in the same desired compound, **[Sngr$_4$-SH-APAP$_3$];[32]**, Scheme 2.16.

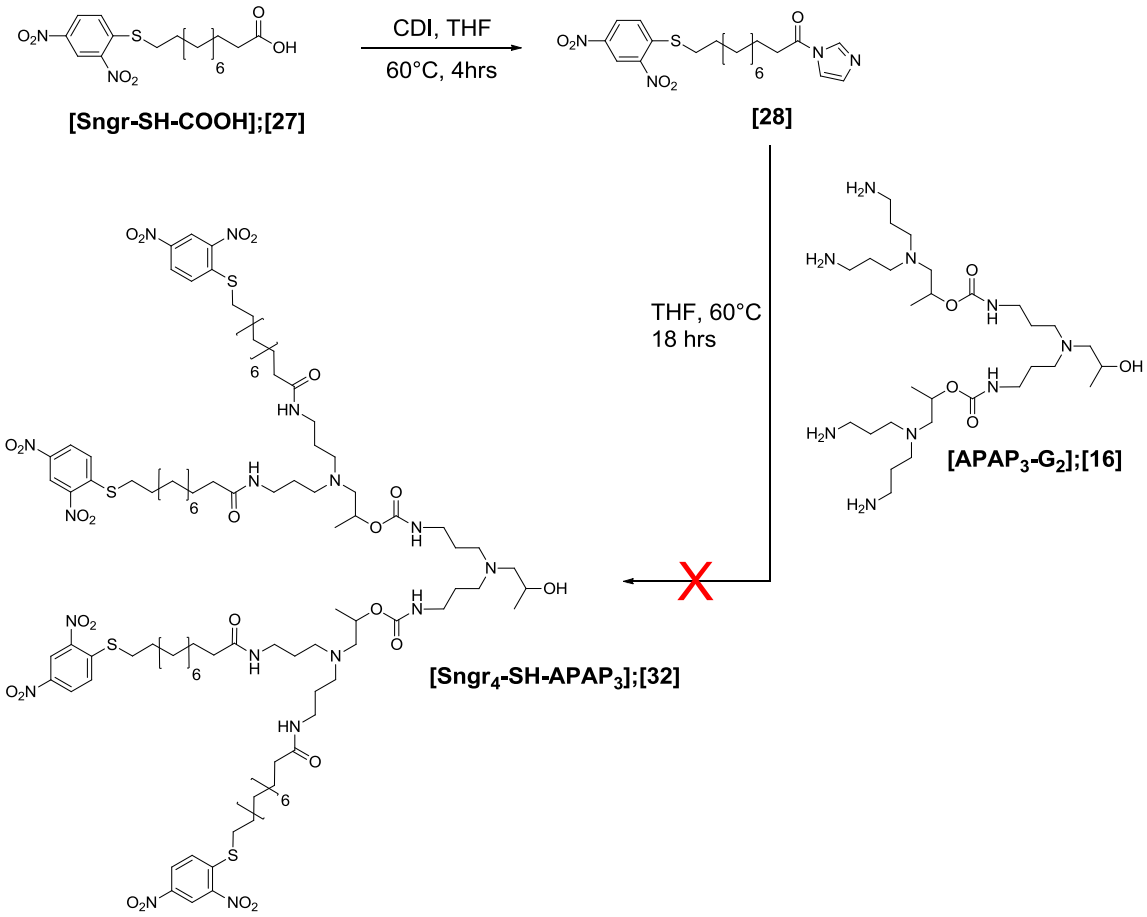

Scheme 2.16 Attempted synthesis of **[Sngr$_4$-SH-APAP$_3$];[32]** using **[APAP$_3$-G$_2$];[16]**

[27] was reacted in a 1:1 molar ratio with CDI, and left for 4 hours to generate the imidazolide intermediate **[28]**, using the same methodology previously used for the synthesis of **[Sngr$_2$-SH-APAP];[29]**. **[APAP$_3$-G$_2$];[16]** was added to the reaction, and the mixture left for 18 hours at 60 °C. After purification of the mixture using aqueous washes, a crude orange paste was obtained. Unfortunately, analysis by ^{1}H or ^{13}C NMR or ESI-MS did not confirm the synthesis of **[Sngr$_4$-SH-APAP$_3$];[32]**, and instead confirmed predominantly intermediate **[28]**.

In one final attempt to synthesise **[32]**, the coupling chemistry was changed. It was suggested that the reaction with imidazolide intermediate **[28]**, may simply not be reactive enough to couple four units of **[28]** to the AB$_4$ branching unit **[16]**. Some care over the choice of the revised chemistry was taken. Since the AB$_4$ branching unit **[16]** contained both primary amines and a secondary hydroxyl, simply

converting **[27]** to an acyl chloride would lead to the reaction at both the primary amine and secondary hydroxyl sites of **[16]**.

N-hydroxysuccinicmide (NHS) is a commonly used activating agent for carboxylic acids, where the activated ester can react with amines to form amides. The reaction is also selective, as it is only reactive towards primary amines and not hydroxyl groups.

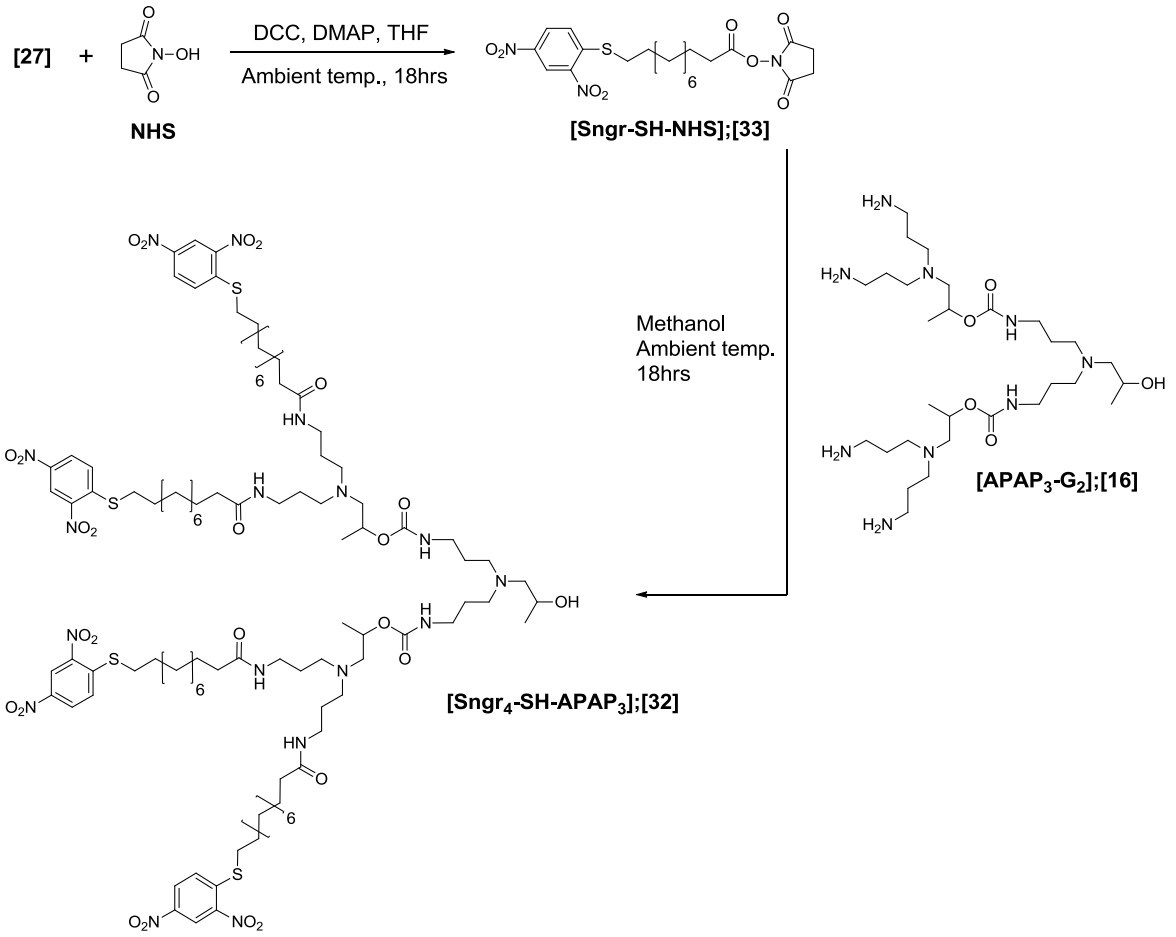

Scheme 2.17 Synthesis of **[Sngr-SH-NHS];[33]** and subsequent reaction to form **[Sngr$_4$-SH-APAP$_3$];[32]**

To synthesise **[Sngr-SH-NHS];[33]**, NHS and **[28]** were reacted together with *N,N'*-dicyclohexylcarbodiimide (DCC) in the presence of a catalytic amount of 4-dimethylaminopyridine (DMAP) in THF at ambient temperature, Scheme 2.17. After filtration of the dicyclohexylurea (DCU) byproduct, and liquid chromatography (silica, eluting chloroform, increasing to chloroform:acetone, 90:10) of the crude mixture, **[Sngr-SH-NHS];[33]** was formed as a yellow powder in 50% yield. The

resulting ester was confirmed using ^{1}H NMR, with the presence of a large singlet at 2.86 ppm for the appearance of the four symmetrical protons from the succinimide ring, Figure S2.32. Analysis using ESI-MS confirmed populations at 504 Da (MNa^{+} = 504 Da) and 520 Da (MK^{+} = 520 Da), Figure S2.33. **[Sngr-SH-NHS];[33]** was reacted in a 6:1 ratio with **[APAP$_3$-G$_2$];[16]** in methanol for 18 hours at ambient temperature, producing the G_2 dendron **[Sngr$_4$-SH-APAP$_3$];[32]** as a yellow powder. The crude product was purified by precipitation into acetone, due to the solubility of **[33]** in acetone relative to the desired product **[32]**. Analysis of the material using ^{1}H NMR, Figure S2.34, suggested a high level of coupling, determined by a 2:4 ratio of 2,4-nitrobenzene peripheral groups relative to the single protons located at the two chiral centres adjacent to the urethane bonds. SEC also indicated a single monomodal distribution for **[32]**, and in comparison to **[29]**, the G_1 dendron, a significant shift to lower retention volume was observed, Figure 2.20.

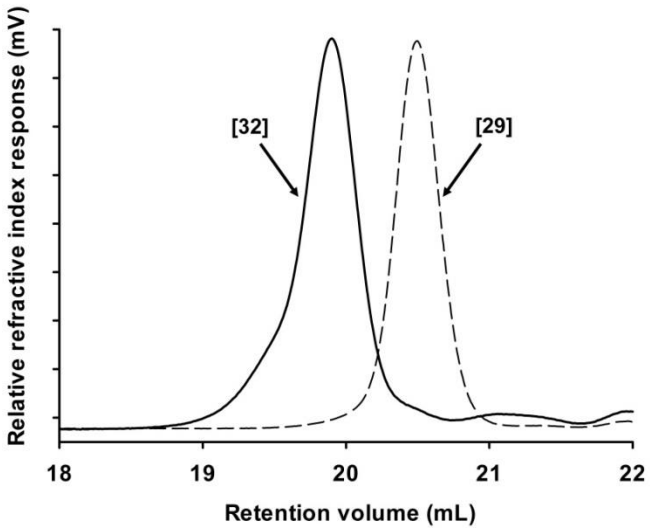

Figure 2.20 SEC chromatograms of **[Sngr$_2$-SH-APAP];[29]** and **[Sngr$_4$-SH-APAP$_3$];[32]**

Unfortunately, mass spectral data by either ESI-MS or MALDI-TOF techniques could not confirm any ion populations for **[32]**.

Although evidence by triple detection SEC suggested that the crude mixture of **[32]** contained higher molecular weight species, SEC was simply not sensitive enough to characterise the actual molecular weights in the mixture. Since mass spectral data was unattainable for **[32]**, it was concluded that

further optimisation was required to synthesise higher generation dendritic macromolecules using this chemistry.

2.3.3 Thiol Michael additions with thiol peripheral dendrons by using Sanger's reagent

Although the G_2 dendron **[32]** could not be fully characterised, **[SH_2-APAP];[30]** was reacted with oligo(ethylene glycol) monomethyl ether acrylate M_n = 480 g/mol [**OEGA]**, Scheme 2.18, as a model reaction to evaluate the potential for thiol Michael addition chemistry.

Recent thiol Michael addition kinetic experiments, analysing the effect of different acrylate/methacrylate substrates and thiol based monomers with both amine and phosphine based catalysts, have shown that both amine and phosphine based catalysts lead to high conversions during thiol Michael additions.[10] In particular, dimethylphenylphopshine (DMPP) was found to achieve high conversions providing the concentration of catalyst was kept to a very low concentration (0.05 eqv) to avoid side reactions. Using similar conditions, 1 equivalent of **[SH_2-APAP];[30]** was reacted with 2 equivalents of [**OEGA**] together with 0.1 equivalents of DMPP in acetone for 4 hours, Scheme 2.18.

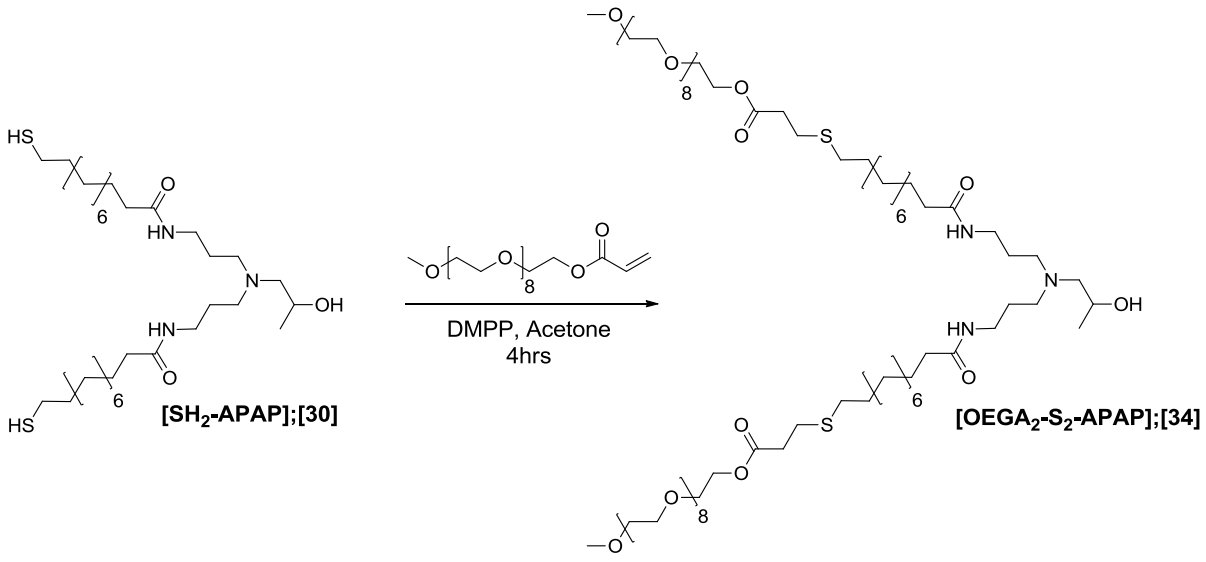

Scheme 2.18 Thiol Michael addition with thiol terminated dendron **[SH_2-APAP];[30]**

The reaction was analysed using ^{1}H NMR after 2 hours and at 4 hours to determine the reaction conversion, Figure 2.21. It was observed that the reaction reached >99% conversion after 2 hours, as indicated by the total disappearance of the acrylate vinyl resonances at 6.44, 6.17 and 5.85 ppm. The appearance of two new triplet resonances at 2.78 and 2.64 ppm also indicated the formation of new C-C bonds, resulting in **[OEGA$_2$-S$_2$-APAP];[34]**.

The results were extremely encouraging, and given the steric bulk of the OEGA substrate, this was a clear testimony of the efficiency of this chemistry.

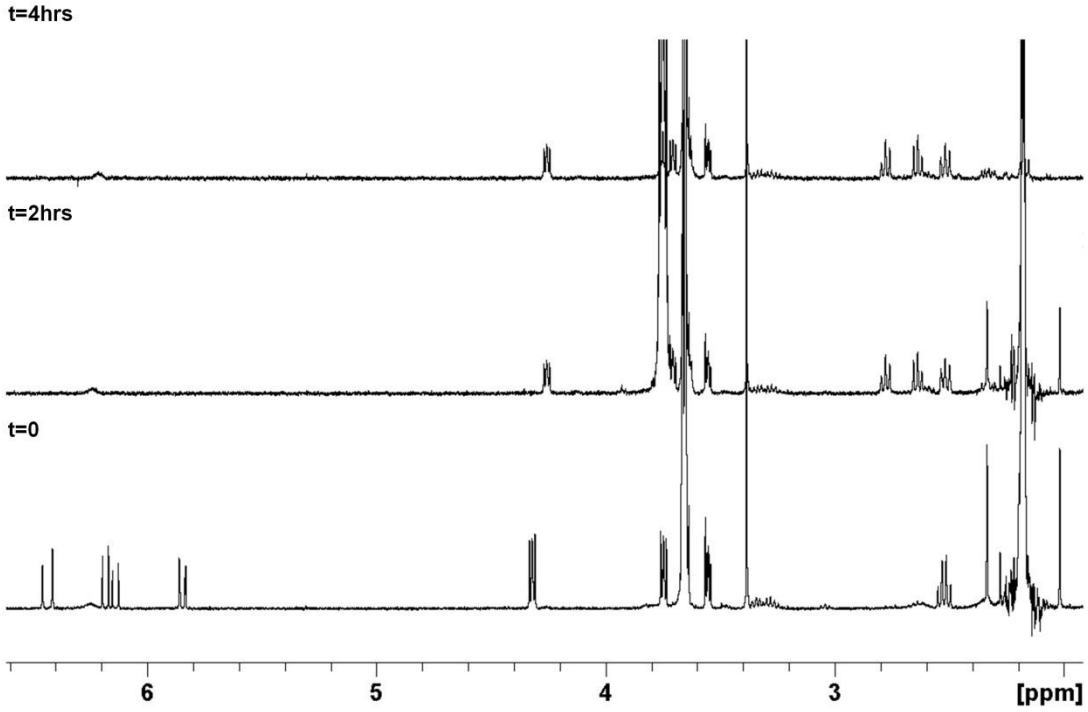

Figure 2.21 ^{1}H NMR spectra (400 MHz, $CDCl_3$) of **[OEGA$_2$-S$_2$-APAP];[34]** at t =0, t= 2hrs, t=4hrs

2.3.4 Conclusions of thiol peripheral dendron synthesis using Sanger's reagent

The thiol protected G_1 dendron, **[Sngr$_2$-SH-APAP];[29]** was synthesised using the AB_2 branching unit [**APAP**]. Deprotection of **[Sngr$_2$-SH-APAP];[29]** using DDT led to the synthesis of **[SH$_2$-APAP];[30]** that was successfully post functionalised by thiol Michael addition chemistry with OEGA, resulting in **[OEGA$_2$-S$_2$-APAP];[34]**. The G_2 materials could not be isolated by using CDI

chemistry, with either [**APAP]** or **[APAP$_3$-G$_2$];[16]**, but by using the activated NHS ester, **[Sngr-SH-NHS];[33]** and **[APAP$_3$-G$_2$];[16]** some evidence of higher molecular weight species by ^{1}H NMR and SEC was shown, suggesting the presence of **[Sngr$_4$-SH-APAP$_3$];[32]**.

The Sanger's protected materials were very difficult to work with, since their solubility was poor in most polar solvents. However, the greatest disadvantage with this route was the removal of the Sanger's (2,4-dinitrobenzene) protecting functionality; an extremely large excess (150 equivalents) of DDT was required. This is not ideal, since it is firstly wasteful (to say the least) and fairly rigorous repetitive precipitations are required to remove such a large excess.

Although the Sanger's route to thiol protected materials is an improvement over the disulfide route, it was by no means a solution to the synthesis of thiol terminated dendritic macromolecules. The last section of this chapter begins a piece of research that will continue throughout the rest of the thesis. It is by far the most efficient and elegant solution to the synthesis of functional dendritic materials via thiol Michael addition.

2.3.5 Synthesis and characterisation of thiol peripheral dendrons using xanthates

Recently, xanthates have been used as thiol protecting groups, to prepare thiol protected polymers that can be readily functionalised using thiol Michael addition chemistry.[11-13] Deprotection of the xanthate protecting group was achieved by aminolysis using a 2.5 molar excess of n-butylamine per pendant xanthate. After successful deprotection, the functional acrylate was added to the same vessel, without purification, for thiol Michael addition functionalisation. This was a very interesting piece of research, since the purification of the thiol functional material was not required, and instead utilised a one-pot process, significantly reducing the chance of disulfide formation.

Building on these findings, the objective was to prepare a model dendritic compound, whereby a similar one-pot strategy could be applied. The xanthate functional carboxylic acid building block, **[Xan-P-COOH];[35]**, was easily prepared via a simple S_N2 alkylation reaction with 1-

bromopropanoic acid and potassium ethyl xanthogenate; both cheap and commercially available reagents, Scheme 2.19.

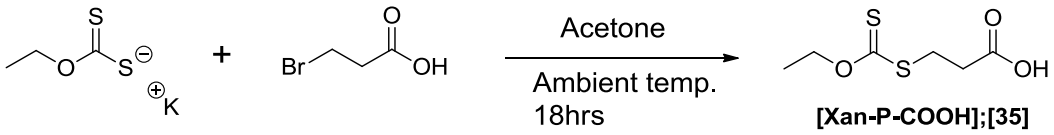

Scheme 2.19 Preparation of Xanthate building block **[Xan-P-COOH];[35]**

Potassium ethyl xanthate was suspended in acetone and 1-bromopanoic acid was added dropwise to the solution via a dropping funnel. Upon addition, the mixture changed colour from yellow to white, indicating the formation of the potassium bromide (KBr) salt. After stirring at ambient temperature for 18 hours, the mixture was filtered and the acetone removed under vacuum to leave a viscous yellow oil. The viscous oil was re-dissolved in CH_2Cl_2 and washed three times with brine to remove trace KBr, dried over $MgSO_4$ and evaporated to dryness resulting in a white solid in 70% yield. The material was characterised by ^{1}H and ^{13}C NMR techniques.

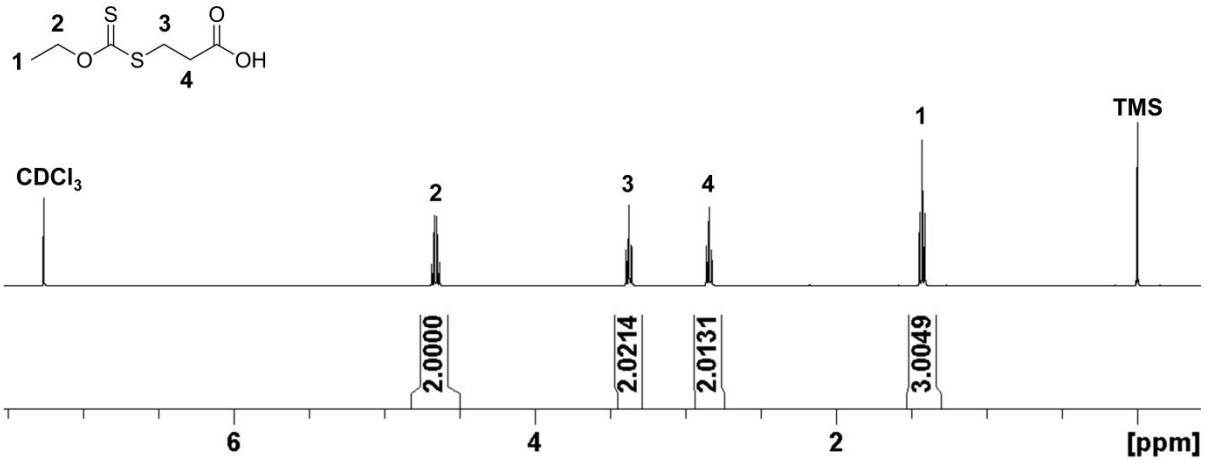

Figure 2.22 ^{1}H NMR spectrum (400MHz, $CDCl_3$) of **[Xan-P-COOH];[35]**

The ^{1}H NMR spectrum of **[Xan-P-COOH];[35]** confirmed that were 4 proton environments, each of which corresponded to the expected integration ratios, Figure 2.22. Analysis by ^{13}C NMR also resulted in 6 carbon environments, including the acid resonance at 177 ppm and the xanthate thiocarbonyl at 214 ppm, Figure S2.35.

Using **[Xan-P-COOH];[35]**, a G_0 dendrimer, **[Xan_3-P-TEA-G_0];[36]** with 3 peripheral xanthates was constructed using triethanolamine (TEA) as a dendrimer core, Scheme 2.20. It was important to only target ester based materials with alcohol reagents, since the introduction of primary or secondary amines, to synthesise amide based compounds, may cause reaction at the xanthate site within **[Xan-P-COOH]**. Initial attempts at using CDI chemistry to generate the required ester bonds resulted in an insoluble viscous oil that could not be characterised. It was suggested that the imidazole byproduct that was generated in the first step of the CDI reaction, may have led to aminolysis with the xanthate functionality. Instead a classical DCC esterification reaction that has been used previously to synthesise dendritic materials in high yields was adopted.[14, 15]

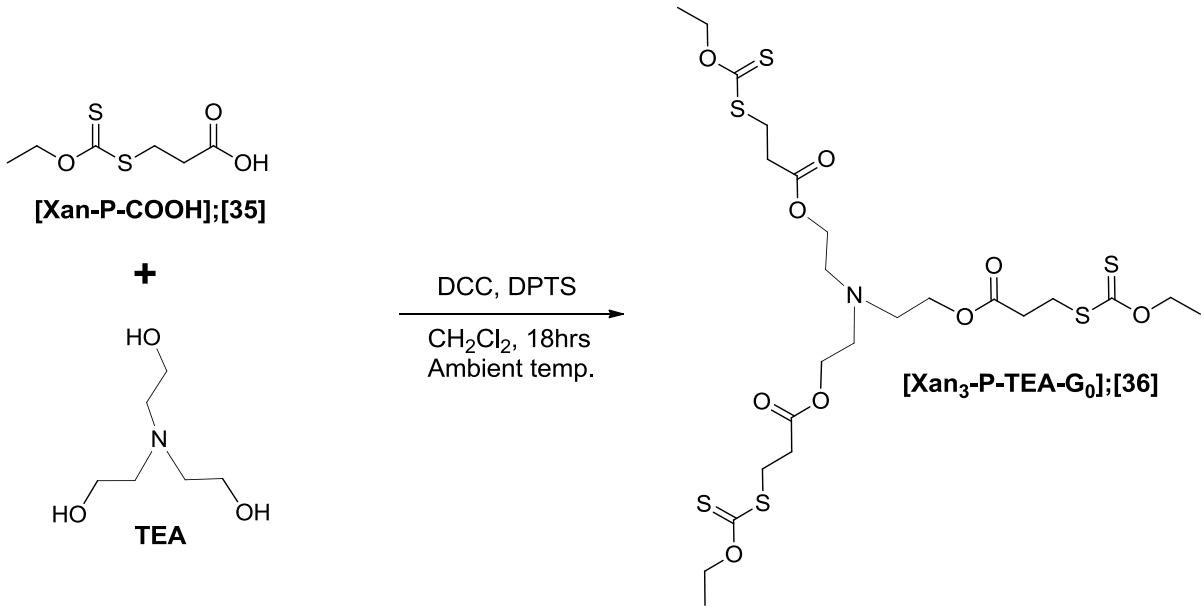

Scheme 2.20 Synthesis of G_0 xanthate dendrimer **[Xan_3-P-TEA-G_0];[36]**

4-(Dimethylamino)pyridinium *p*-toluenesulfonate (DPTS) was chosen as the esterification catalyst since it is known to supress the problematic 1,3 rearrangement of the O-acyl intermediate to a N-acyl urea, by maintaining a low pH during the reaction[14, 16]. See Chapter 3 (section 3.3.4.2) for its synthesis. TEA and **[Xan-P-COOH];[35]** were added in 1:4 ratio, and dissolved in anhydrous CH_2Cl_2 along with DPTS. DCC was added slowly to the mixture in a small volume of CH_2Cl_2, and the reaction was left overnight for 18 hours at ambient temperature. The precipitated DCU byproduct was removed by filtration, washed with CH_2Cl_2, and the product isolated by diluting the mixture with

CH_2Cl_2 and washing twice with 1M $NaHSO_4$ to remove the DPTS catalyst. The organic layer was dried over $MgSO_4$ and evaporated to dryness. The crude mixture required purification by liquid chromatography (silica gel, eluting hexane increasing to hexane/ethyl acetate 40:60) to synthesise the dendrimer **[Xan_3-P-TEA-G_0];[36]** as an orange viscous oil in 60% yield. Characterisation of the trifunctional xanthate dendrimer was obtained by ^1H and ^{13}C NMR as well as ESI-MS. ^1H NMR confirmed six proton environments, indicating the three symmetrical dendritic arms attached to the core, Figure S2.36. Further analysis by ^{13}C confirmed eight carbon environments, including a single ester carbonyl at 171.4 ppm, and a resonance for the xanthate thiocarbonyl at 214.2 ppm, Figure S2.37. ESI-MS confirmed populations at 678 Da (MH^+ = 678 Da), 700 Da (MNa^+ = 700 Da) and 716 Da (MK^+ = 716 Da), Figure 2.23.

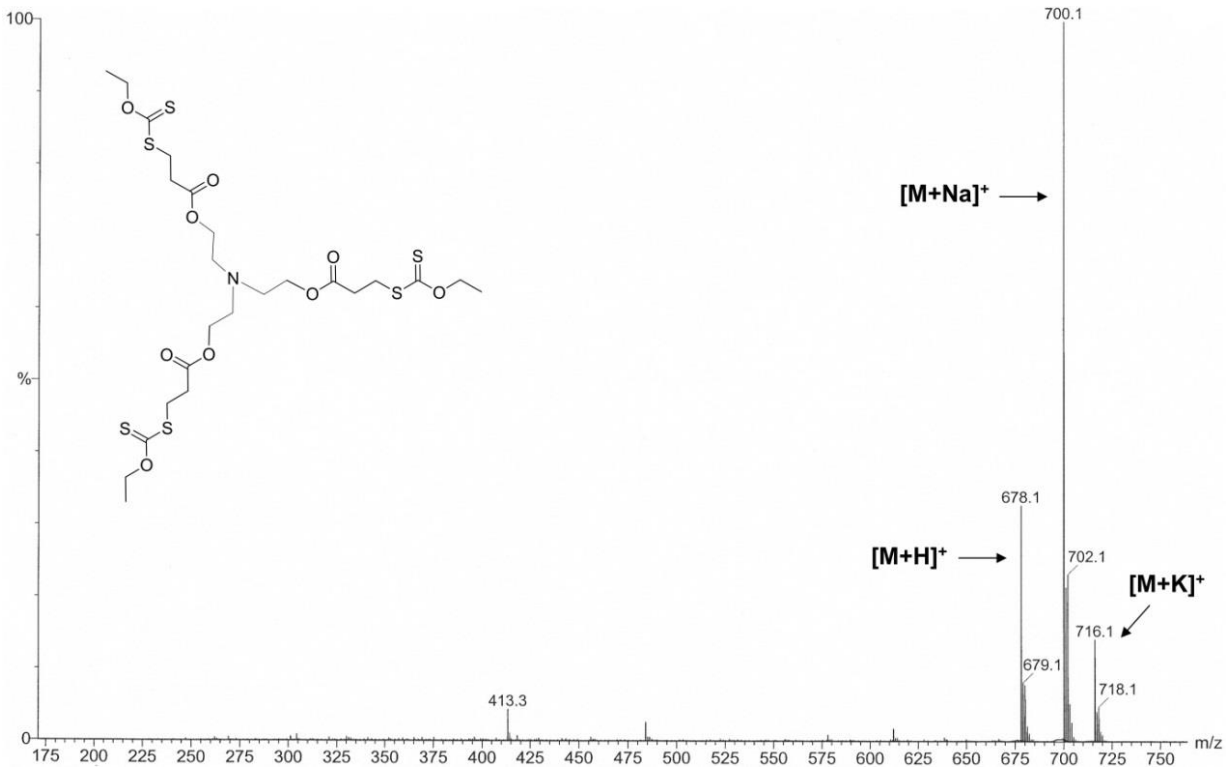

Figure 2.23 ESI-MS (MeOH) spectrum of **[Xan_3-P-TEA];[36]**

Using **[36]**, a one-pot deprotection and functionalisation strategy was evaluated by two model reactions, Schemes 2.21 and 2.22. Following reported procedures, deprotection by aminolysis and subsequent one-pot thiol-acrylate Michael additions were studied in THF, in the presence of n-butylamine.[11] **[36]** was dissolved in THF and vigorously degassed with nitrogen for 10 minutes.

Following this, 3.3 equivalents of n-butylamine amine were slowly added, and the reaction was left sealed under nitrogen for 1.5 hours. TLC analysis (hexane/ethyl acetate 60:40) confirmed total loss of the dendrimer starting material after 1.5 hours, at which point 3 equivalents of **[BA]** were added to the vessel.

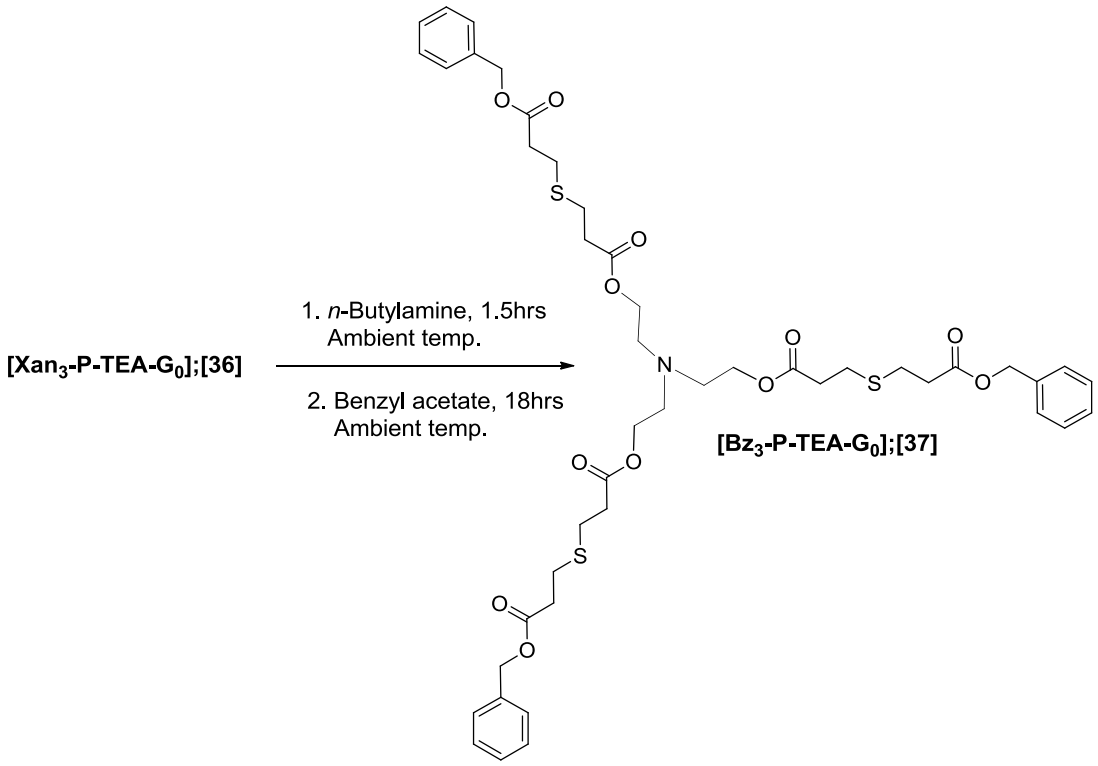

Scheme 2.21 Formation of **[Bz_3-P-TEA];[37]** via a one-pot deprotection and functionalisation strategy using dendrimer **[Xan_3-P-TEA];[36]** and **[BA]**

After 18 hours, purification was achieved by reducing the volume of THF by half under vacuum, and precipitating the mixture twice into hexane. Removal of solvents resulted in **[Bz_3-P-TEA];[37]** as a pale orange oil in 75% yield. Analysis of the functionalised dendrimer by ^{1}H and ^{13}C NMR and ESI-MS confirmed a one-pot deprotection and thiol Michael addition reaction had indeed taken place. As expected, total loss of the characteristic xanthate thiocarbonyl at 214.2 ppm (^{13}C NMR) was observed and the formation of new proton and carbon environments in the ^{1}H and ^{13}C spectra were seen for the Michael adduct, Figure 2.24 and S2.38. ESI-MS confirmed populations at 900 Da (MH^+ = 900 Da), 922 Da (MNa^+ = 922 Da) and 938 Da (MK^+ = 938), Figure 2.25.

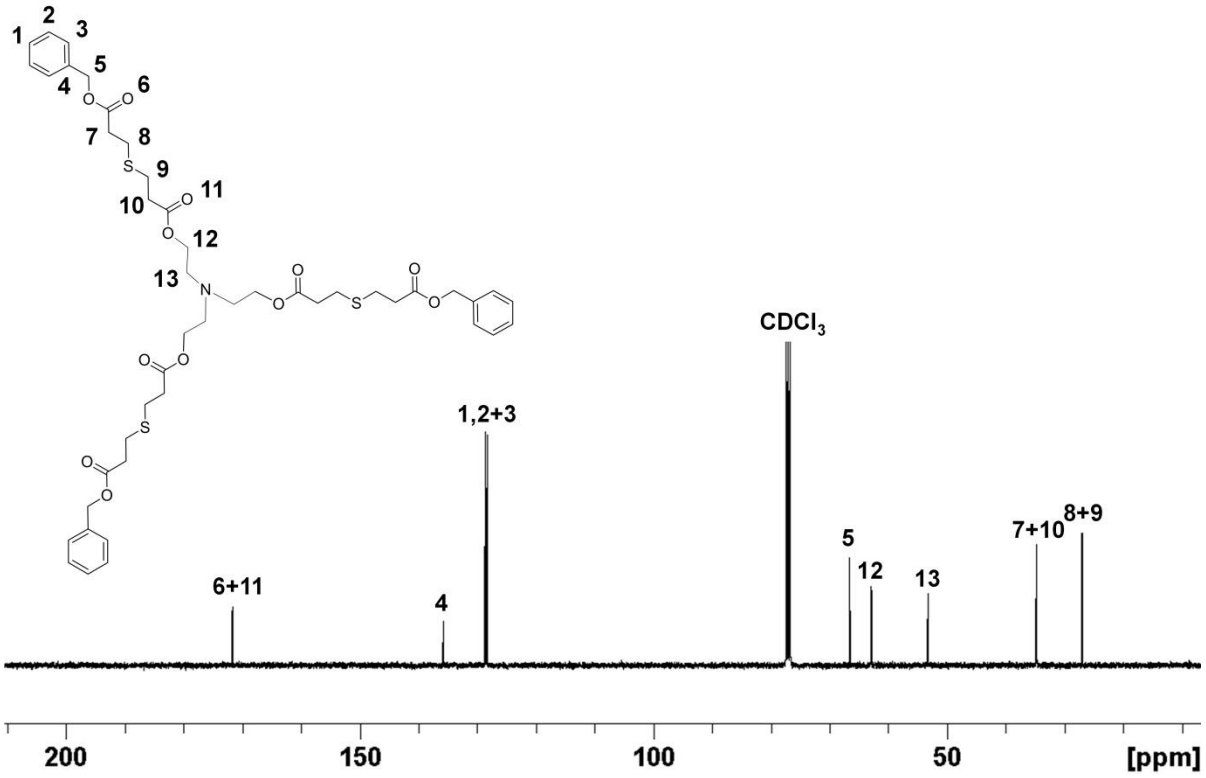

Figure 2.24 ^{13}C NMR spectrum (400MHz, $CDCl_3$) of **[Bz_3-P-TEA-G_0];[37]**

The reaction was repeated using the exact same methodology, but using **[DMAEA]**, as the acrylate substrate, Scheme 2.22.

Purification following the same procedures as **[37]** resulted in **[Am_3-P-TEA];[38]** as a viscous yellow oil in 80% yield. Characterisation by ^{1}H and ^{13}C NMR spectroscopy confirmed the expected total number of resonances, Figure 2.26 and S2.39. ESI-MS confirmed populations at 843 Da (MH^+ = 843 Da), 865 Da (MNa^+ = 865 Da) and 881Da (MK^+ = 881 Da), S2.40. The two model reactions clearly demonstrated the effectiveness of this chemistry, and its potential for a highly efficient synthetic technique for the preparation of surface functional dendritic materials.

Chapter 3 will continue from these final successful findings, and a synthetic route will be designed and implemented to target higher generation materials.

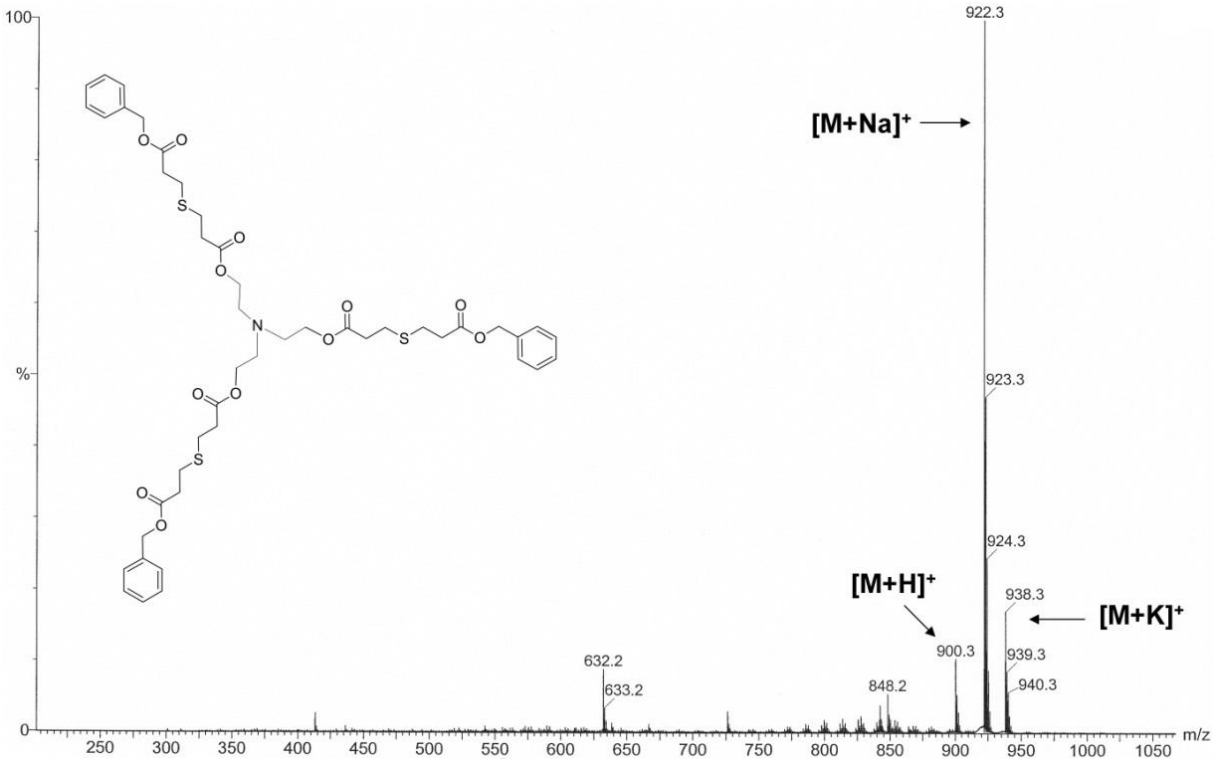

Figure 2.25 ESI-MS (MeOH) spectrum of **[Bz_3-P-TEA-G_0];[37]**

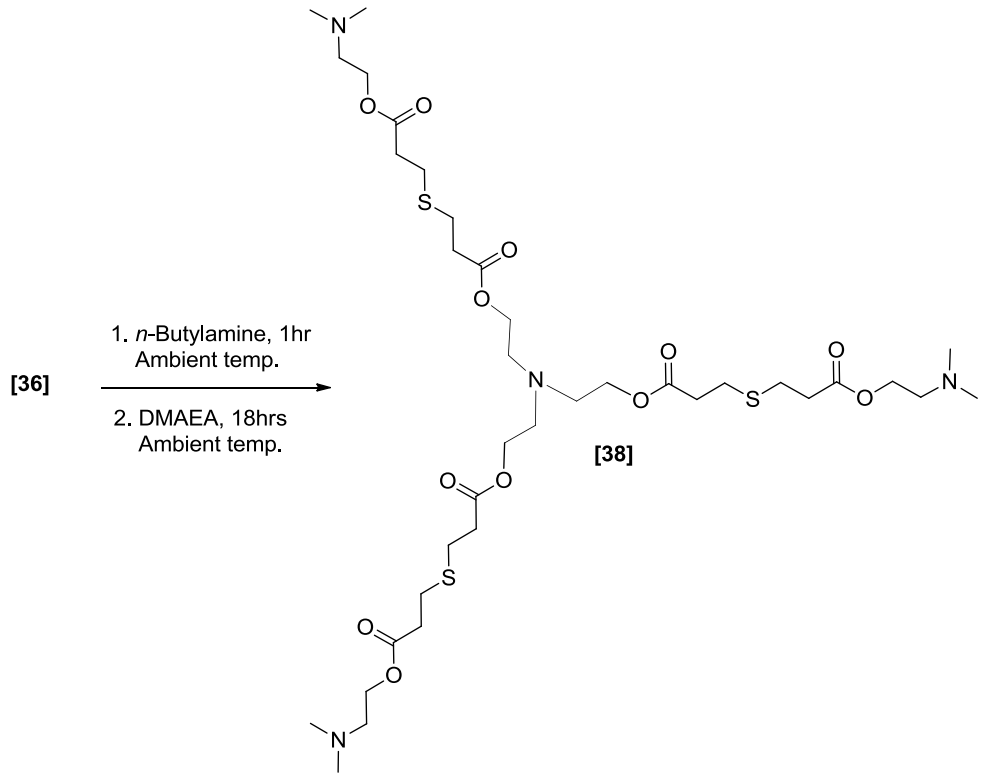

Scheme 2.22 Formation of **[Am_3-P-TEA];[38]** via a one-pot deprotection and functionalisation strategy using dendrimer **[Xan_3-P-TEA];[36]** and **[DMAEA]**

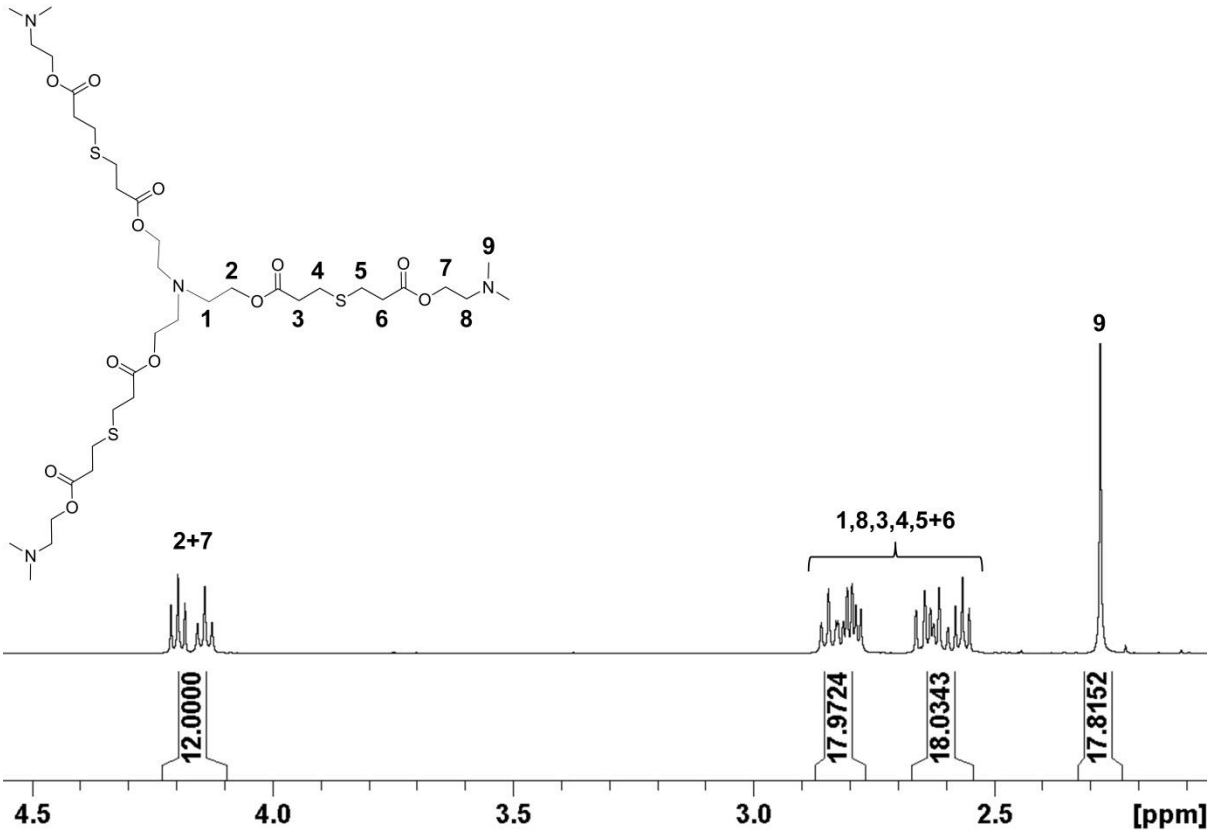

Figure 2.26 ^{1}H NMR spectrum (400MHz, $CDCl_3$) of **[Am_3-P-TEA-G_0];[38]**

2.4 Conclusions

The synthesis of functional dendritic materials using amine and thiol Michael addition was successfully achieved. Dendron functionalisation via amine Michael addition led to pure materials up to G_2, but was found to be inefficient when higher generation materials were targeted. Long reactions times, tedious purification and excess reagents were commonly occurring issues when attempting to target higher generations. As a consequence, thiol Michael addition was investigated as an alternative functionalisation strategy.

Initial attempts to synthesise multi-functional thiol peripheral dendrons resulted in several unsuccessful attempts. In the first attempt, a synthetic strategy utilising a disulfide bond led to complications during the convergent growth steps, resulting in the targeted materials not being isolated. In the second attempt, a synthetic approach using a thiol protecting group, commonly known

as Sanger's reagent, led to multi-functional thiol-protected dendrons to G_1. Higher generation materials were targeted, but without synthetic success. An extensive problem of this strategy was the use of a very large excess of dodecanethiol to remove the Sanger's protecting group; thus an alternative strategy was sought.

In a final attempt, a xanthate group was used as a thiol protecting group. Since the conditions under which xanthate removal and thiol-acrylate Michael addition occurred, were the same, removal of the xanthate functionality and thiol-acrylate Michael addition could be performed in the same pot, eliminating the need to isolate the generated thiol intermediate. A G_0 xanthate functional dendrimer was used as model compound, and fully characterised both before, and after, xanthate removal and thiol-acrylate Michael addition.

Future work may focus on further synthetic improvements to the disulfide and Sanger's protecting group strategy to multi-functional thiol peripheral materials; although it is doubtful these synthetic routes will ever rival the facile nature of the one-pot xanthate deprotection and thiol-acrylate approach.

2.5 References

1. D. A. Tomalia, H. Baker, J. Dewald, M. Hall, G. Kallos, S. Martin, J. Roeck, J. Ryder and P. Smith, *Polymer Journal*, 1985, **17**, 117-132.
2. K. Matyjaszewski, *Macromolecules*, 2012, **45**, 4015-4039.
3. X. Bories-Azeau and S. P. Armes, *Macromolecules*, 2002, **35**, 10241-10243.
4. S. P. Rannard and N. J. Davis, *Organic Letters*, 2000, **2**, 2117-2120.
5. W. J. Feast, S. P. Rannard and A. Stoddart, *Macromolecules*, 2003, **36**, 9704-9706.
6. H. Willcock, *Thesis*, 2008.
7. T. He, D. J. Adams, M. F. Butler, A. I. Cooper and S. P. Rannard, *Journal of the American Chemical Society*, 2009, **131**, 1495-1501.
8. M. Trollsås, C. J. Hawker, J. L. Hedrick, G. Carrot and J. Hilborn, *Macromolecules*, 1998, **31**, 5960-5963.
9. G. Carrot, J. G. Hilborn, M. Trollsås and J. L. Hedrick, *Macromolecules*, 1999, **32**, 5264-5269.
10. G.-Z. Li, R. K. Randev, A. H. Soeriyadi, G. Rees, C. Boyer, Z. Tong, T. P. Davis, C. R. Becer and D. M. Haddleton, *Polymer Chemistry*, 2010, **1**, 1196-1204.
11. R. Nicolaÿ, *Macromolecules*, 2011, **45**, 821-827.
12. M. Le Neindre, B. Magny and R. Nicolay, *Polymer Chemistry*, 2013, **4**, 5577-5584.
13. M. Le Neindre and R. Nicolaÿ, *Polymer International*, 2014, **63**, 887-893.
14. C. J. Hawker and J. M. J. Frechet, *Journal of the American Chemical Society*, 1992, **114**, 8405-8413.
15. H. Ihre, A. Hult, J. M. J. Fréchet and I. Gitsov, *Macromolecules*, 1998, **31**, 4061-4068.
16. J. S. Moore and S. I. Stupp, *Macromolecules*, 1990, **23**, 65-70.

CHAPTER 3

A Facile and Highly Efficient Functionalisation Strategy of Polyester Dendrimers via "One-Pot" Xanthate Deprotection/Thiol- Acrylate Michael Addition Reactions

Publication arising from this chapter: "The First Peripherally Masked Thiol Dendrimers: A Facile and Highly Efficient Functionalization Strategy of Polyester Dendrimers via One-Pot Xanthate Deprotection/Thiol-Acrylate Michael Addition Reactions." See: S. E. R. Auty, O. Andrén, M. Malkoch and S. P. Rannard, *Chem. Commun.*, 2014, 50, 6574 – 6577.

3.1 Introduction

In Chapter 2, a number of different synthetic routes to functionalise dendritic materials were explored, and it was concluded that amine-acrylate Michael addition was inefficient under the studied conditions beyond G_2. Attempts were made to utilise thiol-acrylate Michael addition to synthesise thiol-functional dendrons. After several unsuccessful attempts, it was found that if a xanthate group was used as a thiol protecting group, deprotection of the xanthate to generate the reactive thiol and subsequent functionalisation with an acrylate substrate can be performed in the same reaction vessel. This is an extremely effective methodology, since the one-pot process does not require the reactive thiol intermediate to be isolated, eliminating the use of thiols, and reducing likelihood of disulfide formation.

3.2 Aims

The success of the xanthate-derived thiol acrylate reactions suggest a synthetic route to deriving dendrons and dendrimers of significant molecular weight. The aims of this chapter involved targeting four generations of xanthate peripheral dendrimers (G_0, G_1, G_2, G_3) with full characterisation. Using each of these xanthate functional dendrimers, one-pot deprotection and functionalisation via thiol Michael addition will be performed, to introduce hydrophilic, hydrophobic and polymeric functionalisation. A schematic diagram in Figure 3.1 outlines the aims, as illustrated using a G_2 dendrimer.

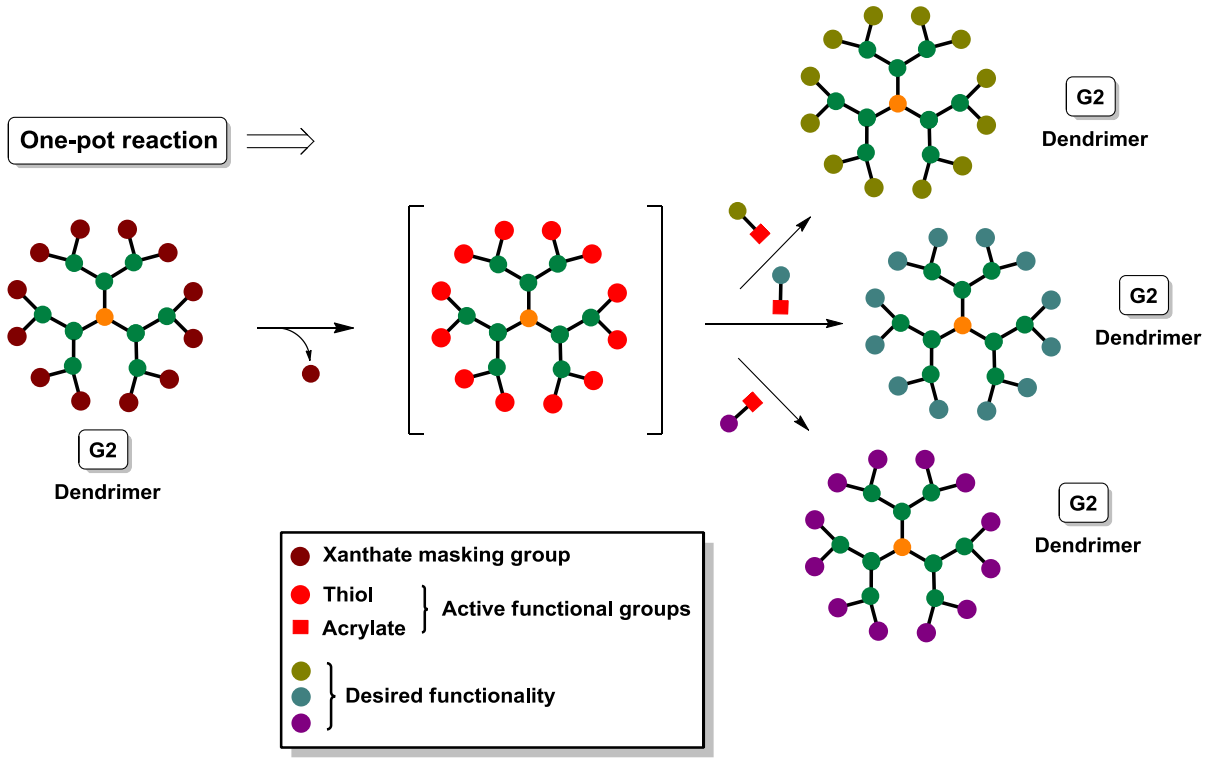

Figure 3.1 Schematic representation of the one-pot xanthate deprotection/Thiol-acrylate functionalisation strategy, illustrated by using a G_2 dendrimer

3.3 Synthetic route: Utilising a convergent approach

Initially a convergent approach for the synthesis of xanthate functional dendrons was adopted, and began with the synthesis of **[35]**, Scheme 3.1, following the procedures described in Chapter 2. Aliphatic polyester chemistry, based on the AB_2 monomer 2,2-bismethylolpropanoic acid (bis-MPA), was chosen for the dendrimer scaffold since the polyester backbone synthesis chemistry is orthogonal to the xanthate peripheral protecting chemistry.

The xanthate functional carboxylic acid **[35]** was activated by conversion to an acid chloride using 2 equivalents of oxalyl chloride and a catalytic amount of DMF in CH_2Cl_2, Scheme 3.1. Particular care was taken since the gases that are generated during this reaction are carbon monoxide and gaseous HCl which are both extremely toxic. After 3 hours at ambient temperature, and confirmation of reaction completion by loss of effervescent, the excess oxalyl chloride was removed by rotary

evaporation using a stripping procedure with chloroform as a co-solvent. Analysis of the dark red oil **[Xan-P-COCl];[39]** by ^{13}C NMR confirmed the acyl chloride formation by the resonance at 172.4 ppm, and the reagent was used immediately to prevent any hydrolysis. To react **[39]** with each of the hydroxyl groups of **bis-MPA**, a 1.1 excess of **[39]** per OH group was used, together with triethylamine and 4-dimethylaminopyridine (DMAP) in CH_2Cl_2. After 16 hours at room temperature, the crude product was filtered, diluted with CH_2Cl_2, washed with water, dried over $MgSO_4$ and purified by liquid chromatography (silica, eluting ethyl acetate:hexane (80:20) increasing the polarity to ethyl acetate:hexane (20:80)) to result in the G_1 xanthate dendron **[Xan$_2$-P-COOH];[40]** as a viscous orange oil in 71% yield, Scheme 3.1.

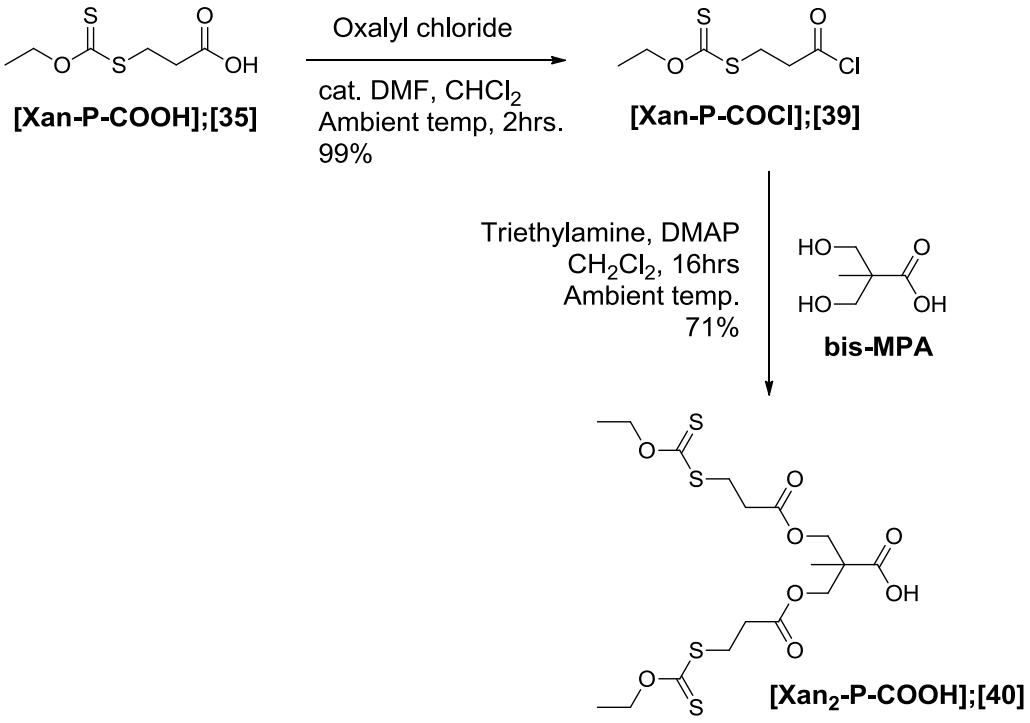

Scheme 3.1 Synthesis of xanthate functional dendron **[Xan$_2$-P-COOH];[40]**

The xanthate functional dendron **[40]** was characterised using ^1H and ^{13}C NMR as well as ESI-MS. ^1H NMR confirmed six environments in the expected ratios, Figure 3.2, and ^{13}C NMR confirmed ten environments, including the newly formed ester carbonyl at 171 ppm, Figure S3.1. ESI-MS confirmed the correct mass at 509 Da (MH^+ = 509 Da).

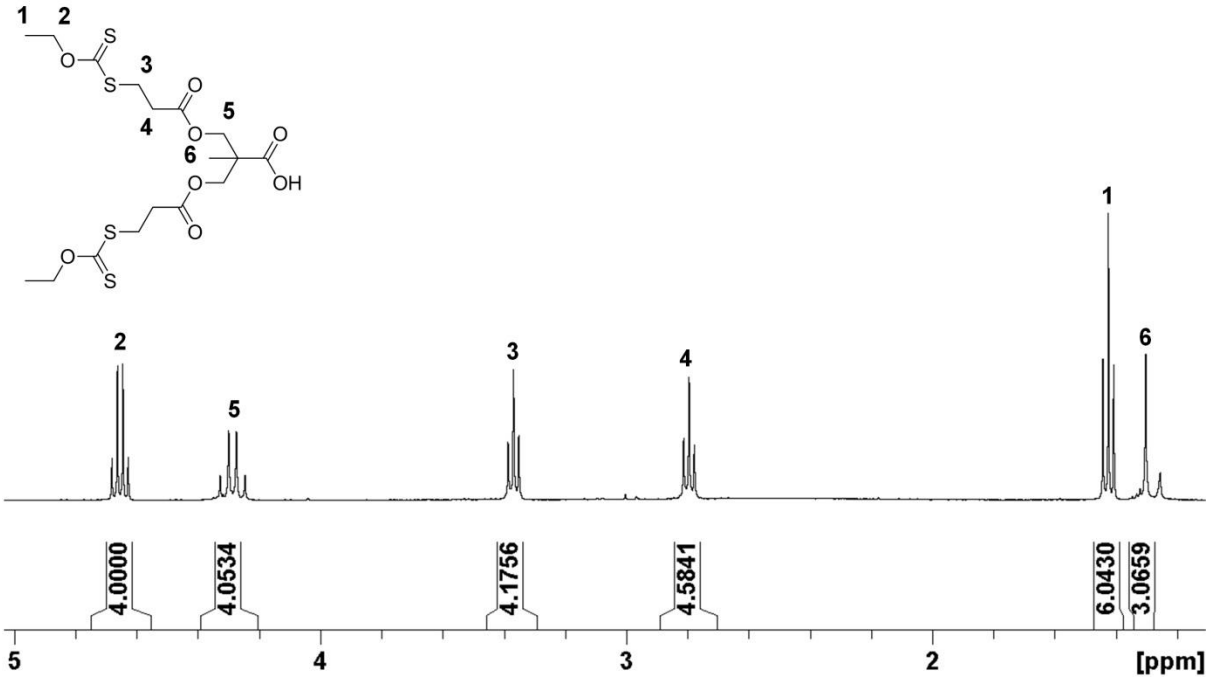

Figure 3.2 ^{1}H NMR spectrum (400 MHz, $CDCl_3$) of xanthate functional dendron **[Xan$_2$-P-COOH];[40]**

The synthesis of the G_2 dendron followed a similar procedure, through activation of the focal point of **[40]**, Scheme 3.2.

Oxalyl chloride was reacted in a 2:1 ratio with the G_1 dendron **[40]** and a catalytic amount of DMF in CH_2Cl_2. Purification was achieved by removing the excess oxalyl chloride after dilution with chloroform on the rotary evaporator, resulting in a red oil in 99% yield. A comparison between the ^{1}H NMR resonances of the three protons attached to the tertiary methyl of **[40]** and **[41]**, showed a downfield shift from 1.30 ppm to 1.40 ppm, confirming the acyl chloride. **[41]** was used immediately, and added dropwise to a mixture of DMAP, triethylamine and bis-MPA in CH_2Cl_2 to enable coupling to both primary hydroxyls of bis-MPA. After 16 hours at room temperature, the crude product was filtered, washed with water, dried over $MgSO_4$ and purified by column chromatography (silica gel, eluent EtOAc/hexane). Unfortunately, analysis of the resulting oil by ESI-MS confirmed partially acylated materials and predominantly starting materials, Figure S3.2. Attempts were made to change the reaction conditions by increasing the ratio of **[41]** to 2 per hydroxyl group of bis-MPA, but ESI-MS still confirmed presence of partial substitution.

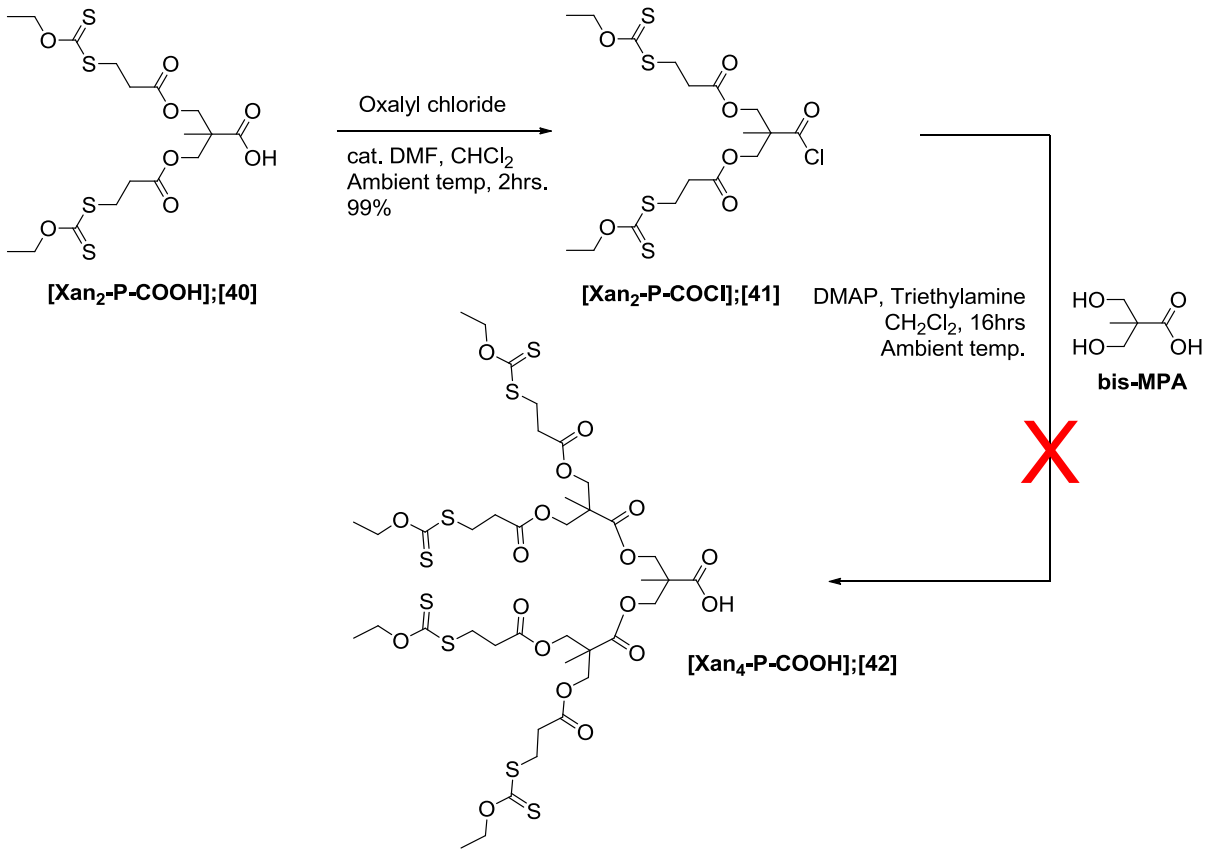

Scheme 3.2 Synthesis of xanthate functional dendron **[Xan$_2$-P-COOH];[42]**

It was noted that in the first convergent synthesis of a bis-MPA dendrimer reported by Ihre *et al.*, the focal point of each bis-MPA dendron was always protected during each convergent growth step by a benzyl ester protecting group.[1] The authors showed that following the growth, the benzyl ester could be selectively removed via hydrogenation without affecting the resulting ester bonds. Adopting the same strategy, a benzyl ester protected bis-MPA, **[43]**, was prepared, Scheme 3.3.

The benzyl ester protected bis-MPA **[OH$_2$-COBz];[43]** was prepared by forming the potassium carboxylate using potassium hydroxide (KOH) in DMF at 100 °C for 1 hour. Benzyl bromide was added, and the reaction was left stirring at 100 °C for 15 hours. The product was isolated by the removal of DMF, redissolving the crude mixture in dichloromethane, washing twice with water, drying the organic layer over $MgSO_4$ and removal of solvents. Further purification obtained by recrystallisation from dichloromethane/hexane generated a cream solid in 65% yield. Analysis of the solid by ^{1}H NMR confirmed **[OH$_2$-COBz];[43]**, Figure S3.3.

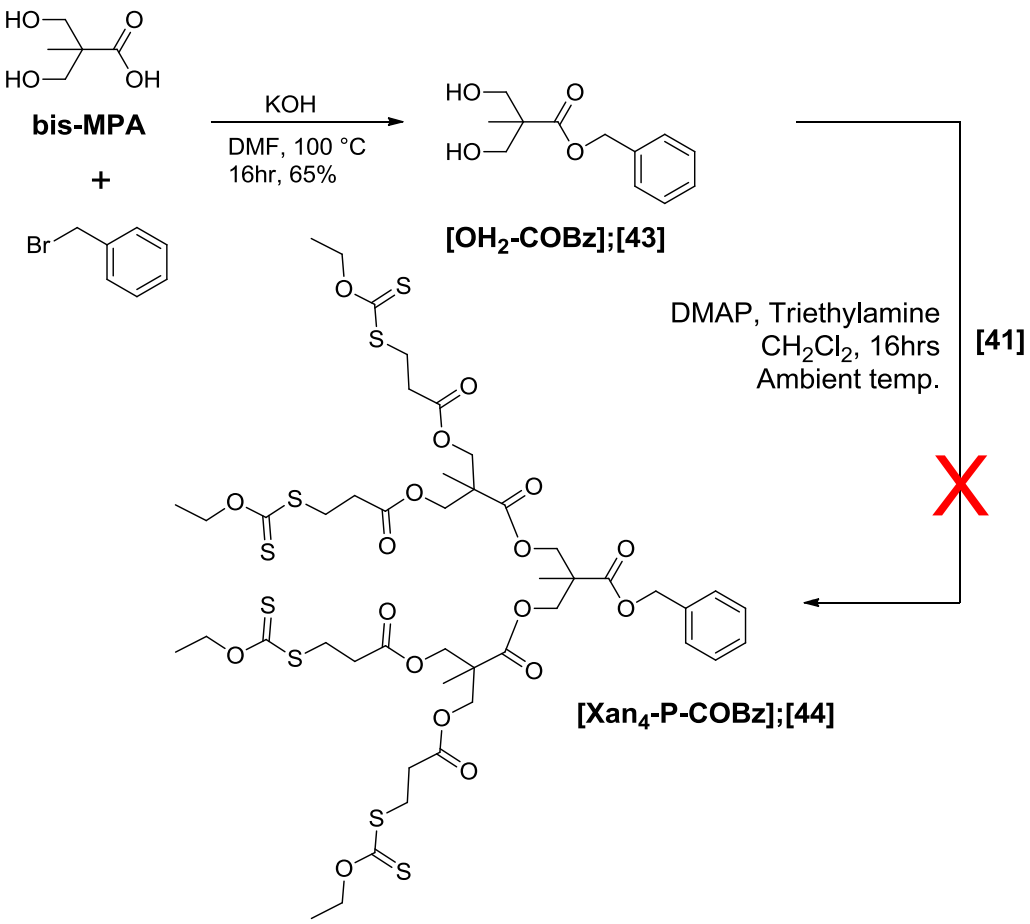

Scheme 3.3 Synthesis of xanthate functional dendron **[Xan$_2$-P-COOH];[44]** utilising a benzyl ester focal point protecting group.

Using **[OH$_2$-COBz];[43]** and 1:4 molar ratio of **[41]**, the synthesis of **[Xan$_2$-P-COOH];[44]** was attempted. After 16 hours at room temperature, the crude product was filtered, washed with water, dried over $MgSO_4$ and purified by liquid column chromatography (silica gel, eluent EtOAc/hexane). Unfortunately, analysis of the resulting oil confirmed no difference in substitution, and the mixture still consisted predominantly of starting materials.

It was concluded that the lack to reactivity to form **[Xan$_2$-P-COOH];[42]** or **[Xan$_2$-P-COOH];[44]** was probably due to the steric bulk of **[41]**. A synthetic route that combined aspects of both the divergent strategy and the convergent strategy was therefore sought.

3.4 Synthetic route: Utilising a divergent approach and convergent approach

3.4.1 Introduction

Both convergent and divergent strategies have their own advantages and disadvantages (Introduction, section 1.2.1 and 1.2.2). It was decided to adopt a divergent growth strategy for the construction of the dendron scaffold and xanthate functionalisation. By selectively removing the focal point functionality, a convergent strategy could be used to couple the xanthate functionalised dendrons to a core to form the resulting dendrimer. By also adopting this route, the focal point functional groups of the resulting dendrons could also be easily modified to initiate polymerisation via a macroinitiator route; discussed later in Chapter 4. The synthetic design is highlighted schematically in Figure 3.3.

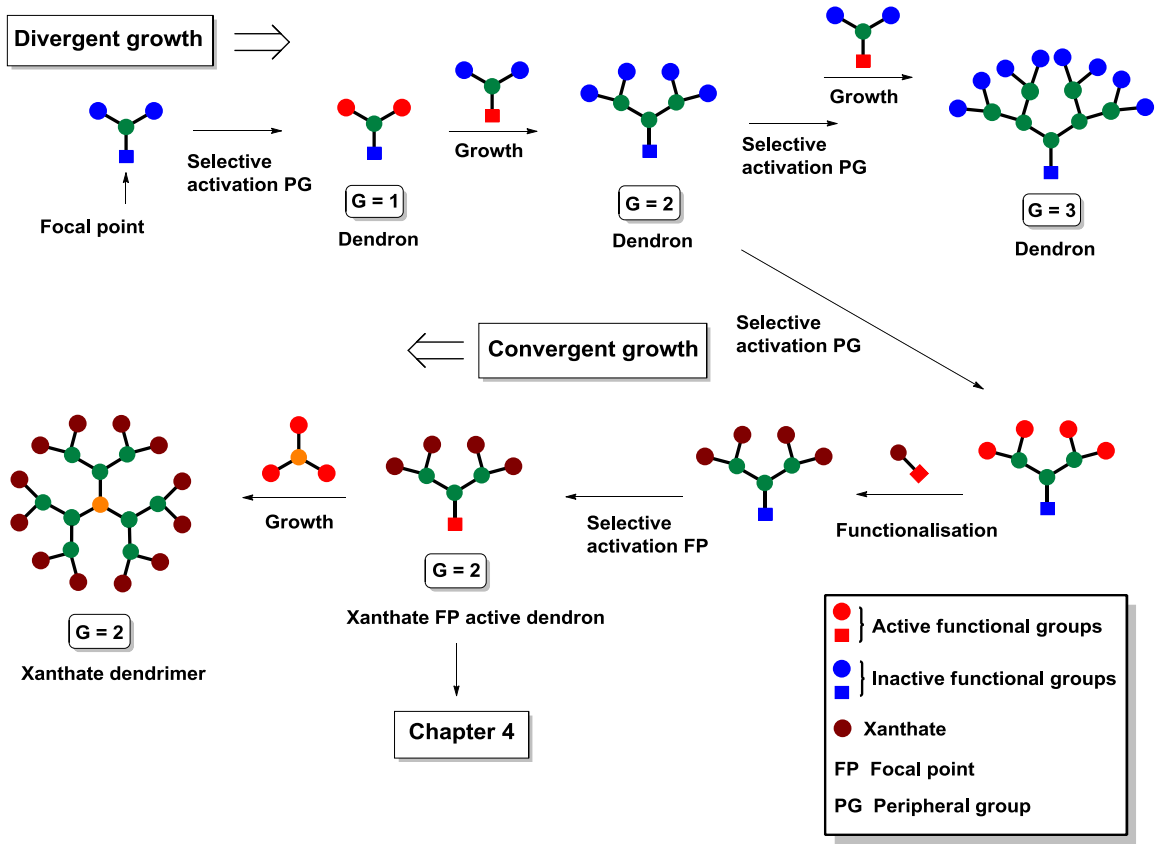

Figure 3.3 Schematic representation of the divergent/convergent approach to xanthate functional dendrimers

3.4.2 Suitability of focal point protecting group

The choice of focal point protection group was crucial to an effective synthesis, since it had to be stable to both the growth/activation chemistry used during the construction of the dendron scaffold, but also be easily removed under conditions that would not degrade the peripheral xanthates, Figure 3.3.

Since the benzyl ester protection group has been shown to be stable to the growth and activation steps used during the construction of bis-MPA dendrimers,[1] a benzyl ester protected xanthate dendron was prepared, whereby a model reaction could be performed to ensure that its removal would not be complicated by the presence of peripheral xanthate groups, Scheme 3.4.

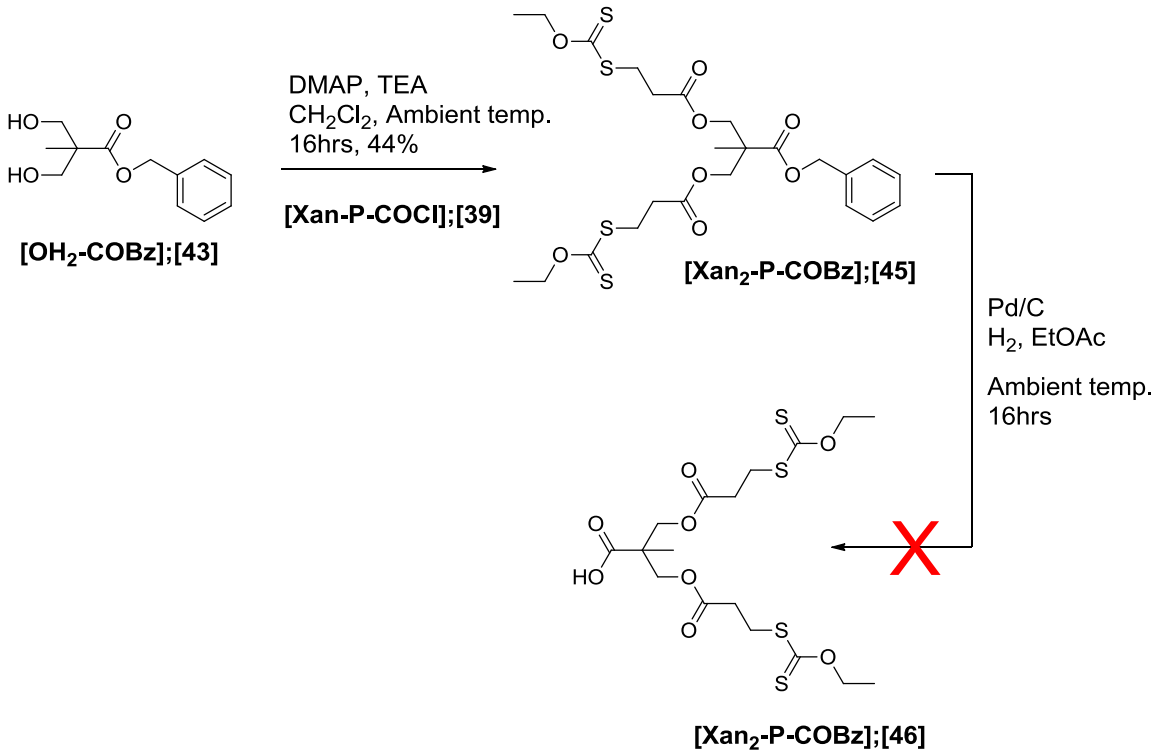

Scheme 3.4 Synthesis of benzyl ester protected xanthate functional dendron **[Xan_2-P-COBz];[45]** and attempted benzyl ester removal

[39] was reacted with each of the hydroxyl groups of **[43]** using a 1.1 excess per OH group, in the presence of triethylamine and DMAP in CH_2Cl_2. After 16 hours at room temperature, the crude product was filtered, washed with water, dried over $MgSO_4$ and purified by column chromatography

(silica gel, eluting with ethyl acetate:hexane 5:95, increasing to 30:70) to result in the G_1 xanthate dendron **[Xan$_2$-P-COBz];[45]** as a viscous orange oil in 44% yield. The material was confirmed using ^{1}H and ^{13}C NMR, Figures S3.4 and S3.5. To remove the protecting group, and generate **[46]**, the compound **[45]** was dissolved in ethyl acetate and palladium on carbon (Pd/C) (10%) added carefully to the reaction vessel. The vessel was backfilled with hydrogen three times and left stirring vigorously under a hydrogen atmosphere (atmospheric pressure), at room temperature for 16 hours.

Unfortunately, analysis by TLC of the reaction after 16 hours showed no evidence of deprotection, and repeating the reaction using a Pd/C catalyst content at 20 wt%, made little difference. It was concluded that catalytic poisoning through the presence of divalent sulfur atoms in the xanthate moieties prevented the hydrogenation reaction from occurring although this was not confirmed.

Following the problems with removal of the benzyl ester protecting group, a new focal point protecting group was chosen. Recently Parrott *et al*. synthesised and radiolabeled a series of bis-mPA polyester dendrons using complexation of ^{99m}Tc and utilising an easily removable *p*-toluenesulfonyl ethyl (TSe) focal point protecting group.[2] This protecting group was shown to be stable throughout the dendron growth and deprotection conditions developed by Ihre *et al.*[3] Furthermore, its facile removal was achieved using the non-nucleophilic base 1,8-diazabicyclo[5.4.0]undec-7-ene (DBU).

A comprehensive search in the literature of xanthate stability towards DBU found no known cases of side reactions, and therefore the formation of bis-MPA dendrons utilising the TSe protecting group was attempted.

3.4.3 Synthesis of bis-MPA scaffold by a divergent route

The monomer that was used was the highly reactive benzylidene protected bis-MPA anhydride, developed by Ihre *et al.*[3] and prepared in two synthetic steps, Scheme 3.5.

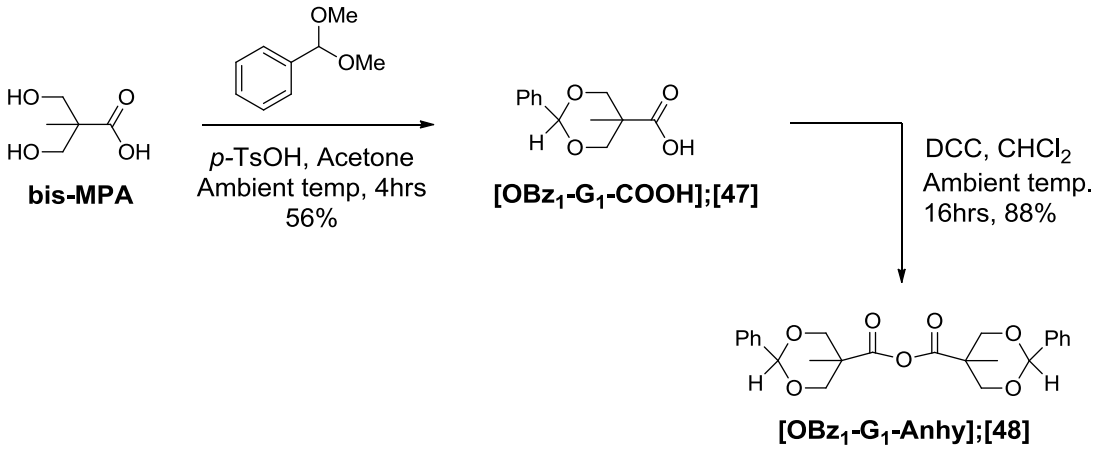

Scheme 3.5 Preparation of anhydride monomer **[OBz_1-G_1-Anhy];[48]**

In the first step, bis-MPA, benzaldehyde dimethyl acetal, and a catalytic amount of *p*-toluenesulfonic acid (TsOH) were dissolved in acetone, and stirred at ambient temperature for 4 hours. After filtration, **[47]** was obtained as white crystals in 56% yield. The anhydride monomer **[OBz_1-G_1-Anhy];[48]** was prepared through the self-condensation of **[47]** by dissolving in CH_2Cl_2 and adding 0.55 equivalents of *N,N'*-dicyclohexylcarbodiimide (DCC) as the dehydrating agent. The reaction was followed using ^{13}C NMR, to monitor the change in the resonance of the carbonyl environment from 179 ppm to 169 ppm, indicative of anhydride formation. After 16 hours, ^{13}C NMR confirmed total loss of the acid resonance, and the crude product was filtered to remove the DCU (*N,N'*-dicyclohexylurea) byproduct. Purification was obtained by precipitating the crude monomer into hexane to result in white crystals in 88% yield and the solid was stored carefully in a desiccator to prevent any degradation of the anhydride. Utilising this monomer, three generations of bis-MPA dendrons were prepared, Scheme 3.6.

The synthesis of the G_1 dendron **[49]** was accomplished by reacting *p*-toluene sulfonyl ethanol (***p*-TSe**) with two equivalents of anhydride monomer **[48]** in the presence of four equivalents of pyridine and 0.2 equivalents of 4-dimethylaminopyridine (DMAP) per hydroxyl group, at ambient temperature for 16 hours. After quenching of the excess anhydride with water for 3 hours, the crude product was diluted with CH_2Cl_2 extracted with 1M $NaHSO_4$, then 1M $NaHCO_3$, and brine to remove the DMAP,

pyridine and benzylidene-protected acid **[47]**. Drying the organic layer over $MgSO_4$ and removal of CH_2Cl_2 yielded the G_1 dendron **[49]** as a white solid in 98%.

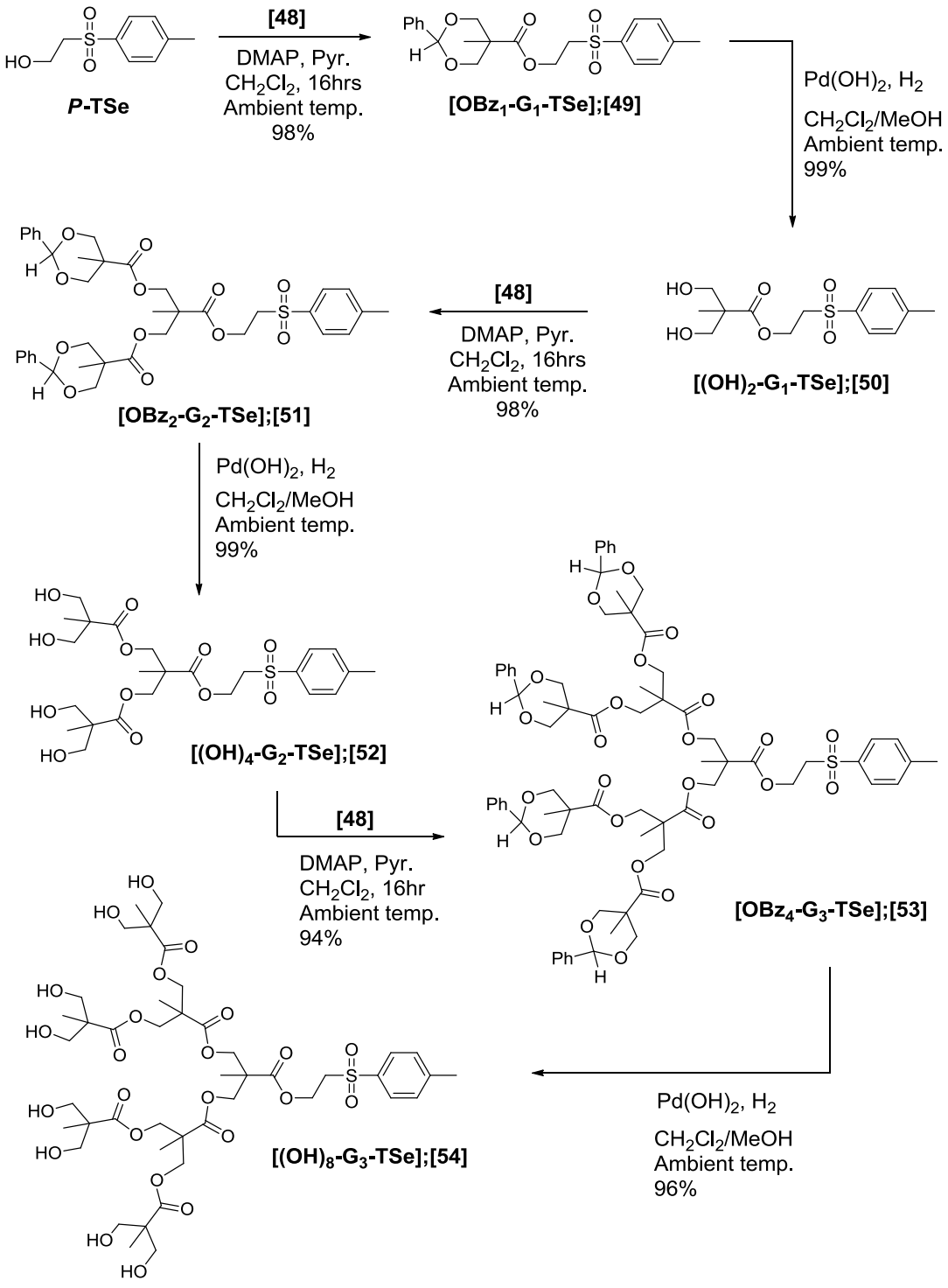

Scheme 3.6 Preparation three generations of bis-MPA dendrons using anhydride monomer **[OBz_1-G_1-Anhy];[48]**

The next step involved a hydrogenation reaction, and used a $Pd(OH)_2$ catalyst (also known as Pearlman's catalyst) under a hydrogen atmosphere (10 bar) for the removal of the benzylidene protecting groups. It was imperative to ensure that all the pyridine and DMAP were removed during the previous extraction steps, otherwise poisoning of the catalyst would result.

The benzylidene protecting groups were readily removed by dissolving **[49]** in a 1:1 mixture of CH_2Cl_2 and methanol, and carefully adding 10% w/w $Pd(OH)_2/C$ (10%) to the mixture. Hydrogenation was carried out using a Parr vessel, which was back-filled with hydrogen 3 times before sealing under hydrogen at medium pressure (10 bar) and leaving the mixture vigorously stirring at ambient temperature overnight. The deprotection was easily monitored by TLC, due to the considerable change in polarity of the product relative to the starting material. After 16 hours, the catalyst was removed by filtering the mixture through a celite plug and after removal of solvents **[50]** resulted as a white solid in 99% yield.

Repetition of the same procedure using esterification and hydrogenation steps led to the synthesis of the G_2 and G_3 hydroxyl-terminated dendrons **[52]** and **[54]**, with yields greater than 90% at each stage.

The only issue that was encountered during the synthesis was the with final hydrogenation step to yield **[54]**, Scheme 3.6, which had to be repeated twice to completely remove all the benzylidene protecting groups.

3.4.4 Characterisation of bis-MPA scaffold by a divergent route

3.4.4.1 Analysis by NMR spectroscopy

^{1}H and ^{13}C NMR spectroscopy during the synthesis of these molecules proved invaluable. The anhydride monomer **[48]** was characterised using both ^{1}H and ^{13}C NMR, but ^{13}C NMR was considerably more useful as it provided the characteristic anhydride resonance at 169.2 ppm, Figure 3.4 and Figure S3.8 (see appendix).

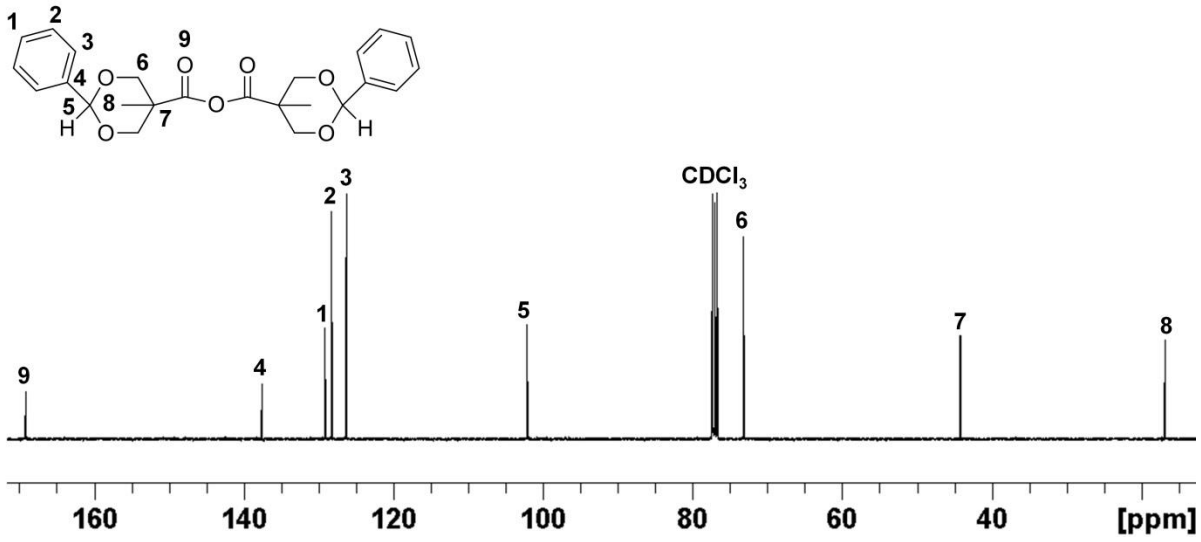

Figure 3.4 ^{13}C NMR spectrum (100 MHz, $CDCl_3$) of anhydride monomer **[OBz$_1$-G$_1$-Anhy];[48]**

NMR spectroscopy with benzylidene protected dendrons **[49]**, **[51]** and **[53]** was performed in deuterated chloroform ($CDCl_3$), but deuterated methanol (CD_3OD) was used with hydroxyl terminated dendrons **[50]**, **[52]** and **[54]** since these materials were not soluble in $CDCl_3$.

Using ^1H NMR, a close examination of the focal point environments relative to the peripheral group environments for dendrons **[49]**, **[51]** and **[53]** was conducted to ensure that complete acylation had taken place. For example, Figure 3.5 illustrates the G_3 benzylidene protected dendron, **[OBz$_3$-G$_3$-TSe];[53]** which when the focal point environment at 7.74 ppm, labelled as environment 13 was calibrated to 2 protons, the integral of the peripheral aromatic resonances at 7.27-7.44 ppm integrated to 22 protons, indicating the four aromatic surface groups (4 x 5 protons) and the additional 2 protons from the TSe protecting group, labelled as environment 14. Similar assignments were made for dendrons **[49]** and **[51]**, see appendix Figures S3.9 and 3.13.

^{13}C NMR was particularly useful to detect the appearance of a new set of monomer environments after each growth step. For example, the ^{13}C NMR spectrum of the G_3 dendron **[OBz$_3$-G$_3$-TSe];[53]** illustrated three different, yet very similar environments for each layer of symmetrical bis-MPA monomers that were present throughout the dendritic backbone, Figure 3.6. The appearance of one new methyl environment, 17.4-21.7 ppm, one new quaternary carbon environment 47.8-51.8 ppm,

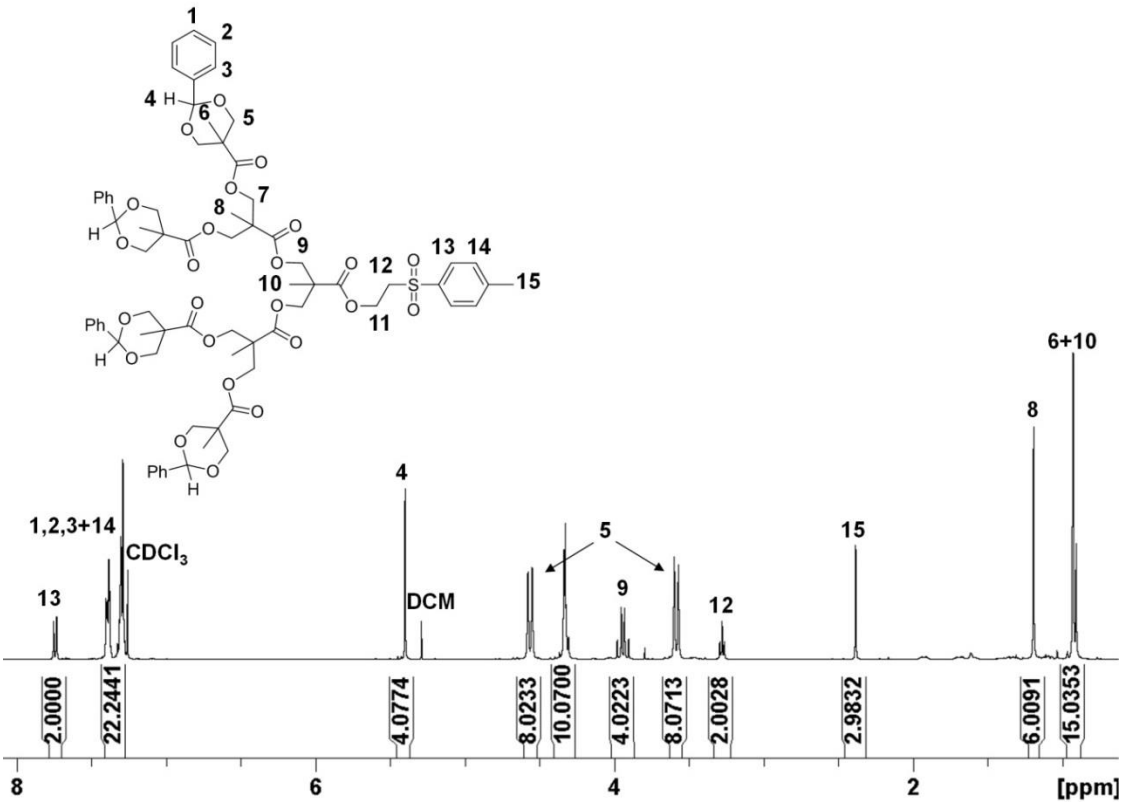

Figure 3.5 ^{1}H NMR spectrum (400 MHz, $CDCl_3$) of benzylidene dendron **[OBz$_3$-G$_3$-TSe];[53]**

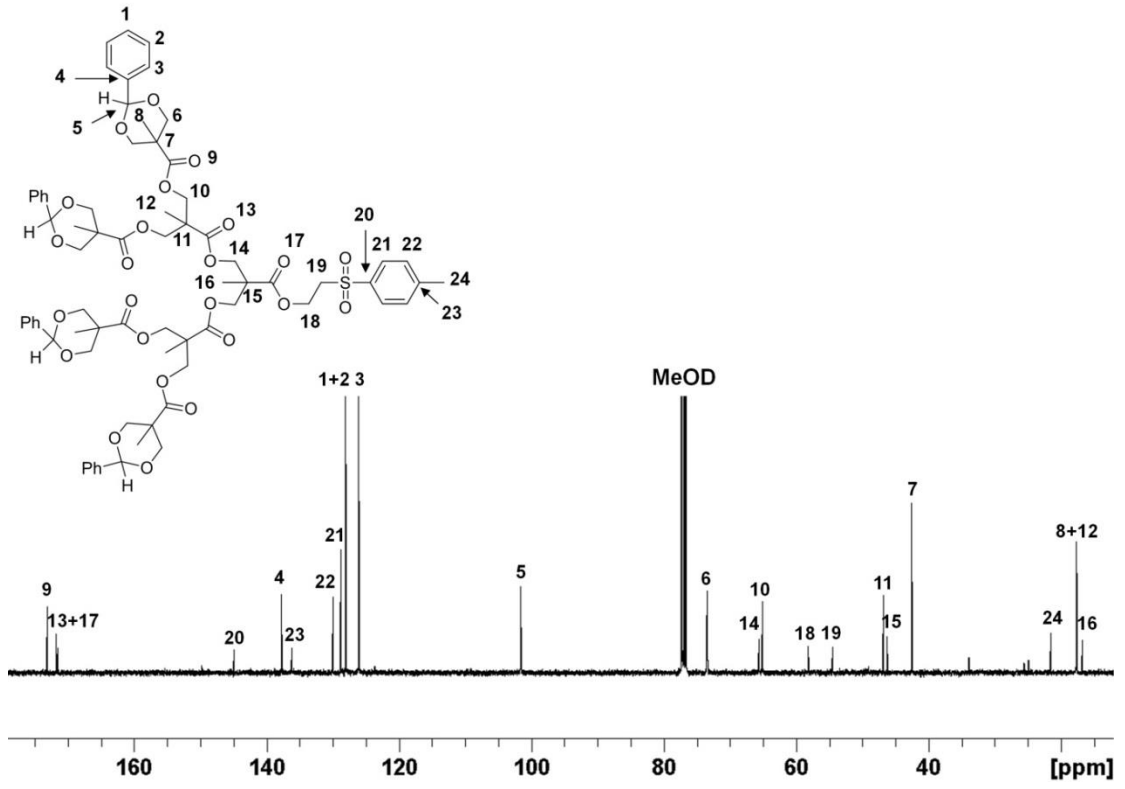

Figure 3.6 ^{13}C NMR spectrum (100 MHz, $CDCl_3$) of benzylidene dendron **[OBz$_3$-G$_3$-TSe];[53]**

one new methylene environment 65.8-67.1 ppm and one new carbonyl environment 171-173 ppm was readily observed after each successive generation, Figure 3.6. Similar assignments were made for dendrons **[49]** and **[51]**, see appendix, Figures S3.10 and S3.14.

Characterisation of the hydroxyl-functional dendrons, **[50]**, **[52]** and **[54]** were also made by using both ^{1}H and ^{13}C NMR spectroscopy. The techniques were used to monitor loss of the benzylidene resonances, and ensure no evidence of backbone degradation had resulted. In each case, ^{1}H NMR analysis of each hydroxyl dendron confirmed total loss of the benzylidene aromatic resonances between 7.27-7.44 ppm and the singlet at 5.42 ppm, **[54]**, Figure 3.7, see appendix for **[50]**, Figure S3.11 and **[52]**, Figure S3.16. No spectroscopic evidence of backbone degradation could be observed. Analysis of the dendrons by ^{13}C NMR also confirmed loss a resonance at 101.7 ppm and also resonances between approximately 120-140 ppm, indicative of the benzylidene environments see appendix for **[54]**, Figure S3.61, **[50]**, Figure S3.12 and **[52]**, Figure S3.14.

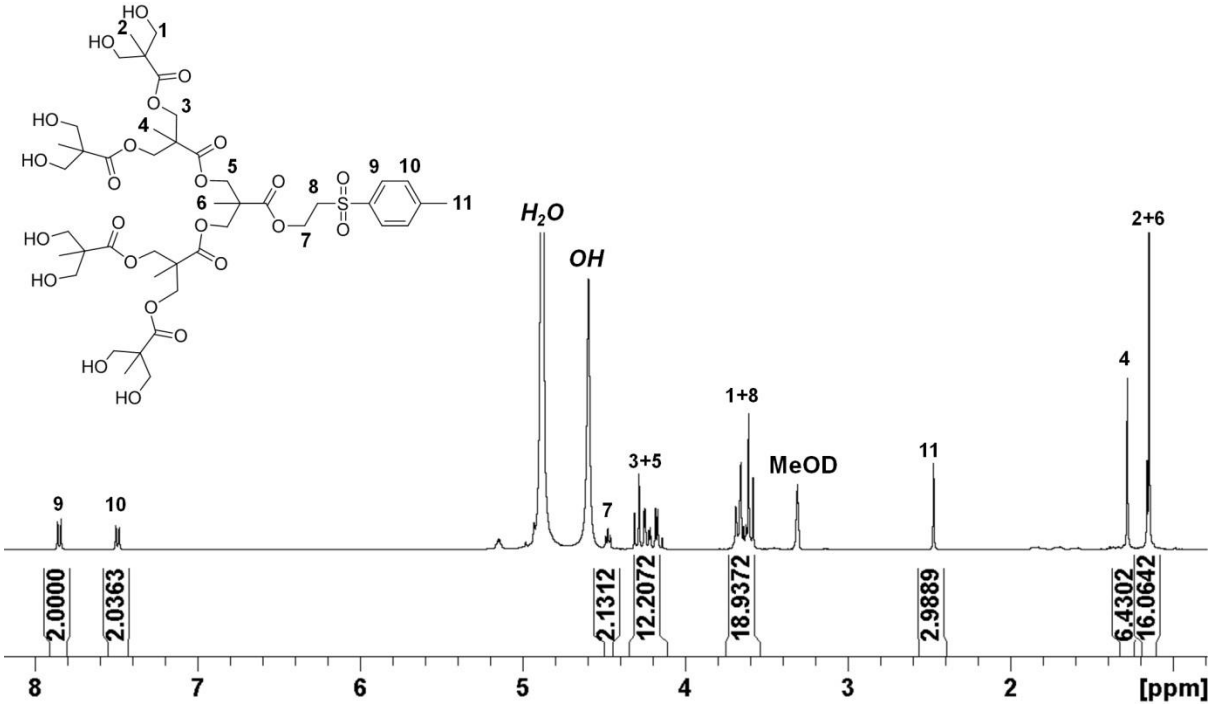

Figure 3.7 ^{1}H NMR spectrum (400 MHz, CD_3OD) of **[$(OH_2)_8$-G_3-TSe];[54]**

3.4.4.2 Analysis by electrospray ionisation mass spectrometry

The G_2 and G_3 dendrons were also analysed by ESI-MS. The G_2 benzylidene, dendron **[OBz$_2$-G$_2$-TSe];[51]** confirmed two populations at 747 Da (MNa^+ = 747 Da) and 763 Da (MK^+ = 763 Da), Figure S3.15. After removal of the peripheral protecting groups, analysis of **[(OH)$_4$-G$_2$-TSe];[52]** indicated no evidence of higher molecular weight species, resulting in two populations at 571 Da (MNa^+ = 571 Da) and 587 Da (MK^+ = 587 Da), Figure S3.18. Observations with the G_3 materials were also similar. Analysis of **[OBz$_3$-G$_3$-TSe];[53]** confirmed two populations at 1387 Da (MNa^+ = 1387 Da) and 1403 Da (MK^+ = 1403 Da), Figure 3.8, and after deprotection via hydrogenation, **[(OH$_2$)$_8$-G$_3$-TSe];[54]** was confirmed by two observed populations at 1035 Da (MNa^+ = 1035 Da) and 1403 Da (MK^+ = 1403 Da), Figure 3.9.

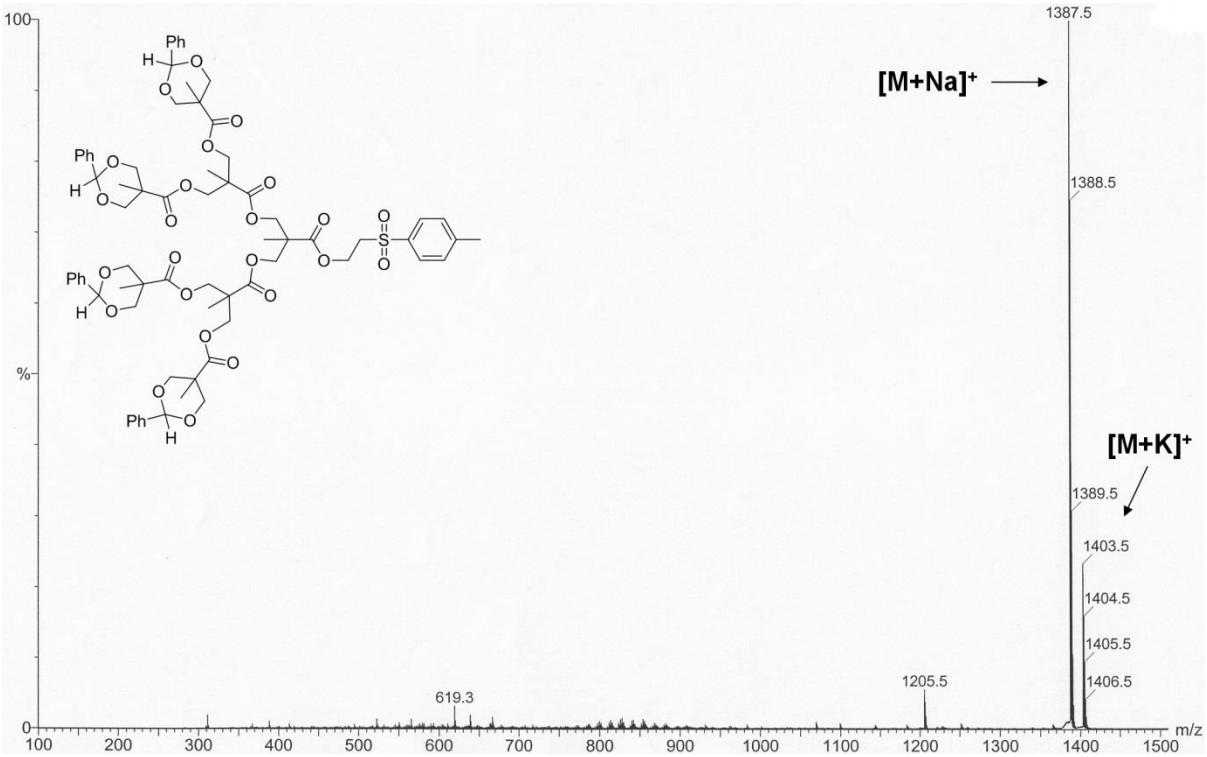

Figure 3.8 ESI-MS (MeOH) of **[OBz$_3$-G$_3$-TSe];[53]**

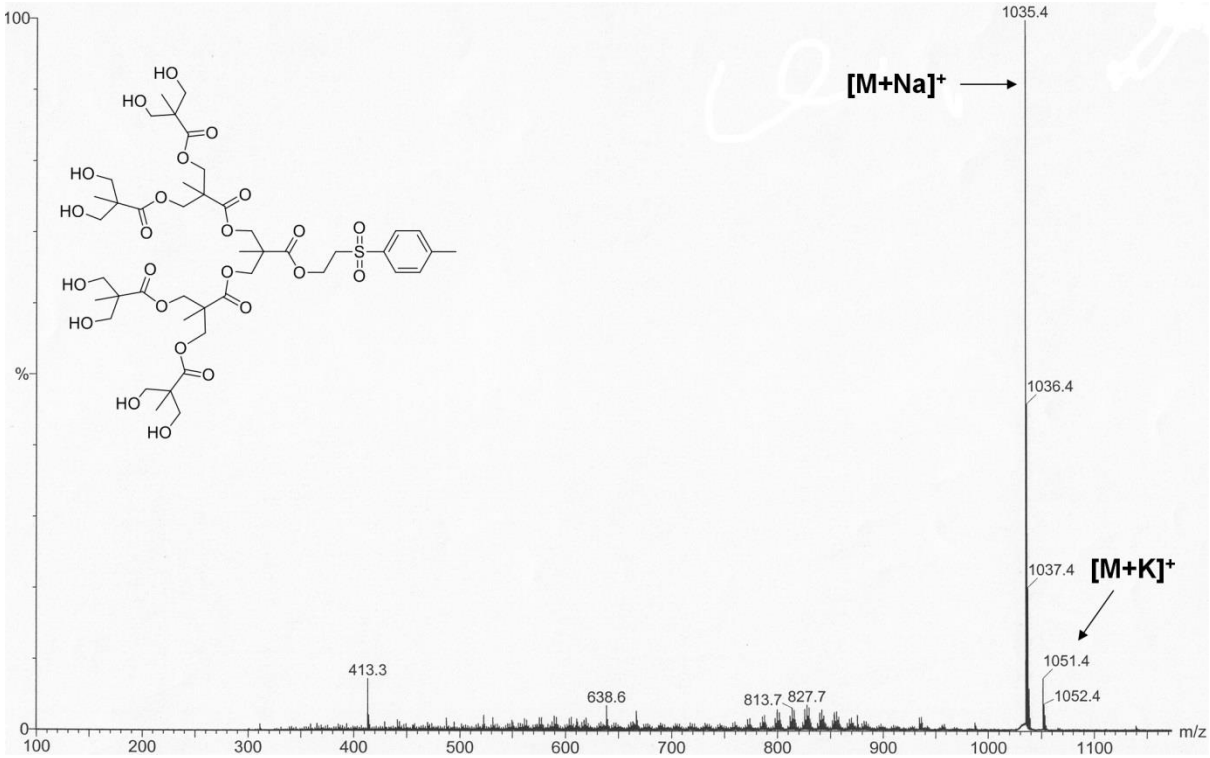

Figure 3.9 ESI-MS (MeOH) of **[OBz$_3$-G$_3$-TSe];[54]**

3.4.4.2 Analysis by SEC

To complete the characterisation, SEC analysis was also performed on the benzylidene dendrons, **[49]**, **[51]** and **[53]**. The hydroxyl terminated dendrons were not soluble in the THF mobile phase, and hence analysis could not be performed using this solvent. The hydroxyl dendrons were soluble in DMF, and attempts were made to study the materials using a DMF SEC system, but due to the high molecular weight column sets fitted to the machine, the samples were too low in molecular weight to obtain good separation. Analysis of the benzylidene protected dendrons **[49]**, **[51]** and **[53]** using SEC with a THF eluent showed narrow dispersity (Đ) in the region of 1.10-1.16 for all samples, Table 3.1. The molecular weights obtained also had good correlation with the expected molecular weights, Table 3.1. Each chromatograph indicated monomodal distributions, Figure 3.10.

Table 3.1 SEC analysis of benzylidene dendrons, **[OBz$_1$-G$_1$-TSe];[49]**, **[OBz$_2$-G$_2$-TSe];[51]** and **[OBz$_3$-G$_3$-TSe];[53]**

Dendron; Entry #	M_{Calc} (Da)	ESI-MS [MNa$^+$] M_{obs} (Da)	SEC[a] M_n	M_w	$Đ$
[OBz$_1$-G$_1$-TSe];[49]	404.1	-	391	428	1.10
[OBz$_2$-G$_2$-TSe];[51]	724.3	747.2	681	764	1.12
[OBz$_3$-G$_3$-TSe];[53]	1364.5	1387.5	1426	1647	1.16

[a]SEC samples were run using a THF mobile phase containing 1% TEA (triethylamine)

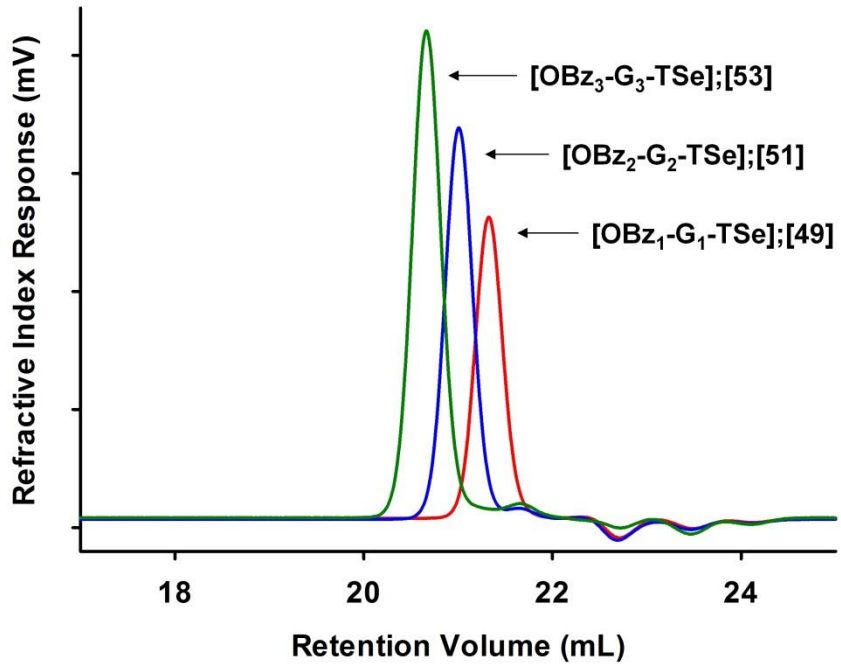

Figure 3.10 SEC analysis (THF) (refractive index detector) of benzylidene dendrons, **[OBz$_1$-G$_1$-TSe];[49]**, **[OBz$_2$-G$_2$-TSe];[51]** and **[OBz$_3$-G$_3$-TSe];[53]**

3.4.5 Functionalisation of the scaffold with xanthate peripheral groups

Previously when a convergent strategy was used, the G_2 dendron could not be obtained. To address this, a divergent/convergent approach was designed. Since the functionalisation of the surface with xanthate requires 2, 4, or 8 multiple esterification reactions it was important to ensure that the acylation chemistry chosen was highly efficient.

3.4.5.1 Xanthate functionalisation via acyl chloride route

Functionalisation of the dendron periphery with xanthates was attempted using the hydroxyl terminated dendron **[$(OH)_4$-G_2-TSe];[52]** and the xanthate acyl chloride **[Xan-P-COCl];[39]**

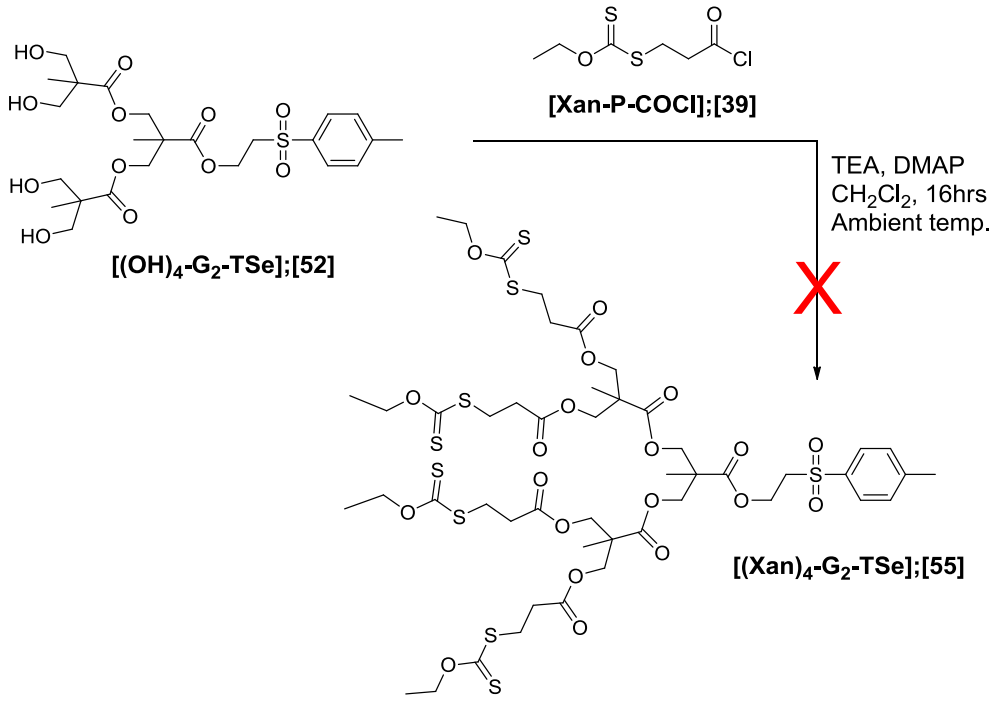

Scheme 3.7 Attempted synthesis of **[$(Xan)_4$-G_2-TSe];[55]** using **[Xan-P-COCl];[39]**

TEA, DMAP and **[52]** were dissolved in CH_2Cl_2 and a 1.2-fold molar excess of **[39]** per hydroxyl group, dissolved in CH_2Cl_2, was added to the vessel and the reaction left stirring under nitrogen for 16 hours. The resulting dark red liquid was filtered, washed with water and purified by using liquid chromatography to form a dark red viscous oil. Unfortunately, analysis of the oil by ESI-MS

confirmed several populations corresponding to partial acylated materials and elimination products, Figure 3.11.

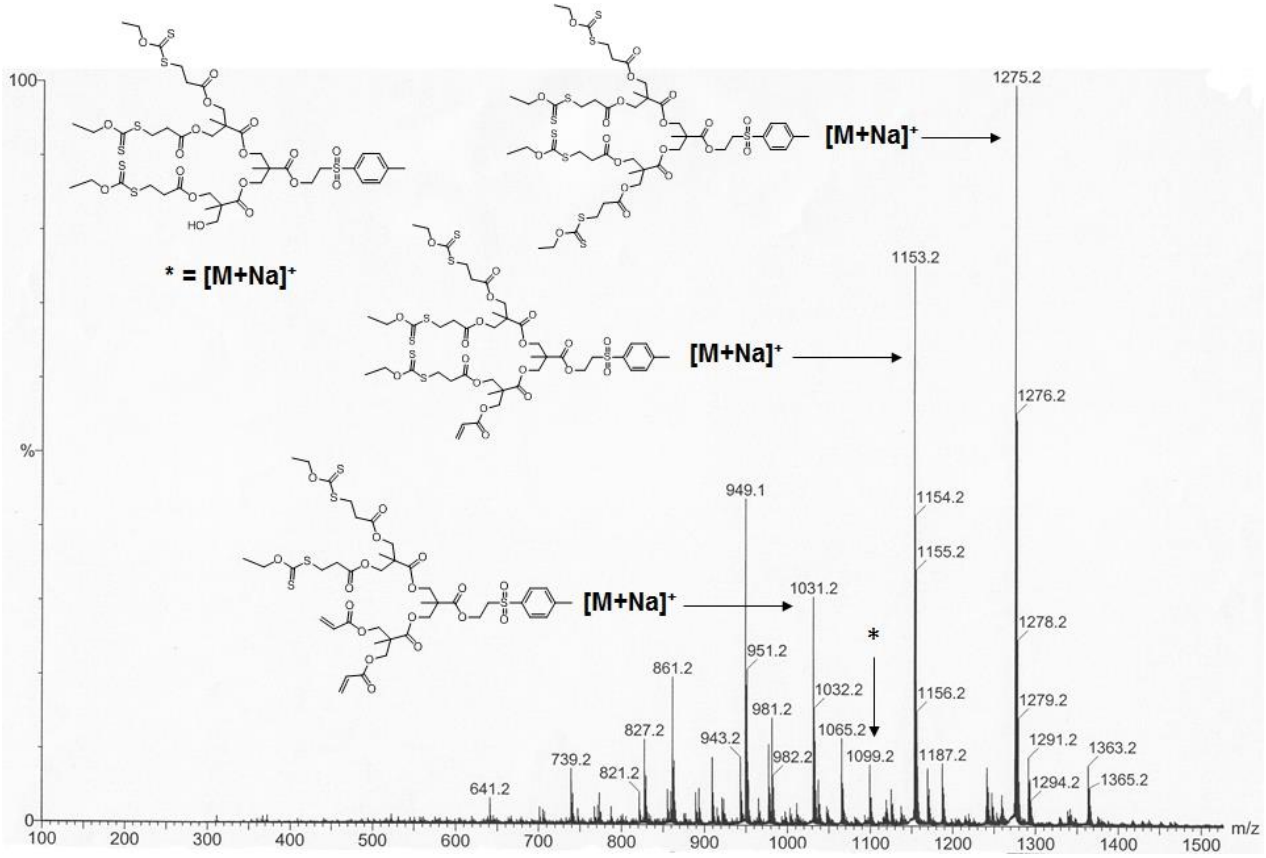

Figure 3.11 ESI-MS analysis of **[(Xan)$_4$-G$_2$-TSe];[55]** via an acyl chloride route

Figure 3.11 shows populations at 1275 Da, 1153 Da and 1031 Da, which all correlate to the sodium adducts of the eliminated structures presented. A population at 1099 Da also confirmed the sodium adduct of a partially acylated product with 3 peripheral xanthates and one hydroxyl group. Further evidence of peripheral acrylate functionalities via elimination was also identified by analysis using ^{1}H NMR, which indicated characteristic proton resonances between 5.88-6.44 ppm, Figure S3.19. A possible explanation of the eliminated side products was the relatively harsh acidic/basic conditions of the acyl chloride reaction, which allowed the acid protons adjacent to the xanthate group to be abstracted, thus resulting in the elimination of the xanthate group.

3.4.5.2 Xanthate functionalisation via DCC esterification

To attempt to resolve these problems, a DCC esterification strategy was attempted, Scheme 3.8.

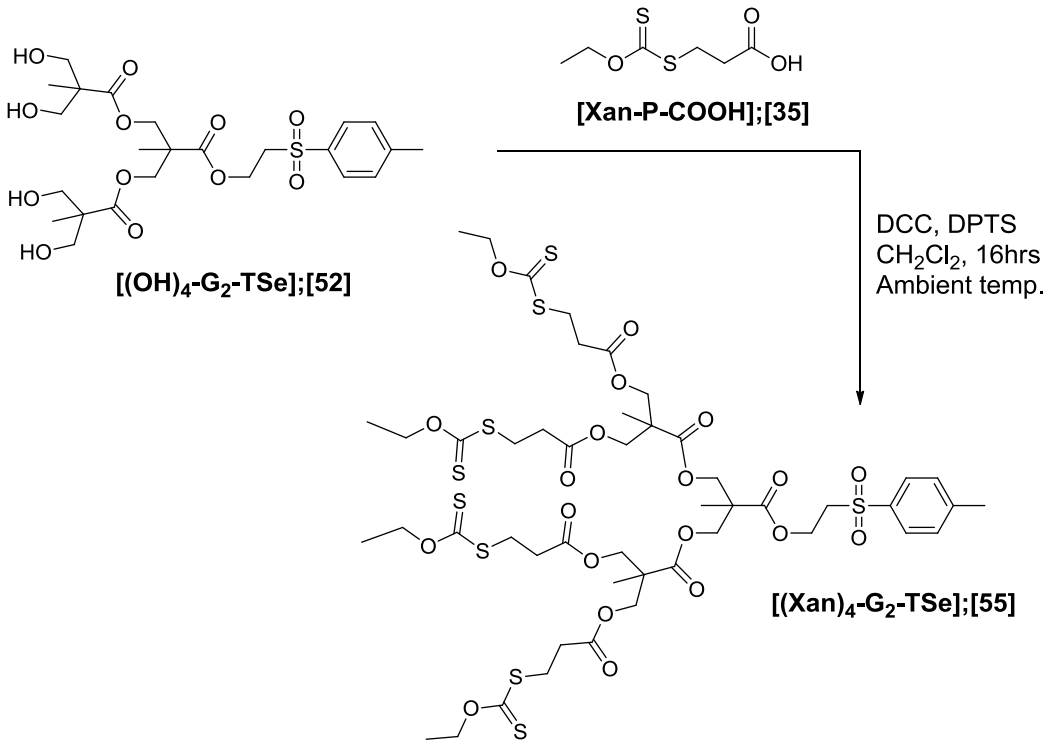

Scheme 3.8 Synthesis of **$[(Xan)_4\text{-}G_2\text{-}TSe];[55]$** using **[Xan-P-COOH];[35]** and DCC/DPTS esterification

The conditions for DCC esterification are much milder, and were expected to prevent elimination via the elimination of harsh acidic or basic conditions. 4-(Dimethylamino)pyridinium *p*-toluenesulfonate (**DPTS**) was chosen as the esterification catalyst since it is known to supress the problematic 1,3 rearrangement of the O-acyl intermediate to a N-acyl urea, by maintaining a low pH during the reaction,[4] Scheme 3.9. The catalyst was prepared by literature procedures,[5] refluxing *p*-toluenesulfonic acid monohydrate (***p*-TsOH monohyd**) in toluene for 4 hours using a Dean-Stark head to remove the water, cooling to 60 °C, adding an equimolar ratio of DMAP, and leaving the mixture to stir for 1 hour to induce the salt formation. After filtration of the solid and recrystallisation from 1,2-dichloroethane, DPTS was obtained as white powder in 81% yield.

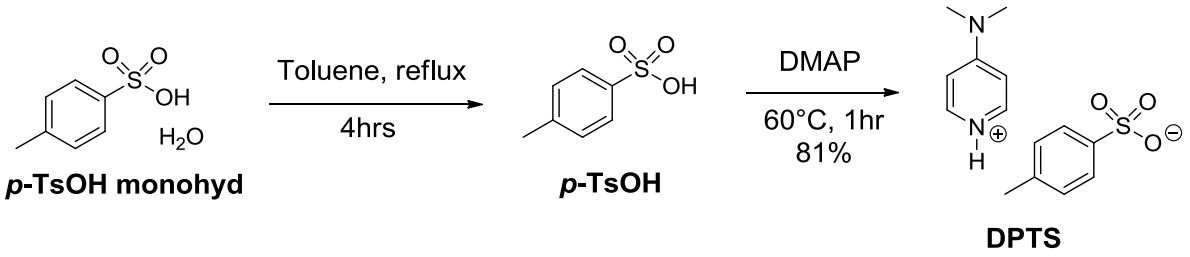

Scheme 3.9 Synthesis of 4-(Dimethylamino)pyridinium *p*-toluenesulfonate (**DPTS**)

Analysis of the catalyst by ^{1}H and ^{13}C NMR, confirmed the correct number of environments and integrals, Figures S3.20 and S3.21.

Using the revised procedure, Scheme 3.8, **[55]** was prepared by dissolving 6 equivalents of **[35]**, 1 equivalent of **[52]** and 4 equivalents of DPTS in CH_2Cl_2. DCC dissolved in CH_2Cl_2 was then added slowly to the mixture, and the reaction was left stirring for 16 hour at ambient temperature. Following this, the crude red liquid was filtered, diluted with CH_2Cl_2, washed twice with water, once with brine and the organic layer dried over $MgSO_4$. After removal of solvents and additional purification by liquid chromatography (silica, eluting hexane increasing to the polarity to hexane:ethyl acetate 80:20), an orange viscous oil was isolated in 72% yield.

Analysis of the resulting oil by ^{1}H and ^{13}C NMR confirmed the correct number of environments and integrals. Presence of the xanthate carbonyl at 214.1 ppm by ^{13}C NMR was indicative of the xanthate functionality, and further ^{1}H NMR resonances at 4.65 ppm and 1.42 ppm confirmed the O-ethyl xanthate moiety. Analysis by ESI-MS resulted in two populations at 1275 Da (MNa^+ = 1275 Da) and 1291 Da (MK^+ = 1291 Da), Figure 3.12. No evidence of elimination adducts or partially acylated materials could be observed in the spectrum, confirming the DCC/DPTS conditions were suitable for the acylation reaction.

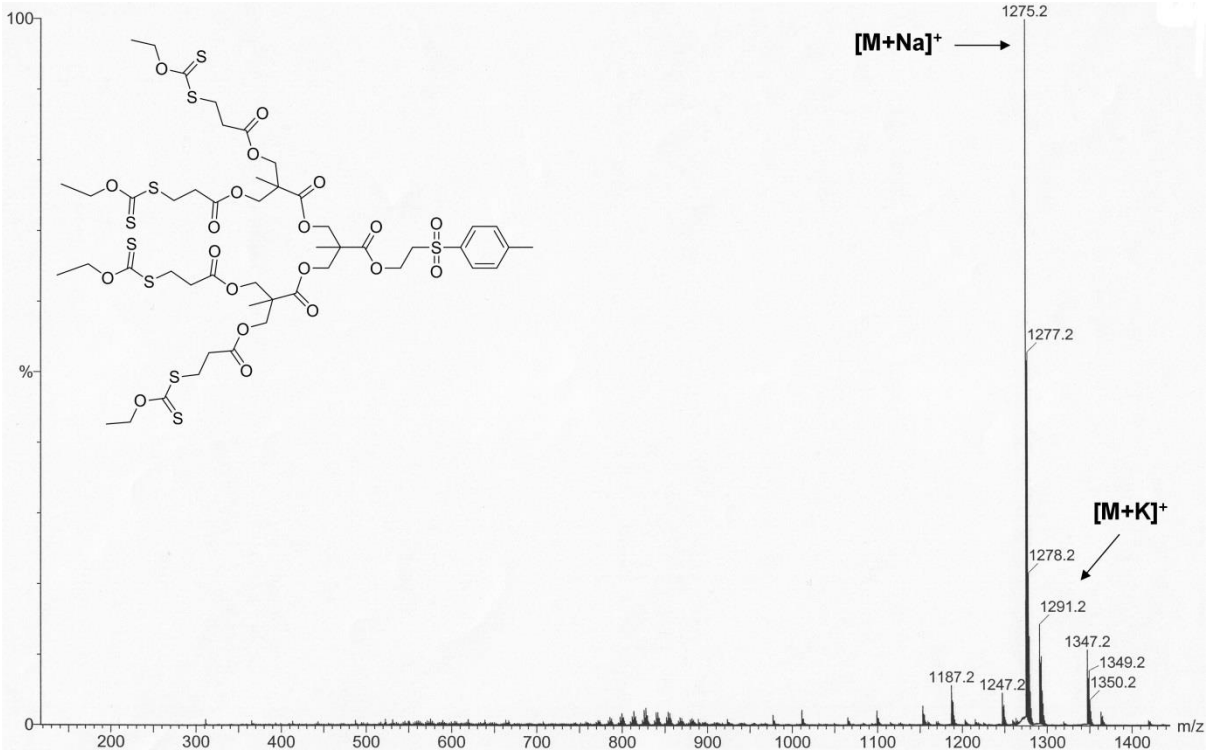

Figure 3.12 ESI-MS analysis of **[(Xan)$_4$-G$_2$-TSe];[55]** via DCC/DPTS route

3.4.5.3 Removal of TSe Protecting group

The next stage was removal of the focal point *p*-toluenesulfonyl ethyl protecting group (TSe), prior to coupling to a trifunctional core, Scheme 3.10. 1,8-Diazabicyclo[5.4.0]undec-7-ene (DBU) has been recently shown to be an effective organic base for the removal of this functionality, without degrading the bis-MPA backbone.[2]

[(Xan)$_4$-G$_2$-TSe];[55] was dissolved in CH_2Cl_2, and 1.2 equivalents of DBU added dropwise to the solution. The mixture proceeded to turn dark red upon addition, and was left stirring overnight at ambient temperature for 16 hours. The product was obtained by diluting with CH_2Cl_2, washing the organic layer twice with 1M $NaHSO_4$, drying the over $MgSO_4$ and removal of solvents to leave a crude red oil. Further purification was achieved by redissolving the oil in a minimum amount of CH_2Cl_2 and precipitating twice into a tenfold excess of hexane:ethyl acetate (10:90) to furnish the purified product as a dark red oil in 86%. Unfortunately upon analysis of the purified oil using ESI-MS, several populations correlating to structures with acrylates, via loss of peripheral xanthates were present, Figure 3.13.

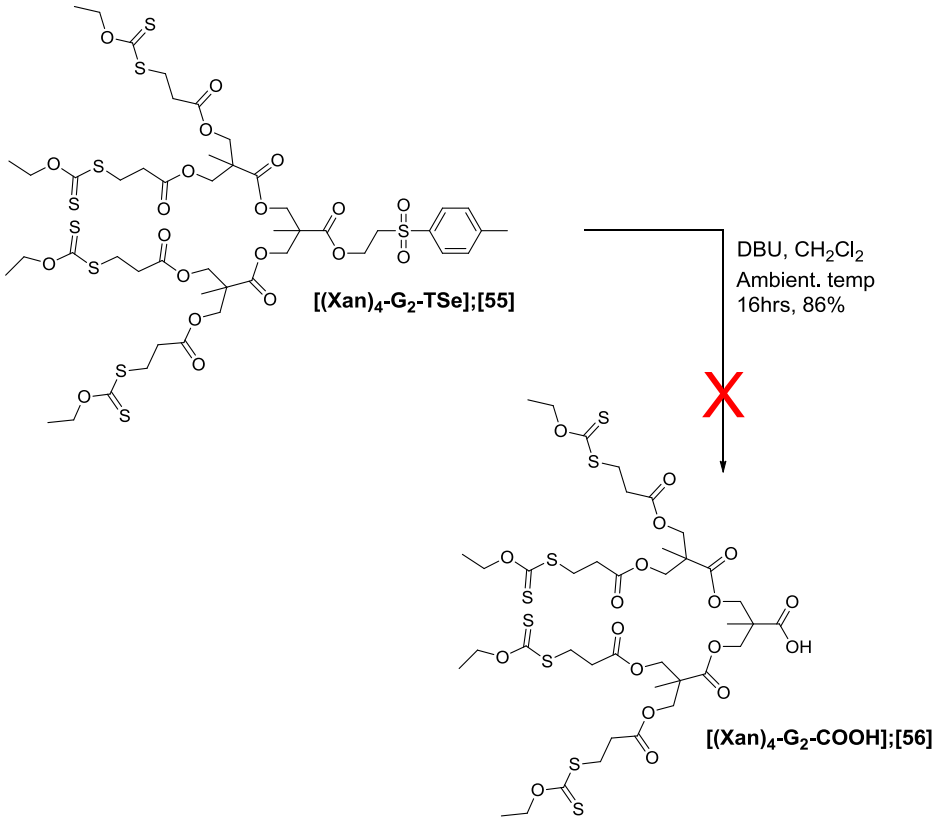

Scheme 3.10 Attempted synthesis of **[(Xan)$_4$-G$_2$-COOH];[56]**

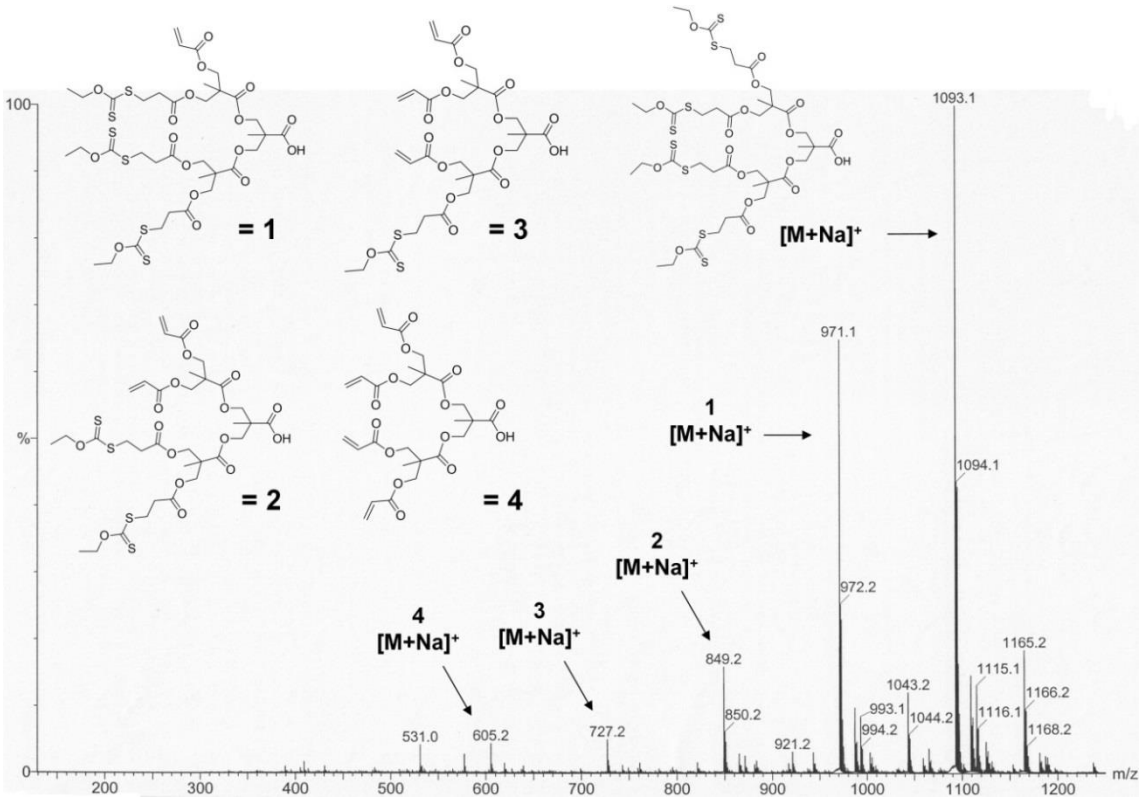

Figure 3.13 ESI-MS analysis of **[(Xan)$_4$-G$_2$-COOH];[56]**

For example, populations at 971 Da (1=MNa^+ = 971 Da), 849 Da (2=MNa^+ = 849 Da), 727 Da (3=MNa^+ = 727 Da) and 605 Da (4=MNa^+ = 605 Da) each confirmed the presence of structures with 1, 2, 3 and 4 acrylate peripheral groups, and the loss of xanthate functionality, Figure 3.13. Further analysis by ^1H NMR also confirmed the presence of acrylate functionality by proton resonances characteristic of acrylates between 5.88-6.44 ppm, Figure S3.22.

Since the protons beta to the xanthate peripherals were reasonably acidic, elimination of the xanthate peripheral groups are likely to have occurred via a mechanism as proposed in Scheme 3.11.

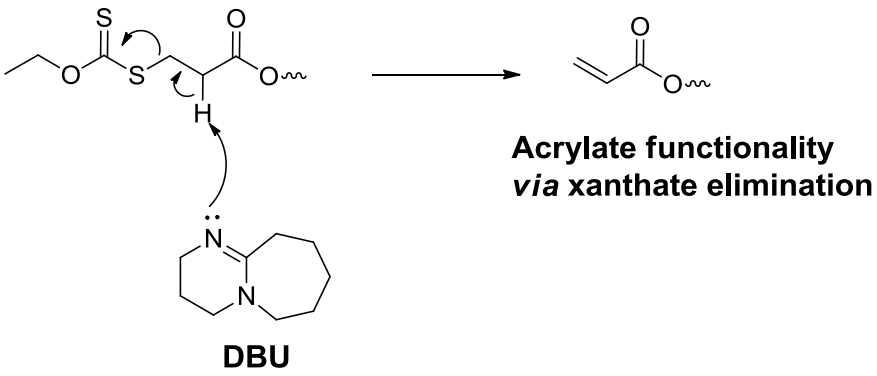

Scheme 3.11 Proposed mechanism of acrylate functionality formation via xanthate elimination

For the elimination reaction to proceed, both the alpha and beta adjoining carbons to the xanthate moiety are required. Hence, by removal of one of these carbon atoms, elimination was expected to not take place.

As a solution, the xanthate building block **[Xan-A-COOH]; [57]** was constructed, by replacing bromopropanic acid, used earlier to synthesise **[Xan-P-COOH];[35]** with bromoacetic acid, reducing the carbon atoms from two to one, Scheme 3.12.

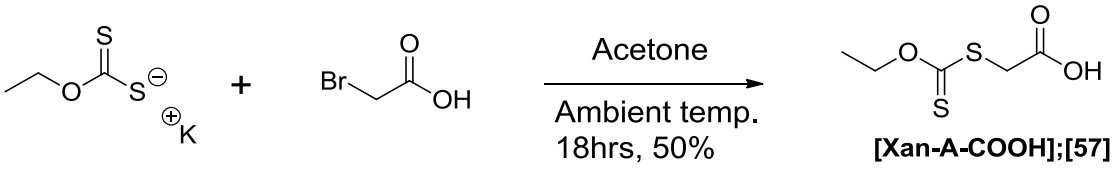

Scheme 3.12 Synthesis of xanthate building block **[Xan-A-COOH];[57]**

Following a similar preparation to compound **[35]**, potassium ethyl xanthate was suspended in acetone and 1-bromoacetic acid added dropwise to the solution. The mixture was left sitting at ambient temperature for 18 hours, which was then filtered and the acetone removed to result in a viscous yellow oil. Purification was obtained by redissolving the oil in CH_2Cl_2, washing the organic layer with brine three times, drying over $MgSO_4$ and evaporating to dryness to result in a white solid in 50% yield. The material was characterised by using ^{1}H and ^{13}C NMR spectroscopy.

The ^{1}H NMR spectrum indicated three proton environments each of which corresponded to the expected ratios, Figure S3.23. Analysis using ^{13}C NMR resulted in five environments, including the acid carbonyl resonance at 174.3 ppm and the xanthate dithiocarbonyl at 212.0 ppm, Figure S3.24.

3.4.6 Synthesis and characterisation of a G_1 xanthate peripheral dendron

To ensure that elimination did not result, **[Xan-A-COOH]; [57]** was used to prepare a G_1 xanthate functional dendron **[Xan_2-G_1-TSe];[58]**, which was treated with DBU to remove the TSe focal point protecting group, Scheme 3.13.

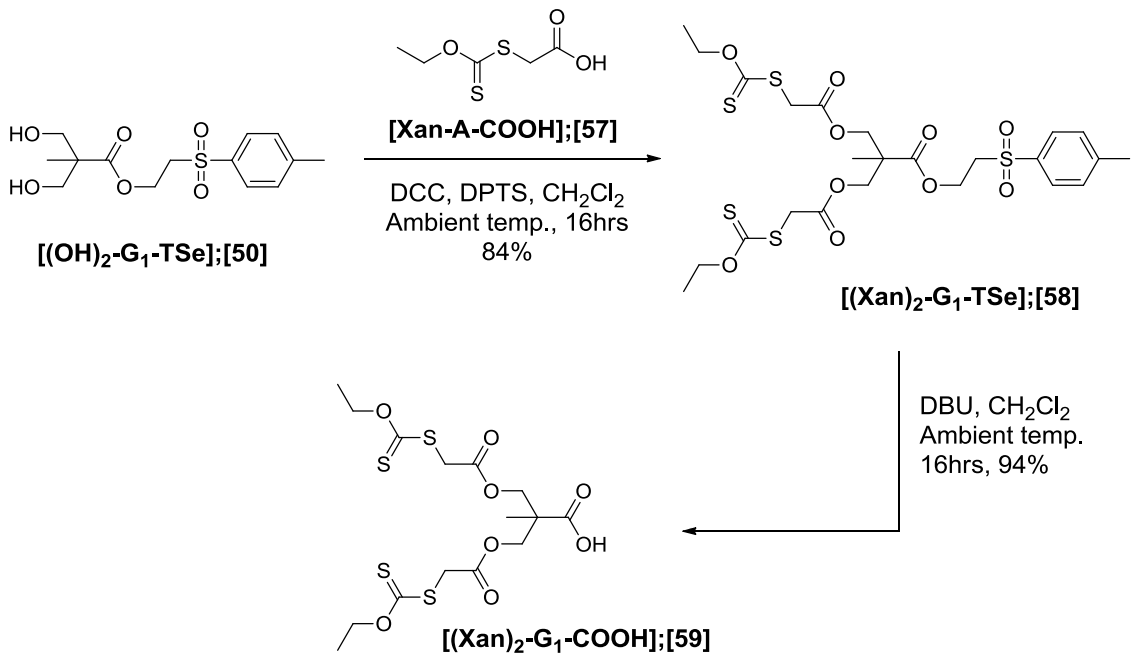

Scheme 3.13 Synthesis of **[Xan_2-G_1-TSe];[58]** and removal of the TSe protecting group to form **[Xan_2-G_1-COOH];[59]**

Using the optimised DCC/DPTS conditions described earlier, **[50]** was dissolved in CH_2Cl_2 with 3 equivalents of **[57]** and 0.4 equivalents of DPTS. A lower amount of DPTS catalyst was used since it was thought 1 equivalent per acylation was excessive, and thus reduced to 0.2 equivalents per acylation. After addition of DCC in CH_2Cl_2, the reaction vessel was sealed and left stirring at ambient temperature for 16 hours. The crude product was filtered, and purified by using liquid chromatography (silica, eluting hexane, increasing to ethyl acetate:hexane, 40:60) resulting in an orange viscous oil in 84%.

^{1}H NMR analysis indicated ten proton environments resulting in the expected integrals, and the presence of a quartet at 4.64 ppm and 1.42 ppm confirmed the xanthate moieties, Figure 3.14. ^{13}C NMR confirmed sixteen carbon environments, including the newly formed ester carbonyl at 167 ppm and the xanthate carbonyl at 214 ppm, Figure S3.25. ESI-MS indicated two populations at 663 Da (MNa^+ = 663 Da) and 679 Da (MK^+ = 679 Da), Figure S3.26.

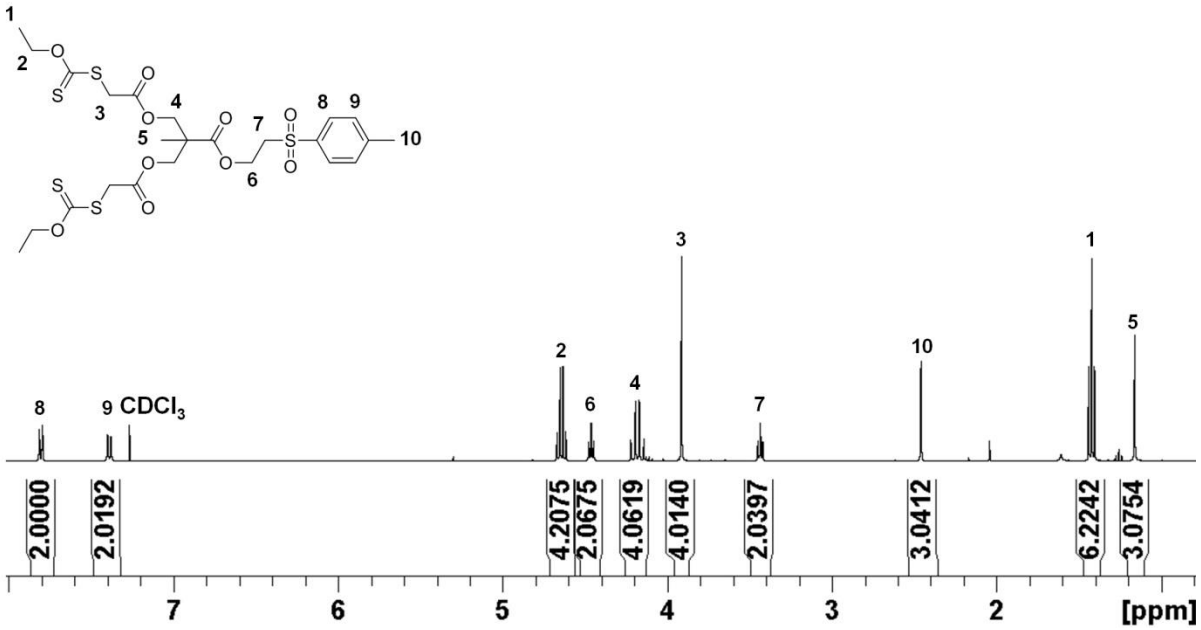

Figure 3.14 ^{1}H NMR (400 MHz, $CDCl_3$) of **[Xan_2-G_1-TSe];[58]**

Following confirmation of **[58]**, the dendron was dissolved in CH_2Cl_2 and 1.3 equivalents of DBU added slowly to the mixture. A colour change from orange to dark red was noted, and the reaction was left stirring for 16 hours at ambient temperature. Isolation of the acid functional dendron was achieved by diluting the mixture, washing twice with 1M $NaHSO_4$, drying over $MgSO_4$, concentrating *in vacuo*

and precipitating twice into a tenfold excess of hexane:ethyl acetate (90:10) to furnish **[Xan_2-G_1-COOH];[59]** as a dark red oil in 94%. Confirmation using ESI-MS confirmed the presence of a population at 481 Da (MNa^+ = 481 Da), and no evidence of populations that could be assigned to eliminated species, Figure 3.15. Analysis by ^1H NMR confirmed the loss of the two CH_2 peaks at 4.46 ppm and 3.44 ppm, and also the aromatic resonances at 7.80 ppm and 7.39 correlating to the TSe protecting group, Figure S3.27. Some evidence of the vinyl sulfone that is generated as the byproduct was noted at 7.77 ppm and 7.35 ppm (aromatic resonances) 6.65, 6.44 and 6.01 ppm (vinyl resonances), however no additional purification was implemented since the byproduct would not result in any side reactions in the next step, and was easily removed via liquid chromatography.

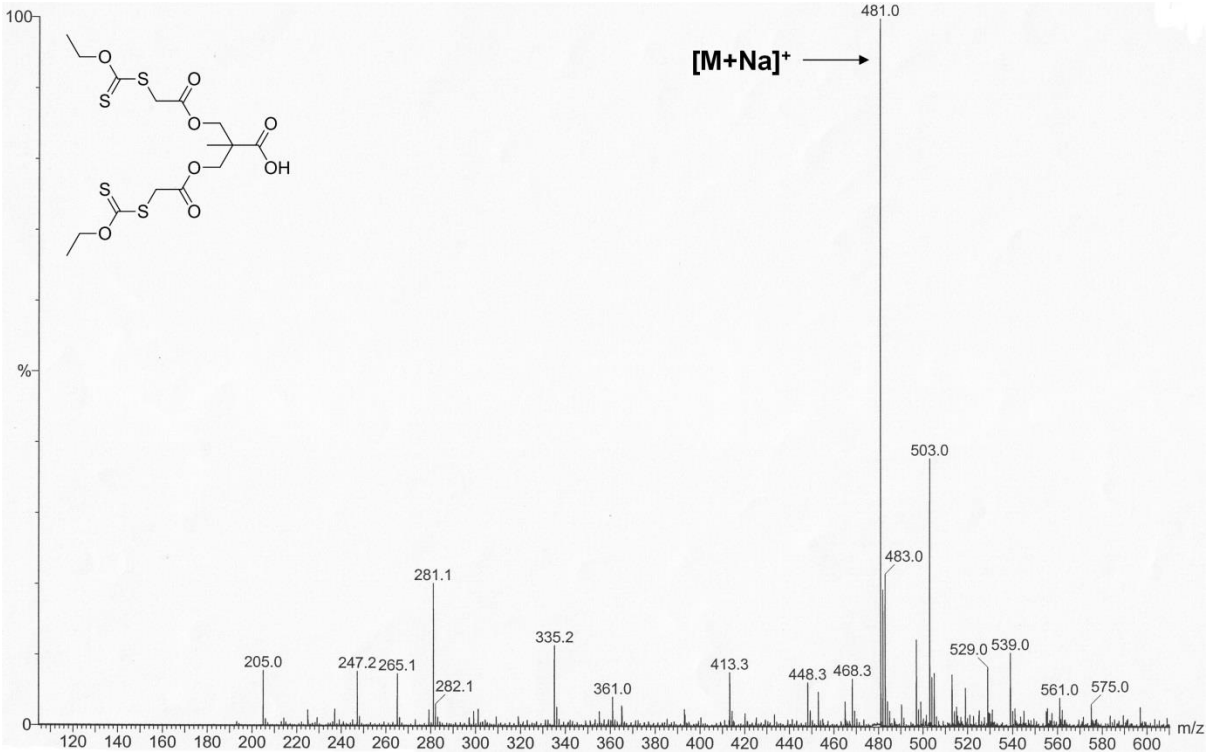

Figure 3.15 ESI-MS analysis of **[Xan_2-G_1-COOH];[59]**

Analysis of **[59]** by ^{13}C NMR confirmed nine carbon environments, including confirmation of the newly formed acid carbonyl resonance at 177.8 ppm, Figure S3.28.

3.4.7 Synthesis and characterisation of G_2 and G_3 xanthate peripheral dendrons

Having successfully shown that xanthate functional dendrons can be synthesised by a divergent growth strategy, the G_2 and G_3 dendrons were synthesised by the same methodology, Scheme 3.14.

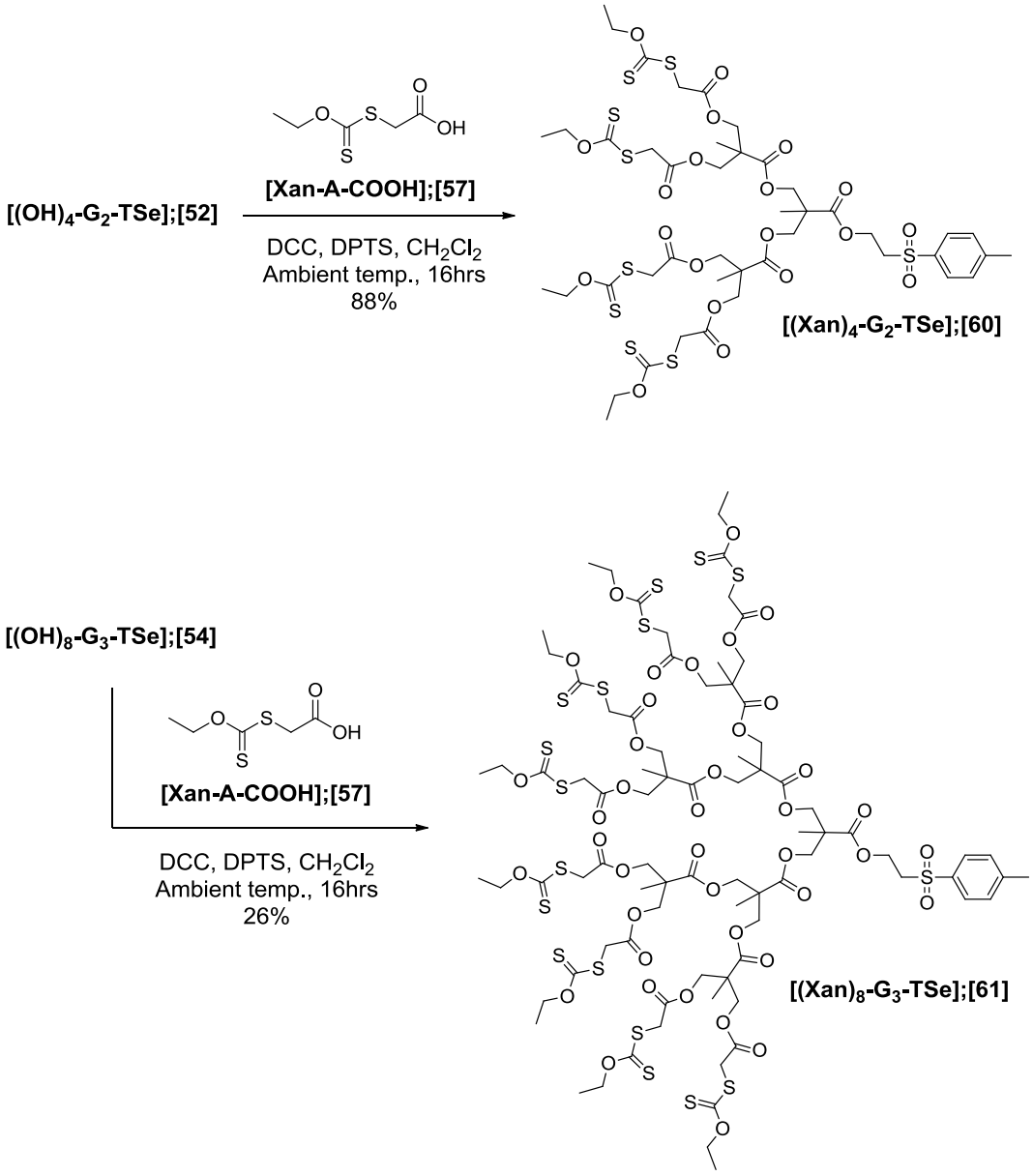

Scheme 3.14 Synthesis of **[Xan_4-G_2-TSe];[60]** and **[Xan_8-G_3-TSe];[61]** via a divergent synthesis

For the synthesis of the G_2 and G_3 xanthate dendrons **[60]** and **[61]**, **[57]** and DCC/DPTS chemistry was again used for the functionalisation. For the G_2 dendron, **[Xan$_4$-G$_2$-TSe];[60]**, **[52]**, DPTS and 6 equivalents of **[57]** were dissolved in CH_2Cl_2. DCC in CH_2Cl_2 was added slowly to the mixture, and the reaction was left stirring overnight at ambient temperature for 16 hours. The crude product was filtered, and purified by using liquid chromatography (silica, eluting hexane, gradually increasing the polarity to ethyl acetate:hexane (50:50)) resulting in **[Xan$_4$-G$_2$-TSe];[60]** as an orange viscous oil in 88%.

A similar strategy was implemented for the synthesis of the G_3 dendron **[Xan$_8$-G$_3$-TSe];[61]**. **[54]**, DPTS and 12 equivalents of **[57]** were dissolved in CH_2Cl_2. However, considerable dilution using CH_2Cl_2 was required due to the polar nature of **[54]**, and hence its unwillingness to dissolve in CH_2Cl_2. DCC in CH_2Cl_2 was slowly added to the mixture, and the reaction at ambient temperature for 16 hours. The crude product was filtered, and purified twice using liquid chromatography (silica, eluting hexane, gradually increasing the polarity to ethyl acetate:hexane (40:60)) resulting in **[Xan$_8$-G$_3$-TSe];[61]** as an orange viscous oil in 26%. The low yield was attributed to the fact that a large proportion of the crude product contained partially acylated materials that required two separate attempts at purification using liquid chromatography. A suggestion for the poor esterification may have been due to the considerable dilution that was required to dissolve the hydroxyl dendron **[54]**.

Both **[60]** and **[61]** were analysed using ^{1}H and ^{13}C NMR techniques as well as MALDI-TOF mass spectrometry.

Analysis of **[60]** by ^{1}H NMR confirmed twelve proton environments each correlating to the expected number of integrations, Figure S3.29. ^{13}C NMR indicated twenty carbon environments, including three ester carbonyl environments at 167.4 ppm, 171.6 ppm and 171.7 ppm, Figure S3.30. Although ESI-MS is an effective technique for analysis of dendritic materials, in some cases of larger dendritic materials (>1500 Da), fragmentation during analysis can occur, making assignments more challenging. MALDI-TOF analysis is a much "softer" technique, and hence fragmentation is much

less likely. Analysis of **[60]** using MALDI-TOF indicated a population at 1291 Da (MNa^+ = 1291 Da) illustrating complete xanthate functionalisation, Figure S3.31.

Analysis of **[61]** using ^1H NMR indicated fourteen proton environments, each correlating to the expected number of integrations, Figure 3.16. For example, calibrating the aromatic focal point resonance at 7.81 ppm to two protons (environment 12), demonstrated an integral of sixteen protons for the OCH_2 xanthate resonance at 4.63 ppm (environment 2). This confirmed the presence of eight peripheral xanthate groups.

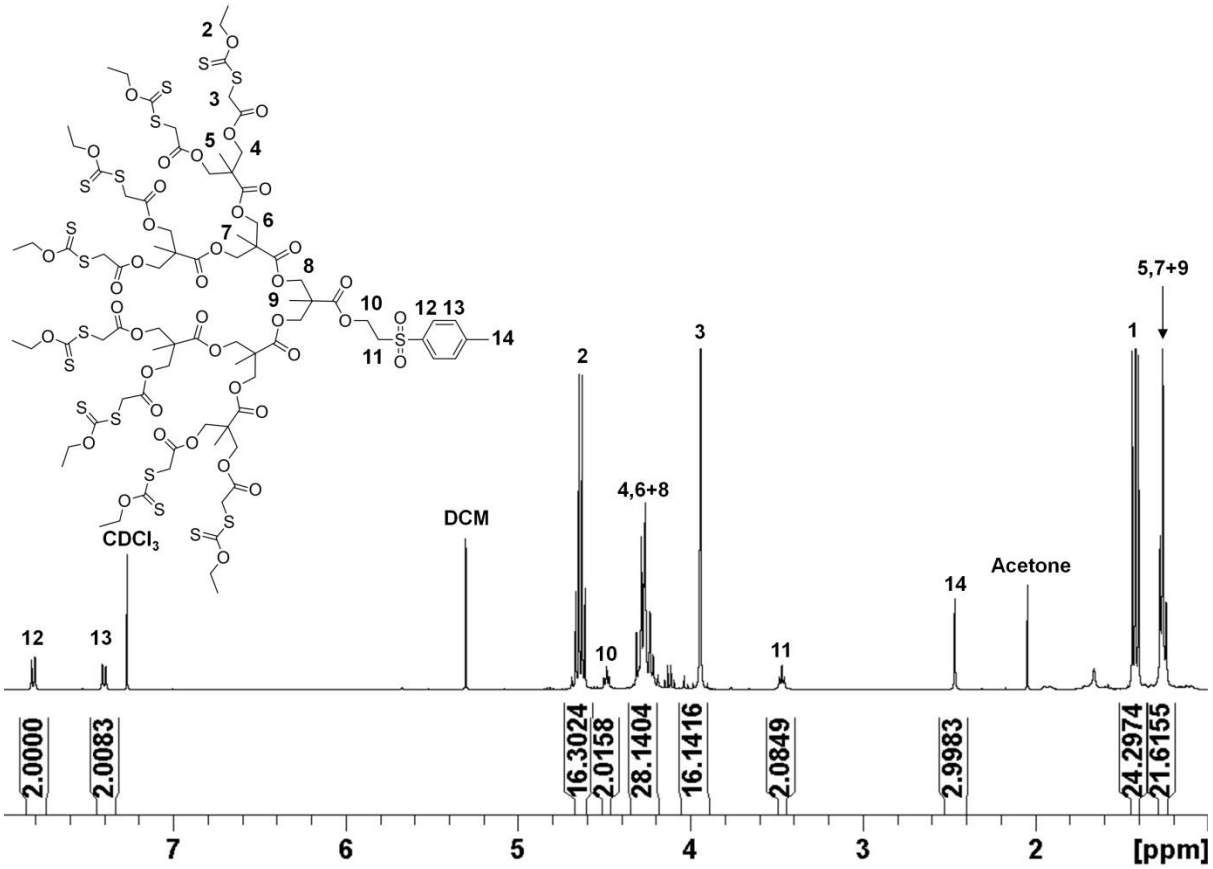

Figure 3.16 ^1H NMR spectrum (400 MHz, $CDCl_3$) of dendron **[Xan_8-G_3-TSe];[61]**

Using ^{13}C NMR confirmed twenty four carbon environments, including the ester carbonyl backbone resonances at 167 ppm, 171.5 ppm, 171.6 ppm and 171.7 ppm, Figure S3.32. MALDI-TOF analysis confirmed a single population at 2331 Da (MNa^+ = 2331 Da), Figure 3.17.

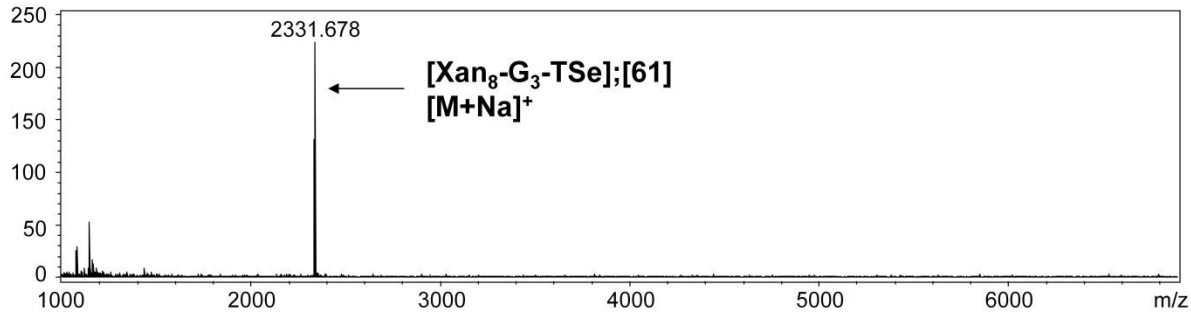

Figure 3.17 MALDI-TOF analysis of **[Xan_8-G_3-TSe];[61]**

After the successful synthesis of **[60]** and **[61]**, both dendrons were activated at their focal points by removing the TSe protecting group, Scheme 3.15. In each case, **[60]** or **[61]** was dissolved in CH_2Cl_2, 1.3 equivalents of DBU slowly added to the mixture, and the reaction left stirring at ambient temperature for 16 hours. After 16 hours total loss of **[60]** resulted, and the product was purified by diluting the mixture, washing twice with 1M $NaHSO_4$, drying over $MgSO_4$, concentrating *in vacuo* and precipitating twice into a tenfold excess of hexane:ethyl acetate (90:10) furnishing **[Xan_4-G_4-COOH];[62]** as a dark red oil in 93%.

For the activated dendron **[Xan_8-G_3-COOH];[63]**, the reaction did not achieve 100% completion, and TLC confirmed evidence of the starting material **[61]** after 16 hours. The product was therefore washed and precipitated in the same way as **[Xan_4-G_4-COOH];[62]**, but with an additional purification step using liquid chromatography (silica, eluting hexane/ethyl acetate 70/30 increasing to 60/40) to remove the TSe protected dendron **[61]**. After removal of solvents, **[63]** was obtained as a dark red viscous oil in 74%.

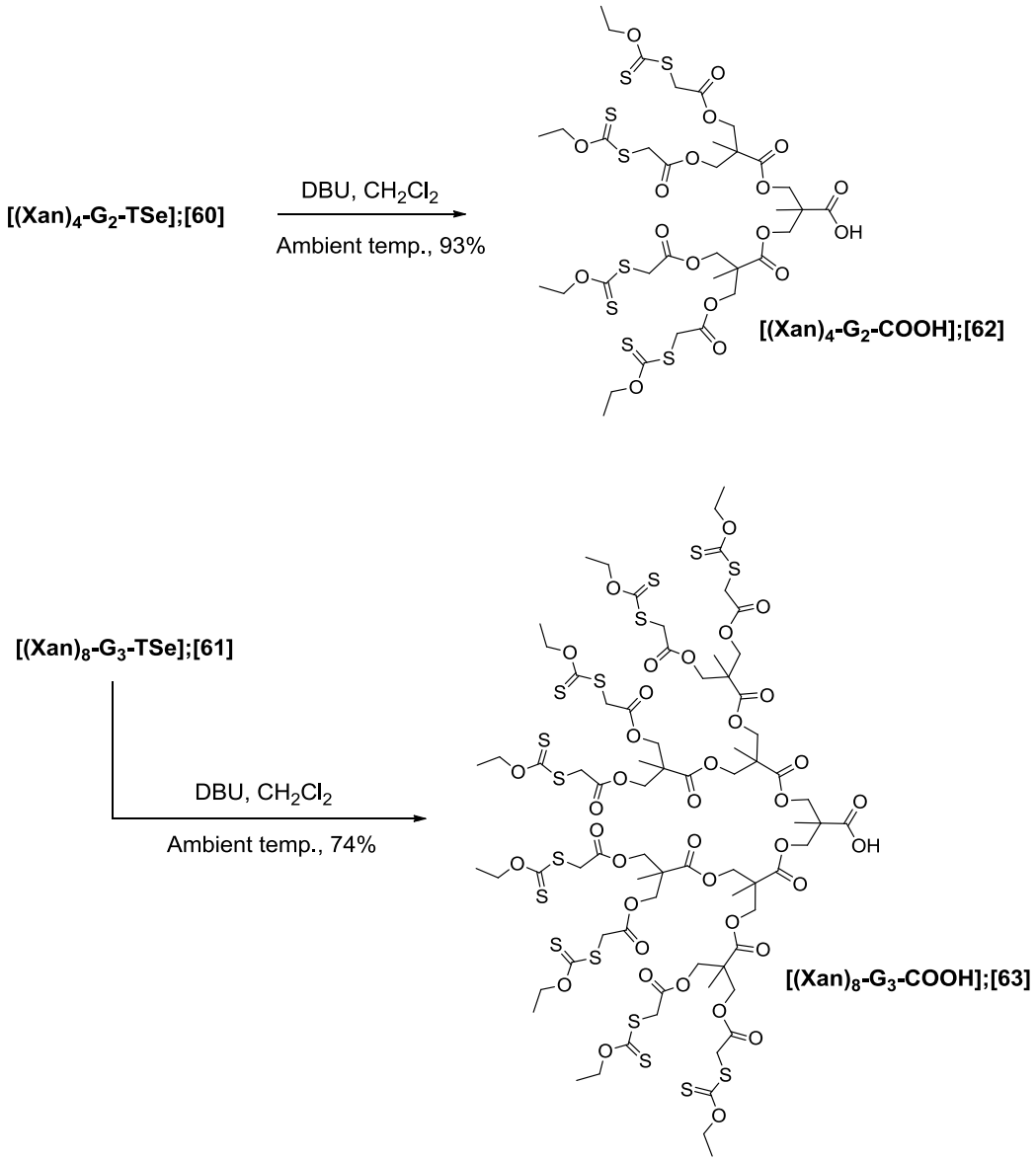

Scheme 3.15 Removal of TSe protecting functionality resulting in activated dendrons **[Xan$_4$-G$_4$-COOH];[62]** and **[Xan$_8$-G$_3$-COOH];[63]**

Once again, ^{1}H NMR, ^{13}C NMR and mass spectrometry techniques proved the most useful characterisation tools. Analysis of **[62]** by ^{1}H NMR illustrated the loss of resonances at 3.44, 4.46, 7.39 and 7.39 ppm correlating to the TSe protecting group, Figure S3.33. ^{13}C NMR confirmed thirteen carbon environments, including the newly formed acid carbonyl resonance at 176 ppm, Figure S3.34. No degradation of the polyester backbone or xanthate elimination could be observed by NMR. ESI-MS indicated a population at 1037 Da (MH^+ = 1037 Da) confirming the activated dendron **[62]**, Figure S3.35; similar analysis was performed for **[63]**. ^{1}H NMR confirmed nine proton environments,

all of which were in agreement with the expected integrations, Figure 3.18. A particularly interesting environment was the tertiary CH_3 methyl singlet at 1.35 ppm labelled as environment 9, Figure 3.18. Prior to deprotection, this resonance is buried amongst the backbone CH_3 methyl singlets at approximately 1.26 ppm. However, after deprotection, and since the adjacent functionality changes from an ester to an acid carbonyl, this resonance shifts to its own separate environment and is readily observed at 1.35 ppm (environment 9), Figure 3.16

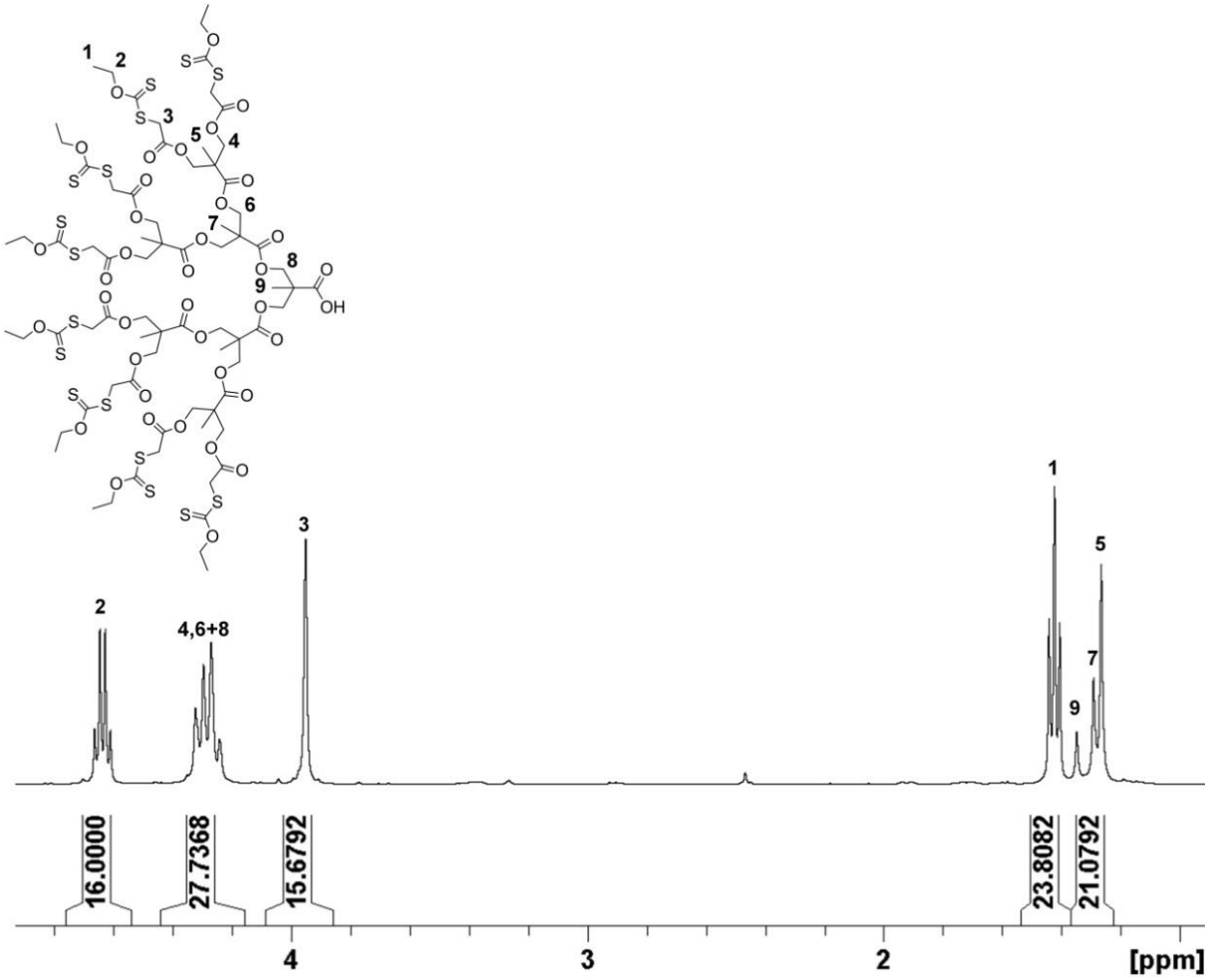

Figure 3.18 ^{1}H NMR spectrum (400 MHz, $CDCl_3$) of **[Xan$_8$-G$_3$-COOH];[63]**

Further evidence of the removal of the TSe functionality was also observed using ^{13}C NMR, which indicated sixteen carbon environments, including the characteristic acid carbonyl resonance at 173 ppm, Figure S3.36. Analysis by MALDI-TOF mass spectrometry confirmed a single population at

2151 Da (MNa^+ = 2149 Da) and no evidence of higher population species, indicating total removal of the TSe functionality, Figure 3.19.

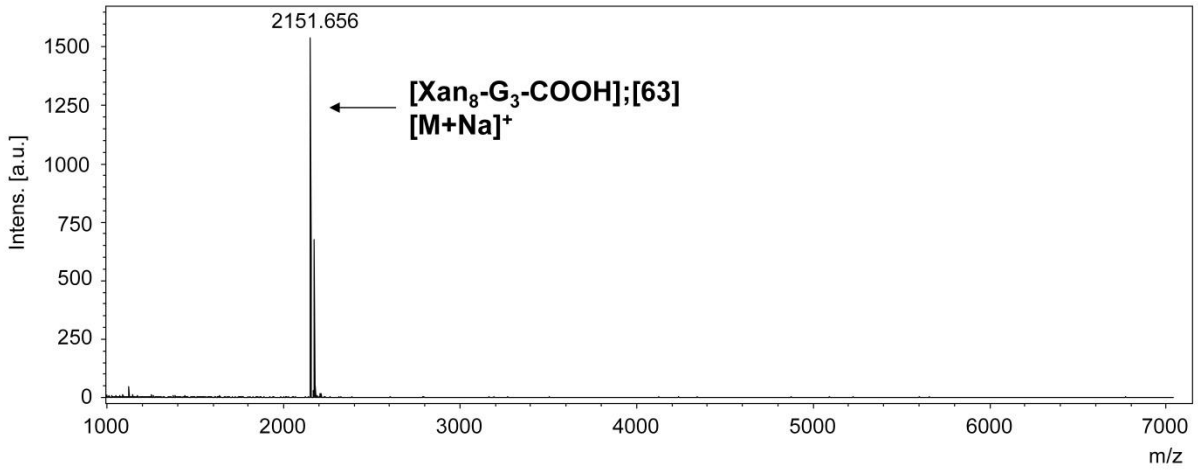

Figure 3.19 MALDI-TOF analysis of **[Xan_8-G_3-COOH];[63]**

3.5 Synthesis of xanthate peripheral dendrimers

After the successful synthesis of G_1, G_2 and G_3 xanthate functional dendrons, each dendron was reacted via a convergent coupling method to a trifunctional core. The core that was utilised was triethanolamine (TEA), Schemes 3.16 and 3.17.

For the preparation of the G_0, G_1 and G_2 dendrimers **[Xan_3-G_0-TEA];[64]**, **[Xan_6-G_1-TEA];[65]** and **[Xan_{12}-G_2-TEA];[66]**, Scheme 3.16, 3.8-4 equivalents of xanthate functional building block/dendron **[57]** or **[59]** or **[62]** was reacted with 1 equivalent of TEA core. An excess was used to ensure that complete coupling resulted to the three reactive hydroxyl sites on the trifunctional core. The xanthate functional dendron, DPTS and TEA were dissolved in CH_2Cl_2, and DCC in CH_2Cl_2 added slowly to the reaction mixture. The vessel was sealed and left stirring at ambient temperature for 16 hours. To isolate the pure dendrimer, the crude mixture was filtered, diluted with CH_2Cl_2 washed twice with 1M $NaHSO_4$, the organic layer dried over $MgSO_4$ and evaporated to dryness.

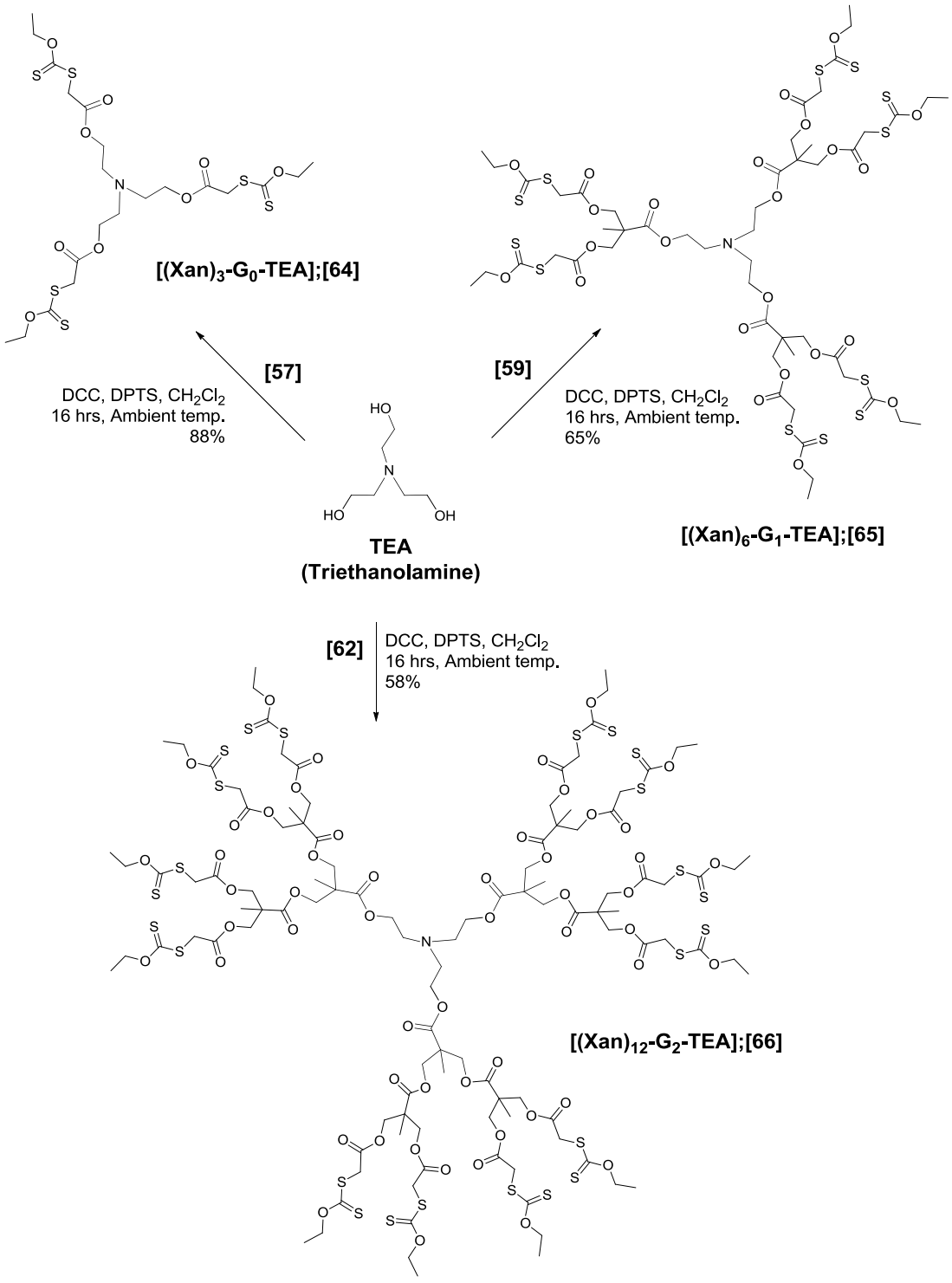

Scheme 3.16 Synthesis of G_0, G_1 and G_2 dendrimers, **[Xan$_3$-G$_0$-TEA];[64]**, **[Xan$_6$-G$_1$-TEA];[65]** and **[Xan$_{12}$-G$_2$-TEA];[66]**

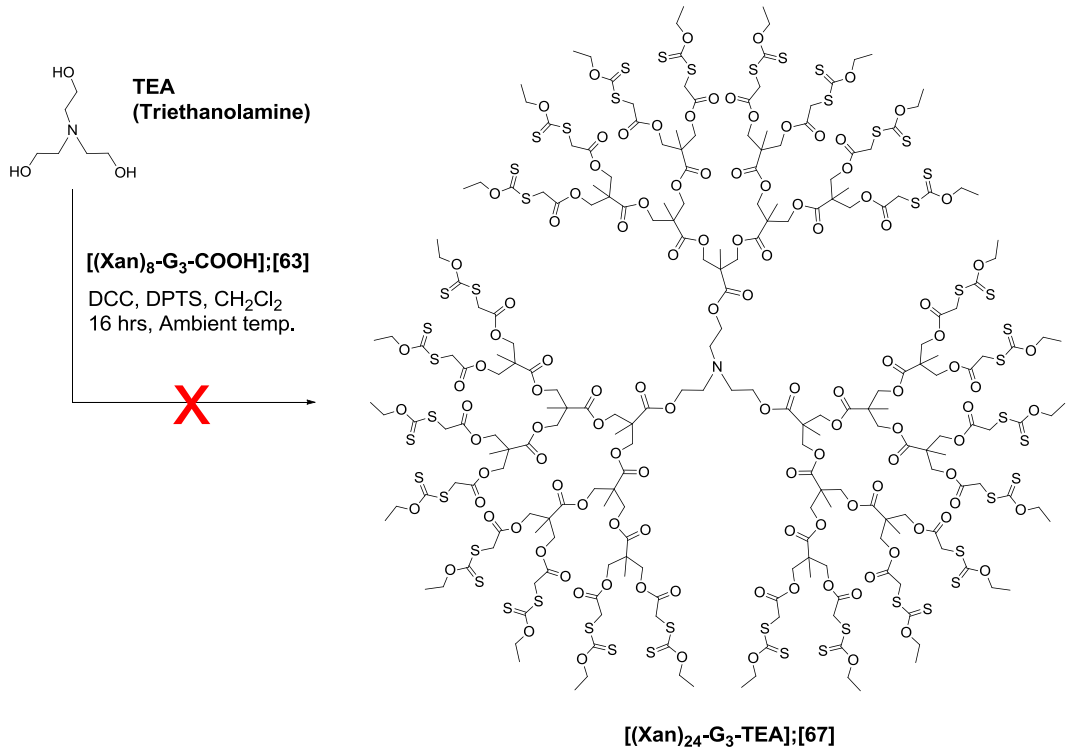

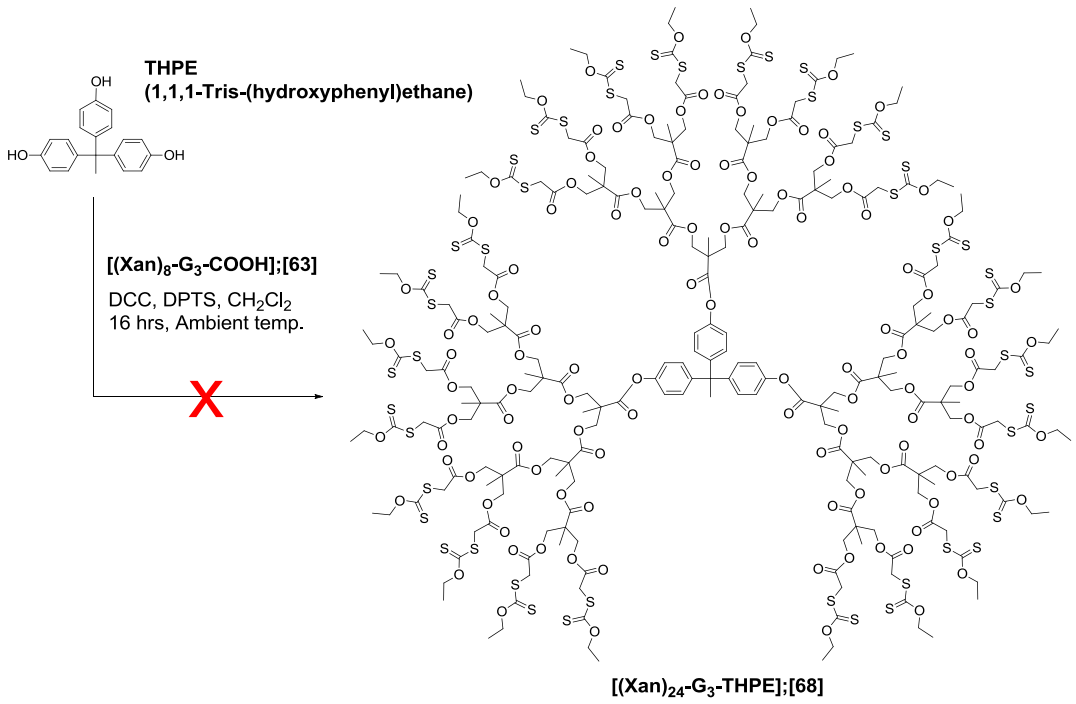

Scheme 3.17 Attempted synthesis of G_3 dendrimers, **[Xan$_{24}$-G$_3$-TEA];[67]** and **[Xan$_{24}$-G$_3$-THPE];[68]**

Additional purification by automated liquid chromatography (silica, eluting hexane increasing to the polarity to hexane:ethyl acetate 40:60) resulted in **[64]** obtained as a viscous orange oil in 88%, **[65]** obtained as a viscous orange oil in 65% and **[66]** as a very viscous orange oil in 58%. The low yield for **[66]** resulted from the poor efficiency of the sterically demanding core coupling step, which led to a considerable amount of mono and di-functional material that was successfully removed via liquid chromatography.

Following a series of unsuccessful attempts the G_3 dendrimers could not be isolated, Scheme 3.17. When initially using TEA as the core to obtain dendrimer **[Xan_{24}-G_3-TEA];[67]** the core to dendron ratio was varied from 1:3 to 1:5 and yet no trace of trifunctional material could be obtained. Increasing the reaction time from 16 hours to 1 week also made no difference, and the trifunctional dendrimer could not be isolated. A final attempt to use a more rigid core, THPE (1,1,1-tris-(hydroxyphenyl)ethane) to obtain dendrimer **[Xan_{12}-G_2-THPE];[68]** did lead to some evidence of tri functional material by MALDI-TOF analysis, but even after rigorous liquid chromatography the di-functional impurity could not be removed. No further attempts were made to isolate the G_3 materials, and the dendron **[Xan_8-G_3-COOH];[63]** was assumed to be too sterically demanding to fit three units around a trifunctional core. A hyper monomer route or a strictly divergent dendrimer synthesis may be the solution to this problem.

3.6 Characterisation of xanthate peripheral dendrimers

Each dendrimer was characterised using ^{1}H NMR, ^{13}C NMR and MALDI-TOF analysis and, although NMR was useful to determine the presence of symmetrical proton and carbon environments, the technique was not sensitive enough to determine slight structural defeats. MALDI-TOF analysis was therefore critical for the dendrimer analysis since the technique could readily identify branching defeats.

3.6.1 Analysis by NMR spectroscopy

The G_0 dendrimer **[Xan$_3$-G$_0$-TEA];[64]** was relatively easy to assign, with five proton environments correlating to the expected integrations, Figure S3.37. The presence of the new triplet resonances at 2.88 ppm and 4.21 ppm each related to the two different, but symmetrical via their dendritic arm, core environments. Analysis by ^{13}C NMR indicated seven carbon environments, including the xanthate carbonyl at 213 ppm and the newly formed ester carbonyl at 168 ppm, Figure S3.38.

Analysis of the G_1 dendrimer, **[Xan$_6$-G$_1$-TEA];[65]** using ^{1}H NMR indicated seven proton environments, including the two new core resonances at 2.87 ppm and 4.17 ppm, Figure S3.40. Integration from the core environment at 4.17 ppm indicated the presence of six peripheral xanthate moieties, and analysis by ^{13}C NMR revealed eleven carbon environments including the two backbone ester carbonyls at 167.4 ppm and 172.2 ppm, Figure S3.41.

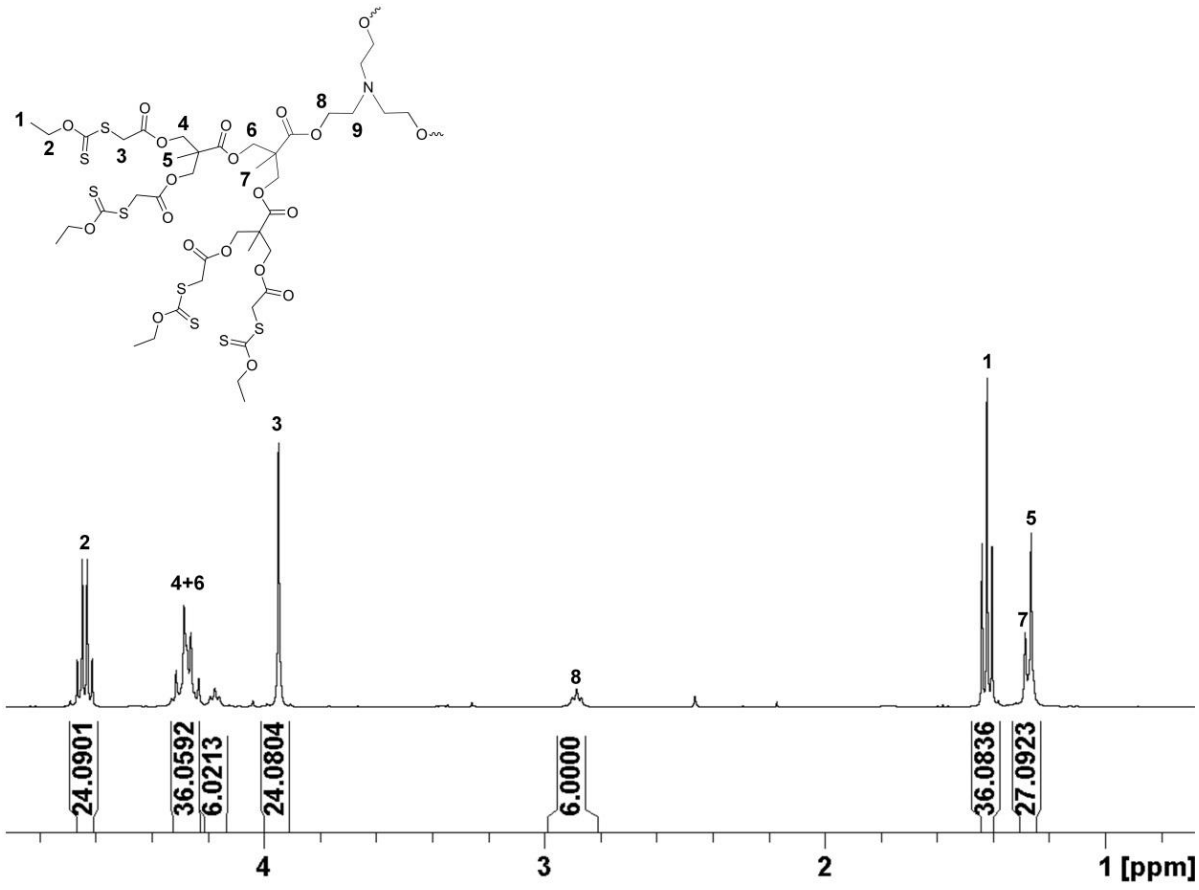

Figure 3.20 ^{1}H NMR spectrum (400 MHz, $CDCl_3$) of **[Xan$_{12}$-G$_2$-TEA];[66]**

G_2 dendrimer **[Xan_{12}-G_2-TEA];[66]** was analysed by ^{1}H NMR and indicated nine different proton environments, Figure 3.20. Integration of the core environment at 2.88 ppm (labelled environment 8, Figure 3.20) indicated the presence of twelve xanthate moieties, confirmed by the O-CH_2 xanthate resonance at 4.64 ppm (labelled environment 2, Figure 3.20). Further confirmation of the dendritic backbone was also illustrated by the slight difference in resonances of the tertiary methyl groups, labelled as environments 7 and 5 at 1.26 ppm and 1.29 ppm.

The ^{13}C NMR spectrum of **[Xan_{12}-G_2-TEA];[66]** confirmed fifteen carbon environments including the three backbone ester carbonyl environments at 167.4, 177.7 and 172.0 ppm, Figure S3.42.

Unfortunately, analysis G_3 dendrimers **[Xan_{24}-G_3-TEA];[67]** and **[Xan_{24}-G_3-THPE];[68]** by ^{1}H NMR indicated evidence of di-substituted species which could not be removed by liquid chromatography. For example, when utilising a TEA core ^{1}H NMR analysis of **[Xan_{24}-G_3-TEA];[67]** revealed additional proton environments at 2.78 ppm and 3.56 ppm, correlating to the presence of an unsymmetrical core and a vacant hydroxyl site, Figure S3.43. When attempting to use a more ridged core, analysis of dendrimer [**Xan_{24}-G_3-THPE];[68]** by ^{1}H NMR also indicated additional unsymmetrical core environments, Figure S3.44. For example, for a fully acylated trifunctional core, two aromatic environments at 6.99 ppm and 7.11 ppm should be present for each of the three symmetrical arms of the dendrimer. However, additional aromatic environments at 6.74, 6.89, 7.78 and 7.37 ppm were observed, readily indicating the presence of di-functional and/or mono-functional dendritic species.

3.6.2 Analysis by mass spectrometry

Each dendrimer was fully analysed by mass spectrometry techniques to ensure structural perfection. For the G_0 dendrimer **[Xan_3-G_0-TEA];[64]** analysis by ESI-MS confirmed three populations at 636 Da (MH^+ = 636 Da), 658 Da (MNa^+ = 658 Da) and 674 Da (MK^+ = 674 Da), indicating the trifunctional xanthate species, Figure S3.39.

The G_1 dendrimer **[Xan_6-G_1-TEA];[65]** was analysed by MALDI-TOF analysis and confirmed a single population at 1492 Da (MNa^+ = 1492 Da), Figure 3.21.

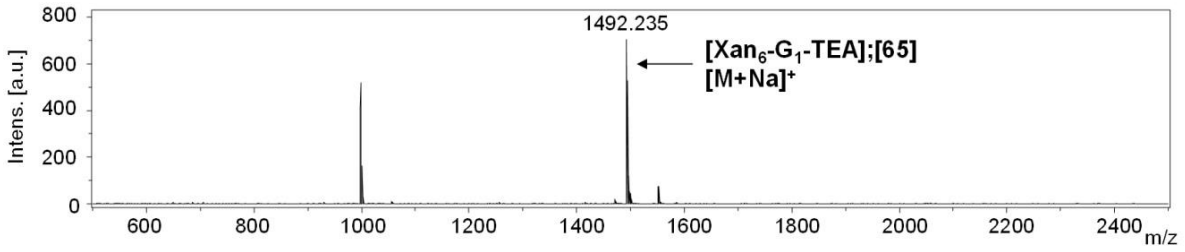

Figure 3.21 MALDI-TOF analysis of **[Xan$_6$-G$_1$-TEA];[65]**

The G_2 dendrimer **[Xan$_{12}$-G$_2$-TEA];[66]** was analysed using MALDI-TOF and indicated a population at 3162 Da (MNa^+ = 3160), Figure 3.22. An additional fragment at 2112 Da was observed, and correlated to the removal of one dendritic arm via cleavage at the CH_2 unit adjacent to the central amine at the core. The fragmentation population did not suggest partial functionalisation of the core, since ^1H or ^{13}C NMR (Figure 3.20, S3.42) confirmed no evidence of mono or di-functional species.

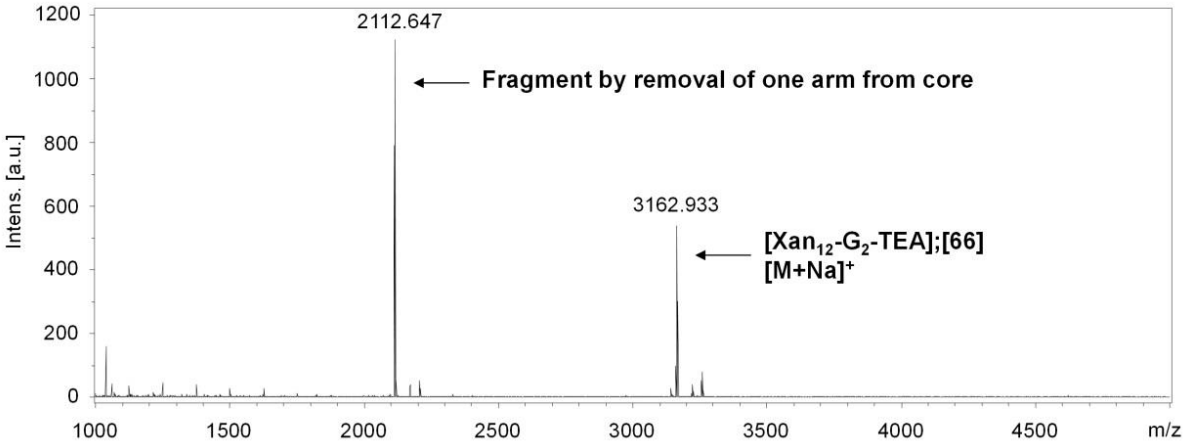

Figure 3.22 MALDI-TOF analysis of **[Xan$_{12}$-G$_2$-TEA];[66]**

Finally the partially functionalised G_3 dendrimers **Xan$_{24}$-G$_3$-TEA];[67]** and **[Xan$_{24}$-G$_3$-THPE];[68]** were analysed by MALDI-TOF analysis, Figures 3.23 and 3.24. Analysis of **[Xan$_{24}$-G$_3$-TEA];[67]** confirmed no evidence of the tri-functional dendrimer, and a single population at 4393 Da (MNa^+ = 4388 Da) which correlated to the di-functional species was confirmed, Figure 3.23.

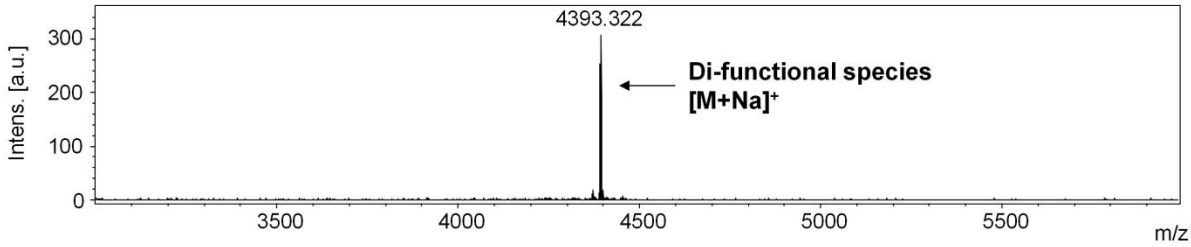

Figure 3.23 MALDI-TOF analysis of **[Xan_{12}-G_2-TEA];[67]** indicating partially acylated materials

Analysis of **[Xan_{24}-G_3-THPE];[68]** by MALDI-TOF indicated some evidence of the tri-functional dendrimer **[68]**, confirmed by a population at 6654 Da (MNa^+ = 6653 Da). However, a significant proportion of di-functional species was also present in the sample, which was readily confirmed by a population at 4547 Da (MNa^+ = 4545 Da), Figure 3.24.

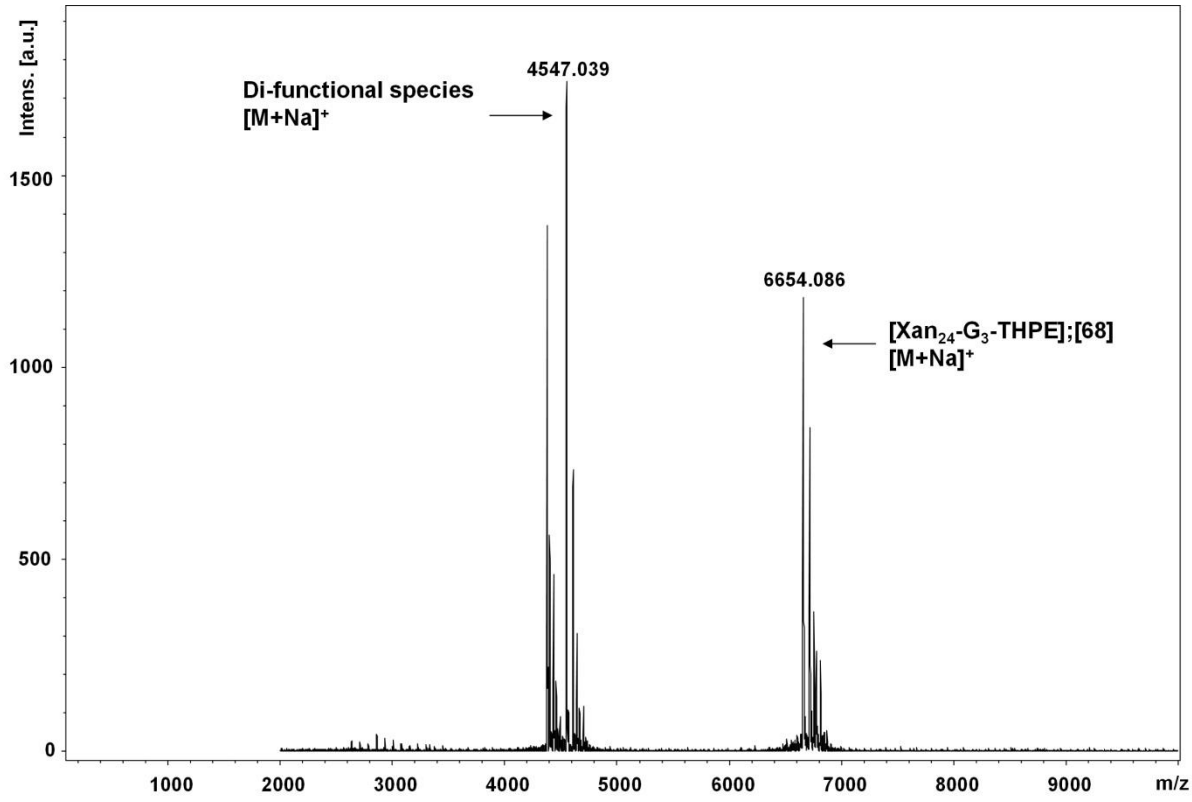

Figure 3.24 MALDI-TOF analysis of **[Xan_{24}-G_3-THPE];[68]** indicating fully and partially acylated material

3.7 One pot xanthate deprotection and thiol Michael addition

3.7.1 Synthesis of functional dendrimers

Having successfully synthesised G_0, G_1 and G_2 xanthate peripheral dendrimers, each dendrimer was functionalised via one-pot xanthate deprotection/thiol-acrylate Michael addition reactions. The G_0 dendrimer **[Xan$_3$-G$_0$-TEA];[64]** was chosen for initial exploratory reactions, and the hydrophobic monomer benzyl acrylate ([**BA]**) was used as the functional substrate, Scheme 3.18.

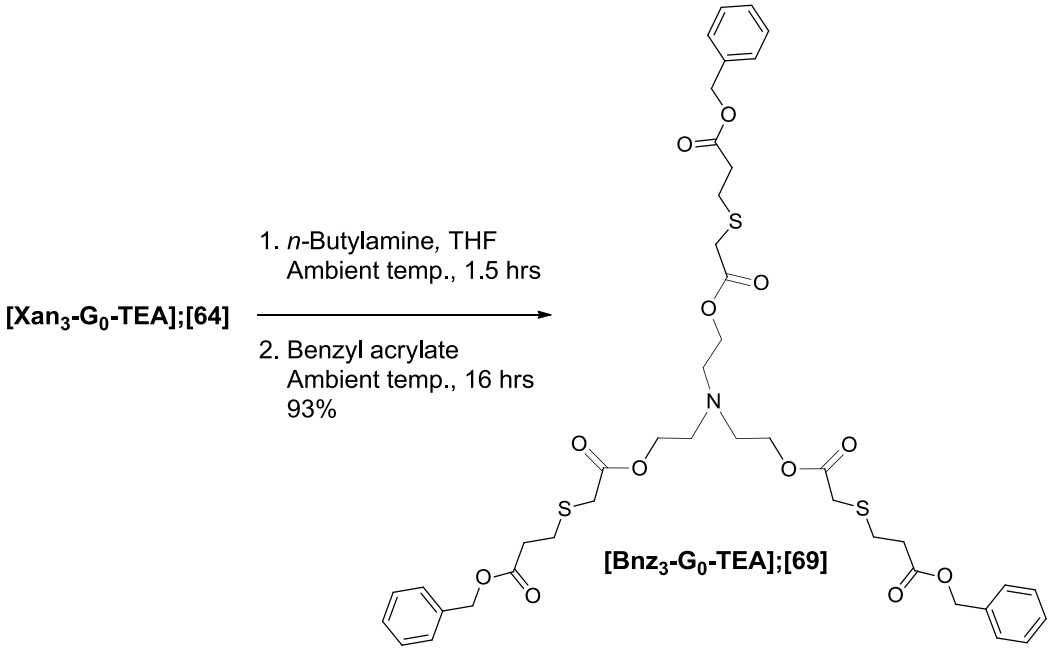

Scheme 3.18 Synthesis of **[Bnz$_3$-G$_0$-TEA];[69]** via a one-pot xanthate deprotection/thiol-acrylate Michael addition reaction

The xanthate functional dendrimer was dissolved in anhydrous THF and vigorously degassed with nitrogen for 10 minutes. Following this, 1.1 equivalents of *n*-butylamine per peripheral xanthate were slowly added, and the reaction left stirring sealed under nitrogen for 1.5 hours. TLC analysis (hexane/ethyl acetate 60:40) confirmed total loss of the xanthate dendrimer starting material after 1.5 hours, at which point 1 equivalent of functional acrylate was added per generated thiol and the mixture left stirring at ambient temperature for 16 hours. Workup of the resulting functionalised

dendrimer was achieved by reducing the volume of THF by half *in vacuo* and precipitating the mixture twice from THF into hexane at ambient temperature. After removal of solvents, **[Bnz$_3$-G$_0$-TEA];[69]** resulted as a pale yellow oil in 93%.

Preparation of G_1 and G_2 functionalised dendrimers were accomplished using the same one-pot methodology, but utilising three different acrylate monomers; **[BA]**; 2-(dimethylamino)ethyl acrylate **[DMAEA]**; and oligo(ethylene glycol) monomethyl ether acrylate M_n = 480 g/mol **[OEGA]**, Schemes 3.19 and 3.20.

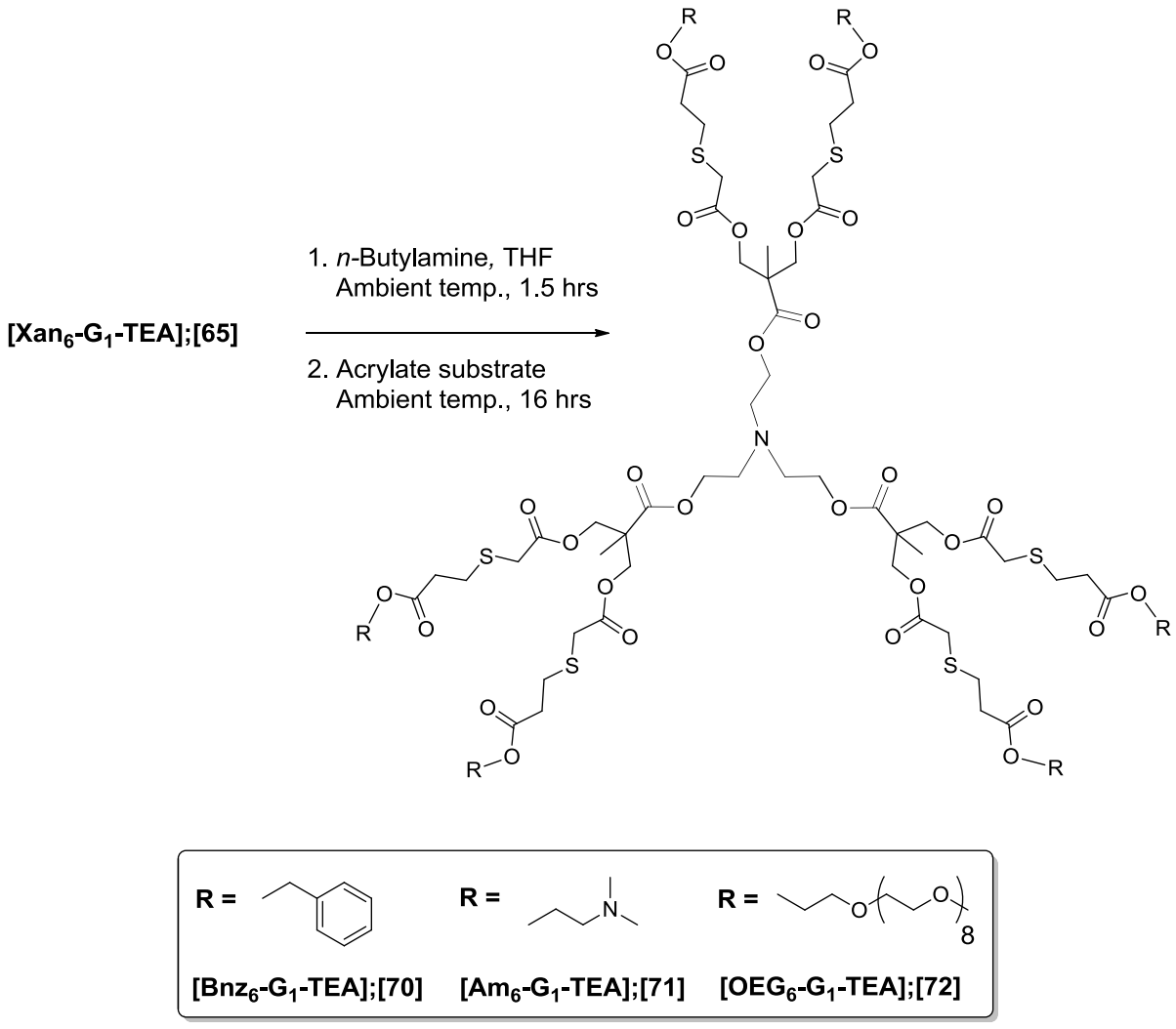

Scheme 3.19 Synthesis of G_1 dendrimers **[Bnz$_6$-G$_1$-TEA];[70], [Am$_6$-G$_1$-TEA];[71], [OEG$_6$-G$_1$-TEA];[72]** via a one-pot xanthate deprotection/thiol-acrylate Michael addition reaction

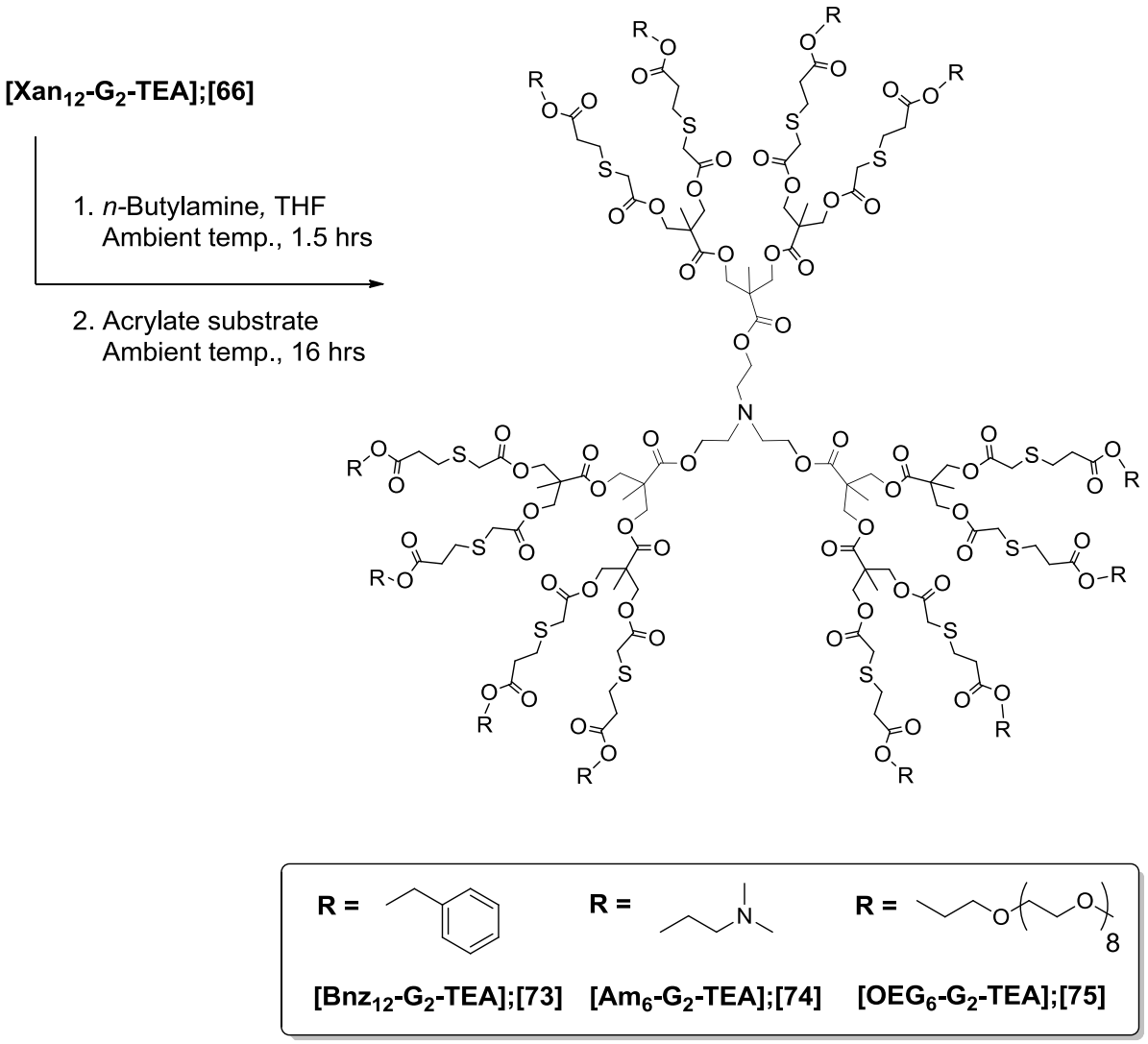

Scheme 3.20 Synthesis of G_2 dendrimers **[Bnz$_{12}$-G$_2$-TEA];[73], [Am$_{12}$-G$_2$-TEA];[74], [OEG$_{12}$-G$_2$-TEA];[75]** via a one-pot xanthate deprotection/thiol-acrylate Michael addition reaction

In each case, recovered yields of functionalised materials exceeded greater than 70%, and were purified by simple precipitation to remove the hexane-soluble dithiocarbamate that was generated as the by-product during the removal of the xanthate group. The resulting dendrimers were yellow or orange viscous oils that were soluble in common organic solvents, with the PEG functionalised materials also soluble in water.

3.7.2 Characterisation of functional dendrimers by NMR

Common for all the functionalised dendrimers was the loss of characteristic xanthate resonances by ^{1}H NMR at 1.42 ppm and 4.64 ppm, illustrated in Figure 3.25 for the G_2 benzyl dendrimer **[Bnz$_{12}$-G$_2$-TEA];[73]**. This was also supported by the loss of the xanthate carbonyl resonance at 221-213 ppm within ^{13}C NMR spectra. A particularly interesting shift was observed for the CH_2 moiety at 3.23 ppm adjacent to the thio-ether, labelled as environment 7, Figure 3.25. Before xanthate deprotection the CH_2 resonates at approximately 3.95 ppm, but upon deprotection and functionalisation the environment shifts to 3.23 ppm. This shift presumably occurs from the loss of the electron withdrawing xanthate group. New ^{1}H NMR resonances at approximately 2.66 and 2.88 ppm confirming the C-C bond via thiol Michael addition were observed in every case for each dendrimer, Figure 3.25, S3.45, S3.48, S3.51, S3.54, S3.57 and S3.59.

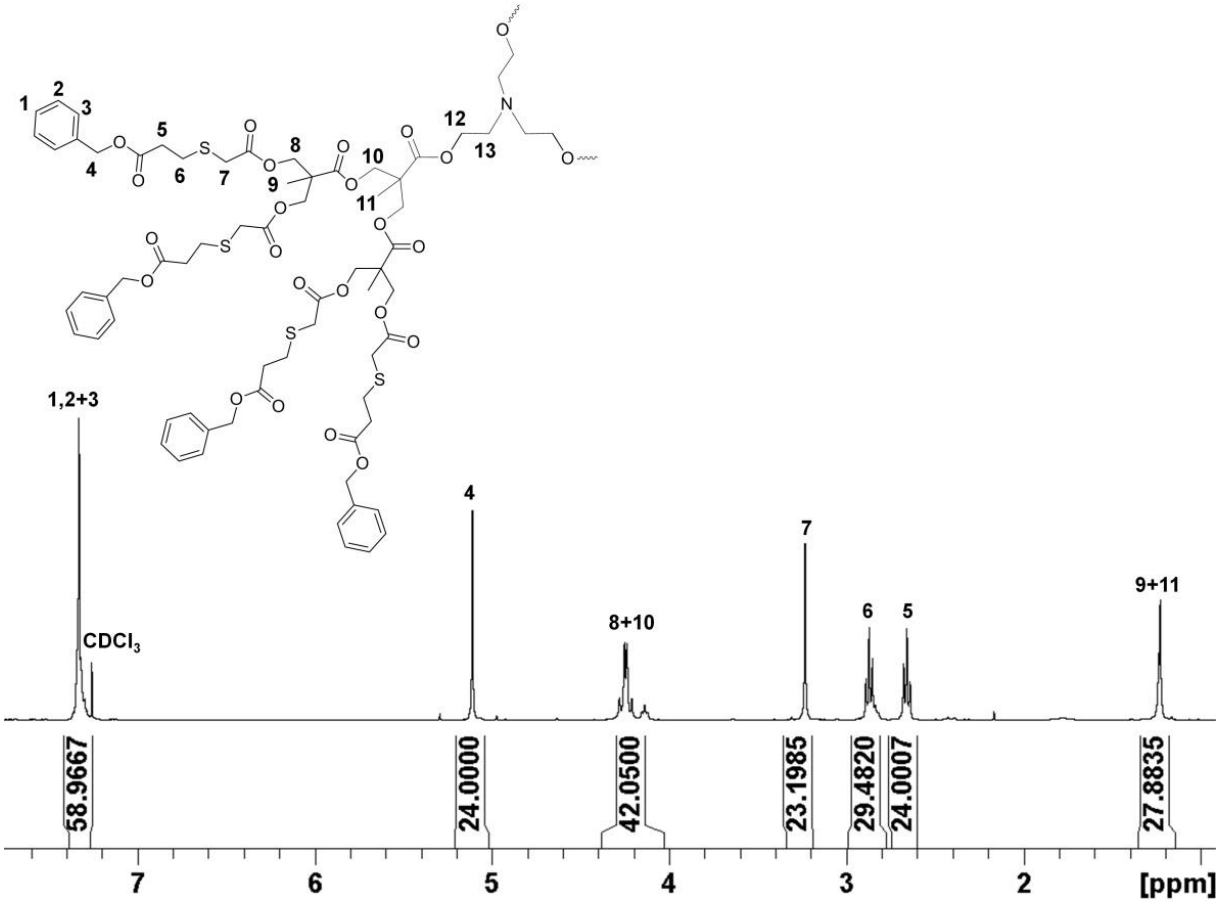

Figure 3.25 ^{1}H NMR spectrum (400 MHz, $CDCl_3$) of **[Bnz$_{12}$-G$_2$-TEA];[73]**

As well as universally common resonances, specific resonances were identified for different peripheral groups.

Analysis of benzyl functionalised dendrimers **[Bnz$_3$-G$_0$-TEA];[69]**, **[Bnz$_6$-G$_1$-TEA];[70]** and **[Bnz$_{12}$-G$_2$-TEA];[73]** by ^{1}H NMR resulted in seven, eleven and thirteen proton environments, including the formation of new environments at 5.13 ppm and 7.35 ppm corresponding the peripheral benzyl functionality, Figures S3.45, S3.48 and Figure 3.25. Further analysis by ^{13}C NMR indicated twelve, sixteen and twenty carbon environments for each benzyl functional dendrimer, Figures S3.46, 3.49 and Figure 3.46. For example, Figure 3.26 shows the ^{13}C NMR spectrum of benzyl dendrimer **[Bnz$_{12}$-G$_2$-TEA];[73]** indicating the aromatic resonances at approximately 128-135 ppm, and also the four ester carbonyl resonances at 169.7, 171.4, 171.8 and 172.0 ppm that represent the dendritic backbone.

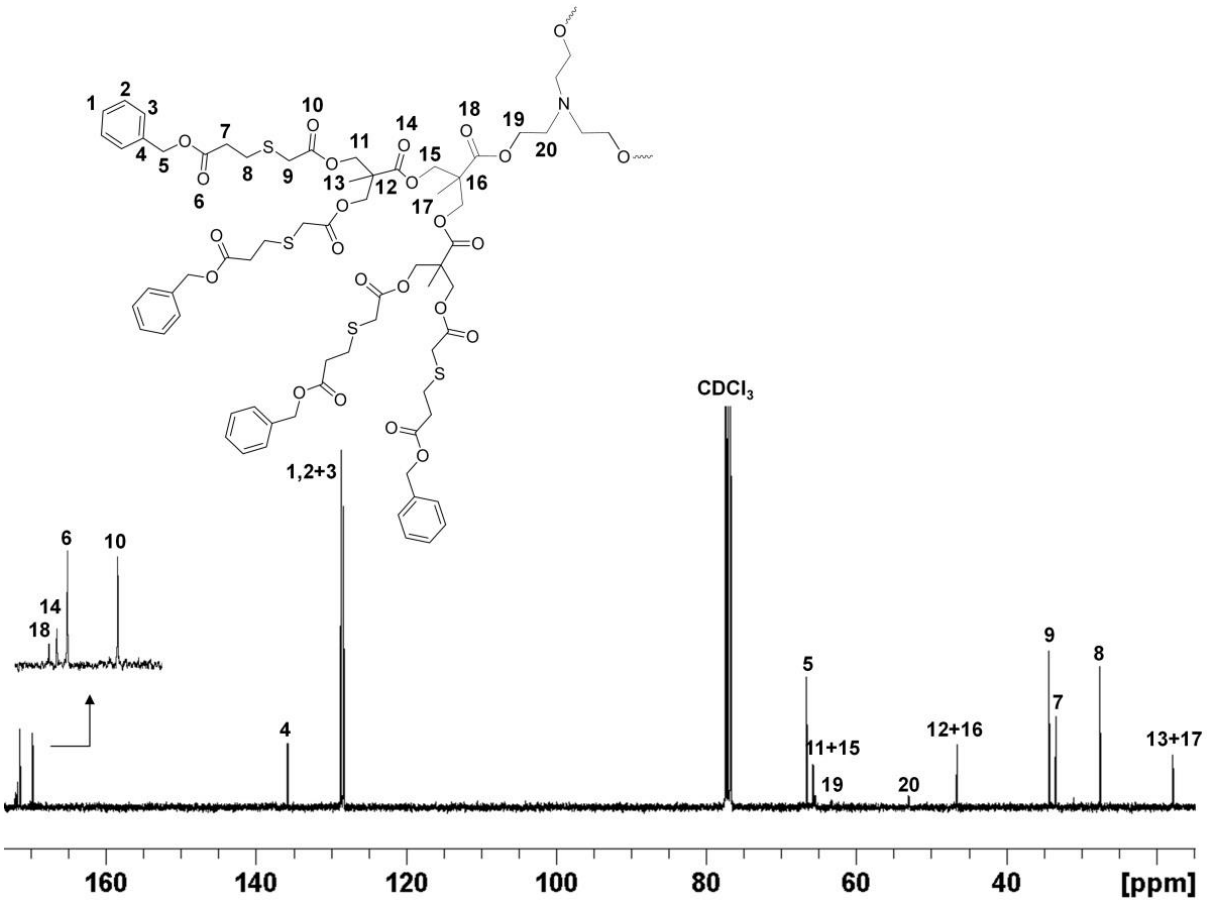

Figure 3.26 ^{13}C NMR spectrum (100 MHz, $CDCl_3$) of **[Bnz$_{12}$-G$_2$-TEA];[73]**

Characteristic resonances were confirmed for the dimethyl amine functional dendrimers. Analysis of both **[Am_6-G_1-TEA];[71]** and **[Am_{12}-G_2-TEA];[74]** confirmed a large singlet at 2.28 ppm by ^{1}H NMR, and a resonance at 45.7 ppm by ^{13}C NMR for the confirmation of the dimethyl amine functionality, Figures S3.51, S3.52, S3.57 and S3.58.

Oligo(ethylene glycol) (OEG) functional dendrimers were slightly more difficult to assign, since the oligo(ethylene glycol) monomethyl ether acrylate monomer was based on a repeat unit number average degree of polymerisation = 9, and therefore comparisons between expected and observed integrations could only be estimated. Analysing the ^{1}H NMR spectra of **[OEG_6-G_1-TEA];[72]** and **[OEG_{12}-G_2-TEA];[75]** confirmed the presence of oligo(ethylene glycol) functionalities at approximately 3.65 ppm and the monomethoxy singlet resonance at 3.38 ppm, Figures S3.54 and S3.59. Further assignments were made to the ^{13}C NMR spectra, but it was challenging to make absolute assignments relating to the oligo(ethylene glycol) backbone, Figures S3.55 and S3.60.

3.7.3 Characterisation of functional dendrimers by mass spectrometry

Each dendritic macromolecule was fully characterised using mass spectrometry techniques. The G_0 benzyl functional dendrimer **[Bnz_3-G_0-TEA];[69]** was characterised by ESI-MS resulting in three populations at 858 Da (MH^+ = 858 Da), 880 Da (MNa^+ = 880 Da) and 896 Da (MK^+ = 896 Da), Figure S3.47. An additional population at 938 Da was also observed corresponding to an increase of approximately 80 Da assumed to be occurring from oxidation at the thio-ether groups. Oxidation at the thio-ether groups generated after Michael addition to sulfoxides has been reported,[6] and it is believed this is occurring during analysis. For example, addition of 5 oxygen atoms would result in a mass increase of approximately 80 Da (16 Da x 5 = 80 Da).

G_1 dendrimers [**[Bnz_6-G_1-TEA];[70], [Am_6-G_1-TEA];[71], [OEG_6-G_1-TEA];[72]** were characterised by MALDI-TOF mass spectrometry, and led to populations at **[70]** = 1914 Da (MH^+ = 1914 Da), 1936 Da (MNa^+ = 1936 Da), 1952 Da (MK^+ = 1952 Da), Figure S3.50; **[71]** = 1801 Da (MH^+ = 1800 Da), 1823 Da (MNa^+ = 1823 Da); Figure 3.53; and **[72]** = 3858 Da (MNa^+ = 3858 Da). In addition to the observed populations correlating to the expected dendrimers, some additional adducts were

observed by increasing by multiples of 16 Da. For example, the population at 1815 Da (MH^++16Da = 1815 Da) was observed for the dimethyl amine peripheral dendrimer **[Am_6-G_1-TEA];[71],** Figure S3.53. Again, this is believed to be due to oxidation at the thio-ether groups during analysis.

Analysis using MALDI-TOF spectroscopy was performed for the G_2 dendrimers **[Bnz_{12}-G_2-TEA];[73], [Am_{12}-G_2-TEA];[74], [OEG_{12}-G_2-TEA];[75]**. In each case molecular weight adducts for the functionalised dendrimers were observed. Analysis of **[Bnz_{12}-G_2-TEA];[73]** resulted in populations at 4049 Da (MNa^+ = 4049 Da) and 4065 Da (MK^+ = 4065 Da), Figure 3.27.

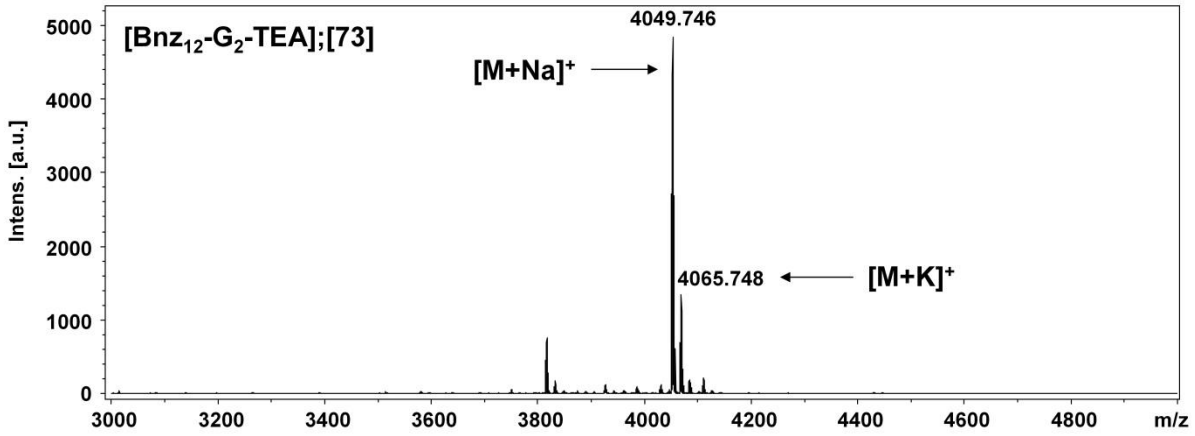

Figure 3.27 MALDI-TOF analysis of **[Bnz_{12}-G_2-TEA];[73]**

Analysis of dimethyl amine peripheral dendrimer **[Am_{12}-G_2-TEA];[74]** by MALDI-TOF resulted in a population at 3822 Da (MNa^+ = 3821 Da), Figure 3.28. Additional populations at 3386 Da and 3605 Da were evident, and can be assigned to fragments, which correlate to the loss of two (3386 Da = MNa^+ = 3386 Da) and one (3605 Da = MNa^+ = 3605 Da) outer peripheral ester units, Figure 3.28.

Finally analysis of the OEG peripheral dendrimer **[OEG_{12}-G_2-TEA];[75]** was conducted by MALDI-TOF, Figure 3.29. Since the OEG monomer is based on a number average degree of polymerisation = 9 a molecular weight distribution was readily observed, Figure 3.29. An enlarged region of the distribution between 6800 and 8000 Da illustrated molecular weight peaks with a molecular weight difference of 44 Da between each population which correlated to the ethylene glycol repeat unit (44 Da).

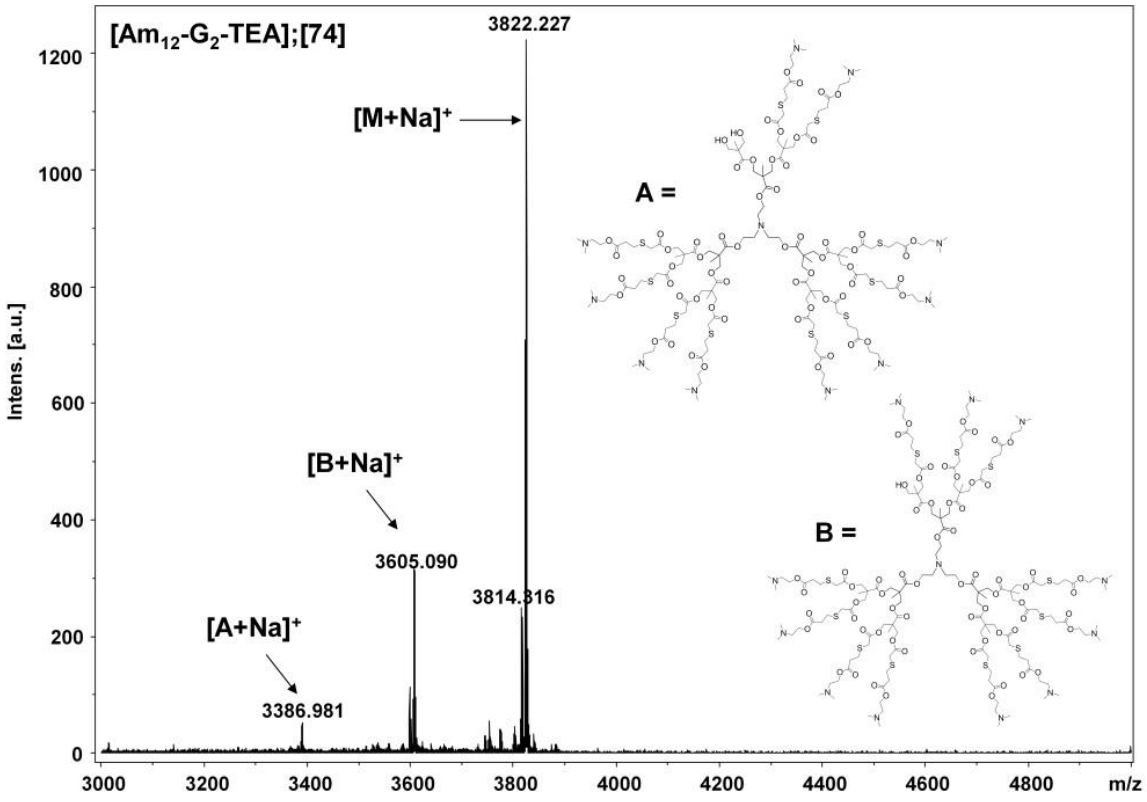

Figure 3.28 MALDI-TOF analysis of **[Am_{12}-G_2-TEA];[74]**

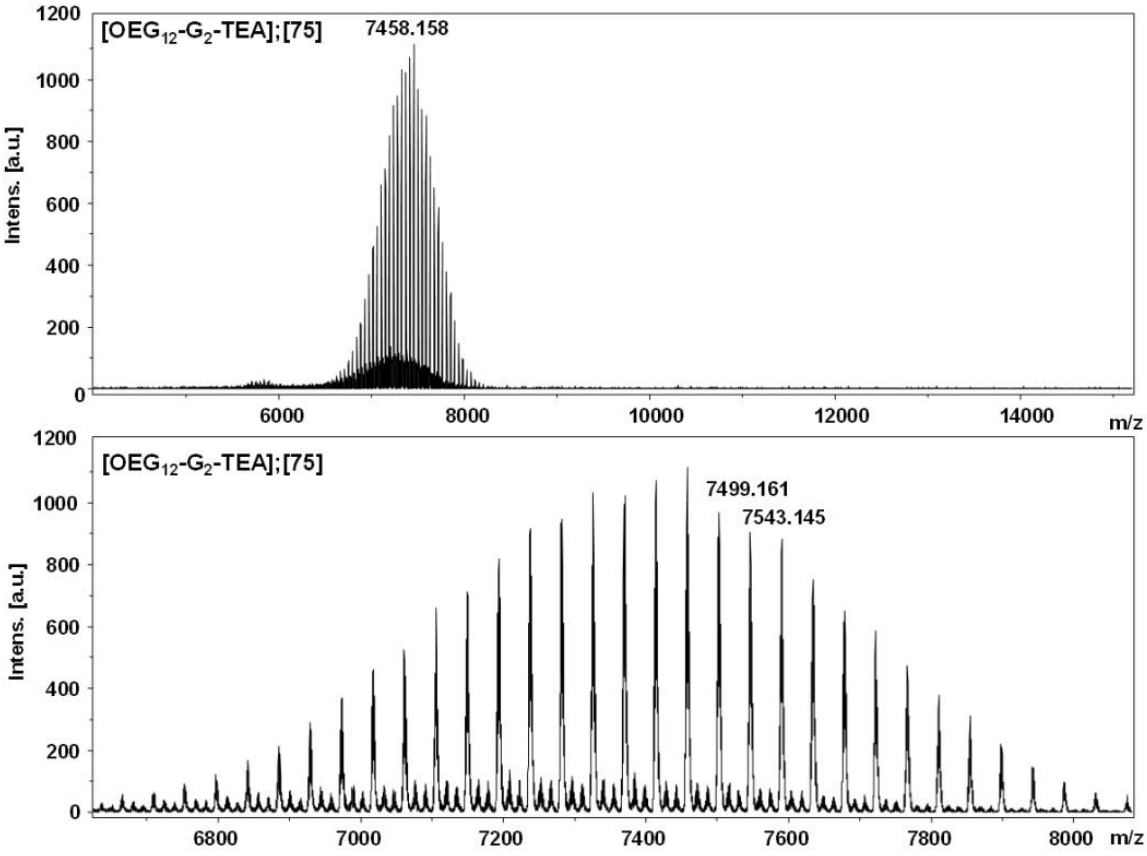

Figure 3.29 MALDI-TOF analysis of **[OEG_{12}-G_2-TEA];[75]**

3.7.4 Characterisation of functional dendrimers by SEC

Dendrimers both before and after Michael addition were analysed by SEC, Table 3.2.

Table 3.2 Analysis of dendrimers before and after Michael addition by MALDI-TOF, ESI-MS and SEC

Dendrimer; Entry #	$M_{calc.}$ (Da)	ESI-MS [MH^+] $M_{obs.}$ (Da)	MALDI-TOF [MNa^+] $M_{obs.}$ (Da)	SEC (THF) M_n (Da)	M_w (Da)	$Đ$
[Xan_3-G_0-TEA];[64]	635.1	636.1	-	890	1400	1.57
[Bnz_3-G_0-TEA];[69]	857.3	858.3	-	1095	1350	1.23
[Xan_6-G_1-TEA];[65]	1469.1	1470.1	1492.2	1540	1795	1.16
[Bnz_6-G_1-TEA];[70]	1913.6	-	1936.8	2145	2320	1.08
[Am_6-G_1-TEA];[71]	1799.7	-	1823.1	2400	2795	1.16
[OEG_6-G_1-TEA];[72]	3834*	-	3858*	3830	4345	1.14
[Xan_{12}-G_2-TEA];[66]	3137.3	-	3161.0	4100	4485	1.09
[Bnz_{12}-G_2-TEA];[73]	4026.1	-	4049.7	4230	4530	1.07
[Am_{12}-G_2-TEA];[74]	3798.5	-	3822.2	5855	6275	1.07
[OEG_{12}-G_2-TEA];[75]	7868*	-	7897*	8585	9795	1.14

*Nominal Molecular weights due to polymer modification

As the reaction of functional acrylates (**[BA]**, **[DMAEA]**, **[OEGA]**), to the xanthate functional dendrimers **[64]**, **[65]** and **[65]** resulted in an increase in total overall molecular weight, an increase in M_n and M_W obtained via SEC was expected.

In every case, functional dendrimers **[69]-[75]** analysed by SEC, Table 3.2, did show an increase in M_n and M_W as expected.

To illustrate the monodisperse nature of the dendrimers before and after functionalisation with **[BA]**, SEC overlays of the chromatograms of G_0, G_1 and G_2 dendrimers are shown in Figure 3.30.

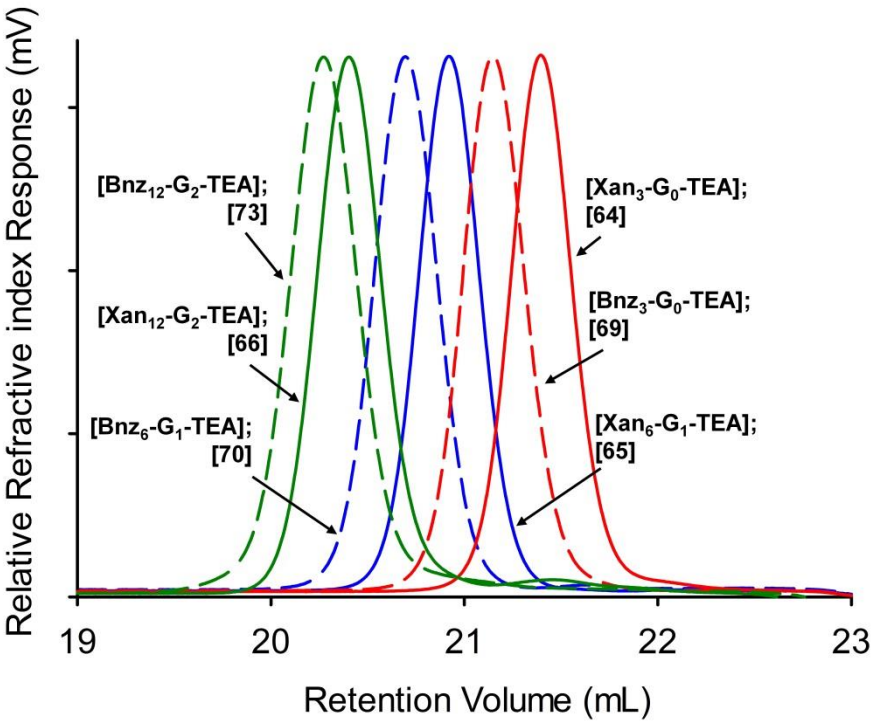

Figure 3.30 SEC chromatograms (refractive index detector, THF eluent) of G_0, G_1, and G_2, dendrimers before and after one-pot deprotection/thiol-Michael addition with **[BA]**. Xanthate peripheral dendrimers (solid lines); **[Xan$_3$-G$_0$-TEA];[64]** (red); **[Xan$_6$-G$_1$-TEA];[65]** (blue); **[Xan$_{12}$-G$_2$-TEA];[66]** (green). Benzyl peripheral dendrimers (dashed lines); **[Bnz$_3$-G$_0$-TEA];[69]** (red); **[Bnz$_6$-G$_1$-TEA];[70]** (blue**)**; **[Bnz$_{12}$-G$_2$-TEA];[73]** (green).

3.8 Conclusions

The first example of xanthate functional dendrimers that can undergo one-pot xanthate deprotection and surface functionalisation via thiol-acrylate Michael addition were presented. From three generations of polyester dendrimers (G_0, G_1, and G_2), a further seven dendrimers resulted, with hydrophobic, hydrophilic and polymeric surface chemistries. All the dendritic materials were fully characterised by ^{1}H and ^{13}C NMR, SEC, and either electrospray or MALDI-TOF mass spectrometry, depending upon the generation and nature of the end groups

Particular attention was paid to the synthetic strategy used to build xanthate functional dendrimers. When initially adopting a strictly convergent strategy, inefficient coupling beyond the synthesis of a G_1 xanthate peripheral dendron resulted. This was solved through the use of an orthogonal divergent strategy; building the dendritic scaffold first, and then successfully functionalising the outer peripheral hydroxyl groups with xanthates, using a new xanthate functional carboxylic acid building block. The xanthate functional dendron was activated at its focal point, and convergently attached to a polyfunctional core. Some complications with the peripheral xanthates did arise when attempting to remove the focal point protecting group. Under the conditions of the focal point removal, elimination of the xanthate functionality, subsequent double bond formation, and generation of acrylate functionality resulted. This was readily observed within the ^{1}H NMR and mass spectral analyses; although the problem was solved by using a modified xanthate functional carboxyl acid building block. Future studies may use this complication for site-specific acrylate placement within functional materials.

3.9 References

1. H. Ihre, A. Hult and E. Söderlind, *Journal of the American Chemical Society*, 1996, **118**, 6388-6395.
2. M. C. Parrott, S. R. Benhabbour, C. Saab, J. A. Lemon, S. Parker, J. F. Valliant and A. Adronov, *Journal of the American Chemical Society*, 2009, **131**, 2906-2916.
3. H. Ihre, O. L. Padilla De Jesús and J. M. J. Fréchet, *Journal of the American Chemical Society*, 2001, **123**, 5908-5917.
4. C. J. Hawker and J. M. J. Frechet, *Journal of the American Chemical Society*, 1992, **114**, 8405-8413.
5. J. S. Moore and S. I. Stupp, *Macromolecules*, 1990, **23**, 65-70.
6. K. Bahrami, M. M. Khodaei and M. Sheikh Arabi, *The Journal of Organic Chemistry*, 2010, **75**, 6208-6213.

CHAPTER 4

Functionalisation of Linear Dendritic hybrid polymers via "One-Pot" Xanthate Deprotection/Thiol-Acrylate Michael Addition Reactions

Publication arising from this Chapter: "One-pot sequential deprotection/functionalisation of linear-dendritic hybrid polymers using a xanthate mediated thiol/Michael addition" See: Sam E. R. Auty, Oliver C. J. Andrén, Faye Y. Hern, Michael Malkoch and Steven P. Rannard, *Polym. Chem.***,** 2015, 6**,** 573-582

4.1 Introduction

In Chapter 3, the first examples of xanthate terminated dendrimers were presented that can undergo xanthate deprotection and peripheral functionalisation by using a one-pot methodology. The chemistry was found to be effective across three generations of dendrimers, generating a further seven materials with hydrophilic, hydrophobic and polymeric surface groups. Building from these successful findings, this Chapter aims to extend the one-pot xanthate deprotection and functionalisation approach beyond the synthesis of functional dendrimers, and towards the synthesis of functional linear dendritic hybrids (LDHs).

4.2 Aims

A synthetic route to deriving functional dendritic macroinitiators (G_1,G_2,G_3 and G_4) that are capable of initiating controlled radical polymerisation by atom transfer radical polymerisation (ATRP) with be designed, implemented and the materials fully characterised.

Using the macroinitiators, xanthate functional LDHs will be constructed via ATRP of tertiary butyl methacrylate (^{t}BuMA), ensuring controlled polymerisation is maintained through kinetic studies. Using the functional LDHs, one-pot deprotection and functionalisation via thiol Michael addition will be performed, to highlight the versatility of this approach. A schematic diagram, Figure 4.1, outlines these aims.

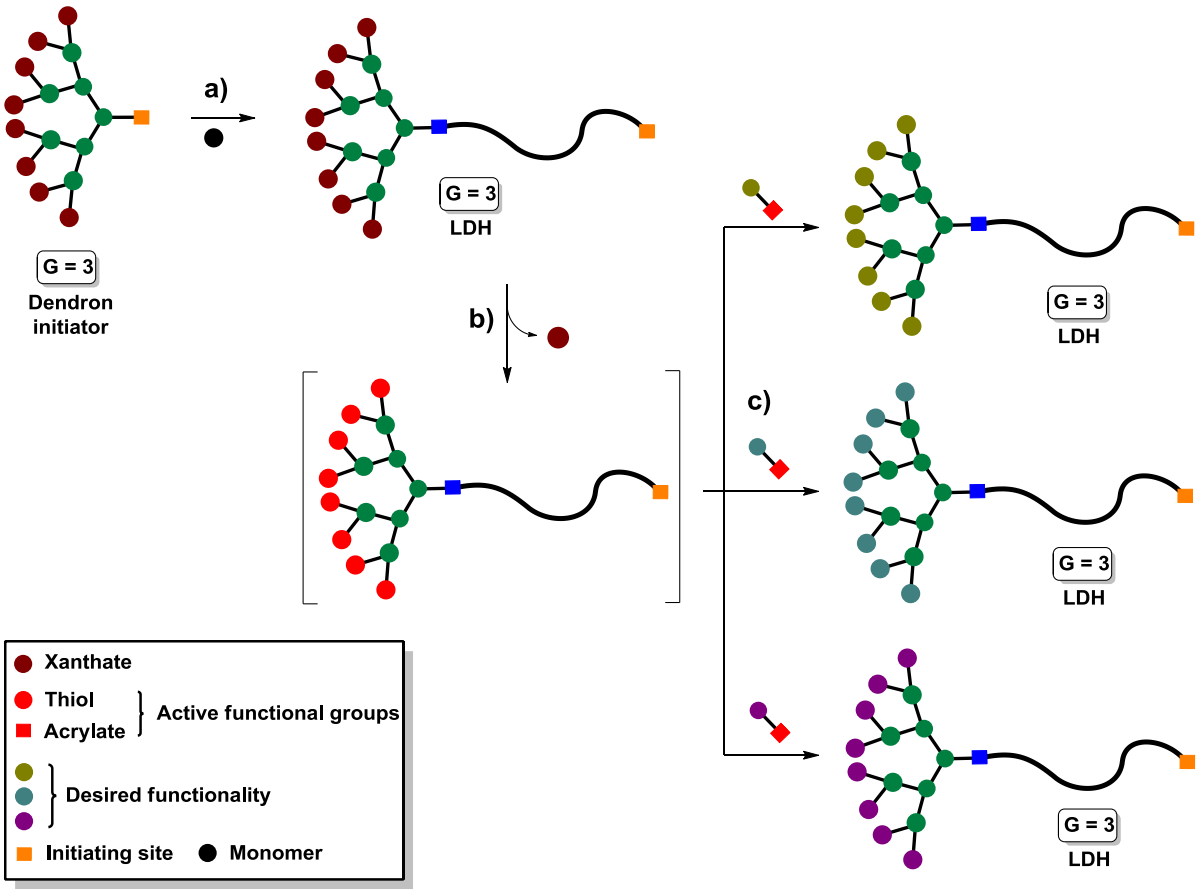

Figure 4.1 Schematic representation of the aims within this Chapter; (a) synthesis of linear dendritic hybrids (LDHs) using xanthate functional dendritic macroinitiators; (b) and (c) one pot xanthate deprotection and thiol Michael addition functionalisation.

4.3 Atom Transfer Radical Polymerisation (ATRP)

The interest in developing novel macromolecular architectures has been largely driven by the significant advances in controlled radical polymerisation (CRP) processes such as nitroxide-mediated polymerisation,[1] ATRP,[2] and reversible addition-fragmentation chain transfer (RAFT) / macromolecular design via the interchange of xanthates (MADIX),[3] which allow control over molecular weight, dispersity, composition, chain architecture and site-specific functionality.

Among the most popular CRP methods is ATRP, developed independently by Kato *et al.*[4] and Wang and Matyjaszewski.[5]

From a mechanistic point of view, ATRP is controlled by an equilibrium between propagating radicals and dormant species, typically in the form of initiating alkyl halides/macromolecular species (P_n-X), Scheme 4.1.[2] The dormant species react with a rate constant of activation (k_{act}) with transition metal complexes in their lower oxidation state acting as activators (Mt^m/L) (where Mt is the transition metal, m is the oxidation state and L is the ligand) to form growing radicals (P_n•) and deactivators-transitional metal complexes in their higher oxidation state, co-ordinated with halide ligands X-Mt^{m+1}/L, Scheme 4.1 The deactivator reacts with the propagating radical in a reverse reaction (k_{deact}) to re-form the dormant species and the activator. (Mechanistic explanation taken from Matyjaszewski).[2] Since ATRP is a catalytic process it can be mediated by many different redox-active transition metal complexes; Cu(I)/L and X-Cu(II)/L is typically the most commonly used system as copper has a low cost and is readily available.

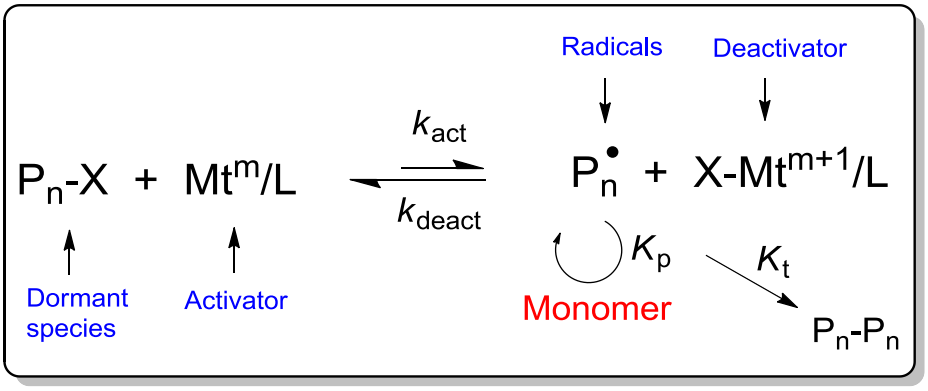

Scheme 4.1 ATRP equilibrium. (Figure adapted from Matyjaszewski).[2]

The rate of an ATRP depends on the rate constant of propagation (k_p) and thus the concentrations of monomer and growing radicals. The radical concentration is affected by the equilibrium constant (K_{ATRP}) between the activation process (generation of radicals, k_{act}) and the deactivation of radicals (formation of alkyl halides, k_{deact}); it is this equilibrium constant ($K_{ATRP} = k_{act}/k_{deact}$) that determines the concentration of radicals. Usually K_{ATRP} is small (10^{-4}-10^{-9}), which ensures a low radical concentration, minimising termination reactions and enabling polymers of uniform length and low dispersity (Đ) (<1.5). The structure of the dormant species (i.e. the initiator or propagating polymer

chain end), ligand, monomer and the reaction conditions (solvent, temperature and pressure) can all strongly influence the values of the rate constants k_{act} and k_{deact}.

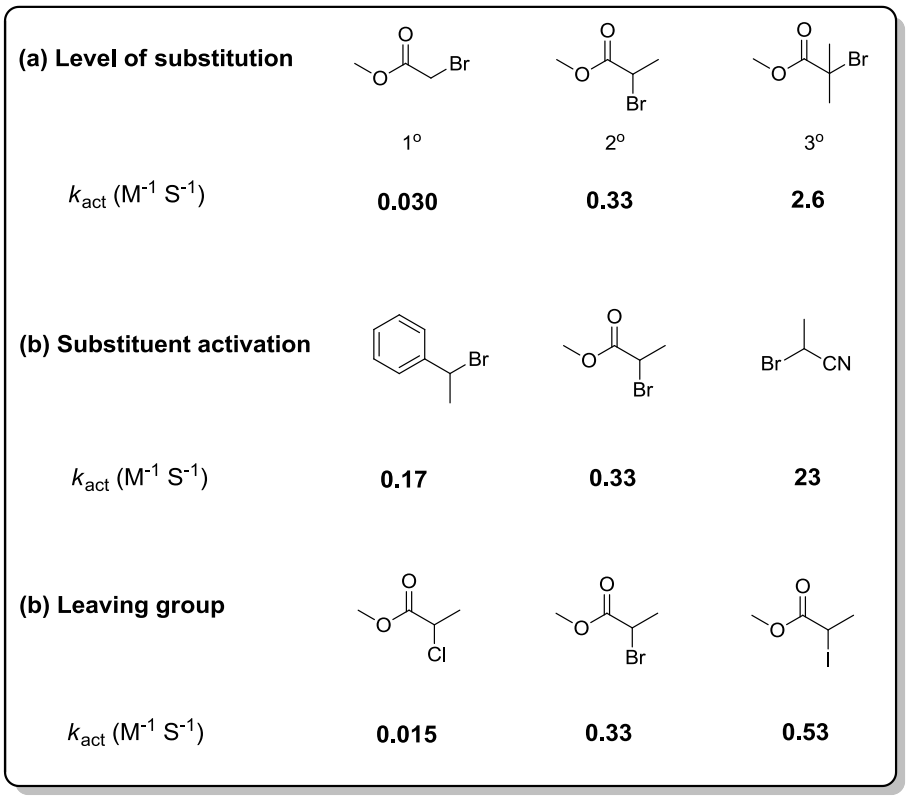

Figure 4.2 Effect on k_{act} by changing the dormant species (initiator) using different; (a) alkyl halide substitution;[6] (b) type of neighbouring substituent;[6] (c) type of halide leaving group.[6]

Changing the initiator structure by the use of different alkyl halide substitutions (primary secondary or tertiary), substituent groups, or different types of alkyl halide has an effect on k_{act}, Figure 4.2.[6] Similar effects on k_{act} are also observed by using different ligand structures, although the variations are significantly greater; for example the tetradentate ligand tris(2-(dimethylamino)ethyl)amine (Me_6TREN), is approximately 68,000 times more active than the bidentate ligand 2,2'-bipyridine (bpy).[7]

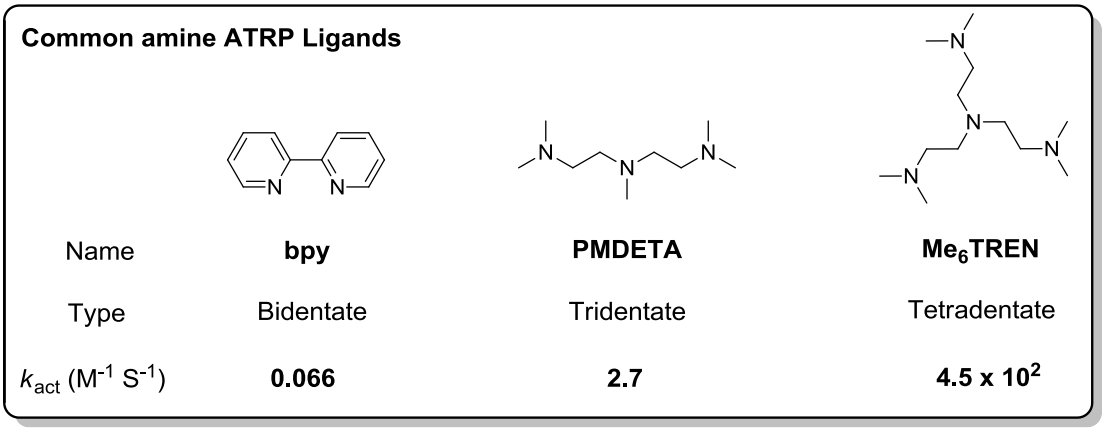

Figure 4.3 Common amine ATRP ligands:[7] 2,2'-Bipyridine (bpy), N,N,N',N'',N''-pentamethyldiethylenetriamine (PMDETA), Tris(2-(dimethylamino)ethyl)amine (Me_6TREN)

One of the disadvantages of ATRP is that the reduced polymer radical concentration can lead to slow polymerisation rates for non-polar monomers such as styrene, even under bulk polymerisation conditions at 110-130 °C.[8] Work by our group and others, has shown that ATRP at ambient temperature of hydrophilic[9] and hydrophobic[10] methacrylates can be polymerised rapidly in polar solvents such as methanol, 2-propanol (IPA) or water/alcohol mixtures, whilst still maintaining low dispersities.

A significant advantage of ATRP is the ability to easily synthesise initiators. The commercially available reagent α-bromoisobutyryl bromide allows a variety of functional groups including alcohols and amines to be easily converted to a tertiary alkyl bromide ATRP initiation site.

Combined with the synthetic ease of initiators, ambient temperature conditions, and good tolerance towards many methacrylate based monomers, throughout this Chapter, and throughout Chapter 5, ATRP will be used as the CRP method for all polymer synthesis.

4.4 Model reaction of xanthate compatibility

Due to the synthetic design of the targeted xanthate peripheral LDHs, Figure 4.1, it was important to ensure that the presence of xanthate functionalities did not inhibit, retard or induce chain transfer during the ATRP of ^{t}BuMA. Recent studies have shown that monomers comprising of similar xanthate functionalities can be polymerised by ATRP without loss of control.[11]

A model polymerisation of ^{t}BuMA was performed in the presence of the xanthate functional acid **[Xan-A-COOH];[57]**, using the commercially available ATRP initiator, ethyl 2-bromoisobutyrate (EBiB) in alcoholic/aqueous media at 40 °C, Scheme 4.2.

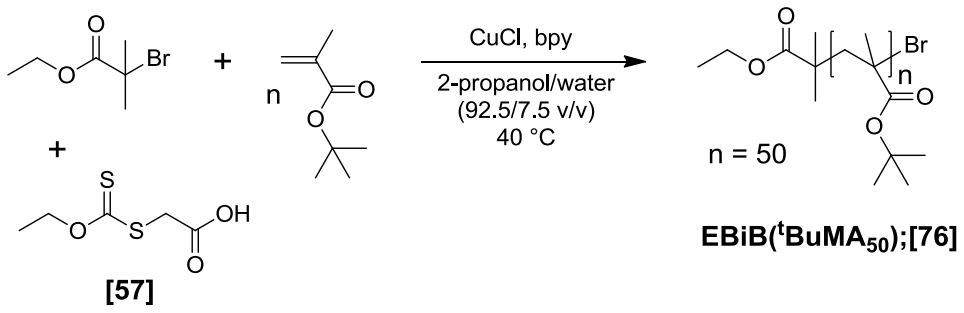

Scheme 4.2 ATRP of ^{t}BuMA under alcoholic conditions, in the presence of xanthate functional acid **[Xan-A-COOH];[57]**

Targeting DP_n = 50 monomer units, ^{t}BuMA, EBiB, **[57]**, IPA/water solvent and bpy were stirred in an oven dried 10 mL round bottom flask (RBF) and deoxygenated using a nitrogen purge for 10 minutes. Cu(I)Cl was added to the flask whilst maintaining a positive flow of nitrogen, and the reaction was left to polymerise at 40 °C for 16 hours. The reaction was terminated by exposure to oxygen when conversion reached >99%, as indicated by the disappearance of the methacrylate vinyl resonances at 5.48 ppm and 6.0 ppm, by ^{1}H NMR analysis. The solution was passed through a neutral alumina column to remove the catalytic system, and precipitated twice into pet ether (30-40 °C) cooled using dry ice. After drying the precipitated sample overnight under high vacuum to remove residual solvents, **EBiB(^{t}BuMA$_{50}$);[76]** was obtained as a white solid.

Analysis of **[76]** by ^{1}H NMR indicated no evidence of xanthate functionality, confirmed by the absence of a resonance at 4.65 ppm (indicative of the xanthate functionality), Figure S4.1. Further analysis by SEC resulted in a number average molecular weight (M_n) of 7900 Da, which was comparable to the theoretical 7100 Da expected, Figure S4.2. The weight average molecular weight (M_w) was slightly high at 12300 Da, resulting in a dispersity (Đ) of 1.56. Since the polymerisation was left at high conversion (>99%) for a long period of time, the high Đ was most likely a result of this.

Coupled with previous reports,[11] the model reaction confirmed the presence of **[57]** was unlikely to be behaving as a chain transfer agent (CTA) during the ATRP of ^{t}BuMA. Further details below also support this.

CTAs are used in RAFT polymerisations to provide control over molecular weight during a free radical polymerisation.[3] In the pre-equilibrium stage of a RAFT polymerisation, which occurs after the generation of propagating monomers (P_m) Scheme 4.3, P_m react with a CTA (a), to form an intermediate radical (b), which can fragment to liberate a new dormant chain (c) and a reinitiating group (d). How affective the CTA (a) is at forming species (b), (c) and (d) is determined by two structural components.

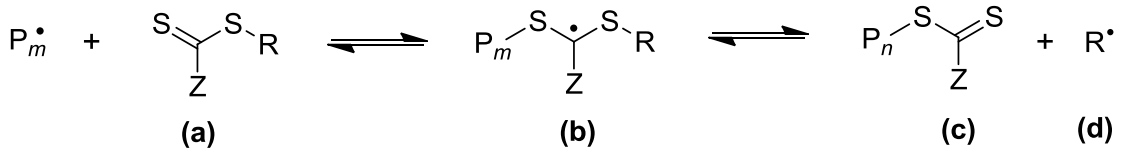

Scheme 4.3 Pre-equilibrium stage of a RAFT polymerisation

The first factor is the Z group, which affects the stability of the S=C bond, and in turn affects the rates of reactions in the pre-equilibrium. The most reactive S=C bonds have Z groups containing carbon (dithioesters) or sulfur (trithiocarbonates).[12] Z groups with oxygen (xanthates) or nitrogen (dithiolcarbamates) are less reactive towards radical addition.[12] The second factor is the R group, which must be able to stabilise a radical so that the right hand side of the pre-equilibrium is favoured, forming intermediate (b), but also provide some instability so that (b) can fragment to reinitiate a new

polymer chain, (d). A good CTA therefore has a reactive S=C bond determined by the choice of the Z group, and a stable, but not too stable (otherwise it will never fragment to (c) and (d)), radical intermediate (b), determined by the R group.

Theory from organic chemistry states that radicals are stabilised by neighbouring atoms that can donate electron density. By increasing the number of neighbouring alkyl groups on the carbon, increases the stability of a radical, Figure 4.4.

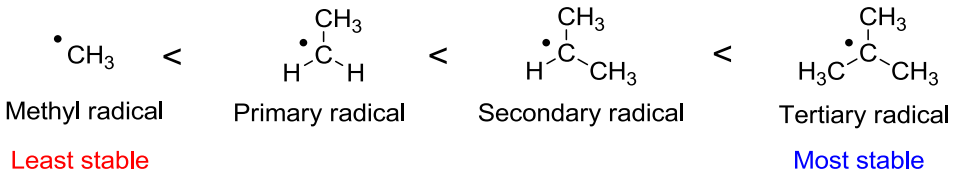

Figure 4.4 Stability of radicals as the neighbouring electron density increases

Using **[57]** as a CTA, Scheme 4.4, it is unlikely that the R group (-CH_2COOH) can provide sufficient stability towards the radical intermediate (e). This is since the primary CH_2 functionality and neighbouring electron withdrawing carboxylic acidic do not donate enough electron density. In fact, since the carboxylic acid is electron withdrawing, this is likely to pull electron density from the primary CH_2 functionality reducing its radical stabilising ability.

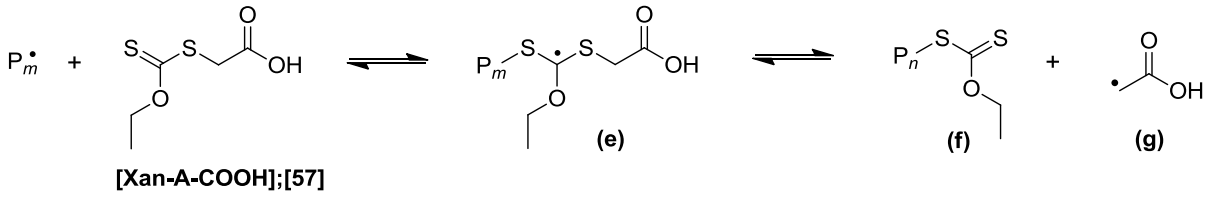

Scheme 4.4 Pre-equilibrium stage of a RAFT polymerisation using **[Xan-A-COOH];[57]**

Even if the intermediate (e) is formed, upon fragmentation to (f) and (g), the reinitiating group (f) is likely to be an equally unstable species. Again, this is since the primary CH_2 functionality and neighbouring electron withdrawing carboxylic acidic do not provide adequate radical stabilisation.

On the basis of the model reaction, organic chemistry principles, and previous reports using similar xanthate functionalities polymerised by ATRP without loss of control,[11] it is unlikely that **[57]** is behaving as a CTA during the polymerisation of ^{t}BuMA by ATRP.

4.5 Dendritic scaffold

4.5.1 Synthesis of bis-MPA dendritic scaffold

The synthesis of high molecular weight dendritic initiators followed a similar strategy to Chapter 3, whereby the dendritic scaffold was constructed by a divergent process. Again, dendrimer macromolecules based on the AB_2 monomer 2,2-bis(methoxy)propionic acid (bis-MPA) were chosen for the scaffold synthesis, due to low toxicity, ease of preparation and reported compatibility with ATRP.[13]

In Chapter 2 the benzylidene protected bis-MPA anhydride **[OBz$_1$-G$_1$-Anhy];[48]** was used for the construction of the bis-MPA scaffold. Although this monomer was extremely efficient, a drawback was that catalytic hydrogenation using $Pd(OH)_2$ under a hydrogen atomosphere (10 bar) was required to remove the benzylidene protecting groups before an additional growth step could occur. Limited by the size of our hydrogenation apparatus, multiple hydrogenations had to be performed to generate a sufficient quantity of material for the next step. Work by Malkoch *et al.*[14] demonstrated that a similar acetonide protected bis-MPA anhydride can be easily prepared, which employs acid hydrolysis for acetonide removal, thus avoiding hydrogenation. Adopting this strategy, the acetonide protected bis-MPA anhydride **[Acet$_1$-G$_1$-Anhy];[78]** was constructed, Scheme 4.5.

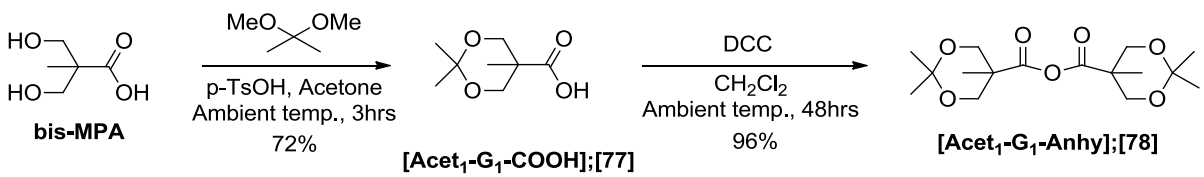

Scheme 4.5 Synthesis of acetonide protected bis-MPA anhydride **[Acet$_1$-G$_1$-Anhy];[78]**

Prepared on a 100g scale, bis-MPA, 2,2-dimethoxypropane, and a catalytic amount of *p*-toluene sulfonic acid (p-TsOH) were suspended in acetone and stirred at ambient temperature for 3 hours. Over the 3 hours the solution became clear as the reaction took place. Following this, the catalyst was neutralised by adding 10 mL of a 1:1 mixture of NH_4OH:EtOH, resulting in salt precipitation. The product was obtained by removal of acetone *in vacuo*, redissolving the crude solid in CH_2Cl_2, washing the organic layer twice with water, drying over $MgSO_4$ and after removal of solvents, resulting in **[Acet$_1$-G$_1$-COOH];[77]** as a white solid in 72% yield.

Similarly to the benzylidene protected anhydride monomer, the acetonide protected anhydride monomer **[Acet$_1$-G$_1$-Anhy];[78]** was prepared through the self-condensation of **[77]** by dissolving in CH_2Cl_2 and adding 0.50 equivalents of *N,N'*-dicyclohexylcarbodiimide (DCC) as the dehydrating agent to the stirring mixture at ambient temperature. The reaction was followed by using ^{13}C NMR spectroscopy, to monitor the change in the shift of the carbonyl environment from 180.3 ppm to 169.5 ppm, indicative of the anhydride formation. After 48 hours, the *N,N'*-dicyclohexylurea (DCU) by-product was removed by filtration, and the crude product precipitated once from the minimum amount of CH_2Cl_2 into hexane cooled using dry ice and left under vigorous stirring for 1 hour. After filtration, and removal of solvents by high vacuum, **[Acet$_1$-G$_1$-Anhy];[78]** was obtained as a grey viscous oil in 96% yield.

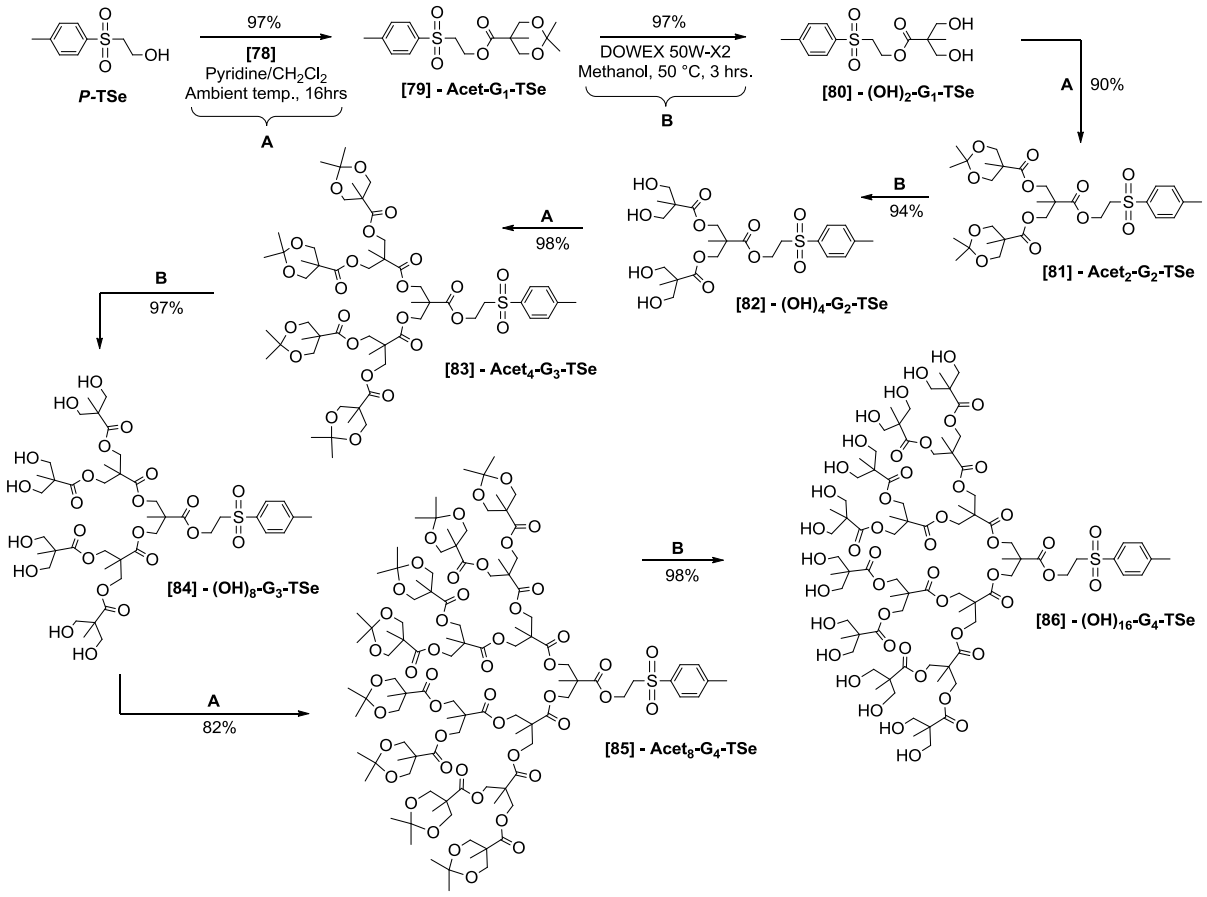

Scheme 4.6 Divergent synthesis of G_1, G_2, G_3 and G_4 hydroxyl terminated dendrons

The construction of G_1, G_2, G_3 and G_4 bis-MPA-derived hydroxyl-functional dendrons **[(OH)$_2$-G$_1$-TSe];[80]**, **[(OH)$_4$-G$_2$-TSe];[82]**, **[(OH)$_8$-G$_3$-TSe];[84]** and **[(OH)$_{16}$-G$_3$-TSe];[86]** were broken into two steps; firstly a growth step by esterification using monomer **[78]**, and secondly an activation step by acid hydrolysis using DOWEX 50W-X2 resin, Scheme 4.6.

For the synthesis of **[(OH$_2$)-G$_1$-TSe];[80]**, growth was achieved by reacting *p*-toluene sulfonyl ethanol (***P*-Tse**) with 1.3 equivalents of **[Acet$_1$-G$_1$-Anhy];[78]**, 0.2 eqv of 4-dimethylaminopyridine (DMAP) and 5 equivalents of pyridine, dissolved in a 1:3 ratio of pyridine:CH_2Cl_2 (v/v). After stirring at ambient temperature for 16 hours, 10 mL of H_2O was added to quench the excess anhydride and the reaction was left stirring for an additional 2 hours. The product was isolated by diluting the mixture with CH_2Cl_2, washing with acid (1M $NaHSO_4$), base (1M $NaHCO_3$), brine, drying the organic layer over $MgSO_4$, and after removal of solvents resulted in **[Acet$_1$-G$_1$-TSe];[79]** as a colourless viscous oil in 97% yield. Removal of the acetonide protecting group was achieved by dissolving **[Acet$_1$-G$_1$-**

TSe];[79] in MeOH, adding DOWEX 50W-X2 resin, and leaving the mixture to stir for 3 hours at 50 °C. Thin-layer chromatography (TLC) confirmed the total disappearance of **[79]** after 3 hours. The product was isolated by the removal of DOWEX resin by filtration, evaporation of MeOH, and after removal of trace solvents by high vacuum overnight, **[$(OH)_2$-G_1-TSe];[80]** was obtained as white solid in 97%.

Hydroxyl terminated dendrons **[82]**, **[84]** and **[86]** were prepared using the same methodology, but required additional purification by liquid chromatography to remove trace impurities.

4.5.2 Characterisation of bis-MPA scaffold

4.5.2.1 Analysis by NMR spectroscopy

Confirmation of the acetonide protected bis-MPA, **[$Acet_1$-G_1-COOH];[77]** was achieved using ^{1}H and ^{13}C NMR spectroscopy, with each spectrum confirming the desired number of environments, Figures S4.3 and S4.4. Similarly to the benzylidene protected monomer **[OBz_1-G_1-Anhy];[48]**, analysis of the acetonide protected anhydride monomer **[$Acet_1$-G_1-Anhy];[78]** was by ^{1}H and ^{13}C NMR spectroscopy, Figures S4.5 and Figure S4.6. Again, the ^{13}C NMR spectrum was considerably more useful, since it provided the characteristic anhydride resonance at 169 ppm.

Dendritic macromolecules **[79]** to **[86]** were fully characterised by ^{1}H and ^{13}C NMR spectroscopy, with the acetonide protected dendrons soluble in $CDCl_3$, and the hydroxyl dendrons soluble in CD_3OD. Analysis of the ^{1}H NMR spectrum of the G_4 acetonide protected dendron **[$Acet_8$-G_4-TSe];[85]** confirmed fourteen different proton environments, with the expected number of integrals relative to the TSe focal point protecting functionality, Figure 4.5. A clear feature of the spectrum was that different generational segments gave rise to unique resonances, such as the methyl groups at 1.14, 1.22, 1.25 and 1.27 ppm (environments, 3, 9, 7 and 5 respectively, Figure 4.4). Similar observations were present in the ^{1}H NMR spectra of lower generation dendrons (G_1, G_2, G_3), **[79]**, **[81]**, **[83]**, Figures S4.7, S4.13 and S4.19.

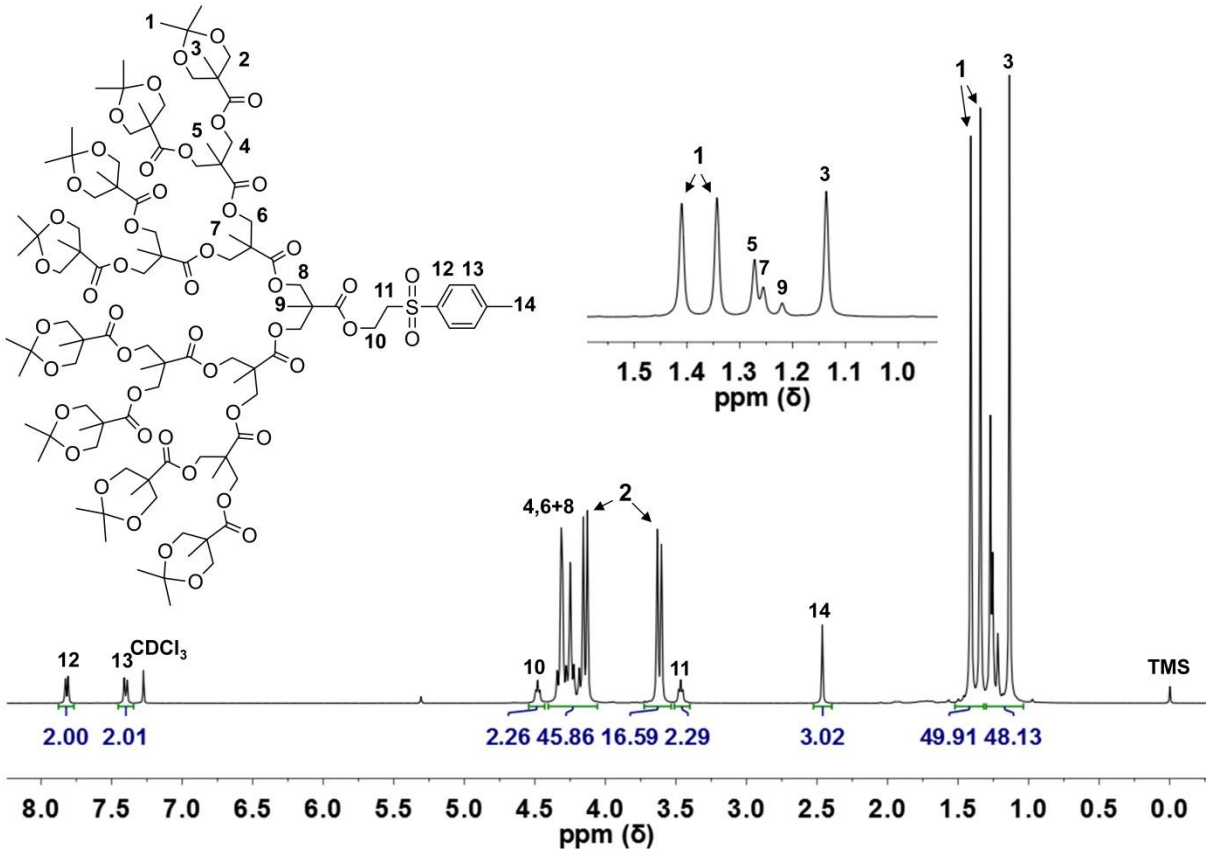

Figure 4.5 ^{1}H NMR spectrum (400 MHz, $CDCl_3$) of **[Acet$_8$-G$_4$-TSe];[85]**

Analysis of the acetonide protected dendrons by ^{13}C NMR spectroscopy resulted in a unique set of resonances after each growth step. For example, the ^{13}C NMR spectrum of acetonide protected dendron **[Acet$_8$-G$_4$-TSe];[85]** confirmed twenty five different carbonyl environments which included four different resonances for each ester carbonyl, methyl, tertiary carbon and methylene environment representative of the different generational segments, Figure S4.25. Similar environments in the ^{13}C NMR spectra of lower generation acetonide protected dendrons (G_1, G_2, G_3), **[79]**, **[81]**, **[83]** were observed, Figures S4.8, S4.14 and S4.20.

Analysis of hydroxyl terminated dendrons **[80]**, **[82]**, **[84]** and **[86]** by ^{1}H and ^{13}C NMR spectroscopy techniques resulted in the expected number of resonances and integrals in each case. A key feature of each ^{1}H NMR spectrum was the disappearance of a large doublet at approximately 1.38 ppm, confirming total removal of the acetonide protecting functionalities; shown in the ^{1}H NMR spectrum

of **[(OH)$_{16}$-G$_3$-TSe];[86]**, Figure 4.6, and also in the spectra of lower generation dendrons, Figures S4.10, S4.16 and S4.22.

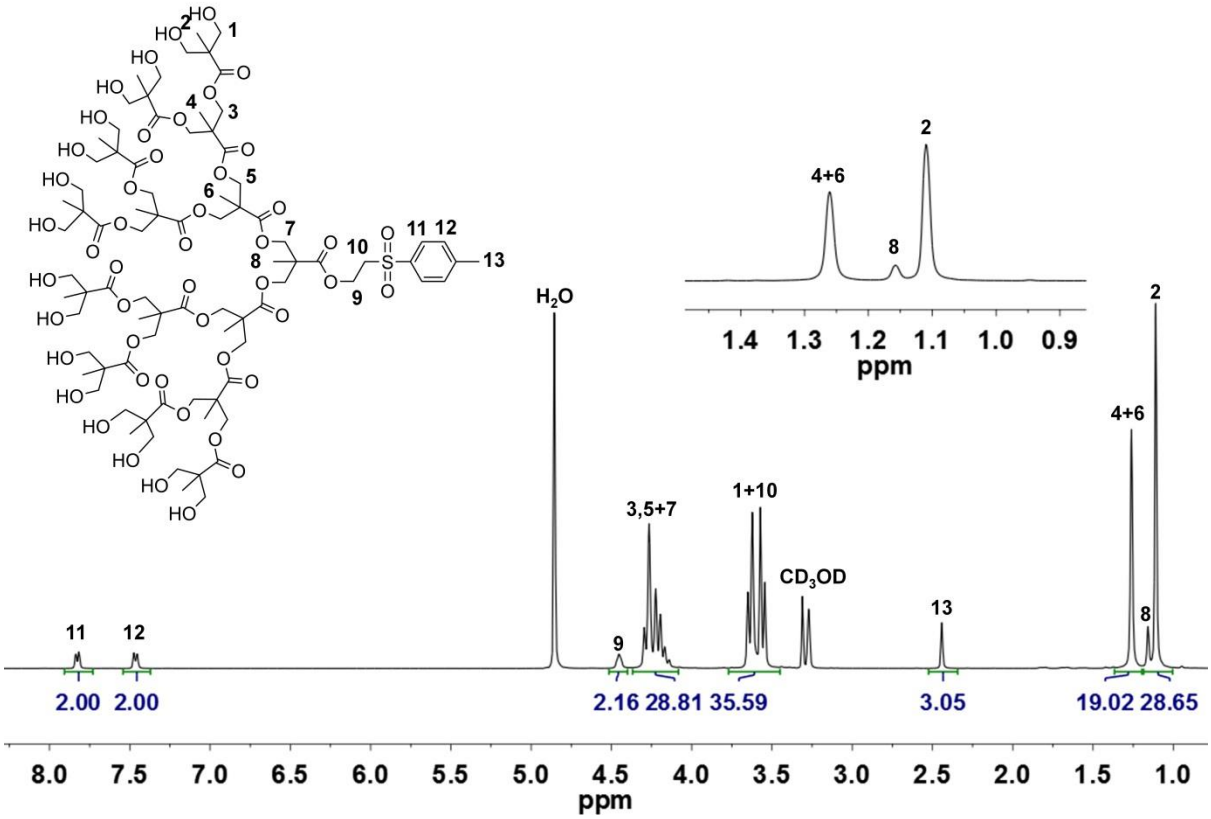

Figure 4.6 ^{1}H NMR spectrum (400 MHz, $CDCl_3$) of **[(OH)$_{16}$-G$_3$-TSe];[86]**

Disappearance of acetonide resonances at approximately 22, 25 and 98 ppm in each ^{13}C NMR spectrum was readily observed for hydroxyl dendrons **[80]**, **[82]**, **[84]** and **[86]**, Figures S4.11, S4.17, S4.23 and S4.26. Importantly, no degradation of TSe functionality was observed in any of the ^{1}H or ^{13}C NMR spectra for hydroxyl dendrons **[80]**, **[82]**, **[84]** and **[86]**.

4.5.2.2 Analysis by mass spectrometry

Each bis-MPA dendron **[79]** to **[86]** was analysed by ESI-MS, resulting in observation of the desired adducts in each case. The acetonide protected G_1 dendron **[Acet$_1$-G$_1$-TSe];[79]** confirmed two populations at 379 Da (MNa^+ = 379 Da) and 395 Da (MK^+ = 395 Da), Figure S4.9. After removal of acetonide functionalities, **[(OH)$_2$-G$_1$-TSe];[80]** three populations at 317 Da (MH^+ = 317 Da), 339 Da

(MNa^+ = 339 Da) and 355 Da (MK^+ = 355 Da) were observed with no populations indicative of starting materials present, Figure S4.12.

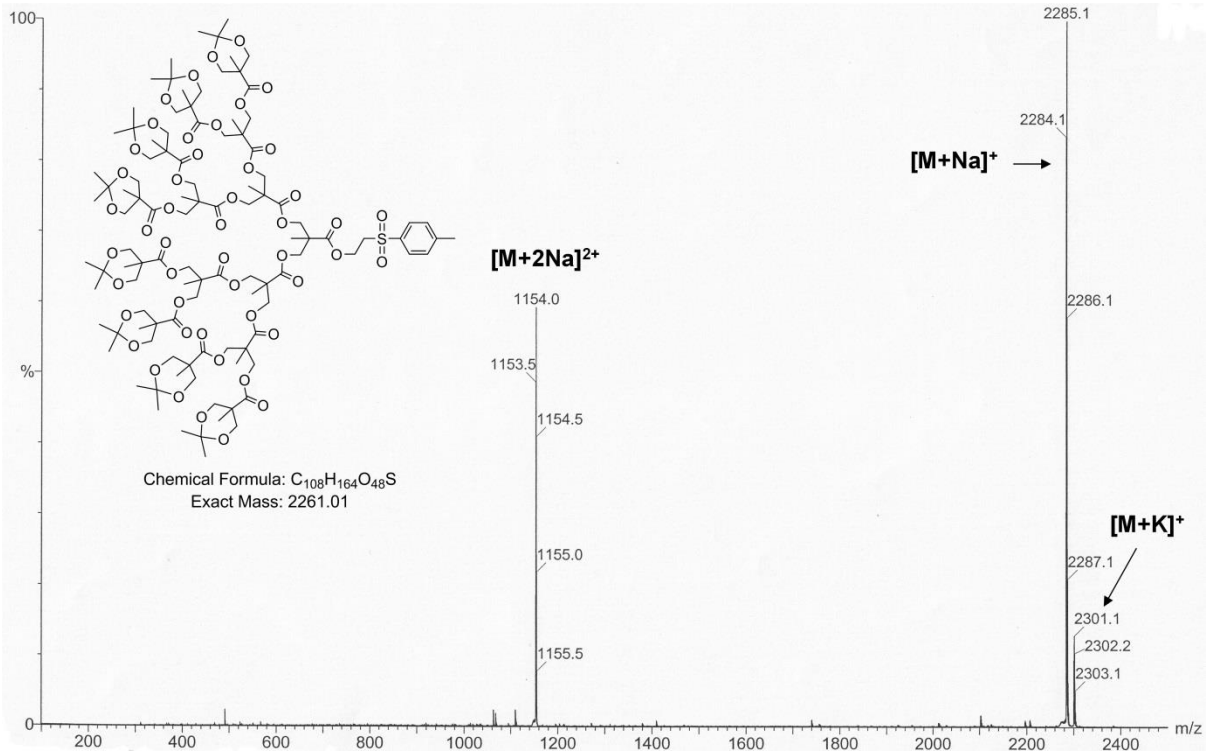

Figure 4.7 ESI-MS (MeOH) of **[Acet$_8$-G$_4$-TSe];[85]**

Populations for the G_2 **[Acet$_2$-G$_2$-TSe];[81]** were confirmed at 651 Da (MNa^+ = 651 Da) and 667 Da (MK^+ = 667 Da), Figure S4.15, and after deprotection, **[(OH)$_4$-G$_2$-TSe];[82]** two populations at 571 Da (MNa^+ = 571 Da) and 587 Da (MK^+ = 587 Da), Figure S4.18.. The G_3 dendron [**Acet$_4$-G$_3$-TSe];[83]** resulted in populations at 1195 (MNa^+ = 1195 Da) and 1211 Da (MK^+ = 1211 Da), Figure S4.21, and following deprotection **[(OH)$_8$-G$_3$-TSe];[84]** was confirmed with two populations at 1035 Da (MNa^+ = 1035 Da) and 1051 Da (MK^+ = 1051 Da), Figure S4.24. The G_4 dendron **[Acet$_8$-G$_4$-TSe];[85]** resulted in populations at 2284 Da (MNa^+ = 2284 Da), 2301 Da (MK^+ = 2301Da), and a double charged species at 1154 Da ($M+2Na^{2+}$ = 1154 Da), Figure 4.7.

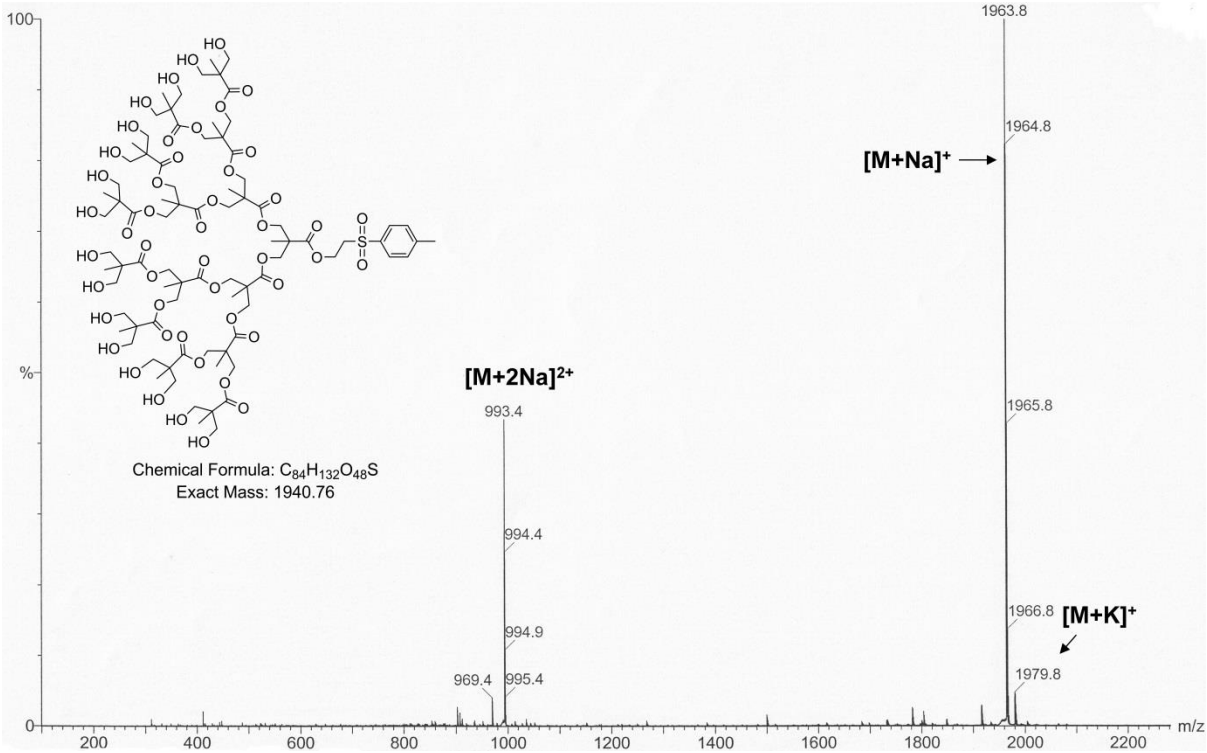

Figure 4.8 ESI-MS (MeOH) of **[(OH)$_{16}$-G$_3$-TSe];[86]**

Deprotection of the eight acetonide functionalities resulted in **[(OH)$_{16}$-G$_3$-TSe];[86]**, with populations confirmed at 1964 Da (MNa^+ = 1964 Da), 1979 Da (MK^+ = 1979 Da) and a double charged species at 993 Da ($M+2Na^{2+}$ = 993 Da), Figure 4.8.

4.6 Dendritic ATRP macroinitiators

4.6.1 Synthesis of xanthate functional macroinitiators

Since G_1 and G_2 hydroxyl dendrons **[(OH)$_2$-G$_1$-TSe];[80]** and **[(OH)$_4$-G$_2$-TSe];[82]** were exactly the same compounds as **[(OH)$_2$-G$_1$-TSe];[50]** and **[(OH)$_4$-G$_2$-TSe];[52]**, prepared earlier in Chapter 3 via the benzylidene protected bis-MPA anhydride, xanthate functionalisation of **[80]** and **[82]**, followed the same esterification procedure using DCC/DPTS and **[Xan-A-COOH]; [57]** resulting in xanthate functional dendrons **[Xan$_2$-G$_1$-TSe];[58]** and **[Xan$_4$-G$_2$-TSe];[60]**.

In Chapter 3, the synthesis of G_3 xanthate functional dendron **[Xan$_8$-G$_3$-TSe];[61]** was achieved by DCC/DPTS esterification with **[(OH)$_8$-G$_3$-TSe];[54]** (also the same as compound **[(OH)$_8$-G$_3$-TSe];[84]**) and **[Xan-A-COOH];[57]**, but was complicated by the poor solubility of **[54]** with CH_2Cl_2 which resulted in a low yield of 26% after purification by liquid chromatography. After its synthesis, it was also found that the solubility of the G_4 hydroxyl dendron **[(OH)$_{16}$-G$_3$-TSe];[86]** in CH_2Cl_2 was very poor.

Pyridine was found to be a good solvent for the hydroxyl terminated dendrons, and is also a catalyst and co-solvent in typical anhydride esterifications. With this in mind, a solution to increase the yield of the G_3 xanthate functional dendron **[Xan$_8$-G$_3$-TSe];[61]** and to synthesise the G_4 xanthate functional dendron, was to prepare the xanthate functional anhydride monomer **[Xan-A-Anhyd];[87]**, Scheme 4.7.

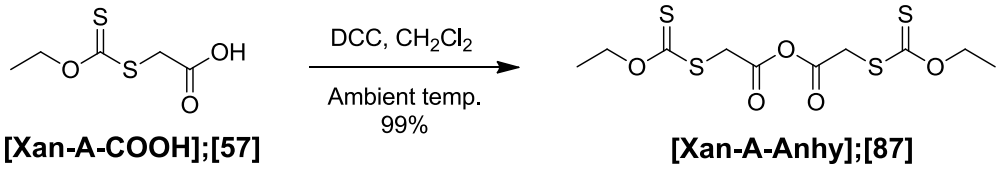

Scheme 4.7 Synthesis of xanthate functional anhydride **[Xan-A-Anhyd];[87]**

To prepare the anhydride monomer, dehydration was achieved by dissolving the functional xanthate monomer **[Xan-A-COOH]; [57]** in CH_2Cl_2, adding DCC, and leaving the mixture to stir for 24 hours at ambient temperature. Determination of reaction completion was followed by using ^{13}C NMR spectroscopy, whereby the ^{13}C NMR spectrum of **[87]** resulted in an anhydride carbonyl resonance at 163 ppm. Workup resulted by filtration of the DCU by-product, removal of CH_2Cl_2 *in vacuo* to result in **[87]** as a red paste in 99% yield.

Using this anhydride monomer, the G_3 **[Xan$_8$-G$_3$-TSe];[61]** and G_4 [**Xan$_{16}$-G$_4$-TSe];[88]** xanthate functional dendrons were successfully prepared, Scheme 4.8.

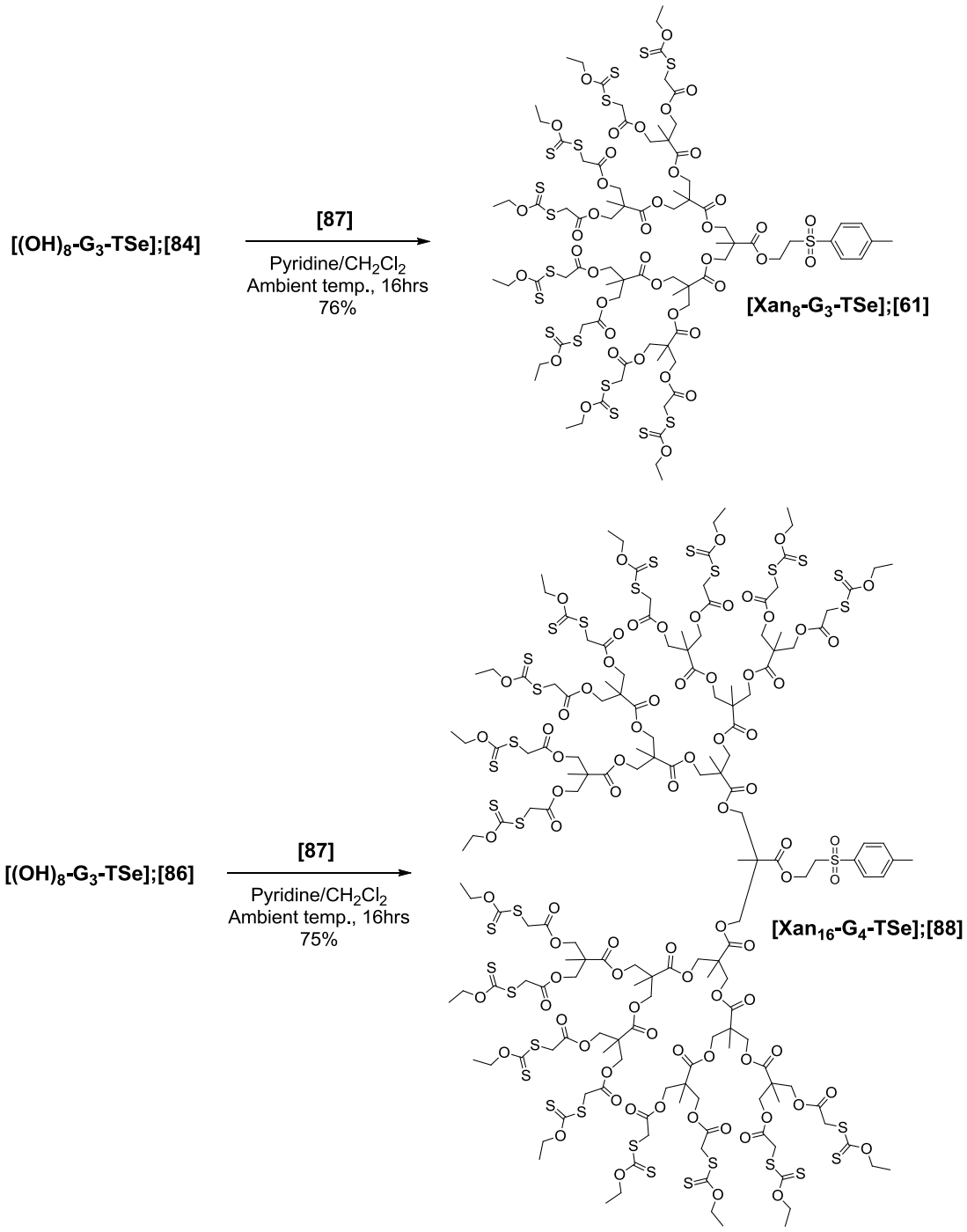

Scheme 4.8 Preparation of xanthate functional dendrons **[Xan_8-G_3-TSe];[61]** and **[Xan_{16}-G_4-TSe];[88]** by esterification using anhydride monomer **[Xan-A-Anhyd];[87]**

For the synthesis of **[Xan_8-G_3-TSe];[61]**, the hydroxyl dendron **[$(OH)_8$-G_3-TSe];[84]** and DMAP were dissolved in a 1:2 (v/v) mixture of pyridine:CH_2Cl_2 and cooled in an ice bath. Xanthate anhydride **[Xan-A-Anhyd];[87]** (1.3 equivalents per OH group), dissolved in a small volume of CH_2Cl_2, was then added slowly to the mixture and left at 0 °C for 30 minutes. Following this, the

reaction was allowed to warm to ambient temperature, and stirred for an additional 16 hours. Before isolation of the product, the excess anhydride was quenched by adding approximately 10 mL of H_2O and stirring the mixture vigorously for an additional 3 hours. The product was isolated by diluting with CH_2Cl_2, washing the organic layer with acid (1M $NaHSO_4$), base (1M $NaHCO_3$), brine, drying over $MgSO_4$, and removal of solvents, resulting in a red viscous oil. Additional purification by liquid chromatography (silica, hexane:ethyl acetate, 15:85, increasing the polarity to 50:50) resulted in **[Xan_8-G_3-TSe];[61]** as viscous red oil in 76% yield. The synthesis of the G_4 xanthate functional dendron was prepared by the same method, resulting in **[Xan_{16}-G_4-TSe];[88]** as a red viscous oil in 75% yield.

To convert the xanthate functional dendrons to ATRP initiators, two steps were performed on each dendron, Scheme 4.9. The first step involved activation of the focal point, by removing the TSe protecting moiety, using the conditions described earlier in Chapter 3, resulting in dendrons **[59], [62], [63]** and **[90]**. In the second step, modification to a suitable tertiary alkyl bromide ATRP initiation site was achieved by synthesising 2-hydroxyethyl-2-bromoisobutyrate **[OH-BiB];[89]**, via an asymmetric modification of ethylene glycol, which was reacted with the acid functional focal point of each xanthate dendron **[59], [62], [63]** and **[90]** under DCC/DPTS esterification conditions, resulting in the ATRP initiators **[91]-[94]**. In a typical esterification reaction; **[OH-BiB];[89]**, the acid functional dendron and DPTS were dissolved in CH_2Cl_2. DCC in a small volume of CH_2Cl_2 was then added to the vessel, and the reaction left stirring at ambient temperature for 16 hours. Workup was achieved by diluting the mixture with CH_2Cl_2, washing the organic layer with H_2O, brine, drying the organic layer over $MgSO_4$, and evaporating to dryness. The viscous oil was purified by liquid chromatography (silica, typically ethyl acetate 10:90, increasing the polarity to ethyl acetate:hexane, 30:70), resulting in a viscous oil. After removal of trace solvents by high vacuum, yields were in the range of 55-67%.

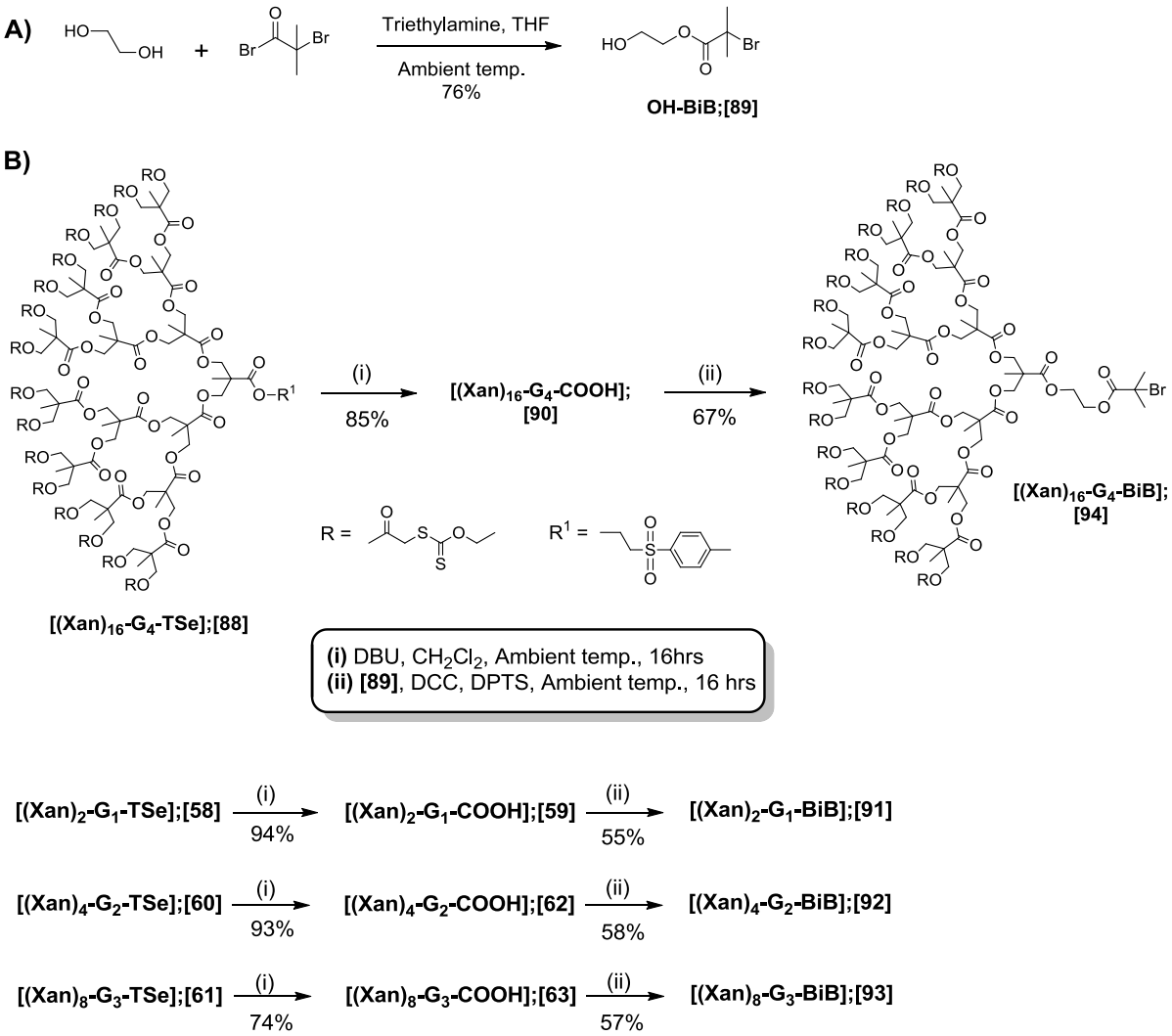

Scheme 4.9 Preparation of xanthate functional dendritic ATRP macroinitiators; A) Synthesis of **[OH-BiB];[89]** via asymmetric modification of ethylene glycol; B) Focal point modification of xanthate functional dendrons using **[OH-BiB];[89]**.

4.6.2 Characterisation of xanthate functional macroinitiators

4.6.2.1 Analysis by NMR spectroscopy

The characterisation of xanthate functional dendrons **[Xan$_2$-G$_1$-TSe];[58]**, [**Xan$_4$-G$_2$-TSe];[60]** and **[Xan$_8$-G$_3$-TSe];[61]** by NMR spectroscopy was described earlier in Chapter 3, and the repeated synthesis of these molecules during the work contributing to this Chapter agreed with the reported spectroscopic data. Analysis of the ^{1}H NMR spectrum of the G$_4$ xanthate functional dendron **[Xan$_{16}$-G$_4$-TSe];[88]** indicated the desired number of environments and the expected number of integrals,

Figure 4.9. For example, relative to the aromatic environments labelled in Figure 4.8 as 14 and 15, the presence of the characteristic xanthate resonance at 4.63 ppm (OCH_2) labelled as environment 2, integrated to 32, suggesting sixteen peripheral xanthate moieties. Analysis of the ^{13}C NMR spectrum of **[Xan$_{16}$-G$_4$-TSe];[88]** indicated twenty seven different carbon environments, although several resonances were very low in intensity, making some assignments more challenging, Figure S4.27.

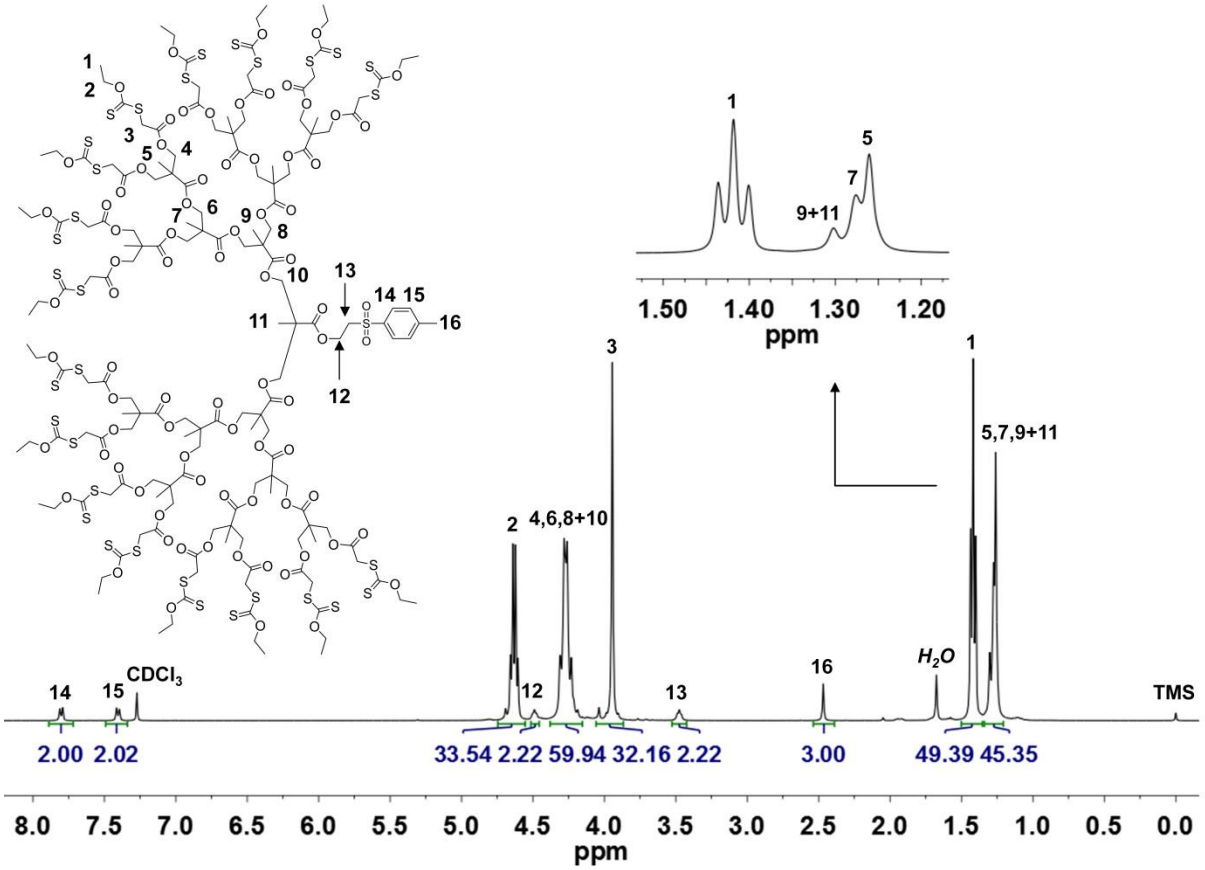

Figure 4.9 ^1H NMR spectrum (400 MHz, $CDCl_3$) of **[Xan$_{16}$-G$_4$-TSe];[88]**

The characterisation of acid functional xanthate dendrons **[Xan$_2$-G$_1$-COOH];[59]**, [**Xan$_4$-G$_2$-COOH];[62]** and **[Xan$_8$-G$_3$-COOH];[63]** by NMR spectroscopy was also described earlier in Chapter 3, and again the spectroscopic data agreed with that reported. Analysis of the ^1H NMR spectrum of the acid functional dendron **[Xan$_{16}$-G$_4$-COOH];[90]** confirmed loss of the TSe protecting functionality, indicated by the loss of resonances at 3.48 and 4.50 ppm, and a significant reduction in the intensity of resonances at 7.40 and 7.80 ppm. Similarly to the analysis of the ^1H NMR spectra of G_3 dendrons **[62]** and **[63]**, (Chapter 3, Figures 3.16 and 3.17) a particularly interesting environment

was the backbone methyl resonances at approximately 1.25 ppm, Figure 4.9 (expanded region). Before deprotection, this environment is split into three singlets, correlating to the different methyl groups that are present, labelled as 5, 7, 9 and 11.

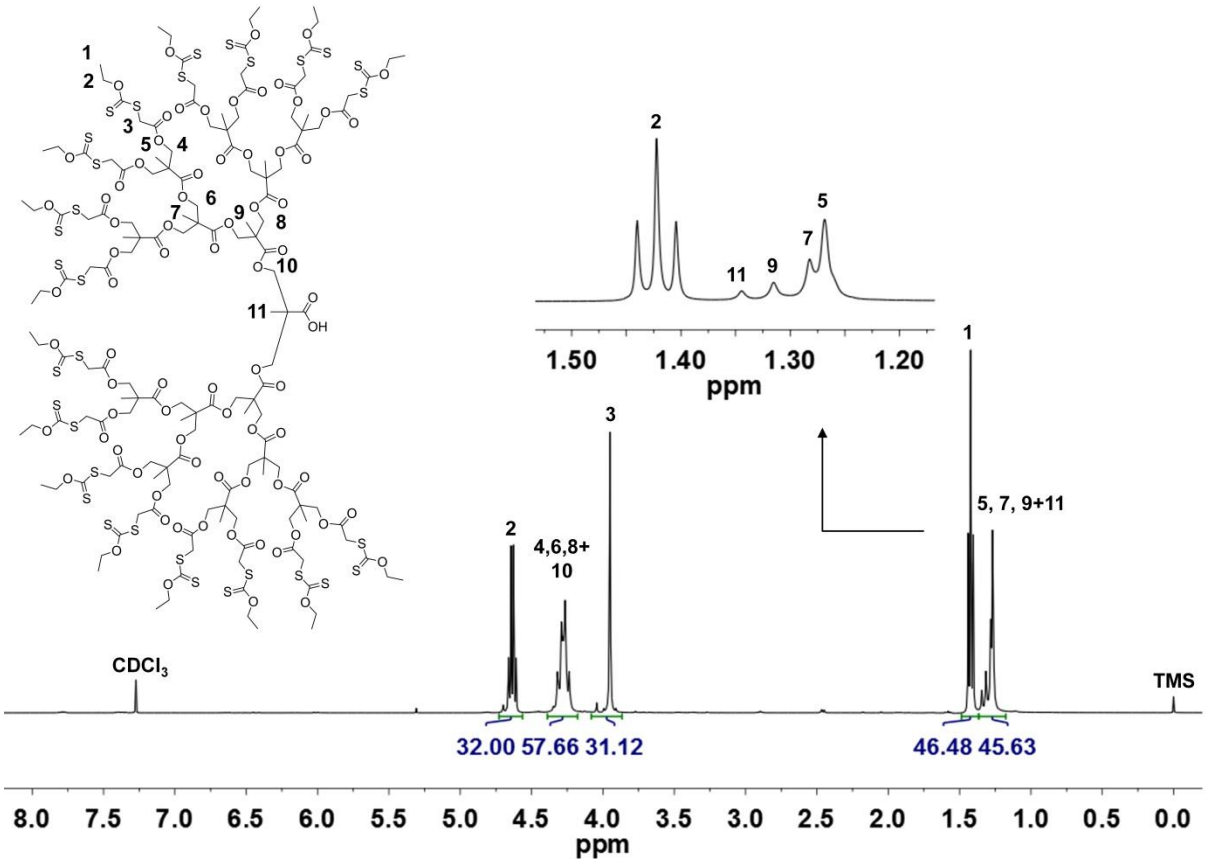

Figure 4.10 ^{1}H NMR spectrum (400 MHz, $CDCl_3$) of **[Xan$_{16}$-G$_4$-COOH];[90]**

After deprotection, this environment shifted slightly to four different singlets, which correlated to the different methyl resonances 5, 7, 9 and 11, Figure 4.10 (expanded region). As expected, this demonstrated that moving from an ester to an acid carbonyl at the focal point had an effect on the adjacent methyl resonance, 11. Analysis of **[89]** by ^{13}C NMR spectroscopy was performed, S4.28, but the intensity of the acid carbonyl resonance was too small to detect.

Synthesis of 2-hydroxyethyl 2-bromoisobutyrate **[OH-BiB];[89]** was readily confirmed by NMR spectroscopy, with the ^{1}H NMR spectrum indicating three different proton environments and the ^{13}C spectrum indicating five different environments, Figures S4.29 and 4.30.

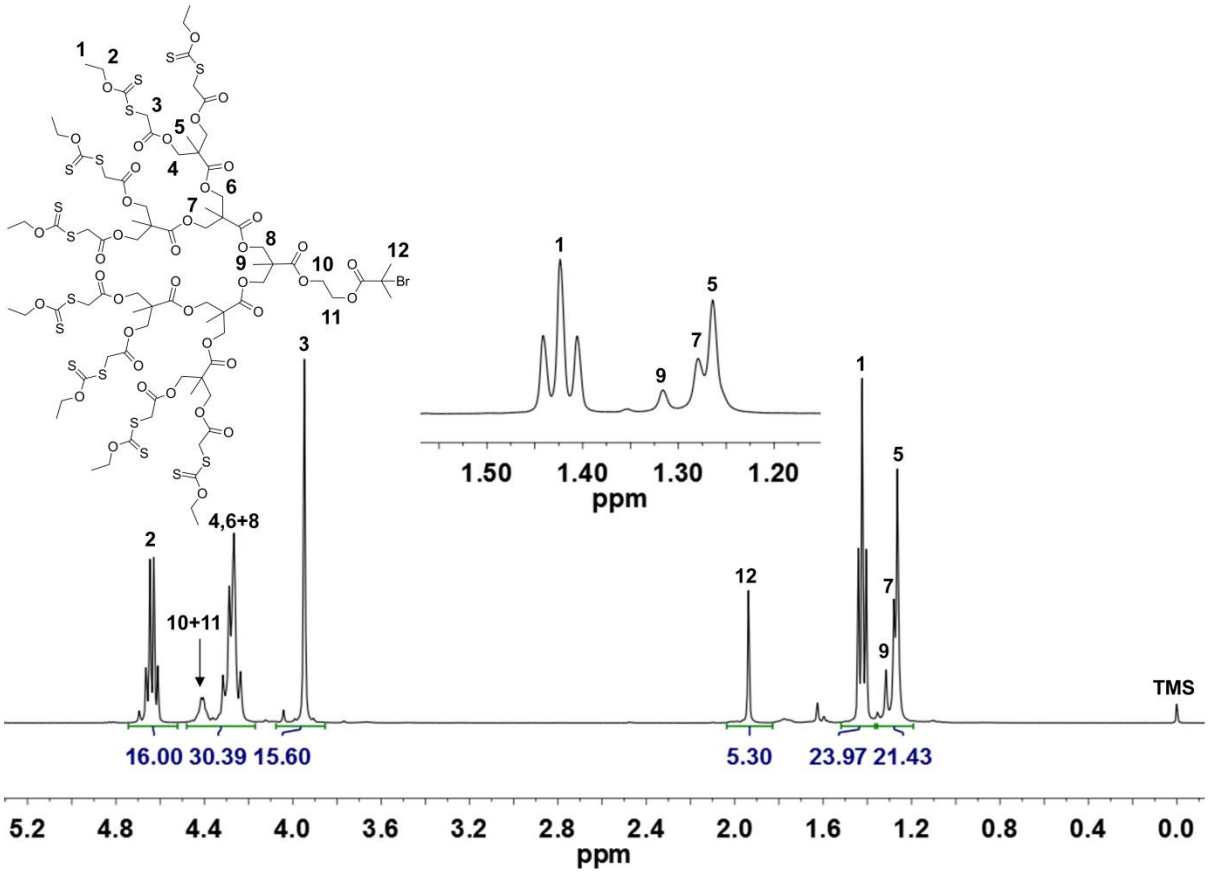

Figure 4.11 ^{1}H NMR spectrum (400 MHz, $CDCl_3$) of **[Xan$_8$-G$_3$-BiB];[93]**

Characterisation of each dendritic initiator, **[91]-[94]** by ^{1}H NMR spectroscopy indicated the formation of a sharp singlet at approximately 1.90 ppm indicating the two symmetrical methyl resonances on the bromisobutyrate moiety, Figures 4.11, S4.32, S4.34 and S4.37. An additional integral of four protons at approximately 4.40 ppm for the two OCH_2 units was also observed, present from the 2-hydroxyethyl-2-bromoisobutyrate unit. Analysis of the macroinitiators by ^{13}C NMR spectroscopy was useful for the first three generations of initiators, **[91]**, **[92]** and **[93]**, indicating the loss of the acid carbonyl resonance at approximately 173 ppm, and the subsequent formation of a new ester carbonyl resonance at approximately 172 ppm, Figure S4.33, S4.35 and S4.36. Neither the acid or the ester carbonyl could be readily observed for the G_4 initiator **[94]**, Figure S4.28 and S4.38, presumably due to the size of the macromolecule and hence insensitivity towards NMR. Instead, analysis by MALDI-TOF became the most valuable technique.

4.6.2.2 Analysis by MALDI-TOF mass spectrometry

The G_4 xanthate dendrons were fully characterised by MALDI-TOF analysis. **[Xan$_{16}$-G$_4$-TSe];[88]** indicated a population at 4555 Da (MNa^+ = 4555 Da), confirming the presence of sixteen xanthate peripheral groups, Figure 4.12. In addition, a peak at 4614 Da was observed, corresponding to an increase of approximately 80 Da. It is assumed that this adduct corresponds to a species whereby oxidation at the thiol-ether has occurred during MALDI-TOF analysis, resulting in sulfoxides. For example the addition of 5 oxygen atoms would result in an increase of 80 Da (16 x 5 = 80 Da).

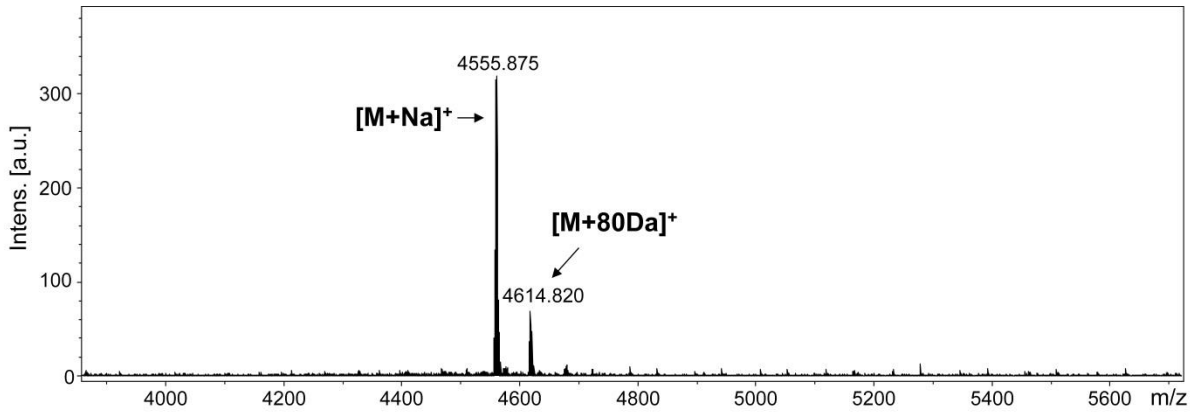

Figure 4.12 MALDI-TOF spectrum of **[Xan$_{16}$-G$_4$-TSe];[88]**

After removal of the TSe protecting functionality, analysis of the MALDI-TOF spectrum of **[Xan$_{16}$-G$_4$-COOH];[90]** confirmed two populations at 4737 Da (MNa^+ = 4373 Da) and 4393 Da (MK^+ = 4389 Da), Figure 4.13. The slight variation in expected and observed masses (approx. 4 Da) was most likely due to the isotropic distribution of xanthate peripheral groups. Sulfur has four stable isotopes (^{32}S, ^{33}S, ^{34}S, ^{36}S; relative abundance (%) 95.02:0.75:4.21:0.02) and, as each xanthate group contains two sulfur atoms, 32 sulfur atoms are present in **[Xan$_{16}$-G$_4$-COOH];[90]**. In addition to the expected populations there were peaks arising from possible thiol-ether oxidations. A population at 4432 Da confirmed an increase of approximately 80 Da, as well as peaks at 4450 and 4490 Da; these further peaks maybe different counter ion populations from the oxidised species. The population arising at 4556 Da did unfortunately suggest the presence of a slight impurity of protected precursor **[Xan$_{16}$-G$_4$-TSe];[88]** (MNa^+ = 4555 Da), but the reaction was not repeated since the impurity was only considered minor.

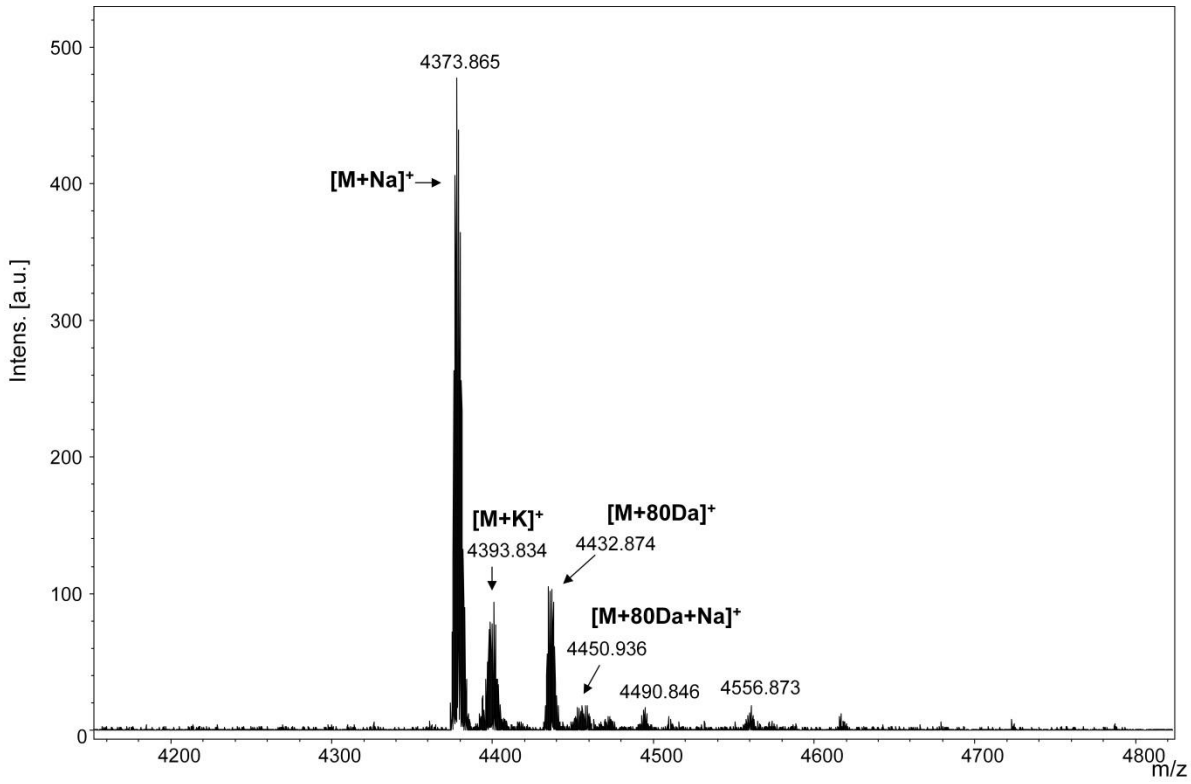

Figure 4.13 MALDI-TOF spectrum of **[Xan$_{16}$-G$_4$-COOH];[90]**

MALDI-TOF analysis was performed on each xanthate dendritic initiator **[91]-[94]**, Figure 4.14. Peaks corresponding to the sodium adducts of the molecular ion were observed at 674 Da (MNa^+ = 673 Da), 1229 Da (MNa^+ = 1229 Da), 2341 Da (MNa^+ = 2341 Da) and 4567 Da (MNa^+ = 4565 Da) for **[Xan$_2$-G$_1$-BiB];[91]**, **[Xan$_4$-G$_2$-BiB];[92]**, **[Xan$_8$-G$_3$-BiB];[93]** and **[Xan$_{16}$-G$_3$-BiB];[94]**. Again, some additional adducts (particularly in the case for **[93]** and **[94]**) were observed by increasing multiples of 16 Da, but were believed to occurring from thiol-ether oxidation during analysis.

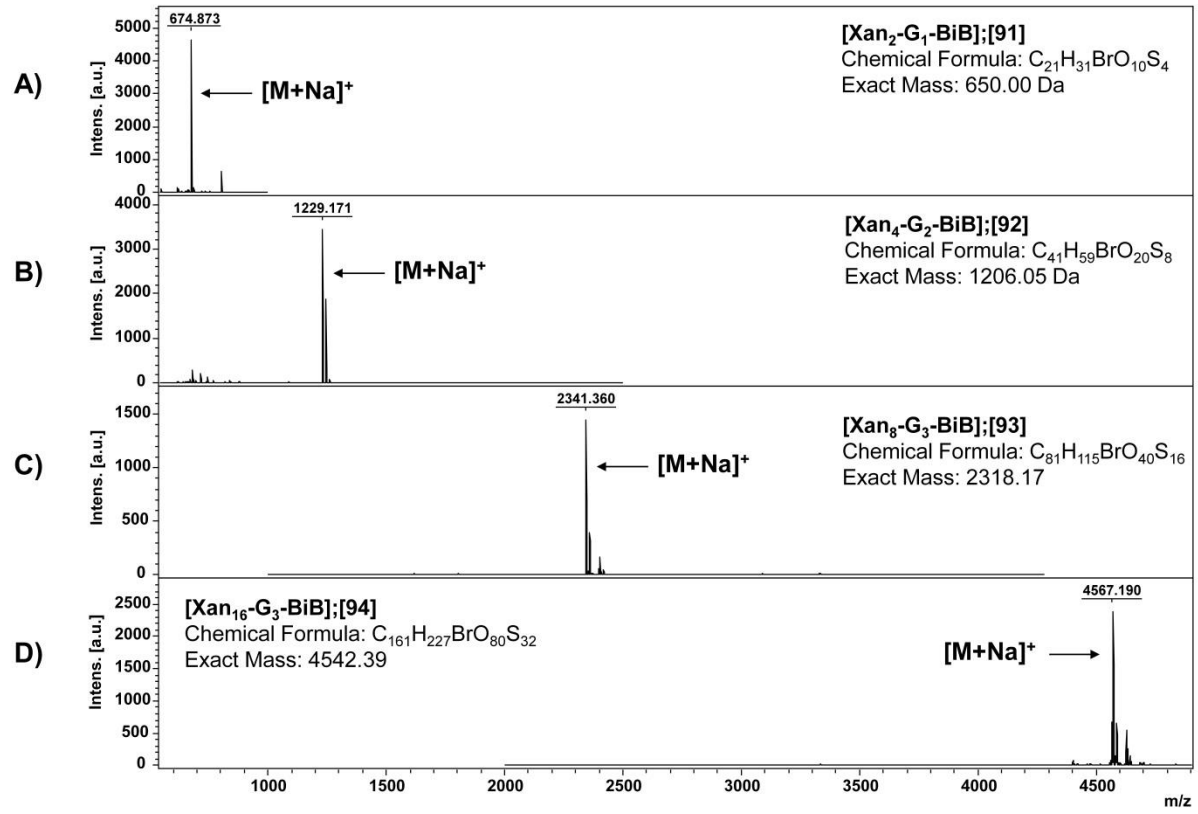

Figure 4.14 MALDI-TOF spectrum of (a) **Xan$_2$-G$_1$-BiB];[91]**; (b) **[Xan$_4$-G$_2$-BiB];[92]**; (c) **[Xan$_8$-G$_3$-BiB];[93]**; (d) **[Xan$_{16}$-G$_3$-BiB];[94]**

4.7 Synthesis and characterisation of xanthate functional LDHs

^{t}BuMA was employed as the monomer for LDH synthesis, since the resulting polymer backbone and pendant tertiary methyl groups all resonate between approximately 0.8-2.2 ppm by ^{1}H NMR spectroscopic analysis. This enabled the use of ^{1}H NMR spectroscopy to observe changes to the structure of the dendritic surface groups after thiol Michael addition click chemistry. The target was to utilise initiators **[Xan$_2$-G$_1$-BiB];[91]**, **[Xan$_4$-G$_2$-BiB];[92]**, **[Xan$_8$-G$_3$-BiB];[93]** and **[Xan$_{16}$-G$_3$-BiB];[94]** to polymerise ^{t}BuMA to a target number average degree of polymerisation (DP_n) of 50 monomer units.

Based on previous reports of ATRP of ^{n}BuMA, an alcoholic IPA/water (92.5/7.5 v/v) solvent system was used in conjunction with the G_1 and G_2 initiators **[Xan$_2$-G$_1$-BiB];[91]** and **[Xan$_4$-G$_2$-BiB];[92]**,

Scheme 4.10. In a typical LDH synthesis, targeting DP_n = 50 monomer units, ^{t}BuMA, the dendritic initiator, IPA/water solvent and bpy were stirred in an oven dried round bottom flask and deoxygenated using a nitrogen purge for 10 minutes. Cu(I)Cl was added to the flask whilst maintaining a positive flow of nitrogen, and the targeted LDH left to polymerise at 40 °C. For studies of polymerisation kinetics, the reaction was sampled regularly (~0.2 mL) and diluted into THF for SEC analysis, and into $CDCl_3$ for ^{1}H NMR analysis.

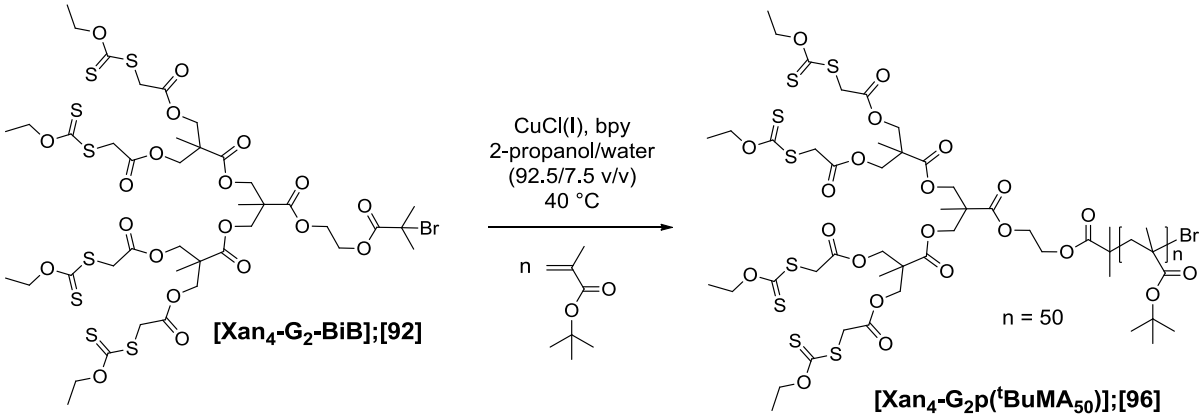

Scheme 4.10 Synthesis of LDH using initiator **[Xan$_4$-G$_2$-BiB];[92]**

The reactions were terminated by exposure to oxygen and addition of THF when conversion reached >90% as indicated by the disappearance of the methacrylate vinyl resonances at 5.48 ppm and 6.0 ppm, by ^{1}H NMR spectroscopic analysis. The polymer solutions were passed through a neutral alumina column to remove the catalytic system, and precipitated twice into hexane, which was cooled using a dry ice bath. After drying the precipitated sample overnight under high vacuum to remove residual solvents, the polymer was obtained as a white solid.

Kinetics studies with initiators **[91]** and **[92]** were performed to ensure controlled polymerisation, Figure 4.15. Using each initiator, a constant concentration of active radicals, through a linear semi-logarithmic plot *vs* time, and a linear relationship with increasing molecular weight *vs* time was observed, Figure 4.14.

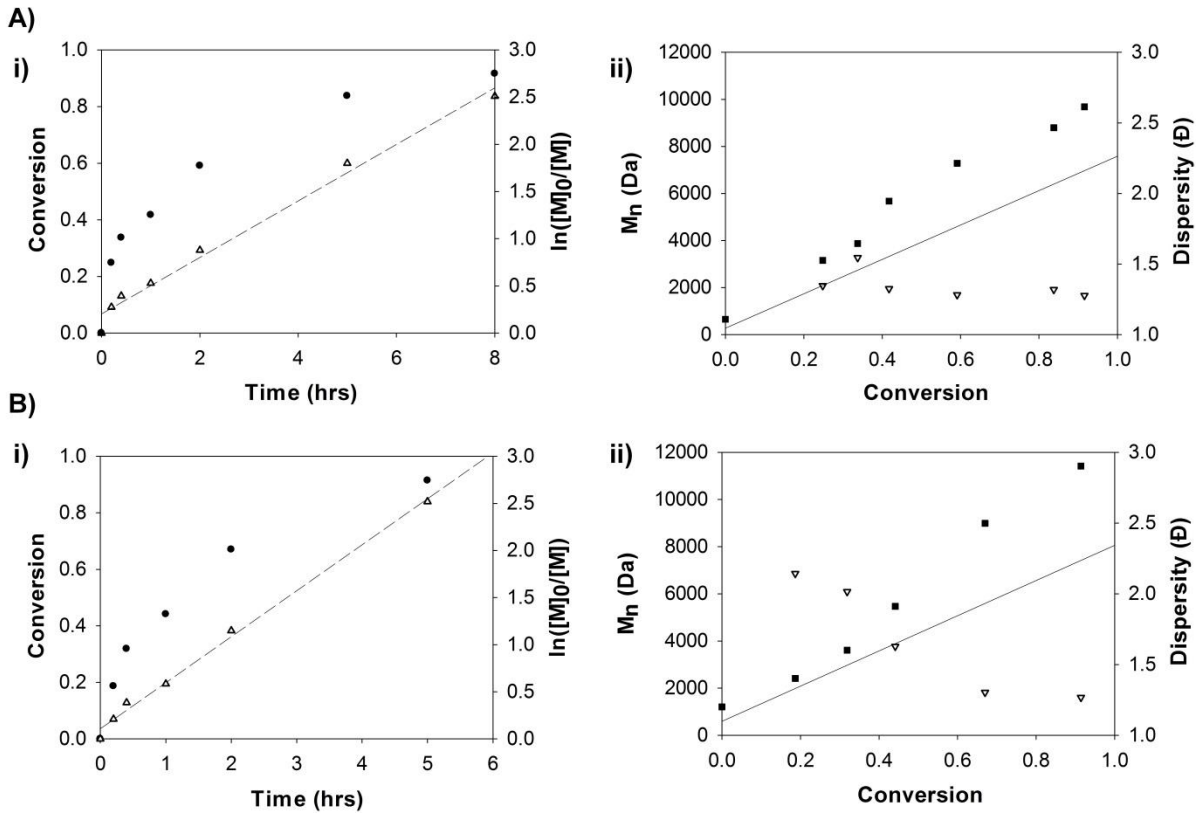

Figure 4.15 Kinetic studies of the ATRP of ^{t}BuMA to a targeted DP_n = 50 monomer units using; A) **[Xan$_2$-G$_1$-BiB];[91]**; B) **[Xan$_4$-G$_2$-BiB];[92]**. Conversion *vs.* time plots are shown (closed black circles) with corresponding semi-logarithmic plots (open black upward triangles); dotted lines represent linear regression of the semi-logarithmic plots. M_n *vs*. conversion plots (closed black squares) and corresponding dispersity (Đ) *vs*. conversion plots are also shown (open black downward triangles); grey lines represent theoretical M_n *vs.* conversion.

Attempting to use the G_3 or G_4 initiators **[Xan$_8$-G$_3$-BiB];[93]** and **[Xan$_{16}$-G$_3$-BiB];[94]** under these conditions found that neither initiator was soluble in the alcoholic IPA/water mixture. Various commonly used ATRP solvents were attempted to solubilise the initiators, including methanol (insoluble), 100% IPA (insoluble), 100% water (insoluble), and ethanol (insoluble). Acetone (100%) was found to solubilise all four generations of initiators, and was used as an alternative solvent to the IPA/water mixture. ^{t}BuMA was polymerised to a DP_n = 50 monomer units, and polymerisation conditions were kept the same, with the exception of a slightly increased temperature at 50 °C, Scheme 4.11.

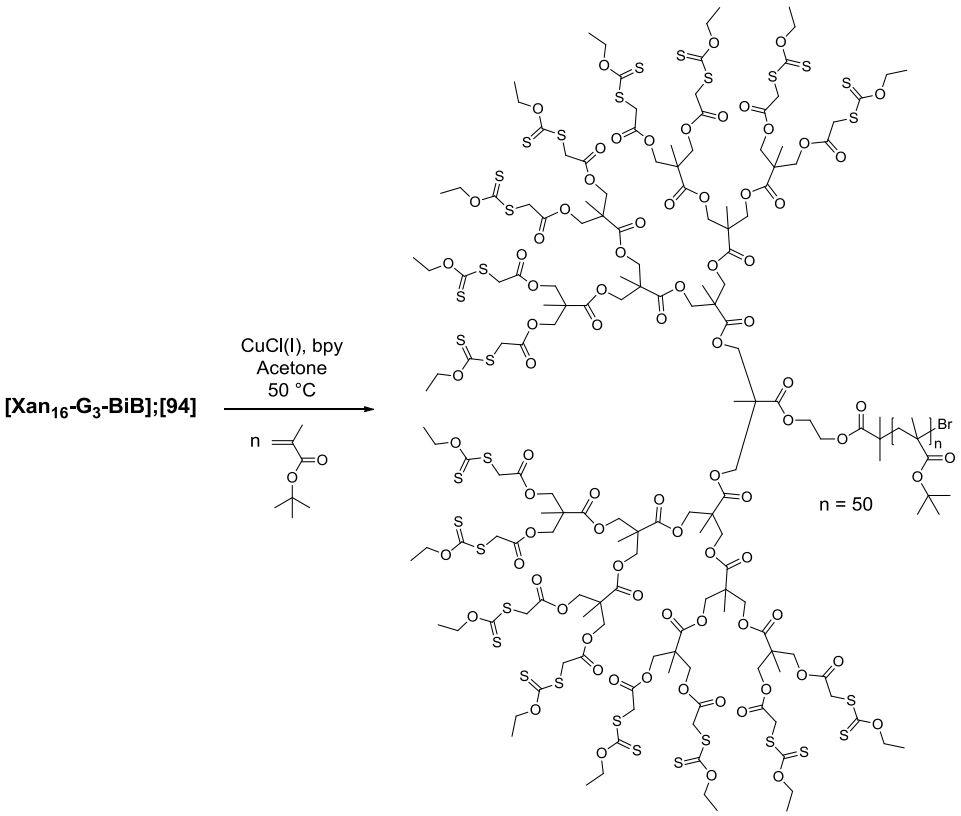

Scheme 4.11 Synthesis of LDH **[Xan$_{16}$-G$_4$p(^{t}BuMA$_{50}$)];[100]** using initiator **[Xan$_{16}$-G$_3$-BiB];[94]**

Kinetic studies were repeated with all four initiators **[91]-[94]** for the ATRP of ^{t}BuMA, Figure 4.16. Polymerisation with each initiator resulted in a constant concentration of active radicals, indicated by a linear semi-logarithmic plot *vs.* time and a linear relationship with increasing molecular weight *vs.* conversion. The experiments revealed that the polymerisation rate appeared to decrease as the size of the dendritic initiator increased, suggesting that the increased dendritic size had an effect on the ATRP equilibrium constant ($K_{ATRP} = k_{act}/k_{deact}$). SEC and ^{1}H NMR spectroscopic analysis of the purified LDHs was performed, Table 3.1. In alcohol, (entries **[95]** and **[96]**, Table 3.1) conversions of each polymerisation reached >90% after 7 hours, and dispersity (Đ) remained relatively low (<1.4) using either the G_1 or G_2 initiator. The resulting LDHs showed a good correlation with theoretical molecular weights by SEC and ^{1}H NMR spectroscopy.

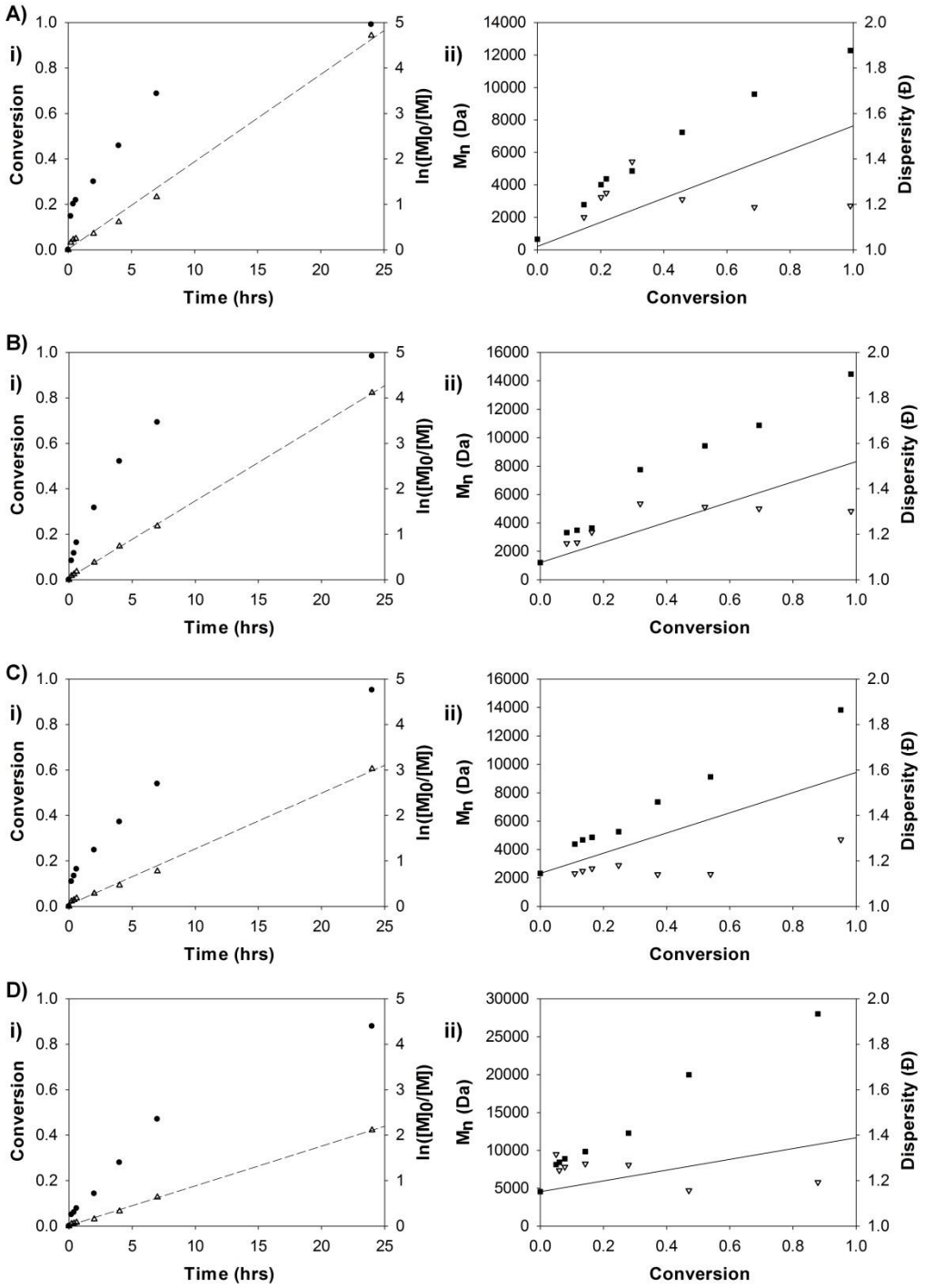

Figure 4.16 Kinetic studies of the ATRP of ^{t}BuMA to a targeted DP_n = 50 monomer units using; A) **[Xan$_2$-G$_1$-BiB];[91]**; B) **[Xan$_4$-G$_2$-BiB];[92]**; C) **[Xan$_8$-G$_3$-BiB];[93]** and D) **[Xan$_{16}$-G$_3$-BiB];[94]**. Conversion *vs.* time plots are shown (closed black circles) with corresponding semi-logarithmic plots (open black upward triangles); dotted lines represent linear regression of the semi-logarithmic plots. M_n *vs*. conversion plots (closed black squares) and corresponding dispersity (Đ) *vs*. conversion plots are also shown (open black downward triangles); grey lines represent theoretical M_n vs. conversion.

Table 3.1 Analysis of LDHs by SEC and ^{1}H NMR spectroscopy **[95]-[100]**

Target polymer; Entry #	Time (h)	Conv (%)	Ther. M_n (Da)	SEC[c] M_n (Da)	SEC[c] M_w (Da)	SEC[c] $Đ$	Calc DP[n] SEC	Calc DP[n] ^{1}H NMR
[Xan$_2$-G$_1$p(^{t}BuMA$_{50}$)];[95][a]	7	92	7100	8700	11900	1.37	57	59
[Xan$_4$-G$_2$p(^{t}BuMA$_{50}$)];[96][a]	6	94	7800	9900	13400	1.35	47	48
[Xan$_2$-G$_1$p(^{t}BuMA$_{50}$)];[97][b]	24	99	7100	11800	15200	1.29	79	60
[Xan$_4$-G$_2$p(^{t}BuMA$_{50}$)];[98][b]	24	98	7800	15300	19100	1.25	99	49
[Xan$_8$-G$_3$p(^{t}BuMA$_{50}$)];[99][b]	28	95	9000	15000	17000	1.13	89	76
[Xan$_{16}$-G$_4$p(^{t}BuMA$_{50}$)];[100][b]	29	99	12000	29000	33000	1.14	172	87

[a]IPA/H_2O (92.5/7.5 v/v), 50 wt%, 40°C; [CuCl];[Bpy];[^{t}BuMA] = [1];[2];[50]. [b]Acetone, 50 wt%, 50°C; [CuCl];[Bpy];[^{t}BuMA] = [1];[2];[50]. [c]THF containing 2% TEA (v/v)

In acetone conditions, (entries **[97]**, **[98]**, **[99]** and **[100]**, Table 3.1) conversions of each polymerisation reached >95% after 24 hours, which was considerably slower than in alcohol, but with dispersity remaining low (<1.3) using either G_1, G_2, G_3, or G_4 initiators. SEC analysis of the LDHs in acetone conditions did show some discrepancy between observed and theoretical molecular weights, which was found to increase as the generation size of the initiator increased. This was not surprising since the ATRP initiating site becomes increasingly "masked" by the steric size of the dendron, which is more prominent at higher generations. The activation and deactivation of the focal point tertiary bromide may therefore be impaired, potentially leading to a lack of radical formation or rapid deactivation and possible termination in the early stages of the reaction. This appears to result in fewer chains being successfully initiated (for example, using initiator **[Xan$_{16}$-G$_3$-BiB];[94]**), and hence higher than expected molecular weights (for example, LDH **[Xan$_{16}$-G$_2$p(^{t}BuMA$_{50}$)];[100]**), but noticeably lower Đ values. ^{1}H NMR analysis of the LDHs in acetone conditions showed a good correlation with theoretical DP_n = 50 when using G_1 and G_2 initiators (entries **[97]**, **[98]**), but some discrepancy when using G_3 or G_4 initiators (entries **[97]**, **[98]**) again, most likely arising from initiator inefficiency. Some variation in molecular weights obtained by SEC was also obtained when using G_1 and G_2 initiators under alcoholic solvent conditions (LDHs, **[95]** and **[96]**) *vs.* polymers obtained in acetone solvent conditions (**[97]** and **[98]**), suggesting that initiation efficiency was reduced in acetone conditions. Analysis of the SEC refractive index (RI) and right angle light scattering (RALS) chromatograms, Figure 4.17, showed monomodal distributions of all LDHs **[95]-[100]**, but some evidence of residual initiator indicated by a slight peak in the refractive index detector at an

approximate elution of 20-21 mL, present in all the samples. The residual initiator was particularly evident in the chromatograms of LDHs **[96]** and **[100]**, and attempts to remove initiator from LDH **[100]** by dialysis (THF/H_2O) were made, but without success. No further purification was attempted.

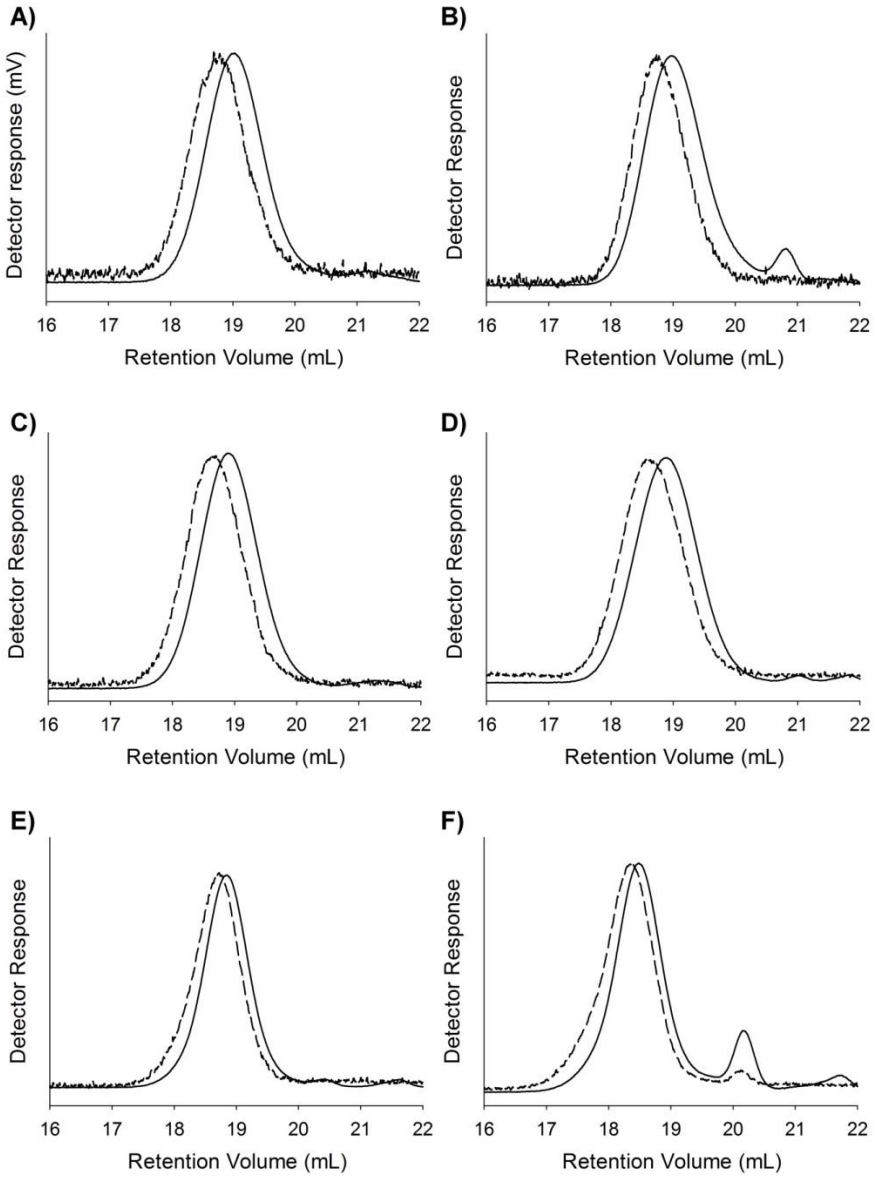

Figure 4.17 Triple detection SEC chromatograms of; (A) **[Xan_2-G_1p(^{t}BuMA$_{50}$)];[95]**; (B) **[Xan_4-G_2p(^{t}BuMA$_{50}$)];[96]**; (C) **[Xan_2-G_1p(^{t}BuMA$_{50}$)];[97]**; (D) **[Xan_4-G_2p(^{t}BuMA$_{50}$)];[98]**; (E) **[Xan_8-G_3p(^{t}BuMA$_{50}$)];[99]**; (F). The figure shows the refractive index (RI) detector response (solid lines) and the right angle light scattering (RALS) detector response (dotted lines).

4.8 One-pot xanthate deprotection and functionalisation via thiol Michael addition of LDHs

LDH polymers **[95]**, **[96]**, **[98]**, **[99]** and **[100]** were used for the one-pot xanthate deprotection and thiol Michael addition reactions. Analysis of each LDH by ^{1}H NMR spectroscopy indicated resonances at 3.95 and 4.64 ppm (labelled as environments 3 and 2), which identified the xanthate peripheral groups, Figure 4.18, S4.39, S4.40 and S4.41. These resonances were particularly important to monitor substrate functionalisation after the one-pot xanthate deprotection and thiol Michael addition reactions.

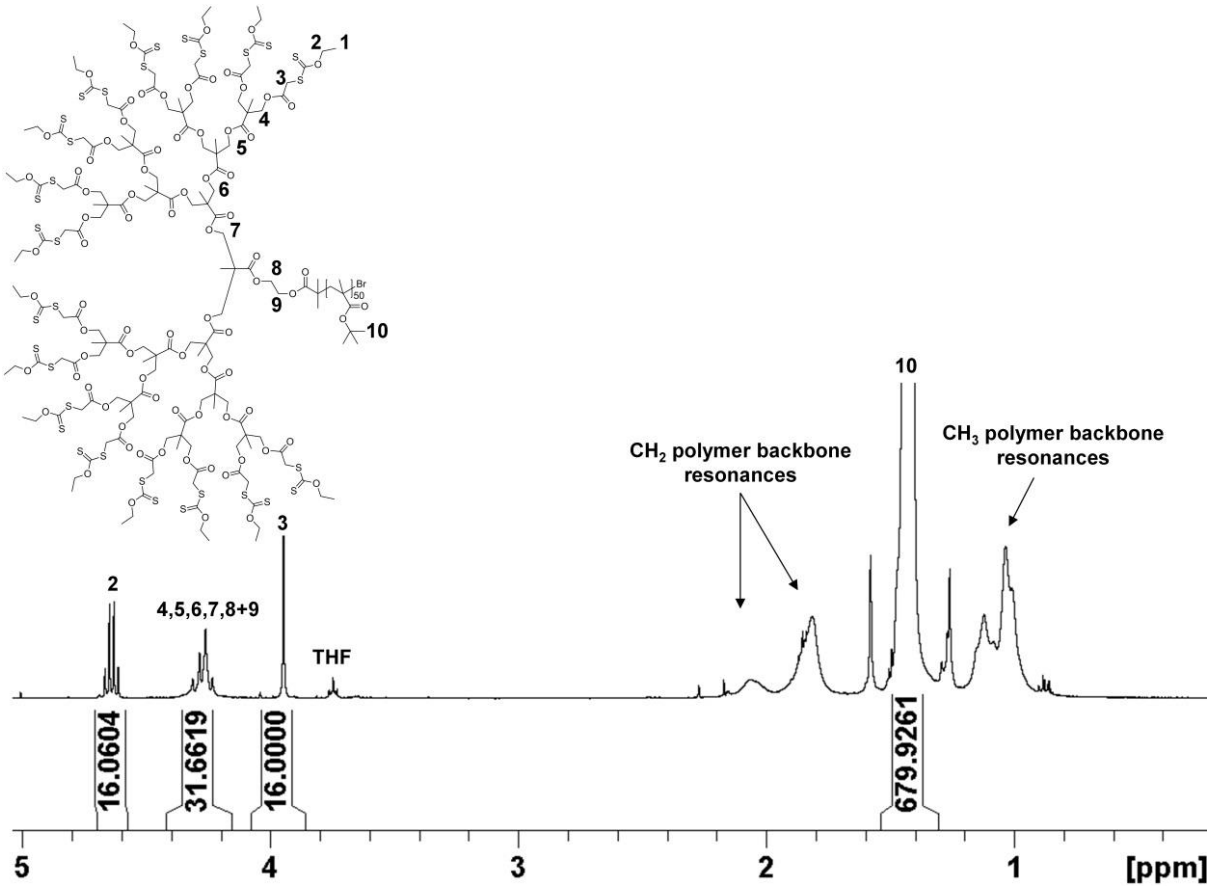

Figure 4.18 ^{1}H NMR spectrum (400 MHz, $CDCl_3$) of **[Xan_{16}-G_2p(^{t}BuMA$_{50}$)];[100]**

To study the versatility of the proposed thiol Michael addition, six acrylate monomers were chosen; five commercially available, and one prepared by a simple esterification reaction using acryloyl

chloride, Scheme 4.12. The monomers that were chosen were commonly used acrylate monomers, enabling hydrophilic, hydrophobic and polymeric functionalities to be attached to the LDHs. The preparation of morpholino propan-2-oyl acrylate **[MPA]** was achieved by the reaction of acryloyl chloride with morpholino propan-2-ol **[MP]** in the presence of triethylamine and a catalytic amount of DMAP. After purification by aqueous washes, the product was obtained as a dark orange oil in 74% yield. Analysis of each ^{1}H and ^{13}C NMR spectrum of **[MPA];[101]** confirmed the expected number of proton and carbon environments, Figures S4.42 and S4.43.

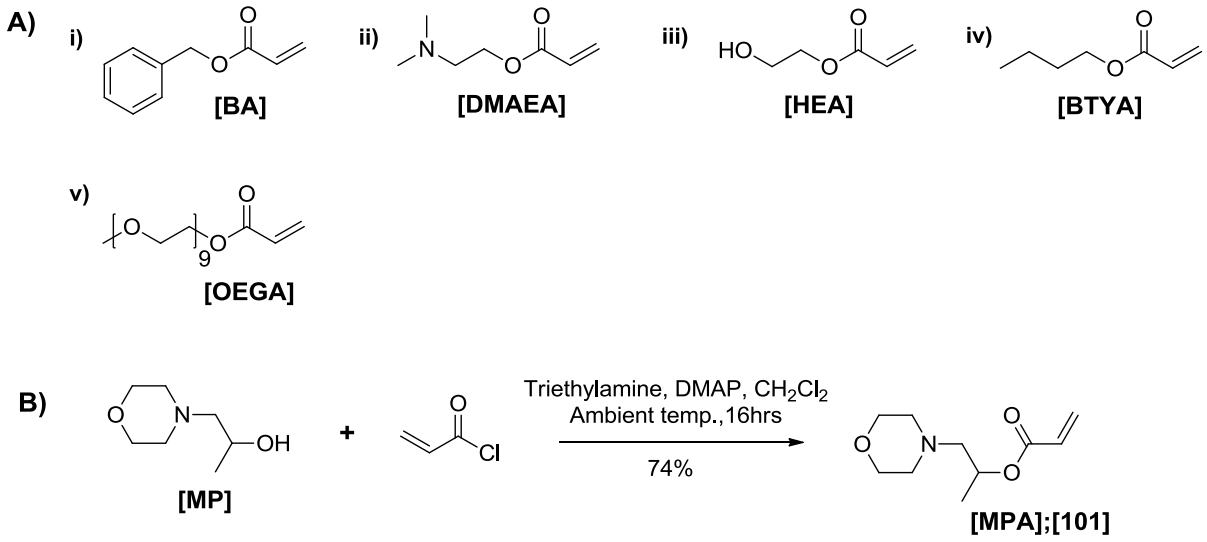

Scheme 4.12 Acrylate functional monomers used in this study. A) Commercially available monomers; i) Benzyl acrylate **[BA]**; ii) 2-(Dimethylamino)ethyl acrylate **[DMAEA]**; iii) 2-Hydroxyethyl acrylate **[HEA]**; iv) Butyl acrylate **[BTYA]**; v) Oligo(ethylene glycol) methyl ether acrylate, average M_n = 480 **[OEGA]**; [37] B) Synthesis of morpholino propanyl acrylate **[MPA];[101]**, prepared by reaction of acryloyl chloride with morpholino propan-2-ol **[MP]**.

In Chapter 3, it was found that a range of surface functional dendrimers can be prepared from xanthate peripheral dendrimers by a one-pot xanthate deprotection and thiol Michael addition procedure. Under similar conditions, two model reactions were performed using LDHs **[96]** and **[98]**

with the monomer **[BA]** to establish the optimum one-pot procedure conditions, including molar ratios of n-butyl amine (for deprotection), and **[BA]** monomer (for functionalisation), Scheme 4.13.

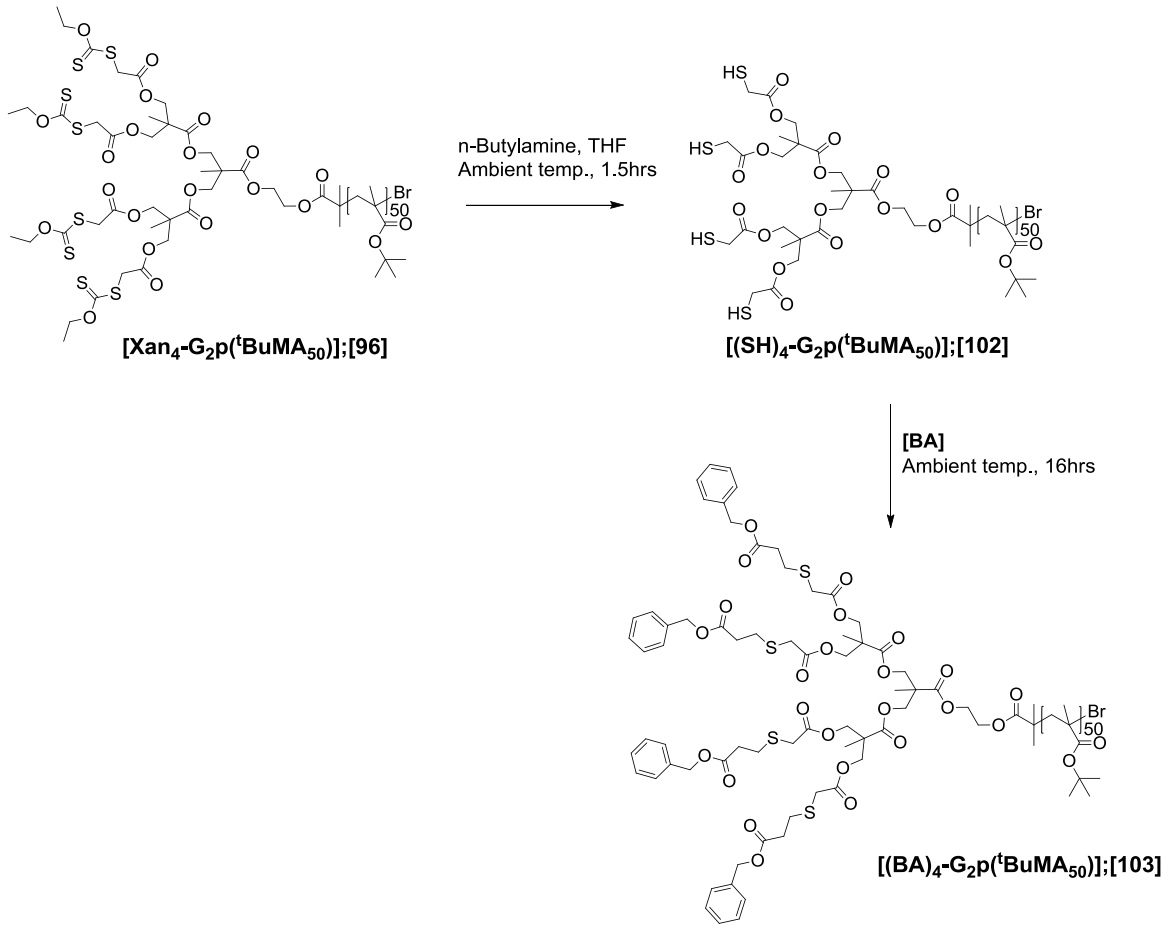

Scheme 4.13 Synthesis of LDH **[(BA)$_4$-G$_2$p(^{t}BuMA$_{50}$)];[103]** by the one-pot xanthate deprotection and thiol Michael addition approach

In the first reaction, LDH **[98]** was dissolved in anhydrous THF (10 wt%) and purged with nitrogen for a period of approximately 10 minutes to remove any residual oxygen. After degassing, a 2.5 molar excess of n-butyl amine per xanthate peripheral group was added to the solution, and the reaction was left stirring at ambient temperature for 1.5 hours. Following this, the mixture was precipitated into cold hexane (cooled using a dry ice bath), to isolate the intermediate (**[(SH)$_4$-G$_2$p(^{t}BuMA$_{50}$)];[102]**).

In the second reaction, the above procedure was repeated using LDH **[96]** (due not having any **[98]** precursor left) and, after xanthate deprotection for 1.5 hours, a 5 molar excess of [**BA]** with respect to each thiol was added, and the mixture left stirring at ambient temperature for 16 hours. Workup of

[(BA)$_4$-G$_2$p(^{t}BuMA$_{50}$)];[103] was achieved by precipitation from the THF mixture into cold hexane, (cooled using a dry ice bath), to result in a white power that was dried under high vacuum overnight.

To ensure total deprotection of the LDH xanthate peripheral groups, analysis of the of thiol intermediate (**[(SH)$_4$-G$_2$p(^{t}BuMA$_{50}$)];[102]**) was crucial. The ^{1}H NMR spectrum, Figure 4.19 (B), confirmed removal of the xanthate peripheral groups, indicated by the loss of the resonance at 4.65 ppm corresponding to outer OCH_2 environment on the xanthate moieties (shown in blue).

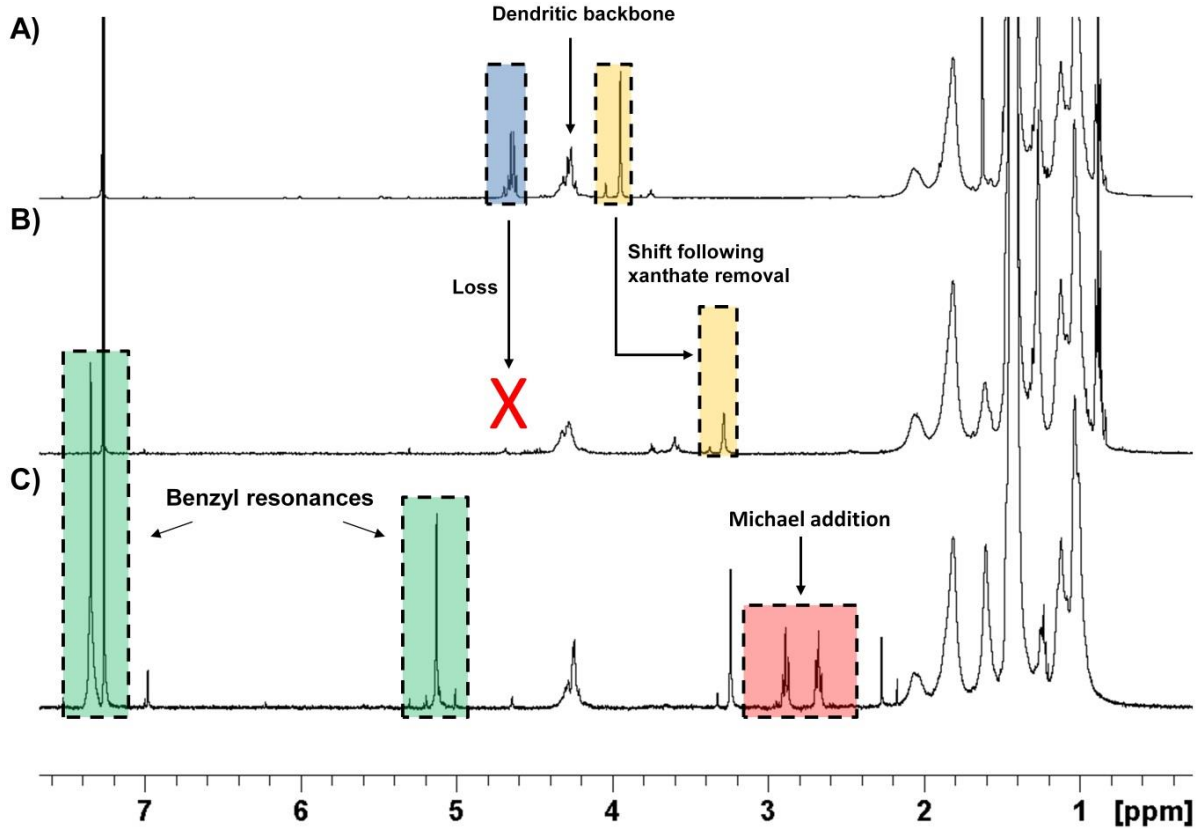

Figure 4.19 ^{1}H NMR spectrum (400 MHz, $CDCl_3$) of (A); **[Xan$_4$-G$_2$p(^{t}BuMA$_{50}$)];[96]**; (B) **([(SH)$_4$-G$_2$p(^{t}BuMA$_{50}$)];[102]**); (C) **[(BA)$_4$-G$_2$p(^{t}BuMA$_{50}$)];[103]**

Further indication of xanthate removal was indicated by the shift of the methylene singlet at 3.95 ppm to 3.28 ppm (shown in yellow) due the lack of the electron withdrawing thiocarbonyl, and subsequent thiol formation, Figures 4.19 (A) and (B). The appearance of triplet resonances indicative of thiol Michael addition (formation of CH_2-CH_2 bond) at 2.68 and 2.89 ppm (shown in red) were observed

for the functionalised LDH **[(BA)$_4$-G$_2$p(^{t}BuMA$_{50}$)];[103]**, along with benzyl resonances at 5.15 and 7.34 ppm (shown in green), Figure 4.19 (C).

Due to the different batches of sample used (albeit nominally the same material, **[96]** *vs.* **[98]**), some evidence of residual initiator peaks were more prominent in the chromatogram of **[(BA)$_4$-G$_2$p(^{t}BuMA$_{50}$)];[103]** as a larger proportion of residual initiator was present in the precursor **[96]** (see Figure 4.17). Substantial broadening from an retention volume of approximately 13 mL was clearly evident in both the RI and RALS detector chromatogram of **[(SH)$_4$-G$_2$p(^{t}BuMA$_{50}$)];[102]**, in contrast to the well-defined chromatogram of **[(BA)$_4$-G$_2$p(^{t}BuMA$_{50}$)];[103]**. Chromatogram broadening suggested evidence of high molecular weight species in **[102]**, presumably from disulfide formation arising from the thiol peripheral groups. This illustrated a clear advantage of the one-pot approach, whereby disulfide formation is considerably suppressed as thiol intermediates are never isolated.

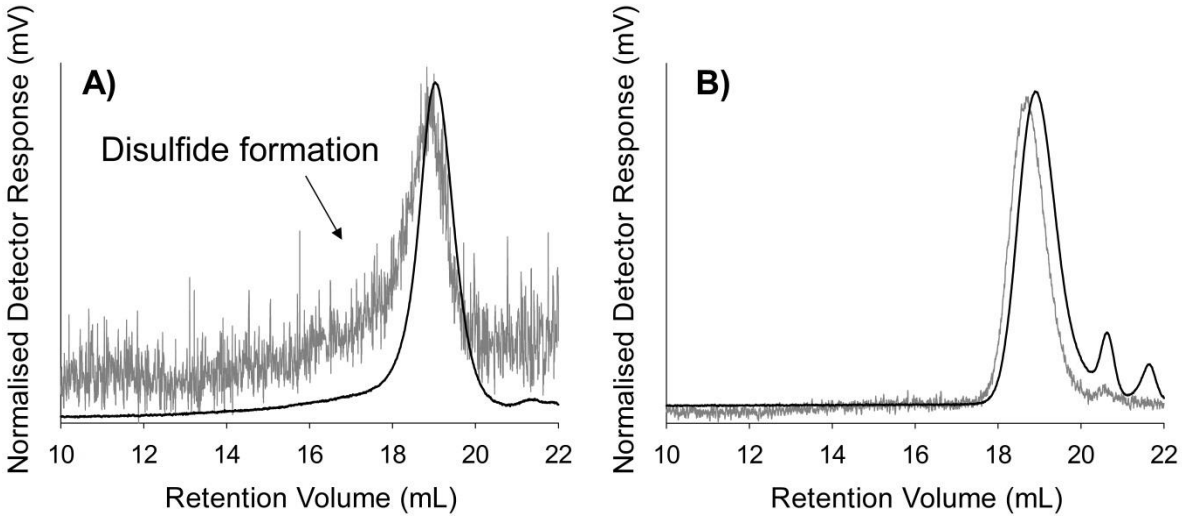

Figure 4.20 Triple detection SEC chromatograms of; (A) **[(SH)$_4$-G$_2$p(^{t}BuMA$_{50}$)];[102]**; (B) **[(BA)$_4$-G$_2$p(^{t}BuMA$_{50}$)];[103]**. The figure shows the refractive index (RI) detector response (solid black lines) and the right angle light scattering (RALS) detector response (solid grey lines).

Using the one-pot xanthate deprotection and thiol Michael additions conditions described, functional LDHs **[104]** to **[122]** were prepared, Table 4.2.

Target LDH; Entry #	LDH precursor	Functional acrylate	Conv (%)	SEC[a]		
				M_n (Da)	M_w (Da)	$Đ$
[$(Bz)_2$-G_1p(^{t}BuMA$_{50}$)];[104]	[95]	[BA]	>99	10300	13200	1.29
[$(Am)_2$-G_1p(^{t}BuMA$_{50}$)];[105]	[95]	[DMAEA]	>99	12000	15300	1.28
[$(OEG)_2$-G_1p(^{t}BuMA$_{50}$)];[106]	[95]	[OEGA]	>99	11200	14700	1.32
[$(Hydx)_2$-G_1p(^{t}BuMA$_{50}$)];[107]	[95]	[HEA]	>99	9900	12800	1.30
[$(Btyl)_2$-G_1p(^{t}BuMA$_{50}$)];[108]	[95]	[BTYA]	>99	11900	15000	1.27
[$(Mp)_2$-G_1p(^{t}BuMA$_{50}$)];[109]	[95]	[MPA]	>99	13700	17400	1.26
[$(Bz)_4$-G_2p(^{t}BuMA$_{50}$)];[103]	[96]	[BA]	>99	11900	14800	1.24
[$(Am)_4$-G_2p(^{t}BuMA$_{50}$)];[110]	[96]	[DMAEA]	>99	12200	16100	1.31
[$(OEG)_4$-G_2p(^{t}BuMA$_{50}$)];[111]	[96]	[OEGA]	>99	14100	17900	1.27
[$(Hydx)_4$-G_2p(^{t}BuMA$_{50}$)];[112]	[96]	[HEA]	>99	11000	15800	1.42
[$(Btyl)_4$-G_2p(^{t}BuMA$_{50}$)];[113]	[96]	[BTYA]	>99	13700	17600	1.28
[$(Mp)_4$-G_2p(^{t}BuMA$_{50}$)];[114]	[96]	[MPA]	>99	27600	45600	1.67
[$(Bz)_8$-G_3p(^{t}BuMA$_{50}$)];[115]	[99]	[BA]	>99	15500	17900	1.17
[$(Am)_8$-G_3p(^{t}BuMA$_{50}$)];[116]	[99]	[DMAEA]	>99	20100	54200	2.70
[$(OEG)_8$-G_3p(^{t}BuMA$_{50}$)];[117]	[99]	[OEGA]	>99	21800	26500	1.22
[$(Hydx)_8$-G_3p(^{t}BuMA$_{50}$)];[118]	[99]	[HEA]	>99	14000	18000	1.28
[$(Btyl)_8$-G_3p(^{t}BuMA$_{50}$)];[119]	[99]	[BTYA]	>99	14600	18400	1.27
[$(Mp)_8$-G_3p(^{t}BuMA$_{50}$)];[120]	[99]	[MPA]	>99	20000	38300	1.91
[$(Bz)_{16}$-G_4p(^{t}BuMA$_{50}$)];[121]	[100]	[BA]	>99	29000	33600	1.16
[$(Mp)_{16}$-G_4p(^{t}BuMA$_{50}$)];[122]	[100]	[MPA]	>99	48800	526600	10.8

[a]THF containing 2% TEA (v/v)

Table 4.2 Analysis of functional LDHs prepared by one-pot xanthate deprotection and thiol Michael addition

Analysis of each ^{1}H NMR spectrum of LDHs **[103]-104]**, with respect to the shift of the singlet at 3.95 ppm to 3.28 ppm, confirmed that xanthate deprotection was >99%, Table 4.2. Common amongst all the LDHs were resonances at 2.68 and 2.89 ppm which were indicative of thiol Michael addition, shown for the G_3 materials **[115]-[120]**, Figures 4.21 and 4.22.

Each LDH resulted in new resonances for the different peripheral substrates; benzyl (Bz) resonances at 5.11 and 7.34 ppm (Figure 4.21, environments, 1 and 2); dimethyl amino (Am) resonances at 2.37 (Figure 4.21, environment 6); oligo(ethylene glycol) (OEG) resonances at 3.65 ppm (Figure 4.21, environments 13 and 14); hydroxyethyl (hydx) resonances at 3.82 ppm (Figure 4.22, environments, 5 and 4); butyl (btyl) resonances at 4.09 ppm (Figure 4.22, environment 9) and morpholino resonances at 2.45, 3.66 and 5.14 ppm (Figure 4.22, environments 13, 14, 15 and 16); it should be noted that these were the only key observable resonances; there are other relevant signals, but they were buried within the polymer or dendritic backbone resonances.

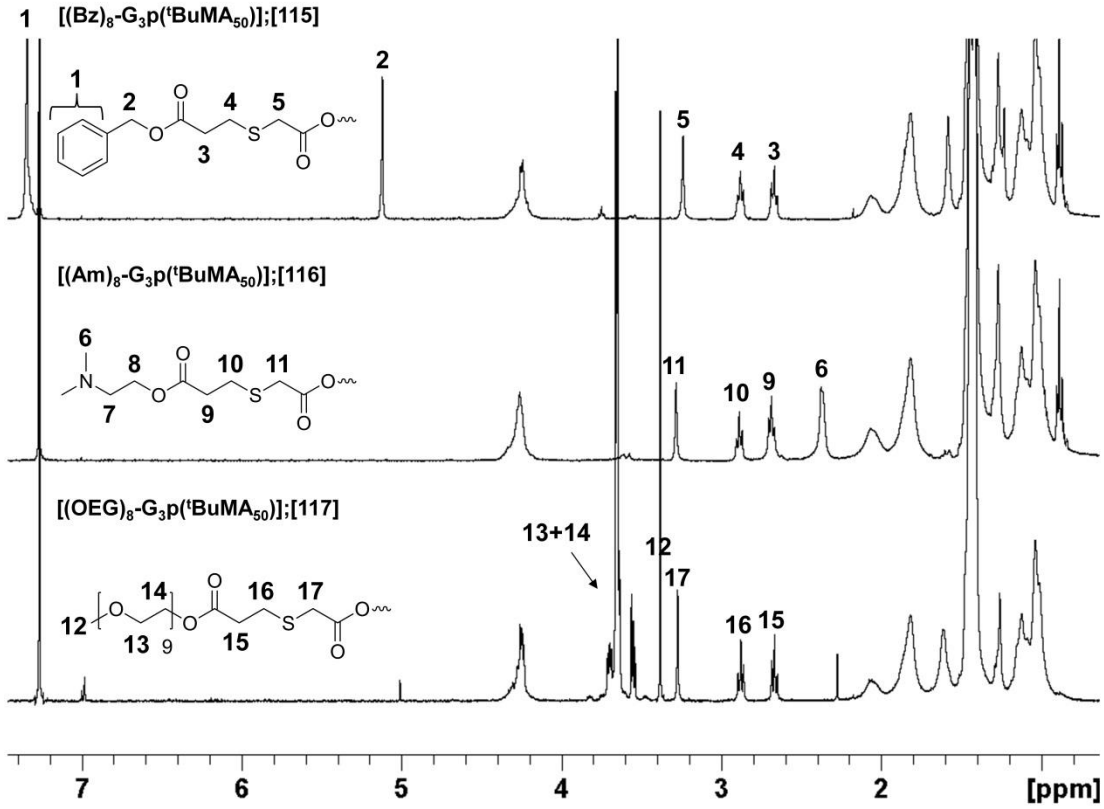

Figure 4.21 ^{1}H NMR spectrums (400 MHz, $CDCl_3$) of functional LDHs **[115]-[117]**

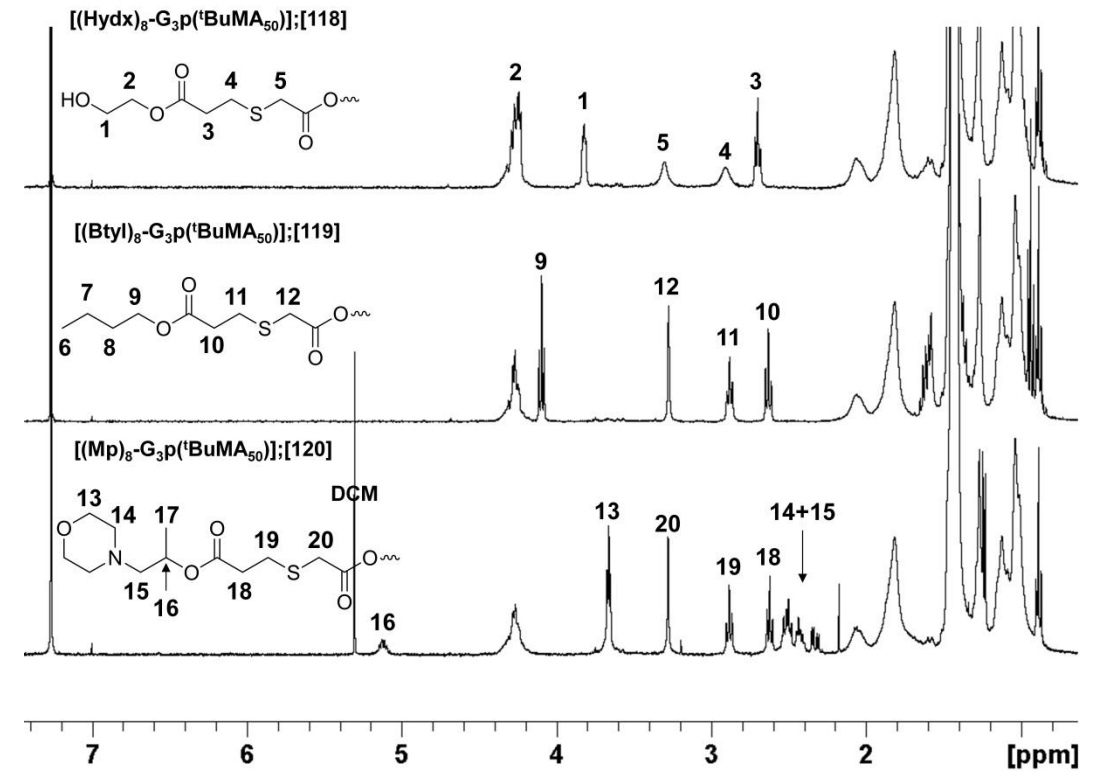

Figure 4.22 ^{1}H NMR spectrums (400 MHz, $CDCl_3$) of functional LDHs **[118]-[120]**

LDHs **[102]-[114]** were analysed by SEC, Table 4.2. Generally, the functionalised LDHs resulted in higher molecular weights by SEC analysis compared to their parent starting materials, with considerable molecular weight increases observed with the oligo(ethyl glycol) functionalised LDHs (entries; **[106]**, **[111]** and **[117]**, Table 4.2).

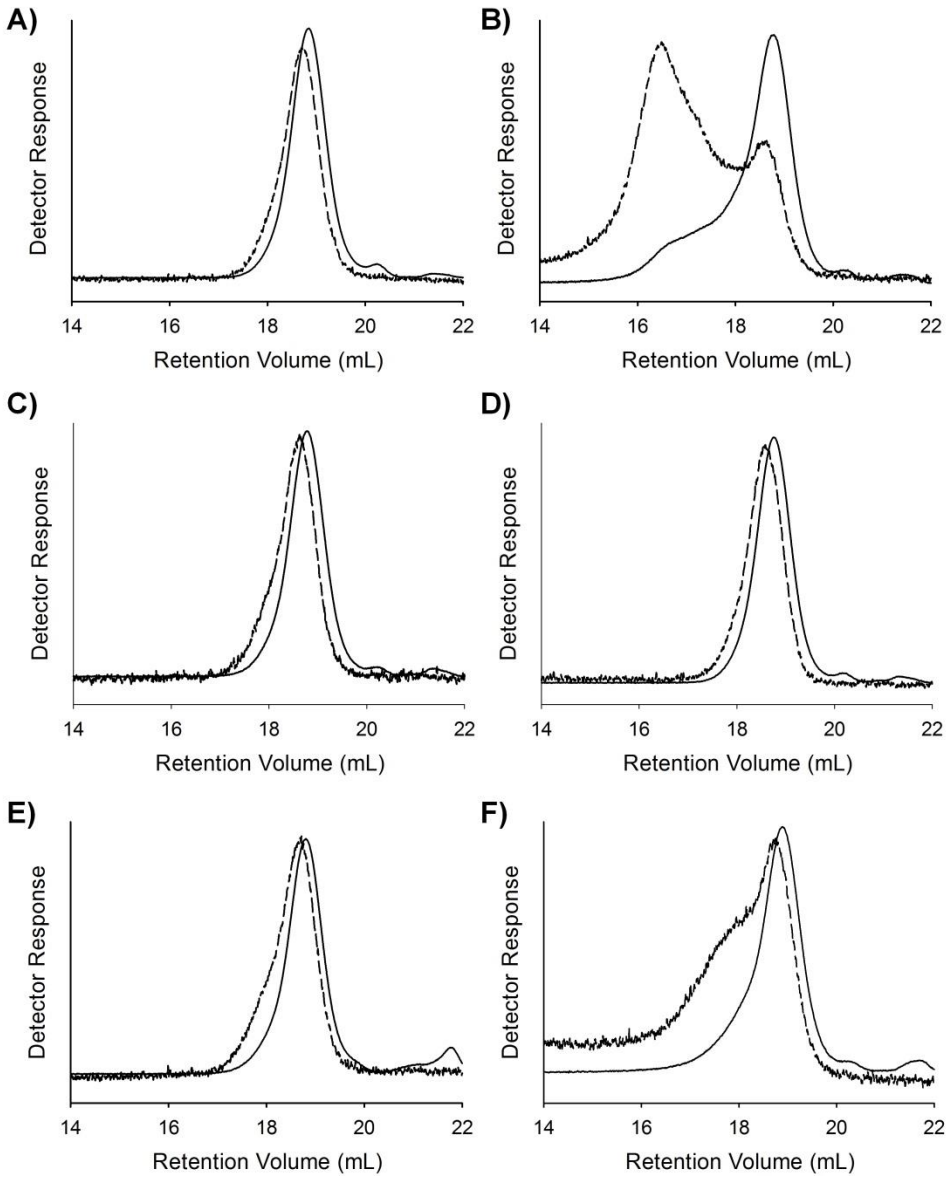

Figure 4.23 Triple detection SEC chromatograms of; (A) **[(Bz)$_8$-G$_3$p(^{t}BuMA$_{50}$)];[115]**; (B) **[(Am)$_8$-G$_3$p(^{t}BuMA$_{50}$)];[116]**; (C) **[(OEG)$_8$-G$_3$p(^{t}BuMA$_{50}$)];[117]**; (D) **[(Hydx)$_8$-G$_3$p(^{t}BuMA$_{50}$)];[118]**; (E) **[(Btyl)$_8$-G$_3$p(^{t}BuMA$_{50}$)];[119]**; (F) **[(Mp)$_8$-G$_3$p(^{t}BuMA$_{50}$)];[120]**.The figure shows the refractive index (RI) detector response (solid lines) and the right angle light scattering (RALS) detector response (dotted lines).

This is to be expected, since an increase in molecular weight is achieved through the addition of functional substrates ([**OEGA]**, average M_n = 480 Da per monomer addition). However, more surprisingly were the considerable molecular weight increases observed with amine based functionalities, including Am and Mp (entries; **[105]**, **[109]**, **[110]**, **[114]**, **[116]**, **[120]** and **[122]**, Table 4.2). The SEC chromatograms of LDHs with amine based functionalities also showed significant broadening in both the RI and RALS detectors, illustrated for LDHs **[116]** and **[120]**, Figure 4.23 (B) and (F), relative to the chromatograms of non-amine based functional LDHs **[115],** **[117]**, **[118]** and **[119]**, Figure 4.22 (A), (C), (D) and (E). The RALS detectors signals for **[116]** and **[120]** showed the presence of very high molecular weight materials indicated by the broad shoulders at low retention volumes. Shoulders were also present in the RI detector signals at low retention volumes, (particularly for **[$(Am)_8$-G_3p(^{t}BuMA$_{50}$)];[116]**, Figure 4.22 (B)) but at reduced intensities stating that the concentration of the high molecular weight materials was low. This suggests that addition of an amine peripheral monomer leads to disulfide formation, thus resulting in high molecular weight species. Without further work this lies somewhat inconclusive, but a suggestion for a future experiment may be to add a reducing agent such as tributylphosphine or dithiolthreitol (DTT) to an amine functional LDH and re-run a SEC experiment to see if the high molecular weight species are lost, therefore confirming the presence of disulfide bonds.

4.9 Conclusion

The first example of xanthate functional LDHs that can undergo one-pot xanthate deprotection and surface functionalisation via thiol-acrylate Michael addition were presented. From four generations of xanthate functional ATRP macroinitiators, used to synthesise four generations of xanthate functional LDHs (G_1, G_2, G_3 and G_4) a further twenty functional LDHs with hydrophobic, hydrophilic and polymeric surface chemistries were obtained. All functional LDHs were characterised by ^{1}H NMR spectroscopy and SEC.

Building from chapter 3, improvements to the synthesis of xanthate functional dendron were made; thus allowing the synthesis of high generation xanthate functional macroinitiators. This was facilitated by the use of a xanthate functional anhydride building block. Kinetic studies showed that the presence of xanthates did not complicate the ATRP of ^{t}BuMA, allowing the controlled synthesis of LDHs.

Some evidence of disulfide formation was found in the SEC chromatograms of functional LDHs when amine functional acrylate monomers were used during one-pot xanthate deprotection and thiol Michael addition chemistry. It is unknown why this specifically occurs when using an amine based monomer, in comparison to a non-amine based monomer is used, but as a suggestion, perhaps the increased nucleophilicity arising from the nitrogen atoms within the amine monomer leads to proton abstraction from the corresponding thiol, thus promoting disulfide formation. Formation of the quaternary salt of the amine monomer may supress disulfide formation. Further studies may also seek to analyse the thermal properties of the synthesised LDHs; for example, does the glass transition temperature of the LDH change as the dendritic peripheral groups are changed? Further self-assembly properties of the functional LDHs may also be interesting.

Research currently ongoing from the described synthetic routes to xanthate functional LDHs has shown that partial deprotection of the peripheral xanthates within LDHs can also be achieved. This has allowed LDHs with mixed functionalities through a two-stage protection and functionalisation strategy to be produced, which is believed to be the first example of such materials, Figure 4.24.

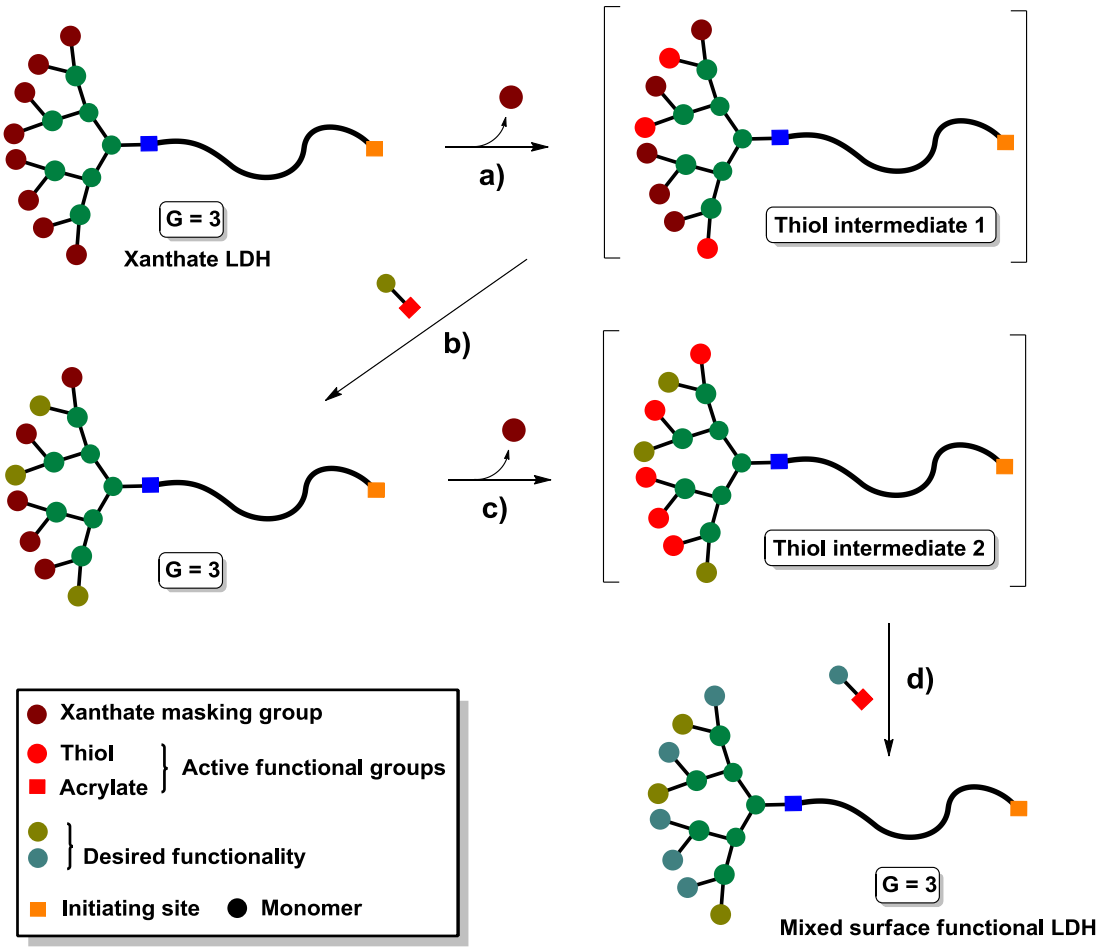

Figure 4.24 Schematic representation for the preparation of mixed surface functional LDHs by a two-stage protection and functionalisation strategy using xanthate deprotection and thiol Michael addition chemistry

4.10 References

1. J. Nicolas, Y. Guillaneuf, C. Lefay, D. Bertin, D. Gigmes and B. Charleux, *Progress in Polymer Science*, 2013, **38**, 63-235.
2. K. Matyjaszewski, *Macromolecules*, 2012, **45**, 4015-4039.
3. S. Perrier and P. Takolpuckdee, *Journal of Polymer Science Part A: Polymer Chemistry*, 2005, **43**, 5347-5393.
4. M. Kato, M. Kamigaito, M. Sawamoto and T. Higashimura, *Macromolecules*, 1995, **28**, 1721-1723.
5. J.-S. Wang and K. Matyjaszewski, *Journal of the American Chemical Society*, 1995, **117**, 5614-5615.
6. W. Tang and K. Matyjaszewski, *Macromolecules*, 2007, **40**, 1858-1863.
7. W. Tang and K. Matyjaszewski, *Macromolecules*, 2006, **39**, 4953-4959.
8. T. E. Patten, J. Xia, T. Abernathy and K. Matyjaszewski, *Science*, 1996, **272**, 866-868.
9. K. L. Robinson, M. A. Khan, M. V. de Paz Báñez, X. S. Wang and S. P. Armes, *Macromolecules*, 2001, **34**, 3155-3158.
10. S. McDonald and S. P. Rannard, *Macromolecules*, 2001, **34**, 8600-8602.
11. M. Le Neindre and R. Nicolay, *Polymer Chemistry*, 2014, **5**, 4601-4611.
12. D. J. Keddie, *Chemical Society Reviews*, 2014, **43**, 496-505.
13. L. A. Connal, R. Vestberg, C. J. Hawker and G. G. Qiao, *Macromolecules*, 2007, **40**, 7855-7863.
14. M. Malkoch, E. Malmström and A. Hult, *Macromolecules*, 2002, **35**, 8307-8314.

CHAPTER 5

Oil in water emulsion stabilisation using dendritic polymer surfactants

5.1 Introduction

Surfactants comprising branched polymer systems have been shown to exhibit greater stability than analogous linear copolymers.[1] This is thought to be due to the multiple hydrophobic chain ends which are provided by the branched architecture in contrast to the weak single chain end droplet adhesion provided by the linear architecture (see Introduction, Chapter 1, section 1.7.4).

Work by Woodward *et al*. has shown that when the chain ends of surfactants comprising a branched architecture were modified to become hydrophilic, demulsification was observed.[2] This confirms that the hydrophobicity of the chain-ends which "anchors" into the oil droplet plays a vital role in emulsion stabilisation.

Unpublished work by our group has shown that the number of chain-ends which anchor into the oil droplet also plays a role in emulsion stabilisation. By using a mixed ATRP initiating system with hydrophobic and hydrophilic initiators, the number of hydrophobic "anchoring groups" per branched polymer were controlled. Results confirmed that the hydrophobic chain end composition could be decreased as low as 25% before any significant change in mean droplet size was observed. This opens up the potential for replacing some of the chain ends with functionalities that are not meant to stabilise the oil droplets, but rather allows functionality to be imparted. This is potentially an extremely advantageous system, as such chain ends may be functionalised with water soluble cell receptors for targeted delivery.

Dendritic hybrid architectures such as linear dendritic hybrids (LDH) and hyperbranched polydendrons (HPD) (see Introduction, Chapter 1, sections 1.5.2 & 1.5.4) offer a means to introduce multiple chain-end functionalities, Figure 5.1. Different surface groups can be easily offered by using different dendritic macroinitiators.

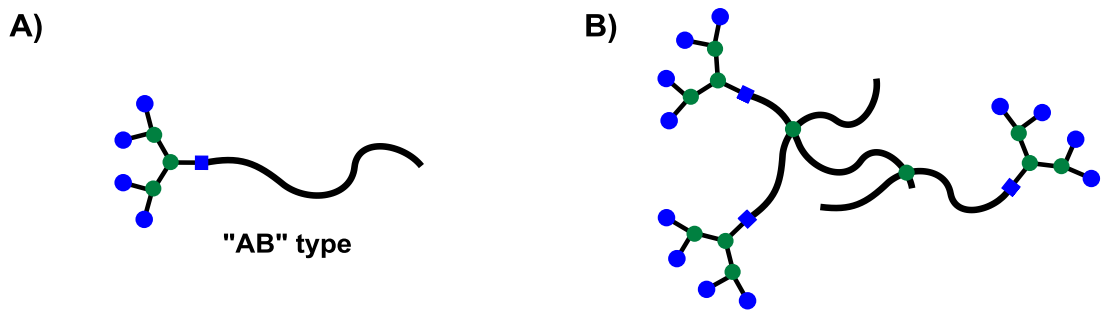

Figure 5.1 Dendritic hybrid architectures; (A) AB type linear dendritic hybrid (LDH); (B) hyperbranched polydendron (HPD)

It can be hypothesised that surfactants based on a HPD architecture will exhibit greater emulsion stability than the analogous LDH architecture. Again this is due to the multiple hydrophobic chain ends provided by the branched architecture (HPD) in contrast to the weak single chain end droplet adhesion provided by the linear architecture (LDH) due to the multiple end group effect.

5.2 Aims

Extending from our unpublished results, showing that the number of chain-ends which anchor into the oil droplet plays a role in emulsion stabilisation, the aim is to perform a similar study and evaluate how effective polymeric surfactants generated from LDHs and HPDs architectures are at stabilising o/w emulsions, based on differences between polymer architecture and changes to the dendritic components. In other words, what happens to the stability of the emulsion when “good” hydrophobic non-dendritic chain ends are replaced with dendritic chain ends?

The study will include changing the generation of the dendron, the dendritic surface chemistry and using mixed dendritic/non-dendritic initiating systems to vary the contribution to stabilisation from the dendritic species.

It should be stated that this is only a preliminary study, and so full characterisation of the surfactant properties will not be carried out.

Both LDHs and HPDs will be synthesised using a macroinitiator approach (see Chapter 1), employing four different functional dendritic ATRP initiators, modified using a one-pot xanthate deprotection thiol Michael addition functionalisation chemistry, drawn schematically for the G_2 initiators in Figure 5.2.

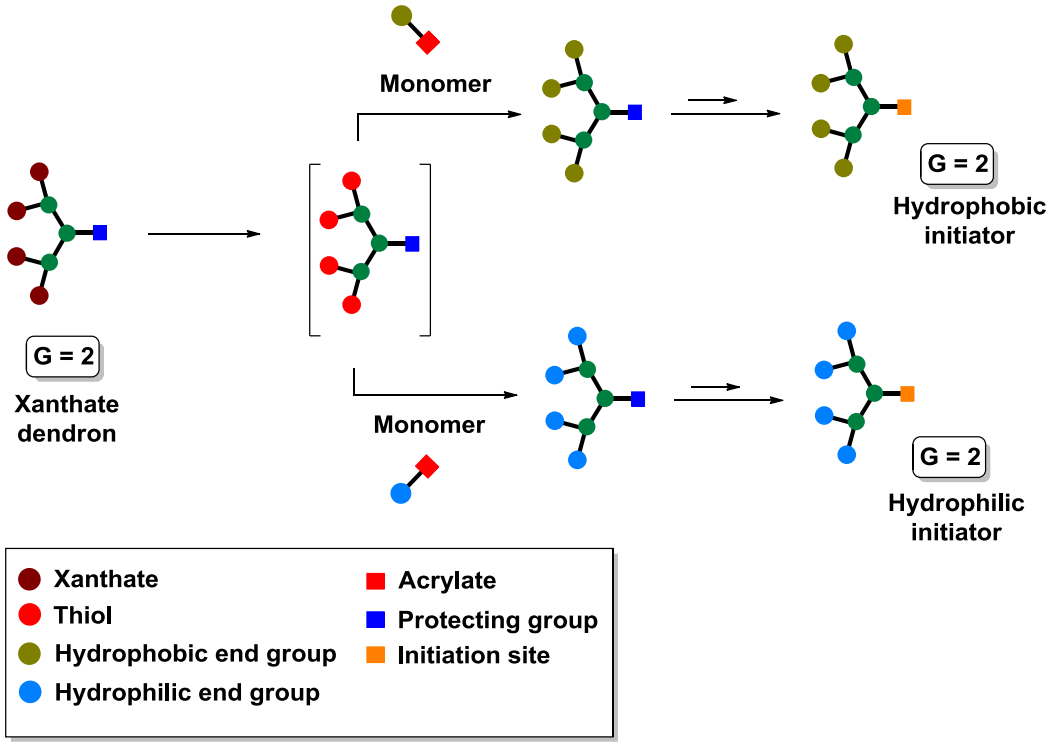

Figure 5.2 Schematic strategy for the synthesis of G_2 dendritic macroinitiators using one-pot thiol xanthate deprotection and thiol Michael addition chemistry

Using each of these initiators and conventional ATRP or branched vinyl polymerisation ATRP, LDHs and HPDs will be synthesised, comprising hydrophobic or hydrophilic dendritic surface groups, Figure 5.3.

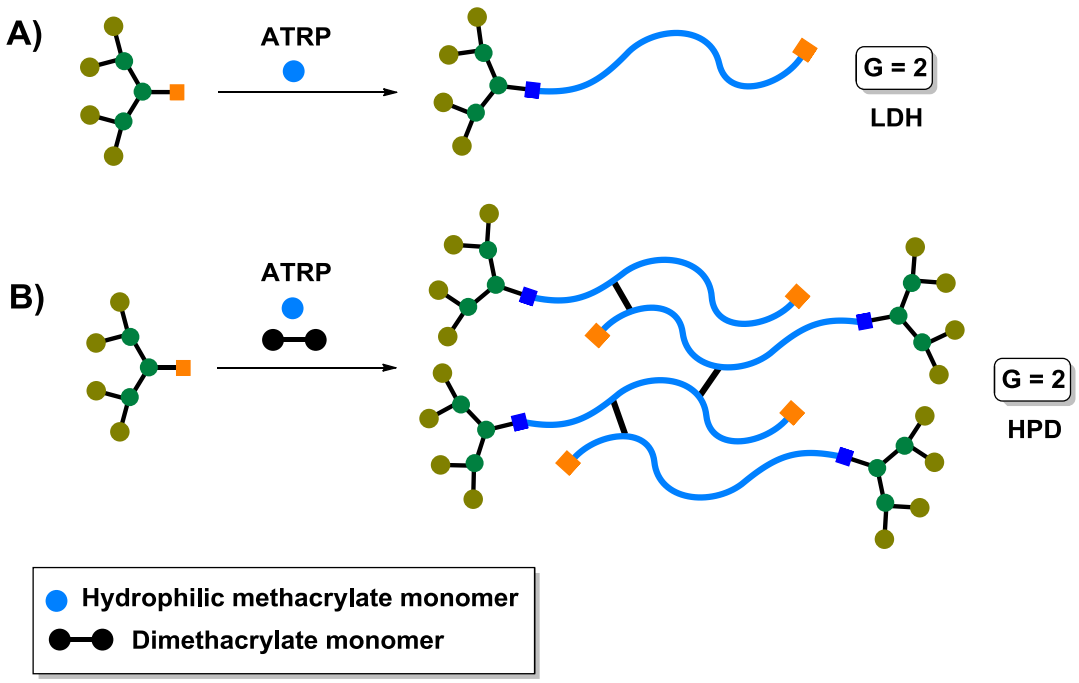

Figure 5.3 Schematic representation using a hydrophobic G_2 initiator to synthesise; (A) linear dendritic hybrids (LDHs); (B) hyperbranched polydendrons (HPDs)

To study the effect of the dendritic component within the emulsion surfactant system, a varying molar % of a non-dendritic component will be added via a mixed ATRP initiator system, to create materials which comprise both dendritic and non-dendritic surface groups. This will be performed at 50% molar increments for the LDH materials, Figure 5.4 and 25% molar increments for the HPDs, Figure 5.5.

Initially, a long term stability test of emulsions comprising the different surfactants will be performed. Following a selection of "good" surfactants, more specific experiments will be performed to probe their performance.

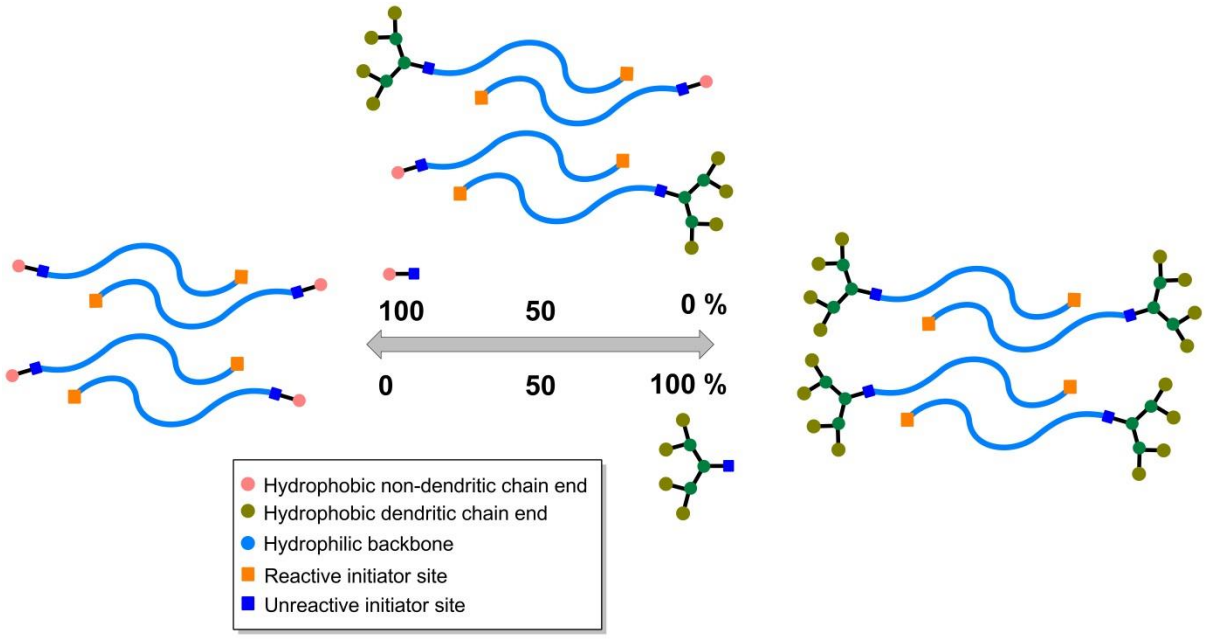

Figure 5.4 Schematic representation of a mixed initiator system for LDH, comprising a G_2 hydrophobic dendron with a non-dendritic component, at 50% molar increments

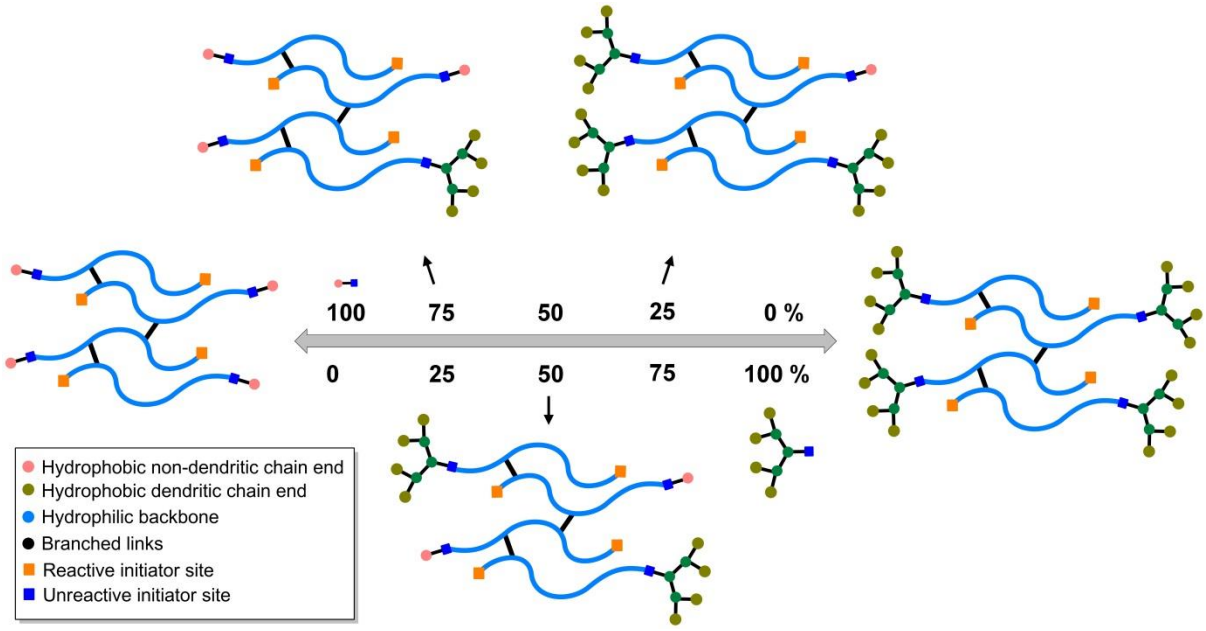

Figure 5.5 Schematic representation of a mixed initiator system for HPD, comprising a G_2 hydrophobic dendron with a non-dendritic component, at 25 % molar increments

5.3 Branched Vinyl Polymerisation by ATRP

As discussed in Chapter 4, the optimum reaction conditions for ATRP of hydrophilic and hydrophobic methacrylate monomers to synthesise linear polymers at ambient temperature are now relatively well understood. Branched polymers are currently of significant interest and, as such, existing conditions for ATRP have been manipulated to synthesise high molecular weight branched materials without gelation.[3-5]

To produce soluble high molecular weight branched polymers by ATRP a low concentration of divinyl branching monomer, in addition to the conventional monomer, is added to the system. The branching monomer concentration must be maintained at a ratio with the initiator, below an effective initiator:brancher of 1:1 to avoid gelation; this is since the incorporation of more than one branching monomers per chain can lead to a cross-linked branched network. Kinetic studies of ATRP of 2-hydroxylpropyl methacrylate (HPMA) in the presence of a low concentration of ethylene glycol dimethacrylate (EGDMA) as the divinyl branching agent, concluded that branched vinyl polymerisation by ATRP can be broken into three stages,[5] Scheme 5.1.

In the first stage, ATRP commenced through the traditional initiation from an alkyl halide initiator (see Chapter 4, section 4.3). In the propagation stage, the number average molecular weight (M_n) of the polymer obtained by SEC, increased more or less linearly up to about 90% conversion, closely resembling ATRP of HPMA in the absence of EGDMA. In the final stages, above 85-90% conversion, a steep increase in M_n was observed, so called "latent branching", illustrating that branching occurs most significantly at high conversion. This is since the primary concentration of free monomer is very low, which leads to linking of the pendent vinyl bonds of the incorporated EGDMA monomer in a statistical manner.

Studies have also shown that concentration of the reaction mixture has a significant influence of the branching process.[6] Under high dilution (10 wt %), intramolecular branching was favoured; leading to

so-called “looping” of the divinyl monomer. Increasing the concentration of the reaction mixture (50 wt %) had the opposite effect, and inter-molecular branching was preferred.

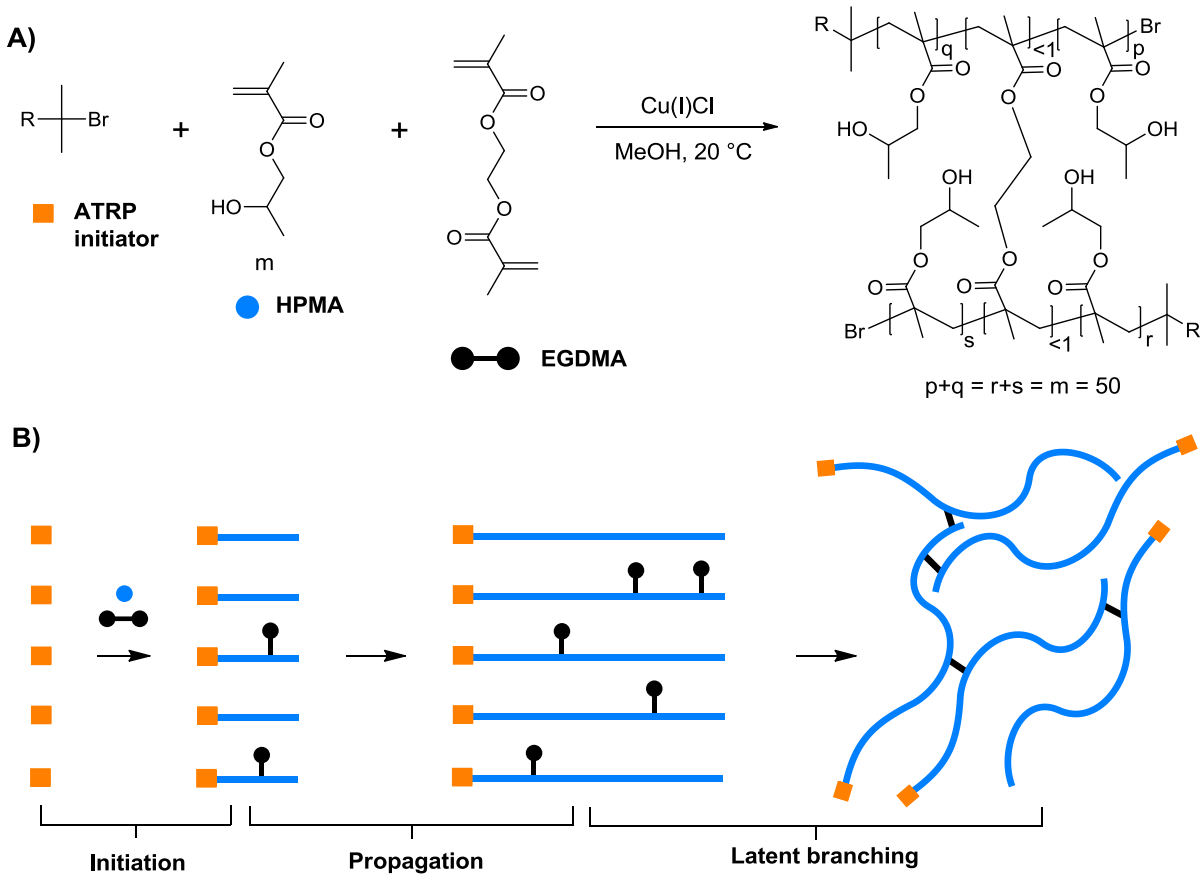

Scheme 5.1 (A) Synthesis of branched poly(2-hydroxylpropyl methacrylate) by statistically linked EGDMA units; (B) Schematic representation of the three stage branched vinyl polymerisation by ATRP

Our group has shown that the above branched vinyl polymerisation by ATRP can be used to synthesise branched copolymers,[7-9] and recently hydrophobic HPDs.[10] In this present study, branched vinyl polymerisation by ATRP will be used to synthesise hydrophobic and amphiphilic HPDs.

5.4 Synthetic strategy

Utilising the xanthate functional macroinitiators in Chapter 4, an elegant synthetic strategy would be to synthesise a single xanthate functional LDH, and a single xanthate functional HPD by conventional ATRP and branched vinyl polymerisation ATRP respectively, and then perform one-pot xanthate deprotection and thiol Michael addition reactions, generating a number of different surface functional LDHs and HPDs.

In early studies this method was adopted, and using initiator **[$(Xan)_4$-G_2-BiB];[92]** (see chapter 4 for its preparation), the successful ATRP of the commercially available hydrophilic monomer oligo(ethyleneglycol) monomethyl ether methacrylate (OEGMA) with a number average degree of polymerisation (DP_n) = 7-8 monomer units (M_n = 300 Da) to synthesise a xanthate functional LDH was achieved. Unfortunately, analysis of the resulting ^{1}H NMR spectrum of the LDH, confirmed that the xanthate peripheral groups were obscured by the OEGMA polymeric backbone resonances, preventing analysis by ^{1}H NMR spectroscopy. Since analysis by ^{1}H NMR spectroscopy is crucial to the effective characterisation of the functionalised dendritic peripheral groups, this method was not pursued any further. Instead, one-pot xanthate functionalisation and thiol Michael addition was performed to synthesise four surface functional ATRP initiators.

5.4.1 Synthesis of dendritic ATRP initiators

In Chapters 2, 3 and 4, thiol Michael addition was shown to work effectively using acrylate functional monomers. Benzyl acrylate **[BA]** was therefore chosen as the hydrophobic monomer to provide hydrophobic benzyl (Bz) peripheral groups, Figure 5.6. Tertiary amine groups are known to be soluble in acidic media due to protonation, and therefore the previously synthesised morpholino propanoyl acrylate **[MPA]** was chosen as the hydrophilic monomer to provide the pH responsive morpholino (Mp) peripheral groups, Figure 5.6. **[MPA]** was also adopted in favour of 2-(dimethylamino) ethyl acrylate as dendritic materials with dimethylamino surface functionalities have been found to be extremely difficult to purify by liquid chromatography, arising from strong silica binding interactions with the peripheral dimethyl amine moieties.

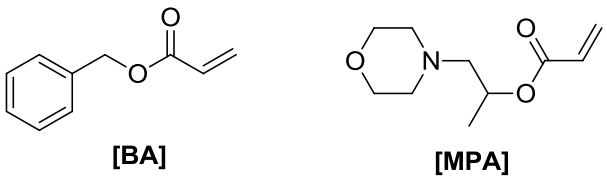

Figure 5.6 Monomers used during the synthesis of dendritic ATRP initiators; benzyl acrylate [BA]; morpholino propanoyl acrylate [MPA]

Initially, one-pot xanthate deprotection and thiol Michael addition reactions were performed with previously synthesised initiators **[(Xan)$_2$-G$_1$-BiB];[91]** and **[(Xan)$_4$-G$_2$-BiB];[92]**, and the hydrophobic monomer **[BA]**, as a synthetic route to hydrophobic Bz functional initiators, illustrated for **[(Xan)$_2$-G$_1$-BiB];[91]**, Scheme 5.2.

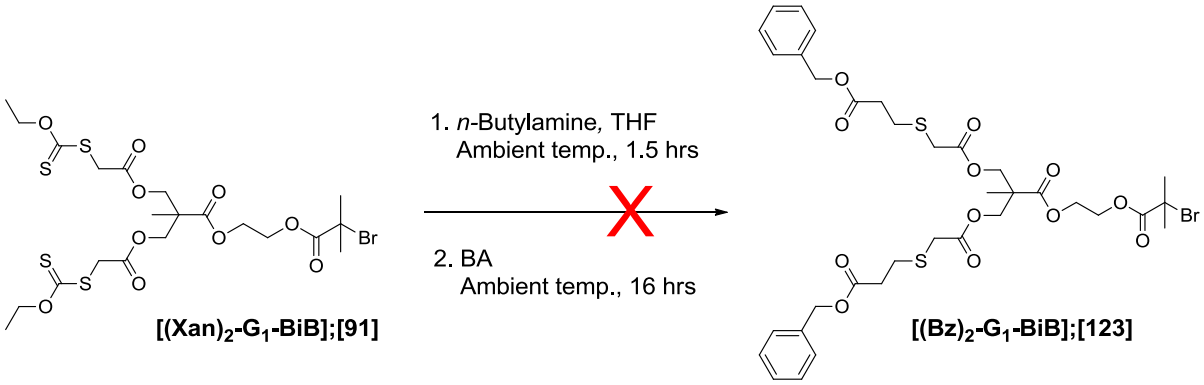

Scheme 5.2 Attempted synthesis of Bz functional initiator **[(Bz)$_2$-G$_1$-BiB];[123]** using the precursor **[(Xan)$_2$-G$_1$-BiB];[91]**

Unfortunately, analysis of the ^{1}H NMR spectra of the Bz functional initiators after one-pot xanthate deprotection and thiol Michael addition, showed multiple resonances in addition to those expected. Since the xanthate functional initiator precursors **[(Xan)$_2$-G$_1$-BiB];[91]** and **[(Xan)$_2$-G$_1$-BiB];[92]** contain bromine atoms, the in-situ generation of thiols during xanthate deprotection, may have complicated the one-pot synthesis leading to competing thiol-bromo click reactions (see Introduction for thiol-bromo reactions). [The results from this complication are somewhat interesting, and this is

now a route that is being investigated as a novel methodology to synthesise high molecular weight hyperbranched polymers using an AB_x monomer]. Instead, a slightly more complex protection and deprotection procedure using the previously synthesised xanthate functional dendrons **[$(Xan)_2$-G_1-TSe];[58]** and **[$(Xan)_4$-G_2-TSe];[60]** from Chapter 2 was employed.

5.4.1.1 Synthesis of G_1 ATRP macroinitiators

The synthetic route to the G_1 dendritic ATRP initiators is highlighted in Scheme 5.3. In the first step, **[$(Xan)_2$-G_1-TSe];[58]** was dissolved in anhydrous THF, and vigorously degassed with nitrogen for 10 minutes. Following this, 1.1 equivalents of *n*-butylamine per peripheral xanthate were slowly added, and the reaction left stirring, sealed under nitrogen for 1.5 hours. TLC analysis (hexane/ethyl acetate 60:40) confirmed total loss of the xanthate starting material after 1.5 hours, after which 1.3 equivalent of functional acrylate (**[BA]** or **[MPA]**) was added per thiol, and the mixture left stirring at ambient temperature for an additional 16 hours.

Workup of the resulting functionalised dendrons was achieved by reducing the volume of THF by half *in vacuo* and precipitating the mixture twice from THF into hexane (2 x 150 mL) at ambient temperature. Following removal of solvents, the Bz peripheral dendron **[$(Bz)_2$-G_1-TSe];[123]** was obtained in 90% yield as an orange viscous oil, and the Mp functional dendron **[$(Mp)_2$-G_1-TSe];[124]** as an orange viscous oil in 92% yield.

The second step involved the removal of the *p*-toluenesulfonyl ethyl protecting group (TSe). This was achieved by dissolving either the dendron **[$(Bz)_2$-G_1-TSe];[123]** or **[$(Mp)_2$-G_1-TSe];[124]** in CH_2Cl_2 and adding 1.3 equivalents of 1,8-diazabicyclo[5.4.0]undec-7-ene (DBU). Both mixtures proceeded to turn dark red upon addition, and were left stirring overnight at ambient temperature for 16 hours. The products were isolated by diluting with CH_2Cl_2, washing the organic layer twice with 1M $NaHSO_4$, drying the over $MgSO_4$ and removal of solvents to result in crude red oils. Additional purification for the Bz peripheral dendron resulted from using automated liquid chromatography (silica) by first using a mobile phase of 100% hexane, increasing the polarity to 100% ethyl acetate, which removed the desired impurities.

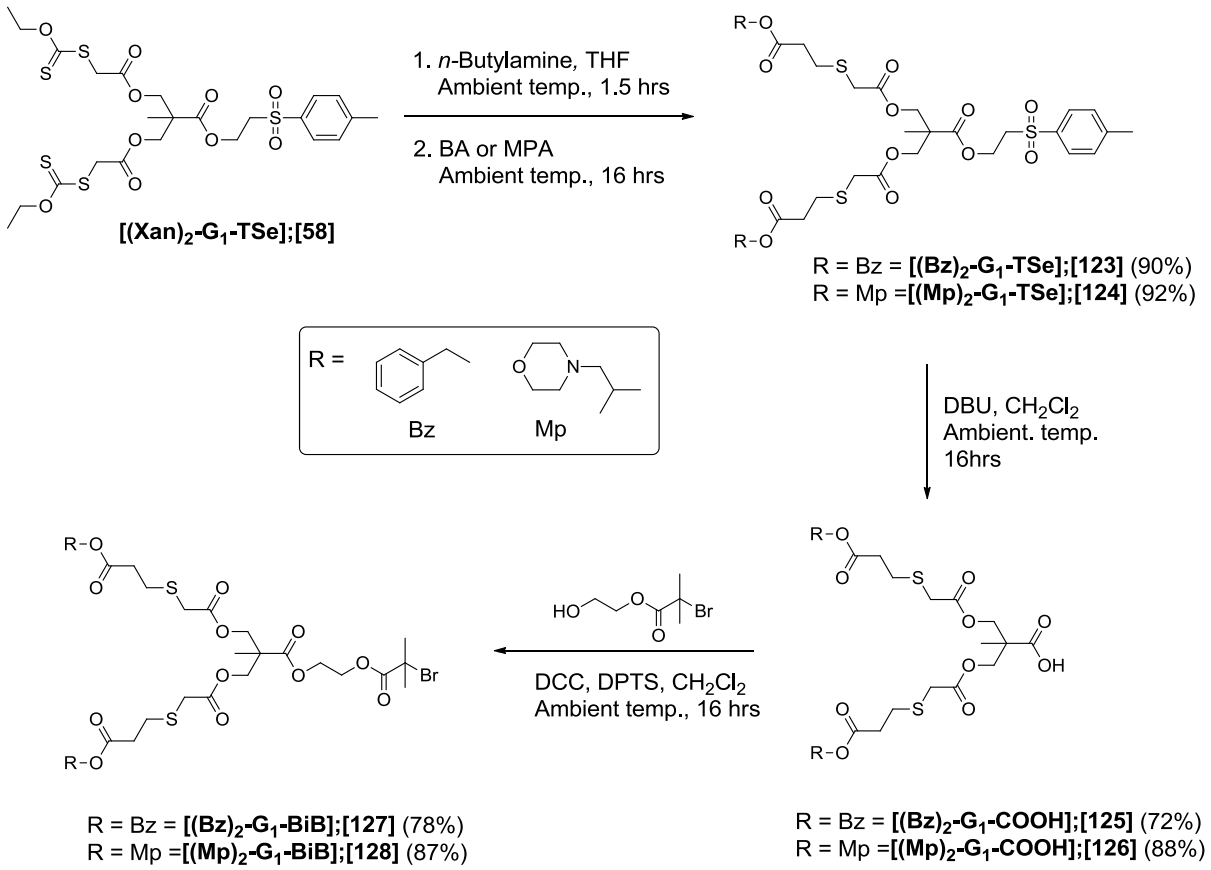

Scheme 5.3 Synthesis of G_1 ATRP initiators using one-pot xanthate deprotection and thiol Michael addition click chemistry to induce the desired peripheral functionality

The mobile phase solvent system was then changed to CH_2Cl_2, increasing to CH_2Cl_2:MeOH 90:10 (product eluted at 7% MeOH), which enabled the product to be removed from the silica column. This methodology was used since the product was not soluble in hexane or ethyl acetate, and enabled the greatest separation between impurities and the product. After removal of solvents, **[(Bz)$_2$-G$_1$-COOH];[125]** was obtained as a red oil in 72% yield. The same methodology was adopted for the Mp functional dendron, using an initial mobile phase solvent system of hexane increasing to hexane:ethyl acetate 50:50, then changing to CH_2Cl_2 and increasing to CH_2Cl_2:MeOH 90:10 (product eluted at 9% MeOH). After removal of solvents, **[(Mp)$_2$-G$_1$-COOH];[126]** was obtained as a red oil in 88% yield.

In the final step, the previously synthesised 2-hydroxyethyl-2-bromoisobutyrate, **[OH-BiB];[89]** (see Chapter 4) was coupled to the reactive carboxylic acid focal points of **[125]** and **[126]**. The dendron

[125] or **[126]**, 4-(dimethylamino)pyridinium *p*-toluenesulfonate (DPTS; see Chapter 3, section 3.3.4.2) and **[OH-BiB];[89]** (see Chapter 4) were dissolved in anhydrous CH_2Cl_2. N,N′-Dicyclohexylcarbodiimide (DCC) dissolved in CH_2Cl_2 was added slowly to the mixture, and the reaction left stirring for 16 hours at ambient temperature. Following this, the crude mixtures were filtered, diluted with CH_2Cl_2, washed twice with water, once with brine and the organic layer was dried over $MgSO_4$. After removal of solvents, the Bz peripheral initiator was purified by automated liquid chromatography (silica, eluting hexane increasing to the polarity to hexane:ethyl acetate 90:10), to result in **[$(Bz)_2$-G_1-BiB];[127]** as an orange viscous oil isolated in 78% yield. The Mp peripheral initiator was also purified by automated liquid chromatography (silica, eluting CH_2Cl_2 increasing to the polarity to CH_2Cl_2:MeOH 95:5), resulting in **[$(Mp)_2$-G_1-BiB];[128]** as red viscous oil in 87% yield.

5.4.1.2 Synthesis of G_2 ATRP macroinitiators

The synthesis of the G_2 initiators followed the same procedure to the G_1 initiators, Scheme 5.4. In the first step, **[$(Xan)_4$-G_2-TSe];[60]** was deprotected with 1.2 equivalents of n-butylamine (increased from 1.1 to account for steric bulk) per xanthate, and functionalised with 1.5 equivalents (increased from 1.3 to account for steric bulk) of **[BA]** or **[MPA]** using exactly the same methodology as the G_1 materials. Following purification the G_2 Bz dendron **[$(Bz)_4$-G_2-TSe];[129]** was obtained as an orange viscous oil in 92% yield. The G_2 Mp dendron **[$(Mp)_4$-G_2-TSe];[130]** was obtained as an orange oil in 96% yield. It should be noted that even at G_2 extremely high yields were observed, highlighting the efficiency of this chemistry. The removal of the TSe protecting group followed the same procedure as the G_1 materials, using 1.3 equivalents of DBU. After liquid chromatography (silica, eluting hexane, increasing the polarity to hexane:ethyl acetate 50:50) resulted in **[$(Bz)_4$-G_2-COOH];[131]** as an orange oil in 79%, and **[$(Mp)_4$-G_2-COOH];[132]** as an orange oil in 75% yield.

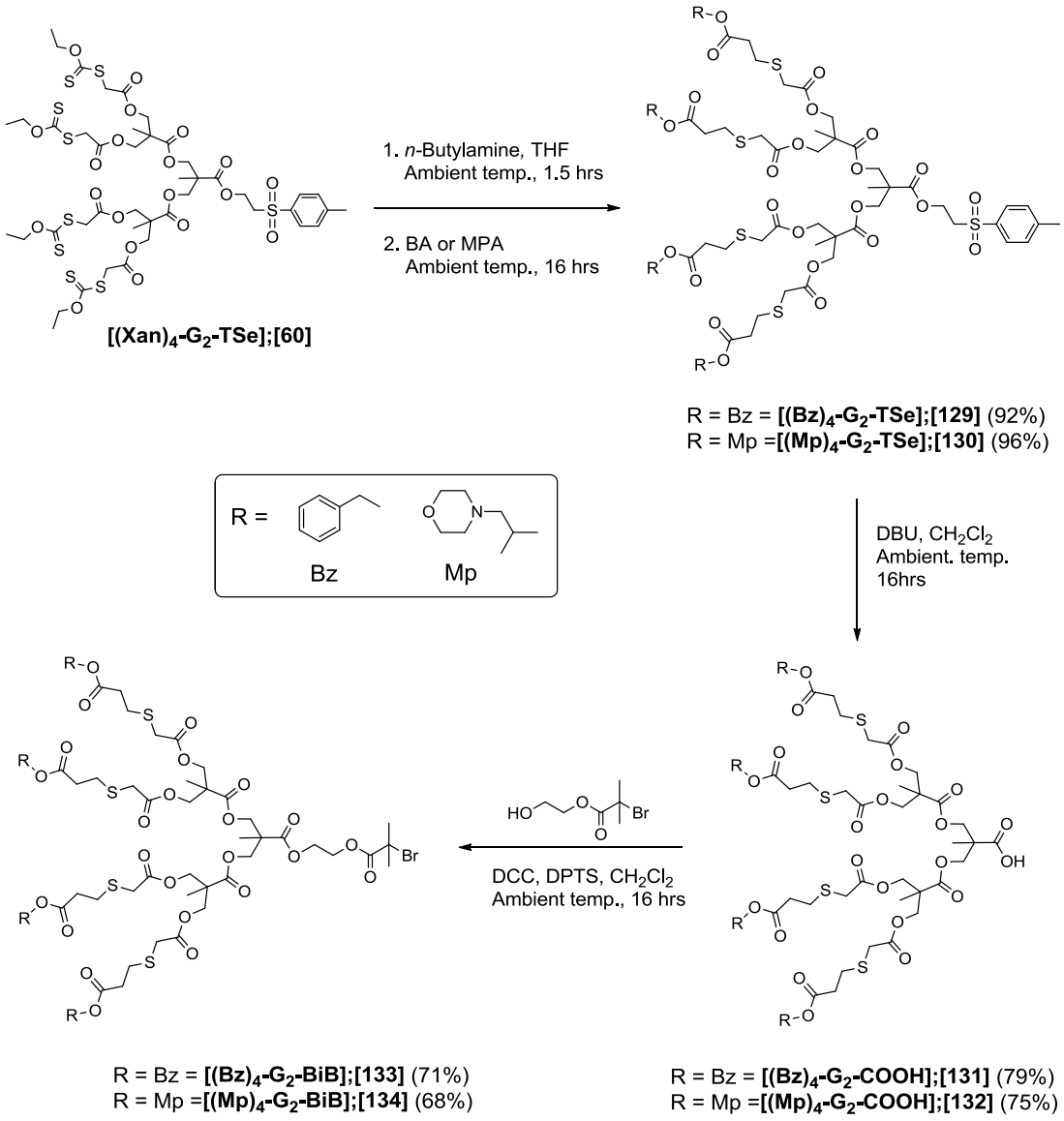

Scheme 5.4 Synthesis of G_2 ATRP initiators by using one-pot xanthate deprotection and thiol Michael addition click chemistry to induce the desired peripheral functionality

In the final step, the focal points of the G_2 dendrons were modified to ATRP initiators, using the same procedure as the G_1 materials. After purification by extraction and liquid chromatography (silica, eluting hexane, increasing the polarity to hexane:ethyl acetate 40:60) **[(Bz)$_4$-G$_2$-BiB];[133]** was obtained as a viscous orange oil in 71% yield, and **[(Mp)$_4$-G$_2$-BiB];[134]** (silica gel, eluting CH_2Cl_2 increasing the polarity to CH_2Cl_2:MeOH 90:10) as a red viscous oil in 68% yield. It is possible that the slight decrease in yields may be a result of steric hindrance during focal point modification.

5.4.1.3 Characterisation of G_1 ATRP macroinitiators

The G_1 dendrons **([123]-[128]**) were analysed by NMR spectroscopy (^{1}H and ^{13}C), electrospray ionisation mass spectrometry (ESI-MS) and microanalysis. Functionalised dendrons [**(Bz)$_2$-G$_1$-TSe];[123]** and **[(Mp)$_2$-G$_1$-TSe];[124]** each resulted in characteristic resonances by NMR spectroscopy to enable easy determination of their structures. Analysis of [**(Bz)$_2$-G$_1$-TSe];[123]** by ^{1}H NMR spectroscopy resulted in fourteen proton environments, with characteristic Bz resonances at approximately 7.35 ppm, Figure S5.1. Similar analysis of **[(Mp)$_2$-G$_1$-TSe];[124]** by ^{1}H NMR spectroscopy resulted in fifteen proton environments, with Mp resonances at 2.37-2.56 ppm and 3.66 ppm, Figure S5.4. Analysis of both [**(Bz)$_2$-G$_1$-TSe];[123]** and **[(Mp)$_2$-G$_1$-TSe];[124]** by ^{13}C NMR spectroscopy gave the expected number of twenty one and fifteen carbon environments, respectively, Figures S5.2 and S5.5. Confirmation of [**(Bz)$_2$-G$_1$-TSe];[123]** by ESI-MS led to three populations at 789 Da (MH^+ = 789 Da), 811 Da (MNa^+ = 811 Da) and 827 Da (MK^+ = 827 Da), Figure S5.3. Analysis of [**(Mp)$_2$-G$_1$-TSe];[124]** by ESI-MS also resulted in three populations 863 Da (MH^+ = 863 Da), 885 Da (MNa^+ = 885 Da) and 901 Da (MK^+ = 901 Da), Figure S5.6.

After removal of the TSe protecting group, loss of the characteristic aromatic signals at 7.40 and 7.80 ppm was observed for both **[(Bz)$_2$-G$_1$-COOH];[125]** and **[(Mp)$_2$-G$_1$-COOH];[126]** by ^{1}H NMR spectroscopy, Figures S5.7 and S5.10. Further confirmation of the acid functionality was confirmed for **[(Bz)$_2$-G$_1$-COOH];[125]** by ^{13}C NMR spectroscopy, resulting in the loss of an ester carbonyl, and the formation of a new acid resonance at approximately 177 ppm, Figure S5.8. A similar acid resonance for **[(Mp)$_2$-G$_1$-COOH];[126]** was confirmed at 176 ppm, although the peaks within the ^{13}C NMR spectrum were relatively broad, suggesting a hydrogen bonding effect, Figure S5.11. Analysis of the acid functional dendrons by ESI-MS resulted in observation of populations at 629 Da (MH^+ = 629 Da) and a sodiated adduct at 651 Da ($[M-H+2Na]^+$ = 651 Da) for **[(Bz)$_2$-G$_1$-COOH];[125]**, Figure S5.9. Sodiated/neutralised adducts are known to occur during ESI-MS analysis of carboxylic acids, and have been readily observed during the ESI-MS analysis of 1,1′-ferrocenedicarboxylic acid.[11] Populations at 681Da (MH^+ = 681 Da), 703 Da (MNa^+ = 703 Da) and 725 Da ($[M-H+2Na]^+$ = 725 Da) were observed for **[(Mp)$_2$-G$_1$-COOH];[126]**, Figure S5.12.

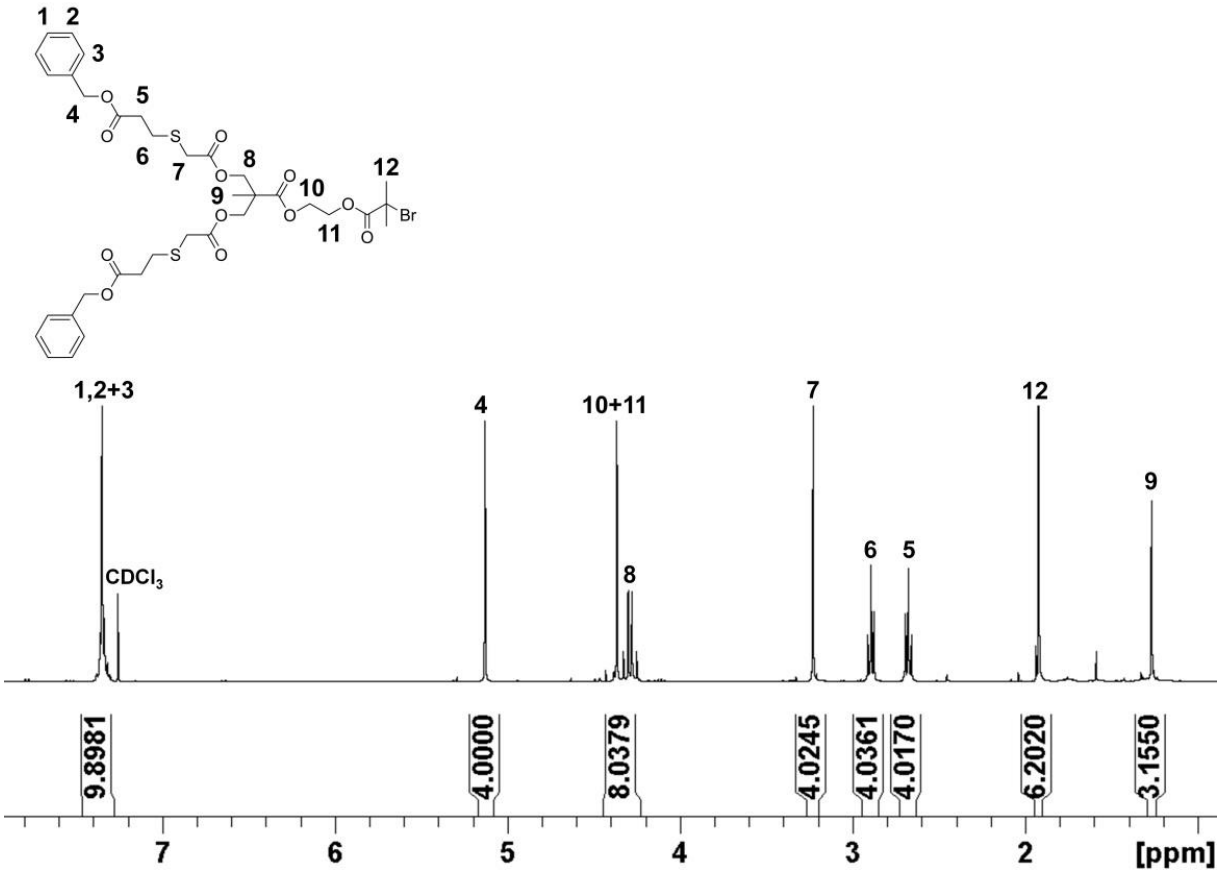

Figure 5.7 ^{1}H NMR spectrum (400MHz, $CDCl_3$) of **[(Bz)$_2$-G$_1$-BiB];[127]**

Modifications to the acid functional focal points with **[OH-BiB];[89]** resulted in the final G_1 ATRP initiators **[(Bz)$_2$-G$_1$-BiB];[127]** and **[(Mp)$_2$-G$_1$-BiB];[128]**.

Analysis of the ^{1}H NMR spectra of both dendrons resulted in the expected number of proton environments and integrations, Figures 5.7 and 5.8.

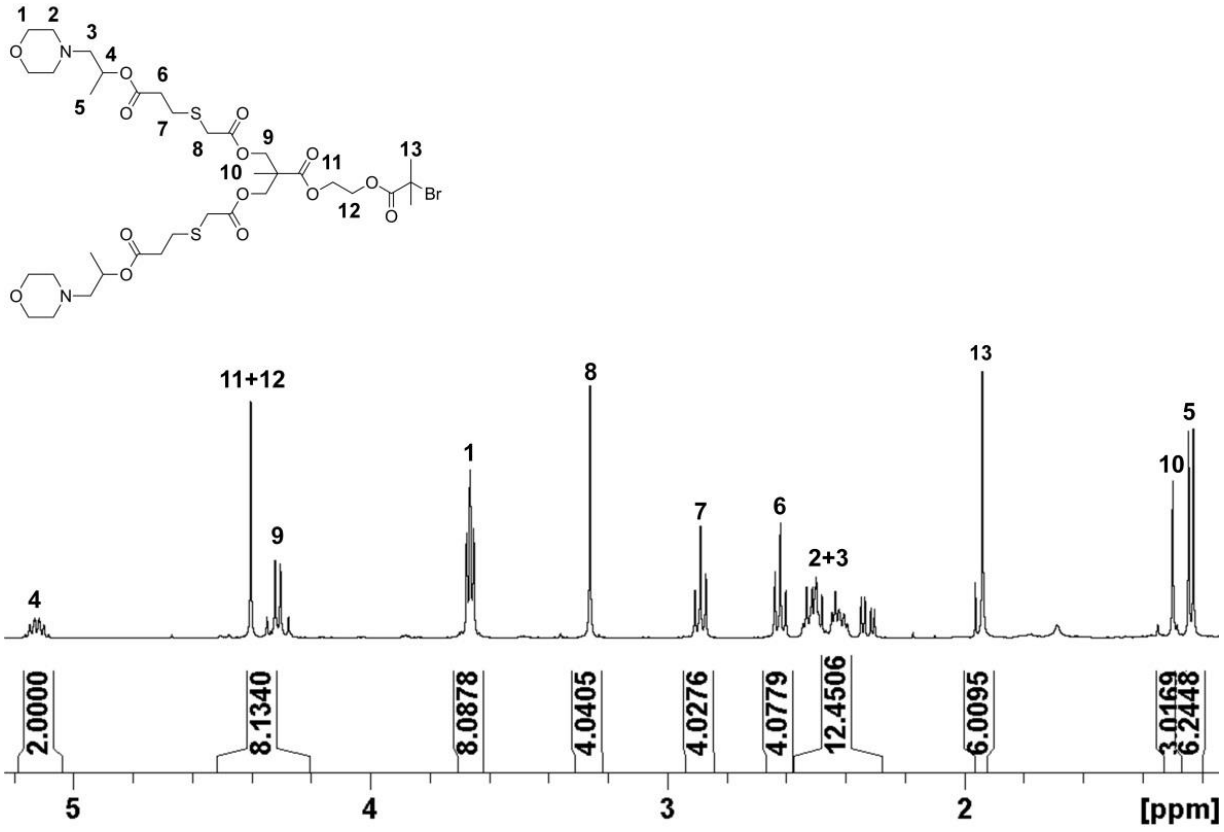

Figure 5.8 ^{1}H NMR spectrum (400MHz, $CDCl_3$) of **[(Mp)$_2$-G$_1$-BiB];[128]**

Further confirmation by ^{13}C NMR analysis indicated the desired number of carbon environments, including four ester carbonyl environments between 169-172 ppm, Figures S5.13 and S5.14. Populations at 801 Da (MH^+ = 801 Da), 821 Da (MNa^+ = 821 Da) and 839 Da (MK^+ = 839 Da) were confirmed by ESI-MS for **[(Bz)$_2$-G$_1$-BiB];[127]**, Figure 5.9. In addition, a population at 879 Da was observed, corresponding to an increase of approximately 80 Da. It is assumed that this adduct corresponds to a species whereby oxidation at the thiol-ether has occurred during ESI-MS analysis, and the product is ionised as the potassium adduct, for example; ((16 x 2)+(39)) = 71 Da). Since there is a large isotopic distribution occurring from S and Br atoms within the molecule, the additional 9 Da may be accounted for by the spread of masses. Similar populations with increasing multiples of 16 Da were observed using MALDI-TOF analysis of functionalised dendrimers in Chapter 3. Populations at 875 Da (MH^+ = 875 Da), 897 Da (MNa^+ = 897 Da) and 898 Da (MK^+ = 898 Da) were confirmed for **[(Mp)$_2$-G$_1$-BiB];[128]**, Figure 5.10.

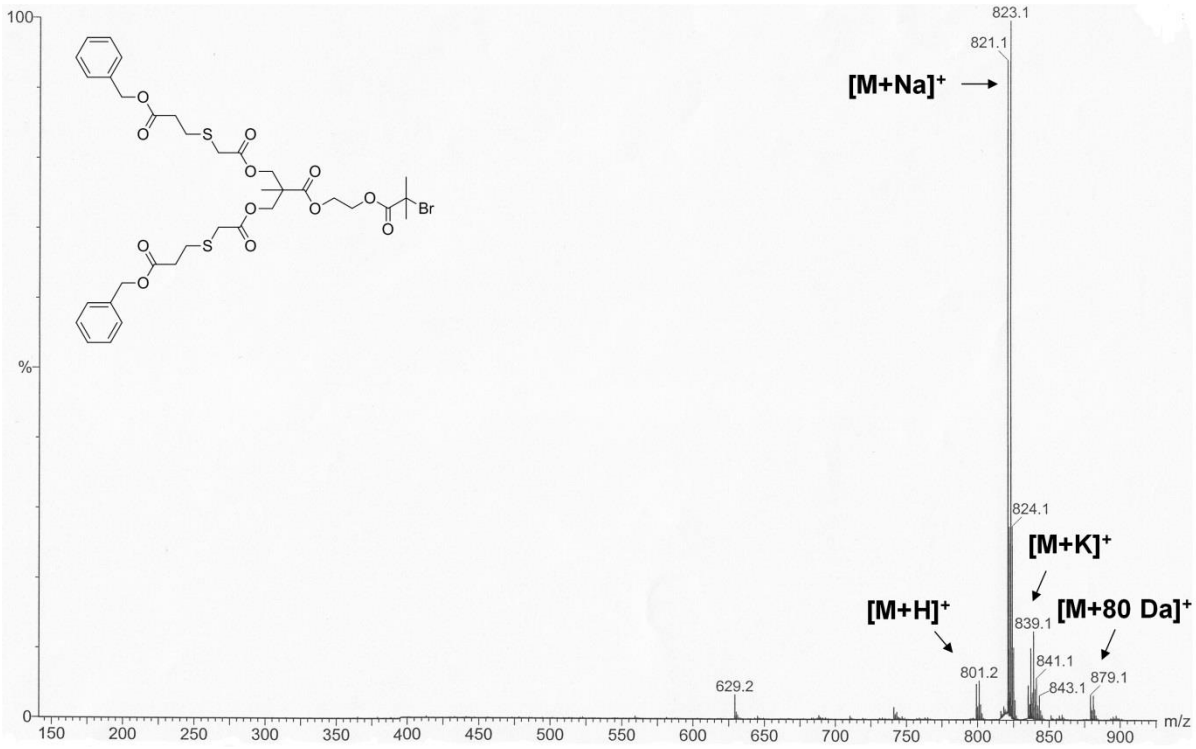

Figure 5.9 ESI-MS (MeOH) spectrum of **[(Bz)$_2$-G$_1$-BiB];[127]**

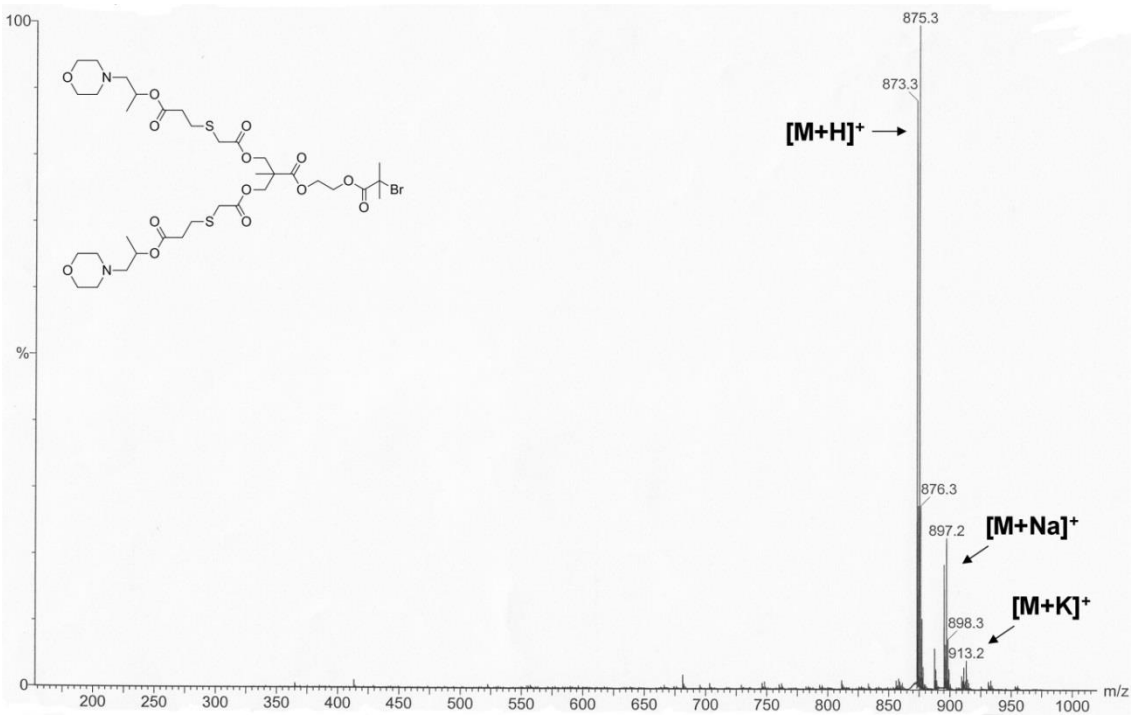

Figure 5.10 ESI-MS (MeOH) spectrum of **[(Mp)$_2$-G$_1$-BiB];[128]**

5.4.1.4 Characterisation of G_2 ATRP macroinitiators

The G_2 dendrons **([129]-[130]**) were also analysed by NMR spectroscopy (^{1}H and ^{13}C), ESI-MS and microanalysis techniques.

The ^{1}H NMR spectrum of Bz dendron **[(Bz)$_4$-G$_2$-TSe];[129]** indicated the expected number of proton environments and integrations after thiol Michael additions. Characteristic resonances, similar to the G_1 Bz dendron [(**Bz)$_2$-G$_1$-TSe];[129]**, confirmed the Bz peripheral groups at 7.35 ppm, Figure S5.15. ^{13}C NMR analysis confirmed the presence of twenty five carbon environments, including four backbone ester carbonyl resonances, Figure S5.16. Analysis of the G_2 Mp dendron **[(Mp)$_4$-G$_2$-TSe];[130]** by ^{1}H NMR spectroscopy, indicated the expected number of seventeen proton environments, Figure S5.18, and twenty five carbon environments by ^{13}C NMR techniques, Figure S5.19. Analysis of **[(Bz)$_4$-G$_2$-TSe];[129]** using ESI-MS resulted in a population at 1515 Da (MNa^+ = 1515 Da), and a population at 1573 Da (again corresponding to an increase of approximately 80 Da), Figure 5.17. Analysis of **[(Mp)$_4$-G$_2$-TSe];[130]** by ESI-MS resulted in populations at 1641 Da (MH^+ = 1641 Da), 1663 Da (MNa^+ = 1663 Da) and a population at 1721 Da (with the same signal corresponding to an increase of approximately 80 Da), Figure S5.20.

Similar to the G_1 dendrons, **[(Bz)$_2$-G$_1$-COOH];[125]** and **[(Mp)$_2$-G$_1$-COOH];[126]**, loss of the TSe moiety was evidential by the loss of characteristic aromatic signals at 7.40 and 7.80 ppm using ^{1}H NMR analysis; both **[(Bz)$_4$-G$_2$-COOH];[131]** and **[(Mp)$_4$-G$_2$-COOH];[132]** displayed total loss of these resonances, Figures S5.21 and S5.24. Another particularly interesting shift was the tertiary methyl resonance at 1.17-1.19 ppm, which shifted to approximately 1.29-1.30 ppm for both **[(Bz)$_4$-G$_2$-COOH];[131]** and **[(Mp)$_4$-G$_2$-COOH];[132]** due to the adjacent acid functionality. The newly formed acid carbonyl resonance was difficult to detect for **[(Bz)$_4$-G$_2$-COOH];[131]** by ^{13}C NMR studies, Figure S5.22, but confirmation of **[(Bz)$_4$-G$_2$-COOH];[131]** by ESI-MS indicated no evidence of protected starting material, with populations observable at 1333 Da (MNa^+ = 1333 Da), 1349 Da (MK^+ = 1349 Da) and 1392 Da (increase of approximately 80 Da), Figure S5.23. Again, the acid carbonyl resonance was difficult to detect by ^{13}C NMR analysis for [(**Mp)$_4$-G$_2$-COOH];[132]**, Figure S5.25, but no evidence of protected species were confirmed by ESI-MS with the expected populations

at 1459 Da (MH^+ = 1459 Da) and 1481 Da (MNa^+ = 1481 Da), Figure S5.26. Finally coupling with **[OH-BiB];[89]** resulted in the G_2 ATRP initiators **[$(Bz)_4$-G_2-BiB];[133]** and **[$(Mp)_4$-G_2-BiB];[134]**.

Analysis of the ^{1}H NMR spectra resulted in the correct number of environments and integrations, Figures 5.11 and 5.12.

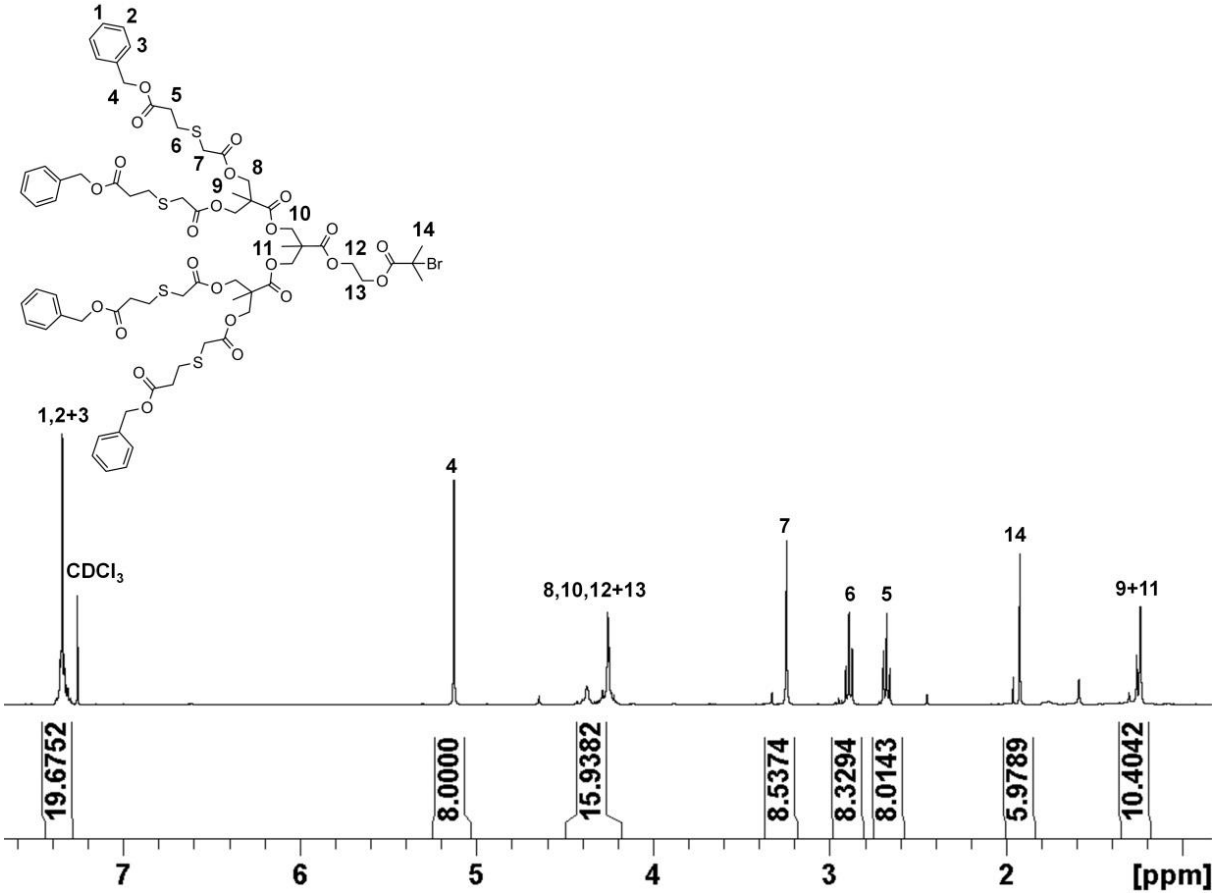

Figure 5.11 ^{1}H NMR (400MHz, $CDCl_3$) of **[$(Bz)_4$-G_2-BiB];[133]**

Appearance of a new singlet at 1.92 ppm, Figures 5.11 and 5.12, confirmed the presence of the 2-bromoisobutyrate moiety. Analysis of the ^{13}C NMR spectrum for **[$(Bz)_4$-G_2-BiB];[133]** resulted in the expected number of twenty five different carbon environments, including five different ester carbonyl environments between 169-172 ppm, Figure S5.27. ESI-MS confirmed a population at 1527 Da (MNa^+ = 1527 Da) and an adduct at 1585 Da (an increase in approximately 80 Da) indicating the presence of **[$(Bz)_4$-G_2-BiB];[133]**, Figure 5.11. The ^{13}C NMR spectrum of [(**$(Mp)_4$-G_2-BiB];[134]** displayed the expected number of twenty three different carbon environments, Figure S5.28. ESI-MS

confirmed populations at 1651 Da (MH^+ = 1651 Da), 1673 Da (MK^+ = 1673 Da) and an adduct at 1733 Da (an increase in approximately 80 Da), Figure 5.12.

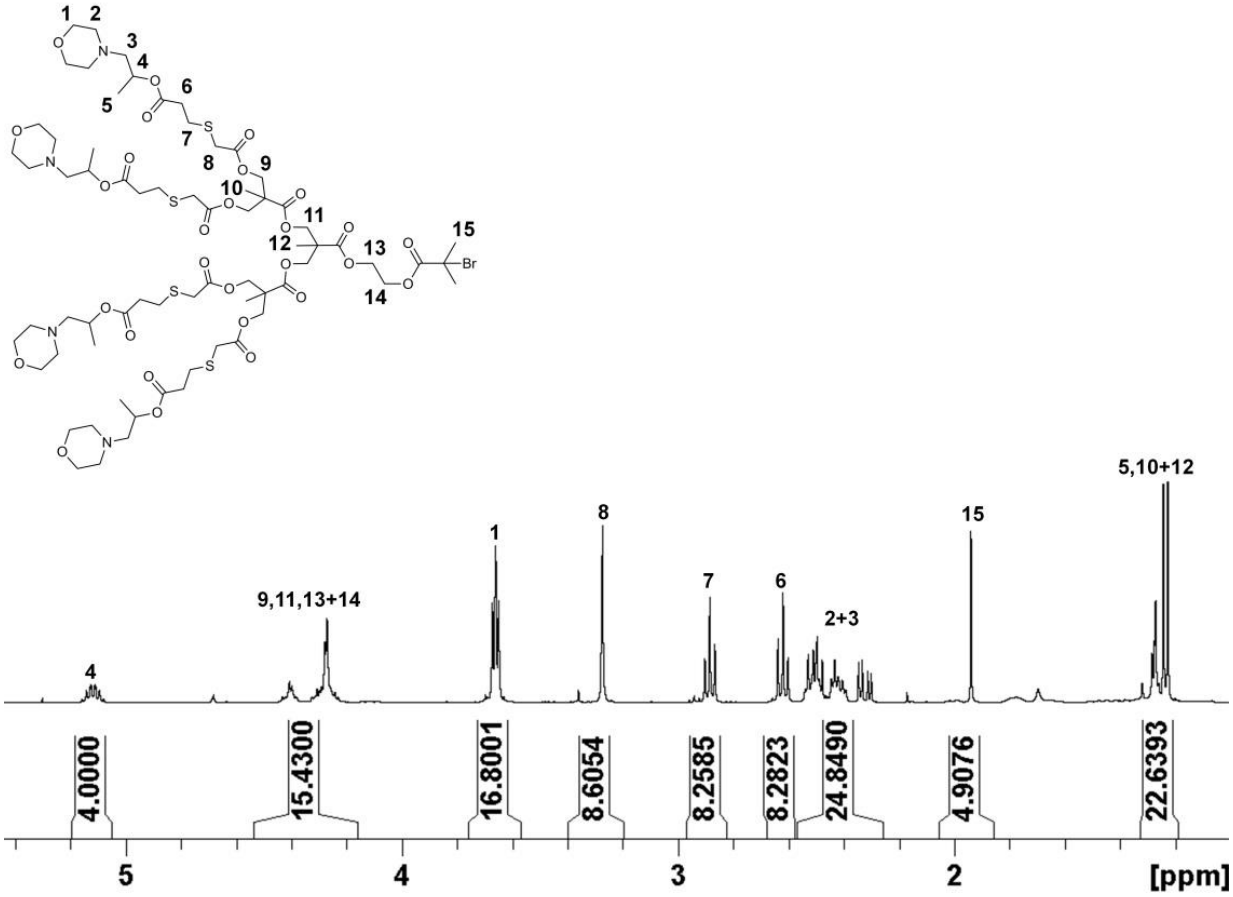

Figure 5.12 ^{1}H NMR (400MHz, $CDCl_3$) of **[$(Mp)_4$-G_2-BiB];[134]**

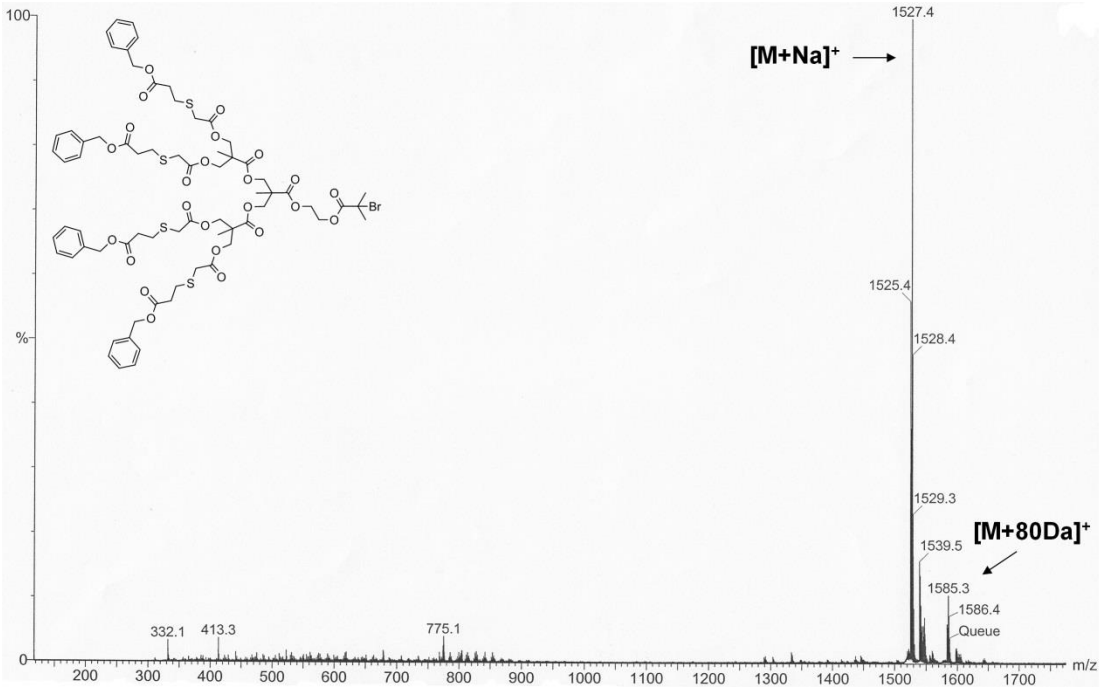

Figure 5.13 ESI-MS (MeOH) spectrum of **[$(Bz)_4$-G_2-BiB];[133]**

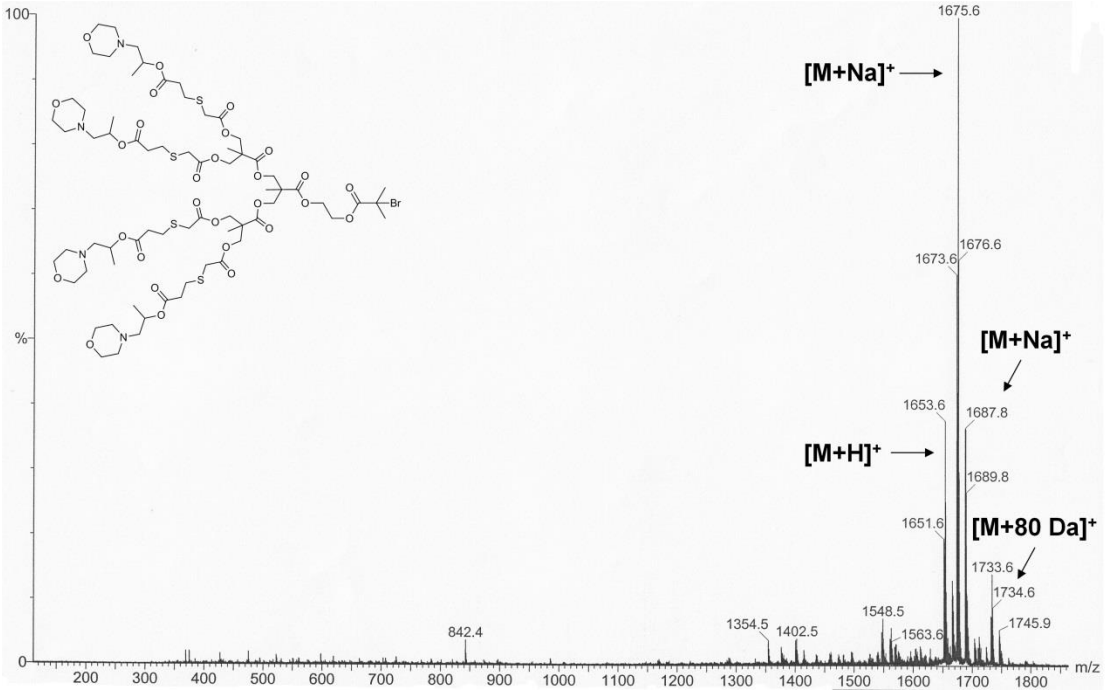

Figure 5.14 ESI-MS (MeOH) spectrum of **[$(Mp)_4$-G_2-BiB];[134]**

5.5 Synthesis of polymeric surfactants

5.5.1 Synthesis and characterisation of LDHs

The polymerisation of the commercially available hydrophilic monomer OEGMA with a DP_n = 7-8 monomer units (M_n = 300 Da) by ATRP has been previously reported under mixed isopropanol/water (92.5/7.5% v/v) solvent conditions at ambient temperature.[8] The target within this section of the research was to utilise the G_1 and G_2 initiators (**[127], [128]**, **[133]** and **[134]**) to polymerise OEGMA to a target DP_n = 80 monomer units. Similar conditions were employed using CuCl(I) and 2,2'-bypyridyl (bpy) as the catalytic system, and isopropanol/water (92.5/7.5 v/v) as the reaction solvent, at a concentration of 50% w/v, (monomer/solvent), Scheme 5.5.

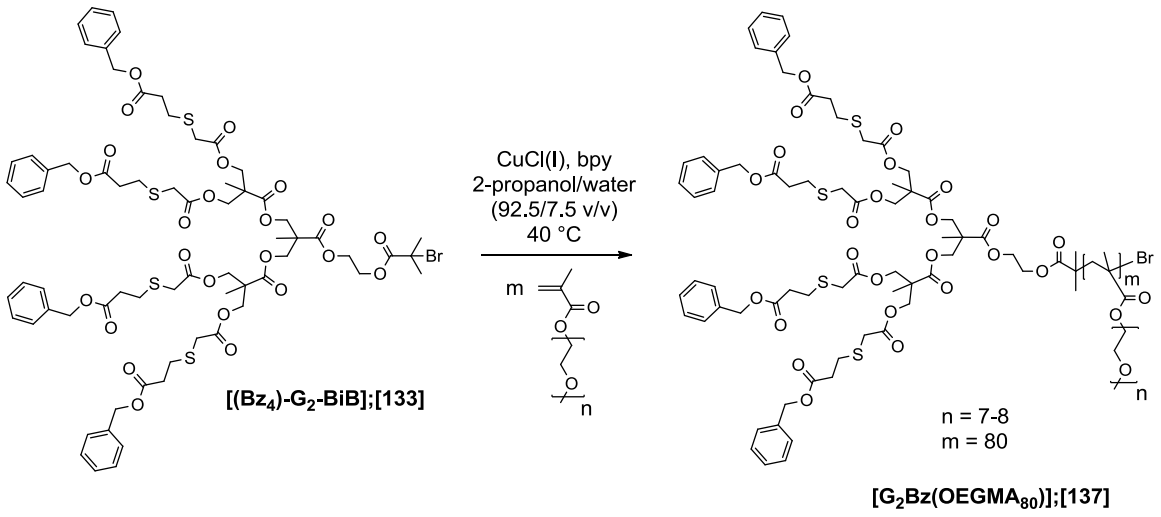

Scheme 5.5 Synthesis of LDH **[G_2Bz(OEGMA$_{80}$)];[137]** using OEGMA and **[(Bz)$_4$-G_2-BiB];[133]** under alcoholic ATRP conditions

In a typical LDH synthesis, targeting DP_n = 80 monomer units, the OEGMA monomer, dendritic initiator, isopropanol/water solvent and bpy were stirred in an oven-dried 10 mL round bottom flask and deoxygenated using a nitrogen purge for 10 minutes. Cu(I)Cl was added to the flask whilst maintaining a positive flow of nitrogen, and the targeted LDH was left to polymerise at 40 °C.

The reactions were terminated by exposure to oxygen and addition of acetone when conversion reached >85% as determined by the OEGMA vinyl resonances at 5.63 ppm and 6.08 ppm by ^{1}H NMR

spectroscopy. Dowex Marathon exchange beads (approx. 2 g) were added to remove the catalytic system, followed by precipitation of the crude polymer once into petroleum ether (40-60 °C) which was cooled using an ice bath. Polymers were dried under high vacuum for approximately one hour. Characterisation of LDHs was achieved by both ^{1}H NMR spectroscopy and triple detection size exclusion chromatography (SEC), Table 5.1.

Table 5.1 Characterisation of LDHs employing G_1 and G_2 initiators **[127], [128]**, **[133]** and **[134]** synthesised under alcoholic ATRP conditions

Target Polymer; Entry #	Time (hrs.)	Conv.[b] (%)	SEC[a] (THF) Target M_n (Da)	M_n (Da)	M_w (Da)	$Đ$	Calc. DP_n SEC	^{1}H NMR[b]
[G_1Bz(OEGMA$_{80}$)];[135]	10	91	24800	34100	66300	1.95	111	108
[G_1Mp(OEGMA$_{80}$)];[136]	12.5	97	24900	50200	108200	2.16	164	-
[G_2Bz(OEGMA$_{80}$)];[137]	18	96	25500	52700	97400	1.85	171	150
[G_2Mp(OEGMA$_{80}$)];[138]	29	87	25700	58200	107100	1.84	188	-

[a] Triple detection SEC. [b] Calculated from ^{1}H NMR spectra ($(CD_3)_2CO$).

Polymer M_n values of < 60 kDa and dispersity (Đ) values of < 2.2 were obtained, as determined by SEC. In all cases, higher than expected Đ values were obtained, with significant shoulders and chromatogram broadening in the refractive index detector (RI) and right angle light scattering (RALS) detector signals for polymers **[135]-[138]**, particularly evident for LDH **[G_1Mp(OEGMA$_{80}$)];[136]**, Figure 5.15.

LDH **[G_1Mp(OEGMA$_{80}$)];[136]** was repeated and terminated after 10 hours, leading to a lower conversion of 80%. Analysis of the resulting polymer by SEC led to a significantly lower Đ equal to 1.53 (M_n = 29906 Da; M_w = 45719), which suggested that the high Đ values for LDHs **[135]-[138]**, were due to loss of control through termination by disproptionation at high conversion. However, since an accurate comparison between LDH materials and HPD materials was required, (i.e. a target DP_n of 80 monomer units) it was decided to target higher conversion polymers, at the expensive of high Đ (i.e. >1.5).

Bz functional LDHs, [**135]** and **[137]** were analysed by ^{1}H NMR spectroscopy. Initiator Bz resonances at 5.18 ppm (OCH_2) and 7.35 ppm (Bz) were used to calculate the DP_n, relative to the

pendant OEGMA monomethyl resonances at 3.34 ppm. No initiator resonances could be observed for the Mp functional LDHs **[136]** and **[138]** by ^{1}H NMR spectroscopy.

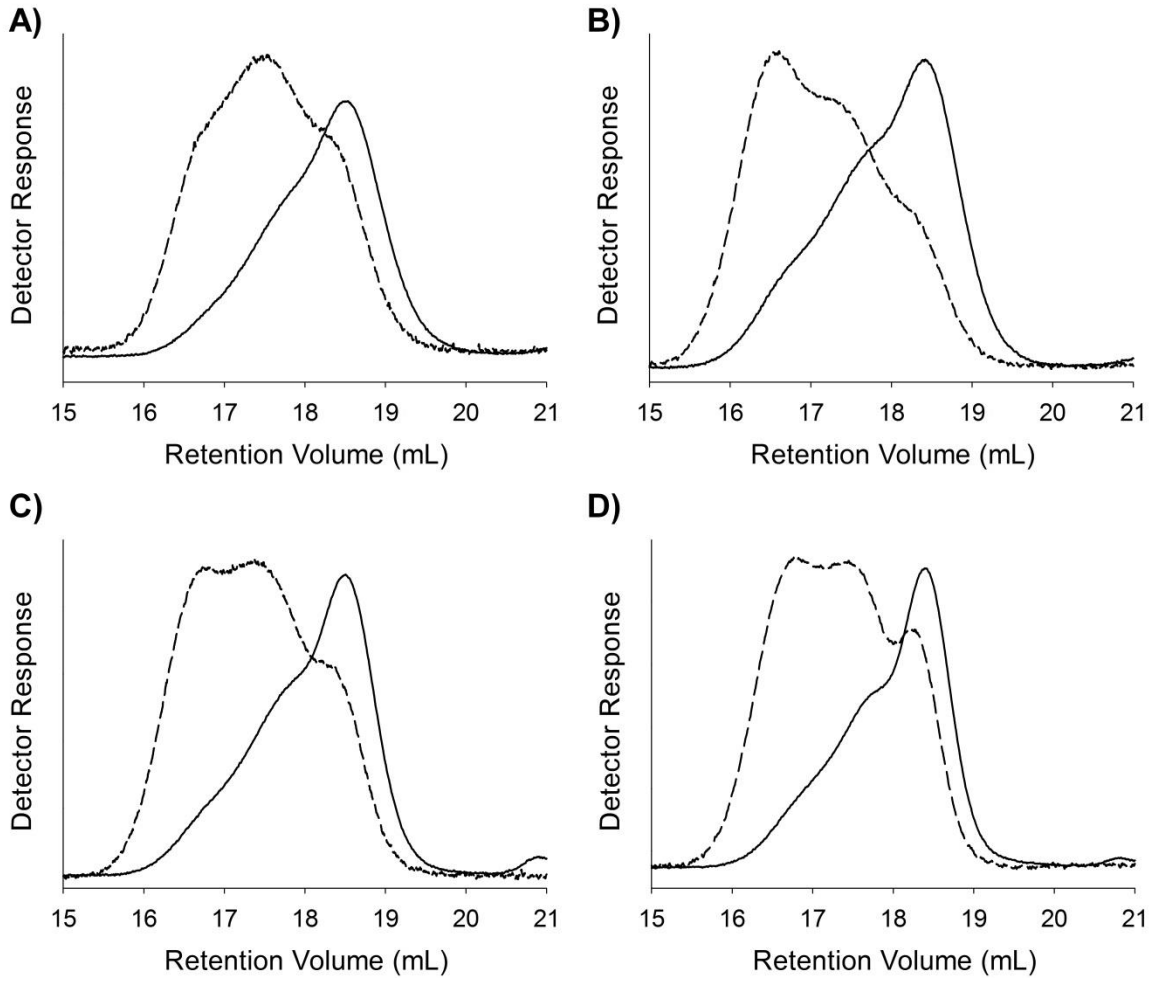

Figure 5.15 Triple detection SEC chromatograms of; (A) **[G_1Bz(OEGMA$_{80}$)];[135]**; (B) **[G_1Mp(OEGMA$_{80}$)];[136]**; (C) **[G_2Bz(OEGMA$_{80}$)];[137]**; (D) **G_2Mp(OEGMA$_{80}$)];[138]**. The figure shows the refractive index (RI) detector response (solid lines) and the right angle light scattering (RALS) detector response (dotted lines).

DP_n calculated using ^{1}H NMR spectroscopy was found to be in agreement with DP_n calculated by SEC for **[135]**. In contrast, a slightly lower DP_n calculated by ^{1}H NMR spectroscopy was found relative to DP_n calculated by SEC for **[137]**. This may suggest the presence of residual initiator within LDH **[137]**, which is also supported by the variation in M_n analysed by SEC between LDH **[135]** and **[137]**, suggesting reduced initiator efficiency. Further variations of the obtained M_n and Đ values by

SEC suggested differing initiator efficiencies, with initiator **[(Bz)$_2$-G$_1$-BiB];[127]** appearing to be the most efficient.

5.5.2 Synthesis and characterisation of HPDs

The synthesis of HPDs involved the polymerisation of a mixture containing a monofunctional monomer and a low concentration of bifunctional monomer. G_1 and G_2 initiators (**[127], [128]**, **[133]** and **[134]**) were utilised to initiate the polymerisation of OEGMA in the presence of the branching monomer ethylene glycol dimethacrylate (EGDMA). A target DP_n of 80 monomer units for the primary OEGMA chains combined with an initiator:brancher ratio of 1:0.9 was used when polymerising via the G_1 initiators **[127]** and **[128]** and an initiator:brancher ratio of 1:0.8 was used when utilising the G_2 initiators **[133]** and **[134]**, Scheme 5.6.

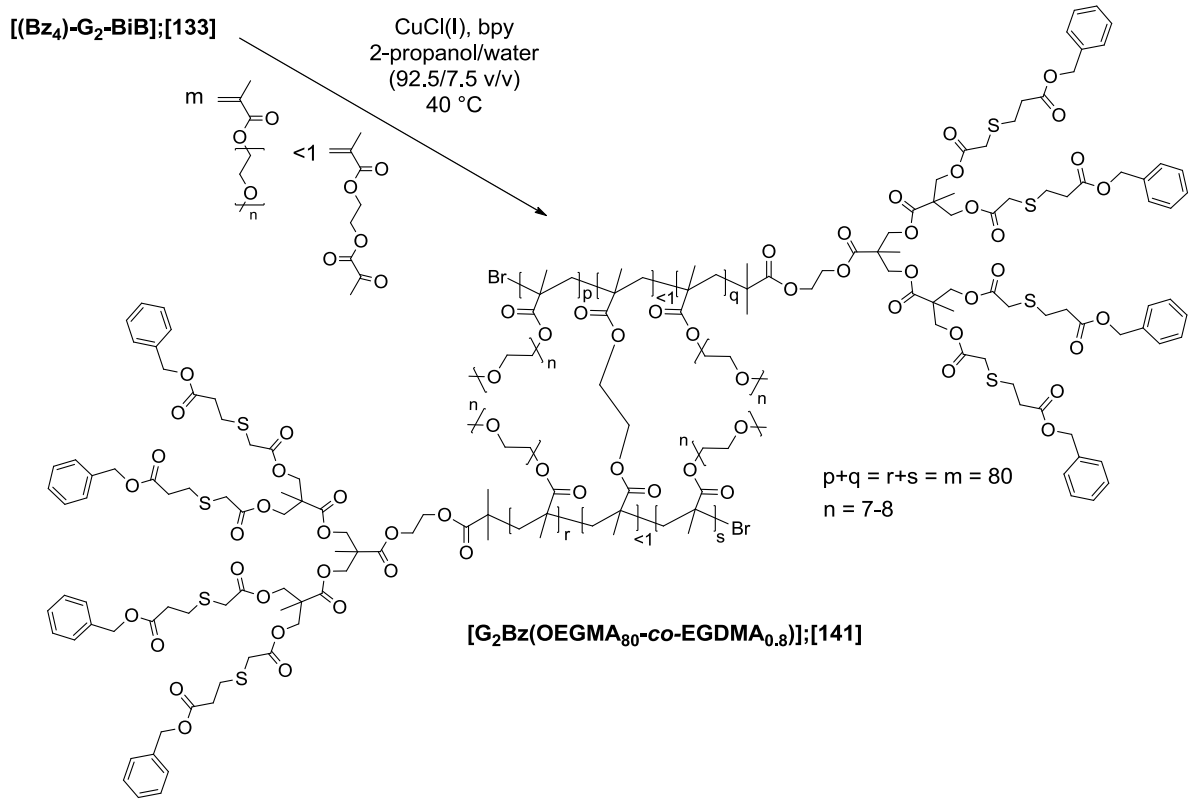

Scheme 5.6 Synthesis of HPD [**G$_2$Bz(OEGMA$_{80}$-*co*-EGDMA$_{0.8}$)];[141]** using OEGMA, **[(Bz)$_4$-G$_2$-BiB];[133]** and statistically linked EGDMA units under alcoholic ATRP conditions

The lower brancher concentration was used with the G_2 initiators, to avoid gelation, since reduced initiation efficiency was shown when synthesising LDHs earlier, Table 5.1.

In a typical polymerisation, targeting primary chains of a DP_n = 80 monomer units, the OEGMA monomer, EGDMA, dendritic initiator, isopropanol/water solvent and bpy were stirred in an oven dried 10 mL round bottom flask and deoxygenated using a nitrogen purge for 10 minutes. Cu(I)Cl was added to the flask whilst maintaining a positive flow of nitrogen, and the targeted HPD was left to polymerise at 40 °C. The mixtures became very viscous at conversions >90% (good indication of branching occurring), and the reactions were terminated when conversion reached >95% as determined by the OEGMA vinyl resonances at approximately 5.63 ppm and 6.08 ppm using ^{1}H NMR spectroscopy.

Workup was achieved by using the same methodology as the LDH materials, by addition of Dowex Marathon exchange beads (approx. 2 g) to remove the catalytic system, followed by precipitation of the crude polymer once into petroleum ether (40-60 °C) cooled using an ice bath. Polymers were dried under high vacuum for approximately one hour.

Table 5.2 Characterisation of HPDs using initiators [**127], [128]**, **[133]** and **[134]** under alcoholic ATRP conditions

Target Polymer; Entry #	Conv.[b] (%)	Time (hrs.)	SEC[a] (THF) M_n (Da)	SEC[a] (THF) M_w (Da)	SEC[a] (THF) $Đ$	Calc. DP_n SEC	Calc. DP_n ^{1}H NMR[b]
[G_1Bz(OEGMA$_{80}$-*co*-EGDMA$_{0.9}$)];[139]	99	18	204700	1478000	7.22	-	93
[G_1Mp(OEGMA$_{80}$-*co*-EGDMA$_{0.9}$)];[140]	98	18	661500	1800000	2.72	-	-
[G_2Bz(OEGMA$_{80}$-*co*-EGDMA$_{0.8}$)];[141]	99	39	680000	2603000	3.83	-	147
[G_2Mp(OEGMA$_{80}$-*co*-EGDMA$_{0.8}$)];[142]	95	26	224500	1371000	6.11	-	-

[a] Triple detection SEC. [b] Calculated from ^{1}H NMR spectra ($(CD_3)_2CO$).

In all cases, the presence of 0.8 or 0.9 equivalents of EGDMA with respect to the dendritic initiator led to dramatic increase in the observed M_n, M_w and dispersities of the resulting polymers by SEC, Table 5.2.

Weight average molecular weights as high as 1.80 MDa were observed for the G_1 initiated HPDs, and 2.60 MDa for G_2 initiated HPDs. It was also evident from the SEC chromatograms that materials of significantly higher molecular weights were present, in contrast to the LDH materials, Figure 5.16. ^{1}H NMR analysis of the precipitated Bz HPDs **[139]** and **[141]** allowed a determination of the DP_n of the primary OEGMA polymer chains. The targeted number average chain length of 80 monomer units and that determined by ^{1}H NMR spectroscopy were significantly different, but comparable to the chain lengths determined by ^{1}H NMR spectroscopy of the LDHs, Table 5.1.

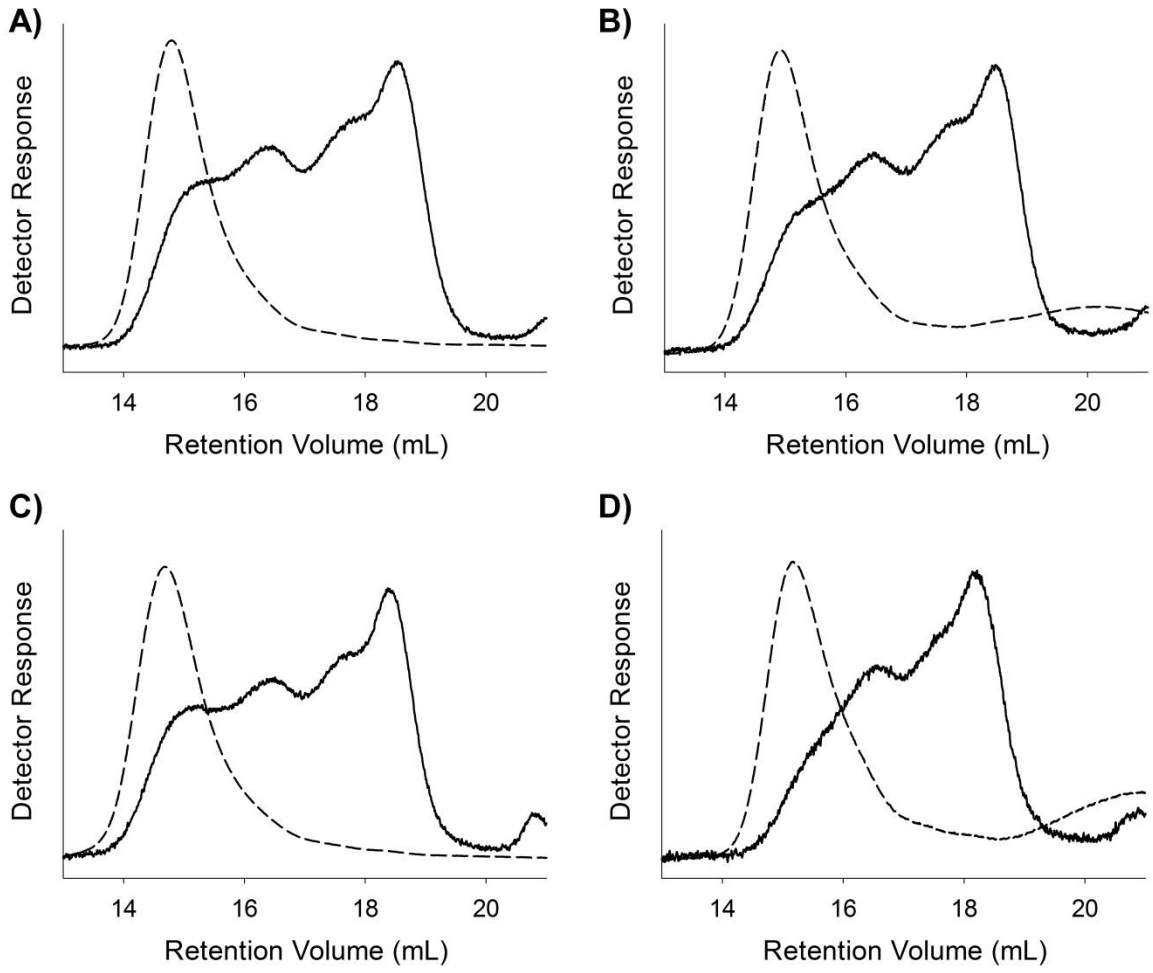

Figure 5.16 Triple detection SEC chromatogram of; (A) **[G_1Bz(OEGMA$_{80}$-*co*-EGDMA$_{0.9}$)];[139]**; (B) **[G_1Mp(OEGMA$_{80}$-*co*-EGDMA$_{0.9}$)];[140]**; (C) **[G_2Bz(OEGMA$_{80}$-*co*-EGDMA$_{0.8}$)];[141]**; (D) **[G_2Mp(OEGMA$_{80}$-*co*-EGDMA$_{0.8}$)];[142]**. The figure shows the refractive index (RI) detector response (solid lines) and the right angle light scattering (RALS) detector response (dotted lines)

5.5.3 Synthesis and characterisation of mixed initiated LDHs

In order to assess the effect of the dendritic end group on the properties of the polymeric surfactant, a mixed initiator system was utilised, targeting LDHs which comprised both dendritic and non-dendritic end group functionalities. These materials were synthesised to ensure that a mixed initiator systems did not lead to complications, such as initiator – initiator interference, and that comparisons of polymeric surfactants comprised of mixed initiated LDHs could be made between polymeric surfactants comprised of HPDs. For example, does a polymeric surfactant comprised of a mixed initiated LDH stabilise an emulsion in the same way as a polymeric surfactant comprised of an HPD architecture?

Dodecyl bromisobutyrate **[DBiB];[143]** has been recently shown to effectivity initiate the polymerisation of OEGMA,[12] and was therefore chosen as the non-dendritic initiator component. Since the oil phase used during the emulsion studies is dodecane (see later), a dodecyl chain end also seemed reasonable as a potential hydrophobic stabilising group. The **[DBiB];[143]** initiator was synthesised by an undergraduate research student within our research group,[12] and analysis of the compound using ^{1}H and ^{13}C NMR, and mass spectrometry was found to be as expected, Figures S5.29, S5.30 and S5.31.

The synthesis of a mixed initiated LDH involved initiating the polymerisation of OEGMA using two initiators at the same time. **[DBiB];[143]** and dendritic initiators (**[127], [128]**, **[133]** and **[134]**) were utilised to initiate the polymerisation of OEGMA, targeting a DP_n of 80 monomer units for the primary OEGMA chains, combined with a dendritic initiator:**[DBiB];[143]** ratio of 0.5:0.5, Scheme 5.7. As a comparable standard to a mixed initiated LDH, a linear polymer initiated by **[DBiB];[143]** comprised of 100% dodecyl end groups was also synthesised. The polymerisation and workup procedures were identical to the synthesis of LDHs, with the exception of the required quantity of **[DBiB];[143]** added to the reaction vessel prior to deoxygenation.

Significant loss of control was again evident indicated by the significantly high dispersities (>1.5) and broad SEC chromatograms, due to targeting high monomer conversions, Figure 5.17.

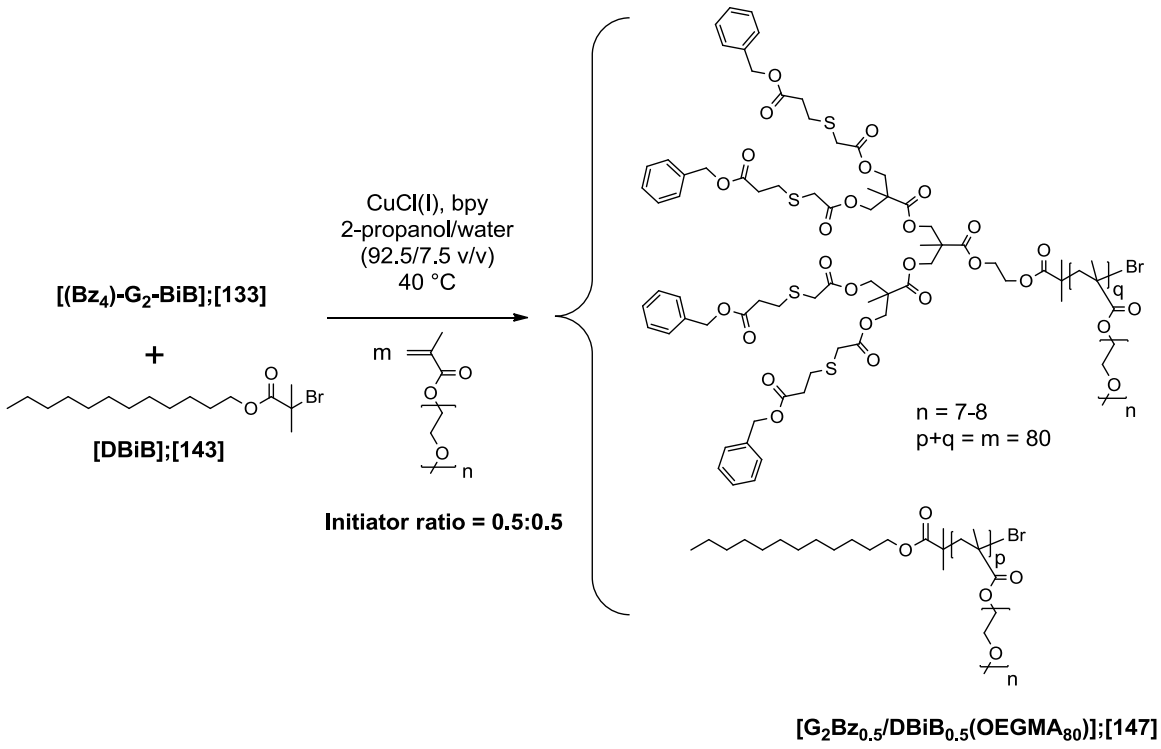

Scheme 5.7 Synthesis of mixed initiated LDH **[$G_2Bz_{0.5}$/$DBiB_{0.5}$($OEGMA_{80}$)]; [147]** using **[$(Bz)_4$-G_2-BiB];[133]** and **[DBiB];[143]** under alcoholic ATRP conditions

However, analysis of M_n, M_w and dispersity by SEC under mixed initiated LDH conditions, Table 5.3, were found to be in good agreement with the M_n, M_w and dispersity analysed by SEC from singularly initiated LDHs, Table 5.1, suggesting no negative impact of the presence of two initiators.

Unfortunately, analysis of the actual % compositions of the dendritic to non-dendritic ends groups within the purified mixed initiated LDHs, **[145]-[148]** could not be conducted by ^{1}H NMR spectroscopy, since the non-dendritic dodecyl resonances were obstructed by the poly(OEGMA) backbone resonances. This was further complicated for Mp mixed initiated LDHs, since the Mp resonances by ^{1}H NMR spectroscopy were not observed either.

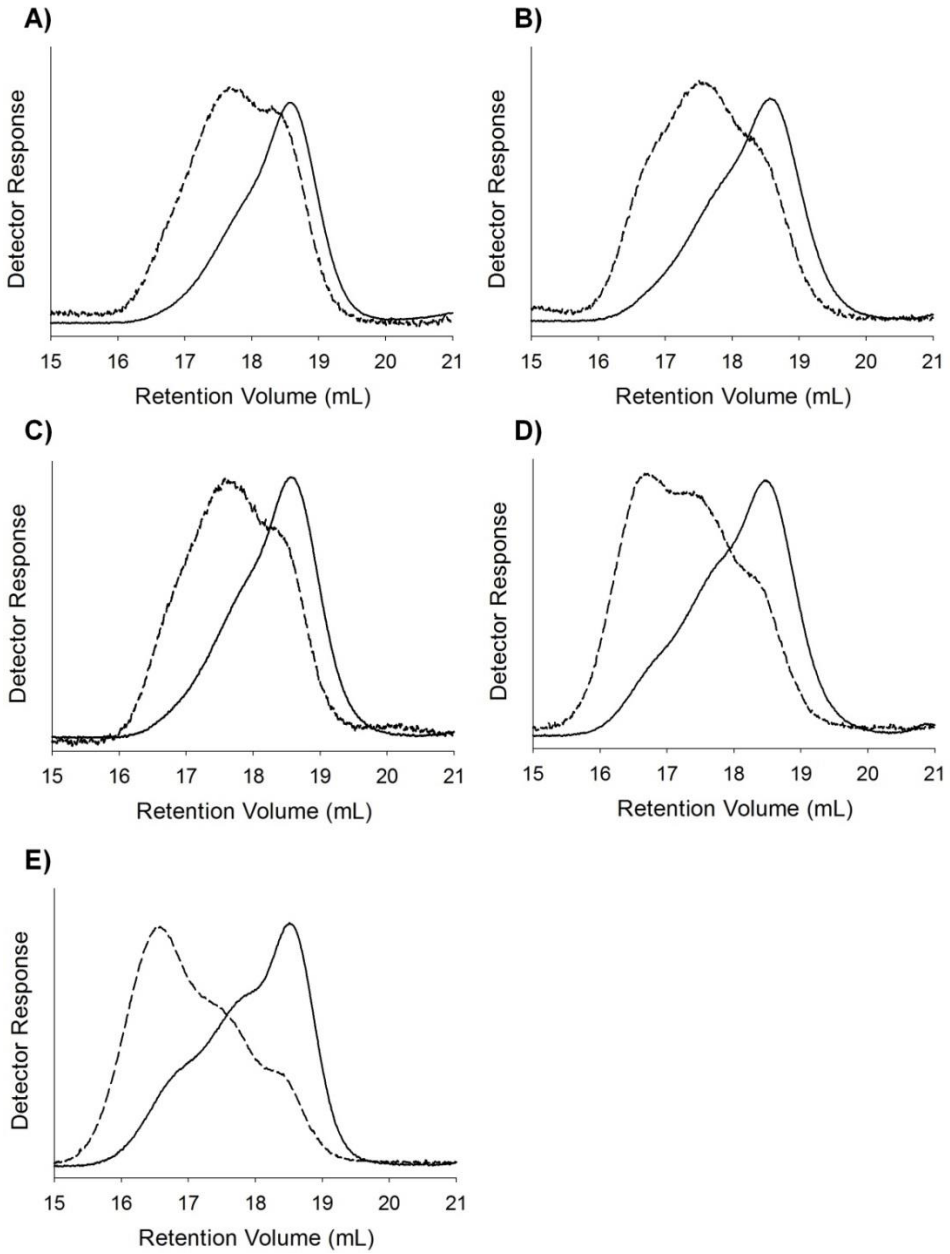

Figure 5.17 Triple detection SEC chromatograms of; (A) **[DBiB(OEGMA$_{80}$)];[144]**; (B) **[G$_1$Bz$_{0.5}$/DBiB$_{0.5}$(OEGMA$_{80}$)];[145]**; (C) **[G$_1$Mp$_{0.5}$/DBiB$_{0.5}$(OEGMA$_{80}$)];[146]**; (D) **[G$_2$Bz$_{0.5}$/DBiB$_{0.5}$(OEGMA$_{80}$)];[147]**; E) **[G$_2$Mp$_{0.5}$/DBiB$_{0.5}$(OEGMA$_{80}$)];[148]**. The figure shows the refractive index (RI) detector response (solid lines) and the right angle light scattering (RALS) detector response (dotted lines).

5.5.4 Synthesis and characterisation of mixed initiated HPDs

[DBiB];[143] was used to synthesise mixed initiated HPDs comprised of both dendritic and non-dendritic end group functionalities. **[DBiB];[143]** and dendritic initiators (**[127], [128]**, **[133]** and **[134]**) were utilised to initiate the copolymerisation of OEGMA and EGDMA, targeting a DP_n of 80 monomer units for the primary OEGMA chains, combined with dendritic initiator:DBiB ratios of 0.75:0.25; 0.5:0.5 and 0.25:0.75, Again, an initiator:brancher ratio of 1:0.9 was employed when using the G_1 initiators **[127]** and **[128]** and an initiator:brancher ratio of 1:0.8 was utilised when using the G_2 initiators **[133]** and **[134]**.

As a comparable standard to a mixed initiated HPD, a branched polymer initiated by **[DBiB];[143]** comprised of 100% dodecyl end groups was also synthesised. The polymerisation and workup procedures were identical to the synthesis of HPDs, with the exception of the required quantity of **[DBiB];[143]** added to the reaction vessel prior to deoxygenation. Characterisation of the resulting polymers was obtained by using SEC, Table 5.4. Again comparable to the LDH materials (Tables 5.1 and 5.3), the presence of 0.8 or 0.9 equivalents of EGDMA led to a dramatic increase in the observed M_n, M_w and dispersities of the resulting polymers by SEC, Table 5.4. M_w values as high as 2.56 MDa were observed for the mixed G_1/DBiB initiated HPDs, and 1.89 MDa for the mixed G_2/DBiB initiated HPDs. SEC chromatograms are shown for the branched polymer **[143]** comprised of 100% dodecyl end groups, and mixed initiated HPDs, **[156]**, **[157]** and **[158]**, Figure 5.18.

Table 5.3 Characterisation of mixed initiated LDHs under alcoholic ATRP conditions

Target Polymer; Entry #	Target composition (equivalents)		Conv.[b]	Time	SEC[a] (THF)		
	Dendritic initiator	DBiB	(%)	(hrs.)	M_n (Da)	M_w (Da)	$Đ$
[DBiB(OEGMA$_{80}$)];[144]	-	1.0	85	10	29000	51200	1.77
[G$_1$Bz$_{0.5}$/DBiB$_{0.5}$(OEGMA$_{80}$)];[145]	0.5	0.5	93	10	30900	60900	1.97
[G$_1$Mp$_{0.5}$/DBiB$_{0.5}$(OEGMA$_{80}$)];[146]	0.5	0.5	90	10	36500	64500	1.77
[G$_2$Bz$_{0.5}$/DBiB$_{0.5}$(OEGMA$_{80}$)];[147]	0.5	0.5	97	18	51900	109200	2.10
[G$_2$Mp$_{0.5}$/DBiB$_{0.5}$(OEGMA$_{80}$)];[148]	0.5	0.5	98	26	57100	132100	2.31

[a] Triple detection SEC. [b] Calculated from ^{1}H NMR spectra ($(CD_3)_2CO$).

Table 5.4 Characterisation of mixed initiated HPDs under alcoholic ATRP conditions

Target Polymer; Entry #	Target composition (equivalents)		Conv.[b]	Time	SEC[a] (THF)		
	Dendritic initiator	DBiB	(%)	(hrs.)	M_n (Da)	M_w (Da)	$Đ$
[DBiB(OEGMA$_{80}$-*co*-EGDMA$_{0.9}$)];[149]	-	1.0	98	19	110726	913363	8.25
[G$_1$Bz$_{0.25}$/DBiB$_{0.75}$(OEGMA$_{80}$-*co*-EGDMA$_{0.9}$)];[150]	0.25	0.75	97	18	108028	792733	7.34
[G$_1$Bz$_{0.5}$/DBiB$_{0.5}$(OEGMA$_{80}$-*co*-EGDMA$_{0.9}$)];[151]	0.5	0.5	96	18	64178	373783	5.82
[G$_1$Bz$_{0.75}$/DBiB$_{0.25}$(OEGMA$_{80}$-*co*-EGDMA$_{0.9}$)];[152]	0.75	0.25	99	18	845722	2565000	3.03
[G$_1$Mp$_{0.25}$/DBiB$_{0.75}$(OEGMA$_{80}$-*co*-EGDMA$_{0.9}$)];[153]	0.25	0.75	97	18	210839	1164000	5.52
[G$_1$Mp$_{0.5}$/DBiB$_{0.5}$(OEGMA$_{80}$-*co*-EGDMA$_{0.9}$)];[154]	0.50	0.50	98	19	357850	1427000	3.99
[G$_1$Mp$_{0.75}$/DBiB$_{0.25}$(OEGMA$_{80}$-*co*-EGDMA$_{0.9}$)];[155]	0.75	0.25	96	18	69103	497405	7.20
[G$_2$Bz$_{0.25}$/DBiB$_{0.75}$(OEGMA$_{80}$-*co*-EGDMA$_{0.8}$)];[156]	0.25	0.75	98	24	72386	840564	11.6
[G$_2$Bz$_{0.5}$/DBiB$_{0.5}$(OEGMA$_{80}$-*co*-EGDMA$_{0.8}$)];[157]	0.5	0.5	97	24	61659	709537	11.5
[G$_2$Bz$_{0.75}$/DBiB$_{0.25}$(OEGMA$_{80}$-*co*-EGDMA$_{0.8}$)];[158]	0.75	0.25	98	39	332756	1892000	5.69
[G$_2$Mp$_{0.25}$/DBiB$_{0.75}$(OEGMA$_{80}$-*co*-EGDMA$_{0.8}$)];[159]	0.25	0.75	96	34	70647	492415	6.97
[G$_2$Mp$_{0.5}$/DBiB$_{0.5}$(OEGMA$_{80}$-*co*-EGDMA$_{0.8}$)];[160]	0.50	0.50	96	50	136353	1013000	7.43
[G$_2$Mp$_{0.75}$/DBiB$_{0.25}$(OEGMA$_{80}$-*co*-EGDMA$_{0.8}$)];[161]	0.75	0.25	96	50	136495	844575	6.19

[a] Triple detection SEC. [b] Calculated from ^{1}H NMR spectra ($(CD_3)_2CO$).

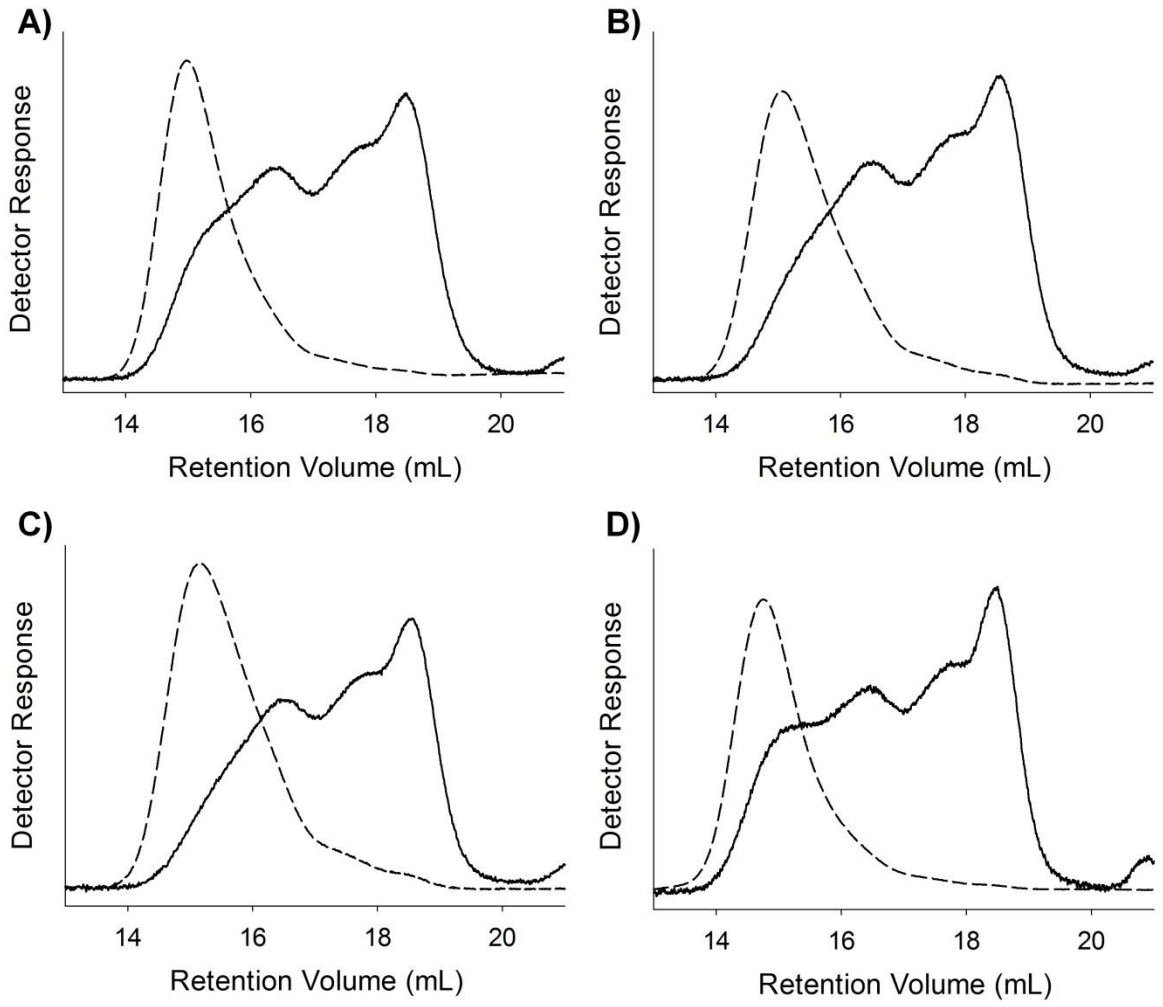

Figure 5.18 Triple detection SEC chromatograms of; (A) **[DBiB(OEGMA$_{80}$-*co*-EGDMA$_{0.9}$)];[149]**; B) **[G$_2$Bz$_{0.25}$/DBiB$_{0.75}$(OEGMA$_{80}$-*co*-EGDMA$_{0.8}$)];[156]**; (C) **[G$_2$Bz$_{0.5}$/DBiB$_{0.5}$(OEGMA$_{80}$-*co*-EGDMA$_{0.8}$)];[157]**; (D) **[G$_2$Bz$_{0.75}$/DBiB$_{0.25}$(OEGMA$_{80}$-*co*-EGDMA$_{0.8}$)];[158]**. The figure shows the refractive index (RI) detector response (solid lines) and the right angle light scattering (RALS) detector response (dotted lines).

5.6 Oil-in-Water emulsions stabilised by LDHs and HPDs

To form o/w emulsions, aqueous solutions (3 mL) of each of the synthesised polymeric surfactants **[135]-[142]**, **[144-161]** (2.5 mg/mL), were homogenised for two minutes (24,000 revolutions per minute (rpm)) with 3 mL of dodecane. The emulsions were left to equilibrate for 1 day before any measurements were taken. Emulsion droplet sizes were measured using laser diffraction, and selected samples were measured by optical microscopy.

5.6.1 Long term stability of emulsions at natural pH

A long term stability study of the o/w emulsions was performed over a 50 day period. 3 separate emulsion samples were prepared using each emulsifier to enable the standard deviation between samples to be measured. The distilled water used to prepare the aqueous polymer solution was pH 7.37. Each polymer resulted in a dodecane o/w emulsion, confirmed by the addition of an emulsion sample (100 µL) to a large volume of water (100 mL) resulting in the sample being dispersed as it was diluted in the water phase.

5.6.1.1 Emulsions stabilised by a linear polymer, LDHs or linear polymer/LDH surfactant

Dodecane o/w emulsions stabilised using a linear polymer, LDHs or a linear polymer/LDH mixture (**E1-E9**), Table 5.5, showed coalescence over the 50 day period, presumably due to a weak interaction with dodecane droplet surfaces via a single dendritic or non-dendritic hydrophobic chain end. The amount of phase separated oil was very difficult to measure, and indistinguishable between emulsion samples (**E1-E9**) but, as an estimate, an approximate 0.5 mm layer was present at the surface of the total emulsion sample (20 mm in length), Figure 5.19. It was also apparent, that no effect of changing the size, composition or type of dendritic component was observed in the stability of the emulsion, confirmed by no significant differences in the amount of oil present between different emulsion samples (**E1-E9**).

Table 5.5 Table of emulsions stabilised by a linear polymer, LDH or linear polymer/LDH mixture surfactant, showing volume-average diameter (D[4,3]) at t=0 after equilibration, and the presence of phase separated oil after a 50 day time period.

Polymer; Entry #	Dendritic equiv.	Emulsion #	D[4,3] at t=1 day (μm)[a]	Oil after 50 days[b]
[DBiB(OEGMA$_{80}$)];[144]	-	**E1**	13.96 ± 0.51	Y
[G$_1$Bz$_{0.5}$/DBiB$_{0.5}$(OEGMA$_{80}$)];[145]	0.5	**E2**	15.46 ± 1.63	Y
[G$_1$Bz(OEGMA$_{80}$)];[135]	1.0	**E3**	15.63 ± 1.33	Y
[G$_1$Mp$_{0.5}$/DBiB$_{0.5}$(OEGMA$_{80}$)];[146]	0.5	**E4**	14.58 ± 1.24	Y
[G$_1$Mp(OEGMA$_{80}$)];[136]	1.0	**E5**	13.19 ± 0.48	Y
[G$_2$Bz$_{0.5}$/DBiB$_{0.5}$(OEGMA$_{80}$)];[147]	0.5	**E6**	15.44 ± 0.33	Y
[G$_2$Bz(OEGMA$_{80}$)];[137]	1.0	**E7**	15.04 ± 0.21	Y
[G$_2$Mp$_{0.5}$/DBiB$_{0.5}$(OEGMA$_{80}$)];[148]	0.5	**E8**	14.71 ± 0.18	Y
[G$_2$Mp(OEGMA$_{80}$)];[138]	1.0	**E9**	12.08 ± 0.49	Y

[a] Measured by laser diffraction after 24 hours to enable equilibration. [d] Determined by visually observing phase separation.

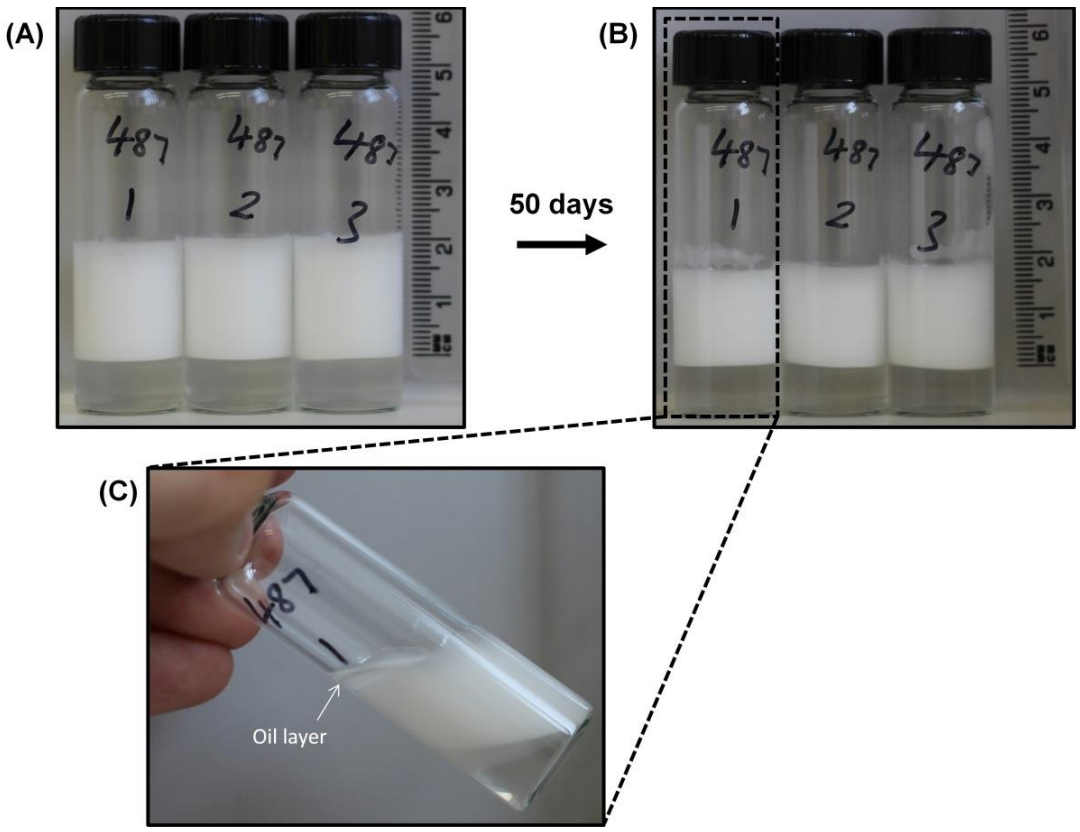

Figure 5.19 Digital images of emulsion **E3** stabilised with surfactant (**[G$_1$Bz(OEGMA$_{80}$)];[135]**); (A) t=1 day; (B) t=50 days (C); Expansion of emulsion **E3** at t=50 days, showing phase separation of oil by coalescence.

5.6.1.2 Emulsions stabilised by a branched polymer, HPDs or branched polymer/HPD surfactant

In contrast, emulsions stabilised by a branched polymer, HPD or a branched polymer/HPD surfactant showed no observable demulsification within the samples over the 50 day period (**E10-E26**), Table 5.6. A digital image shows emulsion **E14** after 50 days, Figure 5.20, stabilised by the HPD surfactant [**G_1Bz(OEGMA$_{80}$-*co*-EGDMA$_{0.9}$)];[139]**. Relative to emulsion **E3** stabilised by the equivalent LDH surfactant (**[G_1Bz(OEGMA$_{80}$)];[135]**), Figure 5.19, the emulsion **E14** showed no sign of oil phase separation.

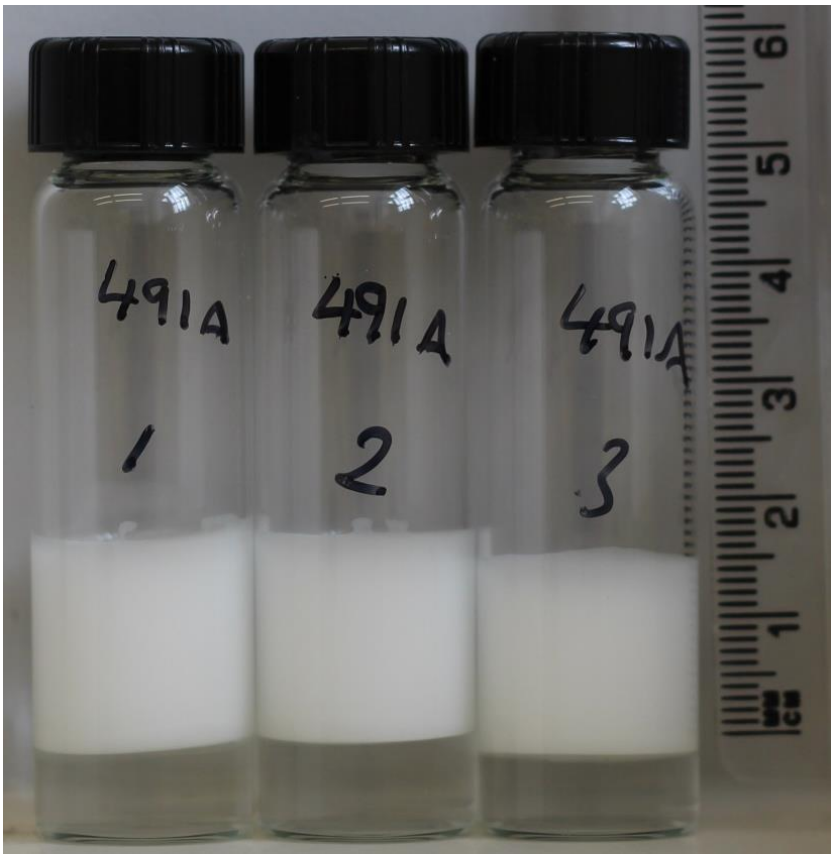

Figure 5.20 Digital image of comparable emulsion **E14** stabilised with the HPD surfactant **[G_1Bz(OEGMA$_{80}$-*co*-EGDMA$_{0.9}$)];[139]** after t=50 days, showing no phase separation of oil by coalescence.

Table 5.6 Table of emulsions stabilised by a branched polymer, HPD or a branched polymer/HPD surfactant, showing volume-average diameter D[4,3] at t=1 days after equilibration, and at t=50 days.

Polymer; Entry #	Dodecyl equiv.	Dendritic equiv.	Emulsion #	D[4,3] (μm)[a] t=1 day	D[4,3] (μm)[a] t=50 days[b]
[DBiB(OEGMA$_{80}$-*co*-EGDMA$_{0.9}$)];[149]	1.0	-	**E10**	15.35 ± 0.53	14.51 ± 1.15
[G$_1$Bz$_{0.25}$/DBiB$_{0.75}$(OEGMA$_{80}$-*co*-EGDMA$_{0.9}$)];[150]	0.75	0.25	**E11**	16.00 ± 1.38	13.54 ± 1.21
[G$_1$Bz$_{0.5}$/DBiB$_{0.5}$(OEGMA$_{80}$-*co*-EGDMA$_{0.9}$)];[151]	0.50	0.50	**E12**	14.93 ± 0.22	14.08 ± 1.56
[G$_1$Bz$_{0.75}$/DBiB$_{0.25}$(OEGMA$_{80}$-*co*-EGDMA$_{0.9}$)];[152]	0.25	0.75	**E13**	17.38 ± 1.03	17.84 ± 1.62
[G$_1$Bz(OEGMA$_{80}$-*co*-EGDMA$_{0.9}$)];[139]	-	1.0	**E14**	16.72 ± 1.16	14.83 ± 1.66
[G$_1$Mp$_{0.25}$/DBiB$_{0.75}$(OEGMA$_{80}$-*co*-EGDMA$_{0.9}$)];[153]	0.75	0.25	**E15**	16.06 ± 0.80	12.77 ± 0.48
[G$_1$Mp$_{0.5}$/DBiB$_{0.5}$(OEGMA$_{80}$-*co*-EGDMA$_{0.9}$)];[154]	0.50	0.50	**E16**	16.13 ± 0.30	16.90 ± 2.49
[G$_1$Mp$_{0.75}$/DBiB$_{0.25}$(OEGMA$_{80}$-*co*-EGDMA$_{0.9}$)];[155]	0.25	0.75	**E17**	16.54 ± 0.61	12.40 ± 1.51
[G$_1$Mp(OEGMA$_{80}$-*co*-EGDMA$_{0.9}$)];[140]	-	1.0	**E18**	16.08 ± 0.38	15.15 ± 0.52
[G$_2$Bz$_{0.25}$/DBiB$_{0.75}$(OEGMA$_{80}$-*co*-EGDMA$_{0.8}$)];[156]	0.75	0.25	**E19**	16.53 ± 0.51	15.05 ± 1.28
[G$_2$Bz$_{0.5}$/DBiB$_{0.5}$(OEGMA$_{80}$-*co*-EGDMA$_{0.8}$)];[157]	0.50	0.50	**E20**	17.05 ± 0.83	15.12 ± 0.57
[G$_2$Bz$_{0.75}$/DBiB$_{0.25}$(OEGMA$_{80}$-*co*-EGDMA$_{0.8}$)];[158]	0.25	0.75	**E21**	18.27 ± 0.33	23.12 ± 1.56
[G$_2$Bz(OEGMA$_{80}$-*co*-EGDMA$_{0.8}$)];[141]	-	1.0	**E22**	20.30 ± 0.86	18.92 ± 1.26
[G$_2$Mp$_{0.25}$/DBiB$_{0.75}$(OEGMA$_{80}$-*co*-EGDMA$_{0.8}$)];[159]	0.75	0.25	**E23**	16.45 ± 1.12	13.45 ± 0.94
[G$_2$Mp$_{0.5}$/DBiB$_{0.5}$(OEGMA$_{80}$-*co*-EGDMA$_{0.8}$)];[160]	0.50	0.50	**E24**	15.86 ± 0.47	14.96 ± 2.21
[G$_2$Mp$_{0.75}$/DBiB$_{0.25}$(OEGMA$_{80}$-*co*-EGDMA$_{0.8}$)];[161]	0.25	0.75	**E25**	16.38 ± 0.94	14.07 ± 0.48
[G$_2$Mp(OEGMA$_{80}$-*co*-EGDMA$_{0.8}$)];[142]	-	1.0	**E26**	21.21 ± 0.94	18.00 ± 0.46

[a]Emulsions were measured by laser diffraction; results based on an average of 3 separate samples, with 3 measurements per sample. Error is based on the standard deviation between the 3 separate samples. [b]Emulsions showed no phase separated oil after the 50 day period.

This remarkable difference in emulsion stabilisation between polymer surfactants of varying architecture may be due to strong adhesion of the polymers to the droplets arising from the multiple hydrophobic chain ends within the branched systems. A similar study of o/w emulsions stabilised by branched polymeric surfactants found no change to droplet size by laser diffraction, whereas the linear equivalents coalesced over several weeks.[1] As such, the remainder of this long term stability study will focus on the analysis of emulsions stabilised by a branched polymer, HPD or a branched polymer/HPD surfactant, using emulsions **E10-E26**, Table 5.6.

To provide a comparable reference to discuss the effect of introducing a dendritic component within the emulsion surfactant system emulsion **E10**, stabilised by a branched polymer containing 100% dodecyl chain ends **[DBiB(OEGMA$_{80}$-*co*-EGDMA$_{0.9}$)];[149]**, was used as the reference, unless otherwise stated. More specifically, the moment mean diameter of the emulsion droplets (D[4,3]) of **E10** (14.51 ± 1.15 μm) after 50 days was compared to emulsions **E11-E26**. A grey bar drawn horizontally in graphs A, B, C and D, Figures 5.21 and 5.22, visually highlights this reference (inclusive of standard deviation across three separate samples).

The D[4,3] of emulsions stabilised by surfactants comprising increasing increments of G_1 Bz (25, 50, 75 and 100 %) (**E11-E14**) showed no considerable change over the 50 day period, remaining the same (within error) as t=1day, Figure 5.14 (A). Within this series, emulsion **E13** stabilised by a surfactant comprising 75 % G_1 Bz end groups was slightly larger at both t=1 day and t=50 days (i.e. outside the comparable standard, **E10**, see grey bar), Figure 5.21(A).

In contrast, emulsions stabilised by surfactants comprising increasing increments of G_2 Bz (25, 50, 75 and 100 %) (**E19-E22**) differed considerably by D[4,3] at both t=1 day and t=50 days, Figure 5.21 (B). At t=0, the D[4,3] of the emulsion droplets increased almost linearly, relative to the increasing composition of G_2 Bz and removal of dodecyl composition within the polymeric surfactants. This was a particularly interesting observation, showing that at t=0, the size of emulsion droplets could be "tuned" relative to the removal of dodecyl end groups within the surfactant composition.

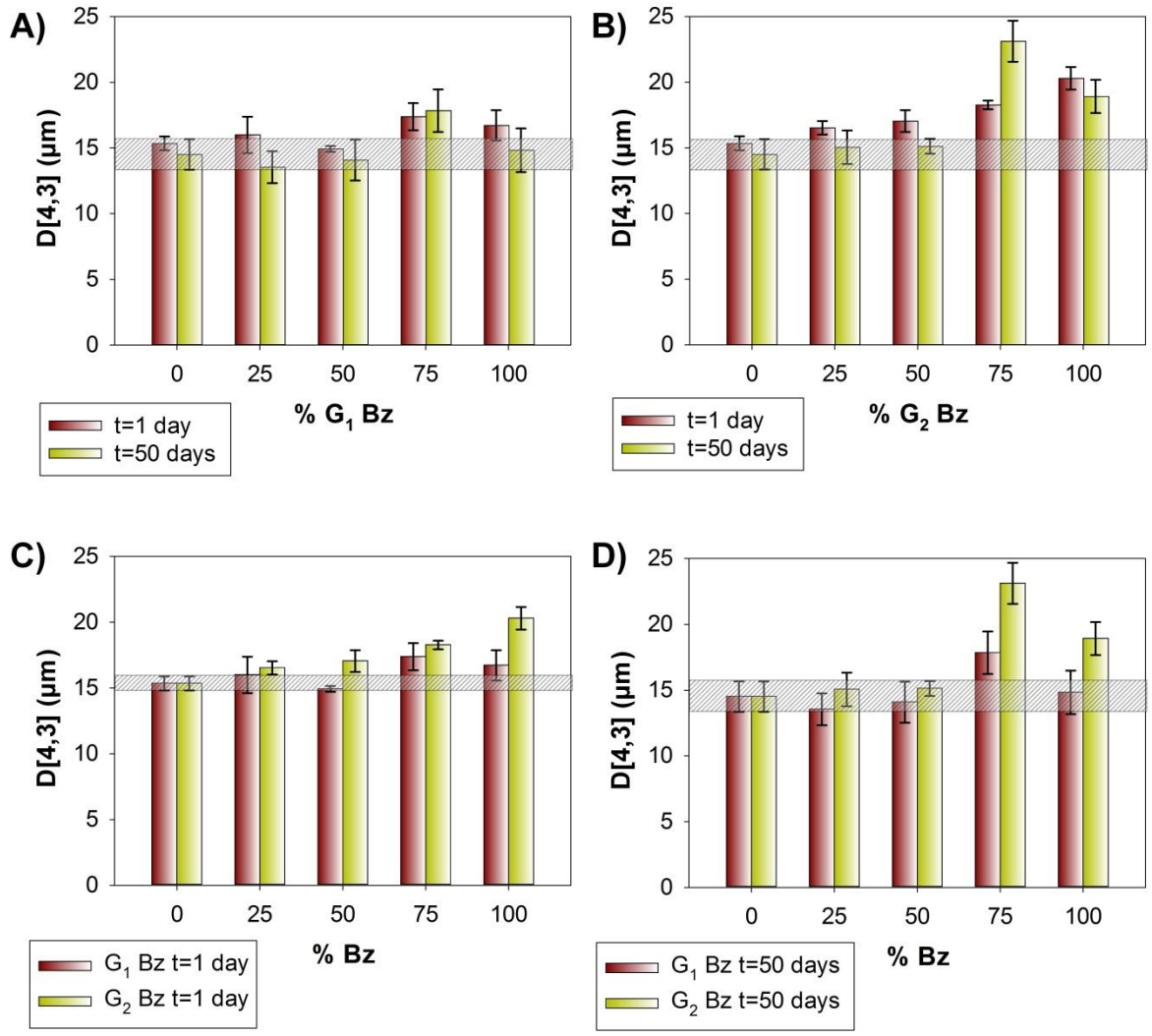

Figure 5.21 Bar chart showing D[4,3] of; (A) Emulsions stabilised by HPD surfactants comprised of increasing increments of G_1 Bz (0, 25, 50, 75 and 100 %) content at t=1 day and t=50 days (B); Emulsions stabilised by HPD surfactants comprised of increasing increments of G_2 Bz (0, 25, 50, 75 and 100 %) content at t=1 day and t=50 days; (C) Emulsions stabilised by HPD surfactants comprised of increasing increments of G_1 and G_2 Bz (0, 25, 50, 75 and 100 %) at t=1 day; (D) Emulsions stabilised by HPD surfactants comprised of increasing increments of G_1 and G_2 Bz (0, 25, 50, 75 and 100 %) at t=50 days. A grey bar is drawn horizontally in graphs A, B, C and D, to highlight the D[4,3] of an emulsion stabilised by a branched polymer comprised of 100 % dodecyl end groups after 50 days (A, B and D) and after 1 day (C).

Unfortunately, although interesting, the result was actually disappointing, illustrating that as dodecyl end groups are replaced with G_2 Bz end groups within the surfactant composition, the emulsion droplet size increases. This is undesirable when stabilising an emulsion with a "good" surfactant, since an effective surfactant should provide and maintain a reduction in interfacial tension within the emulsion system, hence stabilising the oil droplet. As the D[4,3] is increasing through an increasing G_2 Bz surfactant content, this shows that there is a decreasing ability to stabilise the oil-water interface within the emulsion; thus by removing dodecyl end groups and replacing them with G_2 Bz end groups within the surfactant composition the surfactant properties reduces, even 1 day after emulsification.

Analysing the same series of emulsions over the 50 day period, Figure 5.21(B), the D[4,3] appeared to become more uniform, but the variation in D[4,3] in emulsions formed with HPDs containing 75 % (**E21**) and 100 % (**E22**) G_2 Bz end groups were still considerably larger. The larger absolute values of D[4,3] may suggest a steric packing issue for the surfactants at the droplet interface, more noticeable using surfactants with a higher G_2 Bz content. It was also apparent that the D[4,3] values were considerably larger when using a surfactant containing 75 % G_2 Bz end groups (**E21**) specifically; greater even than when the surfactant containing 100 % G_2 Bz groups (**E22**) was used. Interestingly, this observation was repeated when using G_1 Bz surfactants, Figure 5.21(A), although the differences in the D[4,3] between emulsions stabilised with surfactants comprised of 75% G_1 dendron (**E13**) and other G_1 Bz samples (**E11**, **E12** and **E14**) was smaller Figure 5.21(B).

Plotting the two different generations on the same graph allow comparisons between emulsions stabilised using G_1 or G_2 Bz functional HPDs to be made, Figures 5.21 (C) and (D), and essentially reiterates the above discussions. At t=1, Figure 5.21 (C) emulsions formed with G_2 Bz HPDs showed an increase in D[4,3] with increasing G_2 Bz surfactant content, whereas emulsions formed with G_1 Bz HPDs appeared to result in little change in D[4,3] relative to increasing G_1 Bz surfactant content. After 50 days, Figure 5.21 (D), there was little difference across either the emulsion series stabilised with surfactants containing G_1 or G_2 Bz dendrons, apart from at surfactant compositions of 75 %, G_1 Bz , 75% G_2 Bz, and 100 % G_2 Bz content where the D[4,3] was larger (inclusive of error) than the

comparable emulsion, **E10**, stabilised by a branched polymer surfactant comprised of 100 % dodecyl chain ends.

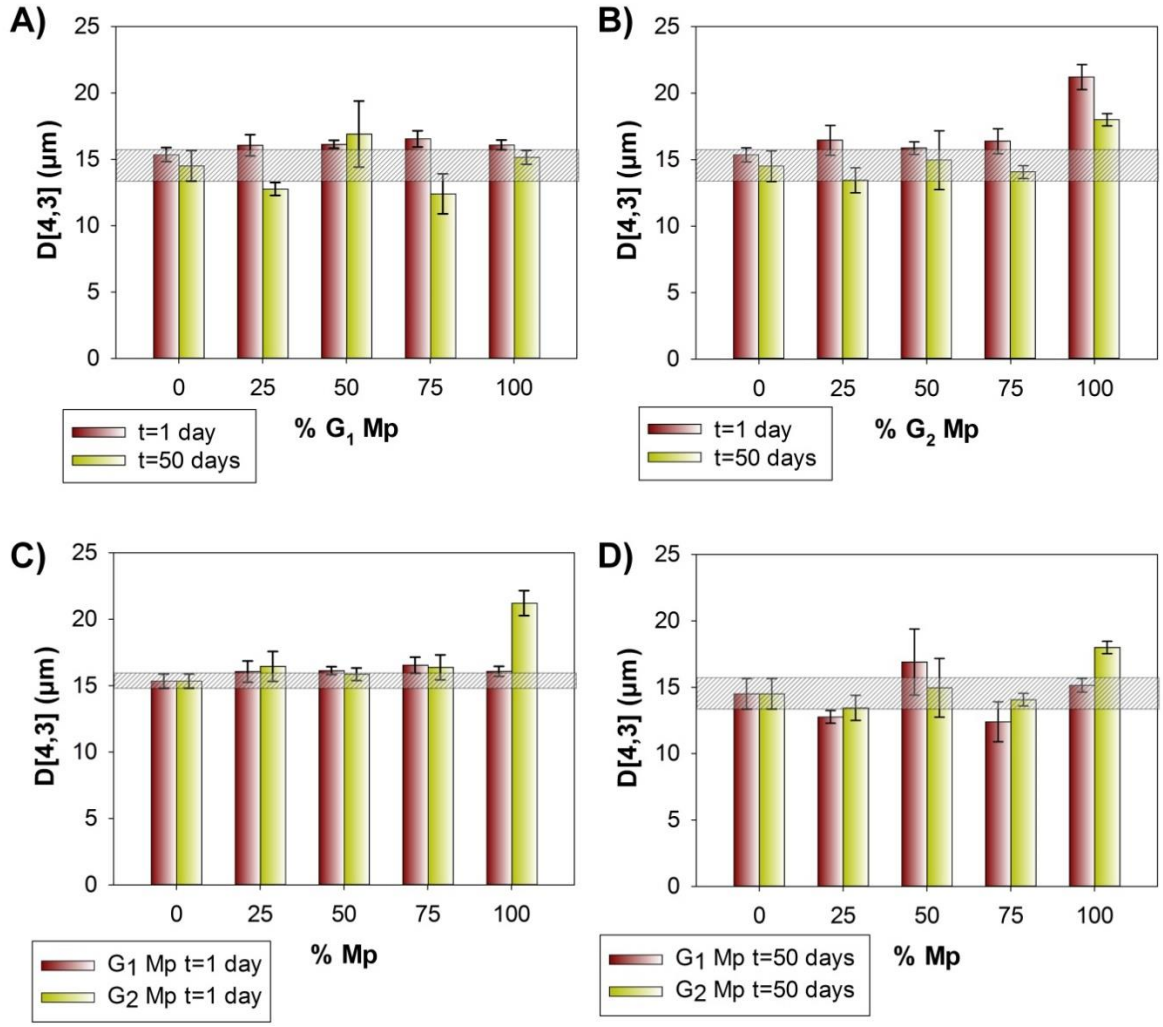

Figure 5.22 Bar chart of; (A) Emulsions stabilised by HPD surfactants comprised of increasing increments of G_1 Mp (0, 25, 50, 75 and 100 %) content at t=1 day and t=50 days (B); Emulsions stabilised by HPD surfactants comprised of increasing increments of G_2 Mp (0, 25, 50, 75 and 100 %) content at t=1 day and t=50 days; (C) Emulsions stabilised by HPD surfactants comprised of increasing increments of G_1 and G_2 Mp (0, 25, 50, 75 and 100 %) at t=1 day; (D) Emulsions stabilised by HPD surfactants comprised of increasing increments of G_1 and G_2 Mp (0, 25, 50, 75 and 100 %) at t=50 days. A grey bar is drawn horizontally in graphs A, B, C and D, to highlight the D[4,3] of an emulsion stabilised by a branched polymer comprised of dodecyl end groups after 50 days (A, B and D) and after 1 day (C).

The D[4,3] of emulsions stabilised by surfactants comprising increasing increments of G_1 Mp (25, 50, 75 and 100 %) (**E15-E18**) showed no considerable change over the 50 day period, remaining the same (within error) as t=1day, Figure 5.22(A). Within this series, emulsion **E15** stabilised by a surfactant comprising 25 % G_1 Mp end groups was slightly smaller at t=50 days (i.e. outside the comparable standard, **E10**, see grey bar, Figure 5.22(A). The reasons for this decrease in size are not entirely apparent as one explanation would be that demuslification had occurred, but no free oil was observable at the surface of the samples after storage for 50 days. Error bars of emulsions formed with HPDs containing 50 % (**E21**) and 75 % (**E22**) G_1 Mp end groups increased considerably at t=50 days, relative to t=1 day, suggesting that the uniformity in the size of the droplet diameters between different samples of the same emulsion has reduced over time. It must be noted however, that the height at which a sample of emulsion was taken for laser diffraction measurements was not standardised.

The D[4,3] of emulsions stabilised by surfactants comprising increasing increments of G_2 Mp (25, 50 and 75 %) (**E23-E25**) showed no considerable change over the 50 day period, remaining the same (within error) as t=1day, Figure 5.22(B). However, emulsion **E26** formed with a HPD containing 100 % G_2 Mp end groups was considerably larger at both t=1 and t= 50 days, also showing a decrease in droplet size over this period.

Plotting the two different generations on the same graph allow comparisons between emulsions stabilised with either G_1 or G_2 Mp functional HPDs to be made, Figures 5.22 (C) and (D).

At t=1 day and t=50 days, Figure 5.22 (C) and (D), the D[4,3] of emulsions stabilised using G_1 and G_2 Mp functional HPDs at 25-75% dendritic content were almost the same (within error), suggesting that there was little difference in the D[4,3] based on different dendron sizes, which is in contrast to emulsions stabilised by G_1 and G_2 Bz functional HPDs. Emulsions **E26** formed with a 100% G_2 Mp HPD had a significantly larger D[4,3] at t= 1 day and t= 50 days, possibly suggesting that packing of an emulsion stabilised by a 100% G_2 Mp HPD is problematic, resulting in a larger D[4,3].

Optical microscopy was used to measure selected emulsion samples, but due to the extremely similar sizes of **E10**-**E26**, the technique provided little information. As an example, an optical microscope image of emulsion **E26** stabilised by a HPD surfactant comprised of 100% G_2 Mp after 50 days is shown in Figures 5.23(A) and (B) at different magnifications (x10, x50). A histogram of the diameter of 100 emulsion droplets from Figure 5.16(B) is shown in Figure 5.16(C).

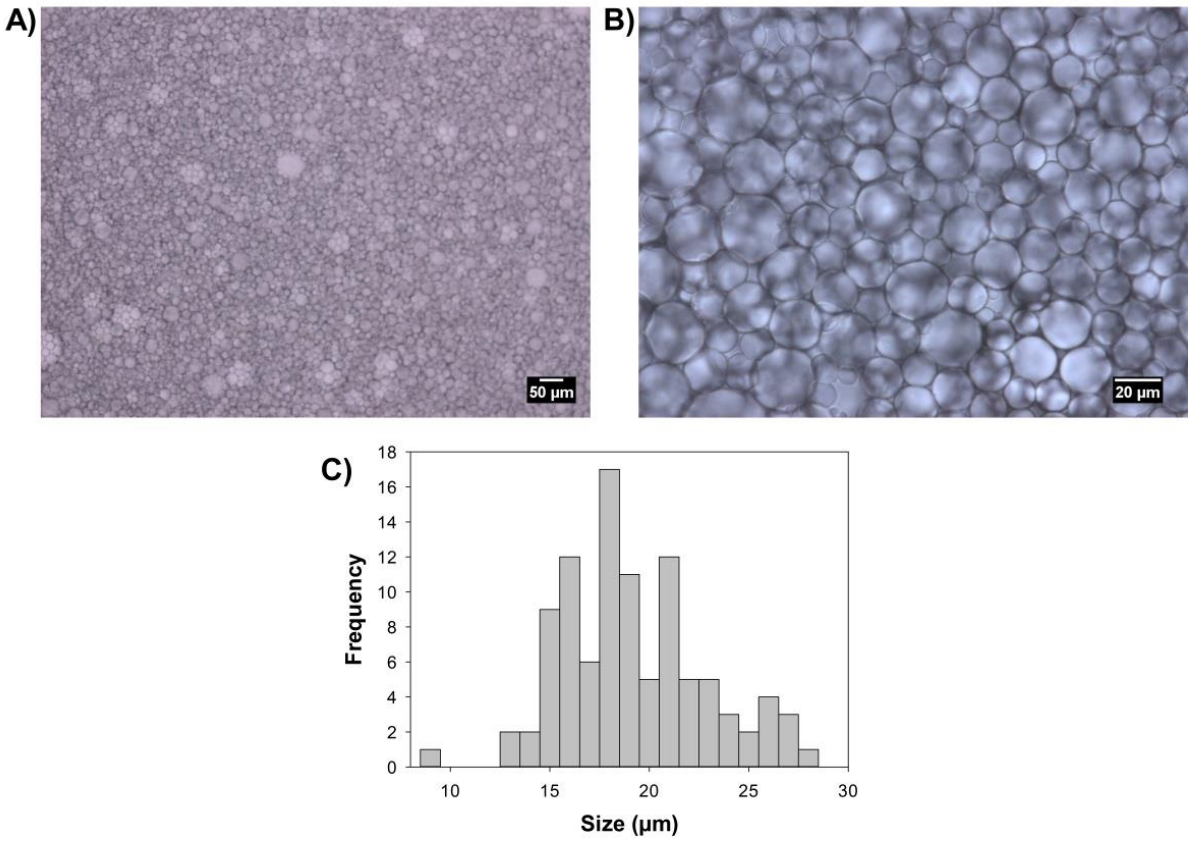

Figure 5.23 An optical microscope image of **E26** stabilised by a HPD surfactant comprised of 100% G_2 Mp after 50 days; (A) at x10 magnification; (B) at x 50 magnification. (C) Shows a histogram plot of 100 oil droplet sizes of from image (A).

5.6.2 Long term stability of emulsions at low pH

In the previous stability study, the amphiphilic polymers were dissolved in aqueous solutions (2.5 mg/mL) at the natural pH of the distilled water (pH 7.37), meaning that both the dendron end groups with Mp and Bz functionalities were hydrophobic and the effect of exchanging different fractions of

dodecyl end groups with dendron initiators could be established with respect to the ability of functionalised HPDs to act as emulsion stabilisers.

Under acidic conditions, the tertiary amine present in the Mp functionality is protonated, and thus the dendron end groups within the HPDs become hydrophilic and potentially less able to interact with the oil droplet surface. As a simple test of pH response, Bz initiators **[127]** and **[133]** and Mp initiators **[128]** and **[134]** were added to aqueous media (5 mg/mL) at pH 7.37 and pH 1.64. After stirring gently for 16 hours at room temperature, visual observations were made, Figure 5.24. The Bz initiators **[127]** and **[133]** were not soluble in water at either pH 7.37 or pH 1.64, Figure 5.24(A) and (B). In contrast to this, the Mp initiators **[128]** and **[134]** were not soluble in the aqueous solution at pH 7.37, but were soluble at pH 1.64, clearly visible in Figure 5.24(B).

A long term stability study of the o/w emulsions was performed over a 29 day period under acidic conditions (pH 1.64). The methodology for emulsion preparation was identical to the previous stability study but each polymer was first dissolved in aqueous acid prior to emulsification.

5.6.2.1 Emulsions stabilised by a linear polymer, LDHs or linear polymer/LDH surfactant at low pH

All dodecane o/w emulsions stabilised using a linear polymer, LDHs or a linear polymer/LDH mixture (**E27**-**E34**) under acidic conditions showed coalescence over the 29 day period, with emulsions comprised of Mp peripheral functionalities showing considerable oil phase separation, Table 5.7.

Emulsion **E31** stabilised via an LDH surfactant comprised of 100% G_1 Mp chain ends, resulted in coalescence after l day, with 90% demulsification occurring after 7 days, and total phase separation after 14 days, Figure 5.25 (A). Significant coalescence of emulsion **E30** stabilised via a mixed LDH surfactant comprised of 50% G_1 Mp and 50% dodecyl chain was observed, after 29 days, Figure 5.25 (C). Interestingly, emulsion **E35** stabilised via a LDH surfactant comprised of 100% G_2 Mp chain ends coalesced slower than **E31** comprised stabilised of 100% G_1 Mp chain ends, (see digital image 14 days **E31**, Figure 5.25(A), vs digital image 29 days **E35**, Figure 5.25 (B)). This may suggest that

although there are twice as many hydrophilic Mp groups present in the G_2 materials verses the G_1 materials, the larger hydrophobic polyester dendron present at G_2, perhaps provides some hydrophobicity leading to extended, but limited, stability. However, generally, the decreased concentration of hydrophobic end groups at this pH, were clearly not able to stabilise the oil/water interface when using the LDH materials with G_1 and G_2 Mp functional dendrons.

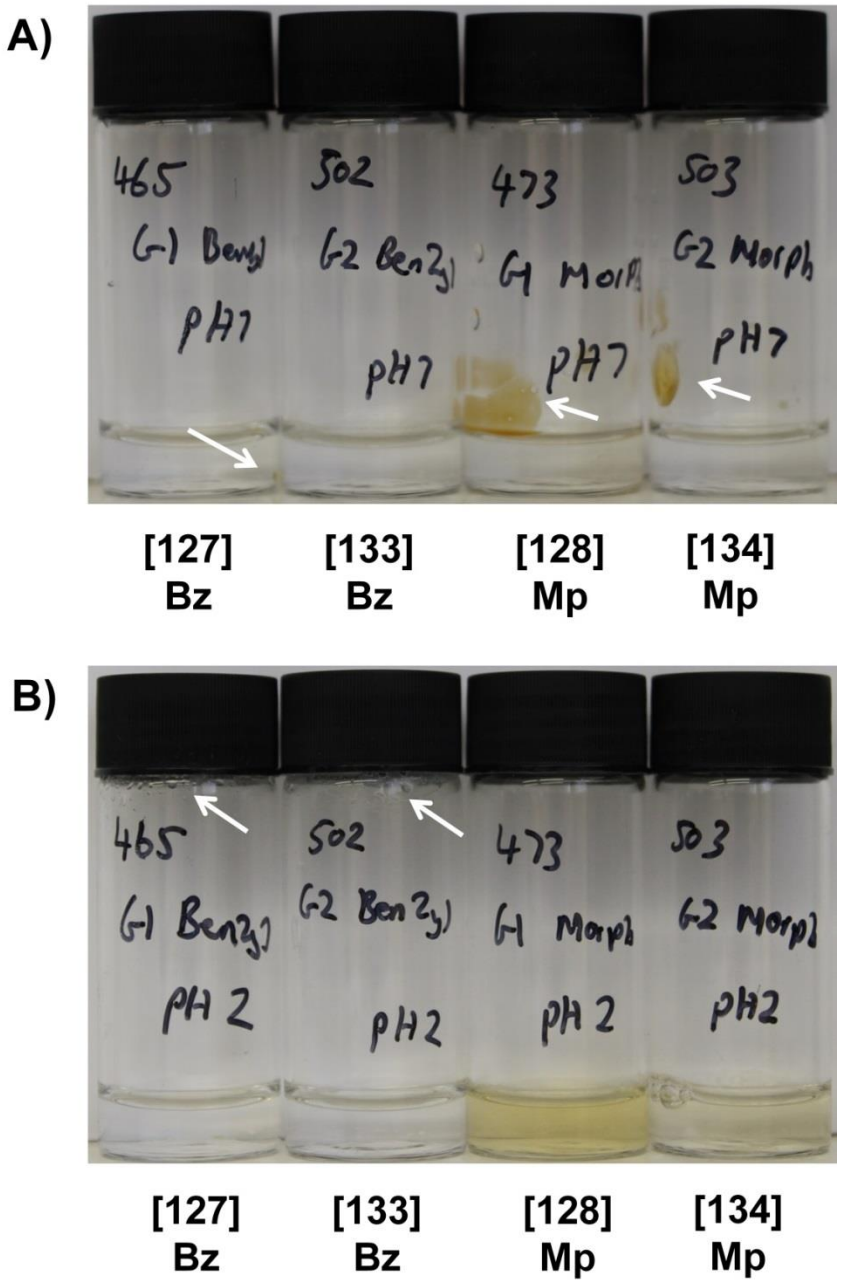

Figure 5.24 Digital images of 5.0 mg/mL aqueous solutions of Bz and Mp initiators after stirring for 16 hours at; (A) pH 7.47; (B) pH 1.64. The white arrows aim to highlight the insoluble materials.

Table 5.7 Table of emulsions stabilised with a surfactant comprised of a linear polymer, LDH or a linear polymer/LDH mixture (**E27-E34**) under acidic conditions (pH 1.64) showing D[4,3] at t=1 after equilibration, and the presence of phase separated oil after a 29 day time period.

Polymer; Entry #	Dendritic equiv.	Emulsion #	D[4,3] at t=1day (μm)[a]	Oil 7 days[b]	Oil 29 days[b]
[DBiB(OEGMA$_{80}$)];[144]	-	**E27**	19.07 ± 2.92	N	Y
[G$_1$Bz$_{0.5}$/DBiB$_{0.5}$(OEGMA$_{80}$)];[145]	0.5	**E28**	18.57 ± 4.36	N	Y
[G$_1$Bz(OEGMA$_{80}$)];[135]	1.0	**E29**	23.87 ± 2.18	N	Y[d]
[G$_1$Mp$_{0.5}$/DBiB$_{0.5}$(OEGMA$_{80}$)];[146]	0.5	**E30**	18.52 ± 1.80	Y	Y[d]
[G$_1$Mp(OEGMA$_{80}$)];[136]	1.0	**E31**	21.42 ± 5.98	Y[c]	Y
[G$_2$Bz$_{0.5}$/DBiB$_{0.5}$(OEGMA$_{80}$)];[147]	0.5	**E32**	16.58 ± 3.73	N	Y
[G$_2$Bz(OEGMA$_{80}$)];[137]	1.0	**E33**	15.35 ± 2.80	N	Y
[G$_2$Mp$_{0.5}$/DBiB$_{0.5}$(OEGMA$_{80}$)];[148]	0.5	**E34**	15.66 ± 0.29	N	Y
[G$_2$Mp(OEGMA$_{80}$)];[138]	1.0	**E35**	26.48 ± 3.41	Y	Y[d]

[a]Measured by laser diffraction after 24 hours to enable equilibration. [b] Determined by visually observing phase separation. [c]90% total oil phase separation after 7 days. [d]Significant oil phase separation after 29 days.

Since Bz surface groups are hydrophobic at low pH, it was surprising to see evidence of significant demulsification occurring. Figure 5.25 (D) illustrates the oil phase separation of emulsion **E29** stabilised via a LDH comprised of 100 % G_1 Bz end chains after 29 days. This perhaps suggested that the low pH had resulted in some hydrolysis of the hydrophobic end groups, resulting in fewer oil droplet interactions. Further analysis would be required to confirm this hypothesis.

5.6.2.2 Emulsions stabilised by a branched polymer, HPDs or branched polymer/HPD surfactant at low pH

In contrast, for the branched polymer stabilised emulsions, under acidic conditions, no demulsification was observed in any of the samples over the 29 day period (**E36-E44**), Table 5.8. This again would suggest the branching effect causes multiple end group adhesions to oil droplets, and thus greater stability. The D[4,3] of emulsion **E36** after 29 days stabilised by a branched polymer comprised of 100% dodecyl chain ends was used as the comparable standard against emulsions stabilised via HPDs and mixed HPDs (**E37-E44**), represented as a grey bar in Figures 5.26 and 5.27.

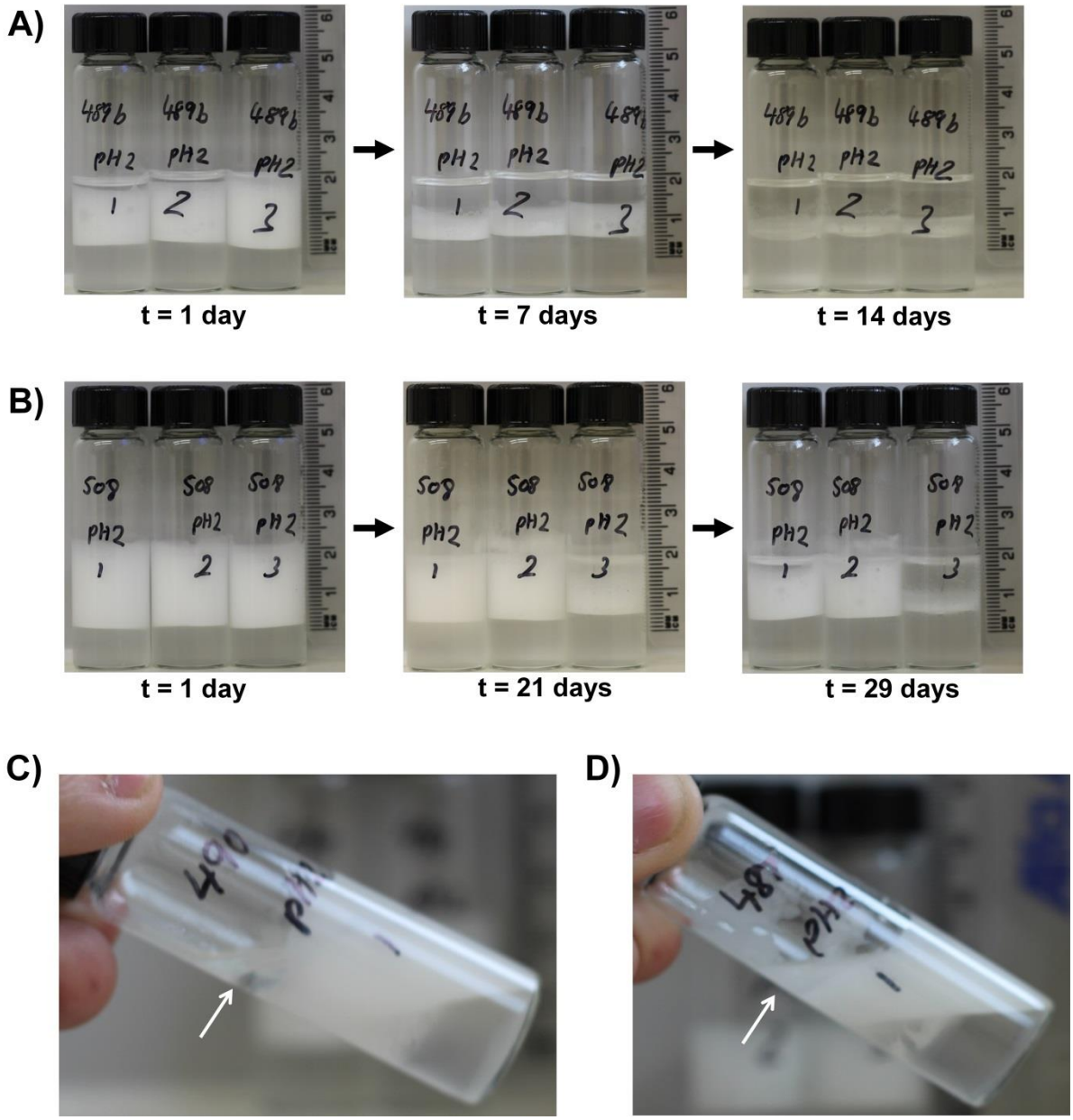

Figure 5.25 Digital images of emulsions stabilised with LDHs at pH 1.64; (A) Oil phase separation over 14 days of emulsion **E31** stabilised by a LDH surfactant comprised of 100% G_1 Mp chain ends; (B); Oil phase separation over 29 days of emulsion **E35** stabilised by a LDH surfactant comprised of 100% G_2 Mp chain ends; (C) Oil phase separation over 29 days of emulsion **E30** stabilised by a mixed LDH surfactant comprised of 50% G_1 Mp and 50% dodecyl chain ends (d); Oil phase separation over 29 days of emulsion **E29** stabilised by a LDH surfactant comprised of 100% G_1 Bz chain ends.

Table 5.8 Table of emulsions stabilised with a surfactant comprised of a branched polymer, HPDs or branched polymer/HPD mixture (**E27-E34**) under acidic conditions (pH 1.64) showing D[4,3] at t=1 after equilibration and after a 29 day time period.

Polymer; Entry #	Dodecyl equiv.	Dendritic equiv.	Emulsion #	D[4,3] (μm)[a] t=1 day	D[4,3] (μm)[a] t=29 days[b]
[DBiB(OEGMA$_{80}$-*co*-EGDMA$_{0.9}$)];[149]	1.0	-	**E36**	16.93 ± 0.92	17.13 ± 3.12
[G$_1$Bz$_{0.5}$/DBiB$_{0.5}$(OEGMA$_{80}$-*co*-EGDMA$_{0.9}$)];[151]	0.5	0.5	**E37**	18.43 ± 3.42	17.67 ± 2.32
[G$_1$Bz(OEGMA$_{80}$-*co*-EGDMA$_{0.9}$)];[139]	-	1.0	**E38**	18.22 ± 0.31	22.36 ± 3.89
[G$_1$Mp$_{0.5}$/DBiB$_{0.5}$(OEGMA$_{80}$-*co*-EGDMA$_{0.9}$)];[154]	0.5	0.5	**E39**	19.22 ± 1.39	19.64 ± 4.77
[G$_1$Mp(OEGMA$_{80}$-*co*-EGDMA$_{0.9}$)];[140]	-	1.0	**E40**	18.16 ± 0.27	20.47 ± 2.52
[G$_2$Bz$_{0.5}$/DBiB$_{0.5}$(OEGMA$_{80}$-*co*-EGDMA$_{0.8}$)];[157]	0.5	0.5	**E41**	17.03 ± 2.16	18.82 ± 1.85
[G$_2$Bz(OEGMA$_{80}$-*co*-EGDMA$_{0.8}$)];[141]	-	1.0	**E42**	21.08 ± 0.58	22.53 ± 3.27
[G$_2$Mp$_{0.5}$/DBiB$_{0.5}$(OEGMA$_{80}$-*co*-EGDMA$_{0.8}$)];[160]	0.5	0.5	**E43**	20.83 ± 1.07	16.60 ± 0.11
[G$_2$Mp(OEGMA$_{80}$-*co*-EGDMA$_{0.8}$)];[142]	-	1.0	**E44**	22.38 ± 3.07	21.02 ± 4.84

[a]Emulsions were measured by laser diffraction; results based on an average of 3 separate samples, with 3 measurements per sample. Error is based on the standard deviation between the 3 separate samples. [b]Emulsions showed no sign of phase separated oil after the 29 day period.

The D[4,3] of emulsions stabilised by surfactants comprising increasing increments of G_1 Bz (50, 100 %) (**E37** and **E38**) under acidic conditions showed no considerable change over the 29 day period, remaining the same (within error) as t=1day, Figure 5.26 (A). Similarly, emulsions stabilised by surfactants comprising increasing increments of G_2 Bz (50, 100 %) (**E41** and **E42**) under acidic conditions also showed no considerable change over the 29 day period, remaining the same (within error) as t=1day, Figure 5.26(B).

Plotting the D[4,3] of emulsions stabilised using G_1 or G_2 Bz functional HPDs on the same graph, did allow some comparisons to be made, Figures 5.26 (C) and (D). At t=1, Figure 5.26(C) emulsion **E42** stabilised by a surfactant comprising 100 % G_2 Bz end groups was slightly larger at t=1 day a (i.e. outside the comparable standard, **E36**, at t=1 day). A general trend in both the G_1 and G_2 materials was that the error bars increased over time, suggesting that the uniformity of the droplet sizes decreased over the 29 day period, Figure 5.26 (D). No other D[4,3] differences were observed at t=29 days (relative to **E36**, see grey bar, Figure 5.26 (D)).

The D[4,3] of emulsions stabilised by surfactants comprising increasing increments of G_1 Mp (50, 100 %) (**E39** and **E40**) under acidic conditions showed no considerable change over the 29 day period, remaining the same (within error) as t=1day, Figure 5.27 (A). The D[4,3] of emulsions stabilised by surfactants comprising increasing increments of G_2 Mp (50, 100 %) (**E43** and **E44**) emulsions did show an increase in droplet size, with respect to increasing Mp content, at t=1 day, Figure 5.27(B). This was perhaps due to an increased charged effect, as an increasing increment of G_2 Mp is added to the surfactant composition, resulting in a packing issue at the oil droplet interface. The D[4,3] of the same emulsions over the 29 day period, appeared to become more uniform.

Plotting the two different generations on the same graph allowed comparisons between emulsions stabilised using G_1 or G_2 Mp functional HPDs to be made, Figures 5.27(C) and (D). At t=1 day, the increasing D[4,3] of emulsions stabilised by surfactants comprising increasing increments of G_2 Mp was clearly noticeable, Figure 5.27(C) and this trend became more uniform over the 29 day period, Figure 5.27(D).

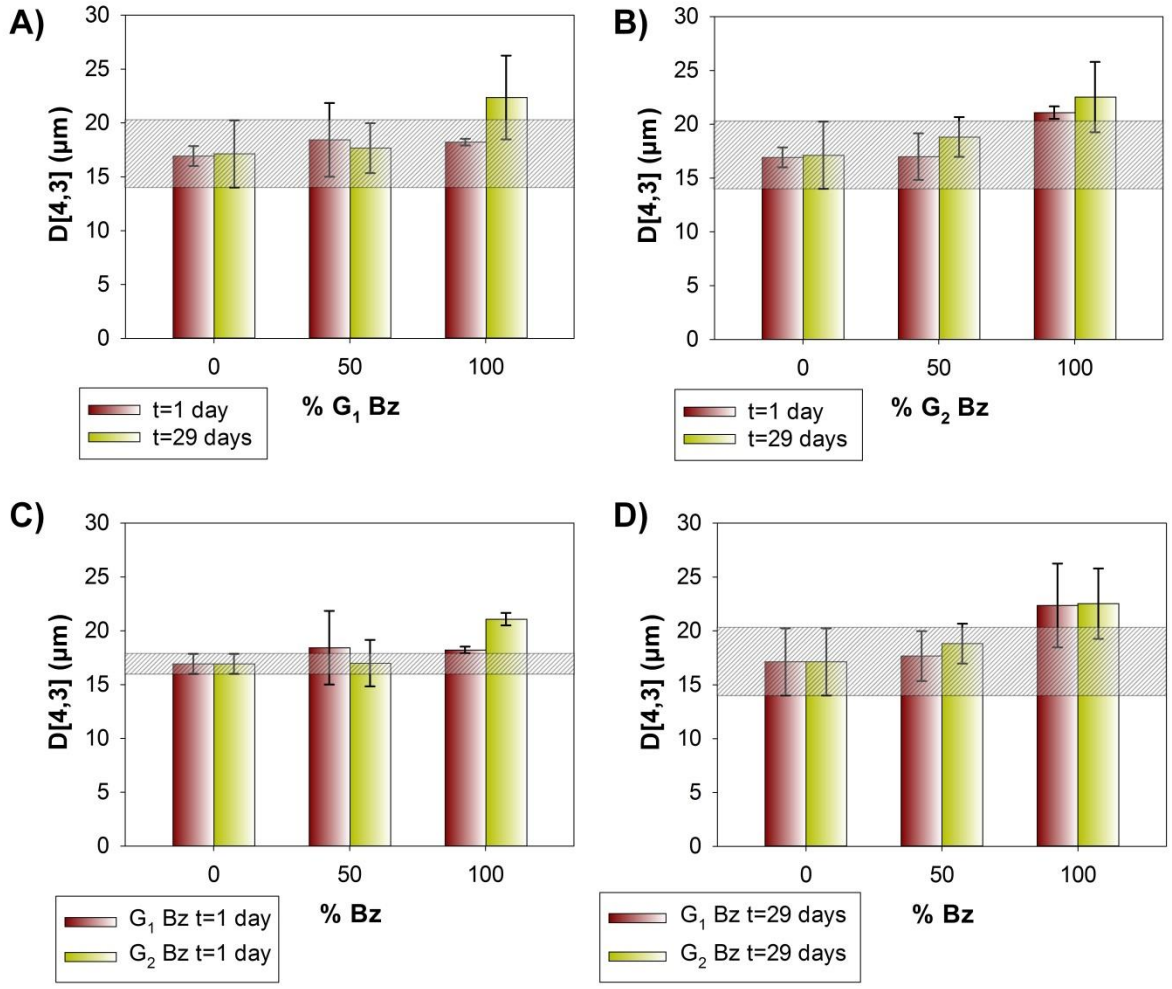

Figure 5.26 Bar charts showing D[4,3] of; (A) Emulsions stabilised by HPD surfactants comprised of increasing increments of G_1 Bz (50 and 100 %) content at t=1 day and t=29 days under acidic conditions (B); Emulsions stabilised by HPD surfactants comprised of increasing increments of G_2 Bz (50 and 100 %) content at t=1 day and t=29 days under acidic conditions; (C) Emulsions stabilised by HPD surfactants comprised of increasing increments of G_1 and G_2 Bz (50 and 100 %) content at t=1 day under acidic conditions; (D) Emulsions stabilised by HPD surfactants comprised of increasing increments of G_1 and G_2 Bz (50 and 100 %) content at t=29 days under acidic conditions. A grey bar is drawn horizontally in graphs A, B, C and D, to highlight the D[4,3] of an emulsion stabilised by a branched polymer comprised of 100% dodecyl end groups after 29 days (A, B and D) and after 1 day (C) under acidic conditions.

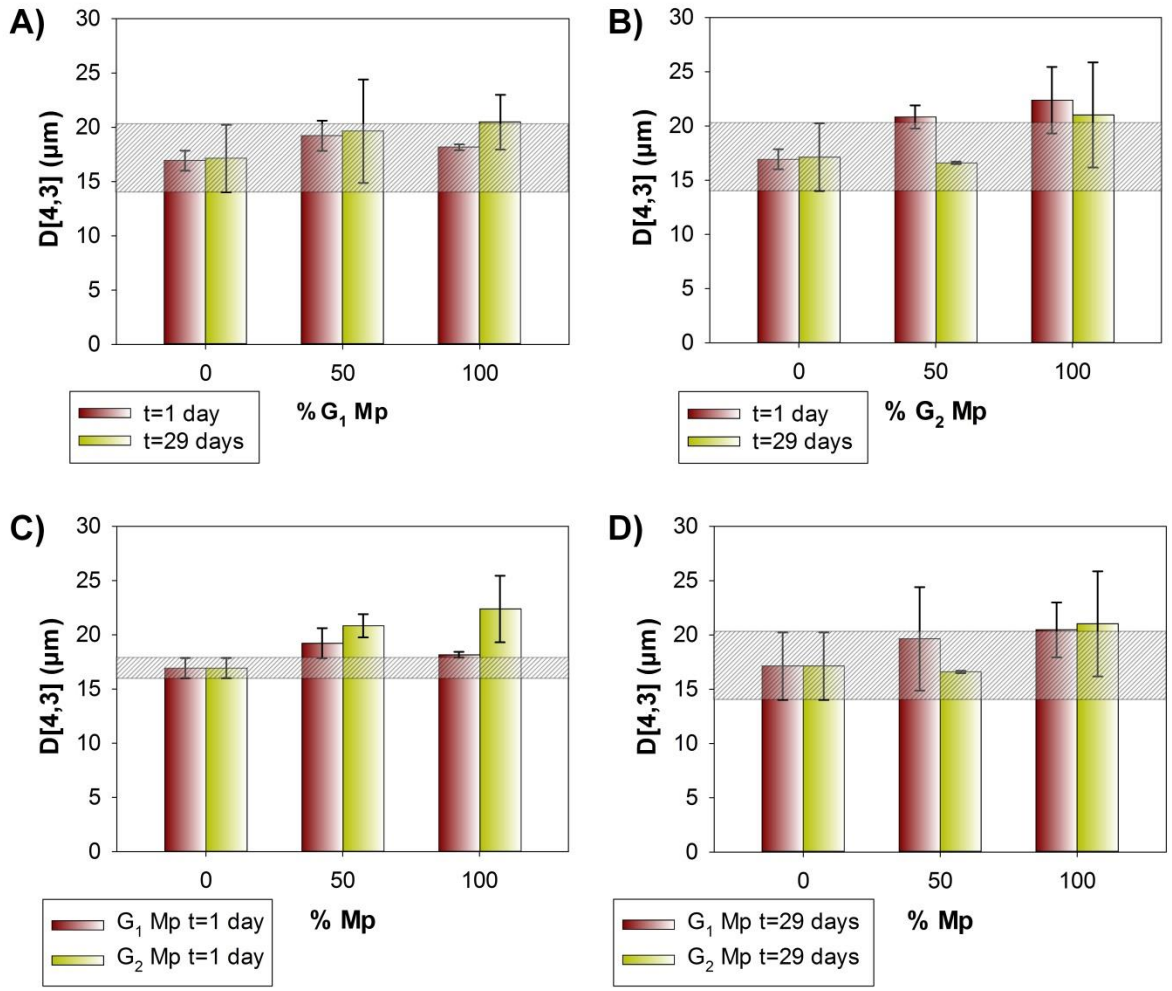

Figure 5.27 Bar charts showing D[4,3] of; (A) Emulsions stabilised by HPD surfactants comprised of increasing increments of G_1 Mp (50 and 100 %) content at t=1 day and t=29 days under acidic conditions (B); Emulsions stabilised by HPD surfactants comprised of increasing increments of G_2 Mp (50 and 100 %) content at t=1 day and t=29 days under acidic conditions; (C) Emulsions stabilised by HPD surfactants comprised of increasing increments of G_1 and G_2 Mp (50 and 100 %) content at t=1 day under acidic conditions; (D) Emulsions stabilised by HPD surfactants comprised of increasing increments of G_1 and G_2 Mp (50 and 100 %) content at t=29 days under acidic conditions. A grey bar is drawn horizontally in graphs A, B, C and D, to highlight the D[4,3] of an emulsion stabilised by a branched polymer comprised of 100% dodecyl end groups after 29 days (A, B and D) and after 1 day (C) under acidic conditions.

There were no observable D[4,3] differences between emulsions stabilised using surfactants containing G_1 Mp functionality over the 29 day period Figures 5.27(C) and (D), however in most of the samples, significantly greater error bars were observed, illustrating the lack of uniformity between emulsions of the same type.

Comparing between acidic and non-acidic emulsions over the 29 day period, in all cases the acidic emulsions were either the same size or larger than the neutral emulsions, Figures S5.32 and S5.33. A suggestion could be that the OEGMA block behaves differently at acidic and neutral pH; this is since the emulsion stabilised by a branched polymer surfactant comprising 100% dodecyl chain ends, also displayed a slight increase in size (within error) at t=0.

5.6.3 Conclusions from long term stability tests at natural and low pH

To conclude, all emulsions prepared using linear polymer surfactants failed through coalescence regardless of end group composition and the pH of the aqueous continuous phase. Emulsion instability was considerably accelerated when the end groups were changed to become hydrophilic by protonation of the Mp functionality under acidic conditions.

In contrast, regardless of end group composition at either neutral or acidic pH, emulsions prepared by branched surfactants showed no sign of coalescence. There are a number of suggestions as to why this may occur, but it is very important to state that the presence of large variations in the polymer architectures, compositions and molecular weights of the HPD materials makes definitive explanations difficult without considerable extra research.

The most probable explanation for the enhanced stability of emulsions stabilised with the branched polymer systems may simply be the large number of end-groups. The linear polymer systems used have mixtures of un-linked polymer chains that are able to move to and from oil droplet interfaces in a dynamic process similar to small molecule surfactants, Figure 5.28(A). Over time, the movement of linear polymer chains from the oil-droplet interface to the aqueous solution and back to an oil droplet may lead to an increasing concentration of polymer chains in solution, especially if the rate of leaving the oil droplet is more rapid than the adsorption of a polymer chain onto another oil/water interface.

In contrast, the branched nature of the HPDs and dodecyl functional branched vinyl polymer means that the individual primary chains are “locked” together, Figure 5.28 (B). Simultaneous release of all of the chain ends of a HPD from the oil-water interface is highly unlikely and would lead to exposure of a large oil surface area and the generation of a significant increase in interfacial tension. This is similar to the energy barriers present within the removal of particles from the interfaces of Pickering-emulsions. It is probable that small numbers of chain ends are moving from the interface, analogous to the linear systems studied here, but the mobility of the primary polymer chain is dramatically reduced, possibly leading to eventual adsorption back onto oil-droplet surface, rather than movement away from the interface into solution.

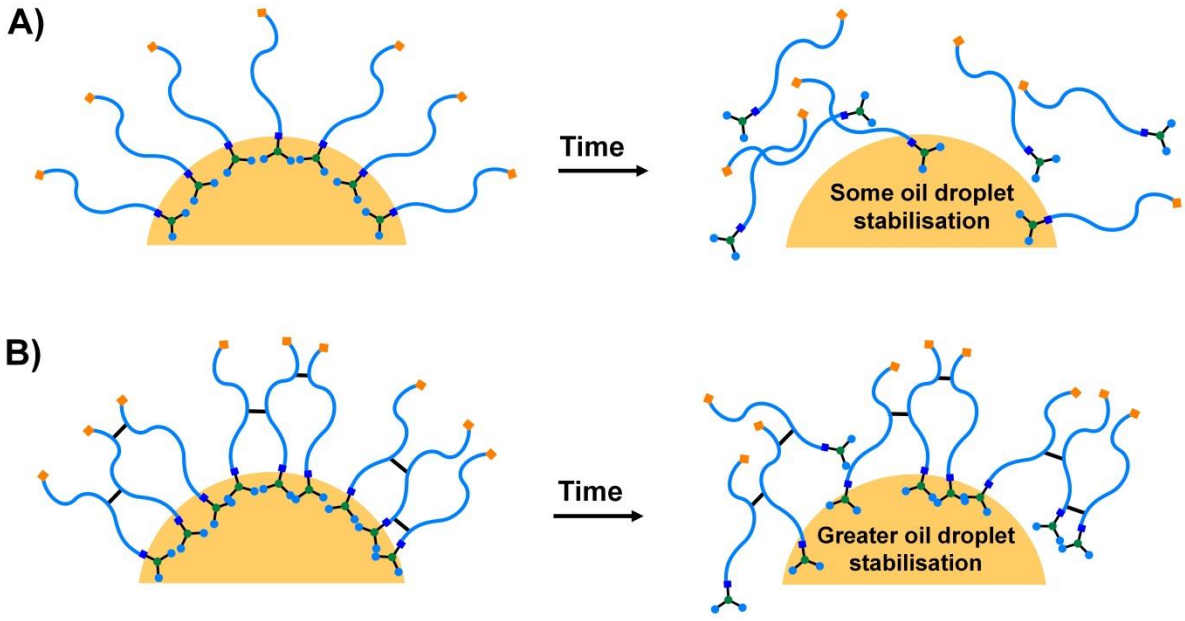

Figure 5.28 Schematic representation of; (A) Emulsion breakdown from chain mobility by a surfactant comprised of a linear system; (B) Emulsion stabilisation from reduced chain mobility by a surfactant comprised of a branched system.

5.7 Dilution study of emulsions stabilised by branched polymer, HPDs or branched polymer/HPD surfactant at natural pH

To assess the performance of emulsions stabilised by a branched polymer, HPDs or branched polymer/HPD surfactant, a 10-fold dilution study was performed. Selected emulsion samples were chosen from the previous long term stability study, Table 5.6. These included emulsion **E10** as the comparable reference, stabilised by a branched polymer surfactant comprised of 100% dodecyl chain ends. Emulsions **E20** and **E22**, stabilised by mixed HPD and HPD surfactants comprised of increasing increments of G_2 Mp (50 and 100 %). And finally, emulsions **E24** and **E26**, stabilised by mixed HPD and HPD surfactants comprised of increasing increments of G_2 Mp (50 and 100 %), Table 5.9.

The emulsions were individually poured into 40 mL test tubes and 27 mL of water was added (new concentration of surfactant 0.25 mg/mL; pH 7.37) followed by homogenisation for 2 minutes at 24,000 rpm. The emulsions were left for 24 hours at room temperature and visual observations were made. Emulsions sizes were recorded by laser diffraction before (t=0) and after (t=1 day) dilution, Table 5.9. It is important to note that this process is considerably different to the dilution, relatively gentle mixing and rapid measurement conducted during the laser diffraction studies.

After dilution and homogenisation at t=0, it was interesting to observed the highly "detergent" like properties of the emulsions, even at very low concentrations of polymeric surfactant (0.25 mg/mL), Figure 5.29 (A).

Unfortunately, oil phase separation was observed after 1 day in all the emulsions in Table 5.9 following dilution. The different amounts of oil between emulsion samples were indistinguishable, but as an approximation a 0.5 mm layer of oil was present on each sample. Digital images in Figures 5.29 (B) and (C) show the presence of phase separated oil in emulsions **E22** and **E26** stabilised by HPDs comprised of 100% G_2 Bz and Mp chain ends respectively. Analysis of each emulsion by laser diffraction after 1 day concluded that with the exception of emulsion **E24**, stabilised by a mixed HPD surfactant comprised of 50% dodecyl and 50% G2 Mp chain ends, the D[4,3] of each emulsion

droplet decreased following dilution, Figure 5.30 (A) and (B),probably due to a reduction in the total volume of oil in the emulsion system arising from demulsification.

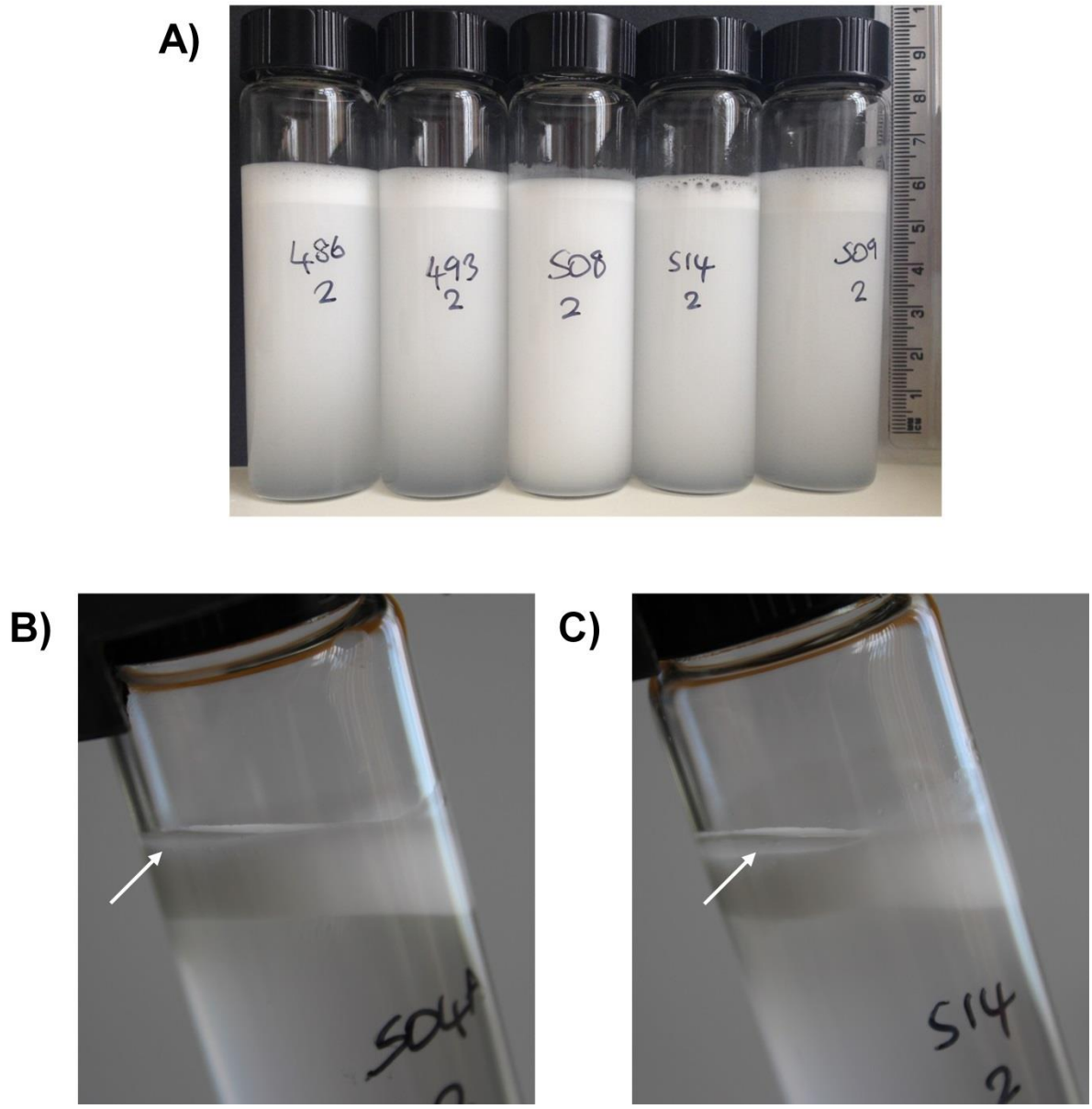

Figure 5.29 Digital images of (A) Emulsions from Table 5.9 after dilution and homogenisation at t=0; (B) Emulsion **E22** stabilised by a HPD surfactant comprised of 100% G_2 Bz chain ends after dilution and 1 day; (C) Emulsion **E26** stabilised by a HPD surfactant comprised of 100% G_2 Mp chain ends after dilution and 1 day; Emulsion E43 after 1 day. The white arrows direct the presence of oil phase separation.

Table 5.9 Dilution Study. Emulsions stabilised with a surfactant comprised of a branched polymer, HPDs or branched polymer/HPD mixture, showing volume-average diameter (D[4,3]) at t=0 before dilution, and t=1 day, after dilution.

Polymer; Entry #	Dodecyl equiv.	Dendritic equiv.	Emulsion #	D[4,3] (μm)[a] t=0	D[4,3] (μm)[a] t=1 day	Oil after 1 day
[DBiB(OEGMA$_{80}$-*co*-EGDMA$_{0.9}$)];[149]	1.0	-	**E10**	15.37 ± 0.04	13.41 ± 0.13	Y
[G$_2$Bz$_{0.5}$/DBiB$_{0.5}$(OEGMA$_{80}$-*co*-EGDMA$_{0.8}$)];[157]	0.5	0.5	**E20**	16.24 ± 0.09	15.03 ± 0.06	Y
[G$_2$Bz(OEGMA$_{80}$-*co*-EGDMA$_{0.8}$)];[141]	-	1.0	**E22**	17.79 ± 0.32	13.03 ± 0.02	Y
[G$_2$Mp$_{0.5}$/DBiB$_{0.5}$(OEGMA$_{80}$-*co*-EGDMA$_{0.8}$)];[160]	0.5	0.5	**E24**	15.44 ± 0.07	19.74 ± 0.12	Y
[G$_2$Mp(OEGMA$_{80}$-*co*-EGDMA$_{0.8}$)];[142]	-	1.0	**E26**	18.21 ± 0.03	14.71 ± 0.04	Y

[a]Emulsions were measured by laser diffraction; results based on one sample with 3 measurements. Error is based on the standard deviation between the 3 measurements.

Table 5.10 Thermal Study. Emulsions stabilised with a surfactant comprised of a branched polymer, HPDs or branched polymer/HPD mixture, showing volume-average diameter (D[4,3]) at t=0 before heating, and t=1 hour, after heating at 60 °C.

Polymer; Entry #	Dodecyl equiv.	Dendritic equiv.	Emulsion #	D[4,3] (μm)[a] t=0	D[4,3] (μm)[a] t= 1 hour @ 60 °C	Oil after 1 hour
[DBiB(OEGMA$_{80}$-*co*-EGDMA$_{0.9}$)];[149]	1.0	-	**E10**	16.35 ± 0.09	15.83 ± 0.04	Y
[G$_2$Bz$_{0.5}$/DBiB$_{0.5}$(OEGMA$_{80}$-*co*-EGDMA$_{0.8}$)];[157]	0.5	0.5	**E20**	18.36 ± 0.69	15.96 ± 0.08	Y
[G$_2$Bz(OEGMA$_{80}$-*co*-EGDMA$_{0.8}$)];[141]	-	1.0	**E22**	19.14 ± 0.31	17.91 ± 0.13	Y
[G$_2$Mp$_{0.5}$/DBiB$_{0.5}$(OEGMA$_{80}$-*co*-EGDMA$_{0.8}$)];[160]	0.5	0.5	**E24**	16.00 ± 0.05	15.78 ± 0.21	Y
[G$_2$Mp(OEGMA$_{80}$-*co*-EGDMA$_{0.8}$)];[142]	-	1.0	**E26**	19.91 ± 0.05	23.30 ± 0.90	Y

[a]Emulsions were measured by laser diffraction; results based on one sample with 3 measurements. Error is based on the standard deviation between the 3 measurements

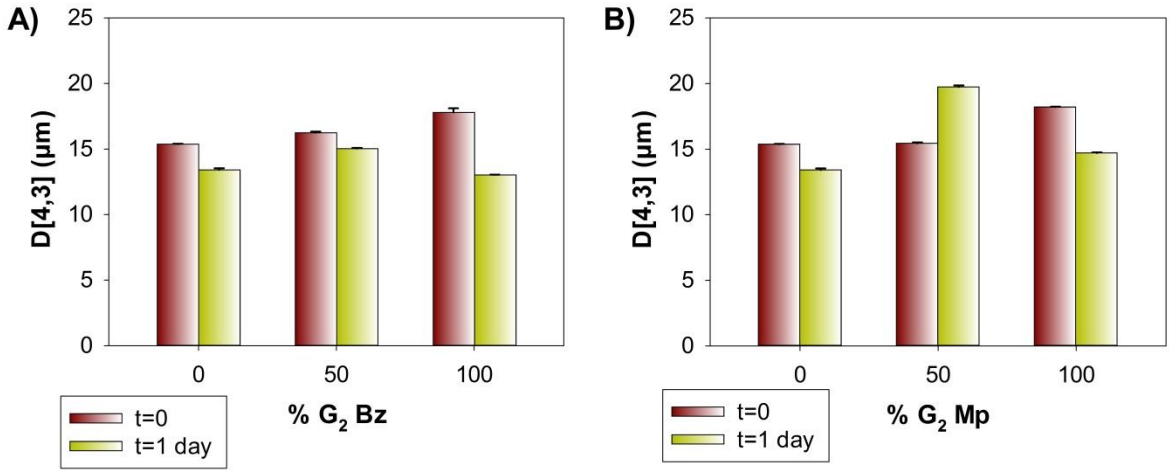

Figure 5.30 Bar charts showing D[4,3] of; (A) Emulsions stabilised by HPD surfactants comprised of increasing increments of G_2 Bz (50 and 100 %) content at t=0 and t=1day after a 10-fold dilution (B); Emulsions stabilised by HPD surfactants comprised of increasing increments of G_2 Mp (50 and 100 %) content at t=0 and t=1 day after a 10-fold dilution

5.8 Thermal study of emulsions stabilised by branched polymer, HPDs or branched polymer/HPD surfactant at natural pH

In this final study, the effect of increasing temperature was examined on emulsions stabilised by a branched polymer, HPDs or branched polymer/HPD surfactant. Selected emulsion samples were chosen from the previous long term stability study, Table 5.6. These included emulsion **E10** as the comparable reference, stabilised by a branched polymer surfactant comprised of 100% dodecyl chain ends, emulsions **E20** and **E22**, stabilised by mixed HPD and HPD surfactants comprised of increasing increments of G_2 Bz (50 and 100 %), and finally, emulsions **E24** and **E26**, stabilised by mixed HPD and HPD surfactants comprised of increasing increments of G_2 Mp (50 and 100 %), Table 5.10.

Each emulsion was clamped in an oil bath, and heated for 1 hour at 60 °C (without stirring). Visual observations were made before and after the heating period.

Visual observations of each emulsion in Table 5.10 indicated no phase separated oil before heating, but the presence of phase separated oil (approx.0.5 mm) after heating. Digital images in Figure 5.31 (A) and (B) show emulsions **E20** and **E24** stabilised by HPDs comprised of 50 % G_2 Bz and 50% dodecyl (**E20**) and 50 % G_2 Mp and 50% dodecyl (**E24**) before and after heating, illustrating the presence of phase separated oil.

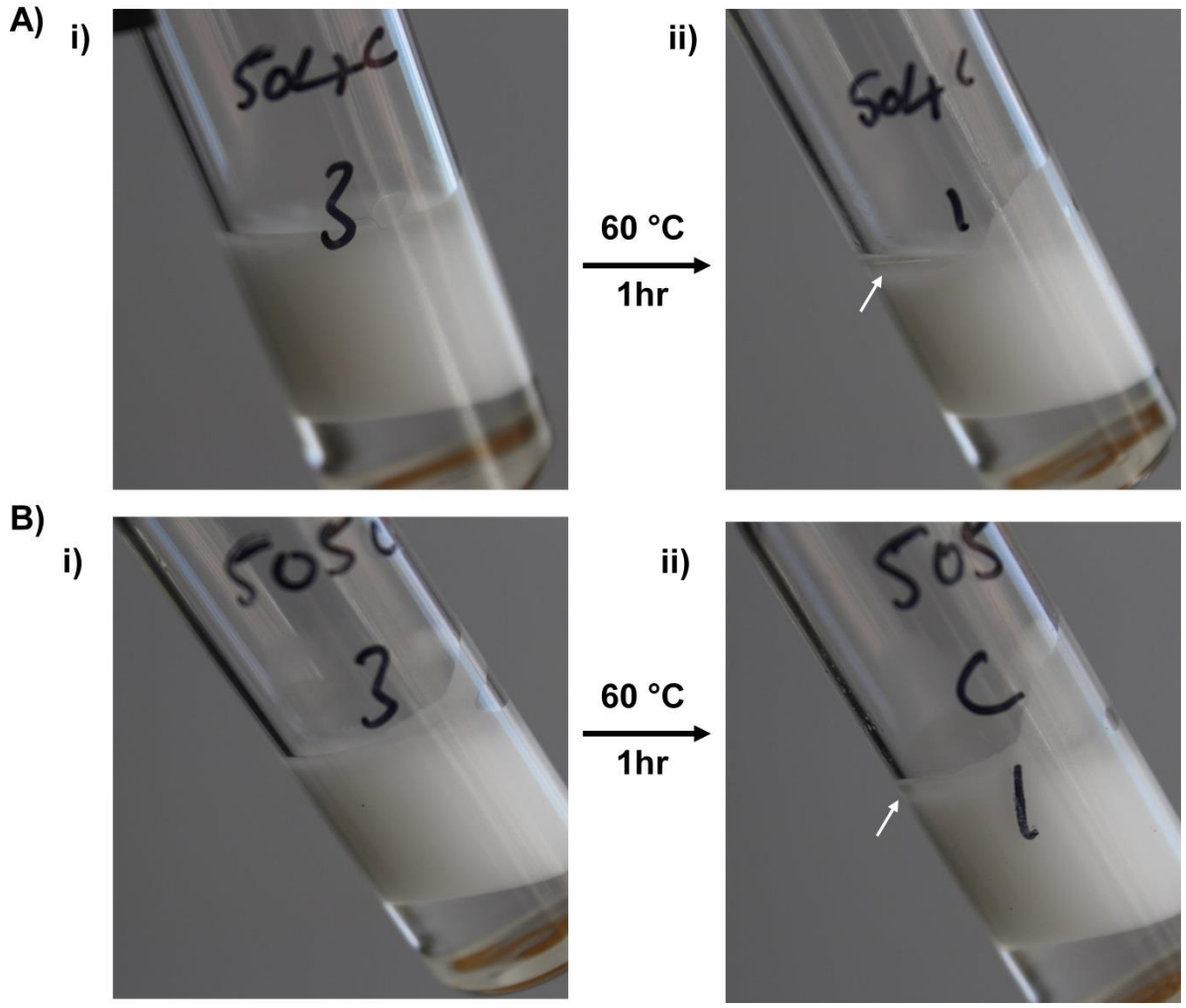

Figure 5.31 Digital images of (A) Emulsion **E20** stabilised by a stabilised by HPDs comprised of 50 % G_2 Bz and 50% dodecyl (i) at t=0; (ii) after heating for 1 hour at 60 °C; (B) Emulsion **E24** stabilised by a stabilised by HPDs comprised of 50 % G_2 Mp and 50% dodecyl (i) at t=0; (ii) after heating for 1 hour at 60 °C. The white arrows direct the presence of oil phase separation.

Analysis of the emulsions after heating by laser diffraction indicated a slight decrease in droplet sizes for emulsions stabilised with branched polymer dodecyl chain ends and HPDs containing G_2 Bz chain ends, Figure 5.32 (A). Droplet sizes of emulsions stabilised using HPDs containing G_2 Mp chain ends, showed a slight decrease in D[4,3] at 50% composition, but a D[4,3] increase at 100% composition, Figure 5.32 (B).

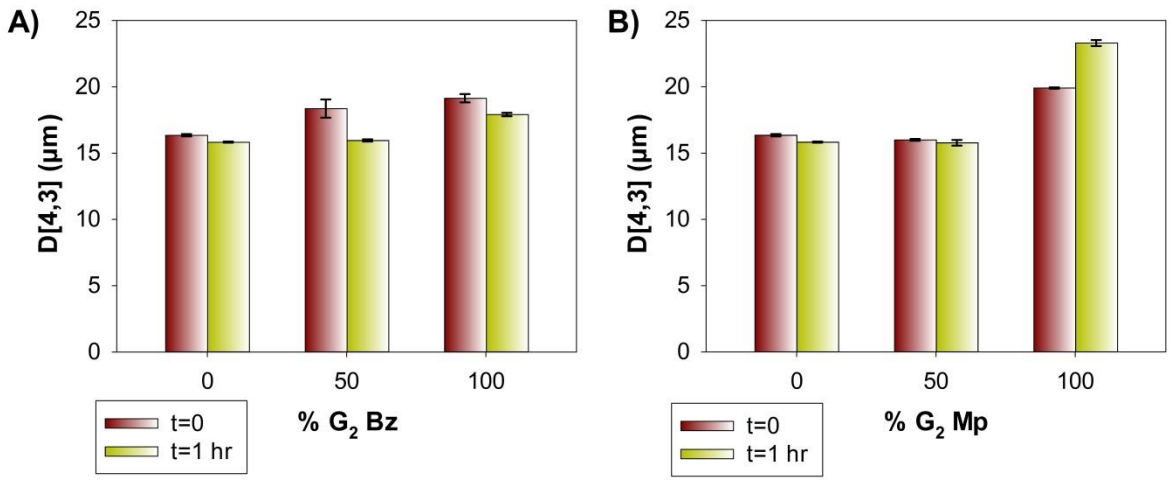

Figure 5.32 Bar charts showing D[4,3] of; (A) Emulsions stabilised by HPD surfactants comprised of increasing increments of G_2 Bz (50 and 100 %) content at t=0 and t=1hour after heating at 60 °C; (B); Emulsions stabilised by HPD surfactants comprised of increasing increments of G_2 Mp (50 and 100 %) content at t=0 and t=1hour after heating at 60 °C.

In an early example of shell cross-linked micelles with tunable hydrophilic/hydrophobic cores, the authors showed that the characteristics of a N-(morpholino)ethyl methacrylate (MEMA) segment of a diblock copolymer can exhibit temperature solubility behaviour.[13] At 60 °C, the MEMA segment was hydrophobic, thus allowing micelles with dehydrated cores, but by cooling to 25 °C, the MEMA segment became hydrophilic, allowing micelles with hydrated cores, and hence an observed increase in size. Although these observations may not be directly applicable to these emulsion systems, this reference does show that morpholino functionalities have been reported to have temperature

dependant properties. Although slight demulsification was seen, the samples were remarkably robust and emulsions of this type may benefit from future studies, allowing potentially thermoresponsive emulsion systems to be developed.

5.9 Conclusions

The synthesis of four dendritic macroinitiators were synthesised with both hydrophobic and pH responsive peripheral functionalities using one-pot xanthate deprotection and thiol Michael addition chemistry. Using each macroinitiator, polymeric surfactants comprised of LDHs and HPDs were prepared, along with more complex architectures comprised of linear polymers, mixed LDHs, branched polymers and mixed HPDs, which varied in end group composition through the use of a mixed initiating system, using a non-dendritic component.

O/w emulsions stabilised by surfactants comprised of linear polymers, LDHs, or mixed linear polymers/LDHs architectures showed coalescence over a long term stability study under neutral and acid conditions. In comparison, o/w emulsions stabilised by surfactants comprised of branched polymers, HPDs, or mixed branched polymer/HPDs architectures showed no coalescence over a long term stability study under neutral and acid conditions. The most probable explanation for the enhanced stability with the branched polymer systems may be the large number of end-groups, which are "locked" together aiding greater oil droplet stabilisation.

Analysis of the D[4,3] of emulsions stabilised using surfactants comprised of mixed branched polymer/HPDs and HPDs architectures showed a few interesting droplet size variations. Arguably the most interesting trend was under neutral pH conditions, after 1 day. A linear increase in emulsion droplet D[4,3] was observed across the surfactant series when the surfactant architecture was changed by removing branched dodecyl chain ends, and replacing them with dendritic G_2 Bz chain ends. This suggested that as the dendritic content was increased, the ability for the surfactant to stabilise an emulsion droplet was reduced; although over time (50 days), the D[4,3] of the emulsion droplets did appear to get more uniform.

In the final study, emulsions stabilised using surfactants comprised of mixed branched polymer/HPDs and HPDs architectures were probed with both thermal and dilution experiments. In both cases, emulsion breakdown by coalescence resulted. This concluded that emulsions comprised of mixed branched polymer/HPDs and HPDs architectures were not stable to significant changes in concentration or temperature.

5.10 References

1. J. V. M. Weaver, S. P. Rannard and A. I. Cooper, *Angewandte Chemie International Edition*, 2009, **48**, 2131-2134.
2. R. T. Woodward, R. A. Slater, S. Higgins, S. P. Rannard, A. I. Cooper, B. J. L. Royles, P. H. Findlay and J. V. M. Weaver, *Chemical Communications*, 2009, 3554-3556.
3. F. Isaure, P. A. G. Cormack, S. Graham, D. C. Sherrington, S. P. Armes and V. Butun, *Chemical Communications*, 2004, 1138-1139.
4. Y. Li and S. P. Armes, *Macromolecules*, 2005, **38**, 8155-8162.
5. I. Bannister, N. C. Billingham, S. P. Armes, S. P. Rannard and P. Findlay, *Macromolecules*, 2006, **39**, 7483-7492.
6. J. Rosselgong, S. P. Armes, W. R. S. Barton and D. Price, *Macromolecules*, 2010, **43**, 2145-2156.
7. T. He, D. J. Adams, M. F. Butler, C. T. Yeoh, A. I. Cooper and S. P. Rannard, *Angewandte Chemie International Edition*, 2007, **46**, 9243-9247.
8. T. He, D. J. Adams, M. F. Butler, A. I. Cooper and S. P. Rannard, *Journal of the American Chemical Society*, 2009, **131**, 1495-1501.
9. R. A. Slater, T. O. McDonald, D. J. Adams, E. R. Draper, J. V. M. Weaver and S. P. Rannard, *Soft Matter*, 2012, **8**, 9816-9827.
10. F. L. Hatton, P. Chambon, T. O. McDonald, A. Owen and S. P. Rannard, *Chemical Science*, 2014, **5**, 1844-1853.
11. N. Kubota, T. Fukuo and R. Akawa, *Journal of the American Society for Mass Spectrometry*, 1999, **10**, 557-560.
12. S. Flynn, MChem Research Project, Rannard Group, 2014.
13. V. Bütün, N. C. Billingham and S. P. Armes, *Journal of the American Chemical Society*, 1998, **120**, 12135-12136.

CHAPTER 6

Experimental

6.1 Materials and Methods

6.1.1 Materials

All compounds were purchased from Sigma Aldrich unless otherwise stated and were used without further purification. 2-(Dimethylamino)ethyl acrylate, 2-bromoacetic acid, pyridine (anhydrous), 4-dimethylaminopyridine (DMAP), hydroxyethyl acrylate and N,N′-dicyclohexylcarbodiimide (DCC) were purchased from Alfa Aesar and were used without further purification. Para-toluene sulfonyl ethanol (*P*-TSe) was purchased from Fluorochem. HPLC grade dichloromethane, acetone, pet ether (30-40°C), hexane and ethyl acetate were supplied by Fisher Scientific. Analytical TLC was performed on commercial Merck plates coated with silica gel. Flash chromatography was performed using a Grace Reveleris flash system with 80 g Silica Reveleris flash cartridges.

6.1.2 Methods

Nuclear magnetic resonance (NMR) spectra were collected using a Bruker Avance 400 MHz. ^{1}H Spectra were recorded at 400 MHz and ^{13}C spectra were recorded at 100 MHz. $CDCl_3$ and CD_3OD containing tetramethylsilane (TMS) purchased from Goss Scientific were used as NMR solvents. Chemical shifts (δ) are reported in parts per million (ppm) and TMS was used as an internal standard for both ^{1}H and ^{13}C spectra. Electrospray mass spectrometry data was obtained using a MicroMass LCT mass spectrometer using Electron ionisation and direct infusion syringe pump sampling. All samples were diluted with methanol. Elemental analyses were recorded in the Microanalytical Laboratory at the University of Liverpool. Size Exclusion Chromatography (SEC) was carried out using a Malvern Viscotek SEC Max connected to a Viscotek 270 Light Scattering detector, Viscometer and Refractive index (RI) triple detection system. HPLC grade tetrahydrofuran THF (Fisher) containing 2% triethylamine (Sigma Aldrich) was used as the eluent, with a flow rate of 1mL/min. SEC Columns were mixed bed columns supplied by Viscotek. The column oven was set at 35 °C. The obtained spectra were analyzed using Malvern OmiSec software calibrated by a universal calibration calculation relative to a narrow linear polystyrene standard (105k). Matrix-assisted laser desorption/ionization - time of flight mass spectrometry (MALDI-TOF) sample solutions were

prepared with a 2 mg/ml concentration in THF. Matrix solution was prepared at a concentration of 10mg/ml in THF and a 1mg/ml NA counter ion solution was prepared. 5 µl of sample solution, 20 µl of matrix solution and 1.5 µl of counter ion was added to a eppendorf sample tube and homogenized. Solution was deposited on a stainless steel sample plate and the solvent allowed to evaporate. Spectrum acquisitions were conducted on a Bruker UltraFlex MALDI-TOF with SCOUT-MTP Ion Source (Bruker Daltonics, Bremen) equipped with a N_2-laser (337nm), a grid less ion source and reflector design. All spectra were acquired using a reflector-positive method with an acceleration voltage of 25 kV and a reflector voltage of 26,3 kV. The detector mass range was set to exclude everything under 1000 Da in order to exclude high intensity peaks from the lower mass range. A total of 1000 shots were performed per sample and the laser intensity was set to the lowest possible value for acquisition of high resolution spectra. The instrument was calibrated using SpheriCalTM calibrants purchased from Polymer Factory Sweden AB. The obtained spectra were analyzed with FlexAnalysis Bruker Daltonics, Bremen, version 2.2.

6.2 Chapter 2 compounds

[**Am_6-TAEA-G_1];[3]** – Tris(2-aminoethyl)amine (TAEA) (0.5 g, 3.42 mmol, 1 equiv.) was dissolved in 5 mL 2-propanol and degassed with nitrogen for 10 minutes. Dropwise, 2-(dimethylamino)ethyl acrylate (DMAEA) (4.67 mL, 30.78 mmol, 9 equiv.) was added to the solution, and the mixture left stirring sealed under nitrogen at ambient temperature for 24 hours. The product was isolated by removing the solvent and excess reagents by high vacuum overnight at 40 °C. Yield: 2.90 g, yellow viscous oil, (84%). ^{1}H NMR (400 MHz, $CDCl_3$): δ = 2.29 (s, 36H), 2.40-3.00 (m, 48H), 4.17 (t, 12H). ^{13}C NMR (100 MHz, $CDCl_3$): δ = 32.50, 45.76, 49.58, 53.19, 53.46, 57.80, 62.17, 172.53. Calcd: $[M+H]^+$ ($C_{48}H_{97}N_{10}O_{12}$) m/z = 1005.7. Found: ESI-MS: $[M+H]^+$ m/z = 1005.7. Anal. Calcd for $C_{48}H_{96}N_{10}O_{12}$: C, 57.35; H, 9.62; S, 13.93. Found: C, 57.58; H, 9.68; N, 14.33.

[**Bz_6-TAEA-G_1];[4]** – Tris(2-aminoethyl)amine (TAEA) (0.5 g, 3.42 mmol, 1 equiv.) was dissolved in 5 mL 2-propanol and degassed with nitrogen for 10 minutes. Dropwise, benzyl acrylate (BA) (4.71

mL, 30.78 mmol, 9 equiv.) was added to the solution, and the mixture left stirring sealed under nitrogen at ambient temperature for 24 hours. The product was isolated by removing the solvent and excess reagents by high vacuum overnight at 40 °C, resulting in a pale yellow oil. ^{1}H NMR (400 MHz, $CDCl_3$): δ = 2.37-2.92 (m, 36H), 5.09 (s, 12H), 7.27-7.40 (m, 30H). ^{13}C NMR (100 MHz, $CDCl_3$): δ = 32.74, 49.75, 52.17, 53.10, 66.20, 128.19, 128.27, 128.32, 128.53, 128.58, 135.98, 172.30. Calcd: $[M+H]^+$ ($C_{66}H_{78}N_4O_{12}$) m/z = 1119.6. Found: ESI-MS: $[M+H]^+$ m/z = 1119.6.

[Bz_2-IPLA-G_1];[5] - Isopropanolamine (0.5 g, 6.66 mmol, 1 equiv.) was dissolved in 5 mL 2-propanol and degassed with nitrogen for 10 minutes. Dropwise, benzyl acetate (BA) (3.06 mL, 19.97 mmol, 3 equiv.) was added to the solution, and the mixture left stirring sealed under nitrogen at ambient temperature for 24 hours. The product was isolated by removing the solvent and excess reagents by high vacuum overnight at 40 °C. Yield: 2.50 g, pale yellow viscous oil, (94%). ^{1}H NMR (400 MHz, $CDCl_3$): δ = 1.08 (d, 3H), 2.16-2.56 (m, 6H), 2.70 (m, 2H), 2.90 (m, 2H), 3.20 (s, br, OH), 3.78 (m, 1H), 5.10 (s, 4H), 7.28-7.40 (m, 10H). ^{13}C NMR (100 MHz, $CDCl_3$): δ = 19.60, 32.69, 49.56, 62.48, 63.61, 66.46, 128.32, 128.44, 128.59, 135.80, 172.31. Calcd: $[M+H]^+$ ($C_{23}H_{30}NO_5$) m/z = 400.2. Found: CI-MS: $[M+H]^+$ m/z = 400.21. Anal. Calcd for $C_{23}H_{29}NO_5$: C, 69.15; H, 7.32; N, 3.51. Found: C, 68.93; H, 7.30; N, 3.47.

[Am_2-IPLA-G_1];[6] - Isopropanolamine (0.5 g, 6.66 mmol, 1 equiv.) was dissolved in 5 mL 2-propanol and degassed with nitrogen for 10 minutes. Dropwise, 2-(dimethylamino)ethyl acrylate (DMAEA) (3.03 mL, 19.97 mmol, 3 equiv.) was added to the solution, and the mixture left stirring sealed under nitrogen at ambient temperature for 24 hours. The product was isolated by removing the solvent and excess reagents by high vacuum overnight at 40 °C. Yield: 1.97 g, yellow viscous oil, (82%). ^{1}H NMR (400 MHz, $CDCl_3$): δ = 1.10 (d, 3H), 2.23 (m, 1H), 2.28 (s, 12H), 2.41 (m, 1H), 2.49 (t, 4H), 2.56 (t, 4H), 2.70 (m, 2H), 2.90 (m, 2H), 3.79 (m, 1H), 4.18 (m, 4H). ^{13}C NMR (100 MHz, $CDCl_3$): δ = 20.03, 32.85, 45.88, 58.09, 62.40, 62.76, 63.97, 172.90. Calcd: $[M+H]^+$ ($C_{17}H_{36}N_3O_5$) m/z = 362.3. Found: ESI-MS: $[M+H]^+$ m/z = 362.3. Anal. Calcd for $C_{17}H_{35}N_3O_5$: C, 56.49; H, 9.76; N, 11.62. Found: C, 56.50; H, 9.83; N, 11.55.

[^{t}BOC$_2$-BAPA-G$_1$];[9] - CDI (39.14 g, 0.241 mol) was added to an oven-dried 500mL 2-neck RBF fitted with a reflux condenser, magnetic stirrer and a dry N_2 inlet. 350 mL of anhydrous toluene was added and the flask purged with N_2 for 10 minutes. The solution was stirred at 60 °C and tertiary butanol (35.7 g, 46 mL, 0.483 mol) added via a warm syringe. The mixture was left stirring at 60 °C for 4 hours under a positive flow of nitrogen. Bis(3-aminopropyl)amine (BAPA) (16.077 g, 17.14 mL, 0.121 mol) was added dropwise, and the reaction was left stirring for a further 18 hours at 60°C under a positive flow of nitrogen. Following this, the solution was allowed to cool to room temperature, and the pale yellow solution was filtered to remove any solid imidazole, and concentrated *in vacuo*. The resulting viscous oil was dissolved in dichloromethane (300 mL) washed with distilled water (2 x 200 mL) and once with brine (150 mL). The organic layer was dried with anhydrous Na_2SO_4, filtered, and concentrated *in vacuo*. Yield: 38 g, white solid, (95%). ^{1}H NMR (400 MHz, $CDCl_3$): δ = 1.44 (s, 18H), 1.65 (m, 4H), 2.65 (t, 4H), 3.21 (t, 4H), 5.19 (s, br, NH – disappears on addition of D_2O). ^{13}C NMR (100 MHz, $CDCl_3$): δ = 28.79, 30.11, 39.29, 47.78, 79.34, 156.48. Calcd: $[M+H]^+$ ($C_{16}H_{34}N_3O_4$) m/z = 332.3. Found: ESI-MS: $[M+H]^+$ m/z = 332.3. Anal. Calcd for $C_{16}H_{33}N_3O_4$: C, 57.98; H, 10.04; N, 12.68. Found: C, 57.84; H, 10.45; N, 12.91.

[^{t}BOC$_2$-APAP-G$_1$];[10] - [9] (20g, 0.06 mol) was added to a 500 mL 2-necked RBF fitted with a reflux condenser, magnetic stirrer and a dry N_2 inlet. The flask was degassed with dry nitrogen for 10 minutes, and dissolved in 200 mL dry ethanol. Whilst stirring, and maintaining the temperature at 30 °C, propylene oxide (10.51g, 11.21mL, 0.181 mol) was added dropwise to the solution over a period of 10 minutes. Under a positive flow of dry N_2, the reaction was left stirring at 30 °C for 18 hours. After this time, the solvent and excess propylene oxide were removed *in vacuo*, and the crude product purified by liquid chromatography (silica gel, eluting with EtOAc:MeOH, 80:20). Yield: 19.90 g, pale yellow oil at ambient temperature, solidifying to an off white solid upon cooling (85%). ^{1}H NMR (400 MHz, $CDCl_3$): δ = 1.11 (d, 3H), 1.44 (s, 18H), 1.62 (m, 4H), 2.61-2.88 (m, 6H), 3.15 (m, 4H), 3.76 (m, 1H), 4.93 (s, br, NH). ^{13}C NMR (100 MHz, $CDCl_3$): δ = 20.14, 27.47, 28.43, 38.75, 51.76, 62.55, 63.45, 79.18, 156.08. Calcd: $[M+H]^+$ ($C_{19}H_{41}N_3O_5$) m/z = 390.3. Found: ESI-MS: $[M+H]^+$ m/z

= 390.3. Anal. Calcd for $C_{19}H_{40}N_3O_5$: C, 58.58; H, 10.09; N, 10.79. Found: C, 58.50; H, 10.19; N, 10.82.

1-[N, N-bis (2-aminopropyl)-amino]-2-propanol;[APAP] - To a 1000 mL RBF, [10] (33.70g) was dissolved in 300 mL of ethyl acetate, and concentrated HCl (35.03g, 30mL, d=1.18, 36% active) added very slowly. CO_2 began to rapidly evolve. The reaction vessel was left open to the atmosphere, and stirred vigorously for 6 hours. After concentration *in vacuo*, to remove the solvents, the remaining oil was analysed by ^{1}H NMR (D_2O). ^{1}H NMR analysis confirmed incomplete decarboxylation; hence the oil was re-dissolved in 300 mL ethyl acetate and heated to 50 °C for a further 5 hours. After removal of ethyl acetate *in vacuo*, ^{1}H NMR (D_2O) confirmed complete decarboxylation and formation of **APAP3HCl.**

For the formation of [**APAP]**, the crude oil was dissolved very slowly in 4M NaOH (300 mL), and reduced by approximately half its volume on the rotary evaporator (60°C). A yellow oily substance formed on the surface of the NaOH solution. The mixture was extracted with $CHCl_3$ (2 x 300mL), the organic layers combined, dried with anhydrous Na_2SO_4, filtered, and concentrated *in vacuo*. Yield: 15.27 g, pale yellow oil (94%). ^{1}H NMR (400 MHz, $CDCl_3$): δ = 1.11 (d, 3H), 1.60 (m, 4H), 1.89 (s, br, OH), 2.31 (m, 4H), 2.40-2.68 (m, 4H), 2.76 (t, 4H), 3.78 (m, 1H). ^{13}C NMR (100 MHz, $CDCl_3$): δ = 20.03, 30.80, 40.31, 52.10, 62.56, 63.95. Calcd: $[M+H]^+$ ($C_9H_{24}N_3O$) m/z = 190.2. Found: CI-MS: $[M+H]^+$ m/z = 190.3. Anal. Calcd for $C_9H_{23}N_3O$: C, 57.10; H, 12.25; N, 22.20 Found: C, 55.18; H, 12.15; N, 20.53.

[Bz_4-APAP-G_2];[11] - APAP (0.5 g, 2.64 mmol, 1 equiv.) was dissolved in 5 mL 2-propanol and degassed with nitrogen for 10 minutes. Dropwise, benzyl acrylate (BA) (2.42 mL, 15.84 mmol, 6 equiv.) was added to the solution, and the mixture left stirring sealed under nitrogen at ambient temperature for 24 hours. The product was isolated by removing the solvent and excess reagents by high vacuum overnight at 40 °C. Yield: 1.79 g, yellow viscous oil, (87%). ^{1}H NMR (400 MHz, $CDCl_3$): δ = 1.07 (d, 3H), 1.53 (m, 4H), 2.28 (s, 24H), 2.10-2.60 (m, 20H), 2.76 (t, 8H), 3.72 (m, 1H), 5.09 (s, 8H), 7.26-7.39 (m, 20H). ^{13}C NMR (100 MHz, $CDCl_3$): δ = 19.92, 24.62, 32.44, 49.08, 51.66,

52.11, 62.27, 63.53, 66.22, 128.20, 128.25, 128.54, 135.97, 172.36. Calcd: $[M+H]^+$ ($C_{49}H_{64}N_3O_9$) m/z = 838.5. ESI-MS: $[M+H]^+$ m/z = 838.5. Anal. Calcd for $C_{49}H_{63}N_3O_9$: C, 70.23; H, 7.58; N, 5.01. Found: C, 70.85; H, 7.68; N, 5.10.

[Am_4-APAP-G_2];[12] - APAP (0.5 g, 2.64 mmol, 1 equiv.) was dissolved in 5 mL 2-propanol and degassed with nitrogen for 10 minutes. Dropwise, 2-(dimethylamino)ethyl acrylate (DMAEA) (2.41 mL, 15.84 mmol, 6 equiv.) was added to the solution, and the mixture left stirring sealed under nitrogen at ambient temperature for 24 hours. The product was isolated by removing the solvent and excess reagents by high vacuum overnight at 40 °C. Yield: 1.79 g, yellow viscous oil, (89%). ^{1}H NMR (400 MHz, $CDCl_3$): δ = 1.10 (d, 3H), 1.57 (m, 4H), 2.28 (s, 24H), 2.31-2.62 (m, 26H), 2.77 (t, 8H), 3.74 (m, 1H), 4.17 (t, 8H). ^{13}C NMR (100 MHz, $CDCl_3$): δ = 19.98, 24.57, 32.21, 45.71, 48.95, 51.62, 52.14, 57.78, 62.15, 62.29, 63.59, 172.58. Calcd: $[M+H]^+$ ($C_{37}H_{76}N_7O_9$) m/z = 762.6. Found: ESI-MS: $[M+H]^+$ m/z = 762.6. Anal. Calcd for $C_{37}H_{76}N_7O_9$: C, 58.32; H, 9.92; N, 12.87. Found: C, 58.49; H, 10.03; N, 12.93.

[^{t}BOC$_4$-APAP$_3$-G_2];[14]- CDI (0.42 g, 2.57 mmol, 1 equiv.) was added to an oven-dried 100mL 2-neck RBF fitted with a reflux condenser, magnetic stirrer and a dry N_2 inlet. 20 mL of anhydrous toluene was added and the flask purged with N_2 for 10 minutes. The solution was stirred at 60 °C and [10] (1.0 g, 2.57 mmol, 1 equiv.) added. The mixture was left stirring at 60 °C for 4 hours under a positive flow of nitrogen. After confirmation of the intermediate species by TLC, APAP (0.243 g, 1.28 mmol, 0.5 equiv.) was added dropwise, and the reaction was left stirring for a further 18 hours at 60°C under a positive flow of nitrogen. Following this, the solution was allowed to cool to room temperature, and the pale yellow solution was filtered to remove any solid imidazole, and concentrated *in vacuo*. The resulting viscous oil was dissolved in dichloromethane (60mL) washed with distilled water (3 x 40 mL) and with brine (1 x 40 mL). The organic layer was dried with anhydrous Na_2SO_4, filtered, and concentrated *in vacuo*. Yield: 1.03 g, colourless glass, (78%). ^{1}H NMR (400 MHz, $CDCl_3$): δ = 1.11 (m, br, 3H), 1.21 (m, br, 6H), 1.44 (s, br, 36H), 1.52-1.88 (m, br, 12H), 2.09-2.85 (m, br, 18H), 3.76 (m, br, 1H), 4.93 (m, br, 2H). ^{13}C NMR (100 MHz, $CDCl_3$): δ = 18.82, 20.17, 27.43, 28.49, 38.92, 51.73, 52.33, 59.36, 62.47, 63.52, 68.53, 78.89, 156.15, 156.78 .

Calcd: $[M+H]^+$ ($C_{49}H_{98}N_9O_{13}$) m/z = 1020.7. Found: ESI-MS: $[M+H]^+$ m/z = 1020.7, $[M+Na^+]$ m/z = 1042.7, $[M+K^+]$ m/z = 1058.7.

[APAP$_3$-G$_2$];[16] - To a 50 mL RBF, [14] (0.225 g, 1 equiv.) was dissolved in 10 mL of ethyl acetate, and concentrated HCl (0.15 mL, 1.76 mmol, 36% active, 8 equiv.) added very slowly. CO_2 began to rapidly evolve. The reaction was stirred vigorously for 3 hours at 50 °C. The resulting oil was analysed by ^{1}H NMR (D_2O). ^{1}H NMR (D_2O) confirmed complete decarboxylation and formation of **[HCl.APAP$_3$-G$_2$];[15]**. For the formation of **[16]**, the crude oil was dissolved very slowly in 4M NaOH (5 mL), and reduced by approximately half its volume on the rotary evaporator (60°C). A yellow oily substance formed on the surface of the NaOH solution. The mixture was extracted with $CHCl_3$ (3 x 10mL), the organic layers combined, dried with anhydrous Na_2SO_4, filtered, and concentrated *in vacuo*. Yield: 0.12 g, viscous yellow oil (86%). ^{1}H NMR (400 MHz, $CDCl_3$): δ = 1.11 (d, br, 3H), 1.20 (d, br, 6H), 1.46-2.02, (m, br, 12H), 2.17-2.85 (m, br, 30H), 3.21 (m, br, 4H), 3.81 (m, br, 1H), 4.89 (m, br, 2H). ^{13}C NMR (100 MHz, $CDCl_3$): δ = 18.83, 27.20, 30.65, 32.64, 39.31, 40.26, 40.52, 47.39, 50.38, 52.32, 52.89, 56.27, 59.43, 62.44, 63.99, 69.06, 156.60. Calcd: $[M+H]^+$ ($C_{29}H_{66}N_9O_5$) m/z = 620.5. Found: ESI-MS: $[M+H]^+$ m/z = 620.5.

[Bz$_8$-APAP$_3$-G$_3$];[17] – [16] (0.2 g, 0.32 mmol, 1 equiv.) was dissolved in 5 mL 2-propanol and degassed with nitrogen for 10 minutes. Dropwise, benzyl acrylate (BA) (0.98 mL, 6.4 mmol, 20 equiv.) was added to the solution, and the mixture left stirring sealed under nitrogen at ambient temperature for 5 days. The product was isolated by removing the solvent and excess reagents by high vacuum overnight at 40 °C. Yield: 0.431 g, yellow viscous oil, (71%). ^{1}H NMR (400 MHz, $CDCl_3$): δ = 1.07 (d, 6H), 1.16 (d, 3H), 1.39-1.74 (m, br, 12H), 2.02-2.60 (m, br, 46H), 2.76 (t, 16H), 2.97-3.28 (m, br, 4H), 3.68 (m, br, 2H), 4.81 (m, br, 1H), 5.08 (s, 16H), 7.27-7.40 (m, 40H). ^{13}C NMR (100 MHz, $CDCl_3$): δ = 18.87, 19.91, 24.58, 24.81, 25.61, 30.93, 32.41, 32.57, 49.06, 49.19, 51.63, 51.77, 52.06, 52.73, 61.93, 63.51, 66.20, 66.97, 128.19, 128.21, 128.53, 135.94, 156.42, 172.36, 172.46. Calcd: $[M+2H]^+$ ($C_{109}H_{147}N_9O_{21}$) m/z = 1918.1. Found: CI-MS: $[M+2H]^{2+}$ m/z = 959.03.

[Am_8-$APAP_3$-G_3];[18] – [16] (0.2 g, 0.32 mmol, 1 equiv.) was dissolved in 5 mL 2-propanol and degassed with nitrogen for 10 minutes. Dropwise, 2-(dimethylamino)ethyl acrylate (DMAEA) (0.97 mL, 6.4 mmol, 20 equiv.) was added to the solution, and the mixture left stirring sealed under nitrogen at ambient temperature for 5 days. The product was isolated by removing the solvent and excess reagents by high vacuum overnight at 40 °C. Yield: 0.41 g, yellow viscous oil, (73%). ^{1}H NMR (400 MHz, $CDCl_3$): δ = 1.11 (d, 6H), 1.19 (d, 3H), 1.40-1.73 (m, br, 12H), 2.28 (s, 48H), 2.33-2.64 (m, br, 62H), 2.77 (t,16H), 3.74 (m, br, 2H), 4.17 (t, 16H), 4.83 (m, 1H). ^{13}C NMR (100 MHz, $CDCl_3$): δ = 18.91, 20.00, 24.55, 25.59, 28.43, 30.93, 32.19, 32.34, 45.42, 45.73, 48.94, 49.09, 51.64, 52.14, 57.78, 62.14, 62.28, 63.65, 67.98, 172.63, 172.72. Calcd: $[M+2H]^+$ ($C_{85}H_{171}N_{17}O_{21}$) m/z = 1766.3. Found: CI-MS: $[M+2H]^{2+}$ m/z = 883.14.

Asymmetric disulfide;[22] - 3,3'-Dithiodipropionic acid (3.574 g, 17.0 mmol, 1 equiv.) was added to an oven-dried 250 mL 2-neck RBF fitted with a reflux condenser, magnetic stirrer and a dry N_2 inlet. 100 mL of anhydrous THF was added and the flask purged with N_2 for 10 minutes. The solution was stirred at 35 °C and CDI (2.90 g, 17.90 mmol, 1 equiv.) added slowly in portions. [NOTE: CO_2 evolved quickly when CDI was added; therefore it is best to add slowly in portions]. The mixture was left stirring at 35 °C for 4 hours under a positive flow of nitrogen. After confirmation of the intermediate species by TLC, the solution was purged well with nitrogen to remove traces of CO_2 and 4-tert butyl amine (0.99 mL, 5.63 mmol, 0.33 equiv.) added dropwise. The reaction was left stirring for a further 18 hours at 35 °C under a positive flow of nitrogen. After 18 hours, the solution was concentrated *in vacuo*, and the resulting viscous oil dissolved in dichloromethane (100mL), washed with 0.5M HCl (2 x 50 mL), Na_2CO_3 (2 x 50mL) and brine (1 x 50 mL). The organic layer was dried with anhydrous Na_2SO_4, filtered, concentrated *in vacuo*, and the crude product purified by liquid chromatography (silica gel, eluting with dichloromethane increasing to dichloromethane/methanol, 90:10). Yield: 0.80 g, white solid, (40%). ^{1}H NMR (400 MHz, $CDCl_3$): δ = 1.31 (s, 9H), 2.62 (t, *J* = 7.4 Hz, 2H), 2.75 (t, *J* = 7.2 Hz, 2H), 2.93 (t, *J* = 7.2 Hz, 2H), 3.00 (t, *J* = 7.4 Hz, 2H), 3.95 (s, br, COO*H*), 4.42 (s, 2H), 7.22 (d, 2H), 7.36 (d, 2H). ^{13}C NMR (100 MHz, $CDCl_3$): δ = 31.33, 33.31,

33.77, 34.11, 34.54, 35.92, 43.54, 125.69, 127.71, 134.76, 150.69, 171.05, 175.81. Calcd: $[M+Na]^+$ ($C_{17}H_{25}NNaO_3S_2$) m/z = 378.1. Found: ESI-MS: $[M+Na]^+$ m/z = 378.1

[Sngr-SH-COOH];[27] - 1-Fluoro-2,4-dinitrobenzene (3.41 g, 18.3 mmol, 1 equiv.) and triethylamine (7.66 mL, 54.9 mmol, 3 equiv.) were dissolved in 30 mL of dichloromethane under a nitrogen atmosphere. 11-Mercaptoundecanoic acid (4 g, 18.3 mmol, 1 equiv.) in 20 mL dichloromethane was added dropwise to the solution, and the resulting orange solution left stirring at ambient temperature for 16 hours. The product was isolated by washing the mixture with 1M HCl (1 x 50 mL) and H_2O (2 x 50 mL), which resulted in a yellow solid that was separated by bückner filtration. The yellow solid was recrystallized twice from hot chloroform, rinsed once with water, and dried under high vacuum overnight. Yield: 4.60 g, yellow solid, (65%). ^{1}H NMR (400 MHz, $CDCl_3$): δ = 1.23-1.88 (m, br, 16H), 2.35 (t, *J* = 7.4 Hz, 2H), 3.04 (t, *J* = 7.5 Hz, 2H), 7.55 (d, *J* = 9.0 Hz, 1H), 8.37 (dd, *J* = 2.5 Hz, *J* = 9.0 Hz, 1H), 9.09 (d, *J* = 2.5 Hz, 1H). ^{13}C NMR (100 MHz, $CDCl_3$): δ = 24.66, 27.47, 28.99, 29.07, 29.15, 29.26, 29.29, 32.72, 33.75, 121.80, 126.81, 126.98, 143.67, 144.86, 147.56, 178.28.

[Sngr$_2$-SH-APAP];[29] – [27] (5 g, 13.0 mmol, 1 equiv.) was added to an oven-dried 250 mL 2-neck RBF fitted with a reflux condenser, magnetic stirrer and a dry N_2 inlet. 80 mL of anhydrous THF was added and the flask purged with N_2 for 10 minutes. The solution was stirred at 60 °C and CDI (2.11 g, 13.0 mmol, 1 equiv.) added slowly in portions. [NOTE: CO_2 evolved quickly when CDI was added; therefore it is best to add slowly in portions]. The mixture was left stirring at 60 °C for 4 hours under a positive flow of nitrogen. After confirmation of the intermediate species by TLC, [28], the solution was purged well with nitrogen to remove traces of CO_2 and APAP (1.23g, 6.50 mmol, 0.5 equiv.) added dropwise. The reaction was left stirring for a further 18 hours at 60 °C under a positive flow of nitrogen. After 18 hours, the solution was concentrated *in vacuo*, and the resulting viscous oil dissolved in dichloromethane (60 mL), washed with H_2O (3 x 60 mL) and brine (1 x 60 mL). The organic layer was dried with anhydrous Na_2SO_4, filtered, concentrated *in vacuo*, and the crude product recrystallized once from hot methanol. Yield: 4.46 g, yellow solid, (74%). ^{1}H NMR (400 MHz, $CDCl_3$): δ = 1.13 (d, 2H), 1.23-1.88 (m, br, 36H), 2.11-2.43 (m, 8H), 2.61 (m, 2H), 3.04 (t, *J* = 7.5

Hz, 4H), 3.31 (m, 4H), 3.77 (m, 1H), 6.23 (t, br, NH), 7.56 (d, *J* = 9.0 Hz, 2H), 8.37 (dd, *J* = 2.5 Hz, *J* = 9.0 Hz, 2H), 9.10 (d, *J* = 2.5 Hz, 2H). ^{13}C NMR (100 MHz, $CDCl_3$): δ = 20.33, 25.78, 27.13, 27.46, 28.96, 29.08, 29.32, 32.73, 36.71, 37.51, 51.64, 62.43, 63.52, 121.79, 126.88, 127.02, 143.68, 144.85, 147.55, 173.60. Calcd: $[M+H]^+$ ($C_{43}H_{68}N_7O_{11}S_2$) m/z = 922.4. Found: ESI-MS: $[M+H]^+$ m/z = 922.4, $[M+Na^+]$ m/z = 944.4,

[SH_2-APAP];[30] – [29] (0.1 g, 0.11 mmol, 1 equiv.) was dissolved in the minimum amount of DMF (approx. 0.5 mL), and 2 drops of triethylamine added. The vessel was degassed with nitrogen for 10 minutes, dodecanethiol (3.29 g, 16.5 mmol, 150 equiv.) added, and left sealed under nitrogen, stirring vigorously for 18 hours at ambient temperature. The product was purified by precipitating the mixture into hexane, re dissolving the crude oil in 10 mL of chloroform, washing the organic layer with H_2O (2 x 30mL), drying over anhydrous Na_2SO_4 and concentrating *in vacuo*. Yield: 30 mg, dark red oil (40%). ^{1}H NMR (400 MHz, $CDCl_3$): δ = 1.13 (d, 3H), 1.21-1.81 (m, br, 36H), 2.17 (t, *J* = 7.5 Hz, 4H), 2.22-2.43 (m, br, 4H), 2.52 (q, *J* = 7.4 Hz, 4H), 2.61 (m, br, 2H), 3.31 (m, 4H), 3.78 (m, br, 1H), 6.15 (s, br, NH). Calcd: $[M+H]^+$ ($C_{31}H_{64}N_3O_3S_2$) m/z = 590.4. Found: ESI-MS: $[M+H]^+$ m/z = 590.4, $[M+Na^+]$ m/z = 612.3.

[Sngr-SH-NHS];[33] – [27] (1.60 g, 4.15 mmol, 1 equiv.), N-hydroxysuccinicmide (0.48 g, 4.15 mmol, 1 equiv.) and a catalytic amount of DMAP were dissolved in 15 mL of THF. The vessel was degassed with nitrogen for 10 minutes, cooled using an ice bath, and DCC (0.94 g, 4.57 mmol, 1.1 equiv.) dissolved in 10 mL of THF, was added slowly to the mixture. The reaction was sealed under nitrogen, and left stirring at ambient tempernature for 18 hours. The precipitated urea byproduct was removed by filtration and the product purified by liquid chromatography (silica gel, eluting with chloroform gradually increasing to chloroform/acetone 90:10). Yield: 1 g, yellow solid (50%). ^{1}H NMR (400 MHz, $CDCl_3$): δ = 1.23-1.85 (m, br, 16H), 2.60 (t, *J* = 7.4 Hz, 2H), 2.85 (s, br, 4H), 3.04 (t, *J* = 7.4 Hz, 2H), 7.55 (d, *J* = 9.0 Hz, 1H), 8.37 (dd, *J* = 2.5 Hz, *J* = 9.0 Hz, 1H), 9.09 (d, *J* = 2.5 Hz, 1H). Calcd: $[M+Na]^+$ ($C_{21}H_{27}N_3NaO_8S$) m/z = 504.1. Found: ESI-MS: $[M+Na]^+$ m/z = 504.1, $[M+K]^+$ m/z = 520.1.

[Sngr$_4$-SH-APAP$_3$];[32] – [33] (0.26 g, 0.54 mmol, 6 equiv.) was dissolved in 1 mL chloroform, and [APAP$_3$-G$_2$];[16] (56 mg, 0.09 mmol, 1 equiv.) added. The mixture was left stirring for 18 hours at ambient temperature. The compound was purified by adding 3 mL of chloroform, passing through a plugged glass pipette to remove the precipitates, precipitated into 50 mL of ice cold acetone and dried under high vacuum overnight. Yield: 7.3 mg, yellow solid (0.15%). ^{1}H NMR (400 MHz, $CDCl_3$): δ = 1.0-3.37 (m, br, 190H), 4.97 (m, br, 2H), 7.57 (d, 4H), 8.37 (d, 4H), 9.08 (d, 4H).

[OEGA$_2$-S$_2$-APAP];[34]– [30] (30 mg, 0.051 mmol, 1 equiv.), 2-Oligo(ethylene glycol) methyl ether acrylate 480 (OEGA) (49 mg, 1.02 mmol, 2 equiv.) and dimethylphenylphopshine (DMPP) (0.7 mg, 0.005 mmol, 0.1 equiv.) were dissolved in 2 mL of dry acetone, degassed with nitrogen for 10 minutes, and stirred at ambient temperature for 4 hours. ^{1}H NMR ($CDCl_3$) time points were taken at 120 and 240 minutes, to determine the reactions conversion. The product was purified by precipitation into hexane, and dried overnight at room temperature to leave a viscous dark red oil. ^{1}H NMR (400 MHz, $CDCl_3$): δ = 1.13 (d, 3H), 1.20-1.43 (m, br), 2.52 (t, *J* = 7.6 Hz, 4H), 2.64 (t, *J* = 7.6 Hz, 4H), 2.78 (t, *J* = 7.8 Hz, 4H), 3.52-3.82 (m, br), 4.26 (t, *J* = 4.70 Hz, 4H), 6.24 (s, br, NH).

[Xan-P-COOH];[35] - Potassium ethyl xanthogenate (14.91 g, 93 mmol, 1.2 equiv.) was suspended in 60 mL of dry acetone and a solution of 1-bromopropanoic acid (11.78 g, 77 mmol, 1 equiv.) in 30 mL of acetone added dropwise over a period of 15-20 minutes. The mixture was left stirring at ambient temperature for 18 hours. The precipitated white salt (potassium bromide) was removed by filtration and washed with a small volume of acetone to afford a clear pale yellow solution. The filtrate was concentrated *in vacuo* resulting in a yellow viscous liquid that was re dissolved in dichloromethane (300 mL) and washed with brine (3 x 100 mL). The organic phase was dried over $MgSO_4$ and evaporated to dryness. Yield: 10.45 g, white solid (70%). ^{1}H NMR (400 MHz, $CDCl_3$): δ = 1.43 (t, *J* = 7.2 Hz, 3H), 2.84 (t, *J* = 7.0 Hz, 2H), 3.38 (t, *J* = 7.0 Hz, 2H), 4.66 (q, *J* = 7.2 Hz, 2H). ^{13}C NMR (100 MHz, $CDCl_3$): δ = 13.78, 30.20, 33.11, 70.20, 176.80, 214.07.

[Xan$_3$-P-TEA-G$_0$];[36] - [35] (5.73 g, 29.52 mmol, 4 equiv.), **t**riethanolamine (TEA) (1.10 g, 7.38 mmol, 1 equiv.) and 4-(Dimethylamino)pyridinium 4-toluenesulfonate (DPTS) (1.30 g, 4.43 mmol,

0.6 equiv.) were dissolved in 50 mL of CH_2Cl_2 under a nitrogen atmosphere. Dicyclohexylcarbodiimide (DCC) was added in 10 mL of CH_2Cl_2 and the reaction mixture stirred overnight for 18 hours. The precipitated urea DCC byproduct was removed by filtration and washed with a small volume of CH_2Cl_2. The product was isolated by diluting the mixture with CH_2Cl_2 (100 mL) and washing with 1 M $NaHSO_4$ (2 x 100 mL). The organic layer was dried over $MgSO_4$ and evaporated to dryness. The product was purified by automated liquid chromatography (silica gel, eluting with hexane gradually increasing to 40:60 ethyl acetate/hexane) to give a viscous oil. Yield: 3 g, orange viscous oil (60%). ^{1}H NMR (400 MHz, $CDCl_3$): δ = 1.42 (t, *J* = 7.2 Hz, 9H), 2.77 (t, *J* = 7.1 Hz, 6H), 2.85 (t, *J* = 6.1 Hz, 6H), 3.37 (t, *J* = 7.1 Hz, 6H), 4.15 (t, *J* = 6.1 Hz, 6H), 4.65 (q, *J* = 7.2 Hz, 6H). ^{13}C NMR (100 MHz, $CDCl_3$): δ = 13.81, 30.60, 33.41, 53.26, 62.99, 70.14, 171.43, 214.22. Calcd: $[M+Na]^+$ ($C_{24}H_{39}NNaO_9S_6$) m/z = 700.1. Found: ESI-MS: $[M+H]^+$ m/z = 678.1, $[M+Na]^+$ m/z = 700.1, $[M+K^+]$ m/z = 716.1.

[Bz_3-P-TEA];[37] – [36] (0.20 g, 0.295 mmol, 1 equiv.) was dissolved in 3 mL anhydrous THF and degassed for 10 minutes under a nitrogen atmosphere. *n*-butylamine (96μL, 0.974 mmol, 3.3 equiv.) was added, and the reaction left stirring, sealed under nitrogen for 1.5 hour at ambient temperature. TLC analysis (hexane/ethyl acetate 60:40) confirmed total loss of [36]. Benzyl acrylate (BA) (136 μL, 0.885 mmol, 3 equiv.) was added, and the reaction left stirring, sealed under nitrogen for 18 hours at ambient temperature. The product was isolated by precipitating the crude mixture from THF twice into hexanes. Residual solvents were removed under high vacuum overnight. Yield: 0.2 g, orange viscous oil (75%). ^{1}H NMR (400 MHz, $CDCl_3$): δ = 2.60 (t, *J* = 7.4 Hz, 6H), 2.66 (t, *J* = 7.2 Hz, 6H), 2.75-2.85 (m, 18H), 4.13 (t, *J* = 6.1 Hz, 6H), 5.13 (s, 6H), 7.27-7.42 (m, 15H). ^{13}C NMR (100 MHz, $CDCl_3$): δ = 26.97, 26.98, 34.67, 34.79, 53.26, 62.86, 66.56, 128.29, 128.33, 128.59, 135.72, 171.64, 171.68. Calcd: $[M+Na]^+$ ($C_{45}H_{57}NNaO_{12}S_3$) m/z = 922.3. Found: ESI-MS: $[M+H]^+$ m/z = 900.3, $[M+Na]^+$ m/z = 922.3, $[M+K^+]$ m/z = 938.3.

[Am_3-P-TEA-G_0];[38] – [36] (0.20 g, 0.295 mmol, 1 equiv.) was dissolved in 3 mL anhydrous THF and degassed for 10 minutes under a nitrogen atmosphere. *n*-butylamine (96μL, 0.974 mmol, 3.3 equiv.) was added, and the reaction left stirring, sealed under nitrogen for 1 hour at ambient

temperature. 2-(Dimethylamino)ethyl acrylate (DMAEA) (135 μL, 0.885 mmol, 3 equiv.) was added, and the reaction left stirring, sealed under nitrogen for 18 hours at ambient temperature. The product was isolated by precipitating the crude mixture from THF twice into hexanes. Residual solvents were removed under high vacuum overnight. Yield: 0.2 g, orange viscous oil (80%). ^{1}H NMR (400 MHz, $CDCl_3$): δ = 2.28 (s, 18H), 2.54-2.67 (m, 18H), 2.77-2.87 (m, 18H), 4.14 (t, *J* = 6.1 Hz, 6H), 4.19 (t, *J* = 5.7 Hz, 6H). ^{13}C NMR (100 MHz, $CDCl_3$): δ = 26.94, 26.97, 34.67, 34.70, 45.72, 53.26, 57.78, 62.49, 62.84, 171.69, 171.90. Calcd: $[M+H]^+$ ($C_{36}H_{67}N_4O_{12}S_3$) m/z = 843.4. Found: ESI-MS: $[M+H]^+$ m/z = 843.4, $[M+Na]^+$ m/z = 865.4, $[M+K^+]$ m/z = 881.4.

6.3 Chapter 3 compounds

4-(Dimethylamino)pyridinium *p*-toluenesulfonate [**DPTS]** – *p*-toluenesulfonic acid monohydrate (7.80 g, 41 mmol, 1 equiv) was dissolved in 50 mL anhydrous toluene and refluxed using a dean-stark head until no further water could be extracted (approximately 4 hours). [Note: the solution turned slightly pink during the loss of water]. Following this, the mixture was cooled to 60 °C and 4-dimethylaminopyridine (DMAP) (5 g, 41 mmol, 1 equiv.) in 30 mL of anhydrous toluene at 60 °C added slowly. A precipitate immediately formed upon addition, and the solution was left to stir at 60 °C for 1 hour. The mixture was then cooled and filtered to yield DPTS. The slightly off-white crystals were recrystallized once from dichloroethane to yield white crystals. Yield: 9.82 g (81%). ^{1}H NMR (400 MHz, $CDCl_3$): δ = 2.35 (s, 3H), 3.21 (s, 6H), 6.76 (d, *J* = 7.7 Hz, 2H), 7.17 (d, *J* = 8.2 Hz, 2H), 7.83 (d, *J* = 8.2 Hz, 2H), 8.21 (d, *J* = 7.7 Hz, 2H). ^{13}C NMR (100 MHz, $CDCl_3$): δ = 21.33, 40.12, 106.79, 126.00, 128.75, 139.77, 142.69, 157.32. Anal. Calcd for $C_{14}H_{18}N_2O_3S$: C, 57.12; H, 6.16; N, 9.52; S, 10.89. Found: C, 57.30; H, 6.12; N, 9.51; S, 10.84. This compound was prepared by the procedure reported by Moore and Stupp.[1] The above spectroscopic data agreed with that reported.

[Xan-P-COCl];[39] – [35] (10 g, 51.5 mmol, 1 equiv.) was dissolved in 100 mL CH_2Cl_2, 5 drops of DMF added, and very slowly oxalyl chloride (8.84 mL, 103 mmol, 2 equiv.) added. CO and HCl gases began to rapidly evolve. [Note: Care: perform in well-equipped fume hood; CO and gaseous

HCl are very toxic]. The mixture was left stirring for 3 hours, until all the gases seized to evolve. The crude product was purified by removing the CH_2Cl_2 *in vacuo* and a repetitive redissolving/removal of solvents procedure with $CHCl_3$ (3 x 50mL) to furnish a viscous red oil. Yield: 10.96 g (99%). ^{1}H NMR (400 MHz, $CDCl_3$): δ = 1.43 (t, *J* = 7.2 Hz, 3H), 3.31-3.43 (m, 4H), 4.66 (q, *J* = 7.2 Hz, 2H). ^{13}C NMR (100 MHz, $CDCl_3$): δ = 13.78, 30.14, 45.99, 70.52, 172.39, 213.41.

[Xan$_2$-P-COOH];[40] – 2,2-Bis(hydroxymethyl)-propionic acid (bis-MPA) (3.22 g, 24 mmol, 1 equiv.), triethylamine (8.64 mL, 62 mmol, 2.6 equiv.) and DMAP (0.15 g, 1.2 mmol, 0.05 equiv.) were dissolved in 40 mL of anhydrous CH_2Cl_2 and the mixture cooled using an ice bath. [Xan-P-COCl];[39] (10.96g, 52 mmol, 2.2 equiv.) diluted in 5 mL anhydrous CH_2Cl_2 was then slowly added to the mixture, and the reaction was left stirring at ambient temperature for 16 hours. The product was isolated by filtering the mixture, diluting with CH_2Cl_2 (100mL), washing with water (3 x 100 mL), drying the organic layer over $MgSO_4$ and removal of solvents *in vacuo*. The crude oil was purified by liquid chromatography (silica, eluting ethyl acetate:hexane (80:20) increasing the polarity to ethyl acetate:hexane (20:80)) to obtain a red viscous oil that was dried by high vacuum overnight. Yield: 8.06 g (71%). ^{1}H NMR (400 MHz, $CDCl_3$): δ = 1.30 (s, 3H), 1.42 (t, *J* = 7.1 Hz, 3H), 2.79 (t, *J* = 7.0 Hz, 4H), 3.37 (4H, *J* = 7.0 Hz, 4H), 4.28 (m, 4H), 4.65 (q, *J* = 7.1 Hz, 4H). ^{13}C NMR (100 MHz, $CDCl_3$): δ = 13.80, 17.86, 30.47, 33.33, 46.06, 65.31, 70.21, 171.00, 179.02, 214.08. Calcd: $[M+Na]^+$ ($C_{17}H_{26}NaO_8S_4$) m/z = 509.04. Found: ESI-MS: $[M+Na]^+$ m/z = 509.0.

[OH$_2$-COBz];[43] – 2,2-Bis(hydroxymethyl)-propionic acid (bis-MPA) (9.00 g, 67.10 mmol) and potassium hydroxide (4.30 g, 77 mmol, 1.14 equiv.) were dissolved in 100 mL DMF and heated at 100 °C for 1 hour. Benzyl bromide (9.60 mL, 80.68 mmol, 1.2 equiv.) was then added, and the reaction left stirring for 15 hours at 100 °C. The mixture was then cooled, the DMF removed in vacuo, and the crude produced dissolved in 200 mL CH_2Cl_2. The organic layer was washed with water (2 x 100 mL), dried over $MgSO_4$ and the solvents evaporated to leave a dark cream solid. The solid was recrystallized twice from hot hexane/CH_2Cl_2 to furnish the product as a cream solid. Yield: 9.72 g (65%). ^{1}H NMR (400 MHz, $CDCl_3$): δ = 1.09 (s, 3H), 3.73 (d, *J* = 11.2 Hz, 2H), 3.92 (d, *J* = 11.2 Hz,

2H), 5.19 (s, 2H), 7.28-7.50 (m, 5H). This compound was prepared by the procedure reported by Ihre et al.[2] The above spectroscopic data agreed with that reported.

[Xan_2-P-COBz];[45] – [OH_2-COBz];[43] (0.54 g, 2.4 mmol, 1 equiv.), triethylamine (0.87 mL, 6.24 mmol, 2.6 equiv.) and DMAP (0.015 g, 0.12 mmol, 0.05 equiv.) were dissolved in 10 mL of anhydrous CH_2Cl_2 and the mixture cooled using an ice bath. [Xan-P-COCl];[39] (1.096g, 5.2 mmol, 2.2 equiv.) diluted in 1 mL anhydrous CH_2Cl_2 was then slowly added to the mixture, and the reaction was left stirring at ambient temperature for 16 hours. The product was isolated by filtering the mixture, diluting with CH_2Cl_2 (20mL), washing with water (3 x 15 mL), drying the organic layer over $MgSO_4$ and removal of solvents *in vacuo*. The crude oil was purified by liquid chromatography (silica, eluting ethyl acetate:hexane (5:95) increasing the polarity to ethyl acetate:hexane (30:70)) to obtain a red viscous oil that was dried by high vacuum overnight. Yield: 0.61 g (44%). ^{1}H NMR (400 MHz, $CDCl_3$): δ = 1.27 (s, 3H), 1.41 (t, J = 7.1 Hz, 6H), 2.68 (t, *J* = 7.0 Hz, 4H), 3.30 (t, *J* = 7.0 Hz, 4H), 4.27 (m, 4H), 4.64 (q, *J* = 7.1 Hz, 4H), 5.17 (s, 2H), 7.29-7.40 (m, 5H). ^{13}C NMR (100 MHz, $CDCl_3$): δ = 13.79, 17.88, 30.42, 33.24, 46.32, 65.68, 66.97, 70.16, 128.30, 128.49, 128.63, 135.49, 170.93, 172.33, 214.09.

[OBz_1-G_1-COOH];[47] – 2,2-Bis(hydroxymethyl)-propionic acid (bis-MPA) (100 g, 0.756 mol, 1 equiv.), benzaldehyde dimethyl acetal (170.20 g, 1.12 mol, 1.5 equiv.), and *p*-toluenesulfonic acid monohydrate (7.10 g, 37.3 mmol, 0.05 equiv.) were added to 750 mL of acetone. The reaction mixture was stirred for 4 hours at ambient temperature. After storage of the reaction mixture in the refrigerator overnight, the solids were filtered off and washed with cold acetone to result in the product as white crystals. Yield: 92.50 g (56%). ^{1}H NMR (400 MHz, $CDCl_3$): δ = 1.11 (s, 3H), 3.70 (d, *J* = 11.7 Hz, 2H), 4.63 (d, *J* = 11.6 Hz), 5.49 (s, 1H), 7.34 (m, 3H), 7.47 (m, 2H). ^{13}C NMR (100 MHz, $CDCl_3$): δ = 17.75, 42.15, 73.44, 101.95, 126.17, 128.29, 129.09, 137.49, 178.69. This compound was prepared by the procedure reported by Ihre et al.[3] The above spectroscopic data agreed with that reported.

[OBz_1-G_1-Anhy];[48] – [OBz_1-G_1-COOH];[47] (92 g, 0.414 mol, 1 equiv.) and N,N'-Dicyclohexylcarbodiimide (DCC) (47.04 g, 0.228 mol, 0.55 equiv.) were added to 700 mL of CH_2Cl_2.

The reaction mixture was stirred overnight for 24 hours. The precipitated urea byproduct was removed by filtration and washed with a small volume of CH_2Cl_2. The crude product was purified by precipitating the filtrate into 2.5 L of hexane at ambient temperature under vigorous stirring for 30 minutes. After filtration the product was isolated as white crystals. Yield: 84.82 g (88%). ^{1}H NMR (400 MHz, $CDCl_3$): δ = 1.11 (s, 6H), 3.68 (d, *J* = 11.7 Hz, 2H), 4.65 (d, *J* = 11.7 Hz, 2H), 7.32 (m, 6H), 7.44 (m, 4H). ^{13}C NMR (100 MHz, $CDCl_3$): δ = 16.90, 44.23, 73.21, 102.15, 126.31, 128.27, 129.14, 137.61, 169.16. This compound was prepared by the procedure reported by Ihre et al.[3] The above spectroscopic data agreed with that reported.

General procedure for divergent dendron growth using anhydride coupling - [OBz_1-G_1-Anhy];[48], the hydroxyl substrate, and 4-dimethylaminopyridine (DMAP) were dissolved in an anhydrous 1:1 ratio of CH_2Cl_2:Pyridine (v/v) under a nitrogen atmosphere and stirred at ambient temperature for 16 hours. After this time, approximately 2 mL of water was added and the reaction was stirred for an additional 2 hours in order to quench the excess anhydride. The product was isolated by diluting the mixture with CH_2Cl_2 (150 mL) and washing with 1 M $NaHSO_4$ (3 x 150 mL), 1M $NaHCO_3$ (3 x 150 mL), and brine (2 x 150 mL). The organic layer was dried over $MgSO_4$ and evaporated to dryness. Any residual solvents were removed under high vacuum overnight.

General procedure for removal of benzylidene protecting groups by hydrogenation - To a Parr vessel suitable for catalytic hydrogenation, the benzylidene protected dendron was dissolved in a 1:1 mixture of CH_2Cl_2:MeOH (v/v). $Pd(OH)_2$ on Carbon (20%) was added and the apparatus was evacuated and back-filled with hydrogen three times (H_2 pressure: 10 atm). The mixture was left under a hydrogen atmosphere, vigorously stirring for 16 hrs at ambient temperature. After hydrogenation, the catalyst was filtered off through a celite plug and *carefully* washed with methanol. The filtrate was evaporated to dryness to result in the desired hydroxyl terminated dendron as a white solid.

[OBz_1-G_1-TSe];[49] - The dendron growth step was carried out as described above, specifically using para-toluene sulfonyl ethanol (*p*-TSe) (10 g, 50 mmol, 1 equiv.), [OBz_1-G_1-Anhy]; [48**]** (42.65 g, 100

mmol, 2 equiv.) and DMAP (2.57 g, 21 mmol, 0.40 equiv.) that was dissolved in 220 mL of dry CH_2Cl_2 and 120 mL of pyridine. Yield: 19.78 g, white foam (98%). ^{1}H NMR (400 MHz, $CDCl_3$): δ = 0.96 (s, 3H), 2.43 (s, 3H), 3.46 (t, *J* = 6.2 Hz, 2H), 3.60 (d, *J* = 11.6 Hz, 2H) 4.47 (t, *J* = 6.2 Hz, 2H), 4.52 (d, *J* = 11.6 Hz, 2H), 5.43 (s, 1H), 7.27-7.44 (m, 7H).^{13}C NMR (100 MHz, $CDCl_3$): δ = 17.52, 21.64, 42.46, 55.13, 58.20, 73.32, 101.72, 126.15, 128.19, 128.23, 129.01, 130.09, 136.01, 145.11, 149.86, 173.52. SEC: M_n = 390, M_w = 430, M_w/M_n = 1.10. This compound was prepared by the procedure reported by Parrott et al.[4] The above spectroscopic data agreed with that reported.

[$(OH)_2$-G_1-TSe];[50] – The hydrogenation step was carried out as described above, specifically using [OBz_1-G_1-TSe];[49] (5.5 g, 13.60 mmol, 1 equiv.), 210 mL of CH_2Cl_2:MeOH (1:1, v/v) and 0.55 g $Pd(OH)_2$. Yield: 4.3 g, white foam (99%). ^{1}H NMR (400 MHz, CD_3OD): δ = 1.03 (s, 3H), 2.45 (s, 3H), 3.49 (dd, *J* = 10.9 Hz, 4H), 3.59 (t, *J* = 5.9 Hz, 2H), 4.40 (t, *J* = 5.8 Hz, 2H), 7.47 (d, *J* = 8.2 Hz, 2H), 7.83 (d, *J* = 8.6 Hz, 2H). ^{13}C NMR (100 MHz, CD_3OD): δ = 17.07, 21.61, 51.58, 55.90, 58.93, 65.66, 129.30, 131.22, 137.76, 146.71, 175.89. Anal. Calcd for $C_{14}H_{20}O_6S$: C, 53.15; H, 6.37; S, 10.14. Found: C, 53.12; H, 6.37; S, 10.08. This compound was prepared by the procedure reported by Parrott et al.[4] The above spectroscopic data agreed with that reported.

[OBz_2-G_2-TSe];[51] - The dendron growth step was carried out as described above, specifically using [$(OH)_2$-G_1-TSe];[50] (4.10 g, 12.96 mmol, 1 equiv.), [OBz_1-G_1-Anhy]; [48**]** (16.58 g, 39 mmol, 3 equiv) and DMAP (0.71 g, 5.38 mmol, 0.45 equiv.)) that was dissolved in 70 mL of dry CH_2Cl_2 and 35 mL of pyridine. Yield: 8.68 g, white foam (93%). ^{1}H NMR (400 MHz, $CDCl_3$): δ = 0.95 (s, 6H), 1.09 (s, 3H), 2.37 (s, 3H), 3.10 (t, *J* = 5.8 Hz, 2H), 3.60 (d, *J* = 12.4 Hz, 4H) 4.20 (m, 6H), 4.56 (m, 4H), 5.42 (s, 2H), 7.27-7.43 (m, 12H), 7.68 (d, *J* = 8.3 Hz, 2H). ^{13}C NMR (100 MHz, $CDCl_3$): δ = 17.33, 17.72, 21.56, 42.60, 46.70, 54.65, 58.32, 65.20, 73.46, 73.53, 101.63, 126.12, 128.05, 128.16, 128.91, 130.00, 136.29, 137.78, 145.00, 172.00, 173.17. Calcd: $[M+Na]^+$ ($C_{38}H_{44}NaO_{12}S$) m/z = 747.25. Found: ESI-MS: $[M+Na]^+$ m/z = 747.2, $[M+K]^+$ m/z = 763.2. Anal. Calcd for $C_{38}H_{44}O_{12}S$: C, 62.97; H, 6.12; S, 4.42. Found: C, 63.11; H, 6.20; S, 4.42. SEC: M_n = 680, M_w = 760, M_w/M_n = 1.12. This compound was prepared by the procedure reported by Parrott et al.[4] The above spectroscopic data agreed with that reported.

[$(OH)_4$-G_2-TSe];[52] - The hydrogenation step was carried out as described above, specifically using [OBz_2-G_2-TSe];[51] (7.90 g, 10.90 mmol, 1 equiv.), 190 mL of CH_2Cl_2:MeOH (1:1, v/v) and 0.40 g $Pd(OH)_2$. Yield: 5.93 g, white foam (99%). ^{1}H NMR (400 MHz, CD_3OD): δ = 1.15 (s, 9H), 2.48 (s, 3H), 3.57-3.69 (m, 10H), 4.09 (d, *J* = 11.2 Hz) 2H), 4.14 (d, *J* = 10.6 Hz, 2H), 4.46 (t, *J* = 5.2 Hz, 2H), 7.49 (d, *J* = 8.4 Hz, 2H), 7.85 (d, *J* = 8.2 Hz, 2H). ^{13}C NMR (100 MHz, CD3OD): δ = 17.31, 17.86, 21.67, 47.68, 51.82, 55.84, 59.68, 65.97, 66.20, 129.29, 131.36, 137.81, 146.82, 173.79, 175.95. Calcd: $[M+Na]^+$ ($C_{24}H_{36}NaO_{12}S$) m/z = 571.18. Found: ESI-MS: $[M+Na]^+$ m/z = 571.2, $[M+K]^+$ m/z = 587.2. Anal. Calcd for $C_{24}H_{36}O_{12}S$: C, 52.54; H, 6.61; S, 5.84. Found: C, 53.02; H, 6.65; S, 5.63. This compound was prepared by the procedure reported by Parrott et al.[4] The above spectroscopic data agreed with that reported.

[OBz_4-G_3-TSe];[53] - The dendron growth step was carried out as described above, specifically using [$(OH)_4$-G_2-TSe];[52] (2.50 g, 4.56 mmol, 1 equiv.), [OBz_1-G_1-Anhy]; [48**]** (11.67 g, 27.36 mmol, 6 equiv) and DMAP (0.35 g, 2.83 mmol, 0.62 equiv.)) that was dissolved in 70 mL of dry CH_2Cl_2 and 35 mL of pyridine. Yield: 5.87 g, white foam (94%). ^{1}H NMR (400 MHz, $CDCl_3$): δ = 0.88-0.98 (m, 15H), 1.19 (s, 6H), 2.38 (s, 3H), 3.28 (t, *J* = 6.2 Hz, 2H), 3.58 (d, *J* = 11.8 Hz, 8H), 3.95 (dd, 4H), 4.34 (m, 10H), 4.56 (d, *J* = 11.8 Hz, 8H), 5.40 (s, 4H), 7.27-7.43 (m, 22H), 7.74 (d, 2H). ^{13}C NMR (100 MHz, CD_3OD): δ = 16.85, 17.66, 21.59, 42.59, 46.30, 46.87, 54.58, 58.22, 65.14, 65.70, 73.44, 73.52, 101.68, 126.20, 128.07, 128.13, 128.88, 130.04, 136.26, 137.824, 145.00, 171.63, 171.83, 173.20. Calcd: $[M+Na]^+$ ($C_{72}H_{84}NaO_{24}S$) m/z = 1387.5. Found: ESI-MS: $[M+Na]^+$ m/z = 1387.5, $[M+K]^+$ m/z = 1403.5. Anal. Calcd for $C_{24}H_{36}O_{12}S$: C, 63.33; H, 6.20; S, 2.35. Found: C, 63.49; H, 6.30 S, 2.00. SEC: M_n = 1430, M_w = 1650, M_w/M_n = 1.15. This compound was prepared by the procedure reported by Parrott et al.[4] The above spectroscopic data agreed with that reported.

[$(OH)_8$-G_3-TSe];[54] – The hydrogenation step was carried out as described above, specifically using [OBz_4-G_3-TSe];[53] (5.80 g, 4.25 mmol, 1 equiv.), 200 mL of CH_2Cl_2:MeOH (1:1, v/v) and 0.60 g $Pd(OH)_2$. Yield: 4.14 g, white foam (96%). ^{1}H NMR (400 MHz, CD_3OD): δ = 1.10-1.20 (m, 15H), 1.28 (s, 6H), 2.47 (s, 3H), 3.54-3.75 (m, 18H), 4.11-4.35 (m, 12H), 4.48 (t, 3H), 7.49 (d, 2H), 7.85 (d, 2H). ^{13}C NMR (100 MHz, CD_3OD): δ = 17.35, 17.75, 18.26, 21.70, 47.79, 47.95, 51.83, 55.74,

59.86, 65.82, 65.95, 66.23, 67.13, 129.30, 131.34, 137.83, 146.82, 173.40, 173.80, 176.01. Calcd: $[M+Na]^+$ ($C_{44}H_{68}NaO_{24}S$) m/z = 1035.4. Found: ESI-MS: $[M+Na]^+$ m/z = 1035.4, $[M+K]^+$ m/z = 1051.4. Anal. Calcd for $C_{44}H_{68}O_{24}S$: C, 52.17; H, 6.77; S, 3.17. Found: C, 52.27; H, 6.81 S, 2.85. This compound was prepared by the procedure reported by Parrott et al.[4] The above spectroscopic data agreed with that reported.

[$(Xan)_4$-G_2-TSe];[55] – [35] (0.70 g, 3.29 mmol, 6 equiv), [$(OH)_4$-G_2-TSe];[52] (0.30 g, 0.55 mmol, 1 equiv.) and DPTS (0.65 g, 2.20 mmol, 4 equiv.) were dissolved in 15 mL CH_2Cl_2 under a nitrogen atmosphere. Dicyclohexylcarbodiimide (DCC) (0.75 g, 3.62 mmol, 6.6 equiv.) was added slowly in a small volume of CH_2Cl_2, and the reaction mixture was stirred for 16 hours at ambient temperature. The urea byproduct was removed by filtration and washed with a small volume of CH_2Cl_2. After removal of solvents, the crude oil was purified by liquid chromatography (silica, eluting hexane, increasing the polarity to ethyl acetate:hexane (20:80)) to obtain a red viscous oil that was dried by high vacuum overnight. Yield: 0.50 g (72%). ^{1}H NMR (400 MHz, $CDCl_3$): δ = 1.18 (s, 3H), 1.24 (s, 6H), 1.42 (t, *J* = 7.10 Hz, 3H), 2.46 (s, 3H), 2.78 (t, *J* = 7.0 Hz, 8H), 3.35 (t, *J* = 7.0 Hz, 8H), 3.45 (t, *J* = 6.0 Hz, 2H), 4.16-4.28 (m, 12H), 4.47 (t, *J* = 6.0 Hz, 2H), 4.65 (q, *J* = 7.1 Hz, 8H), 7.40 (d, 2H), 7.82 (d, 2H). ^{13}C NMR (100 MHz, $CDCl_3$): δ = 13.80, 17.30, 17.88, 21.68, 30.45, 33.23, 46.35, 46.55, 54.79, 58.33, 65.40, 65.53, 70.19, 128.10, 130.16, 136.27, 145.21, 170.97, 171.63, 171.78, 214.08. Calcd: $[M+Na]^+$ ($C_{48}H_{68}NaO_{20}S_9$) m/z = 1275.2. Found: ESI-MS: $[M+Na]^+$ m/z = 1275.2, $[M+K]^+$ m/z = 1291.2.

[Xan-A-COOH];[57] – Potassium ethyl xanthate (53.06 g, 276 mmol, 1.2 equiv.) was added to 400 mL acetone. A solution of 2-bromoacetic acid (38.35 g, 331 mmol, 1 equiv.) in acetone (100 mL) was added dropwise at ambient temperature over a period of 20 min. Stirring was continued overnight at ambient temperature. The precipitated byproduct was removed by filtration and washed with a small volume of acetone to afford a clear pale yellow solution. The filtrate was concentrated under vacuum leaving a yellow viscous liquid that was dissolved in dichloromethane (300 mL) and washed with brine (3 x 100 mL). The organic phase was dried over $MgSO_4$ and evaporated to dryness to afford a white solid. Yield: 24.23 g (50%). ^{1}H NMR (400 MHz, $CDCl_3$): δ = 1.43 (t, *J* = 7.1 Hz, 3H), 3.98 (s,

2H) 4.67 (q, *J* = 7.1 Hz, 2H), 4.53. ^{13}C NMR (100 MHz, $CDCl_3$): δ = 13.68, 37.60, 70.93, 174.30, 212.0.

General procedure for dendron functionalisation with xanthate surface groups - The hydroxyl-terminated dendron, [Xan-A-COOH];[57], and DPTS were dissolved in CH_2Cl_2 under a nitrogen atmosphere. Dicyclohexylcarbodiimide (DCC) was added slowly to the mixture in a small volume of CH_2Cl_2 and the reaction was stirred overnight at ambient temperature for 16 hours. The urea byproduct was removed by filtration and washed with a small volume of CH_2Cl_2. The product was purified by liquid chromatography (silica gel, eluting with hexane gradually increasing the polarity to 40:60 ethyl acetate/hexane) to give a viscous oil.

General procedure for deprotection of para-toluene sulfonyl ester (TSe) - The xanthate functionalised dendron was dissolved in dry CH_2Cl_2 and 1.3 equivalents of 1,8-diazabicyclo[5.4.0]undec-7-ene (DBU) added. The reaction was stirred under a nitrogen atmosphere for 16 hours and monitored by using TLC (60:40 hexane:ethyl acetate). The product was isolated by diluting the mixture with CH_2Cl_2 (100 mL) and washing with 1 M $NaHSO_4$ (2 x 100 mL). The organic layer was dried over $MgSO_4$ and evaporated to dryness. The product was then precipitated three times into hexanes and ethyl acetate (9:1). Any residual solvent was removed under high vacuum to yield a viscous oil.

[Xan_2-G_1-TSe];[58] – The xanthate functionalisation step was carried out as described above, specifically using [Xan-A-COOH];[57] (4.65 g, 25.80 mmol, 3 equiv.), [$(OH)_2$-G_1-TSe];[50] (2.72 g, 8.60 mmol, 1 equiv.), DPTS (1.01 g, 3.44 mmol, 0.4 equiv.) , and DCC (5.86 g, 28.38 mmol, 3.3 equiv.). The crude product was purified by liquid chromatography (silica, eluting hexane, gradually increasing the polarity to ethyl acetate:hexane (40:60)). Yield: 4.60 g, orange viscous oil (84%). ^{1}H NMR (400 MHz, $CDCl_3$): δ = 1.16 (s, 3H), 1.42 (t, *J* = 7.1, 6H), 2.46 (s, 3H), 3.44 (t, *J* = 6.0 Hz, 2H), 3.91 (s, 4H), 4.16 (d, *J* = 11.0, 2H), 4.21 (d, *J* = 11.0 Hz), 4.46 (t, *J* = 6.0 Hz, 2H), 4.64 (q, *J* = 7.1 Hz, 4H), 7.39 (d, *J* = 8.0, 2H), 7.81 (d, *J* = 8.3, 2H). ^{13}C NMR (100 MHz, $CDCl_3$): δ = 13.74, 17.56, 21.67, 37.70, 46.19, 54.97, 58.36, 66.13, 70.91, 128.12, 130.18, 136.18, 145.28, 167.33, 171.80,

212.57. Calcd: $[M+Na]^+$ ($C_{24}H_{32}NaO_{10}S_5$) m/z = 663.05. Found: ESI-MS: $[M+Na]^+$ m/z = 663.0, $[M+K]^+$ m/z = 679.0. Anal. Calcd for $C_{24}H_{32}O_{10}S_5$: C, 44.98; H, 5.03; S, 25.02. Found: C, 45.66; H, 5.08 S, 25.60. SEC: M_n = 700, M_w = 910, M_w/M_n = 1.30

[Xan$_2$-G$_1$-COOH];[59] – The removal of the para-toluene sulfonyl (*p*-TSe) protecting group was carried out as described above, specifically using [Xan$_2$-G$_1$-TSe];[58] (4.60 g, 7.18 mmol, 1.0 equiv), and DBU (1.40 mL, 9.33 mmol, 1.3 equiv). Yield: 3.10 g, orange viscous oil (94%). ^{1}H NMR (400 MHz, $CDCl_3$): δ = 1.32 (s, 3H), 1.42 (t, *J* = 7.10, 6H), 2.47 (s, 3H), 3.94 (s, 4H), 4.30 (d, *J* = 11.1 Hz, 2H), 4.36 (d, *J* = 11.1 Hz, 2H), 4.64 (q, *J* = 7.1 Hz, 4H). ^{13}C NMR (100 MHz, $CDCl_3$): δ = 13.74, 17.86, 37.74, 46.06, 66.13, 70.87, 167.45, 177.80, 212.53. Calcd: $[M+Na]^+$ ($C_{15}H_{22}NaO_8S_4$) m/z = 481.01. Found: ESI-MS: $[M+Na]^+$ m/z = 481.0. Anal. Calcd for $C_{15}H_{22}O_8S_4$: C, 39.29; H, 4.84; S, 27.97. Found: C, 40.06; H, 5.06 S, 25.82.

[Xan$_4$-G$_2$-TSe];[60] – The xanthate functionalisation step was carried out as described above, specifically using [Xan-A-COOH];[57] (9.97 g, 55.32 mmol, 6 equiv.), [(OH)$_4$-G$_2$-TSe];[52] (5.06 g, 9.22 mmol, 1 equiv.), DPTS, (2.17 g, 7.38 mmol, 0.8 equiv.), and DCC (12.56 g, 60.85 mmol, 6.6 equiv.). The crude product was purified by liquid chromatography (silica, eluting hexane, gradually increasing the polarity to ethyl acetate:hexane (50:50)). Yield: 9.65 g, orange viscous oil (88%). ^{1}H NMR (400 MHz, $CDCl_3$): δ = 1.20 (s, 3H), 1.25 (s, 6H), 1.42 (t, *J* = 7.1, 12H), 2.46 (s, 3H), 3.46 (t, *J* = 5.9 Hz, 2H), 3.94 (s, 8H), 4.17-4.33 (m, 12H) 4.46 (t, *J* = 5.9 Hz, 2H), 4.64 (q, *J* = 7.1 Hz, 8H), 7.40 (d, *J* = 9.2, 2H), 7.82 (d, *J* = 8.3, 2H).^{13}C NMR (100 MHz, $CDCl_3$): 13.75, 17.37, 17.86, 21.69, 37.72, 46.36, 46.58, 54.81, 58.41, 65.58, 66.24, 70.89, 128.12, 130.16, 136.28, 145.20, 167.43, 171.64, 171.68, 212.61. Calcd: $[M+Na]^+$ ($C_{44}H_{60}NaO_{20}S_9$) m/z = 1219.11. Found MALDI-TOF: $[M+Na]^+$ = 1219.1. Anal. Calcd for $C_{44}H_{60}O_{20}S_9$: C, 44.13; H, 5.05; S, 24.10. Found: C, 44.21; H, 5.04 S, 24.30. SEC: M_n = 1080, M_w = 1235, M_w/M_n = 1.14

[Xan$_8$-G$_3$-TSe];[61] – The xanthate functionalisation step was carried out as described above, specifically using [Xan-A-COOH];[57] (8.53 g, 47.32 mmol, 12 equiv.), [(OH)$_8$-G$_3$-TSe];[54] (4.00 g, 3.94 mmol, 1 equiv.), DPTS, (1.85 g, 6.3 mmol, 1.6 equiv.), and DCC (10.73 g, 52.00 mmol, 13.2

equiv.). The crude product was purified by liquid chromatography (silica, eluting hexane, gradually increasing the polarity to ethyl acetate:hexane (40:60)). Yield: 2.37 g, orange viscous oil (26%). ^{1}H NMR (400 MHz, $CDCl_3$): δ = 1.22-1.29 (m, 21H), 1.42 (t, *J* = 7.1 Hz, 24H), 2.47 (s, 3H), 3.47 (t, *J* = 6.0 Hz, 2H), 3.94 (s, 16H), 4.18-4.35 (m, 28H), 4.49 (t, *J* = 6.0 Hz, 2H), 4.64 (q, *J* = 7.1 Hz, 16H). ^{13}C NMR (100 MHz, $CDCl_3$): 13.76, 17.29, 17.62, 17.85, 21.70, 37.76, 46.36, 46.52, 46.76, 54.74, 58.40, 65.47, 66.22, 70.88, 128.10, 130.17, 136.50, 145.30, 167.42, 171.47, 171.62, 171.68, 212.63. Calcd: $[M+Na]^+$ ($C_{44}H_{116}NaO_{40}S_{17}$) m/z = 2331.22. Found MALDI-TOF: $[M+Na]^+$ = 2331.68. Anal. Calcd for $C_{44}H_{116}O_{20}S_{17}$: C, 43.87; H, 5.20; S, 23.43. Found: C, 43.99; H, 5.09 S, 23.76.

[Xan$_4$-G$_2$-COOH];[62] – The removal of the para-toluene sulfonyl (*p*-TSe) protecting group was carried out as described above, specifically using [Xan$_4$-G$_2$-TSe];[60] (9.50 g, 7.93 mmol, 1.0 equiv), and DBU (1.54 mL, 9.33 mmol, 1.3 equiv). Yield: 7.44 g, orange viscous oil (93%). ^{1}H NMR (400 MHz, $CDCl_3$): δ = 1.27 (s, 6H), 1.33 (s, 3H), 1.42 (t, *J* = 7.1 Hz, 12H), 3.94 (s, 8H), 4.21-4.36 (m, 12H), 4.64 (q, *J* = 7.1 Hz, 4H). ^{13}C NMR (100 MHz, CDCl3): δ = 13.75, 17.65, 17.85, 37.72, 46.37, 65.71, 66.33, 70.90, 167.50, 171.68, 175.89, 212.62. Calcd: $[M+Na]^+$ ($C_{35}H_{50}NaO_{18}S_8$) m/z = 1037.07. Found ESI-MS: $[M+Na]^+$ = 1037.1. Anal. Calcd for $C_{35}H_{50}O_{18}S_8$: C, 41.40; H, 4.96; S, 25.27. Found: C, 42.30; H, 5.11 S, 25.30. SEC: M_n = 1690, M_w = 2570, M_w/M_n = 1.52

[Xan$_8$-G$_3$-COOH];[63] – The removal of the para-toluene sulfonyl (*p*-TSe) protecting group was carried out as described above, specifically using [Xan$_8$-G$_3$-TSe];[61] (7.21 g, 3.12 mmol, 1.0 equiv), and DBU (0.61 mL, 4.06 mmol, 1.3 equiv). Yield: 4.97 g, orange viscous oil (74%).^{1}H NMR (400 MHz, $CDCl_3$): δ = 1.27 (s, 12H), 1.29 (s, 6H), 1.35 (s, 3H), 1.42 (t, *J* = 7.2 Hz, 24H), 3.95 (s, 16H), 4.28 (m, 28H), 4.64 (t, *J* = 7.2 Hz, 2H). ^{13}C NMR (100 MHz, $CDCl_3$): δ = 13.77, 17.48, 17.72, 17.90, 37.50, 46.20, 46.33, 46.80, 65.58, 66.26, 66.72, 70.92, 167.69, 171.49, 171.67, 173.18, 212.61. Calcd: $[M+Na]^+$ ($C_{75}H_{106}NaO_{38}S_{16}$) m/z = 2149.18. Found: MALDI TOF MS: $[M+Na]^+$ m/z = 2149.10. Anal. Calcd for $C_{75}H_{106}O_{38}S_{16}$: C, 42.32; H, 5.02; S, 24.10. Found: C, 42.69; H, 5.02; S, 23.86.

General procedure for dendrimer synthesis by convergent growth - The xanthate functional material, triethanolamine (TEA) and DPTS were dissolved in CH_2Cl_2 under a nitrogen atmosphere.

Dicyclohexylcarbodiimide (DCC) was added slowly to the mixture in a small volume of CH_2Cl_2 and the reaction was stirred overnight at ambient temperature for 16 hours. The urea byproduct was removed by filtration and washed with a small volume of CH_2Cl_2. The product was isolated by diluting the mixture with CH_2Cl_2 (100 mL) and washing with 1 M $NaHSO_4$ (2 x 100 mL). The organic layer was dried over $MgSO_4$ and evaporated to dryness. The product was purified by liquid chromatography (silica gel, eluting with hexane gradually increasing the polarity to 40:60 ethyl acetate/hexane) to give a viscous oil.

[Xan_3-G_0-TEA];[64] – The dendrimer synthesis was carried out as described above, specifically using [Xan-A-COOH];[57] (1.54 g, 8.54 mmol, 4 equiv.), TEA, (0.32 g, 2.14 mmol, 1 equiv.), DPTS, (1.51 g, 5.13 mmol, 2.4 equiv.), and DCC (1.94 g, 9.40 mmol, 4.4 equiv.). The crude product was purified by liquid chromatography (silica, eluting hexane, gradually increasing the polarity to ethyl acetate:hexane (40:60)). Yield: 1.01 g, orange viscous oil (88%). ^{1}H NMR (400 MHz, $CDCl_3$): δ = 1.43 (t, *J* = 7.1 Hz, 9H), 2.88 (t, *J* = 5.8 Hz, 6H), 3.95 (s, 6H), 4.21 (t, *J* = 5.8 Hz, 2H), 4.65 (q, *J* = 7.1 Hz, 6H). ^{13}C NMR (100 MHz, $CDCl_3$): δ = 13.76, 37.93, 53.18, 64.10, 70.76, 167.86, 212.72. Calcd: $[M+H]^+$ ($C_{21}H_{33}NO_9S_6$) m/z = 635.05. Found: ESI-MS: $[M+H]^+$ m/z = 636.1, $[M+Na]^+$ m/z = 658.0, $[M+H]^+$ m/z = 674.0. SEC: M_n = 890, M_w =1400, M_w/M_n = 1.57

[Xan_6-G_1-TEA];[65] – The dendrimer synthesis was carried out as described above, specifically using [Xan_2-G_1-COOH];[59] (3.01 g, 6.56 mmol, 3.8 equiv.), TEA, (0.258 g, 1.73 mmol, 3 equiv.), DPTS, (1.53 g, 5.19 mmol, 3 equiv.), and DCC (1.50 g, 7.27 mmol, 4.2 equiv.). The crude product was purified by liquid chromatography (silica, eluting ethyl acetate:hexane (10:90), gradually increasing the polarity to ethyl acetate:hexane (40:60)). Yield: 1.65 g, orange viscous oil (65%).^{1}H NMR (400 MHz, $CDCl_3$): δ = 1.27, (s, 9H), 1.43 (t, *J* = 7.1 Hz, 18H), 2.87 (t, *J* = 6.3 Hz, 6H), 3.93 (s, 12H), 4.17 (t, *J* = 6.3 Hz, 6H), 4.25 (d, *J* = 11.0 Hz, 6H), 4.33 (d, *J* = 11.0 Hz, 6H), 4.64 (q, *J* = 7.1 Hz, 12H). ^{13}C NMR (100 MHz, CDCl3): δ = 13.76, 17.92, 37.75, 46.21, 53.09, 63.38, 66.30, 70.90, 167.39, 172.19, 212.55. Calcd: $[M+Na]^+$ ($C_{51}H_{75}NNaO_{24}S_{12}$) m/z = 1492.12. Found: MALDI-TOF: $[M+Na]^+$ m/z = 1492.24. Anal. Calcd for $C_{51}H_{175}NO_{24}S_{12}$: C, 41.64; H, 5.14; N, 0.95; S, 26.16. Found: C, 42.14; H, 5.13; N, 0.94; S, 26.30. SEC: M_n = 1540, M_w =1795, M_w/M_n = 1.16

[Xan_{12}-G_2-TEA];[66] – The dendrimer synthesis was carried out as described above, specifically using [Xan_4-G_2-COOH];[62] (7.28 g, 7.17 mmol, 3.8 equiv.), TEA, (0.282 g, 1.89 mmol, 1 equiv.), DPTS, (1.67 g, 5.67 mmol, 3 equiv.), and DCC (1.64 g, 7.94 mmol, 4.2 equiv.). The crude product was purified by liquid chromatography (silica, eluting ethyl acetate:hexane (10:90), gradually increasing the polarity to ethyl acetate:hexane (50:50)). Yield: 3.71 g, orange viscous oil (58%). ^{1}H NMR (400 MHz, $CDCl_3$): δ = 1.27 (s, 18H), 1.29 (s, 9H), 1.42 (t, *J* = 7.1 Hz, 26H), 2.88 (t, *J* = 6.4 Hz, 6H), 3.95 (s, 24H), 4.18 (t, *J* = 6.4 Hz, 6H), 4.22-4.33 (m, 36H), 4.64 (q, *J* = 7.1 Hz, 24H). ^{13}C NMR (100 MHz, $CDCl_3$): δ = 13.77, 17.75, 17.90, 37.73, 46.35, 46.57, 52.97, 63.37, 65.51, 66.21, 70.89, 167.40, 171.66, 172.02, 212.61. Calcd: $[M+Na]^+$ ($C_{111}H_{159}NNaO_{54}S_{24}$) m/z = 3160.29. Found: MALDI-TOF: $[M+Na]^+$ m/z = 3162.93. Anal. Calcd for $C_{111}H_{159}NO_{54}S_{24}$: C, 42.44; H, 5.10; N, 0.45; S, 24.50. Found: C, 43.67; H, 5.24; N, 0.66; S, 23.96. SEC: M_n = 4095, M_w = 4485, M_w/M_n = 1.09.

General procedure for one pot xanthate deprotection and thiol Michael addition - The xanthate peripheral dendrimer was dissolved in anhydrous THF and degassed for 10 minutes under a nitrogen atmosphere. *n*-butylamine (1.1 equiv. per Xanthate group) was added and the reaction left for 1.5 hours, and followed using TLC (60:40 hexane:ethyl acetate). The acrylate monomer (1.1 equiv. per thiol) was added and the reaction mixture stirred overnight at ambient temperature for 16 hours. The product was isolated by diluting the mixture with CH_2Cl_2 (100 mL) and washing with 1 M $NaHSO_4$ (2 x 100 mL). The organic layer was dried over $MgSO_4$ and evaporated to dryness. The product was then precipitated twice into hexanes, and any residual solvent was removed under high vacuum to yield a viscous oil.

[Bnz_3-G_0-TEA];[69] – The one pot xanthate deprotection and thiol Michael addition was carried out as described above, specifically using [Xan_3-G_0-TEA];[64], (0.2 g, 0.315 mmol, 1 equiv.), *n*-butylamine (0.076 g, 103 µL, 1.04 mmol, 3.3 equiv.) benzyl acrylate (0.154 g, 145 µL, 0.95 mmol, 3 equiv.) and 3 mL anhydrous THF. Yield: 0.25 g, pale yellow oil (93%). ^{1}H NMR (400 MHz, $CDCl_3$): δ = 2.69 (t, *J* = 7.2 Hz, 6H), 2.85 (t, *J* = 5.9 Hz, 6H), 2.92 (t, *J* = 7.2 Hz, 6H), 3.24 (s, 6H), 4.16 (t, *J* = 5.9 Hz, 6H), 5.13 (s, 6H), 7.35 (m, 15H). ^{13}C NMR (100 MHz, $CDCl_3$): δ = 27.53, 33.59, 34.31, 53.16, 63.37, 66.59, 128.29, 128.33, 128.59, 135.70, 170.14, 171.45. Calcd: $[M+H]^+$ ($C_{42}H_{52}NO_{12}S_3$)

m/z = 858.3. Found: MALDI-TOF: $[M+H]^+$ m/z = 858.3, $[M+Na]^+$ m/z = 880.2, $[M+K]^+$ m/z = 896.2. SEC: M_n =1095, M_w =1350, M_w/M_n = 1.23

[Bnz_6-G_1-TEA];[70] – The one pot xanthate deprotection and thiol Michael addition was carried out as described above, specifically using [Xan_6-G_1-TEA];[65], (0.2 g, 0.136 mmol, 1 equiv.) and *n*-butylamine (89 µL, 0.90 mmol, 6.6 equiv.), benzyl acrylate (125 µL, 0.816 mmol, 6 equiv.) and 3 mL anhydrous THF. ^{1}H NMR (400 MHz, $CDCl_3$): δ = 1.25 (s, 9H), 2.67 (t, *J* = 7.2 Hz, 12H), 2.88 (t, *J* = 7.2 Hz, 12H), 3.22 (s, 12H), 4.27 (m, 18H), 5.12 (s, 12H), 7.34 (m, 30H). ^{13}C NMR (100 MHz, $CDCl_3$): δ = 17.73, 27.51, 33.41, 34.26, 46.33, 52.94, 62.47, 65.83, 66.60, 128.27, 128.33, 128.59, 135.69, 169.75, 171.44, 172.22. Calcd: $[M+H]^+$ ($C_{93}H_{112}NO_{30}S_6$) m/z = 1914.6. Found: MALDI-TOF: $[M+H]^+$ m/z = 1914.8, $[M+Na]^+$ m/z = 1936.8, $[M+K]^+$ m/z = 1952.8. SEC: M_n = 2145, M_w = 2320, M_w/M_n = 1.08

[Am_6-G_1-TEA];[71] – The one pot xanthate deprotection and thiol Michael addition was carried out as described above, specifically using [Xan_6-G_1-TEA];[65], (0.2 g, 0.136 mmol, 1 equiv.), *n*-butylamine (89 µL, 0.90 mmol, 6.6 equiv.), 2-(Dimethylamino)ethyl acrylate (125 µL, 0.816 mmol, 6 equiv.) and 3 mL anhydrous THF. Yield: 0.216 g, pale yellow oil (88%). ^{1}H NMR (400 MHz, $CDCl_3$): δ = 1.28 (s, 9H), 2.28 (s, 36H), 2.56 (t, *J* = 5.8 Hz, 12H), 2.67 (t, *J* = 7.2 Hz, 12H), 2.80-2.98 (m, *J* = 7.4 Hz, 18H), 3.26 (s, 12H), 4.12-4.23 (m, *J* = 5.7 Hz, 18H), 4.27 (d, *J* = 11.1 Hz, 6H), 4.33 (d, *J* = 11.1 Hz, 6H).^{13}C NMR (100 MHz, $CDCl_3$): δ = 17.82, 27.48, 33.38, 34.19, 45.73, 46.37, 53.04, 57.77, 62.53, 63.30, 65.81, 169.71, 171.66, 172.29. Calcd: $[M+Na]^+$ ($C_{79}H_{129}N_7NaO_{30}S_6$) m/z = 1822.7. Found: MALDI-TOF: $[M+Na]^+$ m/z = 1823.1. SEC: M_n = 2400, M_w =2795, M_w/M_n = 1.16

[OEG_6-G_1-TEA];[72] – The one pot xanthate deprotection and thiol Michael addition was carried out as described above, specifically using [Xan_6-G_1-TEA];[65], (0.2 g, 0.136 mmol, 1 equiv), *n*-butylamine (89 µL, 0.90 mmol, 6.6 equiv), 2 oligo(ethylene glycol) methyl ether acrylate (0.394g, 0.816 mmol) and 3 mL anhydrous THF. Yield: 0.40 g, pale yellow oil (77%). ^{1}H NMR (400 MHz, CDCl3): δ = 1.27 (s, 9H), 2.67 (t, J = 7.2 Hz, 12H), 2.80-2.97 (m, J = 7.0 Hz, 18H), 3.26 (s, 12H), 3.38 (s, 18H), 3.51-3.77 (m, 193H), 4.16 (t, J = 6.5 Hz, 6H), 4.21-4.39 (m, 24H). 13C NMR (100

MHz, CDCl3): δ = 17.83, 27.41, 33.38, 34.11, 46.36, 53.03, 59.04, 63.29, 63.87, 65.78, 69.04, 70.53, 71.94, 169.69, 171.55, 172.29. Found MALDI-TOF: $[M+Na]^+$ m/z = 3858.5. SEC: M_n = 2400, M_w =2795, M_w/M_n = 1.14.

[Bnz_{12}-G_2-TEA];[73] – The one pot xanthate deprotection and thiol Michael addition was carried out as described above, specifically using [Xan_{12}-G_2-TEA];[66] (0.1 g, 0.032 mmol, 1 equiv.), *n*-butylamine (46 µL, 0.461 mmol, 14.1 equiv.), benzyl acrylate (88.2 µL, 0.576 mmol, 18 equiv.) and 2 mL anhydrous THF. Yield: 0.11 g, pale yellow oil (89%). ^{1}H NMR (400 MHz, $CDCl_3$): δ = 1.23 (s, 27H), 2.66 (t, *J* = 7.2 Hz, 24H), 2.79-2.93 (m, *J* = 7.3 Hz, 24H), 3.23 (s, 24H), 4.14 (t, *J* = 6.2 Hz, 6H), 4.19-4.22 (m, 36H), 7.27-7.39 (m, 60H). ^{13}C NMR (100 MHz, $CDCl_3$): δ = 17.70, 17.77, 27.47, 33.35, 34.25, 46.50, 52.95, 63.27, 65.42, 65.71, 66.55, 128.27, 128.31, 128.58, 135.73, 169.71, 171.40, 171.75, 172.02. Calcd: $[M+Na]^+$ ($C_{195}H_{231}NNaO_{66}S_{12}$) m/z = 4049.1. Found: MALDI-TOF: $[M+Na]^+$ m/z = 4049.75, $[M+K]^+$ m/z = 4065.75. SEC: M_n = 4235, M_w =4530, M_w/M_n = 1.07.

[Am_{12}-G_2-TEA];[74] – The one pot xanthate deprotection and thiol Michael addition was carried out as described above, specifically using [Xan_{12}-G_2-TEA];[66] (0.1 g, 0.032 mmol, 1 equiv.), *n*-butylamine (46 µL, 0.461 mmol, 14.4 equiv.), 2-(Dimethylamino)ethyl acrylate (88.0 µL, 0.576 mmol, 18 equiv.) and 2 mL anhydrous THF. Yield: 0.107 g, pale orange oil (87%). ^{1}H NMR (400 MHz, $CDCl_3$): δ = 1.27 (s, 27H), 2.28 (s, 72H), 2.56 (t, *J* = 5.8 Hz, 24H), 2.67 (t, *J* = 7.2 Hz, 24H), 2.88 (m, *J* = 7.2 Hz, 30H), 3.28 (s, 24H), 4.13-4.35 (m, 66H). ^{13}C NMR (100 MHz, $CDCl_3$): δ = 17.73, 17.80, 27.45, 33.34, 34.18, 45.72, 46.51, 52.97, 57.74, 62.50, 63.27, 65.41, 65.69, 169.71, 171.65, 171.75, 172.01. Calcd: $[M+Na]^+$ ($C_{159}H_{267}N_{13}NaO_{66}S_{12}$) m/z = 3821.45. Found: MALDI-TOF: $[M+Na]^+$ m/z = 3822.2. SEC: Mn = 5855, Mw =6265, M_w/M_n = 1.07.

[OEG_{12}-G_2-TEA];[75] – The one pot xanthate deprotection and thiol Michael addition was carried out as described above, specifically using [Xan_{12}-G_2-TEA];[66] (0.19 g, 0.061 mmol, 1 equiv.), *n*-butylamine (87 µL, 0.461 mmol, 14.4 equiv.), 2 oligo(ethylene glycol) methyl ether acrylate (0.583g, 1.1 mmol, 18 equiv.) and 2 mL anhydrous THF. Yield: 0.350 g, pale yellow oil (73%) ^{1}H NMR (400 MHz, $CDCl_3$): δ = 1.26 (s, 27H), 2.67 (t, *J* = 7.1 Hz, 24H), 2.88 (t, *J* = 7.2 Hz, 24H), 3.28 (s, 24H),

3.38 (s, 36H), 3.52-3.79 (m, 397H), 4.07-4.42 (m, 48H). ^{13}C NMR (100 MHz, $CDCl_3$): δ = 17.82, 27.39, 33.35, 34.09, 46.50, 59.04, 63.85, 65.66, 69.04, 70.58, 71.95, 169.70, 171.56, 171.75, 172.01. Found MALDI-TOF: $[M+Na]^+$ m/z = 7897.0. SEC: M_n = 8585, M_w =9795, M_w/M_n = 1.14.

6.4 Chapter 4 compounds

EBiB(^{t}BuMA$_{50}$);[76] - Target DP_n = 50 monomer units for the primary chains, EBiB (0.028 g, 0.141 mmol, 1 equiv.), ^{t}BuMA (1 g, 7.03 mmol, 50 equiv.), bpy (0.044 g, 0.282 mmol, 2 equiv.), [Xan-A-COOH];[57] (0.025 g, 0.141 mmol, 1 equiv.) and 2 drops of anisole were placed into a 10 mL round-bottomed flask. IPA/H_2O (92.5/7.5 v/v) was added to the flask (50% wt% based on ^{t}BuMA) and the solution was stirred and deoxygenated using a nitrogen purge for 10 minutes. Cu(I)Cl (0.014 g, 0.141 mmol, 1 equiv) was added to the flask, whilst maintaining a positive flow of nitrogen, and the solution was left to polymerise at 40 °C. The reaction was terminated when conversion reached >99%, indicated by ^{1}H NMR after 16 hours, by exposure to oxygen and addition of THF. The solution was passed through a neutral alumina column to remove the catalytic system, and precipitated twice into cold pet ether (30-40 °C) (cooled using dry ice). After drying the precipitated sample overnight under high vacuum to remove residual solvents, the polymer was obtained as a white solid.

[Acet$_1$-G$_1$-COOH];[77] – 2,2-Bis(hydroxymethyl)-propionic acid (bis-MPA) (100 g, 0.746 mol, 1 equiv.), 2,2-dimethoxypropane (116.7 g, 137.24 mL, 1.12 mol, 1.5 equiv.), and *p*-toluenesulfonic acid monohydrate (7.04 g, 37.0 mmol, 0.05 equiv.) were added to 500 mL of acetone. The reaction mixture was stirred for 3 hours at ambient temperature, and the reaction became clear. Following this, the catalyst was neutralised by adding 10 mL of a 1:1 mixture of NH_4OH:EtOH, resulting in salt precipitation. The product was obtained by removal of acetone *in vacuo*, redissolving the crude solid in CH_2Cl_2 (750 mL), washing the organic layer twice with water (2 x 250 mL), drying over $MgSO_4$ and evaporated to dryness. Yield: 93.80 g, white solid, (72%). ^{1}H NMR (400 MHz, $CDCl_3$): δ = 1.22 (s, 3H), 1.42 (s, 3H), 1.45 (s, 3H), 3.68 (d, *J* = 12.1 Hz, 2H), 4.20 (d, *J* = 12.1 Hz, 2H). ^{13}C NMR (100 MHz, $CDCl_3$): δ = 18.44, 21.96, 25.23, 41.76, 65.87, 98.35, 180.25. This compound was

prepared by the procedure reported by Ihre et al.[5] The above spectroscopic data agreed with that reported.

[Acet$_1$-G$_1$-Anhy];[78] - [Acet$_1$-G$_1$-COOH];[77] (93.80 g, 0.539 mol, 1 equiv.) and N,N'-Dicyclohexylcarbodiimide (DCC) (55.56 g, 0.269 mol, 0.50 equiv.) were added to 500 mL of CH_2Cl_2. The reaction mixture was stirred overnight for 48 hours. The precipitated urea byproduct was removed by filtration and washed with a small volume of CH_2Cl_2. The crude product was purified by precipitating the filtrate into 2.5 L of hexane cooled using dry ice under vigorous stirring for 60 minutes. After filtration the product was isolated as a grey viscous oil. Yield: 85.25 g (96%). ^{1}H NMR (400 MHz, $CDCl_3$): δ = 1.24 (s, 3H), 1.40 (s, 3H), 1.44 (s, 3H), 3.69 (d, *J* = 12.1 Hz, 4H), 4.21 (d, *J* = 12.1 Hz, 4H). ^{13}C NMR (100 MHz, $CDCl_3$): δ = 17.74, 21.68, 25.48, 43.68, 65.69, 98.42, 169.52. This compound was prepared by the procedure reported by Malkoch et al.[6] The above spectroscopic data agreed with that reported.

General esterification procedure for divergent dendron growth, [Acet$_1$-G$_1$-TSe];[79]- [Acet$_1$-G$_1$-Anhy];[78] (21.47 g, 65 mmol, 1.3 equiv.), para-toluene sulfonyl ethanol (*P*-TSe) (10.0 g, 50 mmol, 1 equiv.) and 4-dimethylaminopyridine (DMAP) (1.22 g, 10 mmol, 0.2 equiv.) were dissolved in 20 mL (5 equiv./OH-group) of anhydrous pyridine and 60 mL (1:3 ratio of Pyridine:CH_2Cl_2 (v/v)) of anhydrous CH_2Cl_2 under a nitrogen atmosphere. After stirring at ambient temperature for 16 hours, the solution was monitored using TLC to confirm the loss of the starting alcohol. Following this, approximately 20 mL of water was added and stirred at ambient temperature for an additional 2 hours to quench the excess anhydride. The product was isolated by diluting the mixture with CH_2Cl_2 (500 mL) and washing with 1 M $NaHSO_4$ (3 x 250 mL), 1M $NaHCO_3$ (3 x 250 mL), and brine (1 x 250 mL). The organic layer was dried over $MgSO_4$ and evaporated to dryness. Residual solvent was removed under high vacuum overnight. Purification by liquid chromatography on silica was not required for the isolation of [79]. Yield: 17.20 g, colourless viscous oil, (97%). ^{1}H NMR (400 MHz, $CDCl_3$): δ = 1.06 (s, 3H), 1.36 (s, 3H), 1.41 (s, 3H), 2.46 (s, 3H), 3.46 (t, *J* = 6.2 Hz, 2H), 3.56 (d, *J* = 11.9 Hz, 2H), 4.07 (d, *J* = 11.9 Hz, 2H), 4.46 (t, *J* = 6.2 Hz, 2H), 7.38 (d, *J* = 7.9 Hz, 1H), 7.81 (d, *J* = 7.9 Hz, 1H).^{13}C NMR (100 MHz, $CDCl_3$): δ = 18.23, 21.67, 22.14, 25.09, 41.84, 55.06, 57.98, 65.79,

98.11, 128.17, 130.12, 136.07, 145.22, 173.78. Calcd: $[M+Na]^+$ ($C_{17}H_{24}NaO_6S$) m/z = 379.12. Found: ESI-MS: $[M+Na]^+$ m/z = 379.10. Anal. Calcd for $C_{17}H_{24}O_6S$: C, 57.28; H, 6.79; S, 9.00. Found: C, 57.31; H, 6.72; S, 8.89.

General deprotection procedure for removal of acetonide protecting groups, [$(OH)_2$-G_1-TSe];[80] - Eight spatulas of DOWEX 50W-X2 was added to a solution of [$Acet_1$-G_1-TSe];[79] (17.20 g, 48.3 mmol, 1 equiv.) in 400 mL of methanol. The mixture was stirred at 50 °C for 3 hours, and the deprotection followed using TLC until total disappearance of the starting material resulted. Once complete, the resin was filtered off and the solution evaporated to dryness. Residual solvent was removed under high vacuum overnight. Yield: 14.83 g, white crystals, (97%). ^{1}H NMR (400 MHz, CD_3OD): δ = 1.03 (s, 3H), 2.45 (s, 3H), 3.49-3.57 (dd, 4H), 3.59 (t, *J* = 5.9 Hz, 2H), 4.40 (t, *J* = 5.8 Hz, 2H), 7.47 (d, 2H), 7.83 (d, 2H). ^{13}C NMR (100 MHz, CD_3OD): δ = 17.07, 21.61, 51.58, 55.90, 58.93, 65.66, 129.30, 131.22, 137.76, 146.71, 175.89. Calcd: $[M+Na]^+$ ($C_{14}H_{20}NaO_6S$) m/z = 339.10. Found: ESI-MS: $[M+Na]^+$ m/z = 339.10. Anal. Calcd for $C_{14}H_{20}O_6S$: C, 53.15; H, 6.37; S, 10.14. Found: C, 53.31; H, 6.34; S, 10.01.

[$Acet_2$-G_2-TSe];[81] - [$(OH)_2$-G_1-TSe];[80] (14.73 g, 46.56 mmol, 1 equiv.), DMAP (2.56 g, 20.95 mmol, 0.45 equiv.), 2 (46.15 g, 139.68 mmol, 3 equiv.), 38 mL pyridine and 114 mL CH_2Cl_2 were reacted according to the general esterification procedure, resulting in a viscous colourless oil that was purified by liquid chromatography on silica, eluted from EtOAc:hexane (30:70) increasing the polarity to EtOAc:hexane (50:50). Yield: 26.35 g, colourless viscous oil, (90%). ^{1}H NMR (400 MHz, $CDCl_3$): δ = 1.11 (s, 6H), 1.17 (s, 3H), 1.34 (s, 6H), 1.42 (s, 6H), 2.46 (s, 3H), 3.45 (t, *J* = 6.2 Hz, 2H), 3.62 (d, *J* = 11.9 Hz, 4H), 4.13 (d, *J* = 11.9 Hz, 4H), 4.17-4.23 (m, 4H), 4.45 (t, *J* = 6.2 Hz, 2H), 7.39 (d, 2H), 7.80 (d, 2H).^{13}C NMR (100 MHz, $CDCl_3$): δ = 17.37, 18.46, 21.60, 21.65, 25.63, 42.10, 46.69, 54.88, 58.28, 65.07, 65.98, 66.01, 98.13, 128.11, 130.15, 136.24, 145.24, 172.04, 173.50. Calcd: $[M+Na]^+$ ($C_{30}H_{44}NaO_{12}S$) m/z = 651.25. Found: ESI-MS: $[M+Na]^+$ m/z = 651.20. Anal. Calcd for $C_{30}H_{44}O_{12}S$: C, 57.31; H, 7.05; S, 5.10. Found: C, 57.36; H, 6.99; S, 4.95.

[$(OH)_4$-G_2-TSe];[82] - [$Acet_2$-G_2-TSe];[81] (25.26 g, 40.18 mmol, 1 equiv), five spatulas of DOWEX 50W-X2 and 500 mL methanol was reacted according to the general deprotection procedure. Yield: 20.72 g, white crystals, (94%). ^{1}H NMR (400 MHz, CD_3OD): δ = 1.15 (s, 9H), 2.49 (s, 3H), 3.53-3.77 (m, 10H), 4.08 (d, *J* = 11.2 Hz, 2H), 4.14 (d, *J* = 11.2 Hz, 2H), 4.46 (t, *J* = 5.7 Hz, 2H), 7.50 (d, 2H), 7.85 (d, 2H). ^{13}C NMR (100 MHz, CD_3OD): δ = 17.25, 17.81, 21.61, 47.61, 51.77, 55.77, 59.62, 65.80, 66.10, 129.26, 131.28, 137.85, 146.68, 173.67, 175.80. Calcd: $[M+Na]^+$ ($C_{24}H_{36}NaO_{12}S$) m/z = 571.18. Found: ESI-MS: $[M+Na]^+$ m/z = 571.20. Anal. Calcd for $C_{24}H_{36}O_{12}S$: C, 52.54; H, 6.61; S, 5.84. Found: C, 52.60; H, 6.54; S, 5.77.

[$Acet_4$-G_3-TSe];[83] - [$(OH)_4$-G_2-TSe];[82] (20.64 g, 33 mmol, 1 equiv.), DMAP (2.44 g, 20 mmol, 0.62 equiv.), 2 (65.41 g, 198 mmol, 6 equiv.), 53 mL pyridine and 160 mL CH_2Cl_2 were reacted according to the general esterification procedure, resulting in a viscous colourless oil that was purified by liquid chromatography on silica, eluted from EtOAc:hexane (30:70) increasing the polarity to EtOAc:hexane (60:40). Yield: 37.87 g, colourless viscous oil, (98%). ^{1}H NMR (400 MHz, $CDCl_3$): δ = 1.14 (s, 12H), 1.18 (s, 3H), 1.27 (s, 6H), 1.35 (s, 12H), 1.42 (s, 12H), 2.46 (s, 3H), 3.47 (t, *J* = 6.0 Hz, 2H), 3.62 (d, *J* = 12.1 Hz, 8H) 4.08-4.49 (m, 20H), 4.48 (t, *J* = 6.0 Hz, 2H), 7.39 (d, 2H), 7.82 (d, 2H).^{13}C NMR (100 MHz, $CDCl_3$): δ = 17.25, 17.68, 18.50, 21.67, 21.96, 25.30, 42.05, 46.53, 46.85, 54.74, 58.38, 64.90, 65.76, 65.93, 65.98, 98.11, 128.12, 130.14, 136.26, 145.18, 171.67, 171.83, 173.53. Calcd: $[M+Na]^+$ ($C_{56}H_{84}NaO_{24}S$) m/z = 1195.50. Found: ESI-MS: $[M+Na]^+$ m/z = 1195.50. Anal. Calcd for $C_{56}H_{84}O_{24}S$: C, 57.32; H, 7.22; S, 2.73. Found: C, 58.01; H, 7.20; S, 2.72.

[$(OH)_8$-G_3-TSe];[84] - [$Acet_4$-G_3-TSe];[83] (37.60 g, 32.05 mmol, 1 equiv), five spatulas of DOWEX 50W-X2 and 500 mL methanol was reacted according to the general deprotection procedure. Yield: 31.56 g, white crystals, (97%). ^{1}H NMR (400 MHz, CD_3OD): δ = 1.17 (s, 15H), 1.30 (s, 3H), 2.50 (s, 3H), 3.56-3.73 (m, 18H), 4.14-4.38 (m, 12H), 4.50 (t, *J* = 5.5 Hz, 2H), 7.51 (d, 2H), 7.88 (d, 2H). ^{13}C NMR (100 MHz, CD_3OD): δ = 13.70, 17.71, 18.23, 21.66, 47.74, 47.89, 51.80, 55.68, 59.82, 65.79, 66.15, 67.05, 129.29, 131.28, 137.88, 146.71, 173.33, 173.70, 175.89. Calcd: $[M+Na]^+$ ($C_{44}H_{68}NaO_{24}S$) m/z = 1035.37. Found: ESI-MS: $[M+Na]^+$ m/z = 1035.40. Anal. Calcd for $C_{44}H_{68}O_{24}S$: C, 52.17; H, 6.77; S, 3.17. Found: C, 52.16; H, 6.61; S, 3.15.

[Acet$_8$-G$_4$-TSe];[85] - [(OH)$_8$-G$_3$-TSe];[84] (3.67 g, 3.62 mmol, 1 equiv.), DMAP (0.71 g, 5.80 mmol, 1.6 equiv.), 2 (14.35 g, 43.44 mmol, 12 equiv.), 12 mL pyridine and 24 mL CH_2Cl_2 were reacted according to the general esterification procedure, resulting in a viscous colourless oil that was purified by liquid chromatography on silica, eluted from EtOAc:hexane (30:70) increasing the polarity to EtOAc:hexane (70:30). Yield: 6.67 g, colourless viscous oil, (82%). ^{1}H NMR (400 MHz, $CDCl_3$): δ = 1.14 (s, 24H), 1.20-1.30 (m, 21H), 1.34 (s, 24H), 1.41 (s, 24H), 2.46 (s, 3H), 3.47 (t, *J* = 6.0 Hz, 2H), 3.62 (d, *J* = 12.1 Hz, 16H), 4.14 (d, *J* = 12.1 Hz, 16H) 4.17-4.38 (m, 28H), 4.48 (t, *J* = 6.0 Hz, 2H), 7.40 (d, 2H), 7.82 (d, 2H). ^{13}C NMR (100 MHz, $CDCl_3$): δ = 17.13, 17.49, 17.68, 18.49, 21.66, 22.00, 25.26, 42.02, 46.56, 46.68, 46.81, 54.70, 58.38, 64.80, 65.53, 65.91, 65.96, 66.22, 98.08, 128.10, 130.13, 136.36, 145.14, 171.41, 171.54, 171.85, 173.48. Calcd: $[M+Na]^+$ ($C_{108}H_{164}NaO_{48}S$) m/z = 2284.0, $[M+2Na]^{2+}$ ($C_{108}H_{164}Na_2O_{48}S$) m/z = 1153.5. Found: ESI-MS: $[M+Na]^+$ m/z = 2284.10, $[M+2Na]^{2+}$ m/z = 1153.5. Found: MALDI-TOF MS: $[M+Na]^+$ m/z = 2283.81. Anal. Calcd for $C_{108}H_{164}O_{48}S$: C, 57.33; H, 7.31; S, 1.42. Found: C, 57.27; H, 7.19; S, 1.35.

[(OH)$_{16}$-G$_4$-TSe];[86] - [Acet$_8$-G$_4$-TSe];[85] (6.25 g, 2.76 mmol, 1 equiv), three spatulas of DOWEX 50W-X2 and 100 mL methanol was reacted according to the general deprotection procedure. Yield: 5.28 g, white crystals, (98%). ^{1}H NMR (400 MHz, CD_3OD): δ = 1.11 (s, 24H), 1.16 (s, 3H), 1.26 (s, 18H), 2.44 (s, 3H), 3.50-3.70 (m, 34H), 4.08-4.37 (m, 28H), 4.50 (t, 2H), 7.46 (d, 2H), 7.83 (d, 2H). ^{13}C NMR (100 MHz, CD_3OD): δ = 17.34, 17.74, 18.08, 18.31, 21.71, 47.77, 47.91, 48.36, 51.79, 55.70, 59.86, 65.81, 66.14, 67.08, 67.41, 129.32, 131.31, 137.90, 146.70, 173.27, 173.78, 175.89. Calcd: $[M+Na]^+$ ($C_{84}H_{132}NaO_{48}S$) m/z = 1963.75, $[M+2Na]^{2+}$ ($C_{84}H_{132}Na_2O_{48}S$) m/z = 993.37. Found: ESI-MS: $[M+Na]^+$ m/z = 1963.80, $[M+2Na]^{2+}$ m/z = 993.4. Anal. Calcd for $C_{84}H_{132}O_{48}S$: C, 51.95; H, 6.85; S, 1.65. Found: C, 51.36; H, 6.80; S, 1.69.

[Xan-A-Anhyd];[87] - [Xan-A-COOH];[57] (19.11 g, 106 mmol, 1 equiv.) was dissolved in 100 mL CH_2Cl_2. N,N″-Dicyclohexylcarbodiimide (DCC) (10.94 g, 53.01 mmol, 0.5 equiv.) was added to the mixture, and stirring continued at ambient temperature for 24 hrs. The reaction was monitored by ^{13}C NMR. Determination of reaction completion resulted by the appearance of the anhydride carbonyl carbon at 163.1 ppm and the disappearance of the acid carbonyl carbon at 174.3 ppm. The

Dicyclohexylurea (DCU) byproduct was removed by filtration, and the solvent evaporated. Yield: 18.91 g, pale yellow solid, (99%). ^{1}H NMR (400 MHz, $CDCl_3$): δ = 1.44 (t, *J* = 7.1 Hz, 6H) 4.07 (s, 4H), 4.66 (q, *J* = 7.1 Hz, 4H).^{13}C NMR (100 MHz, $CDCl_3$): δ = 13.73, 38.59, 71.28, 163.11, 211.42.

General procedure for functionalisation with Xanthate surface groups using anhydride chemistry, [Xan$_8$-G$_3$-TSe];[61] [$(OH)_8$-G_3-TSe];[84] (5.17 g, 5.10 mmol, 1 equiv.) and DMAP (1.0 g, 8.16 mmol, 1.6 equiv.) were dissolved in 25 mL of anhydrous pyridine. After cooling the mixture in an ice bath, [Xan-A-Anhyd];[87] (18.17 g, 53.05 mmol, 10.4 equiv.) in 50 mL of anhydrous CH_2Cl_2 was added slowly under a nitrogen atmosphere. After stirring at ambient temperature for 16 hours, approximately 10 mL of water was added and stirred at ambient temperature for an additional 3 hours to quench the excess anhydride. The product was isolated by diluting the mixture with CH_2Cl_2 (250 mL) and washing with 1 M $NaHSO_4$ (3 x 150 mL), 1M $NaHCO_3$ (3 x 150 mL), and brine (1 x 150 mL). The organic layer was dried over $MgSO_4$ and evaporated to dryness resulting in a viscous dark orange oil that was purified by liquid chromatography on silica, eluted from EtOAc:hexane (15:85) increasing the polarity to EtOAc:hexane (50:50). Residual solvent was removed under high vacuum overnight. Yield: 8.95 g, orange viscous oil, (76%). ^{1}H NMR (400 MHz, $CDCl_3$): δ = 1.20-1.30 (m, 21H), 1.42 (t, *J* = 7.2 Hz, 24H), 2.47 (s, 3H), 3.47 (t, *J* = 5.8 Hz, 2H), 3.94 (s, 16H), 4.16-4.36 (m, 28H), 4.49 (t, *J* = 5.8 Hz, 2H), 4.63 (t, *J* = 7.2 Hz, 16H) 7.40 (d, 2H), 7.81 (d, 2H). ^{13}C NMR (100 MHz, $CDCl_3$): δ = 13.77, 17.28, 17.63, 17.86, 21.72, 37.73, 46.35, 46.51, 46.75, 54.73, 58.39, 65.46, 66.22, 70.89, 128.10, 130.18, 136.28, 145.21, 167.43, 171.48, 171.63, 171.69, 212.63. Calcd: $[M+Na]^+$ ($C_{84}H_{116}NaO_{40}S_{17}$) m/z = 2331.22. Found: MALDI-TOF MS: $[M+Na]^+$ m/z = 2331.42. Anal. Calcd for $C_{84}H_{116}O_{40}S_{17}$: C, 43.66; H, 5.06; S, 23.59. Found: C, 44.01; H, 5.04; S, 23.86.

[Xan$_{16}$-G$_4$-TSe];[88] - [$(OH)_{16}$-G_4-TSe];[86] (3.81 g, 1.96 mmol, 1 equiv.), DMAP (1.56 g, 12.74 mmol, 6.5 equiv.), 14 (16.13 g, 47.10 mmol, 24 equiv.), 13 mL pyridine and 40 mL CH_2Cl_2 were reacted according to the general xanthate anhydride functionalisation procedure, resulting in a viscous dark orange oil that was purified by liquid chromatography on silica, eluted from EtOAc:hexane (20:80) increasing the polarity to EtOAc:hexane (60:40). Yield: 6.69 g, dark orange viscous oil, (75%). ^{1}H NMR (400 MHz, $CDCl_3$): δ = 1.21-1.34 (m, 45H), 1.42 (t, *J* = 7.0 Hz, 48H), 2.47 (s, 3H),

3.48 (t, *J* = 5.2 Hz, 2H) 3.94 (s, 32H), 4.27 (m, 60H), 4.49 (t, *J* = 5.2 Hz, 2H), 4.63 (t, *J* = 7.0 Hz, 32H), 7.41 (d, 2H), 7.80 (d, 2H). ^{13}C NMR (100 MHz, $CDCl_3$): δ = 13.78, 17.22, 17.53, 17.64, 17.87, 21.73, 37.73 46.32, 46.66, 46.72, 54.68, 58.40, 65.28, 65.80, 66.19, 66.19, 66.50, 70.90, 128.07, 130.19, 136.39, 145.18, 167.43, 171.40, 171.51, 171.67, 212.63. Calcd: $[M+Na]^+$ ($C_{164}H_{228}NaO_{80}S_{33}$) m/z = 4555.45. Found: MALDI-TOF MS: $[M+Na]^+$ m/z = 4555.85. Anal. Calcd for $C_{164}H_{228}O_{80}S_{33}$: C, 43.41; H, 5.06; S, 23.32. Found: C, 43.84; H, 5.07; S, 23.26.

[OH-BiB];[89] - Ethylene glycol (272 mL, 4.85 mol, 50 equiv.) and triethylamine (28 mL, 200 mmol, 2 equiv.) were dissolved in 100 mL of dry tetrahydrofuran. Using an ice bath to cool the vessel, α-Bromoisobutyryl bromide (12 mL, 97.1 mmol, 1 equiv.) was added slowly, dropwise, to the mixture over 30 minutes. The reaction was left stirring under a nitrogen atmosphere at ambient temperature for 16 hours. The product was isolated by pouring the crude mixture into distilled water (800 mL) and extracting the aqueous phase with CH_2Cl_2 (6 x 100 mL). The combined organic layers were washed with 1M HCl (pH 4) (2 x 300mL), dried over $MgSO_4$ and evaporated to dryness. Residual solvent was removed under high vacuum overnight. Yield: 15.64 g, pale yellow oil, (76%) ^{1}H NMR (400 MHz, $CDCl_3$): δ = 1.96 (s, 6H), 3.88 (m, *J* = 4.7 Hz, 2H), 4.32 (m, *J* = 4.7 Hz, 2H). ^{13}C NMR (100 MHz, $CDCl_3$): δ = 30.70, 55.79, 60.89, 67.41, 171.94. Calcd: $[M+NH_4]^+$ ($C_6H_{15}BrNO_3$) m/z = 228.02. Found: CI MS: $[M+NH_4]^+$ m/z) 228.02. Anal. Calcd for $C_6H_{11}BrO_3$: C, 34.14; H, 5.25. Found: C, 34.63; H, 5.30. This compound was prepared by Matyjaszewski et al.[7] The above spectroscopic data agreed with that reported.

[Xan_{16}-G_4-COOH];[90] - [Xan_{16}-G_4-TSe];[88] (6.44 g, 1.22 mmol, 1 equiv.) was dissolved in 50 mL of anhydrous CH_2Cl_2 and 1,8- diazabicyclo[5.4.0]undec-7-ene (DBU) (0.277mL, 1.85 mmol, 1.3 equiv.)added dropwise to the mixture. The reaction was left stirring under a nitrogen atmosphere at ambient temperature for 16 hours and monitored until completion by TLC (60:40 hexane:ethyl acetate). The product was isolated by diluting the mixture with CH_2Cl_2 (100 mL) and washing with 1 M $NaHSO_4$ (2 x 100 mL) and brine (1 x 100 mL). The organic layer was dried over $MgSO_4$ and evaporated to dryness. The product was precipitated twice into hexanes:ethyl acetate (9:1). Residual solvent was removed under high vacuum overnight. Yield: 5.25 g, orange viscous oil, (85%).^{1}H NMR

(400 MHz, $CDCl_3$): δ = 1.20-1.36 (m, 45H), 1.42 (t, *J* = 7.20 Hz, 48H), 3.95 (s, 32H), 4.11-4.44 (m, 60H), 4.63 (t, *J* = 7.20 Hz, 32H). ^{13}C NMR (100 MHz, $CDCl_3$): δ = 13.79, 17.48, 17.59, 17.65, 17.87, 37.74, 46.30, 46.35, 46.67, 46.72, 65.43, 65.92, 66.21, 66.82, 66.50, 70.92, 167.53, 171.39, 171.45, 171.85, 172.98, 212.63. Calcd: $[M+K]^+$ ($C_{155}H_{218}KO_{78}S_{32}$) m/z = 4389.38. Found: MALDI-TOF MS: $[M+K]^+$ m/z = 4393.83. Anal. Calcd for $C_{155}H_{218}O_{78}S_{32}$: C, 42.74; H, 5.04; S, 23.56. Found: C, 42.99; H, 5.01; S, 23.38.

General procedure for focal point modification to α-bromoisobutyrate moiety, [Xan_2-G_1-BiB];[91] - [Xan_2-G_1-COOH];[59] (8.25 g, 18 mmol, 1 equiv.), [OH-BiB];[89] (5.70 g, 27 mmol, 1.5 equiv.), and DPTS (1.06 g, 3.6 mmol, 0.2 equiv.) were dissolved in 80 mL of anhydrous CH_2Cl_2 under a nitrogen atmosphere. DCC (7.43 g, 36 mmol, 2 equiv.) was added to the mixture in a small volume of CH_2Cl_2, and stirring continued at ambient temperature for 16 hrs. The product was isolated by diluting the mixture with CH_2Cl_2 (150 mL), washed with H_2O (2 x 100 mL) and brine (1 x 100 mL). The organic layer was dried over $MgSO_4$ and evaporated to dryness resulting in a viscous dark orange oil that was purified by liquid chromatography on silica, eluted from EtOAc:hexane (10:90) increasing the polarity to EtOAc:hexane (30:70). Residual solvent was removed under high vacuum overnight. Yield: 6.39 g, yellow viscous oil, (55%). ^{1}H NMR (400 MHz, $CDCl_3$): δ = 1.29 (s, 3H), 1.43 (t, *J* = 7.1 Hz, 6H), 1.94 (s, 6H), 3.93 (s, 4H), 4.28 (d, *J* = 11.1 Hz, 2H), 4.35 (d, *J* = 11.1 Hz, 2H), 4.40 (s, 4H), 4.64 (q, *J* = 7.1 Hz, 4H). ^{13}C NMR (100 MHz, $CDCl_3$): δ = 13.76, 17.86, 30.66, 37.75, 46.26, 55.32, 62.72, 63.34, 66.28, 70.90, 167.42, 171.41, 172.06, 212.58. Calcd: $[M+Na]^+$ ($C_{21}H_{31}BrNaO_{10}S_4$) m/z = 673.0. Found: ESI-MS: $[M+Na]^+$ m/z = 673.0 Anal. Calcd for $C_{21}H_{31}BrO_{10}S_4$: C, 38.71; H, 4.80; S, 19.68. Found: C, 39.99; H, 4.86; S, 19.37.

[Xan_4-G_2-BiB];[92] – [Xan_4-G_2-COOH];[62] (6.52 g, 6.42 mmol, 1 equiv.), [OH-BiB];[89] (2.03 g, 9.63 mmol, 1.5 equiv.), DPTS (0.38 g, 1.28 mmol, 0.2 equiv.), DCC (2.65 g, 12.84 mmol, 2 equiv.) in 60 mL of anhydrous CH_2Cl_2 were reacted according to the general procedure for focal point modification resulting in a viscous orange oil that was purified by liquid chromatography on silica, eluted from EtOAc:hexane (20:80) increasing the polarity to EtOAc:hexane (60:40). Yield: 4.53 g, yellow viscous oil, (58%). ^{1}H NMR (400 MHz, $CDCl_3$): δ = 1.26 (s, 6H), 1.29 (s, 3H), 1.42 (t, *J* = 7.2

Hz, 12H), 1.94 (s, 6H), 3.96 (s, 8H), 4.19-4.36 (m, 12H), 4.36-4.49 (m, 4H), 4.64 (q, *J* = 7.1 Hz, 8H). ^{13}C NMR (100 MHz, $CDCl_3$): δ = 13.75, 17.65, 17.87, 30.67, 37.73, 46.36, 46.67, 55.38, 62.90, 63.25, 65.66, 66.25, 70.88, 167.43, 171.37, 171.66, 171.86, 212.62. Calcd: $[M+Na]^+$ ($C_{41}H_{59}BrNaO_{12}S_8$) m/z = 1229.04. Found: ESI-MS: $[M+Na]^+$ m/z = 1229.17. Anal. Calcd for $C_{41}H_{59}BrO_{20}S_8$: C, 40.75; H, 4.92; S, 21.23. Found: C, 43.22; H, 5.20; S, 21.13.

[Xan$_8$-G$_3$-BiB];[93] – [Xan$_8$-G$_3$-COOH];[63] (4.670 g, 2.21 mmol, 1 equiv.), [OH-BiB];[89] (0.466 g, 2.21 mmol, 1.0 equiv.), DPTS (2.43 g, 2.43 mmol, 1.1 equiv.), DCC (0.501 g, 2.43 mmol, 1.1 equiv.) in 30 mL of anhydrous CH_2Cl_2 were reacted according to the general procedure for focal point modification resulting in a viscous orange oil that was purified by liquid chromatography on silica, eluted from EtOAc:hexane (10:90) increasing the polarity to EtOAc:hexane (50:50). Yield: 2.91 g, yellow viscous oil, (57%). ^{1}H NMR (400 MHz, $CDCl_3$): δ = 1.22-1.34 (m, 21H), 1.42 (t, *J* = 7.2 Hz, 24H), 1.94 (s, 6H), 3.95 (s, 16H), 4.17-4.51 (m, 32H), 4.63 (t, *J* = 7.2 Hz, 16H). ^{13}C NMR (100 MHz, $CDCl_3$): δ = 13.76, 17.52, 17.63, 17.86, 30.64, 46.31, 46.57, 46.73, 55.48, 62.95, 63.22, 65.38, 66.18, 70.89, 167.42, 171.34, 171.44, 171.66, 171.76, 212.64. Calcd: $[M+Na]^+$ ($C_{81}H_{115}NaO_{40}S_{16}$) m/z = 2341.16. Found: MALDI TOF MS: $[M+Na]^+$ m/z = 2341.36. Anal. Calcd for $C_{81}H_{115}BrO_{40}S_{16}$: C, 41.90; H, 4.99; S, 22.10. Found: C, 42.75; H, 5.02; S, 22.29.

[Xan$_{16}$-G$_3$-BiB];[94] – [Xan$_{16}$-G$_4$-COOH];[90] (2.073 g, 0.476 mmol, 1 equiv.), [OH-BiB];[89] (0.10 g, 0.476 mmol, 1.0 equiv.), DPTS (0.154 g, 0.524 mmol, 1.1 equiv.), DCC (0.108 g, 0.524 mmol, 1.1 equiv.) in 10 mL of anhydrous CH_2Cl_2 were reacted according to the general procedure for focal point modification resulting in a viscous orange oil that was purified by liquid chromatography on silica, eluted from EtOAc:hexane (10:90) increasing the polarity to EtOAc:hexane (50:50). Yield: 1.46 g, orange viscous oil, (67%). δ = 1.22-1.34 (m, 45H), 1.42 (t, *J* = 7.20 Hz, 48H), 1.94 (6H, s), 3.95 (s, 32H), 4.17-4.47 (m, 64H), 4.63 (t, *J* = 7.20 Hz, 32H). ^{13}C NMR (100 MHz, $CDCl_3$): δ = 13.78, 17.54, 17.64, 17.88, 30.66, 37.73, 46.30, 46.62, 46.66, 46.71, 60.41, 65.25, 65.76, 66.17, 66.47, 70.90, 167.42, 171.18, 171.28, 171.35, 171.47, 171.66, 212.63. Calcd: $[M+Na]^+$ ($C_{161}H_{227}BrNaO_{80}S_{32}$) m/z = 4565.38. Found: MALDI-TOF MS: $[M+Na]^+$ m/z = 4567.19

[95] and [96] - A**tom transfer radical polymerisation (ATRP) of tertiary butyl methacrylate (tBuMA) in IPA/H_2O with [Xan_2-G_1-BiB];[91] or [Xan_4-G_2-BiB];[92] –** In a typical synthesis, targeting DP_n = 50 monomer units for the primary chains, [Xan_2-G_1-BiB];[91] (0.4581 g, 0.703 mmol, 1 equiv.), ^{t}BuMA (5 g, 35.16 mmol, 50 equiv.), bpy (0.220 g, 1.406 mmol, 2 equiv.) and 2 drops of anisole were placed into a 50 mL round-bottomed flask. IPA/H_2O (92.5/7.5 v/v) was added to the flask (50 wt% based on ^{t}BuMA, 5g, 6.3 mL) and the solution was stirred and deoxygenated using a nitrogen purge for 10 minutes. Cu(I)Cl (0.070 g, 0.703 mmol, 1 equiv) was added to the flask, whilst maintaining a positive flow of nitrogen, and the solution was left to polymerise at 40 °C. The reaction was terminated when conversion reached >90%, indicated by ^{1}H NMR after 8 hours, by exposure to oxygen and addition of THF. The solution was passed through a neutral alumni column to remove the catalytic system, and precipitated twice into cold hexane (cooled using a dry ice bath). After drying the precipitated sample overnight under high vacuum to remove residual solvents, the polymer was obtained as a white solid.

[97]-[100] - A**tom transfer radical polymerisation (ATRP) of tertiary butyl methacrylate (tBuMA) in acetone with [91], [92], [93], or [94] -** In a typical synthesis, targeting DP_n = 50 monomer units for the primary chains, [Xan_8-G_3-BiB];[93] (0.653 g, 0.2812 mmol, 1 equiv.), ^{t}BuMA (2 g, 14.06 mmol, 50 equiv.), bpy (0.088 g, 0.5624 mmol, 2 equiv.) and 2 drops of anisole were placed into a 50 mL round-bottomed flask. Acetone was added to the flask (50 wt% based on ^{t}BuMA, 2g, 2.53 mL) and the solution was stirred and deoxygenated using a nitrogen purge for 10 minutes. Cu(I)Cl (0.070 g, 0.703 mmol, 1 equiv) was added to the flask, whilst maintaining a positive flow of nitrogen, and the solution was left to polymerise at 50 °C. Care was taken to ensure that the vessel was sealed thoroughly to ensure the acetone did not evaporate. The reaction was terminated when conversion reached >94%, indicated by ^{1}H NMR after 28 hours, by exposure to oxygen and addition of THF. The solution was passed through a neutral alumni column to remove the catalytic system and precipitated twice into cold hexane (cooled using a dry ice bath). After drying the precipitated sample overnight under high vacuum to remove residual solvents, the polymer was obtained as a white solid.

[MPA];[101] – Morpholio propan-2-ol [MP] (5 g, 34.44 mmol, 1 equiv.), triethylamine (6.24 mL, 44.77 mmol, 1.3 equiv.) and a catalytic amount of DMAP were dissolved in 40 mL CH_2Cl_2. After cooling the mixture in an ice bath, acryloyl chloride (3.64 mL, 44.77 mmol, 1.3 equiv.) was added slowly, dropwise, to the mixture using a dropping funnel. The mixture turned orange on addition of acryloyl chloride. The ice bath was removed after 1 hour, and the mixture was left stirring at ambient temperature for 16 hours. After filtration to remove the salts, the product was isolated by diluting the mixture with CH_2Cl_2 (100mL) and washing with 1M $NaHCO_3$ (3 x 100mL). The organic layer was dried over $MgSO_4$ and evaporated to dryness. Yield: 5.10 g, dark orange oil, (74%). ^{1}H NMR (400 MHz, $CDCl_3$): δ = 1.26 (d, *J* = 6.1 Hz, 1H), 2.32-2.59 (m, 6H), 3.66 (t, *J* = 4.7 Hz, 4H), 5.16 (m, 1H), 5.80 (dd, *J* = 1.6 Hz, 10.4 Hz, 1H), 6.10 (dd, *J* = 10.4 Hz, 17.2 Hz, 1H), 6.38 (dd, *J* = 1.6 Hz, 17.2 Hz, 1H). ^{13}C NMR (100 MHz, $CDCl_3$): δ = 18.46, 54.05, 63.37, 67.03, 68.00, 128.93, 130.42, 165.71.

[104]-[122] General Procedure for one-pot deprotection and Michael addition of the linear dendritic hybrids – In a typical synthesis, the xanthate functional linear dendritic hybrids (0.1 g) was dissolved in 1 mL of anhydrous THF and deoxygenated using a nitrogen purge for 10 minutes. *n*-Butyl amine (2.5 molar excess relative to each xanthate group on the hybrid) was added and the solution stirred at ambient temperature for 1.5 hours. The functional acrylate (5.0 molar excess relative to each thiol) was added, deoxygenated using a nitrogen purge for 2 minutes, and left stirring overnight at ambient temperature. The functionalised polymer hybrid was obtained by precipitation of the mixture into cold hexane (cooled using a dry ice bath). Precipitated samples were dried overnight by high vacuum and freeze dried to remove residual solvents.

6.5 Chapter 5 compounds

[$(Bz)_2$-G_1-TSe];[123] - [$(Xan)_2$-G_1-TSe];[58] (5.13 g, 8.0 mmol, 1 equiv.) was dissolved in 40 mL of anhydrous THF and vigorously degassed with nitrogen for 10 minutes. n-Butylamine (1.74 mL, 17.60 mmol, 2.2 equiv.) was added slowly, and the reaction left stirring at ambient temperature, sealed under nitrogen for 1.5 hours. After confirmation of xanthate starting material loss by TLC

(hexane/ethyl acetate, 60:40) benzyl acrylate (3.18 mL, 20.80 mmol, 2.6 equiv.) was added, and the mixture left stirring at ambient temperature for an additional 16 hours. The product was isolated by reducing the volume of THF by half *in vacuo*, and precipitating the mixture twice from THF into hexane (2 x 150 mL) at ambient temperature. Trace solvents were removed by high vacuum overnight at ambient temperature. Yield: 5.68 g, orange viscous oil (90%). ^{1}H NMR (400 MHz, $CDCl_3$): δ = 1.16 (s, 3H), 2.44 (s, 3H), 2.67 (t, *J* = 7.4 Hz, 4H), 2.88 (t, *J* = 7.4 Hz, 4H), 3.22 (s, 4H), 3.41 (t, *J* = 6.1 Hz, 2H), 4.17 (dd, 4H), 4.44 (t, *J* = 6.1 Hz, 2H), 5.13 (s, 4H), 7.28- 7.41 (m, 12H), 7.79 (d, 2H). ^{13}C NMR (100 MHz, $CDCl_3$): δ = 17.47, 21.65, 27.52, 33.41, 34.28, 46.35, 54.93, 58.30, 65.75, 66.62, 128.11, 128.30, 128.35, 128.60, 130.15, 135.70, 136.23, 145.25, 169.68, 171.41, 171.92. Calcd: $[M+H]^+$ ($C_{38}H_{45}N_{12}O_3S_3$) m/z = 789.2. Found: ESI-MS: $[M+H]^+$ m/z = 789.2, $[M+Na]^+$ m/z = 811.2, $[M+K]^+$ m/z = 827.2. Calcd for $C_{38}H_{44}N_{12}O_3S_3$: C, 57.85; H, 5.62; S, 12.19. Found: C, 58.61; H, 5.62; S, 12.33.

[$(Mp)_2$-G_1-TSe];[124] - [$(Xan)_2$-G_1-TSe];[58] (5.09 g, 7.94 mmol, 1 equiv.) was dissolved in 40 mL of anhydrous THF and vigorously degassed with nitrogen for 10 minutes. n-Butylamine (1.73 mL, 17.47 mmol, 2.2 equiv.) was added slowly, and the reaction left stirring at ambient temperature, sealed under nitrogen for 1.5 hours. After confirmation of xanthate starting material loss by TLC (hexane/ethyl acetate, 60:40) [MPA];[101] (4.14 g, 20.64 mmol, 2.6 equiv.) was added, and the mixture left stirring at ambient temperature for an additional 16 hours. The product was isolated by reducing the volume of THF by half *in vacuo*, and precipitating the mixture twice from THF into hexane (2 x 150 mL) at ambient temperature. Trace solvents were removed by high vacuum overnight at ambient temperature. Yield: 6.36 g, orange viscous oil (93%). ^{1}H NMR (400 MHz, $CDCl_3$): δ = 1.19 (s, 3H), 1.23 (d, 6H), 2.28-2.56 (m, 15H), 2.61 (t, 4H, *J* = 7.1 Hz), 2.88 (t, 4H, *J* = 7.1 Hz), 3.25 (s, 4H), 3.44 (t, *J* = 6.1 Hz, 2H), 3.66 (t, *J* = 4.60 Hz, 8H), 4.20 (dd, 4H), 4.47 (t, *J* = 6.1 Hz, 2H), 5.12 (m, 2H), 7.39 (d, 2H), 7.81 (d, 2H). ^{13}C NMR (100 MHz, $CDCl_3$): δ = 17.47, 18.43, 21.66, 27.64, 33.38, 34.53, 46.37, 54.02, 54.94, 58.29, 63.41, 65.75, 67.03, 68.06, 128.11, 130.16, 136.22, 145.25, 169.67, 171.05, 171.91. Calcd: $[M+H]^+$ ($C_{38}H_{59}N_2O_{14}S_3$) m/z = 863.3. Found: ESI-MS: $[M+H]^+$ m/z =

863.3, $[M+Na]^+$ m/z = 885.3, $[M+K]^+$ m/z = 901.3. Calcd for $C_{38}H_{58}N_2O_{12}S_3$: C, 52.88; H, 6.77; N, 3.25; S, 11.15. Found: C, 53.43; H, 6.72; N, 3.33; S, 11.29.

[$(Bz)_2$-G_1-COOH];[125] - [$(Bz)_2$-G_1-TSe];[123] (5.47 g, 6.93 mmol, 1 equiv.) was dissolved in 60 mL anhydrous CH_2Cl_2, and diazabicyclo[5.4.0]undec-7-ene (DBU) (1.35 mL, 9.01 mmol, 1.3 equiv.) added. The mixture turned dark red upon addition. The reaction was stirred under a nitrogen atmosphere for 16 hours and monitored by using TLC (60:40 hexane:ethyl acetate) to follow the reaction to completion. The product was isolated by diluting the mixture with CH_2Cl_2 (100 mL) and washing with 1 M $NaHSO_4$ (2 x 100 mL). The organic layer was dried over $MgSO_4$ and evaporated to dryness. Additional purification was achieved by liquid chromatography (silica, eluting hexane increasing the polarity to 100 % ethyl acetate (to remove impurities); then changing the mobile phase to CH_2Cl_2 increasing the polarity to CH_2Cl_2:MeOH (90:10); (product eluted approx. 7% MeOH)). Trace solvents were removed by high vacuum overnight at ambient temperature. Yield: 3.01 g, red viscous oil (72%).^{1}H NMR (400 MHz, $CDCl_3$): δ = 1.31 (s, 3H), 2.70 (t, 4H, *J* = 7.4 Hz), 2.92 (t, 4H, *J* = 7.4 Hz), 3.26 (s, 3H), 4.33 (dd, 4H), 5.16 (s, 4H), 7.31-7.43 (m, 10H). ^{13}C NMR (100 MHz, $CDCl_3$): δ = 17.71, 27.46, 33.46, 34.26, 46.21, 66.04, 66.79, 128.21, 128.34, 128.40, 128.62, 130.15, 135.57, 169.81, 171.86, 176.57. Calcd: $[M+Na]^+$ ($C_{29}H_{34}NaO_{10}S_2$) m/z = 629.2. Found: ESI-MS: $[M+Na]^+$ m/z = 629.1, $[M-H+2Na]^+$ m/z = 651.1. Calcd for $C_{29}H_{34}O_{10}S_2$: C, 57.41; H, 5.65; S, 10.57. Found: C, 57.37; H, 5.72; S, 10.92.

[$(Mp)_2$-G_1-COOH];[126] - [$(Mp)_2$-G_1-TSe];[124] (6.12 g, 7.09 mmol, 1 equiv.) was dissolved in 60 mL anhydrous CH_2Cl_2, and diazabicyclo[5.4.0]undec-7-ene (DBU) (1.27 mL, 8.51 mmol, 1.2 equiv.) added. The mixture turned dark red upon addition. The reaction was stirred under a nitrogen atmosphere for 16 hours and monitored by using TLC (60:40 hexane:ethyl acetate) to follow the reaction to completion. The product was isolated by diluting the mixture with CH_2Cl_2 (100 mL) and washing with 1 M $NaHSO_4$ (2 x 100 mL). The organic layer was dried over $MgSO_4$ and evaporated to dryness. Additional purification was achieved by liquid chromatography (silica, eluting hexane:ethyl acetate (50:50) increasing the polarity to 100 % ethyl acetate (to remove impurities); then changing

the mobile phase to CH_2Cl_2 increasing the polarity to CH_2Cl_2:MeOH (90:10);). Trace solvents were removed by high vacuum overnight at ambient temperature. Yield: 4.27 g, red viscous oil (88%).^{1}H NMR (400 MHz, $CDCl_3$): δ = 1.24 (d, 6H), 1.27 (s, 3H), 2.2-2.98 (m, 20H), 3.25 (m, 4H), 3.70 (t, 8H), 4.33 (m, 4H), 5.22 (m, 2H). ^{13}C NMR (100 MHz, $CDCl_3$): δ = 18.14, 18.32, 18.48, 18.56, 27.13, 27.18, 27.40, 27.43, 32.99, 33.09, 33.22, 34.00, 34.76, 34.77, 46.07, 46.18, 46.30, 53.25, 53.32, 53.35, 53.42, 63.83, 62.88, 62.91, 62.96, 65.86-67.09, 167.00, 171.07, 171.16, 175.73. Calcd: $[M+H]^+$ ($C_{29}H_{49}N_2O_{12}S_2$) m/z = 681.3. Found: ESI-MS: $[M+H]^+$ m/z = 681.3, $[M+Na]^+$ m/z = 703.3, $[M-H+2Na]^+$ m/z = 725.2. Calcd for $C_{29}H_{48}N_2O_{12}S_2$: C, 51.16; H, 7.11; N, 4.11; S, 9.42. Found: C, 51.18; H, 7.02; N, 4.08; S, 9.42.

[(Bz)$_2$-G$_1$-BiB];[127] - [(Bz)$_2$-G$_1$-COOH];[125] (2.79 g, 4.60 mmol, 1.0 equiv.), [OH-BiB];[89] (0.971 g, 4.60 mmol, 1.0 equiv.), and DPTS (0.271 g, 0.92 mmol, 0.2 equiv.) were dissolved in 20 mL of anhydrous CH_2Cl_2 under a nitrogen atmosphere. DCC (1.04 g, 5.06 mmol, 1.1 equiv.) was added to the mixture in a small volume of CH_2Cl_2, and stirring continued at ambient temperature for 16 hrs. The product was isolated by diluting the mixture with CH_2Cl_2 (50 mL), washed with H_2O (2 x 50 mL) and brine (1 x 50 mL). The organic layer was dried over $MgSO_4$ and evaporated to dryness resulting in a viscous dark orange oil that was purified by liquid chromatography on silica, eluted from hexane increasing the polarity to ethyl acetate:hexane (10:90). Residual solvent was removed under high vacuum overnight. Yield: 2.88 g, orange viscous oil, (78%). ^{1}H NMR (400 MHz, $CDCl_3$): δ = 1.27 (s, 3H), 1.92 (s, 6H), 2.68 (t, *J* = 7.4 Hz, 4H), 2.90 (t, *J* = 7.4 Hz, 4H), 3.23 (s, 4H), 4.29 (dd, 4H), 4.37 (s, 4H), 5.13 (s, 4H), 7.28-7.41 (m, 10H). ^{13}C NMR (100 MHz, $CDCl_3$): δ = 17.74, 27.52, 30.65, 33.44, 34.29, 46.45, 55.32, 62.66, 63.34, 65.88, 66.62, 128.31, 128.35, 128.60, 135.69, 169.71, 171.39, 172.15. Calcd: $[M+H]^+$ ($C_{35}H_{44}BrO_{12}S_2$) m/z = 799.1. Found: ESI-MS: $[M+H]^+$ m/z = 801.2, $[M+Na]^+$ m/z = 821.1, $[M+K]^+$ m/z = 839.1, $[M+80Da]^+$ m/z = 879.1.

[(Mp)$_2$-G$_1$-BiB];[128] - [(Mp)$_2$-G$_1$-COOH];[126] (4.07 g, 5.98 mmol, 1.0 equiv.), [OH-BiB];[89] (1.26 g, 5.98 mmol, 1.0 equiv.), and DPTS (0.271 g, 0.92 mmol, 0.2 equiv.) were dissolved in 30 mL of anhydrous CH_2Cl_2 under a nitrogen atmosphere. DCC (1.36 g, 6.58 mmol, 1.1 equiv.) was added to the mixture in a small volume of CH_2Cl_2, and stirring continued at ambient temperature for 16 hrs.

The product was isolated by diluting the mixture with CH_2Cl_2 (50 mL), washed with H_2O (2 x 50 mL) and brine (1 x 50 mL). The organic layer was dried over $MgSO_4$ and evaporated to dryness resulting in a viscous dark orange oil that was purified by liquid chromatography on silica, eluted from CH_2Cl_2 increasing the polarity to CH_2Cl_2:MeOH (95:5). Residual solvent was removed under high vacuum overnight. Yield: 2.88 g, red viscous oil, (87%). ^{1}H NMR (400 MHz, $CDCl_3$): δ = 1.23 (d, 6H), 1.30 (s, 3H), 1.94 (s, 6H), 2.27-2.58 (m, 12H), 2.62 (t, *J* = 7.4 Hz, 4H), 2.89 (t, *J* = 7.4 Hz, 4H), 3.26 (s, 4H), 3.66 (t, 8H), 4.31 (dd, 4H), 4.40 (s, 4H), 5.12 (m, 2H). ^{13}C NMR (100 MHz, $CDCl_3$): δ = 17.73, 18.43, 27.64, 30.65, 33.41, 34.53, 46.47, 54.03, 55.30, 62.67, 63.34, 63.43, 65.89, 67.04, 68.05, 169.71, 171.05, 171.38, 171.14. Calcd: $[M+H]^+$ ($C_{35}H_{58}BrN_2O_{14}S_2$) m/z = 873.3. Found: ESI-MS: $[M+H]^+$ m/z = 873.3, $[M+Na]^+$ m/z = 897.12, $[M+K]^+$ m/z = 913.2. Calcd for $C_{35}H_{57}BrN_2O_{14}S_2$: C, 48.11; H, 6.57; N, 3.21; S, 7.34. Found: C, 49.62; H, 6.85; N, 3.51; S, 7.30.

[$(Bz)_4$-G_2-TSe];[129] - [Xan_4-G_2-TSe];[60] (5.296 g, 4.42 mmol, 1 equiv.) was dissolved in 40 mL of anhydrous THF and vigorously degassed with nitrogen for 10 minutes. n-Butylamine (2.10 mL, 21.23 mmol, 4.8 equiv.) was added slowly, and the reaction left stirring at ambient temperature, sealed under nitrogen for 1.5 hours. After confirmation of xanthate starting material loss by TLC (hexane/ethyl acetate, 60:40) benzyl acrylate (4.06 mL, 26.54mmol, 6 equiv.) was added, and the mixture left stirring at ambient temperature for an additional 16 hours. The product was isolated by reducing the volume of THF by half *in vacuo*, and precipitating the mixture twice from THF into hexane (2 x 150 mL) at ambient temperature. Trace solvents were removed by high vacuum overnight at ambient temperature. Yield: 6.10 g, orange viscous oil (92%). ^{1}H NMR (400 MHz, $CDCl_3$): δ = 1.17 (s, 3H), 1.23 (s, 6H), 2.44 (s, 3H), 2.67 (t, *J* = 7.4 Hz, 8H), 2.88 (t, *J* = 7.4 Hz, 8H), 3.22 (s, 8H), 3.41 (t, *J* = 6.1 Hz, 2H), 4.11-4.35 (m, 12H), 4.44 (t, *J* = 6.1 Hz, 2H), 5.13 (s, 8H), 7.28- 7.41 (m, 22H), 7.79 (d, 2H). ^{13}C NMR (100 MHz, $CDCl_3$): δ = 17.35, 17.74, 21.66, 27.51, 33.39, 34.27, 46.53, 46.55, 54.78, 58.35, 65.59, 65.80, 66.59, 128.10, 128.29, 128.33, 128.60, 130.14, 135.72, 136.33, 145.18, 169.74, 171.42, 171.69, 171.75. Calcd: $[M+H]^+$ ($C_{72}H_{84}NaO_{24}S_5$) m/z = 1515.4. Found: ESI-MS: $[M+Na]^+$ m/z = 1515.4, $[M+80Da]^+$ m/z = 1573.4. Calcd for $C_{72}H_{84}NaO_{24}S_{53}$: C, 57.89; H, 5.67; S, 10.73. Found: C, 58.67; H, 5.68; S, 10.88.

[$(Mp)_4$-G_2-TSe];[130] - [Xan_4-G_2-TSe];[60] (5.76 g, 4.81 mmol, 1 equiv.) was dissolved in 50 mL of anhydrous THF and vigorously degassed with nitrogen for 10 minutes. n-Butylamine (2.28 mL, 23.07 mmol, 4.8 equiv.) was added slowly, and the reaction left stirring at ambient temperature, sealed under nitrogen for 1.5 hours. After confirmation of xanthate starting material loss by TLC (hexane/ethyl acetate, 60:40) [MPA];[101] (5.75 g, 28.84 mmol, 6 equiv.) was added, and the mixture left stirring at ambient temperature for an additional 16 hours. The product was isolated by reducing the volume of THF by half *in vacuo*, and precipitating the mixture twice from THF into hexane (2 x 150 mL) at ambient temperature. Trace solvents were removed by high vacuum overnight at ambient temperature. Yield: 7.53 g, orange viscous oil (96%). ^{1}H NMR (400 MHz, $CDCl_3$): δ = 1.17-1.30 (m, 21H), 2.26-2.57 (m, 27H), 2.61 (t, 8H, *J* = 7.1 Hz), 2.88 (t, 8H, *J* = 7.1 Hz), 3.27 (s, 8H), 3.46 (t, *J* = 6.1 Hz, 2H), 3.66 (t, *J* = 4.60 Hz, 16H), 4.11-4.39 (m, 12H), 4.47 (t, *J* = 6.1 Hz, 2H), 5.11 (m, 4H), 7.39 (d, 2H), 7.81 (d, 2H). ^{13}C NMR (100 MHz, $CDCl_3$): δ = 17.35, 17.75, 18.43, 21.68, 27.62, 33.35, 34.51, 46.54, 54.02, 54.78, 58.35, 63.40, 65.59, 65.76, 67.02, 68.04, 128.10, 130.15, 136.33, 145.19, 169.73, 171.05, 171.67, 171.72. Calcd: $[M+H]^+$ ($C_{72}H_{113}N_4O_{28}S_5$) m/z = 1641.6. Found: ESI-MS: $[M+H]^+$ m/z = 1641.6, $[M+Na]^+$ m/z = 1663.6, $[M+80Da]^+$ m/z = 1721.7. Calcd for $C_{72}H_{112}N_4O_{28}S_5$: C, 52.67; H, 6.88; N, 3.41; S, 9.76. Found: C, 53.53; H, 6.85; N, 3.60; S, 9.40.

[$(Bz)_4$-G_2-COOH];[131] - [$(Bz)_4$-G_2-TSe];[129] (5.781 g, 3.87 mmol, 1 equiv.) was dissolved in 55 mL anhydrous CH_2Cl_2, and diazabicyclo[5.4.0]undec-7-ene (DBU) (0.752 mL, 5.03 mmol, 1.3 equiv.) added. The mixture turned dark red upon addition. The reaction was stirred under a nitrogen atmosphere for 16 hours and monitored by using TLC (60:40 hexane:ethyl acetate) to follow the reaction to completion. The product was isolated by diluting the mixture with CH_2Cl_2 (100 mL) and washing with 1 M $NaHSO_4$ (2 x 100 mL). The organic layer was dried over $MgSO_4$ and evaporated to dryness. Additional purification was achieved by liquid chromatography (silica, eluting hexane, increasing the polarity to hexane:ethyl acetate 50:50). Trace solvents were removed by high vacuum overnight at ambient temperature. Yield: 4.00 g, red viscous oil (79%).^{1}H NMR (400 MHz, $CDCl_3$): δ = 1.25 (s, 6H), 1.30 (s, 3H), 2.70 (t, 8H, *J* = 7.4 Hz), 2.92 (t, 8H, *J* = 7.4 Hz), 3.25 (s, 3H), 4.18-4.36 (m, 8H), 5.13 (s, 8H), 7.31-7.43 (m, 20H). ^{13}C NMR (100 MHz, $CDCl_3$): δ = 17.67, 17.77, 27.50,

33.43, 34.38, 46.51, 66.02, 66.26, 66.80, 128.32, 128.38, 128.61, 135.57, 169.76, 171.86, 171.94, 171.97. Calcd: $[M+Na]^+$ ($C_{63}H_{74}NaO_{22}S_4$) m/z = 1333.4. Found: ESI-MS: $[M+Na]^+$ m/z = 1333.4, $[M+K]^+$ m/z = 1349.4. Calcd for $C_{63}H_{74}O_{22}S_4$: C, 57.69; H, 5.69; S, 9.78. Found: C, 57.15; H, 5.63; S, 9.98.

[$(Mp)_4$-G_2-COOH];[132] - [$(Mp)_4$-G_2-TSe];[130] (7.267 g, 4.43 mmol, 1 equiv.) was dissolved in 65 mL anhydrous CH_2Cl_2, and diazabicyclo[5.4.0]undec-7-ene (DBU) (0.861 mL, 5.76 mmol, 1.3 equiv.) added. The mixture turned dark red upon addition. The reaction was stirred under a nitrogen atmosphere for 16 hours and monitored by using TLC (60:40 hexane:ethyl acetate) to follow the reaction to completion. The product was isolated by diluting the mixture with CH_2Cl_2 (100 mL) and washing with 1 M $NaHSO_4$ (2 x 100 mL). The organic layer was dried over $MgSO_4$ and evaporated to dryness. Additional purification was achieved by liquid chromatography (silica, eluting hexane, increasing the polarity to hexane:ethyl acetate 50:50). Trace solvents were removed by high vacuum overnight at ambient temperature. Yield: 4.84 g, red viscous oil (75%). ^{1}H NMR (400 MHz, $CDCl_3$): δ = 1.16-1.37 (m, 21H), 2.32-2.77 (m, 32H), 2.88 (t, *J* = 7.4 Hz, 8H), 3.28 (s, 8H), 3.68 (t, 16H), 4.05-4.45 (m, 12H), 5.15 (m, 4H). ^{13}C NMR (100 MHz, $CDCl_3$): δ = 17.79, 18.00, 18.49, 27.62, 30.93, 33.50, 34.55, 34.60, 46.48, 46.51, 53.77, 63.08, 66.01, 66.33, 66.62, 67.79, 67.89, 169.82, 171.14, 171.79, 175.24. Calcd: $[M+H]^+$ ($C_{63}H_{102}N_4O_{26}S_4$) m/z = 1459.6. Found: ESI-MS: $[M+H]^+$ m/z = 1459.6, $[M+Na]^+$ m/z = 1481.5. Calcd for $C_{63}H_{74}O_{22}S_4$: C, 51.84; H, 7.04; N, 3.84; S, 8.79. Found: C, 52.19; H, 6.89; N, 3.81; S, 8.83.

[$(Bz)_4$-G_2-BiB];[133] - [$(Bz)_4$-G_2-COOH];[131] (3.80 g, 2.90 mmol, 1.0 equiv.), [OH-BiB];[89] (0.734 g, 3.48 mmol, 1.2 equiv.), and DPTS (0.171 g, 0.58 mmol, 0.2 equiv.) were dissolved in 35 mL of anhydrous CH_2Cl_2 under a nitrogen atmosphere. N,N′′-Dicyclohexylcarbodiimide (DCC) (0.66 g, 3.19 mmol, 1.1 equiv.) was added to the mixture in a small volume of CH_2Cl_2, and stirring continued at ambient temperature for 16 hrs. The product was isolated by diluting the mixture with CH_2Cl_2 (50 mL), washed with H_2O (2 x 50 mL) and brine (1 x 50 mL). The organic layer was dried over $MgSO_4$ and evaporated to dryness resulting in a viscous dark orange oil that was purified by liquid chromatography on silica, eluted from hexane increasing the polarity to ethyl acetate:hexane (60:40).

Residual solvent was removed under high vacuum overnight. Yield: 3.11 g, orange viscous oil, (71%). ^{1}H NMR (400 MHz, $CDCl_3$): δ = 1.23, (s, 3H), 1.26 (s, 6H), 1.92 (s, 6H), 2.68 (t, *J* = 7.4 Hz, 8H), 2.90 (t, *J* = 7.4 Hz, 8H), 3.24 (s, 8H), 4.18-4.50 (m, 16H), 5.13 (s, 8H), 7.28-7.41 (m, 20H). ^{13}C NMR (100 MHz, $CDCl_3$): δ = 17.60, 17.75, 27.50, 30.65, 33.39, 34.27, 46.52, 46.63, 55.40, 63.23, 65.67, 65.79, 66.60, 128.30, 128.33, 128.60, 135.71, 169.73, 171.35, 171.42, 171.75, 171.86. Calcd: $[M+Na]^+$ ($C_{69}H_{83}BrNaO_{24}S_4$) m/z = 1525.3. Found: ESI-MS: $[M+Na]^+$ m/z = 1525.4, $[M+80Da]^+$ m/z = 821.1, $[M+K]^+$ m/z = 839.1, $[M+80Da]^+$ m/z = 1586.4. Calcd for $C_{69}H_{83}BrO_{24}S_4$: C, 55.08; H, 5.56; S, 8.52. Found: C, 56.28; H, 5.69; S, 8.68.

[$(Mp)_4$-G_2-BiB];[134] - [$(Mp)_4$-G_2-COOH];[132] (4.43 g, 3.03 mmol, 1.0 equiv.), [OH-BiB];[89] (0.768 g, 3.64 mmol, 1.2 equiv.), and DPTS (0.180 g, 0.61 mmol, 0.2 equiv.) were dissolved in 40 mL of anhydrous CH_2Cl_2 under a nitrogen atmosphere. N,N′-Dicyclohexylcarbodiimide (DCC) (0.69 g, 3.34 mmol, 1.1 equiv.) was added to the mixture in a small volume of CH_2Cl_2, and stirring continued at ambient temperature for 16 hrs. The product was isolated by diluting the mixture with CH_2Cl_2 (50 mL), washed with H_2O (2 x 50 mL) and brine (1 x 50 mL). The organic layer was dried over $MgSO_4$ and evaporated to dryness resulting in a viscous dark orange oil that was purified by liquid chromatography on silica, eluted from CH_2Cl_2 increasing the polarity to CH_2Cl_2:MeOH (90:10). Residual solvent was removed under high vacuum overnight. Yield: 3.40 g, orange viscous oil, (68%). ^{1}H NMR (400 MHz, $CDCl_3$): δ = 1.16-1.37 (m, 21H), 1.94 (s, 6H), 2.32-2.77 (m, 24H), 2.62 (t, *J* = 7.4 Hz, 8H), 2.88 (t, *J* = 7.4 Hz, 8H), 3.28 (s, 8H), 3.68 (t, 16H), 4.05-4.45 (m, 16H), 5.15 (m, 4H). ^{13}C NMR (100 MHz, $CDCl_3$): δ = 17.76, 18.44, 27.63, 30.66, 33.36, 34.52, 46.55, 46.65, 54.04, 55.39, 62.87, 63.42, 65.77, 67.04, 68.04, 169.72, 171.05, 171.34, 171.73, 171.85. Calcd: $[M+H]^+$ ($C_{69}H_{112}BrN_4O_{28}S_4$) m/z = 1651.5. Found: ESI-MS: $[M+H]^+$ m/z = 1651.6, $[M+Na]^+$ m/z = 1675.6, $[M+K]^+$ m/z = 1687.8, $[M+80Da]^+$ m/z = 1733.6 . Calcd for $C_{69}H_{112}BrN_4O_{28}S_4$: C, 50.14; H, 6.77; N, 3.39; S, 7.76. Found: C, 51.95; H, 7.03; N, 3.80; S, 7.84

[135]-[138] – Synthesis of LDHs using [127], [128], [133] or [134] **–** In a typical synthesis, targeting DP_n = 80 monomer units for the primary chains, [$(Bz)_2$-G_1-BiB];[127] (0.034 g, 0.042 mmol, 1 equiv.), OEGMA (1 g, 3.33 mmol, 80 equiv.) and bpy (0.0131 g, 0.084 mmol, 2 equiv.) were placed

into a 50 mL round-bottomed flask. IPA/H_2O (92.5/7.5 v/v) was added to the flask (50 wt% based on OEGMA) and the solution was stirred and deoxygenated using a nitrogen purge for 10 minutes. Cu(I)Cl (4.2 mg, 0.042 mmol, 1 equiv) was added to the flask, whilst maintaining a positive flow of nitrogen, and the solution was left to polymerise at 40 °C. The reaction was terminated by exposure to oxygen and addition of THF. Dowex Marathon exchange beads (approx. 2 g) were added to remove the catalytic system, followed by precipitation of the crude polymer once into petroleum ether (40-60 °C) which was cooled using an ice bath. The polymer was dried under high vacuum for approximately one hour.

[139]-[142] – Synthesis of HPDs using [127], [128], [133] or [134] **–** In a typical synthesis, targeting DP_n = 80 monomer units for the primary chains, [$(Bz)_2$-G_1-BiB];[127] (0.034 g, 0.042 mmol, 1 equiv.), OEGMA (1 g, 3.33 mmol, 80 equiv.), EGDMA (7.5 mg, 7uL, 0.038 mmol, 0.9 equiv.) and bpy (0.0131 g, 0.084 mmol, 2 equiv.) were placed into a 50 mL round-bottomed flask. IPA/H_2O (92.5/7.5 v/v) was added to the flask (50 wt% based on OEGMA) and the solution was stirred and deoxygenated using a nitrogen purge for 10 minutes. Cu(I)Cl (4.2 mg, 0.042 mmol, 1 equiv) was added to the flask, whilst maintaining a positive flow of nitrogen, and the solution was left to polymerise at 40 °C. The reaction was terminated by exposure to oxygen and addition of THF. Dowex Marathon exchange beads (approx. 2 g) were added to remove the catalytic system, followed by precipitation of the crude polymer once into petroleum ether (40-60 °C) which was cooled using an ice bath. The polymer was dried under high vacuum for approximately one hour.

[DBiB];[143] – 1-dodecanol (9.32 g, 0.05 mol, 1.0 equiv.) and triethylamine (6.07 g, 0.06 mol, 1.2 equiv.) were dissolved in 70 mL CH_2Cl_2 and cooled using an ice bath. α-bromo isobutyl-bromide (13.80 g, 0.06 mol, 1.2 equiv.) was added dropwise via a pressure equalising dropping funnel. After addition of α-bromoisobutyl bromide the reaction was allowed to warm to room temperature and left stirring for 24 hours. The product was isolated by washing the organic layer with $NaHCO_3$ (1 x 50 mL), water (4 x 50 mL), drying over $MgSO_4$, and evaporating to dryness. Additional purification was achieved by dissolving the compound in $CHCl_3$ and passing the crude product through a basic alumina column. After removal of solvents, the product was obtained as pale yellow oil. ^{1}H NMR

(400 MHz, $CDCl_3$): δ = 0.90 (s, 3H), 1.30-1.45 (m, 18H), 1.65 (2H), 1.92 (s, 6H), 4.15 (t, 2H). ^{13}C NMR (100 MHz, $CDCl_3$): δ = 14.0, 22.5, 26.0, 28.0, 29-30, 30.7, 32.0, 56.0, 66.0, 172.0. Calcd: $[M+NH_4]^+$ ($C_{16}H_{35}BrNO_2$) m/z = 352.19. Found: CI MS: $[M+NH_4]^+$ ($C_{16}H_{35}BrNO_2$) m/z = 352.19. Calcd for $C_{16}H_{31}BrO_2$: C, 57.31; H, 9.32. Found: C, 57.07; H, 9.25.

[144]-[148] – Synthesis of mixed initiated LDHs using [127], [128], [133] or [134] **–** In a typical synthesis, targeting DP_n = 80 monomer units for the primary chains, $[(Bz)_2$-G_1-BiB];[127] (0.0168 g, 0.021 mmol, 0.5 equiv.), [DBiB];[143] (7 mg, 0.021 mmol, 0.5equiv.), OEGMA (1 g, 3.33 mmol, 80 equiv.) and bpy (0.0131 g, 0.084 mmol, 2 equiv.) were placed into a 50 mL round-bottomed flask. IPA/H_2O (92.5/7.5 v/v) was added to the flask (50 wt% based on OEGMA) and the solution was stirred and deoxygenated using a nitrogen purge for 10 minutes. Cu(I)Cl (4.2 mg, 0.042 mmol, 1 equiv) was added to the flask, whilst maintaining a positive flow of nitrogen, and the solution was left to polymerise at 40 °C. The reaction was terminated by exposure to oxygen and addition of THF. Dowex Marathon exchange beads (approx. 2 g) were added to remove the catalytic system, followed by precipitation of the crude polymer once into petroleum ether (40-60 °C) which was cooled using an ice bath. The polymer was dried under high vacuum for approximately one hour.

[149]-[161] – Synthesis of mixed initiated HPDs using [127], [128], [133] or [134] **–** In a typical synthesis, targeting DP_n = 80 monomer units for the primary chains, $[(Bz)_2$-G_1-BiB];[127] (0.0168 g, 0.021 mmol, 0.5 equiv.), [DBiB];[143] (7 mg, 0.021 mmol, 0.5equiv.), OEGMA (1 g, 3.33 mmol, 80 equiv.), EGDMA (7.5 mg, 7uL, 0.038 mmol, 0.9 equiv.) and bpy (0.0131 g, 0.084 mmol, 2 equiv.) were placed into a 50 mL round-bottomed flask. IPA/H_2O (92.5/7.5 v/v) was added to the flask (50 wt% based on OEGMA) and the solution was stirred and deoxygenated using a nitrogen purge for 10 minutes. Cu(I)Cl (4.2 mg, 0.042 mmol, 1 equiv) was added to the flask, whilst maintaining a positive flow of nitrogen, and the solution was left to polymerise at 40 °C. The reaction was terminated by exposure to oxygen and addition of THF. Dowex Marathon exchange beads (approx. 2 g) were added to remove the catalytic system, followed by precipitation of the crude polymer once into petroleum ether (40-60 °C) which was cooled using an ice bath. The polymer was dried under high vacuum for approximately one hour.

Preparation of o/w emulsions at neutral pH - To form o/w emulsions, aqueous solutions (pH 7.37) (3 mL) of each of the synthesised polymeric surfactants **[135]-[142]**, **[144-161]** (2.5 mg/mL), were homogenised for two minutes (24,000 revolutions per minute (rpm)) with 3 mL of dodecane. The emulsions were left to equilibrate for 1 day before any measurements were taken. Emulsion droplet sizes were measured using laser diffraction, and selected samples were measured by optical microscopy.

Preparation of o/w emulsions at low pH – The methodology for emulsion preparation was identical to the above procedure but each polymer was first dissolved in aqueous acid (pH 1.64) prior to emulsification.

Preparation of o/w emulsions under dilution study – Selected emulsions were individually poured into 40 mL test tubes and 27 mL of water was added (new concentration of surfactant 0.25 mg/mL; pH 7.37) followed by homogenisation for 2 minutes at 24,000 rpm. The emulsions were left for 24 hours at room temperature and visual observations were made.

Preparation of o/w emulsions under thermal study – Selected emulsions were clamped in an oil bath, and heated for 1 hour at 60 °C (without stirring). Visual observations were made before and after the heating period.

6.6 References

1. J. S. Moore and S. I. Stupp, *Macromolecules*, 1990, **23**, 65-70.
2. H. Ihre, A. Hult and E. Söderlind, *Journal of the American Chemical Society*, 1996, **118**, 6388-6395.
3. H. Ihre, O. L. Padilla De Jesús and J. M. J. Fréchet, *Journal of the American Chemical Society*, 2001, **123**, 5908-5917.
4. M. C. Parrott, S. R. Benhabbour, C. Saab, J. A. Lemon, S. Parker, J. F. Valliant and A. Adronov, *Journal of the American Chemical Society*, 2009, **131**, 2906-2916.
5. H. Ihre, A. Hult, J. M. J. Fréchet and I. Gitsov, *Macromolecules*, 1998, **31**, 4061-4068.
6. M. Malkoch, E. Malmström and A. Hult, *Macromolecules*, 2002, **35**, 8307-8314.
7. K. Matyjaszewski, Y. Kwak and R. Nicolay, 2011, US20110046324 A1.

CHAPTER 7

Conclusions and further work

The overall aim of this project has been achieved, namely to develop a new synthetic strategy towards the surface functionalisation of dendritic materials. Two publications and a patent application have resulted from this work, and it is hoped that these publications will provide researchers within the field a novel solution to efficient functionalisation of dendritic materials.

In the early stages of the project, some difficulties did arise. Dendron functionalisation by amine Michael addition was found to be inefficient when higher ($>G_2$) generations were targeted and was therefore dropped in pursuit of the more nucleophilic thiol Michael addition.

Finding a successful route to introduce thiols to the surface of a dendritic material was challenging. A disulfide bond was initially used as a thiol protection strategy, but did not result in the synthesis of any thiol terminated dendritic materials. A second attempt at using 2,4-dinitrobenzene as a thiol protecting group (Sanger's reagent) resulted only in low generation materials. An inherent problem of the 2,4-dinitrobenzene protecting group was that to remove it, and generate the subsequent thiol, very large excesses of dodecanethiol were required.

In a final attempt, a xanthate group was found to be an excellent thiol protecting group. It was easily attached to the surface of a dendrimer, easily removed, and since the conditions under which it was removed and thiol-acrylate Michael additions occurred, were the same, removal of the xanthate functionality and thiol-acrylate Michael addition could be performed in the same pot. This eliminated the need to isolate the generated thiol intermediate and represented a significant milestone in the project.

Building from these findings, this strategy was used to produce high generation thiol-masked dendrimers and high generation thiol-masked linear dendritic materials. Bis-mPA was chosen for the dendritic scaffold and the construction of the dendritic materials was successfully achieved. One-pot deprotection and thiol acrylate click reactions were performed on all the materials with different acrylate substrates.

Each functionalised material was fully characterised by NMR, mass spectrometry and SEC techniques.

In the final part of the project, polymeric surfactants comprised of linear dendritic hybrids (LDHs) and hyperbranched polydendrons (HPDs) were synthesised. The initiators used to synthesise the polymeric surfactants were synthesised by the one-pot deprotection and thiol-acrylate chemistry.

O/w emulsions stabilised by surfactants comprised of linear polymers, LDHs, or mixed linear polymers/LDHs architectures showed coalescence over a long term stability study under neutral and acid conditions. In comparison, o/w emulsions stabilised by surfactants comprised of branched polymers, HPDs, or mixed branched polymer/HPDs architectures showed no coalescence over a long term stability study under neutral and acid conditions.

Further experiments probed the mixed branched polymer/HPDs and HPDs surfactant architectures with thermal and dilution experiments. In each case, emulsion breakdown by coalescence resulted.

The analysis of the dendritic materials was significant in this project, but further characterisation could have been achieved. High pressure liquid chromatography (HPLC) was not used at all, and could be have been used to confirm more accurately the purity of some of the compounds.

The syntheses of G_3 xanthate functional dendrimers were targeted, but were not isolated. Future studies may focus on an alternative synthetic strategy to overcome this problem, for example, by adopting a strictly divergent approach or a by hypercore approach (see Introduction).

Future studies may also seek to analyse the reaction kinetics of both the xanthate deprotection and thiol Michael addition. In all xanthate deprotection and thiol-acrylate Michael addition reactions, the reactions were left for 16 hours; although it has been suggested that the reactions may occur much more rapidly. It has also been suggested that RAFT/MADIX polymerisations may be conducted from the multiple xanthate peripheral sites on the dendrimers; producing core-first star type hybrids (see Introduction). Model reactions conducted within our research group have shown that the xanthate functionality used within this thesis is not effective at maintaining the controlled polymerisation of vinyl acetate via a RAFT/MADIX process.

Research currently ongoing from the described synthetic routes to xanthate functional LDHs has shown that partial deprotection of the peripheral xanthates within LDHs can also be achieved. This has allowed LDHs with mixed functionalities through a two-stage protection and functionalisation strategy to be produced, which is believed to be the first example of such materials.

Future work continuing from the emulsion chapter in this thesis is potentially huge, as emulsions have many significant commercial applications, particularly within drug delivery applications. It has been demonstrated that emulsions stabilised by surfactants comprised of branched architectures can remain stable for long periods of time (50 days), even when dodecyl end chains were removed and replaced with "less able" dendritic chain ends. This demonstrated that up to 75% of the polymer chain ends are effectively redundant within the surfactant.

Functionalisation of these chain ends may therefore be utilised for other purposes, such as attachment of drugs, or specific cell receptors to aid drug delivery.

A pH trigger may also be an additional area for exploration as such properties again may have useful biomedical applications.